The role of systemic and local inflammation, the tumour microenvironment and the IL6/JAK/STAT3 pathway in primary operable breast cancer.

Elizabeth Morrow MBChB MRCSEd

A thesis submitted in fulfilment of the requirements for the degree of Doctor of Philosophy.

Institute of Cancer Sciences
College of Medical, Veterinary & Life Sciences
University of Glasgow

March 2021

Abstract

Breast cancer is the second most common cause of cancer death in females in the UK. It is a heterogenous disease with subtypes which behave differently. There are targeted treatments available for luminal and HER2+ cancers but treatment resistance and cancer recurrences occur. There are currently no targeted treatments for triple negative breast cancer (TNBC). New prognostic tools to stratify risk to guide use of the most aggressive treatments, and new therapeutic targets are desirable. The role of the tumour microenvironment in tumour progression is increasingly recognised. Features of the tumour such as necrosis and budding have been reported to have a prognostic role in cancer and may be influenced by the tumour microenvironment. Cell signalling pathways such as the IL6/JAK/STAT3 pathway provide a link between the tumour microenvironment and tumour cells. Better understanding of these features and pathways may lead to identification of new prognostic and predictive tools and of new therapeutic targets.

The work of this thesis is carried out in two cohorts of patients with primary operable breast cancer with mature follow up. Data was available from clinical records for both regarding patient age, tumour pathology, treatment details and survival. Full section slides from surplus tissue were available from both cohorts and a tissue microarray (TMA) had been previously constructed for the largest cohort. The majority of the work in this thesis is carried out using haematoxylin and eosin (H&E)-stained full section slides and TMA slides stained using immunohistochemistry (IHC) techniques for various proteins. Staining for IL6 expression was carried out using RNA scope. Transcriptomics was carried out using TempOSeq to identify genes associated with tumour budding.

The work of this thesis describes a new combined score of tumour necrosis, budding and tumour-stroma percentage (TSP) which has prognostic value in primary operable breast cancer. It identifies a poor prognostic group in oestrogen receptor positive (ER+) disease which could be targeted for more aggressive treatment, and stratifies risk in ER- disease. 9 genes of potential interest for further investigation are identified as being associated with the high budding phenotype in ER- cancers. For the first time in the literature, this work will describe, in luminal A cancers, an association between tumour IL6 and

membranous IL6R expression and worse cancer specific survival (CSS), and an association between pSTAT3(Ser727) and improved CSS, indicating potential roles as prognostic markers in this subtype. It will describe the expression and associations with survival of other members of the pathway, informing further research regarding in which subtypes inhibiting targets in the pathway may be of clinical value.

Table of Contents

List of Tables

List of Figures

List of Publications

Published Abstracts

ES Morrow, F Gujam, Z Mohammed, DC McMillan, J Edwards. Abstract P1-07-06: The relationship between Klintrup-Makinen score and cancer-specific survival in primary operable breast cancer. Cancer Res February 2018 (78) (4 Supplement) P1-07-06; DOI: 10.1158/1538-7445.SABCS17-P1-07-06

ES Morrow, F Gujam, Z Mohammed, DC McMillan, PG Horgan, AK Roseweir, J Edw ards. Abstract P2-08-23: A combined score of tumour budding and tumour necrosis has prognostic value for cancer specific survival in both ER positive and ER negative primary operable breast cancer. Cancer Res February 15 2019 (79) (4 Supplement) P2-08-23; DOI: 10.1158/1538-7445.SABCS18-P2-08-23

E Morrow, A Roseweir, F Gujam, L Romics, A Lannigan, P Horgan, D McMillan, J Edwards. A combined score of tumour necrosis, tumour budding and tumour-stroma percentage predicts cancer specific survival in primary operable breast cancer. European Journal of Surgical Oncology. May 2019. 45.5.884-885.

List of Accompanying Material

TempOSeq data (used in chapter 6). Microsoft Excel file: TempOSeq data.csv

Acknowledgement

Firstly, huge thanks to my primary supervisor, Joanne Edwards. Thank you so much Joanne for all your guidance, support, patience and infectious enthusiasm. I feel very lucky to have you as a supervisor. To my other supervisors, Antonia Roseweir & Laszlo Romics, thank you for your support and advice.

Thank you to all my colleagues in the lab, particularly Jean Quinn for all your help and guidance in the lab and for patiently dealing with all the stupid questions of this lab novice. Thanks also to everyone in the Academic Unit of Surgery at GRI, particularly to Donald McMillan for his mentorship, to Stephen McSorely and Ross Dolan for being my statistics and RevMan gurus and to Hester van Wyk for her advice on budding scoring. I am grateful to Professors Horgan and McMillan for welcoming me, a breast cancer black sheep, into their predominantly colorectal research unit. A huge thanks to Fadia Gujam, my predecessor in the lab, for teaching me the scoring methods and without whose previous hard work I would not have benefited from such a large dataset.

A number of people have helped specifically with the work of this thesis. Grateful thanks go to Clare Orange and Jen Hay at the NHS GGC Biorepository for their time and effort scanning slides, teaching me to use Slidepath, pulling tissue blocks and answering my numerous queries and requests. Thank you also to Dr Elizabeth Mallon for her support and for her expert training in the basics of breast pathology. Thank you to Colin Nixon and his laboratory colleagues in the Beatson Institute for carrying out the IL6 staining for me and to Gemma Thomson for training me in the use of the Halo software. Thanks to Harper Van Steenhouse and Ditte Andersen at Bioclavis for their collaboration for the transcriptomics work.

Finally, thank you Pete for putting up with me, for tolerating the intermittent high jacking of your over-sized computer so that I didn’t have to do everything on a laptop, for maintaining the supply of caffeine and hugs, and for generally being a massive support. A mention should also go to all involved with the Tailenders podcast. Thanks for ensuring that my tears during the seemingly interminable task of slide scoring were tears of laughter rather than despair. Go well.

Author's Declaration

I declare that I am the sole author of this thesis. Unless otherwise acknowledged, all of the work in this thesis was carried out personally. This thesis has not been submitted previously for a degree or diploma at this or any other institution.

Definitions/Abbreviations

ADH	Atypical ductal hyperplasia
ALH	Atypical lobular hyperplasia
ATAC	Arimidex, Tamoxifen, Alone or in Combination
AUC	Area under the curve
B (lymphocytes/cells)	Bone marrow-derived
CAF	Cancer associated fibroblast
CC	Craniocaudal
CD	Cluster of differentiation
CHO	Chinese hamster ovary
CI	Confidence interval
CSS	Cancer specific survival
CT	Computed topography
DC	Dendritic cells
DCIS	Ductal carcinoma in situ
DFS	Disease-free survival
DIEP	Deep inferior epigastric perforator
DLBCL	Diffuse large B-cell lymphoma
DNA	Deoxyribonucleic acid
dNLR	Derived neutrophil/lymphocyte ratio
EMT	Epithelial mesenchymal transition
ER	Oestrogen receptor
ERK	Extracellular signal-regulated kinase
FFPE	Foramlin-fixed paraffin-embedded
FISH	Fluorescence in situ hybridisation
GH	Growth hormone
gp	Glycoprotein
H&E	Haematoxylin and eosin
HER2	Human epidermal growth factor 2
IL	Interleukin
IL6R	Interleukin-6 receptor
JAK	Janus kinase
LCIS	Lobular carcinoma in situ
LD	Latissimus dorsi
LDH	Lactate dehydrogenase
LMR	Lymphocyte/monocyte ratio
MAPK	Mitogen-activated protein kinase
MDT	Multi disciplinary team
MFS	Metastases-free survival
mGPS	Modified Glasgow Prognostic Score
MHC	Major histocompatibility complex
MLO	Mediolateral oblique
MRI	Magnetic resonance imaging
mRNA	Messenger ribonucleic acid
MSC	Mesenchimal stem cells
MYD88	Myeloid differentiation primary response 88
NFκB	Nuclear factor kappa-light-chain-enhancer of activated B cells
NHSBSP	National Health Service Breast Screening Programme
NICE	National Institute of Clinical Excellence

NK	Natural killer
NLR	Neutrophil/lymphocyte ratio
NPI	Nottingham Prognostic Index
OBCS	Oncoplastic breast conserving surgery
OS	Overall survival
pCR	Pathological complete response
PD-1	Programmed death receptor-1
PD-L1	Programmed death ligand-1
PD-L2	Programmed death ligand-2
PLR	Platelet/lymphocyte ratio
PR	Progesterone receptor
pSTAT	Phosphorylated signal transducers and activators of transcription
pT	Pathological tumour stage
qRT-PCR	Quantitative reverse transcription polymerase chain reaction
RNA	Ribonucleic acid
ROC	Receiver operating characteristic
SBCS	Standard breast conserving surgery
Ser	Serine
STAT	Signal transducers and activators of transcription
T (lymphocytes/cells)	Thymus-derived
TIL	Tumour-infiltrating lymphocyte
TNBC	Triple negative breast cancer
TNM	Tumour Nodes Metastases
TRAM	Transverse rectus abdominus myocutaneous
TSP	Tumour-stroma percentage
TYK2	Tyrosine kinase 2
Tyr	Tyrosine
WHS	Weighted histoscore

1 Introduction

This introductory chapter will first describe the epidemiology, diagnosis, pathology and treatment of breast cancer to provide background and context. It will then outline the current tools used to aid individualised treatment decision making and their limitations, and thus the desirability of novel prognostic tools. Finally it will outline current understanding of the tumour microenvironment and of the IL6/JAK/STAT3 pathway to explain why this thesis will focus on these areas in the search for novel prognostic markers which may be of use in clinical practice.

1.1 Breast Cancer Epidemiology

1.1.1 Incidence and trends

Breast cancer is the most common cancer in females in the UK, with approximately 55,200 new cases every year. It accounts for 15% of the total cancer cases diagnosed. In females, breast cancer represents 30% of new cancer cases but in males it is less than 1%. Incidence rates increase with age, with an average of 24% of new cases occurring in those aged over 75 years. Incidence rates have increased by 18% in the UK since the early 1990s (23% in females) and are projected to rise by 2% between 2014 and 2035(1).

1.1.2 Mortality and trends

Overall, breast cancer is the fourth most common cause of cancer-related death in the UK. In females it is the 2nd most common cause of cancer-related death. It accounts for approximately 11,500 deaths every year. Mortality rates from breast cancer have reduced by 39% since the early 1970s in the UK, and by 19% in the last decade. They are projected to fall by a further 26% between 2014 and 2035(1).

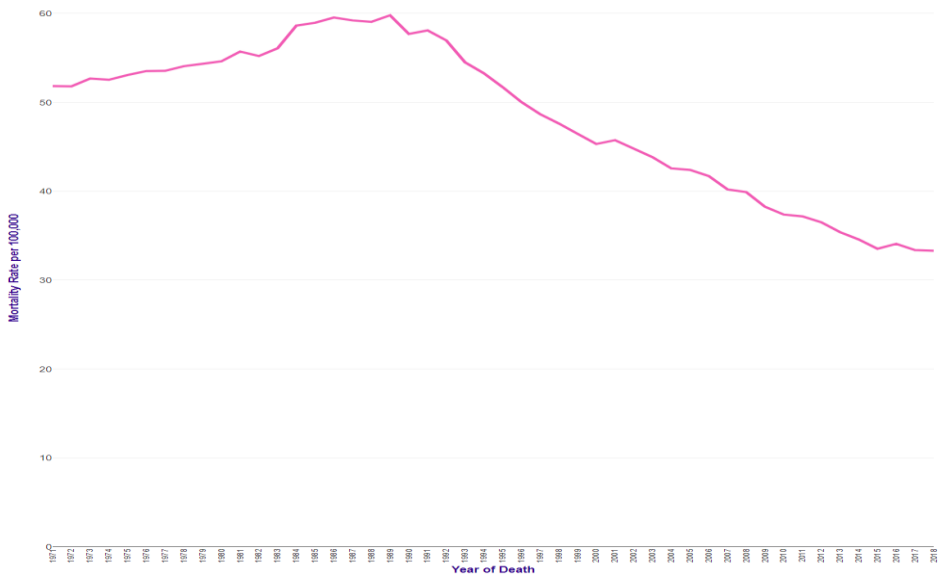

Figure 1-1. Breast cancer European age-standardised mortality rates per 100,000 females in the UK, 1971-2018. Credit: Cancer Research UK.

1.1.3 Risk factors

A woman born after 1960 in the UK has a 15% estimated lifetime risk of developing breast cancer(1). Increasing age is the primary risk factor for breast cancer. Genetics also have an important role to play. Risk of breast cancer increases with each first-degree relative affected, and with relatives affected under 50 years of age. A number of genetic mutations are associated with an increased risk of breast cancer (over 80% lifetime risk in some(2)), of which the most common are BRCA 1, BRCA2 and TP53. However, 23% of breast cancer cases in the UK are preventable(3). Environmental and lifestyle factors which have been shown to contribute to breast cancer risk include being overweight and obesity (8% of cases), alcohol (8%), not breastfeeding (5%), post-menopausal hormone replacement therapy (2%), ionising radiation (1%) and oral contraceptives (<1%)(1).

1.2 Breast cancer diagnosis

1.2.1 Symptomatic clinics and the breast screening programme

The two main routes of presentation with breast cancer in the UK are via symptomatic clinics or the national breast screening programme. Symptomatic patients are referred by their GP to a breast clinic where they undergo triple assessment. This term encompasses clinical assessment, imaging if required, and

biopsy where indicated. The most common presenting symptoms of breast cancer(4) are illustrated below.

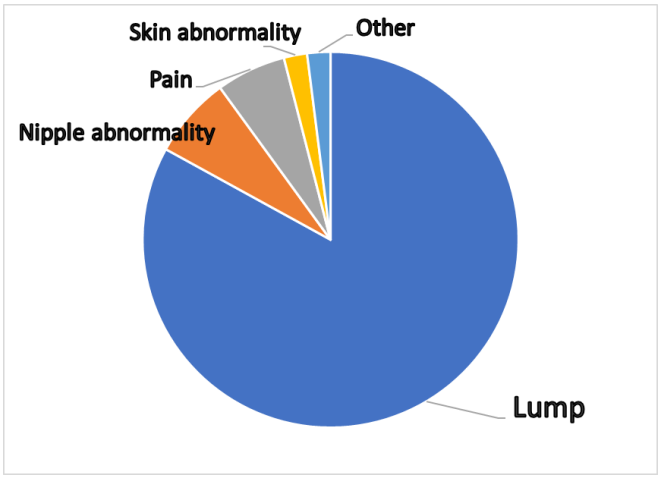

Figure 1-2. Breast cancer presenting symptoms. Chart illustrating the rates of symptoms in patients with a symptomatic presentation of breast cancer (Breast lump 83%, nipple abnormalities 7%, breast pain 6% and breast skin abnormalities 2%)

The UK National Health Service Breast Screening Programme (NHSBSP) was established in 1988. Currently, women aged 50-70 years are invited every three years for screening mammography, though women over the age of 70 years can self-refer for screening and selected patients who have been identified as being at high or moderate risk of developing breast cancer may be offered screening from a younger age and at more frequent time intervals(2). Screening is in the form of two-view digital mammography comprising MLO and CC projections of each breast(2). In the case of an abnormal mammogram, women are recalled to second stage screening when they will undergo clinical examination and further assessment may include further mammographic views, ultrasound and tissue sampling if indicated(2). If biopsy confirms in situ or invasive cancer, the patient is referred on to a breast surgeon for further assessment. In 2015/2016 in Scotland, 1392 breast cancer cases were diagnosed through the screening programme(5).

Where indicated, women presenting to a symptomatic breast clinic will undergo imaging. In women 40 years and over this is in the form of mammography with or without ultrasound. Ultrasound is the imaging modality of choice in women under 40 years due to breast density but mammography may be carried out in younger patients where there is a high degree of suspicion of cancer(6). In selected cases MRI imaging of the breast is also carried out though this does not

form part of the one stop clinic. This is indicated if there is a discrepancy regarding the extent of the disease from other assessment modalities, if accuracy of mammographic assessment is jeopardised by breast density, or if breast conserving surgery (BCS) is being considered for lobular cancer(7).

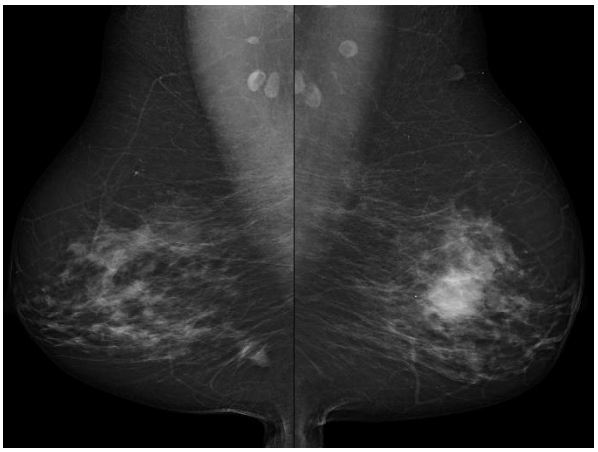

Figure 1-3. Abnormal mammogram. Example of an abnormal bilateral mammogram (MLO view). Case courtesy of Dr Alexandra Stanislavsky, Radiopaedia.org, rID: 62207

Lesions are biopsied using either a 14-gauge spring-loaded core biopsy needle or by a large volume vacuum-assisted biopsy(2). Regardless of whether the lesion is palpable or impalpable, the gold standard is for biopsy to be performed under image guidance(6) though a freehand core biopsy may be required when there is a palpable abnormality but imaging is normal. The core biopsy method allows the pathologist to report on the presence of *in situ* and/or invasive cancer, the grade of the tumour (using the Nottingham Bloom Richardson grading system based on nuclear pleomorphism, tubule formation and mitotic rate(8)), the oestrogen and HER2 receptor status of the tumour, and often the histological type(9).

1.2.2 Breast cancer staging

The stage of breast cancer describes the extent of disease. Currently the TNM system is used, with 'T' representing the local extent of the tumour, 'N' the degree of nodal involvement and 'M' the presence or absence of distant metastatic disease. The tumour extent is assessed using a combination of clinical examination and the imaging techniques described previously. T stage is denoted as shown in **Table 1-1**. In the UK, all patients diagnosed with invasive breast cancer undergo axillary ultrasound, with needle biopsy of any abnormal lymph nodes, as preoperative staging of the axillary nodes(7). Routine imaging for

metastatic disease is not indicated in asymptomatic patients with early (T1/2 and clinically node negative) disease, due to the low rate of metastases at presentation in these patients(10, 11). In symptomatic patients, appropriate investigations are carried out as indicated by the symptom and may include CT scan of chest, abdomen and pelvis. For asymptomatic patients with advanced disease, a CT scan is carried out in the first instance followed by a bone scan and/or liver ultrasound if required(12) though there is slight variation in staging practice regionally(10). The most common sites of breast cancer metastases are bone, lung, brain and liver(13).

Tumour stage	Description
TX	Primary tumour cannot be assessed
T0	No evidence of primary tumour
Tis	Carcinoma in situ
Tis (DCIS)	Ductal carcinoma in situ
Tis (LCIS)	Lobular carcinoma in situ
Tis (Paget's)	Paget's disease of the nipple without invasive carcinoma, DCIS or LCIS
T1	Tumour ≤20mm greatest diameter
T1mi	Tumour ≤1mm
T1a	Tumour >1mm but ≤5mm
T1b	Tumour >5mm but ≤10mm
T1c	Tumour >10mm but ≤20mm
T2	Tumour >20mm but ≤50mm
T3	Tumour >50mm
T4	Tumour any size with direct extension to the chest wall and/or skin
T4a	Extension to the chest wall
T4b	Ulceration and/or ipsilateral satellite nodules and/or skin oedema
T4c	T4a and T4b
T4d	Inflammatory carcinoma
Nodal stage	
cN0	No nodal metastases
cN1	Metastases to moveable level I&II ipsilateral LNs.
cN2	Either of the below.
cN2a	Ipsilateral level I&II axillary LNs matted or fixed.
cN2b	Metastases ONLY in ipsilateral internal mammary nodes.
cN3	Any of the below.
cN3a	Metastases in ipsilateral infraclavicular LN.
cN3b	Metastases in ipsilateral internal mammary AND axillary LNs.
cN3c	Metastases in ipsilateral supraclavicular supraclavicular LN.
Metastases	
M0	No distant metastases
M1	Distant metastases

Table 1-1. Breast cancer staging. Table created using information from Breast Cancer Staging System: AJCC Cancer Staging Manual, Eighth edition, Part XI: Breast. cN = clinical nodal stage. This is specified as post operative pathological lymph node staging uses different definitions. LN = lymph node. Levels I & II = axillary lymph nodes lateral to and behind pectoralis minor respectively.

1.2.3 The role of the multidisciplinary team (MDT)

Multi-disciplinary team-based decision making in breast cancer care has evolved as diagnostic and treatment options have become more complex, as will be outlined later in this chapter. Their role is variable worldwide(14) but in the UK it is mandatory for each patient diagnosed with breast cancer to be discussed within the MDT. These teams comprise breast surgeons, a clinical and a medical oncologist, radiologists, pathologists, breast cancer nurse specialists and a MDT

coordinator/secretary with other optional members(15). This allows for discussion between different health professionals with different areas of expertise, to determine the optimal care pathway for each individual patient. While high quality evidence is lacking, some studies have reported improved patient outcomes with the use of multidisciplinary care(16).

1.3 Breast Cancer Pathology

1.3.1 Histological subtypes

Breast cancer is a heterogenous disease which can be classified by histological or molecular subtype. There are various histological types of breast cancer which differ in pattern of spread and prognosis. The most common is ductal cancer accounting for 70-75% of all breast cancer cases, followed by lobular cancer (5-15%)(17). Less common subtypes include mucinous, medullary and tubular cancers. Pre-invasive cancer which has not breached the basement membrane is termed *in situ* carcinoma(9). It may be ductal (ductal carcinoma in situ, DCIS) or lobular (lobular carcinoma in situ, LCIS).

a) b)

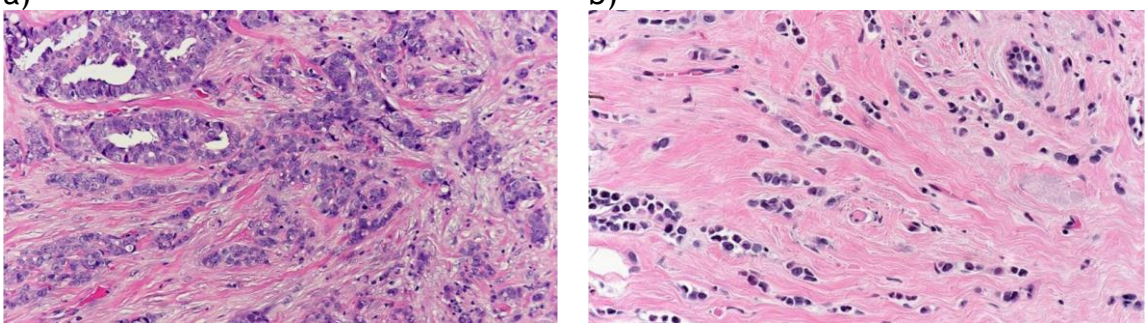

Figure 1-4. Histological subtypes of breast cancer. Images showing examples of the two most common types of breast cancer. H&E-stained slides of a) ductal cancer and b) lobular cancer. Images courtesy of John Hopkins University Department of Pathology https://pathology.jhu.edu/breast/types-of-breast-cancer/

1.3.2 Receptors

Breast cancers may express various receptors. Three of these are routinely reported on pathology reports because of their significance in terms of prognosis and tumour response to systemic treatments.

The oestrogen receptor (ER) is an intracellular, nuclear, oestrogen-binding receptor protein. Upon ligand activation, it regulates target gene expression. ER

is expressed in normal breast tissues and is important for breast development(18). It is upregulated in 70% of breast cancers(19) and is related to tumour cell proliferation. It can be targeted in the treatment of breast cancer by anti-oestrogens such as tamoxifen, which will be covered in greater detail later in this chapter. ER expression is therefore an important predictive factor for response to these therapies. It can be identified by immunohistochemistry techniques using specific antibodies. The results are reported as an Allred score, calculated using the percentage of cells which stain positive and a numerical rating of the staining intensity from 0-3(19). The score ranges from 0-8 and tumours with Allred score >2 are regarded as positive.

a) b)

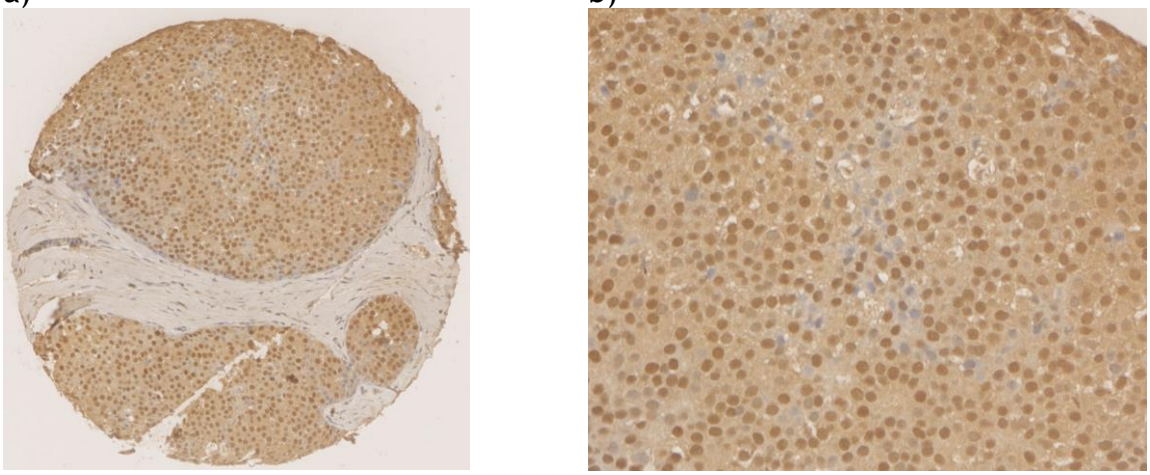

Figure 1-5. ER staining. Images of breast cancer tissue stained using immunohistochemistry for the oestrogen receptor at a) x10 magnification and b) x40 magnification.

Like the ER, the progesterone receptor (PR) is a steroid hormone nuclear receptor which acts as a ligand-activated transcription factor and is involved in pro-proliferative signalling in the breast(20). There is considerable cross talk between the two pathways. The independent predictive power and clinical utility of PR above that of ER alone is controversial and NICE no longer recommend routine measurement. However, a number of studies have reported its prognostic power(21-24). Unlike ER, targeted therapies against the PR have not come into widespread use as early clinical trials reported intolerable side effects due to significant cross-reactivity with the glucocorticoid receptor(20). PR is identified by IHC and reported using the Allred score as described above.

Human epidermal growth factor receptor 2 (HER2 or HER2/neu) is alternatively named receptor tyrosine-protein kinase erbB-2 or protooncogene Neu. It has no identifiable ligand and can undergo ligand-independent dimerization with other

epidermal growth factor receptors leading to tumour promotion(25). HER2 overexpression is present in approximately 15% of breast tumours. It is associated with poorer prognosis but its expression does allow targeted treatment for the tumour by therapies such as the monoclonal antibody trastuzumab. Similarly to the other receptors, HER2 expression is identified using IHC. However, the scoring system is different. It is reported based on the intensity of reaction product and the percentage of membrane positive cells to give a score 0-3+. Scores of 0 or 1+ are reported as negative, 3+ as positive and 2+ as borderline. These latter samples therefore undergo fluorescence in situ hybridisation (FISH) for confirmation(19).

a) b)

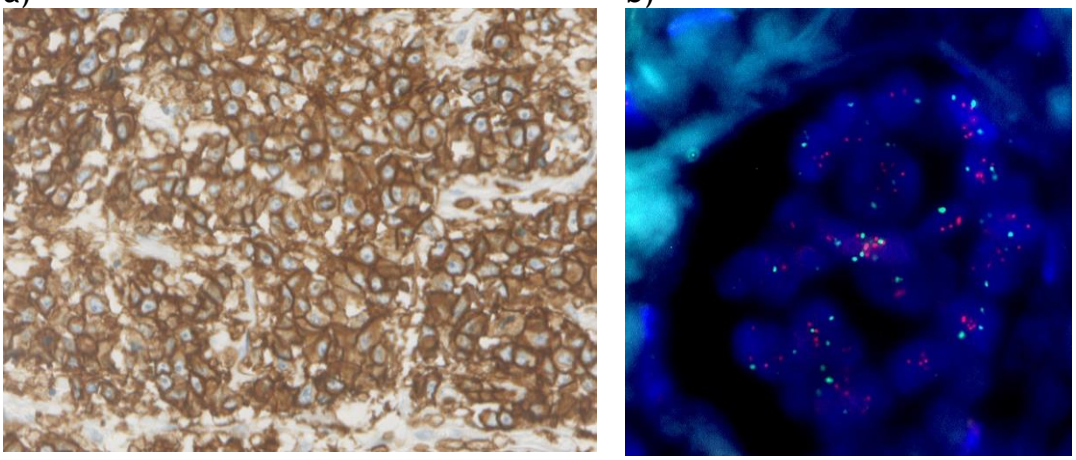

Figure 1-6. HER2 staining. Examples of staining for HER2: a) immunohistochemistry staining of breast cancer tissue at x 40 magnification, b) HER2 amplification by FISH in breast cancer cells. Image b) attributable to IrinaPav, CC BY-SA 4.0 <https://creativecommons.org/licenses/by-sa/4.0>, via Wikimedia Commons

1.3.3 Molecular subtypes

The presence or absence of these receptors, along with other features, allow breast cancers to be categorised into specific molecular subtypes to guide targeted systemic treatments. The different subtypes behave differently and have varying prognosis. The different molecular subtypes, as described in the report of the 12th St Gallen International Breast Cancer Conference (2011) are summarised in Table 2(26).

Intrinsic subtype	ER/PR	HER2	Ki67	Systemic Therapy
Luminal A	Positive	Negative	Low (<14%)	Endocrine therapy. Chemotherapy in few cases.
Luminal B				
HER2-	Positive	Negative	High (>14%)	Endocrine therapy +/- chemotherapy
HER2+	Positive	Positive	Any	Endocrine therapy + anti HER2 therapy + chemotherapy
HER2 overexpression	Negative	Positive	Any	Anti-HER2 therapy + chemotherapy
Basal-like (Triple negative)	Negative	Negative	Any	Chemotherapy

Table 1-2. Molecular subtypes of breast cancer. Table summarising the four main molecular subtypes of breast cancer as determined by the ER/PR, HER2 and Ki67 status of the tumour. The final column summarises the types of systemic treatment which might be offered in each case.

1.4 Breast Cancer Management

1.4.1 Breast surgery

1.4.1.1 Standard breast conserving surgery

Surgical resection of the tumour remains the mainstay of treatment for early breast cancer. Standard breast conserving surgery (SBCS) in the form of a wide local excision aims to resect the tumour with a clear margin of healthy tissue around it. If malignant cells are seen by the pathologist <1mm from the margin of the specimen, then further resection is required due to the risk of residual disease in the breast and therefore an increased risk of recurrence(27). The definition of a clear margin is controversial and varies worldwide, for instance "no tumour on ink" is used to define a clear margin in the USA and in DCIS, a 2mm margin is required(28). With the addition of adjuvant radiotherapy, SBCS has comparable survival outcomes to mastectomy(29). Traditionally SBCS can be carried out for tumours which occupy less than one third of the total volume of the breast. Resecting tumours larger than this is likely to result in considerable deformity.

1.4.1.2 Oncoplastic breast conserving surgery

With improved survival from breast cancer, aesthetic outcome following breast cancer surgery has become almost as important as safe oncological resection of

the tumour. Developments in plastic surgery techniques have led to an increasing role for oncoplastic breast conserving surgery (OBCS). This encompasses a range of therapeutic mammoplasty techniques which allow preservation of the breast shape following resection of larger tumours which would be considered too large for SBCS. OBCS accounted for nearly 3% of the definitive operations for primary breast cancer in Scotland in 2014 and 2015(30). The improved cosmetic outcomes which these techniques provide are important to the psychosocial well-being and quality of life of patients(31, 32) but there are some concerns related to post-operative complications. OBCS is more extensive surgery than SBCS, and complication rates have been reported to be as high as 28.4%(33). Post-operative complications may lead to a delay in adjuvant treatments, though the evidence to date is mixed as to whether OBCS is associated with delay to adjuvant therapies compared to SBCS or mastectomy(34).

1.4.1.3 Mastectomy

For those patients with tumours which are not suitable for breast conserving surgery, mastectomy is required. The modified radical mastectomy involves excision of all of the breast tissue, down to the pectoral fascia, and includes an ellipse of overlying skin with the nipple-areolar complex. To improve cosmetic outcome following breast reconstruction, several skin and/or nipple-preserving mastectomy techniques have been developed which can be used if the patient is to undergo immediate breast reconstruction and when oncologically safe to do so.

1.4.1.4 Breast reconstruction

All patients who undergo mastectomy should be offered breast reconstruction if fit enough(7). This can be performed immediately or in the delayed setting, once adjuvant treatments are complete. There are advantages and disadvantages to each approach. Delayed reconstructions allow more time for decision making and do not risk delay to adjuvant therapies in the event of post-operative complications but may have an inferior aesthetic outcome and incur higher costs(35). Immediate reconstruction, at the time of mastectomy, may be carried out in the context of a skin-sparing or nipple-sparing mastectomy

resulting in superior aesthetic outcome including preserved breast shape, though there is a risk of delay to adjuvant therapy in the event of a complication and the final appearance, particularly in the case of implant reconstruction, may be affected by radiotherapy.

Reconstructions can be implant-based, autologous or a combination of both. Autologous reconstructions utilise musculocutaneous flaps of the patient's own tissue. They may be pedicled flaps, such as the latissimus dorsi (LD) flap and the transverse rectus abdominus myocutaneous (TRAM) flap, or free flaps such as the deep inferior epigastric perforator (DIEP) flap which requires anastomosis of donor site microvessels to the intercostal perforator vessels at the recipient site. For this reason, it may not be suitable for patients at high risk of microvascular disease, such as smokers and diabetics, as they have a much higher risk of postoperative wound necrosis and flap failure.

1.4.2 Radiotherapy

Radiotherapy is given in cancer to administer high doses of radiation to cancer cells, causing radiation-induced cell death(36). Breast radiotherapy is offered to patients who have had breast-conserving surgery as it has been shown to reduce the risk of recurrence(7). For patients who have had mastectomy, radiotherapy is offered to node-positive patients and those with involved resection margins. It may also be given to node-negative patients with T3-4 disease but is not recommended for those at low risk of recurrence(7). Radiotherapy can also be offered to the regional lymph nodes in selected patients, such as supraclavicular fossa irradiation for those with 4 or more involved axillary lymph nodes(7).

1.4.3 Systemic therapy

In early stage (operable) breast cancer, systemic therapy is given in the adjuvant (after surgery) setting with the aim of destroying any circulating tumour cells or micrometastatic deposits. The choice of systemic therapy, in terms of endocrine therapy, chemotherapy, both or neither, is determined by the receptor status of the tumour, the stage of the cancer and the fitness of the patient. Systemic therapy can also be given in the neoadjuvant (before surgery) setting with the aim of reducing the size of the tumour preoperatively to allow less extensive

surgery to be performed. Neoadjuvant chemotherapy also has the advantage that the oncologist is able to observe the response of the tumour to the specific chemotherapy agent, and to alter treatment if necessary.

1.4.3.1 Endocrine therapy

Endocrine therapy is suitable for use against tumours which express the oestrogen receptor, as the growth of these tumours is driven by oestrogen. Currently it is given for 5 or more years following surgical resection of the tumour(7).

Tamoxifen was first tested in the 1970s. It is a non-steroidal anti-oestrogen, otherwise termed a selective oestrogen receptor modulator. It binds the oestrogen receptor, thus disrupting oestrogen-binding which consequently blocks hormone-dependent tumour cell proliferation(18) by blocking the transcription of key growth factors(37). It has been shown in various trials to reduce recurrence of ER positive breast cancer in both pre and post-menopausal women(37). Whilst it blocks the action of oestrogen on breast cancer cells, it seems to have a partial agonist effect in endometrial tissue(37), resulting in increased endometrial cell proliferation and the increased risk of endometrial cancer(18).

Subsequently, aromatase inhibitors such as anastrozole and letrozole were developed and introduced in 1995(37). They act by blocking the conversion of testosterone to oestrogen by inhibiting the enzyme aromatase, and consequently are suitable for use in post-menopausal ER positive breast cancer but have little effect in pre-menopausal breast cancer. The ATAC trial demonstrated superior disease-free survival in post-menopausal breast cancer treated with anastrozole compared to tamoxifen(38). The main side effects of aromatase inhibitors are musculoskeletal problems including osteopenia and osteoporosis with the associated fracture risk.

Aromatase inhibitors are currently the first-line choice of endocrine agent in post-menopausal women at medium or high risk of recurrence, whereas tamoxifen is recommended for those with low recurrence risk, and in pre-menopausal women and all men(7). Premenopausal women may also be offered

ovarian function suppression, particularly if deemed at high risk of disease recurrence(7).

Despite the effectiveness of these therapies, resistance does occur resulting in breast cancer recurrence in some patients whilst on these treatments, or once they have been stopped. There is currently debate, and trials are ongoing, to determine the optimum duration and combination of endocrine treatment for various tumour types and stages. The potential benefits of reduced recurrence rates when extending endocrine therapy beyond 5 years must be weighed against the side effects of the treatment. Currently in the UK, it is recommended to offer extension of endocrine therapy beyond 5 years (by continuation of tamoxifen or switch to/continuation with an aromatase inhibitor) in patients who have been treated with tamoxifen for 2-5 years of those 5 years(7).

1.4.3.2 Chemotherapy

Chemotherapy is offered to patients with ER negative cancer and those with high risk ER positive cancers. In the UK, regimen include an anthracycline with or without a taxane, usually given over 6 cycles(7). Chemotherapy has significant risks and side effects, including nausea, alopecia, cardiotoxicity, neutropenia, neuropathy and hypersensitivity reactions. Therefore these risks must be weighed against the potential benefits, and in patients with multiple or significant comorbidity, the risk may be deemed too high.

In patients with ER positive cancer who are considered to be at an intermediate risk of disease recurrence, the decision regarding whether to give chemotherapy can be challenging. Currently, online tools such as PREDICT(39) can be used to help stratify risk. For patients with ER positive, HER2 negative, node negative cancer stratified as at intermediate risk, tumour gene-profiling tests such as EndoPredict® or Oncotype DX® Breast Recurrence Score can be used to help guide chemotherapy decisions(19). These tools will be considered in more detail later in this chapter.

1.4.3.3 Herceptin

Herceptin, or trastuzumab, is a monoclonal antibody used in the treatment of patients with HER2+ breast cancer. Its mechanism of action is complex and not

fully understood but includes antibody-dependent cellular toxicity, intracellular mechanisms involving apoptosis and cell cycle arrest, inhibition of angiogenesis and prevention of DNA repair following chemotherapy-induced damage(25). The addition of Herceptin to chemotherapy has been shown to improve outcomes in early (in the neoadjuvant and adjuvant settings) and advanced HER2+ breast cancer(25). It is administered at 3-week intervals for 1 year(7). Adverse effects include reversible cardiotoxicity (25) and therefore the presence of significant pre-existing cardiac disease may preclude its use in some patients. Pertuzumab is also a monoclonal antibody which inhibits HER2 dimerisation. It is recommended by NICE, in combination with trastuzumab and chemotherapy, for neoadjuvant treatment of HER2 positive breast cancer which is locally advanced, inflammatory, or early-stage but at high risk of recurrence(40). In the adjuvant setting it is recommended for use in lymph node positive disease(41). More recently, the KATHERINE trial reported that use of T-DM1, a conjugate of trastuzumab and the cytotoxic drug emtansine, in patients with HER2 positive breast cancer with residual invasive disease following neoadjuvant therapy resulted in a 50% reduction in risk of invasive recurrence or death(42).

1.4.3.4 Bisphosphonates

Bisphosphonates have traditionally been used to slow bone thinning and reduce the risk of fractures in people with osteoporosis. In cancer, they are used to reduce the risk of fractures, slow disease progression and reduce pain in the context of malignant bone disease. In breast cancer they have been used to reduce bone thinning in patients receiving aromatase inhibitors. However, they do have effects on T-cell function and so it has been suggested that they could prevent or delay disease recurrence in early breast cancer. A recent review of current evidence has led NICE to recommend that bisphosphonates are offered to postmenopausal women with node-positive breast cancer as there is good evidence for improved disease-free and overall survival in these patients, when treated with zoledronate or sodium clodronate. It can also be considered in those with high-risk node negative cancer(7).

1.4.4 Novel treatments

1.4.4.1 Immune checkpoint inhibitors

In view of the important role of the immune system in the progression of cancer, which will be discussed later in this chapter, there has been considerable focus on the development of therapeutics which enhance the anti-tumour immune response. The most investigated immunotherapy agents in breast cancer to date are PD-1/PD-L1 immune checkpoint inhibitors. Programmed death receptor-1 (PD-1) is a transmembrane receptor found on thymus-derived (T), bone marrow-derived (B) and natural killer (NK) cells which acts to inhibit unrestrained cytotoxic T cell activity in inflammation. Its ligands are programmed death ligand 1(PD-L1), found on many cell types including tumour cells, and programmed death ligand 2 (PD-L2), found predominantly on haematopoietic cells. Blockade of this checkpoint in cancer is aimed at reactivating cytotoxic T lymphocytes, thus improving the anti-tumour activity of the host immune system(43). This may be in the form of PD-1 blockade, for instance with pembrolizumab (a selective monoclonal antibody to PD-1), or PD-L1 blockade, for instance with atezolizumab (a high-affinity monoclonal antibody that inhibits PD-L1 – PD-1 interaction)(43).

Trials have shown a good response to immune checkpoint inhibitors in some cancers including melanoma and non-small cell lung cancer and it is licensed for use in selected patients with these tumour types(44). However, research in breast cancer is at a much earlier stage. Some trials, both those investigating immune checkpoint inhibitors as monotherapy and those which use them in combination with other therapies, have shown promising results in metastatic TNBC with response rates of 5.4-33.3% observed(44). The response tends to be prolonged in those who do respond and the therapy is generally well tolerated. In some studies patients are pre-selected for PD-L1 positivity while in others they are not. However, there is little evidence at this time for their use in ER+ and HER2+ disease(44). Studies of immune checkpoint inhibitors as neoadjuvant therapy in early stage breast cancer have reported particularly promising results with tripling of the pathological complete response (pCR) rates(44). However, these response rates are modest compared to some other tumour types and trials are very much in the early stages. Identifying predictive biomarkers which

aid in the identification of those patients who do respond to immune checkpoint inhibition is therefore important going forwards. Some factors which have been reported as displaying some predictive utility to date include having a normal LDH, high tumour infiltrating lymphocytes (TILs), fewer lines of previous therapy and PD-L1 expression(44).

1.4.5 Current challenges in treatment selection

With these various treatment options come a number of challenges in management decision-making. Both surgical and medical treatments have associated complications, side effects and toxicities. It is therefore important that patients are not exposed to these risks if they will not derive significant benefit from the treatment. Currently, tumour factors such as tumour size, tumour grade, lymph node status and ER status are used to assess the risk of tumour recurrence with small, low grade, lymph node negative, ER positive tumours carrying the best prognosis. However, a proportion of patients with ER positive, lymph node negative cancers will recur and ultimately prove lethal. Therefore, additional prognostic tools are desirable to help identify these patients to be targeted with more aggressive therapy, such as extended endocrine therapy and/or chemotherapy. The current movement within the breast surgical community to carry out less extensive axillary surgery when safe to do so, because of the morbidity associated with this surgery, may mean that less detailed information regarding the burden of axillary disease will be available to oncologists to aid decisions such as post-mastectomy radiotherapy(45). This is another reason why novel prognostic markers are desirable.

1.4.5.1 Current prognostic tools

As already touched on in this chapter, several tools currently exist to aid adjuvant therapy decisions. One of the older and simplest is the Nottingham Prognostic Index (NPI) which calculates a score based on the size of the tumour, tumour grade and lymph node status. This score then stratifies patients into up to 6 prognostic groups. It has been widely validated and its strength lies in its simplicity with no requirement for a computer. However, variability in prognosis

for the different groups has been reported(46). More recently, NPI+ has been developed to incorporate receptor subtypes of the tumour(47).

Various online tools exist, of which the use of Predict is recommended by NICE(7). Predict incorporates tumour pathological characteristics, receptor status, Ki-67, route of presentation and patient age and menopausal status(48). Adjuvant! Online was another alternative but this is no longer available. The benefits of these tools are that they allow an individualised recurrence risk prediction to be calculated in the clinic and the expected benefit of adjuvant treatments can also be calculated. Predict has been widely validated(49, 50). However, there is concern that it is less accurate in patients at the extremes of age (<30 years with ER positive breast cancer or >70 years), women with tumours >50mm or <10mm ER positive tumours, and it has not been validated in men(51). It is also not of use in patients who have been treated with neoadjuvant therapy.

In addition to these online tools, several gene signatures used to predict the risk of distant disease recurrence have been developed, of which EndoPredict, Oncotype DX and Prosigna are currently recommended by NICE(52). They are recommended for use in patients with ER positive, HER2 negative, lymph node negative breast cancer with an intermediate risk prediction using one of the online tools, and in whom the result of the test would affect the decision whether to give chemotherapy. EndoPredict measures expression of 12 genes, Oncotype DX measures 21 genes and Prosigna measure 50 genes. They all require RNA extracted from formalin-fixed, paraffin-embedded (FFPE) breast cancer tissue. As an example, Oncotype DX generates a recurrence score between 0-100(53) with low, intermediate and high risk scores within this range. Evidence in the literature does support the prognostic power of these high and low risk groups(52), though the implications of the intermediate risk group are less clear and are the subject of the TAILORx trial, the initial results of which suggest that chemotherapy can safely be omitted in these intermediate score patients(54). Interestingly, while the different tests do seem to allocate a similar proportion of patients to the different risk groups, on an individual patient basis, variability in the risk group to which a patient is assigned has been reported(52). These tests are also applied to a specific subset of patients, namely those with ER positive, HER2 negative disease and so have no clinical utility for risk stratification in other subtypes. They are made up primarily of proliferative

genes and therefore have very limited utility in highly proliferative breast cancer subtypes such as ER negative, HER2 positive tumours. They are designed for use in lymph node negative and lymph node positive (up to 3 positive nodes) disease but the evidence in lymph node positive or micrometastatic disease is less strong at present. The other limitation of these tests is cost and time. They are expensive, limiting their availability in low resource settings, and Oncotype DX tests, for example, is processed in a central US laboratory so the sample must be sent there and then it will be a further 7-10 days before the result is available(52).

In view of the limitations of the above tests, additional prognostic tools are desirable to help stratify risk and guide treatment. These may be as standalone tests, or factors to add to online tools such as Predict to further refine their prognostic accuracy.

1.4.5.2 Predictive tools and targeted treatments

Another, related factor is the question of which cancers will respond to certain therapies, such as particular chemotherapy drugs or newer therapeutics such as the immune checkpoint inhibitors, and which cancers will not so that patients are not subjected to the side effects unnecessarily. Therefore, predictive biomarkers for use in these situations are also desirable.

There are currently no targeted treatments for triple negative breast cancers and therefore all patients who are fit enough are offered chemotherapy as their only systemic treatment option, with all of its associated toxicities. Therefore targeted treatments for these patients are required, as well as novel treatments for other breast cancer patients who develop resistance to their primary therapy.

In the search for new prognostic and predictive markers and for new treatment targets, interest has developed in the role of the tumour microenvironment in cancer growth.

1.5 The Tumour Microenvironment

The hallmarks of cancer, which a tumour requires in order to grow and spread, include the ability to sustain proliferative signalling, evade growth suppressors, resist cell death, induce angiogenesis, activate invasion and metastasis, and enable replicative immortality(55). Genomic instability and mutations within the cancer cells themselves are important for acquisition of these characteristics, but over the last 2-3 decades it has become increasingly recognised that the tumour microenvironment and the host immune system also play an important role in enabling a tumour to acquire these characteristics and therefore to spread. Various components of the tumour microenvironment will be outlined below.

1.5.1 Tumour-associated stroma

A tumour is made up not just of a collection of malignant cells, but also of tumour-associated stroma contained within which are a number of different cell types(56). These include, endothelial cells, pericytes, cancer-associated fibroblasts and immune inflammatory cells. These components interact with the cancer cells in complex ways which may promote growth of the tumour by secretion of signalling molecules including growth factors, cytokines, chemokines and pro-angiogenic factors. There is evidence that the tumour actively recruits these cells to the tumour microenvironment to help facilitate its progression(56). The role of specific types of immune cell in cancer progression is outlined in more detail below.

1.5.2 Immune cells

1.5.2.1 Innate immune cells

Innate immune cells include mast cells, macrophages, neutrophils, dendritic cells (DC), basophils, eosinophils and NK cells. Their role in immunity includes the identification and removal of foreign substances, recruitment of other immune cells through secretion of cytokines and antigen presentation to adaptive immune cells.

Neutrophils are the first inflammatory effectors recruited, followed by monocytes which differentiate into macrophages in tissues. These are then the main source of growth factors and cytokines which then act on endothelial, epithelial and mesenchymal cells in the local microenvironment(57). Monocytes can also differentiate into DCs which migrate into tissue where they capture antigens then migrate to lymph nodes to stimulate T lymphocyte activation(57).

Tumour associated macrophages may kill neoplastic cells but they also produce angiogenic and lymphangiogenic growth factors, cytokines and proteases which can promote tumour progression, as well as producing IL-10 which blunts the anti-tumour response by cytotoxic T lymphocytes(57). There is also evidence that neutrophils, mast cells and eosinophils may contribute to neoplastic growth through secretion of proteases, pro-angiogenic factors and chemokines(57).

NK cells have been shown to kill tumour cells without MHC restriction(58). Reduced NK cell activity and dysfunction is associated with breast cancer progression and higher disease stage(58). There is also evidence that they potentiate the effects of certain chemo- and immunotherapies(58).

1.5.2.2 Adaptive immune cells

Lymphocytes form the cellular basis of the adaptive immune system. They can broadly be divided into B and T lymphocytes. B lymphocytes originate in the bone marrow and go on to mature in secondary lymphoid tissue such as the lymph nodes and spleen. They express clonally diverse cell surface immunoglobulin receptors recognising specific antigenic epitopes(59). In addition to antibody production, B lymphocytes have a role in T lymphocyte activation, antigen presentation, DC regulation and cytokine production(59). T lymphocytes develop in the thymus from bone-marrow derived progenitors(60). They differentiate initially by progressing from expressing neither to expressing both of the glycoproteins CD8 and CD4 and then become positive for one or the other(60). CD4+ lymphocytes differentiate into different subtypes in response to stimulation by various cytokines. These subtypes include the T helper lymphocytes (Th1, Th2, Th9, Th17 and Th22), T regulatory lymphocytes (Treg) and T follicular helper lymphocytes (Tfh). These different subtypes release different cytokine profiles and play a critical role in immune response(61). On

exposure to an antigen, T lymphocytes proliferate and differentiate into effector cells which migrate to the site of infection and memory cells which ensure a faster immune response on subsequent exposure to that antigen(61). CD8+ effector cells have a cytotoxic function. A much less common type of T lymphocyte, γδT lymphocytes, are proposed to represent a link between the adaptive and innate immune response(62).

In cancer, evidence suggests that lymphocytes may in some contexts have an anti-tumour role, for instance through direct cytotoxicity, but in others may have a pro-tumour role through the secretion of certain cytokines and pro-angiogenic factors(63). As might be expected by their cytotoxic role, there is some evidence that high levels of CD8+ lymphocytes in breast tumours are associated with better outcomes(64-66). On the other hand, there is evidence that CD4+ lymphocytes are associated with worse cancer outcomes(64). Further work is required to better understand their role in primary operable breast cancer.

1.6 Tumour features that may interact with the microenvironment

1.6.1 Tumour necrosis

Tumour necrosis is a feature of solid tumours. It is presumed to be the consequence of rapid tumour growth which exceeds the rate of growth of its blood supply leading to ischaemia(67). However, necrosis can still occur in small tumours and therefore impaired oxygen delivery to tissues may be a factor(68). Tumour necrosis has been reported to be independently associated with poor prognosis in a number of cancers including bladder(69), renal(70), lung(71) and colorectal cancers(67). There are few studies in breast cancer but one small study has reported an association between necrosis and reduced CSS(72). A couple of studies, one in breast(73) and one in colorectal cancer(68), report that this association is not independent of systemic and local inflammation. This has led to the suggestion that inflammation related to tumour necrosis and stimulus of inflammatory pathways by release of mediators by necrotic tissue may be important in the link between necrosis and poor prognosis(68). Further work to

investigate the prognostic role of necrosis in breast cancer and its relationship to inflammation and the tumour microenvironment is warranted.

1.6.2 Tumour budding

Tumour budding is a feature which has been observed in some tumour types, particularly in colorectal cancer, though it was first described in stomach cancer(74). The term refers to single tumour cells or small clusters which are detached from the main tumour(75). They are most commonly observed in the stroma, at the invasive front of the tumour. These buds may show disruption of E-cadherin expression and overexpress markers of invasion, locomotion, migration and EMT, leading to the hypothesis that tumour budding is involved in the process of tumour dissemination(76) and therefore poorer prognosis. Indeed, associations between high numbers of tumour buds and vessel invasion, lymph node and distant metastases have been reported. A role for the tumour stroma in promoting tumour budding has been hypothesised in view of correlations observed between the two(75).

The association between high tumour budding and poorer prognosis has been widely reported in colorectal cancer(74), driving interest in its use clinically as a prognostic marker. However, its adoption in clinical practice has been slowed by the lack of consensus in terms of definition and assessment. For example, tumour buds have been variably defined in the literature as clusters of $\geq$5 malignant cells, clusters of $\leq$4 malignant cells and the definition more recently favoured of isolated cells or clusters $\leq$5 malignant cells(74). Additionally, budding can be assessed either by H&E staining or by pancytokeratin staining. With a view to addressing these issues, the International Tumor Budding Consensus Conference 2016 agreed a standardised method for assessment and reporting of tumour budding and recommended that budding should be included in guidelines and protocols for colorectal cancer reporting(77). Subsequently, it has been included in the College of American Pathologists guidelines for reporting and is included in the Union for International Cancer Control's TNM classification for colorectal cancer(75).

Despite the bulk of literature regarding tumour budding in colorectal cancer, little is known about its role in breast cancer. A few small studies have reported

an association between tumour budding and breast cancer outcomes(78-80). They observe associations between high tumour budding and lymph node metastases, lymphovascular invasion and poorer survival outcomes. However, they are small studies, two of them analysing fewer than 200 patients(79, 80), which limits subtype analysis, and all use a different threshold to define high budding. Therefore, further work in larger cohorts is warranted to validate these observed associations, to define a consistent threshold for high budding and to establish whether there is a potential clinical role for its routine assessment in breast cancer.

1.7 The JAK/STAT3 Cell Signalling Pathway

To affect tumour growth, signals from the tumour microenvironment must be conveyed to the tumour cell nucleus via cell signalling pathways. One of these pathways is the JAK/STAT3 cell signalling pathway.

1.7.1 The pathway

Signalling pathways transmit signals from external stimuli to the cell nucleus to control gene expression. The Janus kinase (JAK)/signal transducers and activators of transcription (STAT) pathway is an evolutionary conserved signalling pathway which facilitates direct communication between transmembrane receptors and the nucleus(81). It is stimulated by a vast array of cytokines and growth factors(82). The pathway mediates numerous cellular processes including proliferation, differentiation, migration and apoptosis which are critical processes in haematopoiesis, immune development, stem cell maintenance and mammary gland development(82, 83). There are 4 JAKs (JAK1, JAK2, JAK3 and TYK2) and 7 STATs (STAT1, STAT2, STAT3, STAT4, STAT5a, STAT5b and STAT6) in mammals(81). STAT3 is recognised as an important factor in mammary epithelial cell growth, differentiation, apoptosis and involution(84, 85).

The JAK/STAT3 pathway is stimulated by IL-6. Il-6 binds to either the membrane-bound or soluble IL-6 receptor, which induces homodimerization of glycoprotein 130 (gp130) and a high affinity functional receptor complex of IL6/IL6R/gp30 is formed(86). This leads to activation of receptor-associated JAKs

which can then phosphorylate each other as well as the intracellular portion of their receptors and cytoplasmic STAT3(83). This phosphorylation occurs at a conserved tyrosine residue (Tyr705) near the C-terminus(82), permitting the dimerisation of STAT3 which then translocates to the nucleus where the dimer binds to regulatory DNA sequences to activate or repress target gene transcription(82).

This pathway in isolation is relatively straightforward. However, it is complicated by interactions with other cell signalling pathways. For example, STAT3 can also undergo phosphorylation of a serine residue (Ser727) within the C terminus via the mitogen-activated protein kinase (MAPK) pathways, particularly the classical extracellular signal-regulated kinase (ERK) pathway(87). The JAK/STAT3 pathway also interacts with the NFκB pathway at multiple levels(88). A further complicating factor is that STAT3 can also localise to mitochondria where it promotes oxidative phosphorylation and membrane permeability(81).

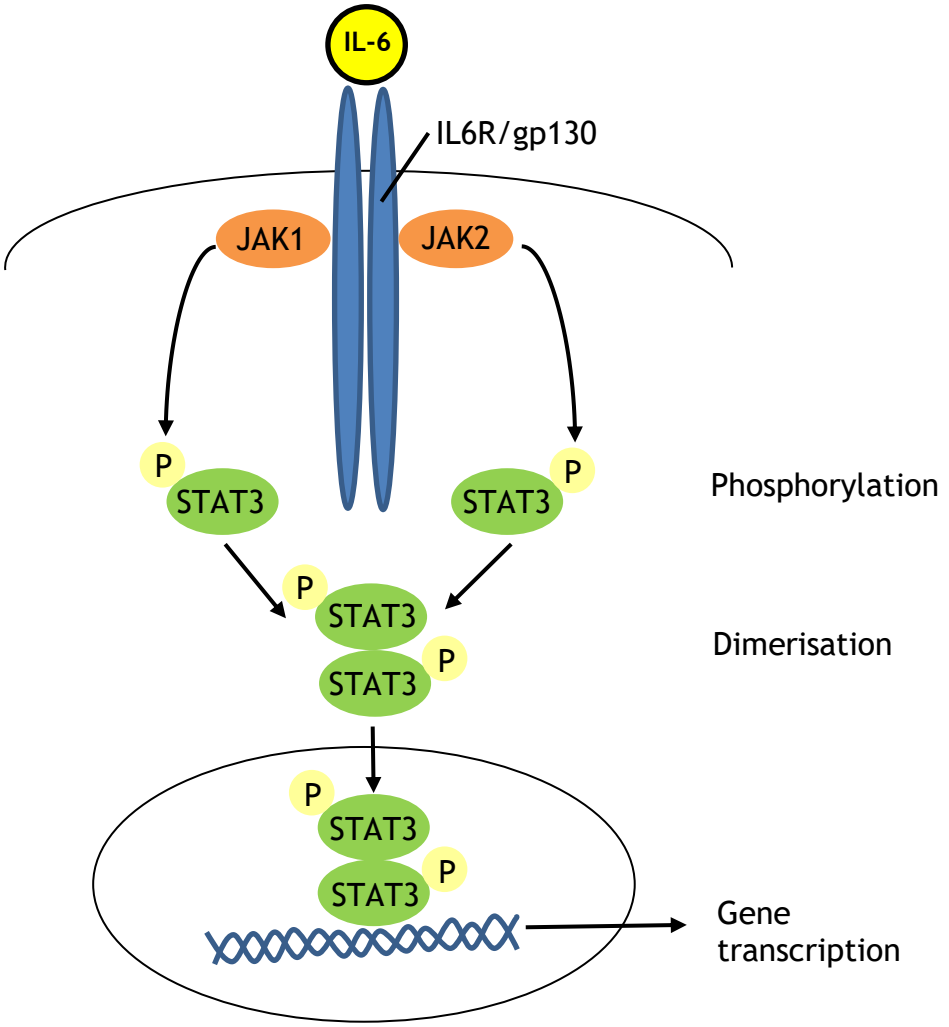

Figure 1-7. The Il-6/JAK/STAT3 pathway. Diagram illustrating the IL6/JAK/STAT3 pathway. IL6 binds with the IL6 receptor leading to activation of JAKs and phosphorylation of STAT3 which dimerises, translocates to the nucleus and regulates gene transcription.

1.7.2 The JAK/STAT3 pathway in solid tumours

The hallmarks of cancer include activating invasion and metastasis, enabling replicative immortality, inducing angiogenesis, resisting cell death, sustaining proliferative signalling and evading growth suppressors(55). Given the influence the JAK/STAT3 pathway has on cell proliferation, migration and apoptosis, it is not surprising that aberrant activation of the pathway has been identified in a number of tumours, both haematological and solid(81). In addition to haematological malignancies, high levels of STAT3 activation have been observed in head and neck, breast, brain, prostate, renal, pancreatic and ovarian tumours and melanoma(85). Several mechanisms support a pro-tumorigenic role for STAT3. Firstly, activation of STAT3 can bring about oncogenesis in cells by inducing permanent changes in gene expression. For

example, constitutive STAT3 activation is required for oncogenic transformation by v-Src(85). Secondly, activation of STAT3 mediates tumour-promoting inflammation by promoting pro-oncogenic inflammatory pathways and opposing anti-tumour immune responses(88).

1.7.3 The JAK/STAT3 pathway in breast cancer

As in other tumours, constitutively activated STAT3 has been observed in breast cancer cell lines but not in non-malignant mammary epithelial cell lines(89, 90). In preclinical studies, high activation of STAT3 has been reported to be associated with increased breast cancer cell proliferation, survival and metastases(91-94). Studies have shown STAT3 to be required for migration and metastases in mice(95, 96). In addition to this, other cell line studies have reported apoptosis, growth inhibition and reduced invasion in breast cancer cells when STAT3 expression is suppressed(97-100).

This preclinical evidence suggests a pro-tumourigenic role for STAT3 in breast cancer. However, studies involving human tissue and cancer outcomes have provided mixed results to date. In human breast cancer tissue, one small study reported no difference in total STAT3 expression levels compared to paired normal tissue from the same patient, but did observe increased pSTAT3(Ser727) expression in the tumour compared to adjacent non-cancer tissue in 62% of patients(101). A positive correlation with cancer stage was observed. Conversely, another study reported that expression levels of pSTAT3(Tyr705) decreased as tumours progressed (normal tissue compared to DCIS, to invasive tumours, to lymph node metastases) in unpaired tissues(102).

Concerning the prognostic role of STAT3, one small study reported high levels of total STAT3 expression (nuclear and/or cytoplasmic) to be associated with worse overall survival (OS)(103) whereas a slightly larger study found no statistically significant association between either nuclear or cytoplasmic expression and OS, though there was an association with better 5yr OS on univariate analysis(104). Other studies have investigated pSTAT3 as an indicator of STAT3 activation rather than total STAT3. Some studies have reported improved patient outcomes in those with high levels of nuclear pSTAT3(Tyr705) expression(104-107) though in one study this association was seen in lymph node positive cancers only(76)

while in another only lymph node negative patients were included(104). On the other hand, one study reported no significant association between nuclear pSTAT3(Tyr705) association and OS, though improved survival was seen in low grade tumours on univariate analysis only(102). In view of this variation in results in the published literature, further studies in large breast cancer cohorts are warranted.

1.8 Summary and thesis aims

Despite significant improvements in breast cancer mortality over the last three to four decades, breast cancer remains the second most common cause of cancer-related death in females in the UK. It is a heterogenous disease with several different subtypes which behave and respond to treatments differently. There are a number of breast cancer treatments available with their own side effects and toxicities. It is important, therefore, to have risk stratification tools to aid treatment decisions. Several tools are already in widespread use, however each has limitations which may include impaired performance in certain groups of patients, cost and logistical issues. It is therefore desirable to identify new prognostic biomarkers which could be used alongside existing prognostic tools to further refine prognostic accuracy and tailor management for the individual patient. As prognostic markers are validated, it can also be anticipated that potential novel targets for treatment may be identified and this is particularly desirable in triple negative breast cancers who currently have no targeted treatments available, and in those other subtypes who develop resistance to initial therapies. To address these challenges, attention has turned towards the tumour microenvironment and the interactions of its components with the tumour. There is evidence that tumour stroma and various immune cells influence tumour progression via various cytokines and growth factors, and that the tumour in turn can recruit tumour-promoting cells to the tumour microenvironment. New prognostic biomarkers may therefore be identified within the tumour microenvironment. One cell signalling pathway which can transmit signals from the microenvironment to the tumour cell nucleus resulting in regulation of transcription of various genes related to tumour growth is the JAK/STAT3 pathway. Activation of this pathway has been observed in breast cancer, and various molecules which target different steps in the pathway are already in existence. Therefore, a better understanding of the role of this

pathway in breast cancer is important, to ascertain whether targeting this pathway would be beneficial in any groups of breast cancer patients. With all of this in mind, the aims of this thesis were as follows:

- to examine the prognostic significance of systemic markers of inflammation and the local inflammatory response in primary operable breast cancer and its molecular subtypes.
- to investigate the prognostic role of tumour necrosis in primary operable breast cancer and its molecular subtypes.
- to investigate the prognostic role of tumour budding in primary operable breast cancer and its molecular subtypes.
- to investigate the prognostic role of tumour stroma, as measured by tumour stroma percentage, in primary operable breast cancer and its molecular subtypes.
- to describe the IL-6/JAK/STAT3 pathway in primary operable breast cancer and its molecular subtypes.
- to investigate the associations between systemic markers of inflammation, tumour necrosis, tumour budding, TSP, T lymphocyte subsets and components of the IL-6/JAK/STAT3 pathway along with known prognostic clinicopathological characteristics in primary operable breast cancer and its molecular subtypes.

2 Materials and Methods

2.1 Patient cohorts

The work in this thesis was carried out using two distinct patient cohorts. Ethical approval for the work was obtained from the West of Scotland Research Ethics Committee 3 (study number 12/WS/0131). Some studies were carried out using the '1800 cohort' of 850 patients, some studies were carried out using the 'FJ cohort' of 450 patients, and some studies were carried out on the two cohorts combined.

2.1.1 1800 cohort

A cohort of 850 breast cancer patients had previously been formed. It is made up of patients who underwent curative resection for primary breast cancer at one of three breast units in Glasgow (Glasgow Royal Infirmary, Western Infirmary Glasgow or the Victoria Hospital Glasgow) between 1995 and 2001. All patients were managed according to the standard local protocols at the time of treatment. A database was available in the Glasgow Safehaven which included clinicopathological details, adjuvant treatment and survival and recurrence data for this cohort (database number GSH/18/ON/008, available at http://researchdata.gla.ac.uk/784/). Details of proteins previously examined in Professor Edwards' laboratory in this cohort were also available in the database. ER, PR and HER2 profiling had all been carried out retrospectively in the lab to ensure standardisation of technique, as techniques had changed in diagnostic labs over the time period of this cohort and routine HER2 testing had not been established. Characteristics of the cohort are summarised in **Table 2-1**.

	1800 cohort n (%)	FJ cohort n (%)
Number of patients	850	451
Years tumours resected	1995-1998	2001-2007
Median follow up (survivors)	162 months	145 months
Events		
Breast cancer death	174 (20.5)	77 (17.1)
Non-breast cancer death	158 (18.6)	100 (22.2)
Missing data	0 (0.0)	3 (0.7)
Age		
<50 years	248 (29.2)	102 (22.6)
≥50 years	602 (70.8)	349 (77.4)
Tumour type		
Ductal	736 (86.6)	451 (100)
Lobular	68 (8.0)	0 (0)
Other	46 (5.4)	0 (0)
Invasive tumour size		
≤20mm	496 (58.4)	226 (50.1)
21-49mm	309 (36.4)	214 (47.5)
≥50mm	44 (5.2)	11 (2.4)
Missing data	1 (0.1)	0 (0)
Grade		
I	161 (18.9)	48 (10.6)
II	382 (44.9)	161 (35.7)
III	305 (35.9)	242 (53.7)
Missing data	2 (0.2)	0 (0)
Nodal status		
Negative	490 (57.6)	253 (56.1)
Positive	348 (40.9)	196 (43.4)
Missing data	12 (1.4)	2 (0.4)
ER		
Positive	570 (67.1)	345 (76.5)
Negative	276 (32.5)	106 (23.5)
Missing data	4 (0.5)	0 (0)
PR		
Positive	396 (46.6)	262 (58.1)
Negative	448 (52.7)	188 (41.7)
Missing data	6 (0.7)	1 (0.2)
HER2		
Negative	699 (82.2)	258 (57.2)
Positive	128 (15.1)	53 (11.8)
Missing data	23 (2.7)	140 (31.0)
Breast Surgery		
Breast conserving surgery	328 (38.6)	236 (52.3)
Mastectomy	521 (61.3)	215 (47.7)
Missing data	1 (0.1)	0 (0)
Axillary Surgery		
Sentinel node biopsy	0 (0)	36 (8.0)
Axillary sample	27 (3.2)	38 (8.4)
Axillary clearance	808 (95.1)	375 (83.1)
None	0 (0)	2 (0.4)
Missing data	1 (0.1)	0 (0)
Adjuvant endocrine therapy		
Yes (tamoxifen)	528 (62.1)	345 (76.5)
Yes (ATAC trial)	32 (3.8)	
No	141 (16.6)	106 (23.5)
Missing data	149 (17.5)	0 (0)
Adjuvant chemotherapy		
Yes	331 (38.9)	205 (45.5)
No	516 (60.7)	245 (54.3)
Missing data	3 (0.4)	1 (0.2)
Adjuvant radiotherapy		
Yes	401 (47.2)	323 (71.6)
No	446 (52.5)	115 (25.5)
Missing data	3 (0.4)	13 (2.9)

Table 2-1. Clinicopathological characteristics of the cohorts. Table detailing the composition and clinicopathological characteristics of the two patient cohorts used for studies in this thesis.

2.1.2 1800 cohort tissue microarray construction

The tissue microarray (TMA) for this cohort had been constructed previously by Clare Orange (currently Greater Glasgow & Clyde Biorepository Manager). Briefly, formalin-fixed paraffin-embedded (FFPE) tissue blocks were obtained from pathology archives and full sections cut. Following haematoxylin and eosin (H&E) staining, they were marked up by Dr Elizabeth Mallon (Consultant pathologist, Queen Elizabeth University Hospital, Glasgow) to identify tumour-rich areas. Three 0.6mm cores were lifted from each block and placed into three separate recipient paraffin blocks. Several cores from other tissue types were also placed into the recipient blocks to act as positive controls during staining. TMA maps were drawn up so that each core could be identified by a unique TMAID which would link it anonymously to the data in the cohort database.

2.1.3 FJ cohort

The FJ cohort was made up of 450 patients who had undergone curative resection for breast cancer in the aforementioned Glasgow hospitals between 2001-2007. Clinicopathological and follow up data for the patients was obtained retrospectively from patient notes (both electronic and physical), and from local laboratory systems. The key characteristics of this cohort are summarised in **Table 2-1**. Unfortunately, despite repeated attempts, over the course of this research it proved impossible to retrieve the tissue blocks for these patients so only previously-stained full section H&E slides were available for analysis in this cohort. Therefore ER, PR and HER2 data for these patients is extracted from the pathology reports.

2.2 Systemic inflammatory markers

For the FJ cohort, the Glasgow laboratory system was used to collect the preoperative haemoglobin, total white cell count, neutrophil, lymphocyte, monocyte and platelet counts for each patient. The closest date to the operation date was used. If this was more than 60 days preoperatively, the patient was excluded from analysis. This data is not available for the 1800-cohort and unable to be obtained due to the cohort age.

2.3 Haematoxylin and eosin staining of full sections

Full section slides were cut from surplus tissue of both the 1800 and FJ cohorts, obtained from the NHS Research Scotland Greater Glasgow and Clyde Biorepository. These slides had been previously stained in the lab using haematoxylin and eosin (H&E) standard protocol. The slides were scanned using a Hamamatsu NanoZoomer (Welwyn Garden City, Hertfordshire, UK) into the Slidepath Digital Image Hub, version 4.0.9 (Slidepath, Leica Biosystems, Milton Keynes, UK) at x20 resolution.

2.3.1 Necrosis scoring

Scoring for the extent of tumour necrosis was carried out in the 1800 cohort by Fadia Gujam and for the FJ cohort by the author. Both scorers were blinded to clinicopathological data and outcomes. Using Slidepath software and a high-definition computer screen, each slide was initially assessed at 10x magnification to look for areas of necrosis. Subsequently, at 20x magnification, the extent of necrosis was visually assessed as the proportion of the visual field occupied by necrotic tissue, using a method adapted from Ikpatt et al(108). This was recorded as none (no necrosis or only single necrotic cells), mild or focal (<25% field occupied by necrotic tissue), moderate (25-50% field occupied by necrotic tissue) or extensive (>50% field occupied by necrotic tissue). For analysis, patients were grouped as low (no or <25% necrosis) and high (>25% necrosis). Only necrosis within the invasive tumour was included, comedo necrosis was visually excluded.

2.3.2 Tumour budding scoring

Scoring for tumour budding was carried out in the 1800 cohort by Fadia Gujam and for the FJ cohort by the author. Using Slidepath software and a high-definition computer screen, the invasive edge was identified at 4x magnification. At 20x magnification, a 10mm^2 grid was placed at the invasive tumour edge. The number of tumour buds within the grid was counted. A tumour bud was defined as an isolated group of 1-5 tumour cells. This process was repeated for 4 further grids placed at different locations along the invasive tumour edge. The highest of the 5 bud counts was used for analysis. Patients were subsequently divided into low budding ($\leq$20 buds) or high budding (>20

buds) for analysis, as this threshold has previously been reported to have the highest prognostic power(78).

2.3.3 Tumour-stroma percentage scoring

Scoring for the tumour-stroma percentage (TSP) was carried out in the 1800 cohort by Fadia Gujam and for the FJ cohort by the author. Using Slidepath software and a high-definition computer screen, at 10% magnification, a representative area of tumour was selected to include tumour cells at all 4 corners of the visual field. The proportion of stroma within the visual field was visually assessed and recorded. For analysis, patients were grouped as TSP $\leq$50% or >50%, as previously described(72).

2.3.4 Klintrup-Makinen scoring

Klintrup Makinen (KM) scoring was carried out in the 1800 cohort by Fadia Gujam and for the FJ cohort by the author. Using Slidepath software and a high-definition computer screen, at 10% magnification the invasive tumour edge was visually assessed for the degree of peri-tumoral inflammatory infiltrate. This was scored as 0 (no inflammatory infiltrate at invasive tumour edge), 1 (patchy inflammatory infiltrate at invasive tumour edge), 2 (continuous layer of inflammatory cells at invasive tumour edge) or 3 ('cup' of inflammatory infiltrate at invasive tumour edge).

2.4 Immunohistochemistry

IHC was used to identify specific types of immune cell, for example different subsets of T lymphocytes, and to visualise levels of expression of various components of the IL-6/JAK/STAT3 pathway. The technique uses a specific antibody to the target antigen of interest. A labelled secondary antibody is then used which reacts with the primary antibody. A chromagen is applied as a signal enhancer so that expression of the antigen can be visualised under a light microscope as a brown stain. The slides are then counterstained with haematoxylin so that the primary stain is more distinct. The various steps in the process are described in more detail below. There was some variation between antibodies in terms of specific timings of stages of the protocol and types of reagents used, because of variability in the optimal conditions for certain

antibodies or changed suppliers to the laboratory. These variations are summarised in **Table 2-2**. A negative control slide was included in each batch of slides. Each TMA slide included a row of cores of liver, kidney, prostate, lung, colon, tonsil and pancreas tissue to act as positive controls for the various antibodies.

Antigen	Make of antibody	Antigen retrieval conditions	Blocking conditions	Antibody concentration and incubation conditions	Secondary antibody & visualisation kit
CD4	Abcam [EPR6855] ab133616 Rabbit monoclonal	Tris-EDTA pH9	10% HS 30mins	1:300 overnight 4˚C	Envision & DAB
CD8	Dako Clone C8/144B, M710301-2 Mouse Monoclonal	Tris-EDTA pH8	10% HS 30mins	1:200 overnight 4˚C	Envision & DAB
IL6R	Abcam Ab128008 Rabbit polyclonal	Citrate pH6	10% HS 30mins	1:500 overnight 4˚C	Envision & DAB
JAK1	Cell Signalling (6G4) #3344 Rabbit monoclonal	Citrate pH6	10% HS 30mins	1:200 overnight 4˚C	Envision & DAB
JAK2	Cell Signaling (D2E12) #3230 Rabbit monoclonal	Citrate pH6	10% HS 30mins	1:200 overnight 4˚C	Envision & DAB
STAT3	Cell Signaling (124H6) #9139 Mouse monoclonal	Tris-EDTA pH8	10% HS 30mins	1:300 overnight 4˚C	Envision & DAB
Phospho-Stat3 (Ser727)	Cell Signaling #9134 Rabbit polyclonal	Tris-EDTA pH8	10% HS 30mins	1:200 overnight 4˚C	ImmPRESS & ImmPACT
Phospho-Stat3 (Tyr705)	Cell Signaling (M9C6) #4113 Mouse monoclonal	Tris-EDTA pH8	10% HS 30mins	1:50 overnight 4˚C	ImmPRESS & ImmPACT

Table 2-2. Antibodies and conditions. Table detailing the antibodies used in the immunohistochemistry studies in this thesis with the retrieval, blocking and incubation conditions and the secondary antibody used for each.

2.4.1 TMA construction and slide preparation

Sections from previously-constructed patient TMAs from the 1800 cohort were requested from the NHS Research Scotland Greater Glasgow and Clyde

Biorepository. TMAs were cut into 2.5µm thick paraffin wax sections and mounted onto slides. They were baked overnight at 56ºC prior to being stored at 4ºC. Before staining they were baked again for 20 minutes at 56ºC to minimise the risk of core loss.

2.4.2 Dewaxing and rehydration

Slides were immersed in histoclear twice for 3 minutes to dewax them. They were then dehydrated by immersion in a series of graded alcohols (100% twice for 3 minutes, 90% once for 2 minutes then 70% once for 2 minutes) before being rinsed in water for 10 minutes.

2.4.3 Antigen retrieval

Antigen retrieval is carried out to break down any protein crosslinks which have formed during the tissue fixation process, unmasking the antigen so that the antibody can bind. Heat-mediated antigen retrieval was carried out using one of two buffer solutions. The TRIS-EDTA buffer is made up of 0.55g Tris Base (Fisher Bioreagents) and 0.37g sodium EDTA (Diaminoethanetetra-acetic acid disodium salt dihydrate, Fisher Scientific) in 1L distilled water. The citrate buffer is made up of 2.41g tri-sodium citrate dihydrate (Fisher Scientific) and 0.346g citric acid (Sigma-Aldrich) in 1L distilled water. The buffer was adjusted to the required pH using 0.1M hydrochloric acid or 0.1M sodium hydroxide. The buffer and pH used for each antibody is detailed in **Table 2-2**.The buffer was heated for 13.5 minutes before the slides were immersed in it within a pressure cooker. They were brought up to pressure before being heated at pressure in a microwave for 5 minutes. The slides were then left to cool in the buffer for 30 minutes prior to rinsing in water.

2.4.4 Blocking endogenous peroxidase and non-specific binding

To block binding of the antibody to endogenous peroxidase, slides were immersed in 3% hydrogen peroxide for 20 minutes. They were then washed in Tris buffer solution (TBS) twice for 5 minutes. TBS was made up of 300g Tris-Base and 438g sodium chloride (VWR Chemicals) in 8L distilled water brought to pH 7.5, and then was further diluted in distilled water 10x prior to use.

Next, a ring was drawn around the tissue on each slide using a Dako Pen (S2002, Dako, Glostrup, Denmark) to create a hydrophobic barrier. To block the binding of antibody to non-specific proteins in the tissue, which would result in background staining, each slide was covered with 500µl of 1.5%, 5% or 10% normal horse serum (Vector) (horse serum diluted in TBS) for either 30 or 60 minutes in a dark box.

2.4.5 Incubation with primary antibody

The blocking solution was tipped off the slides and then each slide covered with 200µl of the appropriate dilution of the primary antibody. Antibody was diluted in antibody diluent (S0809, Dako, Glostrup, Denmark). The negative control slide was covered with antibody diluent only. The slides were then incubated within the dark box either overnight at 4ºC or for 30 minutes at room temperature.

2.4.6 Incubation with secondary antibody

Slides which had been incubated at 4ºC were first brought to room temperature. Slides were washed twice in TBS for 5 minutes. Each slide was then covered with Dako REAL™ EnVision™ (K5007, Dako, Glostrup, Denmark) or ImmPRESS™ HRP Reagent Kit (MP-7500, Vector, Burlingame, CA, USA) and incubated at room temperature in the dark box for 30 minutes before washing twice in TBS for 5 minutes.

2.4.7 Detection and visualisation

The chromogen used for visualisation was 3,3'-Diaminobenzidine (DAB). One of two DAB peroxidase substrate kits was used. When using the DAB Peroxidase Substrate Kit (SK-4100, Vector, Burlingame, CA, USA) 2 drops of buffer, 4 drops of DAB and two drops of hydrogen peroxidase were added to 5mls of distilled water. If the ImmPACT™ DAB Peroxidase Substrate kit (SK-4105, Vector, Burlingame, CA, USA) was used, 1 drop/30µl ImmPACT™ DAB chromogen concentrate was added per 1ml of ImmPACT™ DAB diluent. Each slide was covered in the DAB solution and left for 10 minutes prior to washing in water for 10 minutes.

2.4.8 Counterstaining

Counterstaining was carried out by immersing the slides in Harris haematoxylin for 1 minute then washing in running water. The slides were then immersed in Scott's tap water for 45 seconds before returning to the water. Scott's tap water was made using 40g magnesium sulphate and 7g sodium bicarbonate in 2L distilled water.

2.4.9 Dehydration and mounting

The slides were immersed in a series of graded alcohols (70% for 1 minute, 90% for 1 minute, 100% twice for 1 minute) followed by histoclear twice for 1 minute. Finally, they were mounted on individual cover slips using Omnimount Histological Mounting Medium (National Diagnostics) and allowed to dry. The slides were scanned in the same way as the full sections described above.

2.4.10 Scoring of immune cells

Antibodies to specific cell surface markers for each individual immune cell of interest were used. For example, CD4 was used for helper T lymphocytes and CD8 for cytotoxic T lymphocytes. A quantitative method was used to score the number of specific types of immune cell in each core. At 20x magnification, the number of stained cells in the tumour and in the stroma of each core were counted and recorded separately. For each patient, 3 cores were scored and the mean calculated. For analysis, patients were divided into high and low groups using either a ROC curve-derived threshold or the median.

2.4.11 Weighted histoscore

The weighted histoscore (WHS) was used for scoring of the level of expression of various components of the IL6/JAK/STAT3 pathway, including IL6 receptor, JAK1, JAK2, pSTAT3 (Tyr705), pSTAT3 (Ser727) and total STAT3. Protein expression levels were assessed visually on a single high definition computer monitor at 20x magnification by a scorer blinded to clinicopathological data and outcomes. The proportion of cells with no staining (score 0), weak staining (score 1), moderate staining (score 2) and strong staining (score 3) was recorded. The WHS was calculated as (0x proportion score 0) + (1x proportion

score 1) +(2x proportion score 2) + (3x proportion score 3). A separate score was recorded for tumour nuclear staining, tumour cytoplasmic staining, tumour membranous staining (where applicable) and stromal cell staining. 10% of cores were co-scored independently by a second scorer and the correlation coefficient calculated to ensure good agreement. Three cores were scored for each patient and the mean of the three scores calculated. For analysis, either a ROC-derived threshold, the median or tertiles were used to divide patients into high and low expression groups.

2.5 RNA scope

RNA scope was used to stain for IL-6 RNA expression within cells, as it was not possible to optimise IHC for the IL-6 protein itself. This is an *in situ* hybridisation assay for detection of target RNA. Slides are first pre-treated to make the cells permeable and unmask the target RNA. A target Z probe to the RNA is applied. The lower region of the base probe has an 18-25 base region complementary to the target RNA. To ensure specificity, two Z probes are required to bind to the target RNA before signal amplification will occur. Preamplifiers hybridise to the binding site formed by the double Z probe, then amplifiers bind to the multiple binding sites on the preamplifier. Labelled probes containing a chromogenic enzyme bind to the amplifiers to allow visualisation.

2.5.1 RNA scope for IL-6

Staining of freshly cut (<2weeks) TMA slides was carried out using a Leica Bond RX autostainer, strictly adhering to the manufacturer's instructions, by Colin Nixon (head of histology department, Cancer Research UK Beatson Institute, Glasgow; staining was carried out as a service). Briefly, in situ-hybridisation detection for IL-6 and PPIB (Advanced Cell Diagnostics, Hayward, CA, USA) mRNA was performed using RNA scope 2.5 LS (Brown) detection kit(Advanced Cell Diagnostics, Hayward, CA, USA). This was done for all patients in triplicate. PPIB was selected as a housekeeping (HK) gene.

2.5.2 Scoring of slides stained for IL-6 RNA

Stained slides were scanned using a Leica SCN400f slide scanner. HALO™ Image Analysis Software (PerkinElmer, Waltham, MA, USA) was used to analyse the

slides. Algorithms were set up within the software to distinguish between tumour and stroma. The software quantified the number of probe copies per μm^2 for each tissue core in tumour and stroma separately. This analysis was carried out both for the slides stained with the IL-6 probe and those stained with the HK probe. For each patient, means of the three cores were calculated for IL-6 probe copies in tumour, IL-6 copies in stroma, HK copies in tumour and HK copies in stroma. The quantity of IL-6 was normalised by dividing by the number of HK copies in each location to give a ratio. For example, mean IL-6 copies per μm^2 in tumour / mean HK copies per μm^2 in tumour = tumour IL-6/HK ratio. This ratio value was used in the further analysis. Patients were divided into tertiles of high, medium and low IL-6 expression for analysis.

2.6 Statistical analysis

For each of the variables described above, associations with clinicopathological characteristics were calculated using the appropriate Chi square test. The relationship with oncological outcomes was assed using Kaplan Meier survival analysis and log rank test. 5 and 10 year survival rates were obtained from life tables and recorded as percentage of population surviving. Cox regression survival analysis was carried out for each variable of interest, as well as other known prognostic factors, and recorded as a hazard ratio with 95% confidence interval (CI). Variables which were statistically significant ($p<0.05$) on univariate analysis were entered into the multivariate analysis using a backwards conditional model. For all analysis, statistical significance was defined as $p<0.05$. All analysis was carried out using SPSS software (version 22, IBM Corp, Armonk, NY, USA).

2.7 Transcriptomics

Transcriptomics involves the study of the transcriptome, the RNA transcript of the genome. Comparison of the transcriptome of different populations can lead to the identification of specific genomic sequences associated with a specific phenotype or function. We carried out RNA sequencing for a small sub-cohort of the 1800 cohort with the aim of identifying specific sequences associated with tumour budding.

2.7.1 Patient selection

Due to financial constraints, a cohort of 50 patients was selected to undergo whole transcriptome sequencing. Patients were selected from within the 1800 cohort as these patients had tissue blocks which were easily accessible. Only ER negative patients were selected for reasons related to our tumour budding results which will be fully explained later in this thesis. Within these specifications, the 25 patients with the highest and the 25 patients with the lowest tumour budding counts, for whom tissue blocks were available, were selected.

2.7.2 Preparation of slides

One 5µm full tissue section per patient was cut from the tissue blocks by Colin Nixon using a Finesse microtome. They were fixed to glass slides and passed on immediately to Ditte Anderson (Scientist, BioClavis Ltd) untreated and unbaked for sequencing. This was to ensure the tissue was as fresh as possible to reduce oxidation.

2.7.3 RNA sequencing using TempOSeq®

This technique involves targeting RNAs with detector oligos and removing excess probes and enzymatic inhibitors. Then, correctly hybridised detector oligos are ligated and amplified through primer landing sites that are shared among all probes. The RNA sequencing was carried out by Ditte Anderson and Harper van Steenhouse of Bioclavis Ltd, using TempOSeq® (BioSpyder, Carlsbad, CA, USA), using the protocol outlined below.

Areas of interest were excised from FFPE slides and added to 80µL BioSpyder 1 x FFPE lysis buffer. Each sample was overlaid with mineral oil and incubated at 95°C for 5 minutes to dissolve paraffin. FFPE lysate was incubated in FFPE protease reagent for 30 minutes at 37°C and homogenized by vortexing. The lysate was combined with annealing buffer and detector oligonucleotides (DOs) and incubated overnight at 45°C following a ramp in temperature from 70°C to 45°C. Unbound DOs were degraded by a nuclease mix followed by ligation of bound DOs into a complete probe sequence. The enzymes were deactivated by

incubation at 80°C for 15 minutes and PCR was performed to amplify ligated probes and samples were purified.

2.7.4 Data analysis

Initial analysis was carried out by Bioclavis using the TempOSeqR data analysis program (BioSpyder technologies, USA). Assay performance metrics were calculated using positive and negative controls. Heatmaps were constructed and principle component analysis was carried out to identify any clustering of samples. Differential expression analysis was carried out using MA plots. Results of this analysis as well as the raw data were transferred back to EM in a Microsoft® Office Excel 16 (Microsoft, Redmond, WA, USA) spreadsheet with the TMAID for each patient. The raw data included the log2 fold change and adjusted p value for 22357 genes and this was used to identify genes with a statistically significant (adjusted $p<0.10$) fold change between cohorts. The data was ordered by log2 fold change to identify the top over-expressed and the top under-expressed genes in the high budding cohort.

3 The prognostic role of preoperative circulating markers of the systemic inflammatory response in primary operable breast cancer

3.1 Introduction

Breast cancer is the most common cancer in females and the second most common cause of cancer death in females in the UK(109). It is a heterogenous disease with considerable variation in tumour behaviour and prognosis. Tumour factors such as tumour size, grade, nodal involvement, ER and PR status and HER2 status are well recognised to be associated with prognosis (110-114). More recently, genomic assays have been used as additional prognostic tools to stratify risk and to aid in treatment decisions, particularly regarding chemotherapy in hormone receptor positive patients(115-117). However, these tests are comparatively expensive and not routinely available in all units worldwide. Therefore, clinical prognostic markers are still required.

Increasingly it is being recognised that the host systemic inflammatory response has a role to play in tumour progression(56, 118, 119). Therefore, a number of serum inflammatory markers, and scores made up of their components, have been investigated as routinely available prognostic markers in several cancers. These include components of the differential white cell count (WCC) such as neutrophils, monocytes and lymphocytes, platelets, and also acute phase proteins such as CRP and albumin. Scores made up of combinations of these markers include the neutrophil-lymphocyte ratio (NLR), the platelet lymphocyte ratio (PLR), the lymphocyte-monocyte ratio (LMR) and the modified Glasgow Prognostic Score (mGPS) which gives a score 0-2 based on elevation of CRP and low albumin. These scores have been shown to have prognostic value, mainly in lung and gastrointestinal cancers, particularly in advanced disease(120, 121).

To date there is little consensus as to the prognostic role and clinical utility of these markers in primary operable breast cancer. In this context, a systematic review and meta-analysis of the literature relating to circulating markers of the systemic inflammatory response as prognostic markers in primary operable breast cancer was carried out. Secondly, a cohort study was carried out to

investigate the prognostic role of these markers in primary operable breast cancer in our population.

3.2 Materials and methods

3.2.1 Systematic review

A search up to July 2017 was made of the databases MEDLINE and Embase (Excerpta Medica Database) using combinations of MeSH terms and keywords. Search terms used were 'breast neoplasms', 'white cell count', 'neutrophils', 'lymphocytes', 'monocytes', 'platelets', 'neutrophil-lymphocyte ratio', 'platelet-lymphocyte ratio', 'lymphocyte-monocyte ratio', 'albumin', 'CRP', and 'Glasgow Prognostic Score'. Titles and abstracts were initially reviewed for suitability. Duplicates were removed. Full text articles of the remaining titles were then obtained and reviewed. Inclusion criteria were, available full English language papers investigating a measurable prognostic outcome (overall survival, disease-free survival, cancer specific survival, or recurrence), relating to one or more preoperative serum inflammatory marker or a related score. To be included in the review they required to have investigated breast cancer patients only or, if several cancers were being studied, have identifiable outcomes for the breast cohort within it. Studies were excluded if they included metastatic patients only, did not have a recordable outcome measure, had fewer than 100 patients (to reduce the risk of bias associated with smaller studies), fewer than 10 outcome events, were published before 2000 (to reflect modern treatment practices), or studied levels of inflammatory markers taken after surgery. Where two papers by the same author appeared to use the same cohort, the more recent paper with the larger cohort and more mature follow up was retained. In addition, references in the included papers were checked for any other relevant studies. Results are presented in a descriptive fashion for each inflammatory marker in turn.

3.2.2 Meta-analysis

Meta-analysis for each inflammatory marker was carried out where there were three or more studies which reported a hazard ratio with a 95% confidence interval, and which used the same outcome measure. The hazard ratio from

multivariate analysis was used unless unavailable, in which case the hazard ratio from univariate analysis was used. Review Manager 5.3 was used for all analysis.

3.2.3 Pilot study

3.2.3.1 Data collection

The FJ cohort was used for this study as patient identifiers were available to allow searching of lab systems, and because this is the more recent of the two cohorts so blood results were more easily retrievable. Preoperative lab results, postoperative pathology and clinical outcome data were collected as described in chapter 2. For OS and CSS, patients were censored at the time of data collection (August 16).

3.2.3.2 Analysis

Components of the full blood count, CRP and albumin were first analysed as continuous variables. Then, for each component of the full blood count analysed, ROC curves were used to determine the threshold value for division into high and low groups. Where this did not produce a clear threshold, tertiles or the median were used. Statistical analysis was carried out, as described in chapter 2, to determine associations between various circulating markers of the systemic inflammatory response, or scores and ratios described in the literature, and CSS and OS.

3.3 Systematic review and meta-analysis results

2542 results were obtained from the initial search. After review of the titles for relevance, abstract review, removal of duplicates and non-English language papers, and application of the inclusion and exclusion criteria, 30 studies were included in the final review as shown in the PRISMA diagram (**Figure 3-1**). 18 studies were suitable for inclusion in meta-analysis**.**

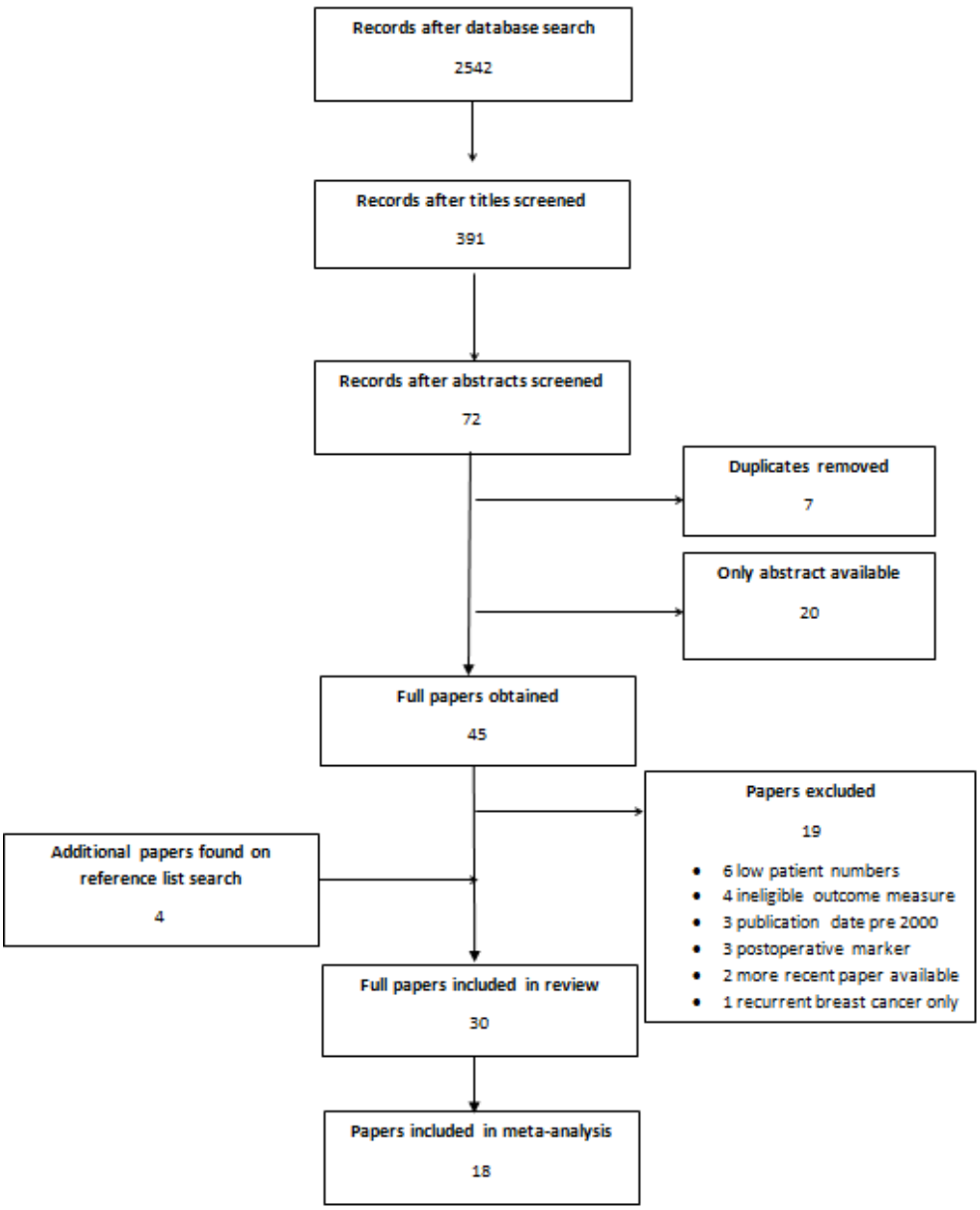

Figure 3-1. PRISMA flow diagram. **Fig.1** PRISMA flow diagram detailing the process of study selection.

3.3.1 The prognostic role of preoperative WCC and its components

Table 3-1 to Table 3-6 summarise the findings of four studies which investigated the WCC or its individual components(122-125). They range from a small retrospective cohort study of 350 patients(122) to a large epidemiological study which included little detail regarding tumour pathology in its report(123). One study analysed each inflammatory marker as a continuous variable while the others selected set thresholds for analysis. None of the studies reported a significant association with survival or cancer recurrence. For WCC and its components there were insufficient studies for meta-analysis.

Author	Year	Country	Study type	Patients	Outcomes	Cancer stage	Subtype	Marker and threshold	No pts >threshold	Outcome measure	Hazard ratio (95% CI)	p
Cihan et al(122)	2014	Turkey	Retrospective cohort	350	48 deaths, 59 rec (14 local + 45 mets)	All primary operable who received adjuvant treatment	**ER+** 55.4% **ER-** 37.7%	WCC (continuous)	N/A	 OS Recurrence	**UV analysis** 0.9 (0.8-1.0) 1.0 (0.9-1.1)	 0.236 0.968
Wulaningsih et al(123)	2015	Sweden	Prospective cohort	6606	736 CDs, 738 NCDs	All stages	Data not shown	WCC$\geq$10x10^9/L	134	 OS CSS	**MV analysis** 1.57 (1.14-2.16) 1.23 (0.75-2.03)	 0.16 0.41

Table 3-1. The prognostic role of preoperative WCC. Papers which investigated the prognostic role of preoperative White Cell Count**.** Rec = recurrences, CDs = cancer deaths, NCDs = non cancer deaths, UV =univariate, MV = multivariate.

Author	Year	Country	Study type	Patients	Outcomes	Cancer stage	Subtype	Marker and threshold	No pts >threshold	Outcome measure	Hazard ratio (95% CI)	p
Cihan et al(122)	2014	Turkey	Retrospective cohort	350	48 deaths, 59 rec (14 local + 45 mets)	All primary operable who received adjuvant treatment	**ER+** 55.4% **ER-** 37.7%	Neutrophils (continuous)	N/A	 OS Recurrence	**UV analysis** 0.9 (0.8-1.0) 0.9 (0.8-1.0)	 0.433 0.638
Wariss et al(124)	2017	Brazil	Retrospective cohort	2288	494 deaths	All stages	**Lum A** 48.9% **Lum B** 9.1% **TNBC**12.7% **Her2** 8.0%	Neutrophils >7.5 x10^9/L	167	OS	**MV analysis** 1.26 (0.92-1.74)	0.150

Table 3-2. The prognostic role of preoperative neutrophils. Papers which investigated the prognostic role of preoperative neutrophils. Rec = recurrences, UV =univariate, MV = multivariate.

Author	Year	Country	Study type	Patients	Outcomes	Cancer stage	Subtype	Marker and threshold	No pts >threshold	Outcome measure	Hazard ratio (95% CI)	p
Cihan et al(122)	2014	Turkey	Retrospective cohort	350	48 deaths, 59 rec (14 local + 45 mets)	All primary operable who received adjuvant treatment	**ER+** 55.4% **ER-** 37.7%	Lymphocytes (continuous)	N/A	 OS Recurrence	**UVanalysis** 0.9 (0.7-1.2) 1.0 (0.8-1.2)	 0.793 0.959
Wen et al(125)	2015	China	Retrospective cohort	2000	326 deaths	All primary operable ILC &IDC	**ER+** 36.8% **ER-** 63.2%	Lymphocytes >2.20x10^9/L	850	OS	**MV analysis** 1.17 (0.90-1.51)	0.241

Table 3-3. The prognostic role of preoperative lymphocytes. Papers which investigated the prognostic role of preoperative lymphocytes. Rec = recurrences, UV =univariate, MV = multivariate.

Author	Year	Country	Study type	Patients	Outcomes	Cancer stage	Subtype	Marker and threshold	No pts >threshold	Outcome measure	Hazard ratio (95% CI)	p
Cihan et al(122)	2014	Turkey	Retrospective cohort	350	48 deaths, 59 rec (14 local + 45 mets)	All primary operable who received adjuvant treatment	**ER+** 55.4% **ER-** 37.7%	Monocytes (continuous)	N/A	 OS Recurrence	**UV analysis** 0.7 (0.3-1.5) 0.9 (0.5-1.6)	 0.414 0.821
Wen et al(125)	2015	China	Retrospective cohort	2000	326 deaths	All primary operable ILC or IDC	**ER+** 36.8% **ER-** 63.2%	Monocytes >0.48x10^9/L	962	OS	**MV analysis** 1.37 (1.05-1.81)	0.023

Table 3-4. The prognostic role of preoperative monocytes. Papers which investigated the prognostic role of preoperative monocytes. Rec = recurrences, UV =univariate, MV = multivariate.

Author	Year	Country	Study type	Patients	Outcomes	Cancer stage	Subtype	Marker and threshold	No pts >threshold	Outcome measure	Hazard ratio (95% CI)	p
Cihan et al(122)	2014	Turkey	Retrospective cohort	350	48 deaths, 59 rec (14 local + 45 mets)	All primary operable who received adjuvant treatment	**ER+** 55.4% **ER-** 37.7%	Eosinophils (continuous)	N/A	 OS Recurrence	**UV analysis** 1.9 (0.5-7.1) 0.6 (0.1-2.6)	 0.305 0.578

Table 3-5. The prognostic role of preoperative eosinophils. Papers which investigated the prognostic role of preoperative eosinophils. Rec = recurrences, UV =univariate, MV = multivariate.

Author	Year	Country	Study type	Patients	Outcomes	Cancer stage	Subtype	Marker and threshold	No pts >threshold	Outcome measure	Hazard ratio (95% CI)	p
Cihan et al(122)	2014	Turkey	Retrospective cohort	350	48 deaths, 59 rec(14 local + 45 mets)	All primary operable who received adjuvant treatment	**ER+** 55.4% **ER-** 37.7%	Basophils (continuous)	N/A	 OS Recurrence	**UV analysis** 1.3 (0.0-21.9) 0.0 (0.0-1.7)	 0.833 0.089

Table 3-6. The prognostic role of preoperative basophils. Papers which investigated the prognostic role of preoperative basophils. Rec = recurrences, UV =univariate, MV = multivariate.

3.3.2 The prognostic role of preoperative platelets

Three studies investigating the prognostic role of the platelet count met the inclusion criteria (**Table 3-7**). ER positive disease predominated in these studies, particularly in the largest study where 91% of its participants had ER positive disease(126). This and a smaller study(127) which used thresholds for analysis (>400g/L and 350g/L respectively) reported a significant independent association between high platelets and worse cancer outcomes, whilst the smallest study, which analysed platelets as a continuous variable, reported no association(122). There were again insufficient studies for meta-analysis.

Author	Year	Country	Study type	Patients	Outcomes	Cancer stage	Subtype	Marker and threshold	No pts >threshold	Outcome measure	Hazard ratio (95% CI)	p
Taucher et al(126)	2003	Austria	Retrospective multicentre	4300	367 deaths (327 BCDs), 658 rec	All primary operable	**ER+** 91.0% **ER-** 8.4%	Platelets >400x10^9/L	161	 OS CSS DFS	**MV analysis** 1.73 (1.17-2.57) 1.67 (1.10-2.54) 1.29 (0.93-1.79)	 0.0064 0.0162 0.1355
Gu et al(127)	2015	China	Retrospective cohort	447	51 deaths, 113 rec	All stages	**ER+** 58.9% **ER-** 41.1%	Platelets >350x10^9/L	Data not shown.	DFS	**MV analysis** 0.998 (0.996-1.000)	0.042
Cihan et al(122)	2014	Turkey	Retrospective cohort	350	48 deaths, 59 rec (14 local + 45 mets)	All primary operable who received adjuvant treatment	**ER+** 55.4% **ER-** 37.7%	Platelets (continuous)	N/A	 OS Recurrence	**UV analysis** 1.0 (0.9-1.0) 0.9 (0.9-1.0)	 0.81 0.539

Table 3-7. The prognostic role of preoperative platelets. Papers which investigated the prognostic role of preoperative platelets**.** Rec = recurrences, CDs = cancer deaths, UV =univariate, MV = multivariate.

3.3.3 The prognostic role of preoperative NLR

Eighteen papers were included which investigated the relationship of the NLR to outcome in operable breast cancer (**Table 3-8**). All the cohorts were dominated by ER positive disease, except one study which included exclusively ER negative disease(128). All but 5 of them(122, 129-132) (one of which analysed NLR as a continuous variable) reported a significant association between high NLR and at least one of the cancer outcomes studied. Thresholds used ranged from 1.93-5. Therefore, following the overall meta-analysis for the different outcomes, sub-analyses were carried out for different thresholds, where the number of studies allowed.

Author	Year	Country	Study type	Patients	Outcomes	Cancer stage	Subtype	Marker and threshold	No pts >threshold	Outcome measure	Hazard ratio (95% CI)	p
Azab et al(133)	2013	US	Retrospective cohort	437	74 deaths	All stages	**ER+** 76.2% **ER-** 23.8%	NLR≥3.3	119	OS	**MV analysis** 3.60 (2.13-6.09)	<0.001
Noh et al(134)	2013	Korea	Retrospective cohort	442	32 deaths	All primary operable	**ER+** 57.9% **ER-** 24.2%	NLR ≥2.5	115	CSS	**MV analysis** 4.08 (1.62-10.28)	0.003
Forget et al(135)	2014	Belgium	Retrospective cohort	451	32 deaths, 72 rec	All primary operable undergoing BCS	**ER+** 83.5% **ER-** 16.5%	NLR >3.3	111	OS DFS	**MV analysis** 2.35 (1.02-5.43) 1.99 (1.16-3.41)	0.046 0.01
Cihan et al(122)	2014	Turkey	Retrospective cohort	350	48 deaths, 59 rec (14 local + 45 mets)	All primary operable who received adjuvant treatment	**ER+** 55.4% **ER-** 37.7%	NLR ≥3,	122	OS Recurrence	**UV analysis** 0.7 (0.4-1.4) 0.8 (0.5-1.3)	0.432 0.410
Nakano et al(136)	2014	Japan	Retrospective cohort	167	19 deaths, 35 rec	Invasive primary operable	**ER+** 77.8% **ER-** 22.2%	NLR≥2.5	47	CSS DFS	**MV analysis** 2.7 (1.1-7.3) 2.0 (0.9-4.1)	0.045 0.07
Koh et al(137)	2014	S. Korea	Retrospective cohort	157	25 'relapse or death'	ER/PR+, Her2- patients who received NAC	N/A	NLR >2.25	66	OS DFS	**MV analysis** 24.87 (3.08-201.3) 3.87 (1.64-9.14)	0.003 0.002
Dirican et al(138)	2014	Turkey	Retrospective cohort	1527	Not documented	All stages	**ER+** 66.7% **ER-** 31.6%	NLR≥4	138	OS DFS	**MV analysis** 1.91 (1.31-2.79) 1.46 (1.04-2.04)	0.001 0.028
Krenn-Pilko et al(129)	2014	Austria	Retrospective cohort	793	136 deaths, (116 CDs), 167 metastases	All primary operable	**LumA** 51.3% **Lum B** 34.9% **Basal** 9.7% **HER2** 4.2%	NLR ≥2.5	448	CSS	**MV analysis** 1.25 (0.81-1.92)	0.315
Yao et al(139)	2014	China	Retrospective cohort	608	24 deaths, 57 rec	All primary operable	**Lum A** 57.9% **Lum B** 10.4% **HER2** 14.6% **TNBC** 17.2%	NLR >2.56	112	CSS DFS	**MV analysis** 3.63 (1.59-8.26) Not associated DFS, data not shown	0.002
Lee et al(130)	2015	S Korea	Retrospective cohort	3116	Data not given	All primary operable	**Lum A** 58.8% **Lum B** 12.2% **HER2** 11.7% **TNBC** 17.4%	NLR (continuous)	N/A	CSS	**UV analysis** 1.09 (0.94-1.26)	0.516

Koh et al(140)	2015	Malaysia	Retrospective cohort	1435	599	All stages	**ER+** 52.3% **ER-** 42.6%	NLR>3 NLR >4 NLR >5	390 194 119	Relative survival ratio	**MV analysis** 1.20 (0.99-1.45) 1.37 (1.08-1.74)* 1.45 (1.08-1.93)*	Not given, * if stat sig.
Hong et al(141)	2015	China	Retrospective cohort	487	73	All primary operable	**Lum A** 12.7% **Lum B** 50.1% **HER2** 12.1% **TNBC** 19.3%	NLR ≥1.93	189	DFS	**MV analysis** 1.87 (1.16-3.02)	0.011
Jia et al(142)	2015	China	Retrospective cohort	1570	108 deaths, 242 rec	All primary operable	**Luminal** 63.8% **HER2** 21.9% **TNBC** 14.3%	NLR >2,	804	 OS DFS	**MV analysis** 3.05 (1.08-8.61) 2.58 (1.23-5.42)	 0.035 0.012
Suppan et al(131)	2015	Austria	Retrospective cohort	247	95 rec	All early stage who underwent neoadj therapy	**Lum** 53.3%, **HER2** 23.3% **TNBC** 23.3%	NLR (continuous)	N/A	Recurrence	**MV analysis** 1.01 (0.96-1.06)	0.738
Krenn-Pilko et al(143)	2016	Austria	Retrospective cohort	762	133 deaths, 179 rec	All primary operable	**Luminal** 87.6% **HER2** 3.7% **Basal** 8.7%	NLR ≥5	58	 OS DFS	**UV analysis** 1.60 (0.92-2.78 **MV analysis** 1.96 (1.14-3.38)	 0.098 0.015
Liu et al(128)	2016	China	Retrospective cohort	318	234 deaths, 283 rec	HR negative primary operable	**ER-** 100% **HER2+** 49.4%	NLR ≥3	123	 OS DFS	**MV analysis** 2.33 (1.71-3.18) 1.89 (1.42-2.51)	 <0.001 <0.001
Wariss et al(124)	2017	Brazil	Retrospective cohort	2288	494 deaths	All stages	**Lum A** 48.9% **Lum B** 9.1% **Her2** 8.0% **TNBC** 12.7%	NLR 4-5 NLR>5	51 77	OS	**MV analysis** 1.03 (0.57-1.89) 1.66 (1.08-2.55)	0.914 0.021
Takeuchi et al(132)	2017	Japan	Retrospective cohort	296	22 rec	All primary operable	**ER+** 85% **ER-** 15% **HER2+** 83% **HER2-** 17%	NLR≥2.06	137	Recurrence	**UV analysis** 2.03 (0.85-4.84)	0.11

Table 3-8. The prognostic role of preoperative NLR. Papers which investigated the prognostic role of preoperative neutrophil-lymphocyte ratio. Rec = recurrences, CDs = cancer deaths, Lum = luminal, UV =univariate, MV = multivariate.

8 studies used an outcome of DFS(128, 135-138, 141-143), with a total of 5169 patients and 1355 events (one study did not publish event data). This showed a significant association of NLR with DFS (pooled HR 1.87, 95% CI 1.59-2.20, p<0.00001). Heterogeneity was minimal (I^2=0% p=0.58) (**Figure 3-2a**).

When the same analysis was carried out for overall survival, there were 9 eligible studies(122, 124, 128, 133, 135, 137, 138, 142, 143) with 7860 patients and 1148 deaths. Pooled HR in this case was higher (HR 2.04, 95% CI 1.46-2.83, p<0.0001). However, there was substantial heterogeneity (I^2=67%, p=0.002) (**Figure 3-2b**).

Four studies using an outcome of CSS were included in the meta-analysis(129, 134, 136, 139). There were 2010 patients with 191 cancer deaths. There was a significant effect shown (HR 2.46, 95% CI 1.27-4.76, p=0.007). There was substantial heterogeneity between the studies (I^2=67%, p=0.003) (**Figure 3-2c**).

3.3.3.1 Subgroup analysis of the relationship between NLR and DFS by threshold used

Four studies which used a threshold of 1.9-2.9 and an outcome measure of DFS were included in a further meta-analysis(136, 137, 141, 142). This showed NLR to be a significant prognostic factor for worse DFS (HR 2.24, 95% CI 1.62-3.11, p<0.001). There was minimal heterogeneity between these studies (I^2=0%) (**Figure 3-2a**).

Four studies used a threshold of 3-5 and an outcome of DFS. At this threshold also, high NLR was significantly associated with poorer DFS (pooled HR 1.76, 95% CI 1.46-2.13, p<0.001, I^2=0%).

3.3.3.2 Subgroup analysis of the relationship between NLR and OS by threshold used

Meta-analysis was carried out for 4 studies which used a threshold of 3-3.9 and an outcome measure of OS(122, 128, 133, 135). Total number of patients was 1556 with 388 deaths. This showed a significant effect association with OS (HR 1.96, 95% CI 1.04-3.66, p=0.04). There was considerable heterogeneity between studies (I^2=82%, p=0.0010) **(Figure 3-2b)**.

Further meta-analysis was carried out for 3 studies which used a threshold of 4-5 and an outcome of OS(124, 138, 143). Again, a significant association was shown (pooled HR 1.75, 95% CI 1.36-2.26, $p<0.0001$). There was minimal heterogeneity ($I^2=0\%$).

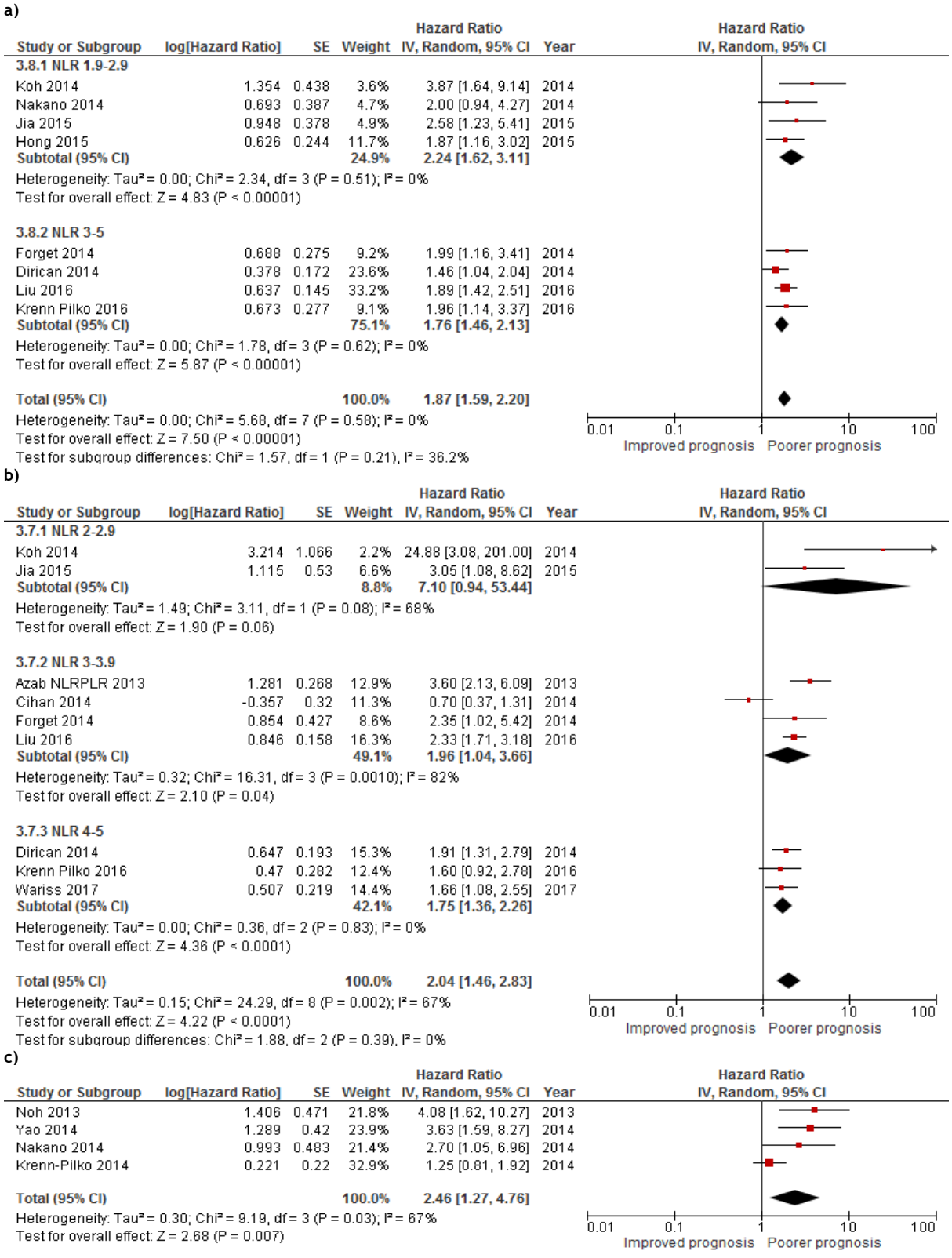

Figure 3-2. Forrest plots of NLR studies. Forrest plots of studies which investigated the neutrophil-lymphocyte ratio with an outcome measure of a) disease free survival oredered by threshold used, b) overall survival ordered by threshold, c) cancer specific survival (all used a threshold of 2-2.5).

3.3.4 The prognostic role of preoperative dNLR

Three papers also investigated the effect of dNLR (derived NLR, defined as the neutrophil count divided by the WCC-neutrophils)(124, 138, 143). Only one of these reported a statistically significant independent association with worse DFS, when dNLR $\geq$3(143). Meta-analysis for these 3 studies showed a significant association of elevated dNLR with OS (HR 1.70, 95% CI 1.39-2.08, p<0.0001). There was minimal heterogeneity between studies (I^2=0%) **(Figure 3-3).**

Author	Year	Country	Study type	Patients	Outcomes	Cancer stage	Subtype	Marker and threshold	No pts >threshold	Outcome measure	Hazard ratio (95% CI)	p
Dirican et al(138)	2014	Turkey	Retrospective cohort	1527	Not documented	All stages	**ER+** 66.7% **ER-** 31.6%	dNLR≥2	397	 OS DFS	**UV analysis** 1.80 (1.40-2.32) 1.71 (1.33-2.19)	 <0.001 <0.001
Krenn-Pilko et al(143)	2016	Austria	Retrospective cohort	762	133 deaths, 179 rec	All primary operable	**Lum** 87.6% **Basal** 8.7% **HER2** 3.7%	dNLR ≥3	93	 OS DFS	**MV analysis** 1.54 (0.91-2.59) 1.70 (1.09-2.65)	 0.106 0.018
Wariss et al(124)	2017	Brazil	Retrospective cohort	2288	494 deaths	All stages	**Lum A** 48.9% **Lum B** 9.1% **Her2** 8.0% **TNBC** 12.7%	 dNLR 2-3 dNLR>3	 278 84	 OS 	**MV analysis** 1.02 (0.76-1.38) 1.53 (0.99-2.38)	 0.869 0.053

Table 3-9. The prognostic role of preoperative dNLR. Papers which investigated the prognostic role of preoperative derived neutrophil-lymphocyte ratio. Rec = recurrences, , Lum= luminal, UV =univariate, MV = multivariate.

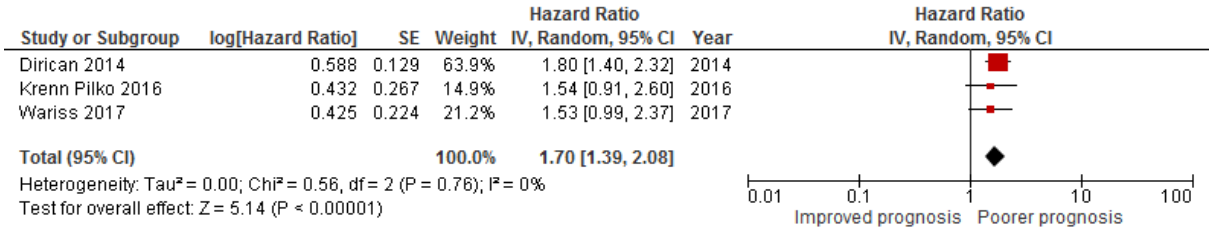

Figure 3-3. Forrest plot for dNLR. Forrest plot of studies which investigated the derived neutrophil-lymphocyte ratio with an outcome measure of overall survival.

3.3.5 The prognostic role of preoperative PLR

Eight studies investigated the prognostic value of the PLR (**Table 3-10**). These cohorts were all made up of predominately ER positive disease, except for one whose cohort was 100% ER negative disease(128). Thresholds used ranged from 107.64 to 300. Two studies using a threshold of >185(133, 140), and one larger study using a threshold of PLR>300(124), reported high PLR to be a significant independent predictor of worse survival.

Five studies(122, 124, 128, 129, 133) used a range of thresholds but all used OS as the outcome measure, so were included in the meta-analysis. There were 4186 patients and 986 deaths). A significant association with OS was shown (HR 1.55, 95% CI 1.04-2.30, p=0.03), but there was substantial heterogeneity between studies (I^2=68%, p=0.01) (**Figure 3-4**).

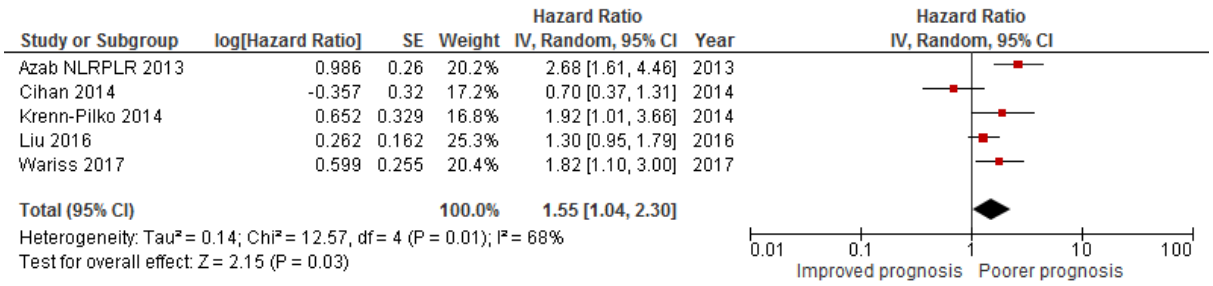

Figure 3-4. Forrest plot for PLR. Forrest plot of studies which investigated the platelet-lymphocyte ratio with an outcome measure of overall survival.

Author	Year	Country	Study type	Patients	Outcomes	Cancer stage	Subtype	Marker and threshold	No pts >threshold	Outcome measure	Hazard ratio (95% CI)	p
Azab et al(133)	2013	US	Retrospective cohort	437	74 deaths	All stages	**ER+** 76.2% **ER-** 23.8%	PLR ≥185	115	OS	**MV analysis** 2.68 (1.61-4.46)	<0.001
Cihan et al(122)	2014	Turkey	Retrospective cohort	350	48 deaths, 59 rec (14 local + 45 mets)	All primary operable who received adjuvant treatment	**ER+** 55.4% **ER-** 37.7%	PLR≥160	50	OS Recurrence	**UV analysis** 0.7 (0.4-1.4) 0.9 (0.5-1.7)	0.414 0.928
Krenn-Pilko et al(129)	2014	Austria	Retrospective cohort	793	136 deaths (116 CDs), 167 mets	All primary operable	**Lum A** 51.3% **Lum B** 34.9% **Basal** 9.7% **HER2** 4.2%	PLR ≥292	48	OS CSS DMFS	**MV analysis** 1.92 (1.01-3.67) 2.03 (1.03-4.02) **UV analysis** 2.02 (1.18-3.44)	0.047 0.042 0.010
Yao et al(139)	2014	China	Retrospective cohort	608	24 deaths, 57 rec	All primary operable	**Lum A** 57.9% **Lum B** 10.4% **HER2** 14.6% **TNBC** 17.2%	PLR >107.64	365	CSS DFS	**UV analysis** Not reported Not reported	0.051 0.273
Koh et al(140)	2015	Malaysia	Retrospective cohort	1435	599	All	**ER+** 52.3% **ER-** 42.6%	PLR >185 PLR>292	424 133	Relative survival ratio	**MV analysis** 1.25 (1.04-1.52)* 1.30 (0.98-1.70)	Not given, *if stat sig
Liu et al(128)	2016	China	Retrospective cohort	318	234 deaths, 283 rec	HR- primary operable	**ER-** 100% **HER2+** 49.4%	PLR ≥147	172	OS DFS	**MV analysis** 1.30 (0.95-1.79) 1.18 (0.90-1.15)	0.104 0.229
Wariss et al(124)	2017	Brazil	Retrospective cohort	2288	494 deaths	All stages	**Lum A** 48.9% **Lum B** 9.1% **Her2** 8.0% **TNBC** 12.7%	PLR 150-300 PLR>300	473 48	OS	**MV analysis** 1.06 (0.84-1.33) 1.82 (1.10-2.99)	0.624 0.019
Takeuchi et al(132)	2017	Japan	Retrospective cohort	296	22 rec	All primary operable	**ER+** 85% **ER-** 15% **HER2+** 83% **HER2-** 17%	PLR ≥162.28	84	Recurrence	**MV analysis** 2.61 (1.07-6.36)	0.035

Table 3-10. The prognostic role of preoperative PLR. Papers which investigated the prognostic role of preoperative platelet-lymphocyte ratio. Rec = recurrences, CDs = cancer deaths, Lum = luminal, UV =univariate, MV = multivariate.

3.3.6 The prognostic role of preoperative LMR

Four studies investigated the role of the LMR in operable breast cancer (**Table 3-11**). Three of the studies comprised patients with predominantly ER positive disease(132, 142, 144) while the largest cohort was made up of 63% ER negative disease(125). Thresholds used for analysis ranged 3.8-4.8. The only study to report a significant association with cancer outcomes evaluated a cohort of 542 locally advanced patients, who received neoadjuvant chemotherapy, and reported that LMR$\geq$4.25 was an independent prognostic factor for improved DFS(144). There were insufficient studies with the same outcome measure to carry out meta-analysis for LMR.

Author	Year	Country	Study type	Patients	Outcomes	Cancer stage	Subtype	Marker and threshold	No pts >threshold	Outcome measure	Hazard ratio (95% CI)	p
Ni et al(144)	2014	China	Retrospective cohort	542	51 rec, deaths not reported	Locally advanced (T3/4 or N2/3), pre neoadj chemo	**Lum** 63.8% **HER2** 27.2% **TNBC** 9.1%	LMR ≥4.25	280	DFS	**MV analysis** 0.68 (0.51-0.92)	0.011
Wen et al(125)	2015	China	Retrospective cohort	2000	326 deaths	All primary operable	**ER+** 36.8% **ER-** 63.2%	LMR > 3.80	590	OS	**MV analysis** 0.84 (0.63-1.12)	0.236
Jia et al(142)	2015	China	Retrospective cohort	1570	108 deaths, 242 rec	All primary operable	**Lum** 63.8% **HER2** 21.9% **TNBC** 14.3%	LMR ≤4.8	759	OS DFS	**MV analysis** 1.33 (0.52-3.45) 1.47 (0.75-2.92)	0.554 0.265
Takeuchi et al(132)	2017	Japan	Retrospective cohort	296	22 rec	All primary operable	**ER+** 85% **ER-** 15% **HER2+** 83% **HER2-** 17%	LMR≥4.56	46	Recurrence	**UV analysis** 0.4 (0.16-1.04)	0.06

Table 3-11. The prognostic role of preoperative LMR. Papers which investigated the prognostic role of preoperative lymphocyte-monocyte ratio. Rec = recurrences, Lum = luminal, UV =univariate, MV = multivariate.

3.3.7 The prognostic role of preoperative CRP

Five papers were identified which met our inclusion criteria (**Table 3-12**). One of these was a large epidemiological study which did not report extensive detail regarding tumour pathology(123) but the other 4 were dominated by ER positive disease. In all but one small study, an association between high CRP and worse cancer outcomes was reported. Thresholds used ranged from 3.25-10mg/L.

Three of the studies(123, 145, 146) were included in a meta-analysis for CRP and overall survival, with a total of 9816 patients and 1896 deaths. There was a non-significant association for elevated CRP with OS (HR 1.34, 95% CI 0.86-2.09, p=0.19). There was considerable heterogeneity between studies (I^2=82%, p=0.004) (**Figure 3-5a**).

A separate meta-analysis was carried out for the same studies with the outcome measure of CSS. There were a total of 986 cancer deaths. Again, a non-significant relationship was observed (HR 1.33, 95% CI 0.90-1.96, p=0.16). Heterogeneity was slightly less for this outcome measure but still substantial (I^2=63%, p=0.07) (**Figure 3-5b**).

Author	Year	Country	Study type	Patients	Outcomes	Cancer stage	Subtype	Marker and threshold	No pts >threshold	Outcome measure	Hazard ratio (95% CI)	p
Al Murri et al(145)	2007	UK	Prospective cohort	300	25 CDs, 14 NCDs, 37 rec	All primary operable	**ER+** 79.3% **ER-** 20.7%	CRP >10mg/L	35	 OS CSS DFS	**UV analysis** 0.60 (0.19-1.95) 0.62 (0.15-2.65) 0.40 (0.10-1.68)	 0.395 0.522 0.211
Allin et al(146)	2011	Denmark	Prospective cohort	2910	225 CDS, 158 NCDs, 118 rec	All primary operable	**ER+** 76.7% **ER-** 15.0%	hsCRP >3.24mg/L	969	 OS CSS DFS Recurrence	**MV analysis** 1.91 (1.46-2.50) 1.78 (1.26-2.52) 1.7 (1.32-2.18) 1.53 (0.98-2.37)	 <0.001 0.001 <0.001 0.06
Sicking et al(147)	2014	Germany	Retrospective cohort	148	13 CDs, 21 NCDs, 30 rec (10 local, 20 mets)	Node negative primary operable, no adjuvant systemic treatment.	**Lum A** 61.9% **Lum B** 17.3% **Her2+** 11.5% **Basal** 9.4%	CRP (continuous) CRP >5mg/L	N/A 31	 OS DFS MFS	**MV analysis** 1.03 (1.00-1.06) 1.03 (1.00-1.07) 1.01 (0.98-1.05) *No sig difference KM for all outcomes.*	 0.023 0.033 0.469
Wulaningsih et al(123)	2015	Sweden	Prospective cohort	6606	736 CDs, 738 NCDs	All stages	Data not shown	Prediagnosis CRP≥10mg/L	1020	 OS CSS	**MV analysis** 1.19 (1.04-1.36) 1.16 (0.95-1.41)	 <0.0001 0.04
Takeuchi et al(132)	2017	Japan	Retrospective cohort	296	22 recurrences	All primary operable	**ER+** 85% **ER-** 15% **HER2+** 83% **HER2-** 17%	CRP≥3.7mg/L	28	 Recurrence	**MV analysis** 2.85 (1.03-7.89)	 0.04

Table 3-12. The prognostic role of preoperative CRP. Papers which investigated the prognostic role of preoperative C-reactive protein. Rec = recurrences, CDs = cancer deaths, NCDs = non cancer deaths, Lum = luminal, UV =univariate, MV = multivariate.

a)

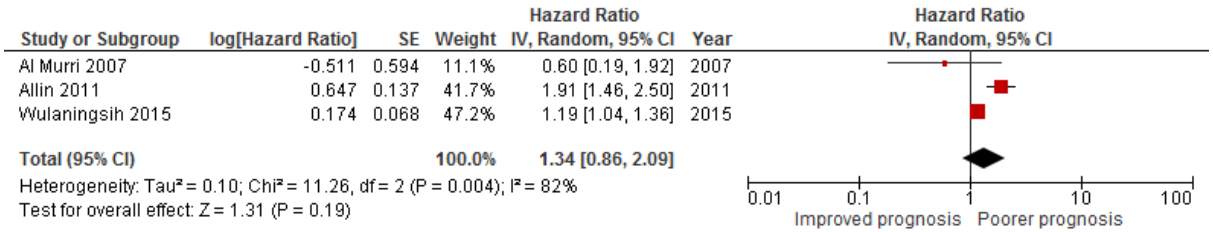

b)

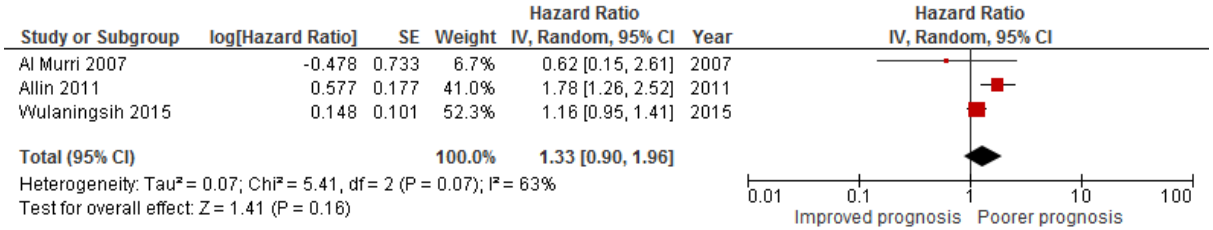

Figure 3-5. Forrest plot for CRP. Forrest plot of studies which investigated CRP with an outcome measure of a) overall survival and b) cancer specific survival.

3.3.8 The prognostic role of preoperative albumin

Five studies were identified, four investigating preoperative albumin with thresholds of 35-43g/L, and one investigating the albumin to globulin ratio (**Table 3-13**). The three which reported data regarding tumour receptors were heavily dominated by ER positive disease. All of the studies reported a significant association between low albumin and cancer outcomes, using thresholds between 35 and 43g/L.

Three studies(123, 145, 148) were entered into the meta-analysis, with a total of 9331 patients and 1725 deaths. This showed a significant association of albumin with OS (HR 1.73, 95% CI 1.01-2.99, p=0.05). There was substantial heterogeneity between studies (I^2=77%, p=0.001) (**Figure 3-6**).

Author	Year	Country	Study type	Patients	Outcomes	Cancer stage	Subtype	Marker and threshold	No pts >threshold	Outcome measure	Hazard ratio (95% CI)	p
Lis et al(149)	2003	USA	Retrospective cohort	170	28 deaths, 9 rec	All stages	Data not given	albumin <35g/L	Not clearly shown, in graph ?10	OS	3.53 (not given)	0.0033
Al Murri et al(145)	2007	UK	Prospective cohort	300	25 CDs, 14 NCDs, 37 rec	All primary operable	**ER+** 79.3% **ER-** 20.7%	Albumin ≤43g/L	114	 OS CSS DFS	**MV analysis** 3.33 (1.60-6.90) 4.44 (1.60-12.3) 3.65 (1.71-7.78)	 0.001 0.004 0.001
Azab et al(150)	2013	USA	Retrospective cohort	354	66 deaths	All stages	**ER+** 95.2%	albumin to globulin ratio <1.21	117	OS	**MV analysis** 3.62 (1.20-10.96)	0.023
Liu et al(148)	2015	US/China	Prospective cohort	2425	212 deaths	All primary operable	**ER+** 77.2% **ER-** 22.2%	albumin >39g/L	419	OS	**MV analysis** 0.55 (0.40-0.75)	0.0002
Wulaningsih et al(123)	2015	Sweden	Prospective cohort	6606	736 CDs, 738 NCDs	All stages	Data not shown	Prediagnosis alb≥40g/L	880	OS CSS	**MV analysis** 0.95 (0.83-1.09) 0.92 (0.75-1.13)	<0.0001 0.23

Table 3-13. The prognostic role of preoperative albumin. Papers which investigated the prognostic role of preoperative albumin. Rec = recurrences, CDs = cancer deaths, NCDs = non cancer deaths, UV =univariate, MV = multivariate.

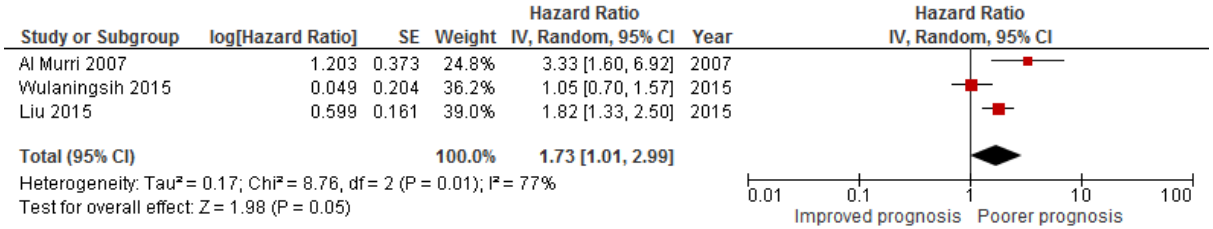

Figure 3-6. Forrest plot for albumin. Forrest plot of studies which investigated albumin with an outcome measure of overall survival.

3.3.9 The prognostic role of other markers of systemic inflammation

Three papers evaluated other systemic markers of inflammation. Wulanansih et al(123) reported haptoglobin $\geq$1.4g/L to be an independent significant prognostic factor for worse OS and CSS. In addition to the role of albumin, as outlined above, Liu et al(148) analysed other liver function tests and showed LDH>469IU/L and total bilirubin >0.2mg/dL to be independently related to worse OS. Watt et al(151) investigated the neutrophil platelet score (NPS, made up of score 0-2 for combination of elevated platelets and elevated neutrophils) in a variety of cancers and reported that this was significantly associated with OS and CSS in the breast cancer cohort of 1921 on Kaplan Meier analysis.

Author	Year	Country	Study type	Patients	Outcomes	Cancer stage	Subtype	Marker and threshold	No pts >threshold	Outcome measure	Hazard ratio (95% CI)	p
Liu et al(148)	2015	US/China	Prospective cohort	2425	212 deaths	All primary operable	**ER+** 77.2% **ER-** 22.2%	 **ALP** >79 IU/L **ALT** >19IU/L **AST** >37IU/L **LDH** >469IU/L **Bilirubin**>0.2mg/dL **Protein** >6.9g/dL	 1017 230 250 1006 2027 1270	 OS	**MV analysis** 1.25 (0.95-1.65) 0.79 (0.59-1.04) 1.40 (0.91-2.15) 1.42 (1.08-1.88) 0.62 (0.45-0.85) 1.02 (0.57-1.81)	 0.11 0.09 0.12 0.01 0.003 0.96
Wulaningsih et al(123)	2015	Sweden	Prospective cohort	6606	736 CDs, 738 NCDs	All stages	Data not shown	Prediagnosis haptoglobin ≥1.4g/L	646	 OS CSS	**MV analysis** 1.34 (1.15-1.55) 1.27 (1.02-1.59)	 <0.0001 0.02
Watt et al(151)	2015	UK	Retrospective cohort	1921	Unknown within tumour type	All stages	Data not shown	NPS 0/1/2	42	OS CSS	Data not shown Data not shown	p<0.001 p<0.001

Table 3-14. The prognostic role of other preoperative inflammatory markers. Papers which investigated the prognostic role of other preoperative inflammatory markers. CDs = cancer deaths, NCDs = non cancer deaths, NPS = neutrophil-platelet score, UV =univariate, MV = multivariate.

3.4 Pilot study results

3.4.1 Patient cohort

Of 451 patients in the FJ cohort, all had preoperative biochemistry available for CRP and albumin analysis and 439 had preoperative full blood count results available. Clinicopathological data for the FJ cohort can be found in chapter 2. All patients had outcome data for overall survival but 3 patients had no cause of death data available so CSS analysis was carried out for 448 patients for biochemistry data and 436 patients for haematology data. There were 77 breast cancer deaths and 100 non breast cancer deaths.

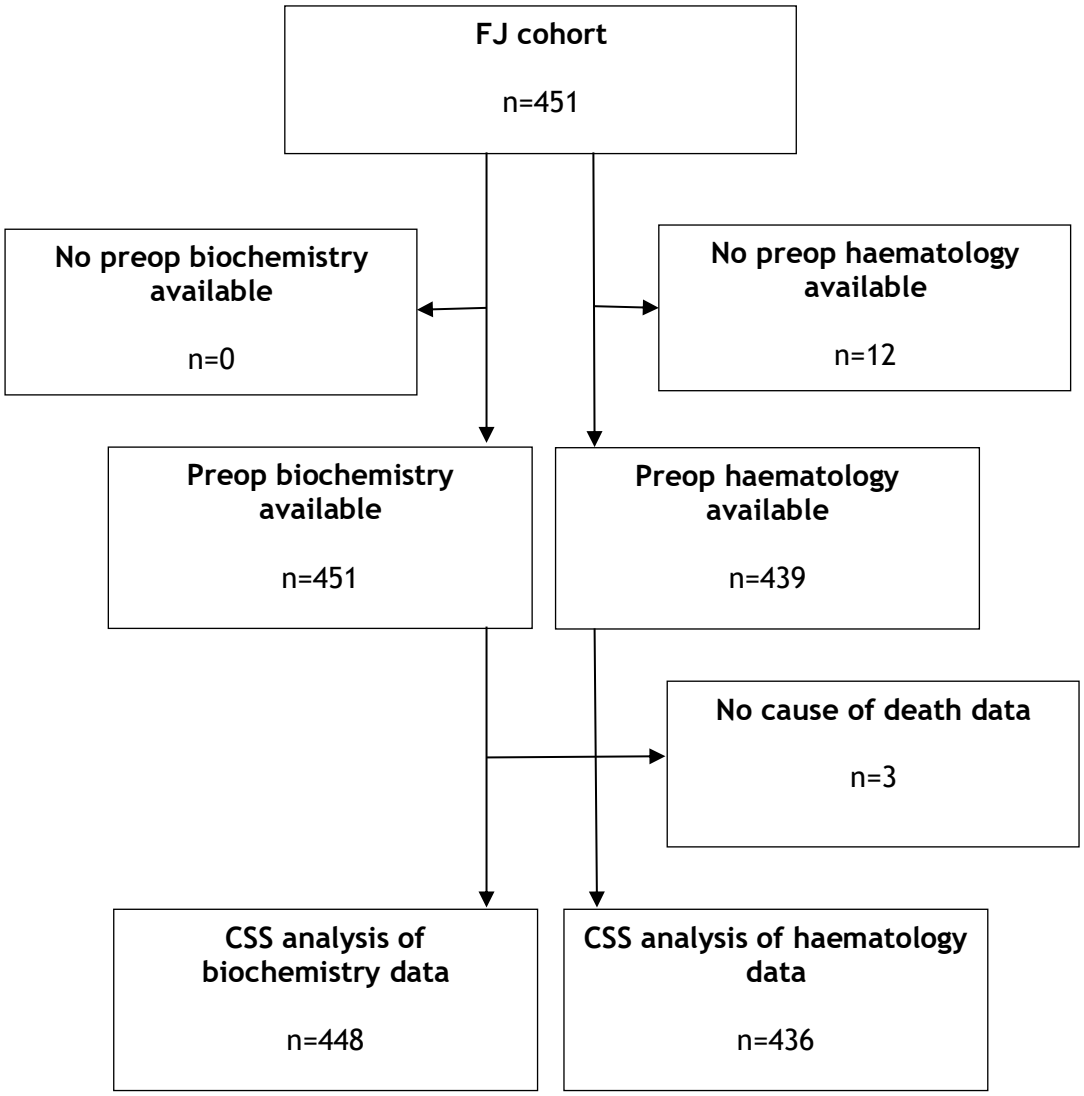

Figure 3-7. Formation of the cohort. Flow diagram detailing how the final cohort for analysis was derived.

3.4.2 Individual circulating markers of the systemic inflammatory response

Median neutrophil count was 4.29 (1.49-14.34) Median lymphocyte count was 1.64 (0.40-4.18). Median monocyte count was 0.48 (0.17-1.48). Median platelet count was 265 (89-617). Median albumin was 43 (31-52). Median CRP was 6 (1-86). Distribution of counts is shown in **Figure 3-8**.

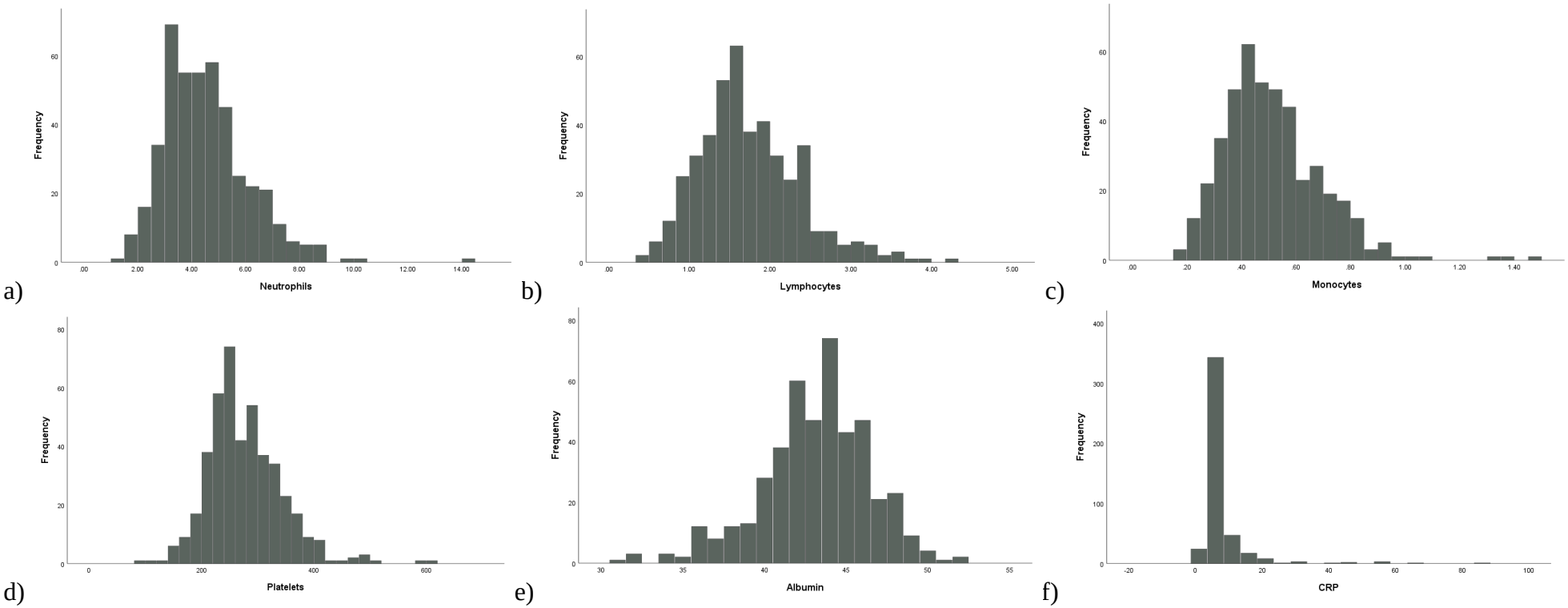

Figure 3-8. Distribution of values for individual circulating markers of the systemic inflammatory response. Histograms illustrating the distribution of preoperative values for a) neutrophils, b) lymphocytes, c) monocytes, d) platelets, e) albumin and f) CRP in the cohort.

ROC curve analysis was carried out to derive thresholds for survival analysis. From this, a threshold of 43g/L was obtained for albumin (incidentally also corresponding to the median) and will be used in all further analysis, but no clear threshold was derived for the other components listed above (**Figure 3-9, Figure 3-10**). Therefore the median was used to divide each of the other components into high and low groups for analysis. Exploratory work (data not shown) demonstrated no greater prognostic power if the components were divided by tertiles instead.

Using these thresholds, 219 (49.9%) patients had high neutrophils, 217 (49.4%) had high lymphocytes, 213 (48.5%) had high monocytes, 219 (49.9%) had high platelets, 227 (50.3%) had low albumin and 108 (23.9%) had a high CRP. High is defined as a value greater than the median meaning that, where a number of patients had the median value for that component, there were fewer than 50% of patients in the high group.

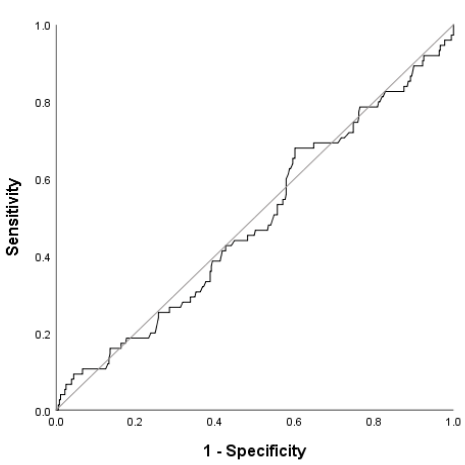

a)

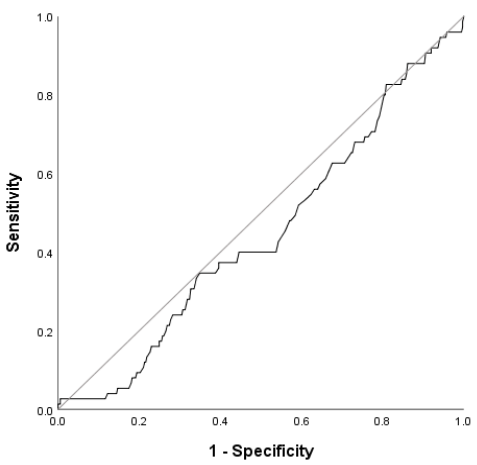

b)

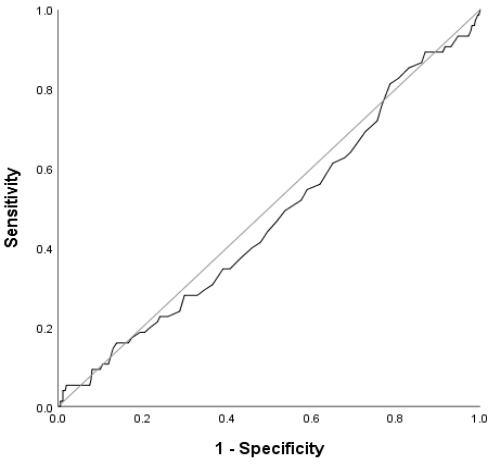

c)

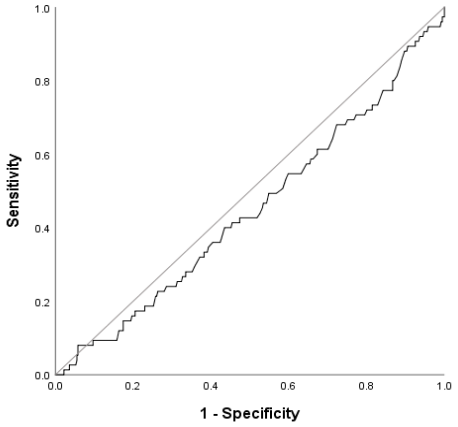

d)

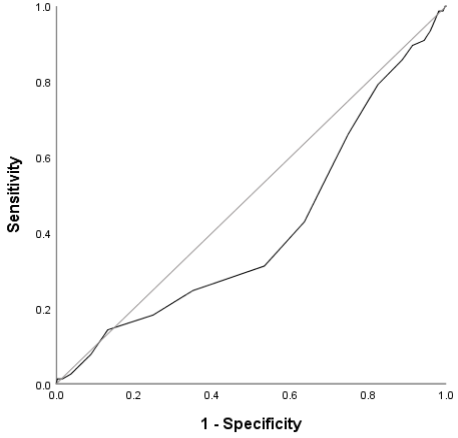

e)

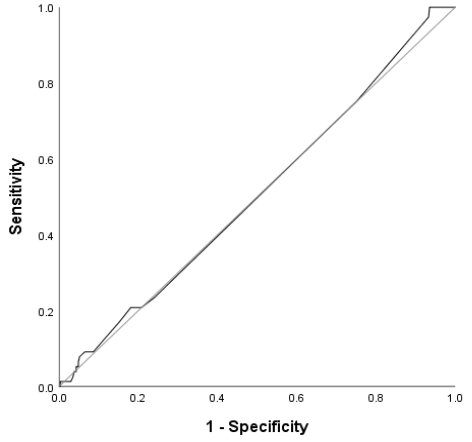

f)

Figure 3-9. ROC curves for individual markers of the systemic inflammatory response and CSS. ROC curves with an outcome of cancer specific survival for a) neutrophils (AUC 0.489), b) lymphocytes (AUC 0.446), c) monocytes (AUC 0.475), d) platelets (AUC 0.448), e) albumin (AUC 0.410) and f) CRP (AUC 0.507).

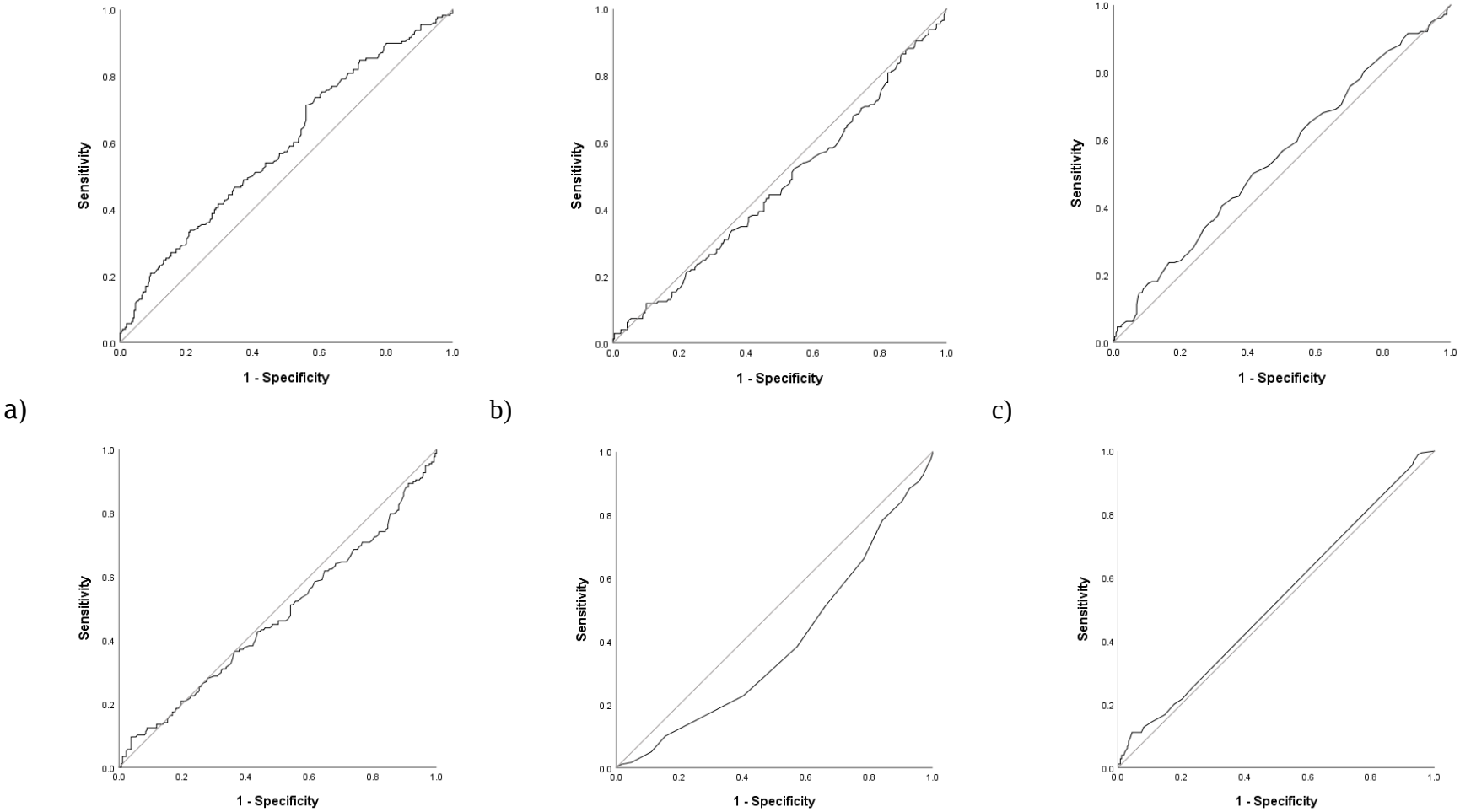

Figure 3-10. ROC curves for individual markers of the systemic inflammatory response and OS. ROC curves with an outcome of OS for a) neutrophils (AUC 0.589), b) lymphocytes (AUC 0.470), c) monocytes (AUC 0.549), d) platelets (AUC 0.472), e) albumin (AUC 0.390) and f) CRP (AUC 0.524).

3.4.2.1 Association between individual markers and CSS

On univariate analysis, albumin ≤43g/L was significantly associated with worse CSS (HR 2.69, 95% CI 1.65-4.37, p<0.001). There was no association between neutrophils (HR 0.93, 95% CI 0.59-1.46, p=0.751), lymphocytes (HR 0.68, 95% CI 0.43-1.08, p=0.103), monocytes (HR 1.13, 95% CI 0.71-1.78, p=0.608), platelets (HR 0.75, 95% CI 0.48-1.19, p=0.223) or CRP (HR 1.10, 95% CI 0.59-1.70, p=0.996) and CSS (**Figure 3-11**).

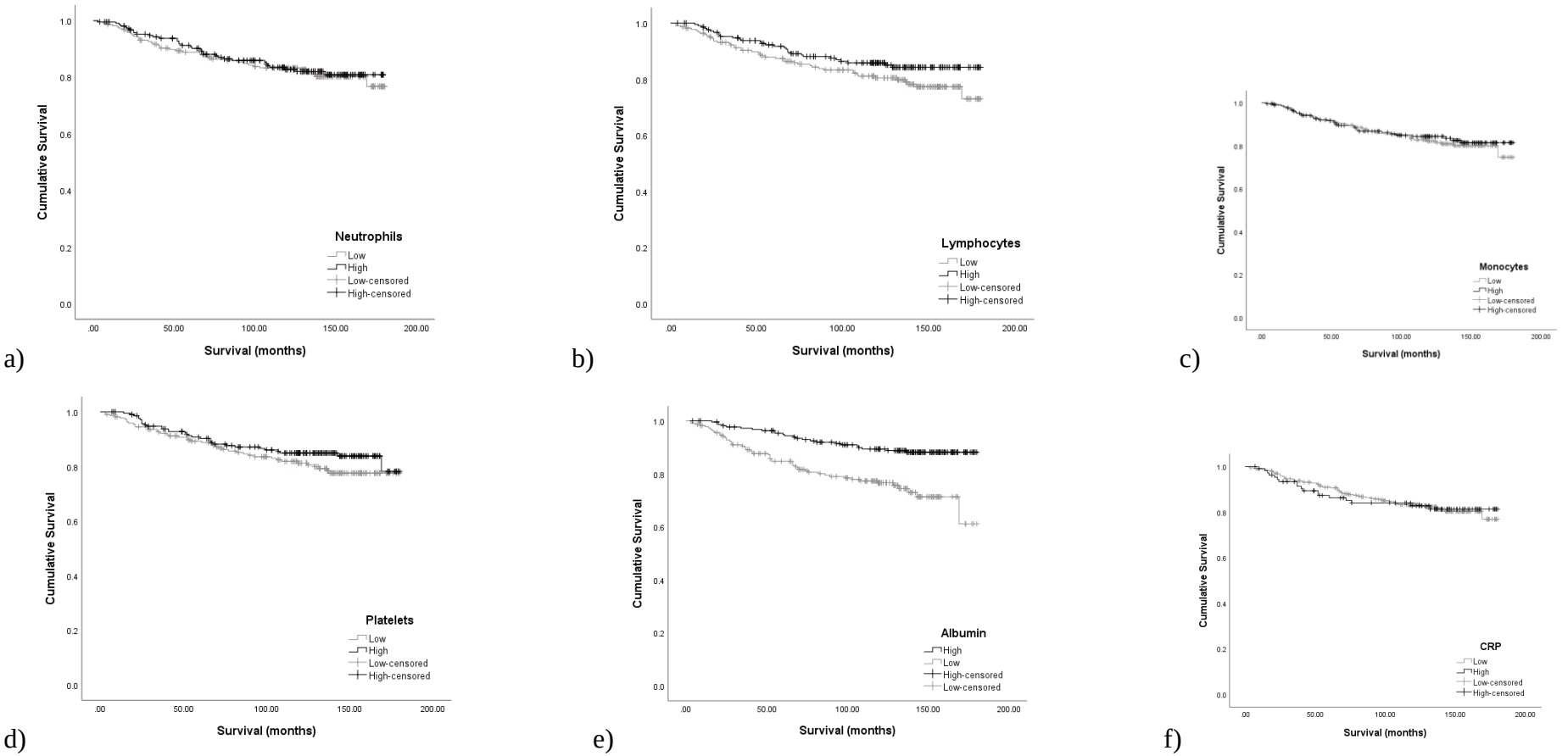

Figure 3-11. Association between individual markers of the systemic inflammatory response and CSS. Kaplan Meier graphs illustrating the relationship between cancer specific survival and a) neutrophils (p=0.751), b) lymphocytes (p=0.100), c) monocytes (p=0.607), d) platelets (p=0.222), e) albumin (p<0.001) and f) CRP (p=0.996)

3.4.2.2 Association between individual markers and OS

On univariate analysis, albumin ≤43g/L was significantly associated with worse OS (HR 2.09, 95% CI 1.54-2.83, p<0.001). There was no association between neutrophils (HR 1.28, 95% CI 0.95-1.72, p=0.103), lymphocytes (HR 0.89, 95% CI 0.66-1.19, p=0.425), monocytes (HR 1.26, 95% CI 0.94-1.69, p=0.127), platelets (HR 0.85, 95% CI 0.63-1.14, p=0.285) or CRP (HR 1.08, 95% CI 0.77-1.52, p=0.649) and OS (**Figure 3-12**).

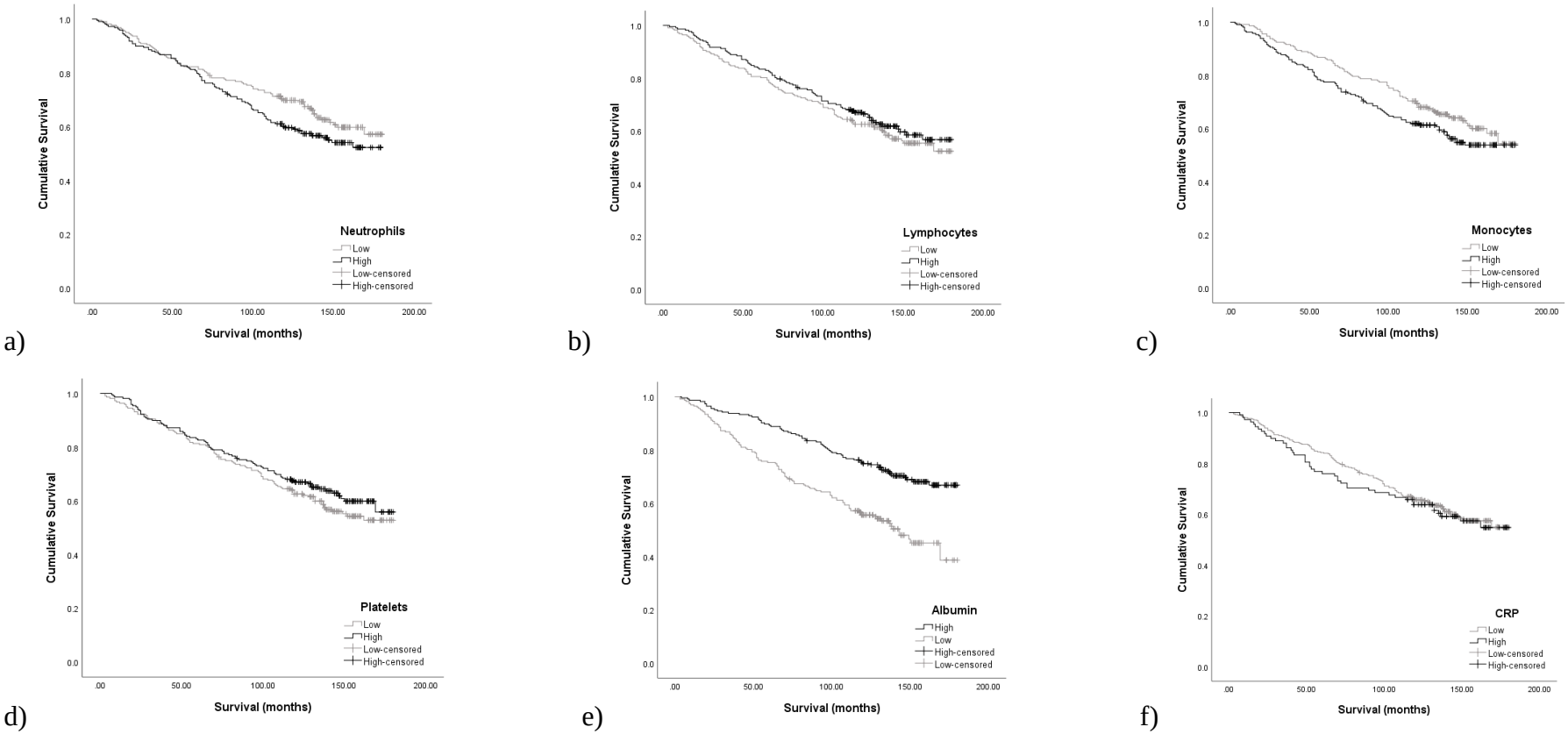

Figure 3-12. Association between individual markers of the systemic inflammatory response and OS. Kaplan Meier graphs illustrating the relationship between overall survival and a) neutrophils (p=0.101), b) lymphocytes (p=0.424), c) monocytes (p=0.126), d) platelets (p=0.283), e) albumin (p<0.001) and f) CRP (p=0.649).

3.4.2.3 Association between individual markers and survival in ER positive and ER negative disease

Neutrophils were not associated with CSS in either ER positive (HR 1.19, 95% CI 0.69-2.04, p=0.534) or ER negative disease (HR 0.50, 95% CI 0.21-1.20, p=0.121), though the Kaplan Meier curve suggested a possible trend to worse CSS for patients with low neutrophils in ER negative disease (**Figure 3-13**). However, high neutrophils were significantly associated with worse OS in ER positive disease (HR 1.46, 95% CI 1.04-2.05, p=0.028), but not in ER negative disease (HR 0.87, 95% CI 0.47-1.59, p=0.641) (**Figure 3-14**).

Low albumin was associated with worse CSS in both ER positive (HR 2.41, 95% CI 1.36-4.25, p=0.002) and ER negative (HR 3.73, 95% CI 1.46-9.56, p=0.006) disease, and with worse OS in ER positive (HR 1.99, 95% CI 1.41-2.82, p<0.001) and ER negative (HR 2.48, 95% CI 1.32-4.66, p=0.005) disease.

None of the other individual factors analysed were significantly associated with CSS or OS in either ER positive or ER negative disease (data not shown).

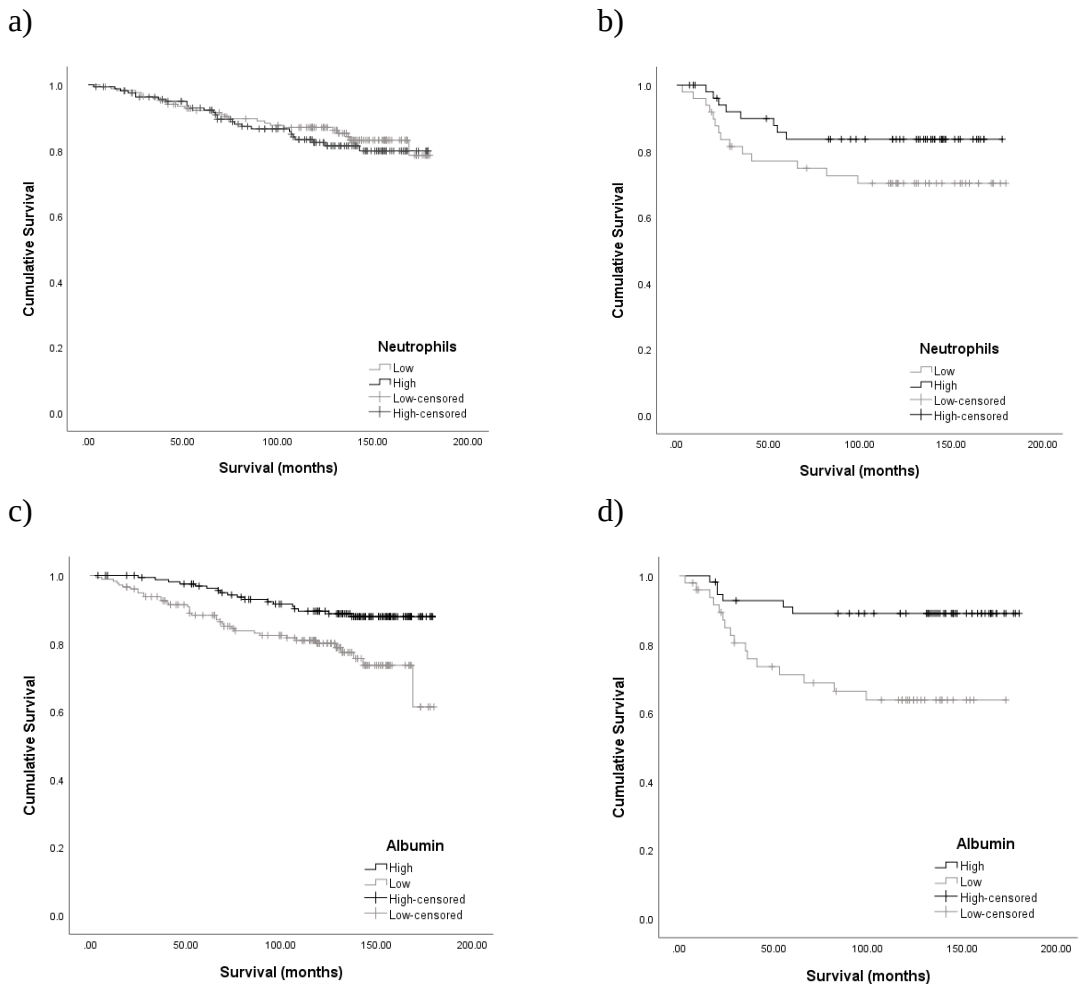

Figure 3-13. Association of neutrophils and albumin with CSS by ER status. Kaplan Meier graphs illustrating the association of neutrophils and albumin with CSS in ER positive (a) neutrophils, p=0.533; c) albumin ,p=0.002) and ER negative disease (b) neutrophils, p=0.113; d) albumin, p=0.003).

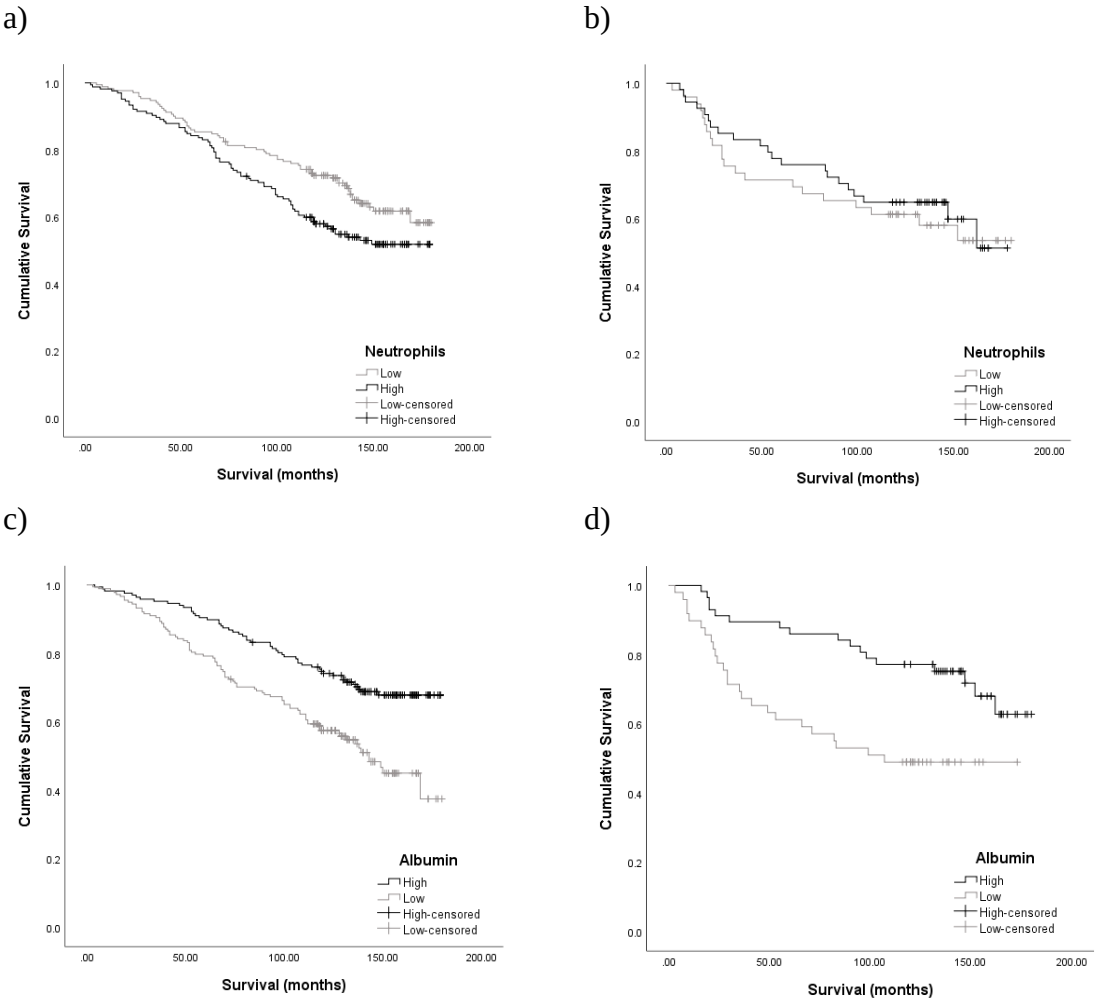

Figure 3-14. Association of neutrophils and albumin with OS by ER status. Kaplan Meier graphs illustrating the association of neutrophils and albumin with OS in ER positive (a) neutrophils, p=0.027; c) albumin ,p<0.001) and ER negative disease (b) neutrophils, p=0.640; d) albumin, p=0.004).

3.4.2.4 Associations of albumin with clinicopathological characteristics

Older age was the only clinicopathological factor significantly associated with low albumin.

Clinicopathological factor	Albumin		p
	Low (≤43) n (%)	High (>43) n (%)	
Age			**<0.001**
≤50yrs	35 (15.4)	67 (29.9)	
51-69yrs	92 (40.5)	109 (48.7)	
≥70yrs	100 (44.1)	48 (21.4)	
Tumour size			0.229
≤20mm	107 (47.1)	119 (53.1)	
21-50mm	116 (51.1)	98 (43.8)	
>50mm	4 (1.8)	7 (3.1)	
Tumour grade			0.473
I	21 (9.3)	27 (12.1)	
II	86 (37.9)	75 (33.5)	
III	120 (52.9)	122 (54.5)	
Nodal involvement			0.967
0	126 (55.8)	127 (57.0)	
1-3	71 (31.4)	68 (30.5)	
>3	29 (12.8)	28 (12.6)	
ER status			0.334
Negative	49 (21.6)	57 (25.4)	
Positive	178 (78.4)	167 (74.6)	
HER2 status			0.878
Negative	149 (83.2)	109 (82.6)	
Positive	30 (16.8)	23 (17.4)	
LVI			0.864
Absent	134 (59.0)	134 (59.8)	
Present	93 (41.0)	90 (40.2)	
CRP			0.888
Low	172 (75.8)	171 (76.3)	
High	55 (24.2)	53 (23.7)	
Neutrophils			0.166
Low	117 (53.4)	103 (46.8)	
High	102 (46.6)	117 (53.2)	
Lymphocytes			0.417
Low	115 (52.5)	107 (48.6)	
High	104 (47.5)	113 (51.4)	
Monocytes			0.666
Low	115 (52.5)	111 (50.5)	
High	104 (47.5)	109 (49.5)	
Platelets			0.535
Low	113 (51.6)	107 (48.6)	
High	106 (48.4)	113 (51.4)	

Table 3-15. Association between preoperative albumin and other clinicopathological factors.

3.4.3 Scores and ratios of circulating markers of the systemic inflammatory response

Next, scores and ratios made up of different combinations of the individual markers of the systemic inflammatory response, previously described in the literature, were analysed. These were the NLR, PLR, LMR and mGPS. Median NLR was 2.58 (0.71-14.67), median PLR was 163.27 (40.84-751.52) and median LMR was 3.53 (0.78-8.76). Distribution of values for these ratios is shown in **Figure 3-15**. 396 (87.8%) patients had a mGPS of 0, 51 (11.3%) had a mGPS of 1 and 4 (0.9%) had a mGPS of 2.

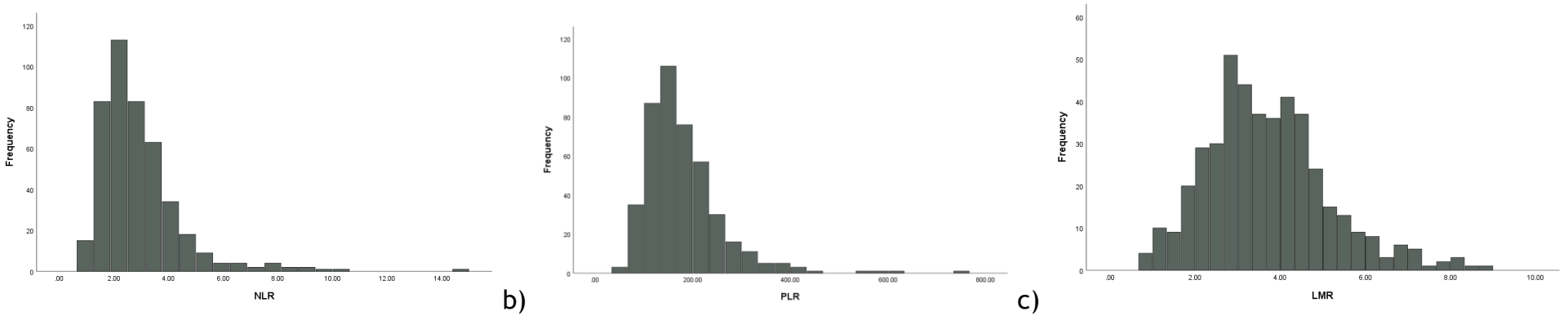

a) b) c)

Figure 3-15. Distribution of values for ratios of markers of the systemic inflammatory response. Histograms illustrating the distribution of preoperative values for a) NLR, b) PLR and c)LMR.

For NLR, PLR and LMR, ROC curves were constructed to identify thresholds to allow division of groups for survival analysis (**Figure 3-16, Figure 3-17**). If these did not demonstrate a clear threshold, Kaplan Meier analysis of tertiles was performed. The ROC derived threshold for NLR was 2.5, which happens to correspond to the median. For further analysis patients were grouped into low NLR (≤2.5) or high NLR (>2.5) groups. Neither ROC nor tertile analysis identified a clear threshold for PLR so the median was used to divide patients into low PLR (≤163) or high PLR (>163) groups. For LMR, the ROC curve did not clearly demonstrate one specific point. Kaplan Meier analysis of tertiles suggested that the cutoff for the lowest tertile would be a suitable threshold for division, and this number did correspond to one of the points furthest from the diagonal line on the ROC curve. Therefore, patients were divided into low (≤2.98) or high (>2.98) LMR groups using this threshold.

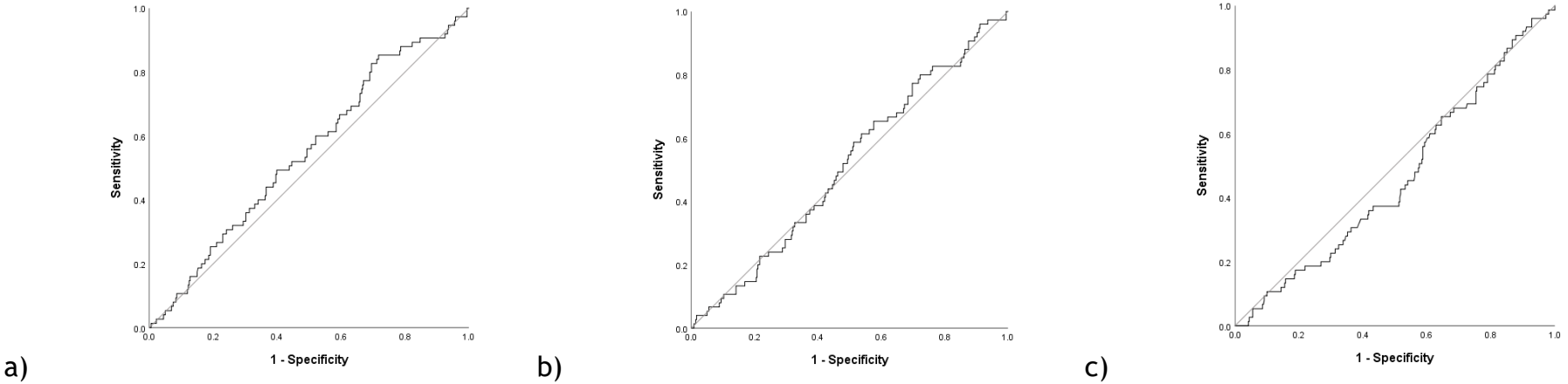

Figure 3-16. ROC curve analysis for ratios of circulating markers of the systemic inflammatory response and CSS. ROC curves with an outcome of CSS for preoperative a) NLR (AUC 0.546), b) PLR (AUC 0.512) and c) LMR (AUC 0.462).

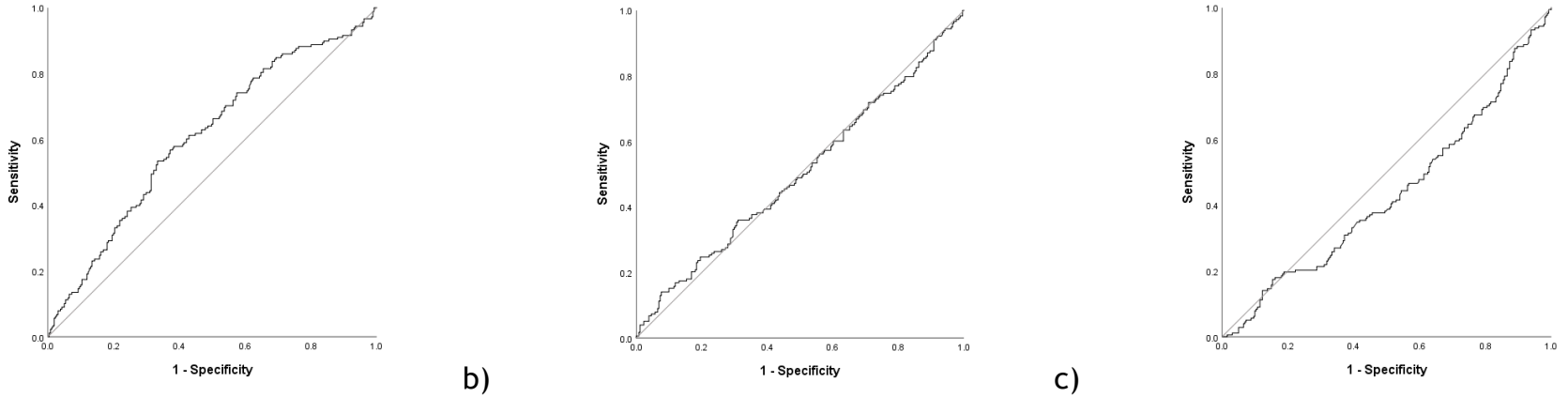

a) b) c)

Figure 3-17. ROC curve analysis for ratios of circulating markers of the systemic inflammatory response and OS. ROC curves with an outcome of OS for preoperative a) NLR (AUC 0.607), b) PLR (AUC 0.502) and c) LMR (AUC 0.433).

3.4.3.1 Associations between scores/ratios and CSS

None of NLR (high v low: HR 1.34, 95% CI 0.85-2.12, p=0.211), LMR (high v low: HR 0.85, 95% CI 0.53-1.37, p=0.511), PLR (high v low: HR 1.14, 95% CI 0.72-1.79, p=0.579) or mGPS (1v0: HR 1.09, 95% CI 0.54-2.19, p=0.804; 2v0: HR 3.20, 95% CI 0.44-23.25, p=0.251) were significantly associated with CSS.

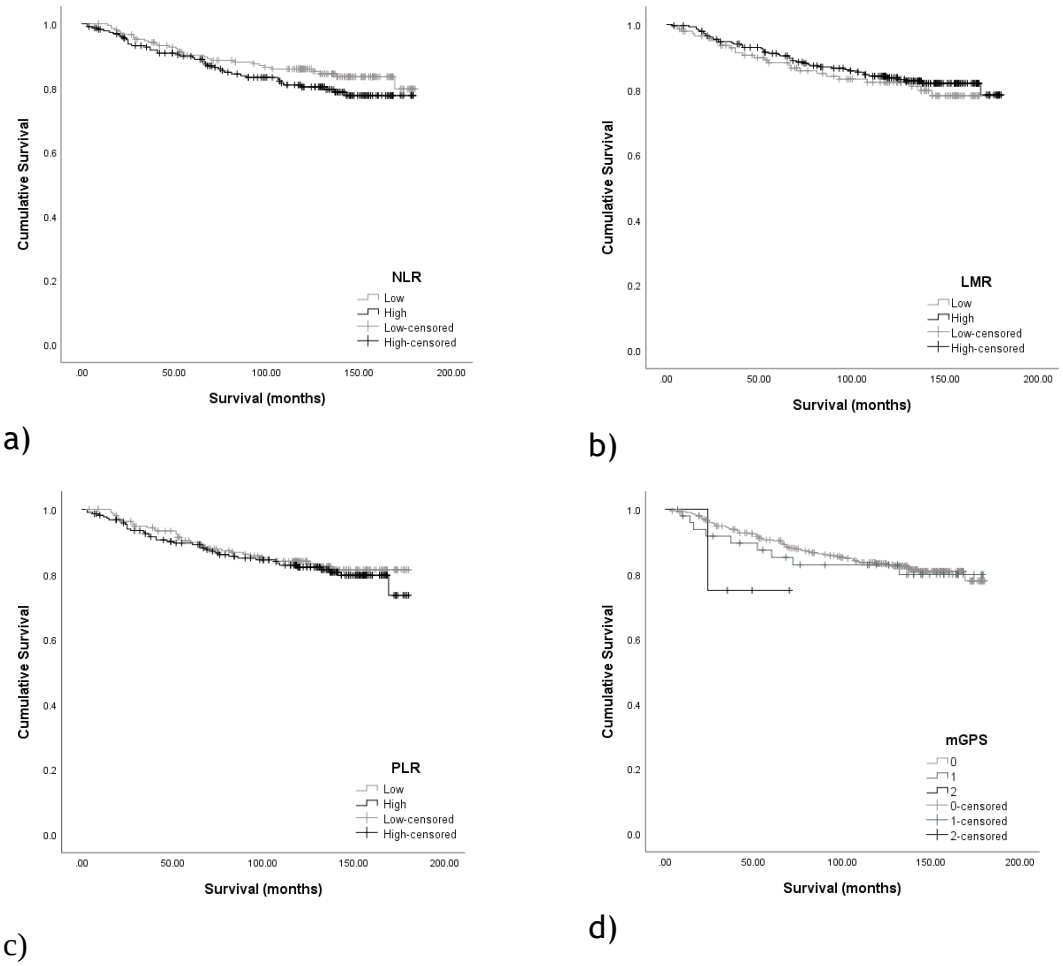

Figure 3-18. Association between ratios/scores of markers of the systemic inflammatory response and CSS. Kaplan Meier graphs illustrating the relationship between cancer specific survival anda) NLR (p=0.209), b) LMR (p=0.510), c) PLR (p=0.578) and d) mGPS (p=0.470).

3.4.3.2 Associations between scores/ratios and OS

High NLR (high v low: HR 1.64, 95% CI 1.21-2.22, p=0.001), low LMR (high v low: HR 0.67, 95% CI 0.49-0.90, p=0.008) and high mGPS (1 v 0: HR 1.13, 95% CI 0.72-1.76, p=0.600; 2 v 0: HR 7.40, 95% CI 2.71-20.25, p<0.001) were all significantly associated with worse OS on univariate analysis. PLR was not significantly associated with OS (high v low: HR. 0.96, 95% CI 0.71-1.29, p=0.773).

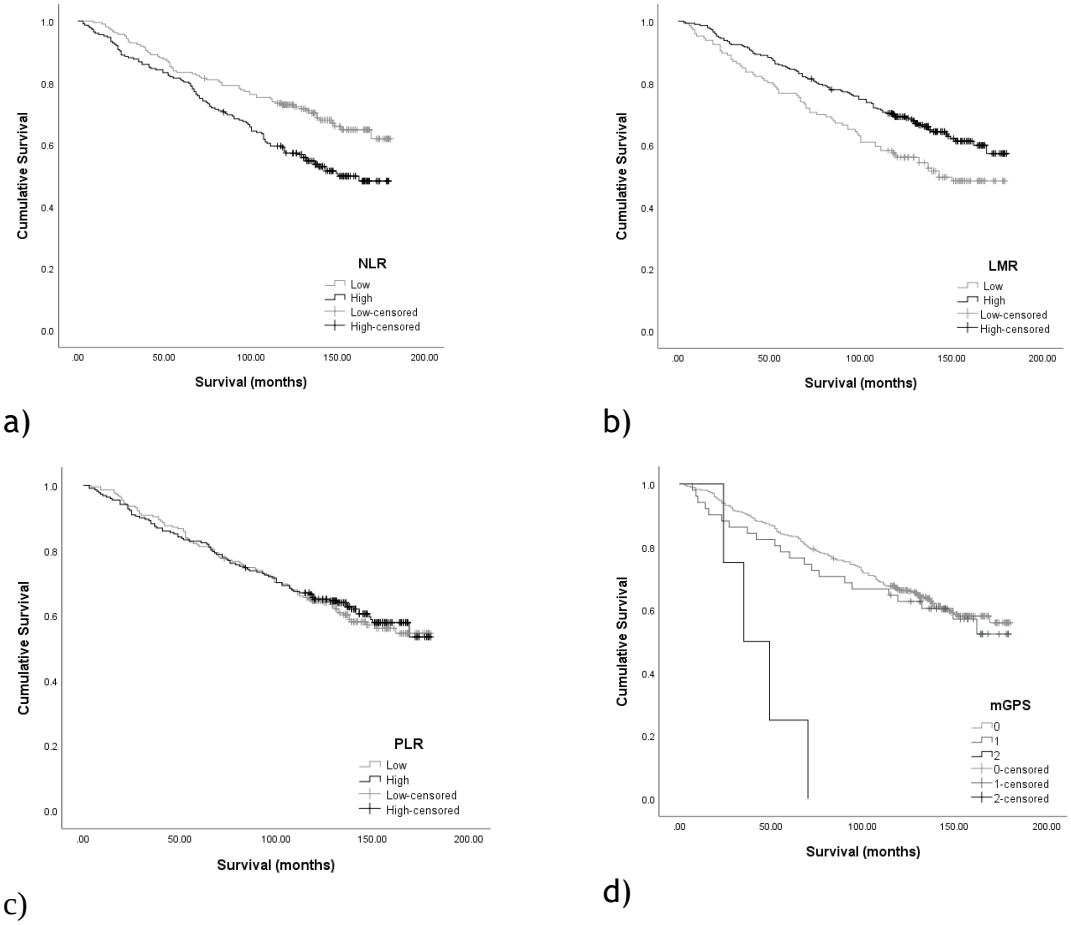

Figure 3-19. Association between ratios/scores of markers of the systemic inflammatory response and OS. Kaplan Meier graphs illustrating the relationship between overall survival anda) NLR (p=0.001), b) LMR (p=0.008), c) PLR (p=0.772) and d) mGPS (p<0.001).

Associations between scores/ratios and survival in ER positive and ER negative disease

High NLR was significantly associated with worse CSS and OS in ER positive (CSS: HR 1.78, 95% CI 1.02-3.11, p=0.042; OS: HR 1.87, 95% CI 1.32-2.66, p<0.001) but not ER negative disease. Neither LMR nor mGPS were significantly associated with CSS but low LMR and high mGPS were associated with worse OS in both ER positive (LMR high v low: HR 0.70, 95% CI 0.50-0.99, p=0.044; mGPS 2v0: HR 6.95, 95% CI 1.70-28.44, p=0.007) and ER negative disease (LMR high v low: HR 0.54, 95% CI 0.29-1.01, p=0.053; mGPS 2v0: HR 5.39, 95% CI 1.25-23.17, p=0.024). PLR was not significantly associated with CSS or OS in either subgroup (data not shown).

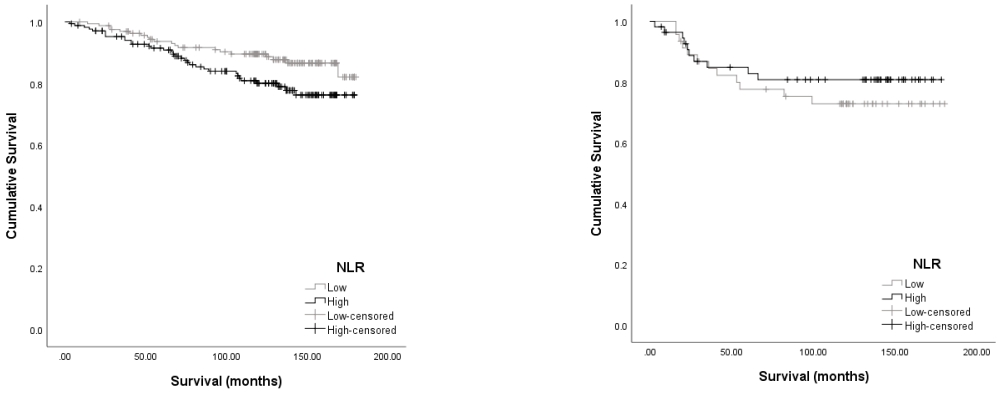

a) b)

Figure 3-20. Association between NLR and CSS by ER status. Kaplan Meier graphs illustrating the association between NLR and CSS in a) ER positive (p=0.040) and b) ER negative disease (p=0.420).

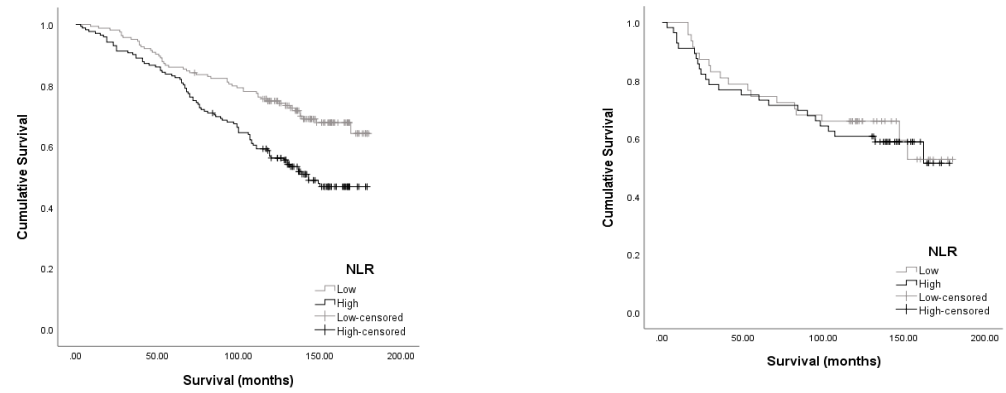

a)

b)

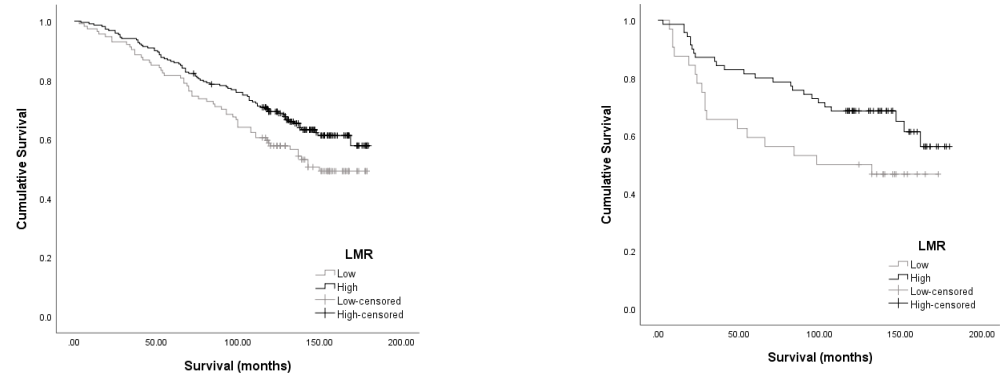

c)

d)

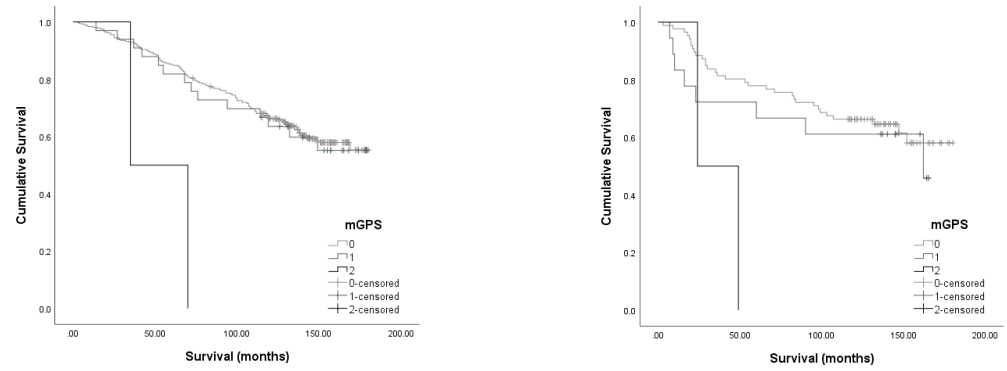

e)

f)

Figure 3-21. Associations between NLR, LMR and mGPS and OS by ER status. Kaplan Meier graphs illustrating the association of NLR, LMR and mGPS with OS in ER positive (a) NLR, p<0.001; c) LMR, p=0.042; e) mGPS, p=0.007) and ER negative disease (b)NLR, p=0.708; d) LMR, p=0.049; f) mGPS, p=0.038).

3.4.3.4 Multivariate analysis

Individual components or ratios/scores significantly associated with either survival outcome on univariate analysis were entered into the multivariate analysis controlling for other known prognostic clinicopathological factors. Ratios/scores with a component in common were not entered into the same analysis. Low albumin was independently associated with worse CSS and OS. mGPS was also independently associated with worse OS but NLR and LMR were not independently associated with CSS or OS.

Clinicopathological factor	CSS		OS		OS		OS		OS	
	HR (95 % CI)	p	HR (95 % CI)	p	HR (95 % CI)	p	HR (95 % CI)	p	HR (95 % CI)	p
Age				**<0.001**		**<0.001**		**<0.001**		**<0.001**
≤50yrs										
51-69yrs			1.30 (0.79-2.15)	0.309	1.26 (0.76-2.08)	0.370	1.37 (0.83-2.26)	0.218	1.40 (0.85-2.32)	0.187
≥70yrs			3.63 (2.25-5.83)	<0.001	3.70 (2.30-5.94)	<0.001	4.35 (2.72-6.95)	<0.001	4.36 (2.73-6.97)	<0.001
Tumour size		**0.035**		**0.015**		**0.015**		0.160		0.166
≤20mm										
21-50mm	2.04 (1.19-3.52)	0.010	1.59 (1.16-2.17)	0.004	1.59 (1.16-2.17)	0.004				
>50mm	1.51 (0.43-5.25)	0.521	1.34 (0.59-3.00	0.484	1.44 (0.64-3.23)	0.374				
Tumour grade		**0.043**		0.187		0.156		**0.049**		0.054
I										
II	1.30 (0.37-4.55	0.679					2.20 (1.09-4.44)	0.028	2.14 (1.06-4.31)	**0.034**
III	2.44 (0.73-8.12)	0.146					2.38 (1.19-4.76)	0.014	2.35 (1.17-4.69)	**0.016**
Nodal involvement		**<0.001**		**<0.001**		**<0.001**		**<0.001**		**<0.001**
0										
1-3	1.78 (0.99-3.20)	0.053	1.43 (1.02-2.02)	0.040	1.43 (1.02-2.02)	0.040	1.47 (1.05-2.06)	0.027	1.47 (1.04-2.06)	0.027
>3	8.25 (4.68-14.54)	<0.001	3.65 (2.43-5.49)	<0.001	3.72 (2.47-5.61)	<0.001	3.42 (2.29-5.09)	<0.001	3.38 (2.27-5.03)	<0.001
LVI		0.556		0.579		0.555		0.746		0.820
Absent										
Present										
Albumin		**<0.001**		**<0.001**		**<0.001**				
>43g/L										
≤43g/L	3.65 (2.21-6.03)		1.84 (1.33-2.54)		1.80 (1.30-2.47)					
mGPS								**0.017**		**0.028**
0										
1							0.95 (0.60-1.49)	0.816	0.89 (0.56-1.41)	0.616
2							4.41 (1.58-12.34)	0.005	3.91 (1.39-11.02)	0.010
NLR				0.054						0.098
≤2.5										
>2.5			1.36 (1.00-1.86)						1.30 (0.95-1.79)	
LMR						0.475		0.606		
≥2.98										
<2.98										

Table 3-16. Multivariate analysis. Multivariate Cox regression survival analysis of individual markers or ratios/scores of markers of the systemic inflammatory response and CSS or OS, controlling for other known prognostic clinicopathological factors. Markers which were significantly associated with survival on univariate analysis were included in the models. Ratios/scores which shared common components were not included in the same model.

3.4.3.5 Associations between NLR and LMR and clinicopathological characteristics

Older age was significantly associated with high NLR and low LMR. There were no other statistically significant associations.

Clinico-pathological characteristic	NLR		p	LMR		p
	Low (≤2.5) n (%)	High (>2.5) n (%)		Low (≤2.98) n (%)	High (>2.98) n(%)	
Age			**0.002**			<0.001
≤50yrs	44 (20.9)	51 (22.4)		25 (17.1)	70 (24.1)	
51-69yrs	111 (52.6)	85 (37.3)		50 (34.2)	144 (49.7)	
≥70yrs	56 (26.5)	92 (40.4)		71 (48.6)	76 (26.2)	
Tumour size			0.573			0.315
≤20mm	111 (52.6)	111 (48.7)		74 (50.7)	147 (50.7)	
21-50mm	96 (45.5)	110 (48.2)		66 (45.2)	138 (47.6)	
>50mm	4 (1.9)	7 (3.1)		6 (4.1)	5 (1.7)	
Tumour grade			0.628			0.386
I	26 (12.3)	22 (9.6)		17 (11.6)	31 (10.7)	
II	76 (36.0)	81 (35.5)		58 (39.7)	98 (33.8)	
III	109 (51.7)	125 (54.8)		71 (48.6)	161 (55.5)	
Nodal involvement			0.464			0.456
0	125 (59.5)	126 (55.5)		83 (56.8)	167 (58.0)	
1-3	64 (30.5)	70 (30.8)		42 (28.8)	91 (31.6)	
>3	21 (10.0)	31 (13.7)		21 (14.4)	30 (10.4)	
ER status			0.572			0.605
Negative	47 (22.3)	56 (24.6)		32 (21.9)	70 (24.1)	
Positive	164 (77.7)	172 (75.4)		114 (78.1)	220 (75.9)	
HER2 status			0.857			0.819
Negative	125 (83.3)	123 (82.6)		75 (82.4)	172 (83.5)	
Positive	25 (16.7)	26 (17.4)		16 (17.6)	34 (16.5)	
LVI			0.294			0.455
Absent	122 (57.8)	143 (62.7)		92 (63.0)	172 (59.3)	
Present	89 (42.2)	85 (37.3)		54 (37.0)	118 (40.7)	
Albumin			0.601			0.223
Low	108 (51.2)	111 (48.7)		79 (54.1)	139 (47.9)	
High	103 (48.8)	117 (51.3)		67 (45.9)	151 (52.1)	
CRP			0.148			0.500
Low	167 (79.1)	167 (73.2)		108 (74.0)	223 (76.9)	
High	44 (20.9)	61 (26.8)		38 (26.0)	67 (23.1)	
Platelets			0.475			0.250
Low	102 (48.3)	118 (51.8)		79 (54.1)	140 (48.3)	
High	109 (51.7	110 (48.2)		67 (45.9)	150 (51.7)	

Table 3-17. Associations between preoperative NLR and LMR and clinicopathological characteristics.

3.5 Discussion

The results of the present systematic review in operable breast cancer showed that the majority of studies examined systemic inflammatory markers in ER positive disease. Of the markers examined, the NLR and albumin were shown to have consistent prognostic value, although the thresholds used were variable. Similarly, the pilot study showed a prognostic role for albumin, NLR and LMR in the cohort of primary operable breast cancer with mature follow up. Therefore, it would appear that the presence of a systemic inflammatory response has prognostic value in patients with primary operable breast cancer.

The marker studied most extensively, NLR, consistently showed prognostic value regardless of threshold used. This finding is in agreement with a large meta-analysis of 100 studies of the NLR in all cancer types, (152) and a meta-analysis of the NLR in all stages of breast cancer(153). The pilot study in the FJ cohort showed an association between NLR and both CSS and OS in ER positive but not ER negative disease. Most studies in the meta-analysis were dominated by ER positive disease. No clinical or pathological characteristic was consistently shown across studies to be associated with raised NLR. The present pilot study reported an association with older age.

The NLR is a ratio made up of the absolute neutrophil count divided by the absolute lymphocyte count. It is not clear whether it is the neutrophil or lymphocyte component of this ratio which is the most significant in terms of its prognostic role though the fact that the PLR, which also involves the lymphocyte count, showed a weaker prognostic effect in this context suggests that it may be the neutrophil count which has the greatest role to play in primary operable breast cancer with a majority of ER positive disease. This is supported by the fact that the present study reported an association between neutrophils and OS in ER positive disease. Previous work in various cancers has shown elevated neutrophils to significantly predict worse outcomes(154-156)whereas the value of low lymphocytes appears to be less clear(157, 158). Mechanisms by which neutrophils promote tumour progression include the remodelling of the extracellular matrix aiding tumour cell migration and angiogenesis, the release of cytokines, chemokines and reactive oxygen species, and the suppression of T cells (119, 159, 160). On the other hand, lymphocytes fulfil a cytotoxic, tumour-

suppressing role (161, 162). The combination of the two in a ratio is felt to result in a magnified and more stable prognostic factor than a single blood cell count. The dNLR was initially described by Proctor el al for use when only the white cell and neutrophil counts were available, such as in chemotherapeutic trial databases(163). This has been less extensively studied but again showed prognostic value on meta-analysis, though less marked than the NLR.

Albumin was consistently associated with prognosis across all studies, although this was most frequently with overall survival rather than cancer-specific outcomes in the literature. In the pilot study it was associate with both OS and CSS in ER positive and ER negative disease. Low albumin has been shown to be a prognostic factor for worse survival in a number of cancers (164). Several mechanisms to explain this have been proposed. These include its role as an antioxidant and as a transporter of common carcinogens (165). Studies have previously demonstrated inhibition of growth of the oestrogen responsive human breast cancer cell line MCF-7 by albumin (166, 167).

NLR/dNLR, PLR and albumin are all markers of the systemic inflammatory response. It was interesting that the other marker of systemic inflammatory response which has consistently shown prognostic value in other cancers(168-172), CRP, did not have a significant prognostic effect in either the meta-analysis or pilot study. Studies show variable results regarding the significance of CRP in primary operable breast cancer and there is certainly no consensus regarding a threshold. The study most suggestive of its prognostic value uses hsCRP (with a threshold of 3.24mg/L) which may not be routinely available in all institutions. As early as 1977, Coombes et al reported that CRP was commonly abnormal in metastatic breast cancer, but rare in localised disease(173), and this may explain the lack of prognostic effect seen in this review of primary operable breast disease. Similarly, whilst investigating potential markers of response to endocrine therapy in breast cancer, Williams et al reported a 13% rate of elevated CRP in stage 3 breast cancer, which rose to 53% in stage four cancer, further supporting this point(174). Interestingly, there were no studies which met our criteria which investigated mGPS, a combined score of CRP and albumin which has been widely validated as a prognostic marker in several cancers. Studies have shown CRP(175) and mGPS(176) to be prognostic in

metastatic breast cancer but evidence in this present review of early-stage breast cancer is limited. Proctor et al(177) did demonstrate an association between mGPS and CSS in a cohort of 1853 breast cancer patients (within a larger study of all cancer types) but this was an unselected cohort with limited availability of staging data. The present study did provide evidence for an association between high mGPS and OS, and a score of 2 does appear to convey greater prognostic power than low albumin alone.

Both the use of NLR and albumin, as described in the studies in this review, have potential limitations in clinical practice. The studies which investigated albumin used thresholds which ranged 35-43g/L, which are within the normal range, and therefore of questionable clinical utility. This was also the case in the pilot study, where ROC curve analysis identified the median value, 43g/L, as the most suitable threshold despite this being in the normal range and meaning that nearly half of the patients would fall into the low albumin category. The use of ROC curves and then, if no suitable threshold was found, carrying out analysis in tertiles before resorting to using the median was done with the aim of avoiding the situation of having half of the patients in either group. Resorting to using the median, having not identified a threshold using the prior two methods, tends to suggest that the factor being analysed is not prognostic anyway, but in the case of albumin it is unfortunate from a clinical utility point of view that the ROC curve identified the median as the most prognostic threshold.

There was variability in the threshold found to be significant in the studies which investigated NLR. Lower values were often used in Asian studies when compared to Western ones and this may reflect population differences in levels of inflammation. Previous studies have demonstrated ethnic variability in levels of inflammation(178-180). Therefore, no consensus has been reached regarding a threshold which could be recommended to stratify prognosis in clinical settings globally. In this meta-analysis there was no relationship seen between NLR threshold used and hazard ratio obtained. NLR is a ratio and therefore has limitations in clinical practice in that it is possible to have a neutrophil count and a lymphocyte count both within the normal range, and still have an elevated NLR, particularly when a lower threshold is used. It could therefore be argued

that a combined score, which increases with each abnormal value, would be more consistently clinically relevant than a ratio.

Some studies carried out sub-analysis for different disease stages. Wen et al(125) found that an elevated monocyte count was an independent significant prognostic factor in stage II-III disease but not stage I. Similarly, Koh et al(137) found that elevated NLR was a significant prognostic factor in stage III and IV disease but not stage II. It may be that in very early-stage breast cancer the inflammatory response is less marked making systemic markers of inflammation less important to prognosis in these early stages. Alternatively, given the better outcome (fewer events) in primary operable breast cancer, it may be that the studies to date have been relatively under powered.

Breast cancer is a heterogeneous disease and the different histological types and molecular subtypes behave differently in terms of progression and response to treatment(181, 182). Despite this, the majority of studies have investigated the prognostic role of inflammatory markers in cohorts of all operable breast cancer. This means, inevitably, that most studies are reported on cohorts with a majority of ER positive disease. Limited studies did carry out sub-analysis for different subtypes. Subgroup analysis for molecular subtypes in NLR studies was conflicting. The findings of several studies support the finding of our pilot study that NLR is associated with prognosis in luminal/ER positive disease(124, 134, 139, 143). The reasons for it to be prognostic in ER positive but not ER negative disease are not clear. One theory could be that ER positive tumours tend to be less inflammatory in general than ER negative tumours and therefore, when inflammation does exist, it is a particularly poor prognostic sign. Alternatively, it may just be that in the case of this small pilot study, the ER negative cohort was underpowered to detect a difference. This theory is supported by the fact that some studies have reported NLR to be prognostic in ER negative subtypes(128, 139-142). Studies which carried out subtype analysis for PLR also reported varying results(124, 129, 140, 147). Therefore, as only limited studies have investigated these markers within different subtypes, there is insufficient data to draw conclusions on this point and further work in this area is certainly warranted.

The studies included in the review and meta-analysis are a heterogeneous group. Many of them are retrospective studies, with the inherent problems of missing data, loss to follow up and potential confounding factors that may result. These issues are shared by the present pilot study. Some studies excluded patients with systemic inflammatory conditions as potential confounders while others did not. A few studies selected patients with a certain type of adjuvant or neoadjuvant therapy whereas most are not selected in terms of treatment. Study size varies greatly between smaller local cohorts of a few hundred patients to large population studies in the thousands. The latter may have the advantage of greater statistical power but may not have as detailed and complete data regarding tumour and patient characteristics and treatment.

Therefore, a pilot studied was conducted on patients from within the host centre, which has the advantage of assessing whether the findings of the meta-analysis are present in the host population but shares the issues of retrospective studies and limited patient numbers. Consistent with the results of the meta-analysis, an association between survival and both NLR and albumin was observed, as well as LMR.

In conclusion, current evidence suggests a potential role for preoperative serum inflammatory markers, which are readily available, in delineating prognosis in primary operable breast cancer, particularly as regards NLR, PLR, LMR and albumin. However, their precise role in clinical practice remains unclear. Further work is warranted to ascertain reproducible thresholds and to ascertain in which subtypes they may be of most value. Large prospective studies would be required to achieve this aim. As currently there is no consensus on thresholds for clinical use, and given the timelines that would be required for a large prospective study, the following chapters of this thesis will instead move on to investigate the role of the local inflammatory response in primary operable breast cancer.

4 The role of the local inflammatory infiltrate in primary operable breast cancer

4.1 Introduction

The findings of the previous chapter suggested a possible prognostic role for markers of the systemic inflammatory response in primary operable breast cancer, although it was acknowledged that there are difficulties in identifying a suitable threshold for clinical use and this was accompanied by the observation that systemic inflammation is not a predominant feature of early-stage breast cancer. Therefore, in primary operable breast cancer, the question arises as to whether the local inflammatory response to the tumour may play a more important role in terms of prognosis or therapeutic targets.

It is now well recognised that the tumour microenvironment has a significant role in the progression of cancer, of which immune cells are a significant component. Increasing evidence supports a role for certain inflammatory cells in suppressing tumour growth, for instance through direct cytotoxicity, while for others they may promote tumour growth through secretion of various cytokines, chemokines and pro-angiogenic factors(63).

The Klintrup-Makinen scoring system was reported in 2005 as a method to classify the inflammatory reaction to a tumour(183). It is a four-point system using H&E-stained tissue which incorporates the overall inflammatory reaction at the invasive margin of the tumour. Using this score, high grade inflammation at the invasive margin has been consistently reported to be associated with improved survival in colorectal cancer(183, 184). However, its role in breast cancer is at present unknown.

Other methods, including IHC, allow assessment of specific inflammatory cell types in and around the tumour, such as CD4+ helper T lymphocytes and CD8+ cytotoxic T lymphocytes. Different subsets of tumour-infiltrating lymphocytes (TILs) have shown varying prognostic roles in different cancers(64, 185-187). In breast cancer, evidence to date suggests that TILs are associated with favourable prognosis in HER2 positive and triple negative breast cancers, as well as improved response to neoadjuvant therapies(188). However, some studies

have reported an association between certain subtypes of CD4+ T lymphocytes and poorer prognosis in breast cancer(64, 189).

The aim of this study was to evaluate the prognostic role of the local inflammatory infiltrate, assessed by the KM score, in primary operable breast cancer, with the hypothesis that a higher KM score would be associated with improved prognosis. A secondary aim was to assess the relationship of KM score to specific TIL subsets.

4.2 Materials and methods

4.2.1 Patient cohort

For this study, both the 1800 and FJ cohorts were used, with characteristics as described in chapter 2. Both cohorts were used for Klintrup-Makinen scoring and analysis, but only the 1800 cohort was used for further analysis related to lymphocyte subsets as TMAs were only available for this cohort.

4.2.2 Slide staining and scanning

4.2.2.1 Klintrup-Makinen score

A single full section slide was cut from surplus tissue blocks, stained with H&E and scanned into Slidepath software as described in chapter 2.

4.2.2.2 Inflammatory cell markers

TMAs for the 1800 cohort were stained in triplicate using the immunohistochemistry technique described in chapter 2. Antibodies for CD4 and CD8 were used as markers of helper T and cytotoxic T lymphocytes respectively, and the slides were scanned into Slidepath software, as detailed in chapter 2.

4.2.3 Scoring

Each slide was scored for Klintrup-Makinen score and each core was scored for CD4 and CD8 positive lymphocytes using the methods described in chapter 2.

4.2.4 Molecular subtyping

Ki67 scoring was available for the 1800 cohort but not for the FJ cohort. For this reason, in this combined cohort, full molecular subtyping could not be carried out. Instead, surrogate receptor subtypes were used for analysis, namely ER+/HER2-, ER+/HER2+, ER-/HER2+ and ER-/HER2- subgroups.

4.2.5 Statistical analysis

Analysis of associations with clinicopathological characteristics and with cancer specific survival was carried out as described in chapter 2. This analysis was carried out initially in the full cohort, then in the ER positive and ER negative cohorts separately, and subsequently in the 4 individual receptor subtypes.

4.3 Results

4.3.1 Patient cohort

1195 patients who underwent surgery for primary operable breast cancer and who had a full section H&E-stained slide suitable for assessing Klintrup-Makinen grade were in included in the study. 1191 patients had full survival data available. Median follow up was 158 months (28-183) during which time there were 234 cancer deaths.

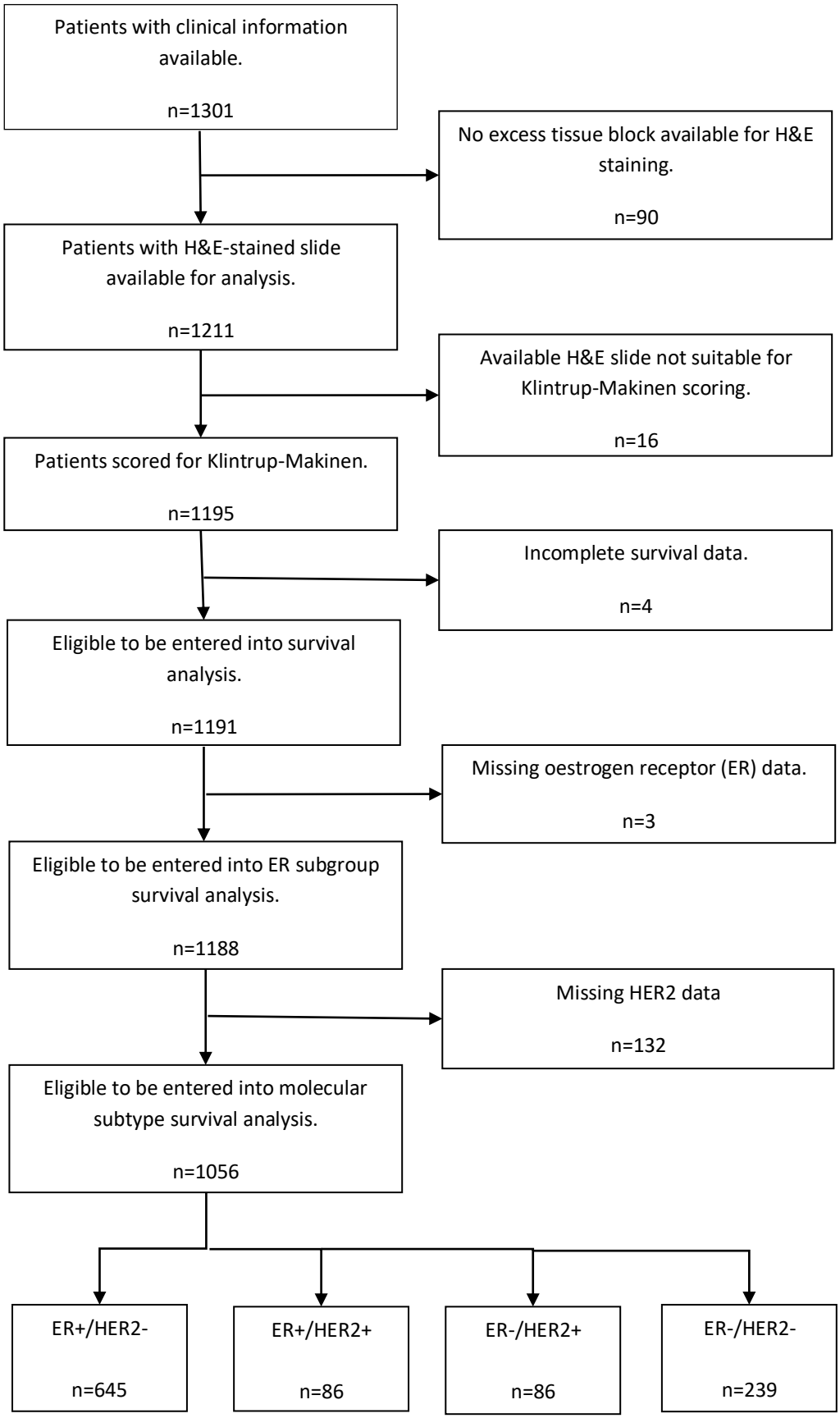

Figure 4-1. Formation of the cohort. Flow diagram showing exclusions from the original cohort and numbers included in the final analysis.

4.3.2 Klintrup-Makinen score

Examples of the 4 different Klintrup-Makinen scores are shown below in **Figure 4-2**. 298 (24.9%) tumours had KM score 0, 589 (49.3%) had KM 1, 238 (19.9%) had KM 2 and 70 (5.9%) had KM 3. The distributions are shown in **Figure 4-3**.

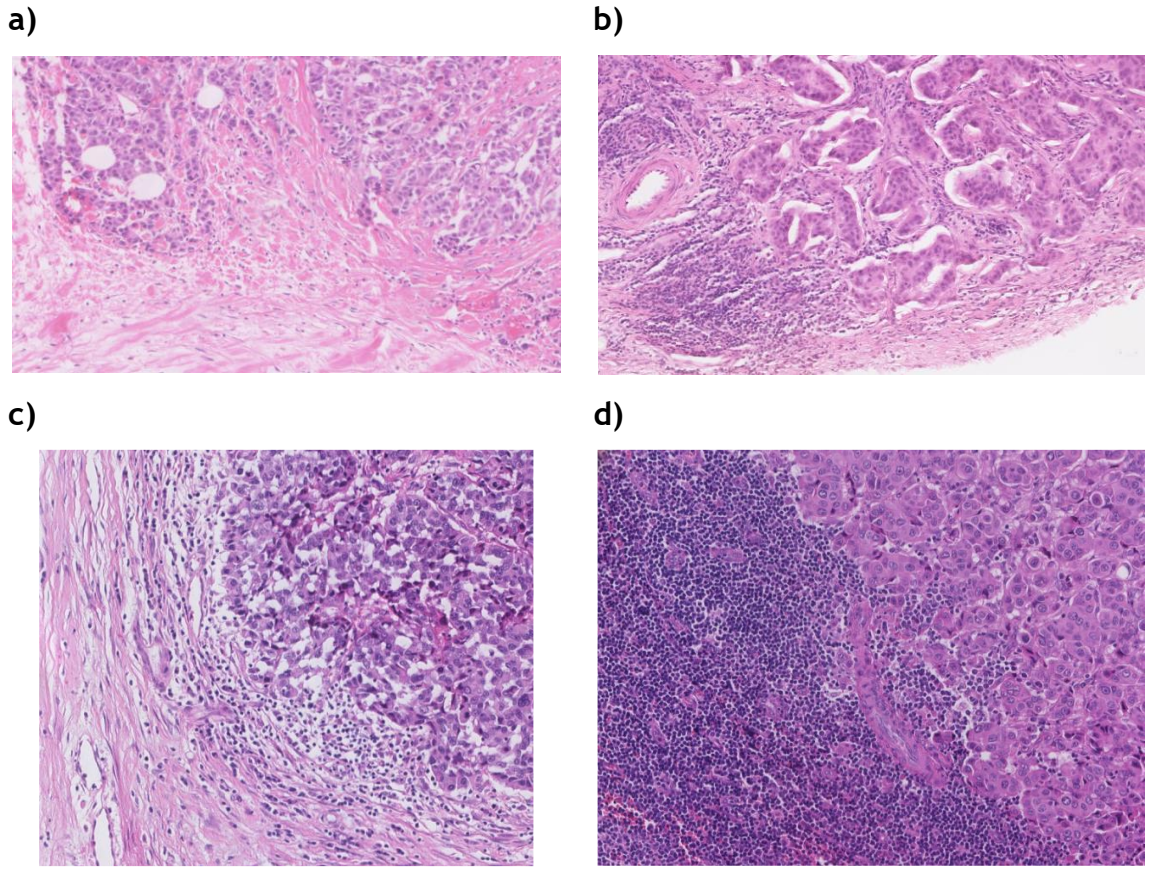

Figure 4-2. Klintrup-Makinen score. Images of breast tumour tissue, stained with H&E, at 20x magnification illustrating examples of a) KM 0 – no inflammatory infiltrate at the invasive tumour edge, b) KM 1 – patchy inflammatory infiltrate at the invasive tumour edge, c) KM 2 – a continuous layer of inflammatory cells at the invasive tumour edge, and d) KM3 – a 'cup' of inflammatory infiltrate at the invasive tumour edge.

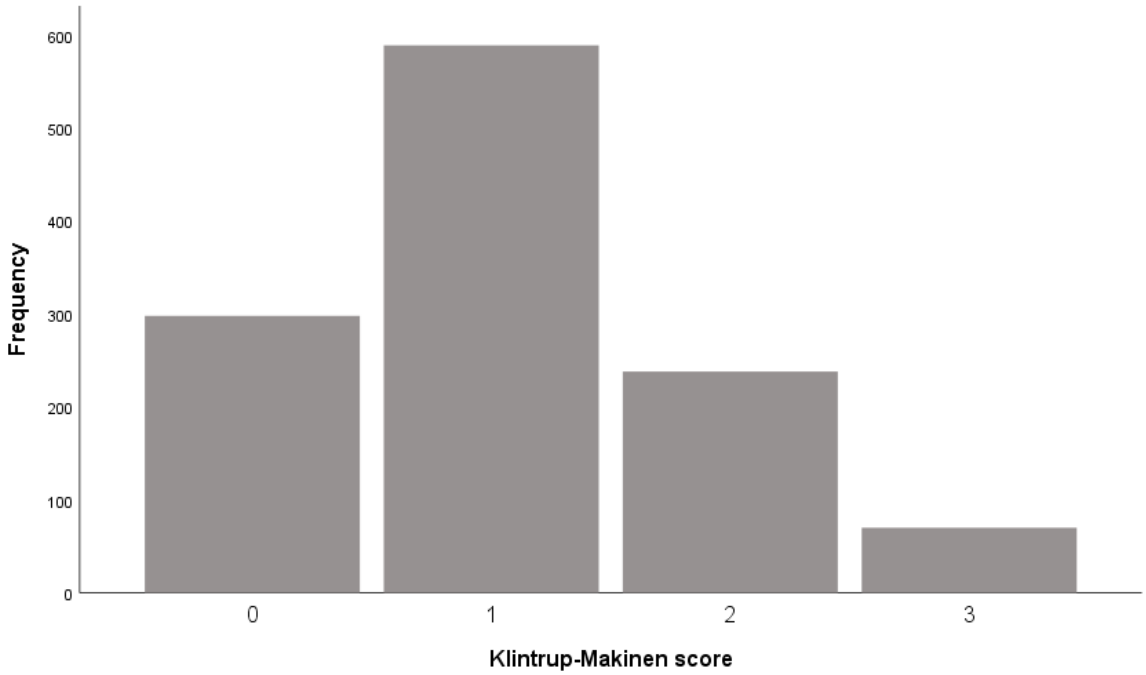

Figure 4-3. Distribution of KM scores. Bar chart illustrating the distribution of Klintrup-Makinen scores within the cohort.

4.3.3 Association between KM score and CSS

In the full cohort, KM score was significantly associated with CSS (p=0.003). However, this association was not straightforward in that patients with both the lowest and highest KM scores had the best CSS while those with a score of 2 had the worst CSS (score 1 v 0: HR 1.46, 95% CI 1.02-2.07, p=0.037; score 2 v 0: HR 1.98, 95% CI 1.34-2.92, p=0.001; score 3 v 0: HR 0.92, 95% CI 0.46-1.83, p=0.807).

When subgroup analysis was carried out, overall KM score was not significantly associated with CSS in ER positive (p=0.116) or ER negative disease (p=0.082). However, in ER positive disease a score of 2 was significantly associated with worse CCS than a score of 0 (score 1 v 0: HR 1.17, 95% CI 0.80-1.72, p=0.409; score 2 v 0: HR 1.70, 95% CI 1.04-2.78, p=0.035; score 3 v 0: HR 0.68, 95% CI 0.24-1.90, p=0.464) but in ER negative disease, whilst there was a trend to scores of 1 and 2 having a worse prognosis, this did not reach statistical significance (score 1 v 0: HR 6.68, 95% CI 0.92-48.52, p=0.060; score 2 v 0: HR 6.92, 95% CI 0.95-50.46, p=0.056; score 3 v 0: HR 3.77, 95% CI 0.45-31.32, p=0.219)(**Figure 4-4**).

a)

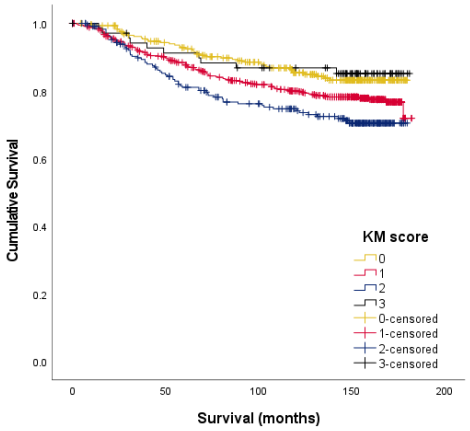

b)

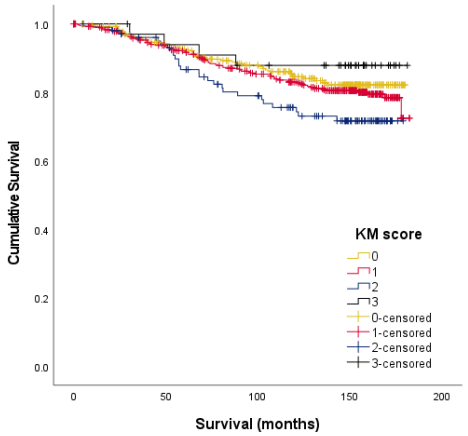

c)

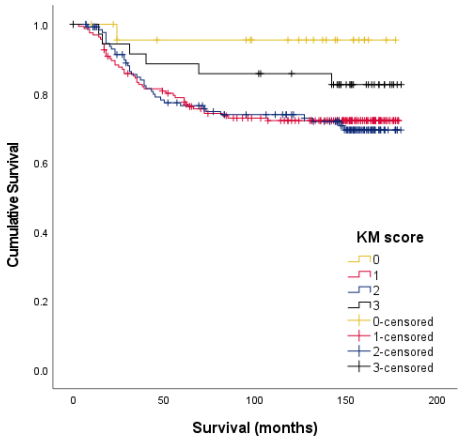

Figure 4-4. KM score and CSS. Kaplan Meier graphs to illustrate the relationship between Klintrup-Makinen score and cancer specific survival in a) the full cohort, (n=1191, **p=0.003**), b) ER positive disease (n=830, p=0.116), c) ER negative disease (n=358, p=0.082).

Overall, KM score was not significantly associated with CSS in any of the 4 receptor subtypes (**Figure 4-5**). Although the pattern of the Kaplan Meier curves suggested the possibility of some variability in terms of which KM scores confer a more favourable prognosis in different subtypes, none of these relationships were statistically significant in ER+/HER2- (score 1 v 0: HR 1.24, 95% CI 0.79-1.95, p=0.342; score 2 v 0: HR 1.62, 95% CI 0.90-2.91, p=0.108; score 3 v 0: HR 0.63, 95% CI 0.19-2.06, p=0.442), ER+/HER2+ (score 1 v 0: HR 0.70, 95% CI 0.27-1.82, p=0.466; score 2 v 0: HR 0.97, 95% CI 0.34-2.80, p=0.954; score 3 v 0: HR 0.47, 95% CI 0.06-3.78, p=0.480), ER-/HER2+ (score 1 v 0: HR 0.44, 95% CI 0.06-3.43, p=0.431; score 2 v 0: HR 0.35, 95% CI 0.05-2.79, p=0.324; score 3 v 0: HR 0.12, 95% CI 0.01-1.91, p=0.132) and ER-/HER2- disease (HRs and 95% CIs incalculable, score 1 v 0: p=0.88; score 2 v 0: p=0.878; score 3 v 0: p=0.885)(**Figure 4-5**).

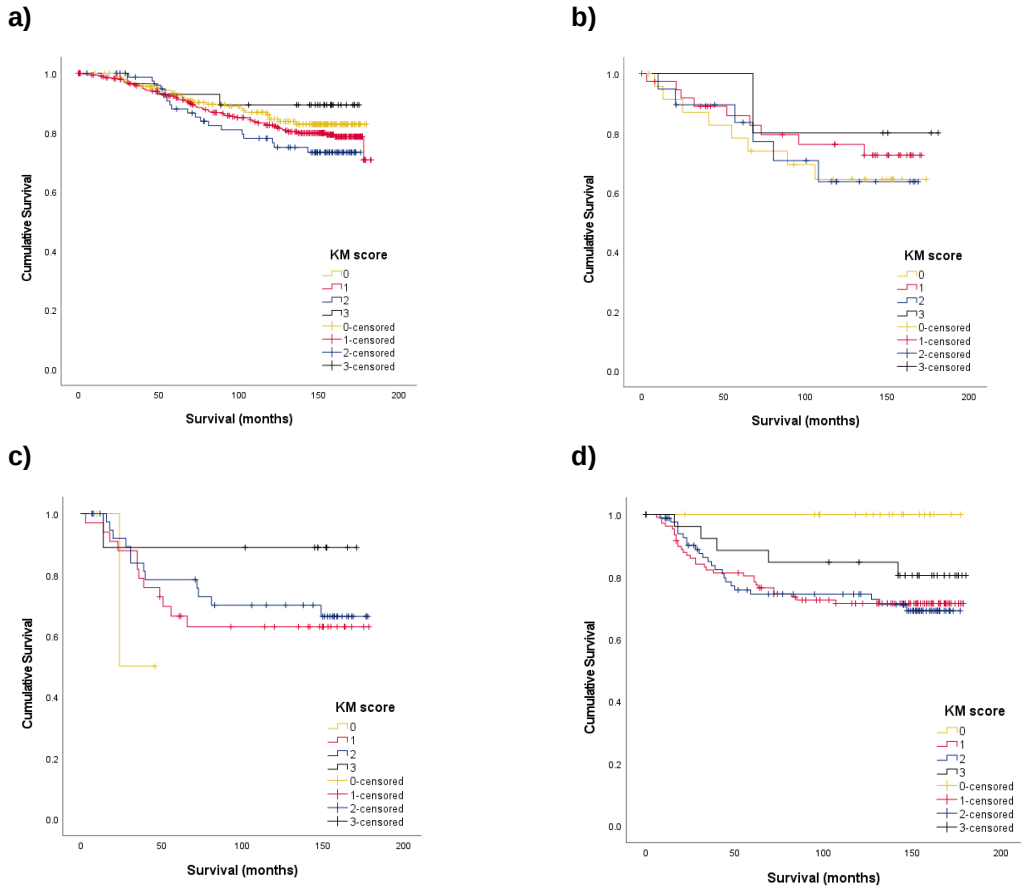

Figure 4-5. KM score and CSS by receptor subtype. Kaplan Meier graphs to illustrate the relationship between Klintrup-Makinen score and cancer specific survival in each of the molecular subtypes. a) ER+/HER2- (n=645, p=0.257), b) ER+/HER2+ (n=86, p=0.799), c) ER-/HER2+ (n=86, p=0.405), d) ER-/HER2- (n=239, p=0.068).

On multivariate analysis controlling for known prognostic clinicopathological factors, KM score was not independently associated with cancer specific survival in the whole cohort (**Table 4-1**).

	Univariate analysis		Multivariate analysis	
	HR (95% CI)	**p**	**HR (95% CI)**	**p**
Tumour size		**<0.001**		**<0.001**
≤20mm	1 (ref)		1 (ref)	
21-49mm	2.31 (1.76-3.05)	**<0.001**	1.54 (1.14-2.06)	**0.004**
≥50mm	4.99 (3.03-8.21)	**<0.001**	3.43 (2.02-5.82)	**<0.001**
Tumour grade		**<0.001**		**<0.001**
I	1 (ref)		1 (ref)	
II	1.84 (1.09-3.10)	**0.023**	1.73 (0.97-3.06)	0.063
III	3.46 (2.09-5.72)	**<0.001**	2.97 (1.68-5.24)	**<0.001**
Nodal status		**<0.001**		**<0.001**
Negative	1 (ref)		1 (ref)	
Positive	3.60 (2.73-4.74)		2.95 (2.20-3.94)	
ER status		**0.003**		0.528
Negative	1 (ref)			
Positive	0.67 (0.51-0.87)			
HER2		**0.001**		0.181
Negative	1 (ref)			
Positive	1.68 (1.23-2.31)			
Klintrup-Makinen		**0.003**		0.112
0	1 (ref)		1 (ref)	
1	1.46 (1.02-2.07)	**0.037**	1.38 (0.94-2.01)	0.097
2	1.98 (1.34-2.92)	**0.001**	1.21 (0.79-1.84)	0.386
3	0.92 (0.46-1.83)	0.807	0.70 (0.34-1.44)	0.334

Table 4-1. Multivariate survival analysis. Table showing KM score and other clinicopathological factors entered into the multivariate analysis for association with cancer specific survival. Significant p values are highlighted in bold.

4.3.4 Association of KM score with clinicopathological characteristics

Higher KM score was associated with younger age, higher tumour grade, ER negativity and HER2 positivity. Tumours with a KM score of 1 or 2 were more likely to be of ductal type, have larger tumours and have nodal involvement compared to those with KM 0 or 3 (**Table 4-2**).

	Klintrup-Makinen score				p
	0 n (%) 298 (24.9%)	1 n (%) 589 (49.3%)	2 n (%) 238 (19.9%)	3 n (%) 70 (5.9%)	
Age					**<0.001**
<50 years	61 (20.5)	145 (24.6)	84 (35.3)	27 (38.6)	
≥50 years	237 (79.5)	444 (75.4)	154 (64.7)	43 (61.4)	
Tumour type					**<0.001**
Ductal	232 (77.9)	571 (96.9)	225 (94.5)	62 (88.6)	
Lobular	44 (14.8)	10 (1.7)	6 (2.5)	0 (0)	
Other	22 (7.4)	8 (1.4)	7 (2.9)	8 (11.4)	
Tumour size					**<0.001**
≤20mm	189 (63.4)	332 (56.5)	92 (38.7)	42 (60.0)	
21-49mm	99 (33.2)	239 (40.6)	134 (56.3)	27 (38.6)	
≥50mm	10 (3.4)	17 (2.9)	12 (5.0)	1 (1.4)	
Tumour grade					**<0.001**
I	64 (21.5)	114 (19.5)	12 (5.0)	1 (1.4)	
II	162 (54.4)	256 (43.7)	65 (27.3)	15 (21.4)	
III	72 (24.2)	216 (36.9)	161 (67.6)	54 (77.1)	
Nodal status					**0.002**
Negative	189 (65.2)	333 (57.2)	117 (49.6)	45 (65.2)	
Positive	101 (34.8)	249 (42.8)	119 (50.4)	24 (34.8)	
ER status					**<0.001**
Negative	25 (8.4)	163 (27.8)	135 (56.7)	36 (51.4)	
Positive	273 (91.6)	423 (72.2)	103 (43.3)	34 (48.6)	
HER2					**<0.001**
Negative	212 (88.7)	454 (86.5)	165 (73.3)	56 (80.0)	
Positive	27 (11.3)	71 (13.5)	60 (26.7)	14 (20.0)	

Table 4-2. Associations between KM score and clinicopathological characteristics. Table describing the associations between Klintrup-Makinen score and important clinicopathological characteristics in primary operable breast cancer.

4.3.5 Associations between KM score and individual TIL subtypes

Frequency of both CD4+ and CD8+ TIL subtypes increased with increasing KM score (**Table 4-3**).

	Klintrup-Makinen score				p
	0	1	2	3	
CD4+					**<0.001**
Low	56 (51.9)	131 (38.3)	27 (15.7)	8 (15.4)	
Medium	30 (27.8)	130 (38.0)	57 (33.1)	12 (23.1)	
High	22 (20.4)	81 (23.7)	88 (51.2)	32 (61.5)	
CD8+					**<0.001**
Low	12 (50.0)	91 (38.7)	17 (19.3)	4 (20.0)	
Medium	11 (45.8)	83 (35.3)	21 (23.9)	2 (10.0)	
High	1 (4.2)	61 (26.0)	50 (56.8)	14 (70.0)	

Table 4-3. Associations between KM score and individual TIL subtypes. Table detailing the associations between KM score and both CD4+ and CD8+ TIL subtypes.

4.3.6 Associations between individual TIL subtypes and CSS

When the inflammatory cell subtypes were analysed individually, low CD8+ lymphocyte infiltrate was associated with worse CSS (medium v low: HR 0.78, 95% CI 0.48-1.26, p=0.307; high v low: 0.33, 95% CI 0.18-0.61, p<0.001). There was no significant association observed between CD4+ lymphocytes and CSS.

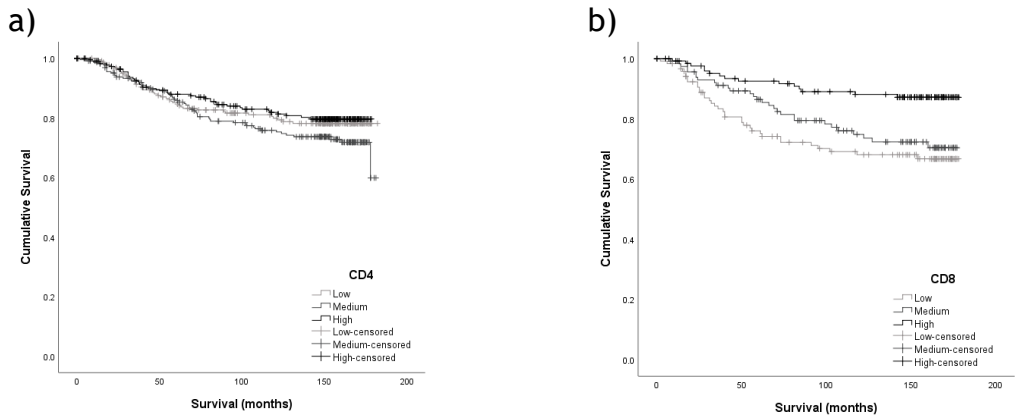

Figure 4-6. Association between TIL subtypes and CSS. Kaplan Meier graphs to illustrate the relationship between CSS and a) CD4+ lymphocytes (n=695, p=0.213) and b) CD8+ lymphocytes (n=371, **p=0.001**).

The individual TIL subtypes were then analysed within each KM score. As might be expected, no individual cell type was significantly associated with CCS in patients with KM0. In patients with KM1 (p=0.025) or KM3 (p=0.039), only high CD8+ T lymphocytes were significantly associated with improved CSS. However, in patients with KM2, CD4+ lymphocytes and CD8+ lymphocytes were both significantly associated with CSS. Within this group, medium levels of CD4+ lymphocytes (overall p=0.021; medium v low: HR 1.88, 95% CI 0.80-4.37, p=0.145; high v low: HR 0.80, 95% CI 0.33-1.91, p=0.612) and lower CD8+ lymphocytes (medium v low: HR 0.84, 95% CI 0.31-2.26, p=0.731; high v low: HR 0.30, 95% CI 0.11-0.83, p=0.021) were associated with worse CSS (**Figure 4-7**).

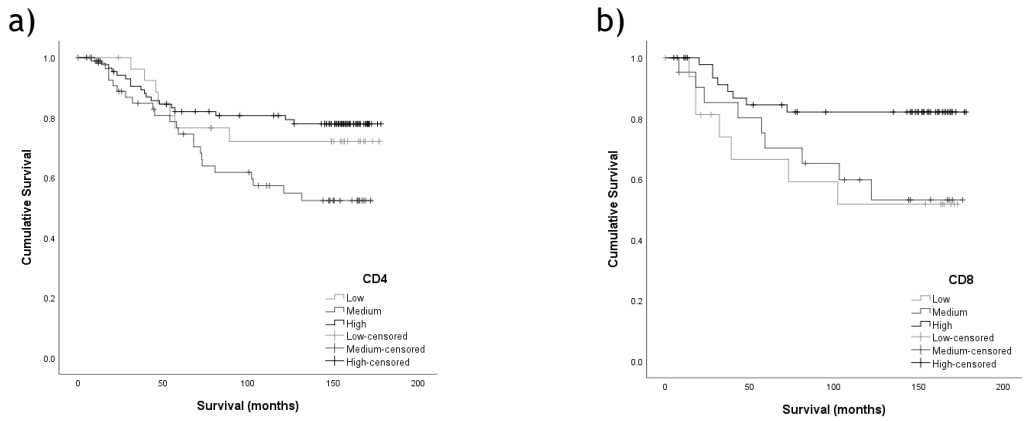

Figure 4-7. The relationship between TIL subtypes and CSS in KM2 patients. Kaplan meier graphs to illustrate the relationship with CSS of a) CD4+ TILs (n=172, p=**0.017**) and b) CD8+ TILs (n=88 p=**0.026**) in patients with a KM score of 2.

4.4 Discussion

In this study it was observed that inflammatory infiltrate at the invasive tumour edge, as measured using the Klintrup Makinen grade, is associated with CSS in primary operable breast cancer, though this was not independent of other known prognostic factors. This association is not straight-forward in that patients with the highest and lowest KM scores have better CSS than those with intermediate scores. These intermediate scores (KM1 and 2) were associated with larger tumours and nodal involvement. Higher KM score was associated with higher numbers of each of the individual TIL subtypes in this study (CD4+ and CD8+ T lymphocytes). Low CD8+ TILs were associated with worse CSS.

There is very little in the published literature regarding the use of the Klintrup Makinen scoring system for assessment of local inflammatory infiltrate in breast cancer. One smaller study (n=461) reported no significant association between KM score and CSS (p=0.069) but the authors divided patients into 2 groups for analysis, weak (0-1) versus strong (2-3) and therefore the more complex relationship with CSS observed in this study would have been hidden with good and poor prognostic groups combined together and cancelling each other out(78). The KM score has been much more widely studied in other cancer types, particularly colorectal cancer, in which it was first described(183). A number of studies have reported improved survival outcomes in colorectal cancer with higher KM score. A recent meta-analysis reported improved DFS, OS and CSS with higher KM score in colorectal cancer(184) A small study reported improved survival in patients with oesophageal cancer with higher KM score on univariate analysis but this did not reach significance on multivariate analysis (p=0.055)(190). No association was seen in a small study of KM in bladder cancer(191).

It is not clear why worse outcomes in intermediate KM groups is observed in this breast cancer study, rather than the positive correlation with outcome seen in colorectal cancer. It may be that it is due to the individual inflammatory cell types that make up the inflammatory infiltrate as the KM does not distinguish between them. However, in this study each of the individual cell types measured using IHC increased with increasing KM score. It may be that the ratios of different cell types change despite them increasing overall in number. There are

also a number of other inflammatory cell types not measured in this study as its focus was on T lymphocytes. It was not possible to reliably calculate ratios in this study as scoring for individual cell types had been carried out at different times by different people. Additionally, it was carried out on TMAs and therefore is more reflective of TIL numbers than inflammatory cells at the invasive tumour edge, which the KM assesses. It would be desirable to carry out multiplex IHC on full section slides to more reliably assess the components of the infiltrate measured by the KM score.

Another measure of the tumour inflammatory infiltrate which has been more extensively covered in the breast cancer literature is measurement of tumour-infiltrating lymphocytes. TILs have been reported to be a favourable prognostic factor in breast cancer(63, 66, 192-194). A 2015 review and meta-analysis reported that total TILs (intraepithelial and stromal) was associated with improved prognosis(66). However, most recent studies report on stromal TILs only(193, 195). This practice is in line with standardised methodology for the assessment of TILs by pathologists proposed initially by an International TILs Working Group in 2014(196) and then updated in 2017 by the renamed International Immuno-Oncology Biomarkers Working Group(197), citing evidence that assessment of intra-tumoural TILs does not add to the prognostic utility of stromal TILs and that the latter is more straightforward and reproducible on H&E-stained slides. This study used total TIL numbers to be consistent with methodology as the CD8+ TILs had been scored this way previously. While most studies have scored stromal TILs throughout the tumour stroma, one study measured total and peripheral sTILs separately and found peripheral sTILs to be associated with survival but not total sTILs(195). This measurement of peripheral sTILs at the invasive tumour edge is probably more reflective of the infiltrate scored by the KM score, so this observed association is interesting in comparison to the KM results in this study. Studies have also reported a predictive role for TILs as higher TILs are associated with higher pCR rates(66, 198-200). Variation in the prognostic and predictive role of TILs depending on molecular subtype has been reported, particularly that they have an association with outcome in triple negative and HER2-enriched subtypes but not in ER positive disease(193, 195, 199).

The advantage of this method of assessing TILs, as well as the KM score, is that they both only require a single H&E-stained full section slide. The disadvantage however is that they do not differentiate between the different lymphocyte subtypes which make up the infiltrate. There is evidence that different lymphocyte subtypes have pro-tumour or anti-tumour actions and it may be that the balance between the actions of these different subtypes partially explains the pattern of survival association seen with our KM data. In our cohort, high CD8+ T lymphocytes were associated with improved CSS. This is in keeping with the findings of numerous other studies(64-66) and is consistent with their cytotoxic action against tumour cells(201). In our study, CD8+ TILs were consistently associated with improved CSS within the different KM scores. Overall, no association between CD4+ T lymphocytes and CSS was observed in this study, though there was an association in patients with a KM score of 2. This is contrary to another study which reported an association with worse cancer outcomes(64). However, it may be due to the more complex roles of CD4+ T lymphocytes with some acting as helper cells, promoting the anti-tumour response, and some acting as Treg cells promoting an immunosuppressive environment in which the tumour can grow(201). This is supported by the complex association with CSS observed in KM2 tumours, mirroring the association of KM with CSS where intermediate numbers are associated with the worst CSS. It should also be noted that CD4 can also be expressed by monocytes and macrophages(202, 203).

In summary, this study has observed a non-independent association between Klintrup Makinen score and CSS, with those patients with intermediate scores having worse outcomes. This is likely to reflect the complex interactions between the tumour and the various inflammatory cells which make up the inflammatory infiltrate. The clinical utility of this score in breast cancer is therefore in doubt, particularly when compared to measurement of TILs which has been much more widely validated as a prognostic and predictive marker in breast cancer studies, particularly in triple negative and HER2-enriched breast cancer, and for which there is standardised methodology. Better understanding of the roles of and interactions between the various immune cells in the tumour microenvironment will be crucial in developing effective breast cancer therapies. This includes progressing our understanding of the more common

subtypes but also further investigating the role of less common subtypes such as FoxP3+ and γδT lymphocytes. Work related to these subtypes is ongoing in our lab.

Although the KM score may have limited clinical utility in breast cancer, the use of a single H&E slide is a considerable advantage for a prognostic score in view of its simplicity and low cost. Therefore, the next chapter of this thesis will go on to investigate other features of the tumour and tumour microenvironment which are assessable on a single H&E slide and which have been reported to have prognostic significance in other cancers.

5 Tumour necrosis, tumour budding and tumour-stroma percentage in primary operable breast cancer

5.1 Introduction

Significant advances in breast cancer diagnosis and treatment over recent decades have been associated with improvements in survival rates from the disease, with breast cancer mortality rates in the UK falling by 22% over the last decade(204). Despite this, breast cancer remains the second highest cause of cancer death in females in the UK, accounting for approximately 31 deaths per day in 2014-2016(204). Consequently, ongoing work is required to identify new prognostic markers and novel therapeutic targets.

Breast cancer is a heterogeneous disease, made up of several different subtypes which are associated with different prognosis and recognised to behave differently (205). There are currently no targeted systemic treatments for triple negative breast cancer. Patients with oestrogen receptor (ER) positive disease receive endocrine therapy, but the more precise benefit of chemotherapy in ER positive patients is yet to be determined. While genomic assays are currently used to aid this decision, their role is under constant refinement and these assays are relatively expensive (115, 116, 206). Therefore, there is a need to establish further prognostic tests, ideally using methods already available in clinical practice.

The tumour microenvironment and its constituent parts, including fibroblasts, tumour-associated stroma and various immune cells, are increasingly recognised to have varied and complex roles in the progression and dissemination of cancer (55, 207). Multiple measures of components of the tumour microenvironment such as tumour necrosis, tumour budding and tumour-stroma percentage (TSP) have shown prognostic value in a number of solid tumours (67-73, 78-80, 208-224). In breast cancer, only one small study has reported an independent association between necrosis and CSS(72) while one historical study found necrosis to be associated with tumour size but was not independently prognostic(73). Three studies have reported an association between high tumour budding and lymph node metastases, lymphovascular invasion and poorer

outcomes(78-80). However, these are small studies with 148, 160 and 474 patients respectively. They each use a different threshold to define high budding, and molecular subtype analysis is limited by the low patient numbers. Similarly, 3 smaller studies have reported an association between high TSP and poorer outcomes in breast cancer, particularly in TNBC(72, 212, 213). The aim of the present study was to validate, in a larger cohort of patients with mature follow up, these previously reported associations with the hypothesis that tumour necrosis, high tumour budding and high TSP would all be associated with poorer CSS but that these associations may vary in the different molecular subtypes and may not be independent of each other. This is with a view to establishing whether these features might have a prognostic role in clinical practice and in which group of patients they could be useful.

5.2 Materials and methods

5.2.1 Patient cohort

For this study, both the 1800 and the FJ cohorts were used, with characteristics as described in chapter 2.

5.2.2 Full section slide staining and scanning

A single full section per patient was cut from surplus tissue blocks, H&E stained and scanned into Slidepath software as described in chapter 2.

5.2.3 Scoring for tumour necrosis, tumour budding and TSP

Each slide was scored for tumour necrosis, tumour budding and TSP as described in chapter 2.

5.2.4 Molecular subtyping

Ki67 scoring was available for the 1800 cohort but not for the FJ cohort. For this reason, in this combined cohort, analysis could not be carried out within the formal molecular subtypes. Subtype analysis was instead carried out in ER+/HER2-, ER+/HER2+, ER-/HER+ and ER-/HER2- subgroups.

5.2.5 Statistical analysis

Analysis of associations with clinicopathological characteristics and with cancer specific survival was carried out as described in chapter 2. This analysis was carried out initially in the full cohort, then in the ER positive and ER negative cohorts separately, and subsequently in the 4 ER/HER2 receptor subtypes. Finally, all of this analysis was repeated in the ductal cancers only, as different pathological subtypes are known to behave differently and ductal cancers are the most common pathological subtype. This ductal analysis is included in the appendices.

5.3 Results

5.3.1 Patient cohort

1188 patients who underwent surgery for primary operable breast cancer and had a score for all three markers were included in the study. 1084 (91.2%) patients had ductal tumours, 498 (41.9%) had grade 3 tumours and 490 (41.2%) had axillary lymph node involvement. 649 (54.6%) cancers were pathological Tumour stage 1 (pT1), 498 (41.9%) were pT2 and 40 (3.4%) were pT3. 826 (69.5%) tumours were ER positive, 173 (14.6%) were HER2 positive and HER2 status was unavailable for 131 patients. Median follow up was 158 months (26-183). Over this time 234 breast cancer deaths were recorded.

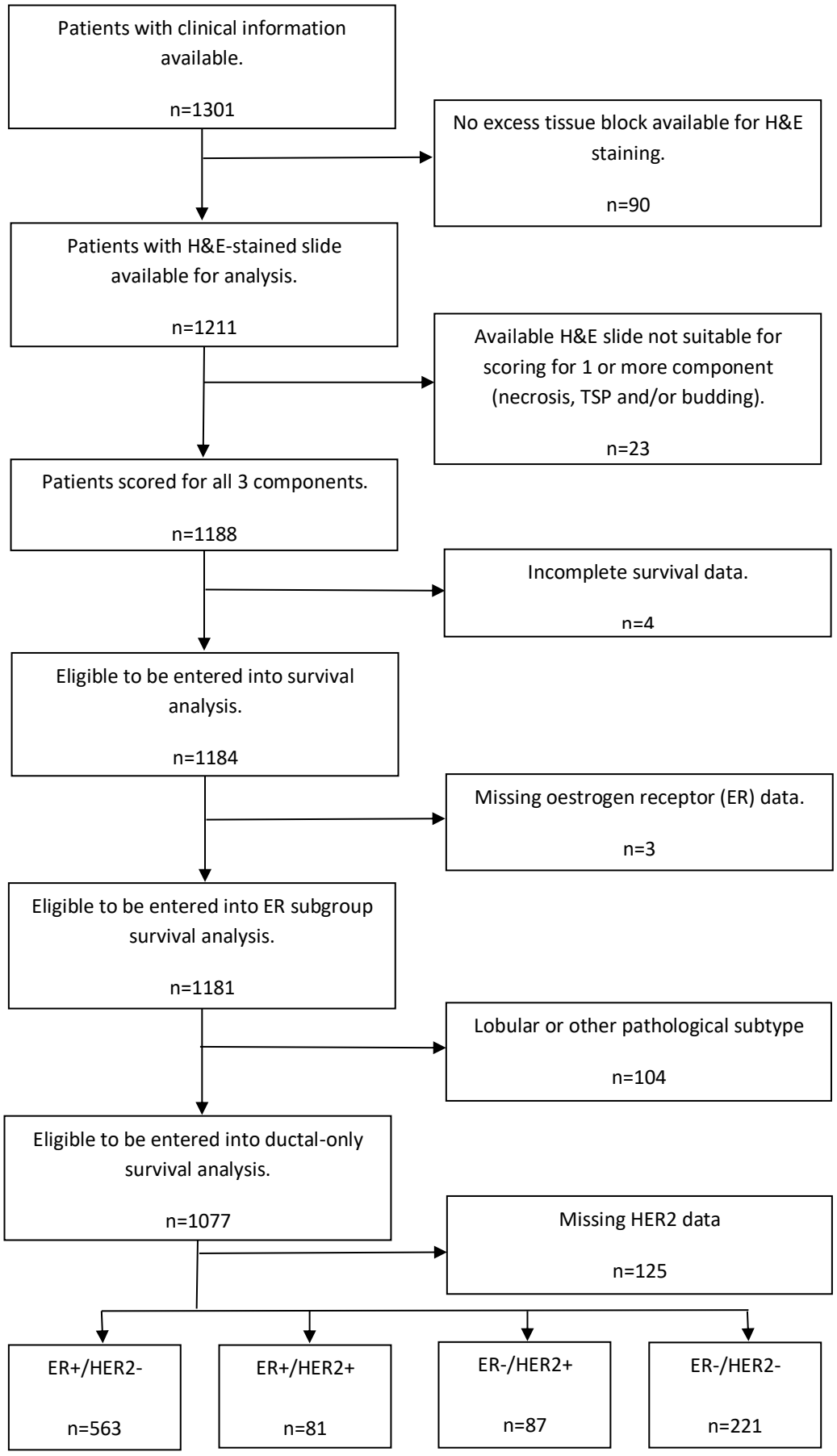

Figure 5-1. Formation of the cohort. Flow diagram showing exclusions from the original cohort and numbers included in the final analysis, by receptor subtype.

5.3.2 Tumour necrosis

700 (58.9%) patients had no or low (<25%) necrosis and 488 (41.1%) patients had high necrosis (>25%).

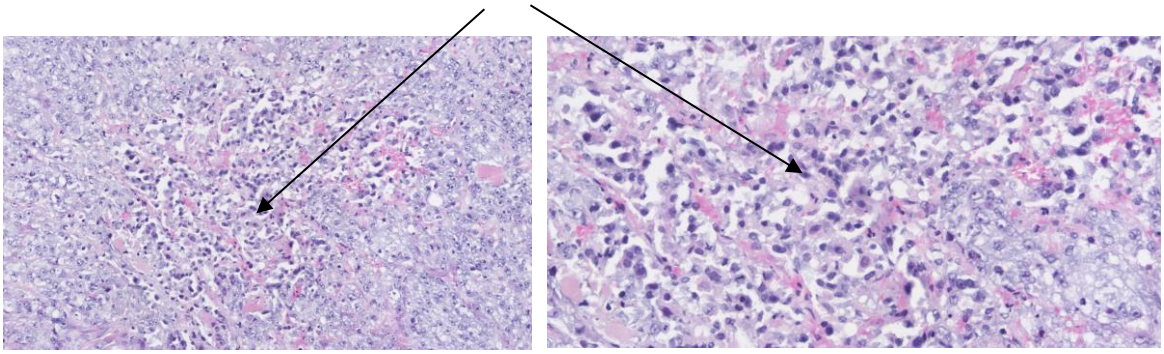

Figure 5-2. Examples of tumour necrosis. Area of necrosis arrowed. Images of breast tumour tissue stained with H&E at 20x and 40x magnification.

5.3.2.1 Associations with cancer specific survival

In the full cohort, high necrosis was associated with worse CSS (10yr CSS 72% high necrosis v 87% no necrosis, p<0.001; HR 2.26, 95%CI 1.74-2.94, p<0.001). High necrosis was associated with worse CSS in both ER positive (10yr CSS 73% high necrosis v 87% no necrosis, p<0.001; HR 2.03, 95% CI 1.46-2.82, p<0.001) and ER negative disease (10yr CSS 70% v 87%, p<0.001; HR 2.77, 95%CI 1.54-4.98, p=0.001) (**Figure 5-3**).

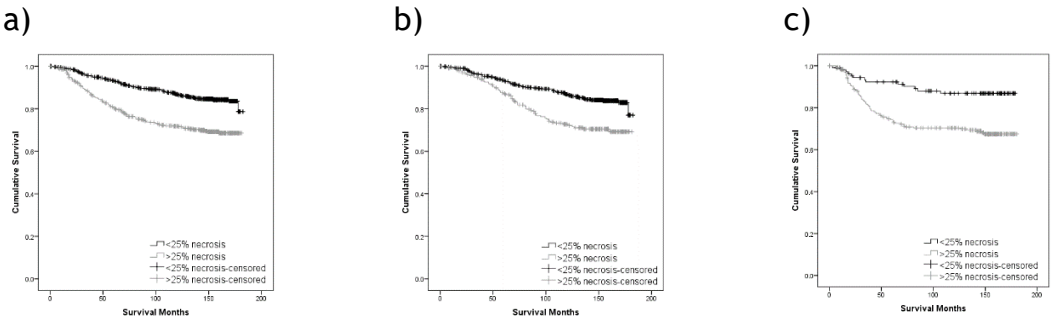

Figure 5-3. The relationship between tumour necrosis and CSS in primary operable breast cancer. Kaplan Meier survival graphs for CSS in patients with high compared to low necrosis in a) the full cohort (n=1184, **p<0.001**), b) ER positive disease (n=823, **p<0.001**), and c) ER negative disease (n=358, **p<0.001**).

In ER+/HER2- disease, high necrosis was associated with worse CSS (10yr CSS 87% v 73%, p<0.001; HR 1.97, 95% CI 1.36-2.86, p<0.001). This was also the case in ER+/HER2+ disease (10yr CSS 76% v 61%, p=0.037; HR 2.24, 95% CI 1.00-5.02, p=0.049) and ER-/HER2- disease (10yr CSS 87% v 71%, p=0.003; HR 2.75, 95% CI

1.35-5.59, p=0.005), but not in ER-/HER2+ cancers (10yr CSS 72% v 67%, p=0.733; HR 1.25, 95% CI 0.43-3.63, p=0.676) (**Figure 5-4**).

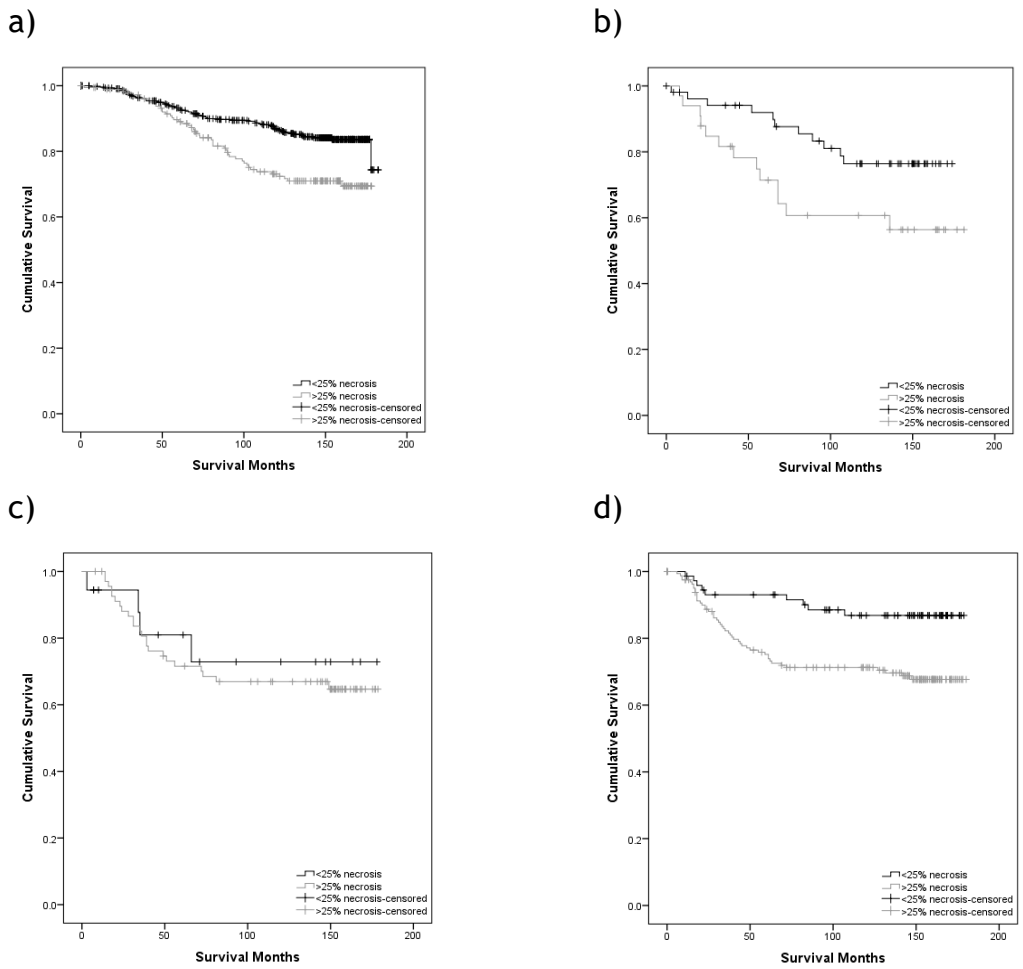

Figure 5-4. The relationship between tumour necrosis and CSS in primary operable breast cancer, by receptor subtype. Kaplan Meier survival graphs for CSS in patients with high compared to low necrosis in a) ER+/HER2- disease (n=643, **p<0.001**), b) ER+/HER2+ disease (n=86, **p=0.043**), c) ER-/HER2+ disease (n=87, p=0.675), and d) ER-/HER2- disease (n=238, **p=0.004**).

5.3.2.2 Associations with clinicopathological characteristics

High tumour necrosis was associated with younger age (p=0.001), ductal subtype (p<0.0001), larger tumour size (p<0.001), higher tumour grade (p<0.001), nodal (p=0.008) and HER2 positivity (p<0.001), ER negativity (p<0.001) and a higher Klintrup Makinen (KM) score (p<0.001) (**Table 5-1**). In smaller cohorts of patients for whom these markers were available, necrosis was associated with high CD4 lymphocytes (n=675, p<0.001) and high CD68 cells (a marker for macrophages, n=369, p<0.001).

	Tumour necrosis		p
	Low (<25%) n=700 (58.9%)	**High (>25%)** n=488 (41.1%)	
Age			**0.001**
<50 years	162 (23.1)	154 (31.6)	
≥50 years	538 (76.9)	334 (68.4)	
Tumour type			**<0.001**
Ductal	610 (87.1)	474 (97.1)	
Lobular	58 (8.3)	2 (0.4)	
Other	32 (4.6)	12 (2.5)	
Invasive tumour size			**<0.001**
≤20mm	437 (62.4)	212 (43.5)	
21-49mm	247 (35.3)	251 (51.5)	
≥50mm	16 (2.3)	24 (4.9)	
Missing data	0	1	
Grade			**<0.001**
I	159 (22.8)	31 (6.4)	
II	339 (48.6)	158 (32.4)	
III	200 (28.7)	298 (61.2)	
Missing data	2	1	
Nodal status			**0.008**
Negative	420 (61.3)	260 (53.6)	
Positive	265 (38.7)	225 (46.4)	
Missing data	15	3	
ER			**<0.001**
Positive	587 (84.0)	239 (49.2)	
Negative	112 (16.0)	247 (50.8)	
Missing data	1	2	
HER2			**<0.001**
Negative	533 (88.2)	351 (77.5)	
Positive	71 (11.8)	102 (22.5)	
Missing data	96	35	
Tumour budding			0.067
≤20 buds	517 (73.9)	383 (78.5)	
>20 buds	183 (26.1)	105 (21.5)	
TSP			0.075
≤50%	477 (68.1)	356 (73.0)	
>50%	223 (31.9)	132 (27.0)	
Klintrup-Makinen			**<0.001**
0	235 (33.9)	58 (11.9)	
1	371 (53.5)	214 (43.9)	
2	72 (10.4)	164 (33.7)	
3	16 (2.3)	51 (10.5)	
Missing data	6	1	

Table 5-1. Associations between tumour necrosis and clinicopathological characteristics. Table detailing the associations between tumour necrosis and other clinicopathological characteristics. ER – oestrogen receptor, TSP – tumour-stroma percentage. Significant p values are highlighted in bold.

5.3.3 Tumour budding

The median highest bud count was 11 (0-45). The distribution of highest bud counts is illustrated below.

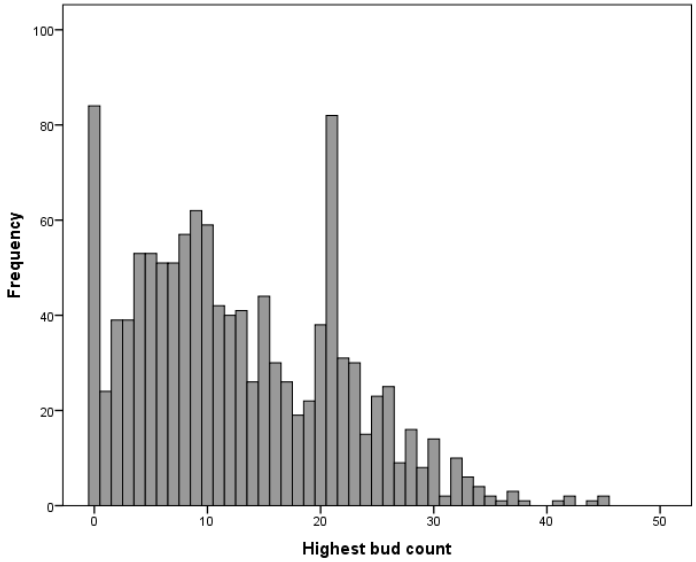

Figure 5-5. Budding count distribution. Histogram showing the distribution of highest bud counts within the whole cohort.

900 (75.9%) tumours had low budding (highest bud count <20) and 288 (24.1%) had high budding. The threshold of 20 buds had been determined as the most prognostic in a previous smaller study(78) but ROC curve analysis supported the use of this threshold in our data also.

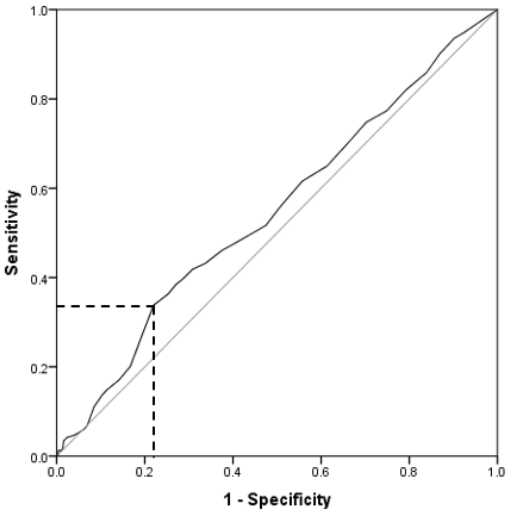

Positive if greater than or equal to	Sensitivity	1-specificity
17.50	0.396	0.285
18.50	0.383	0.269
19.50	**0.362**	**0.252**
20.50	**0.336**	**0.218**
21.50	0.200	0.166
22.50	0.170	0.141

Figure 5-6. ROC curve analysis for highest budding count. ROC curve plotting sensitivity against 1-specificity of highest budding count for the outcome of CSS. Point furthest away from the diagonal line marked with a dotted line. Relevant coordinates highlighted in the table, confirming 20 buds as an appropriate threshold for division of high and low budding groups.

An example of tumour budding is shown in below.

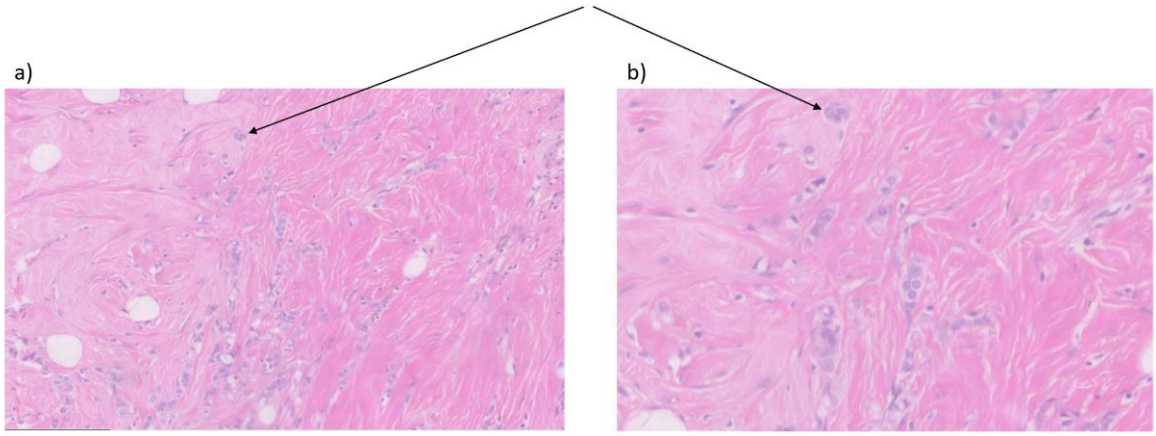

Figure 5-7. Example of tumour budding. Individual tumour bud arrowed. Image of breast cancer tissue stained with H&E at a) 20x magnification and b) 40x magnification.

5.3.3.1 Associations with CSS

In the full cohort, patients with high tumour budding had worse CSS than those with low tumour budding (10yr CSS 72% v 83%, p<0.001; HR 1.69, 95%CI 1.29-2.22, p<0.001). This effect on CSS was negated in the ER positive cohort (10yr CSS 79% high budding v 84% low budding, p=0.143; HR 1.33, 95%CI 0.94-1.89, p=0.102) but potentiated in the ER negative cohort (10yr CSS 49% high budding v 81% low budding, p<0.001; HR 3.05, 95%CI 1.97-4.73, p<0.001) (**Figure 5-8**).

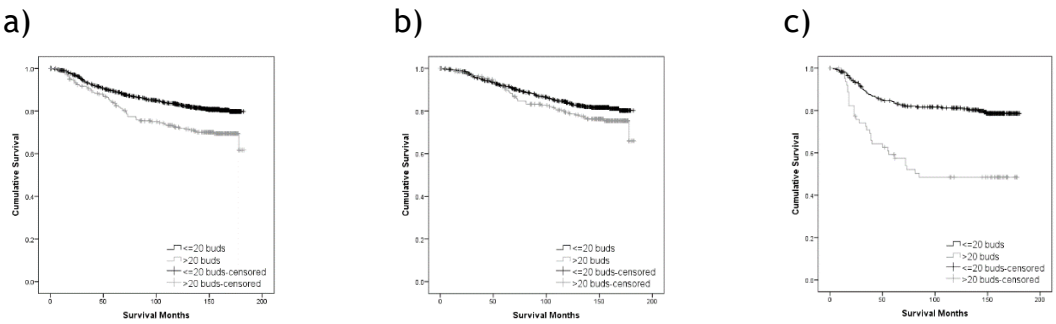

Figure 5-8. The relationship between tumour budding and CSS in primary operable breast cancer. Kaplan Meier survival graphs for CSS in patients with high compared to low tumour budding in a) the full cohort (n=1184, **p<0.001**), b) ER positive disease (n=823, p=0.101), and c) ER negative disease (n=358, **p<0.001**).

High budding was not significantly associated with CSS in either ER+/HER2- (10yr CSS 84% v 82%, p=0.689; HR 1.14, 95% CI 0.77-1.69, p=0.509) or ER+/HER2+ disease (10yr CSS 74% v 61%, p=0.220; HR 1.64, 95% CI 0.72-3.76, p=0.241). High budding was associated with worse CSS in ER-/HER2+ cancers, (10yr CSS 76% v

36%, p=0.003; HR 3.38, 95% CI 1.56-7.32, p=0.002) and in ER-/HER2- cancers (10yr CSS 81% v 55%, p=0.001; HR 2.44, 95% CI 1.41-4.23, p=0.001) (**Figure 5-9**).

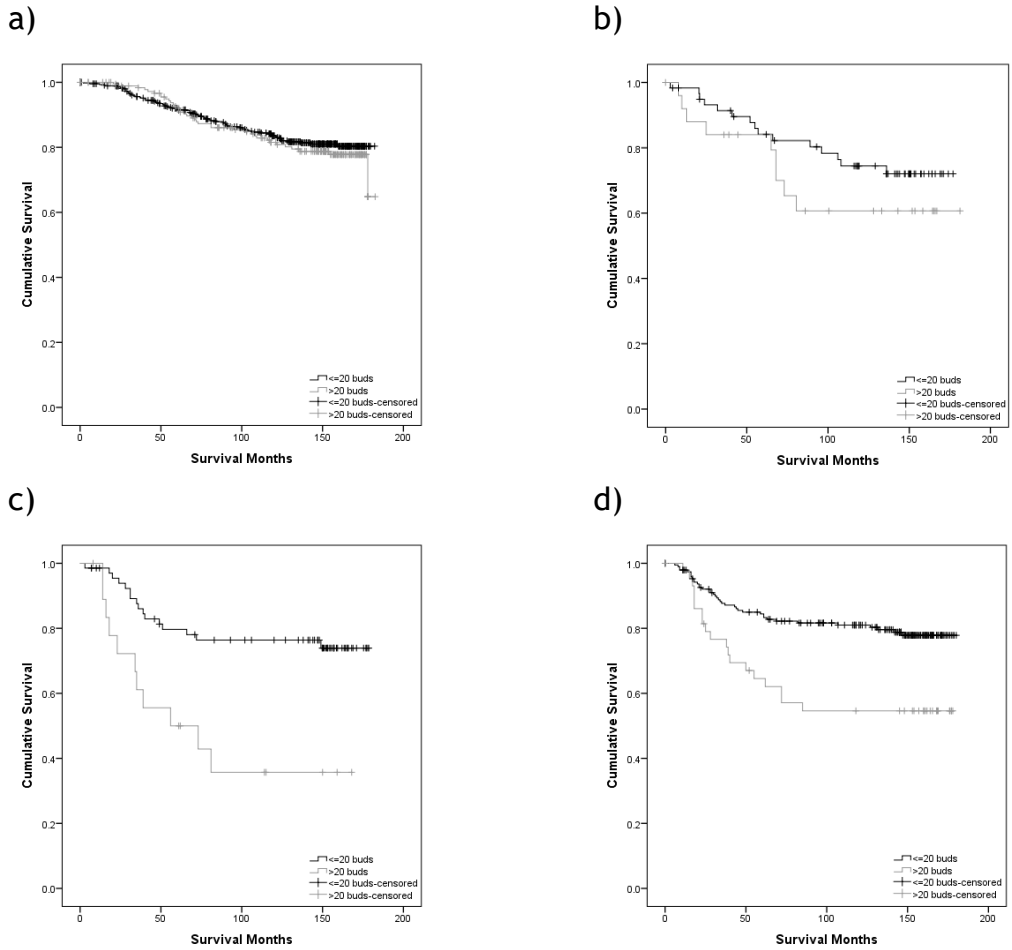

Figure 5-9. The relationship between tumour budding and CSS in primary operable breast cancer, by receptor subtype. Kaplan Meier survival graphs for CSS in patients with high compared to low tumour budding in a) ER+/HER2- disease (n=643, p=0.508), b) ER+/HER2+ disease (n=86, p=0.235), c) ER-/HER2+ disease (n=87, **p=0.001**), and d) ER-/HER2- disease (n=238, **p=0.001**).

5.3.3.2 Associations with clinicopathological characteristics

High tumour budding was associated with lobular subtype (p<0.001), lower tumour grade (p<0.001), nodal (p<0.0001) and ER positivity (p=0.001), high TSP (p<0.001) and lower KM score (p=0.001)(**Table 5-2**). In those patients where the markers were available, high budding was associated with low CD4+ lymphocytes (n=679, p=0.002) and lower CD8+ lymphocytes (n=371, p=0.027).

	Tumour budding		p
	Low (≤20 buds) n=900 (75.9%)	**High (>20 buds)** n=288 (24.1%)	
Age			0.480
<50 years	244 (27.1)	72 (25.0)	
≥50 years	656 (72.9)	216 (75.0)	
Tumour type			**<0.001**
Ductal	831 (92.3)	253 (87.8)	
Lobular	31 (3.4)	29 (10.1)	
Other	38 (4.2)	6 (2.1)	
Invasive tumour size			0.441
≤20mm	492 (54.7)	157 (54.7)	
21-49mm	381 (42.3)	117 (40.8)	
≥50mm	27 (3.0)	13 (4.5)	
Missing data	0	1	
Grade			**<0.001**
I	135 (15.1)	55 (19.1)	
II	343 (38.2)	154 (53.5)	
III	419 (46.7)	79 (27.4)	
Missing data	3	0	
Nodal status			**<0.001**
Negative	541 (61.1)	139 (48.8)	
Positive	344 (38.9)	146 (51.2)	
Missing data	15	3	
ER			**0.001**
Positive	602 (67.1)	224 (77.8)	
Negative	295 (32.9)	64 (22.2)	
Missing data	3	0	
HER2			0.876
Negative	649 (83.5)	235 (83.9)	
Positive	128 (16.5)	45 (16.1)	
Missing data	123	8	
Necrosis			0.067
<25%	517 (57.4)	183 (63.5)	
>25%	383 (42.6)	105 (36.5)	
TSP			**<0.001**
≤50%	665 (73.9)	168 (58.3)	
>50%	235 (26.1)	120 (41.7)	
Klintrup-Makinen			**0.001**
0	228 (25.5)	65 (22.6)	
1	416 (46.5)	169 (58.9)	
2	192 (21.5)	44 (15.3)	
3	58 (6.5)	9 (3.1)	
Missing data	6	1	

Table 5-2. Associations between tumour budding and clinicopathological characteristics. Table detailing the associations between tumour budding and other clinicopathological characteristics.

5.3.4 Tumour-stroma percentage

The median TSP was 40 (0-90). The distribution of TSP across the cohort is illustrated below.

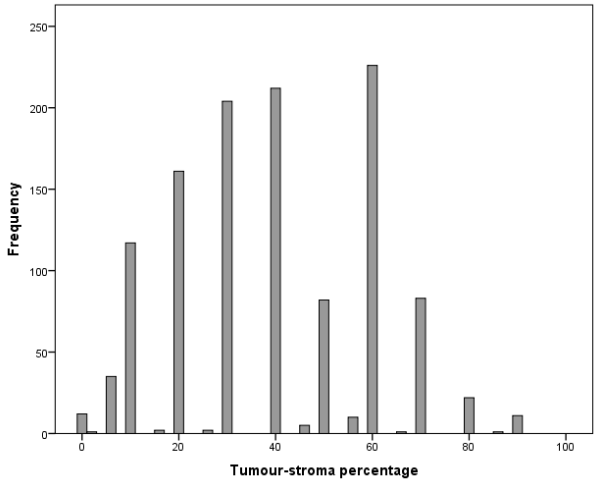

Figure 5-10. TSP distribution. Histogram showing the distribution of TSP within the whole cohort.

Patients were divided into high (>50%) and low (<50%) TSP groups at the 50% threshold as previously described(212, 218). ROC curve analysis supported the use of this threshold in this cohort.

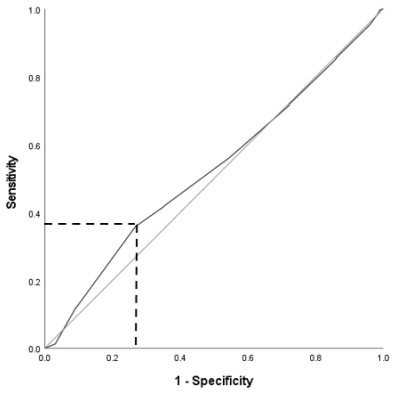

Positive if greater than or equal to	Sensitivity	1-Specificity
35.00	0.562	0.546
42.50	0.421	0.356
47.50	**0.417**	**0.351**
52.50	**0.366**	**0.279**
57.50	0.362	0.270
62.50	0.119	0.093

Figure 5-11. ROC curve for TSP. ROC curve plotting sensitivity against 1-specificity of TSP for the outcome of CSS. Point furthest away from the diagonal line marked with a dotted line. Relevant coordinates highlighted in the table, confirming TSP of 50% as an appropriate threshold for division of high and low TSP groups.

833 (70.1%) tumours had low TSP and 355 (29.9%) had high TSP. Examples of tumours with high and low TSP are shown below.

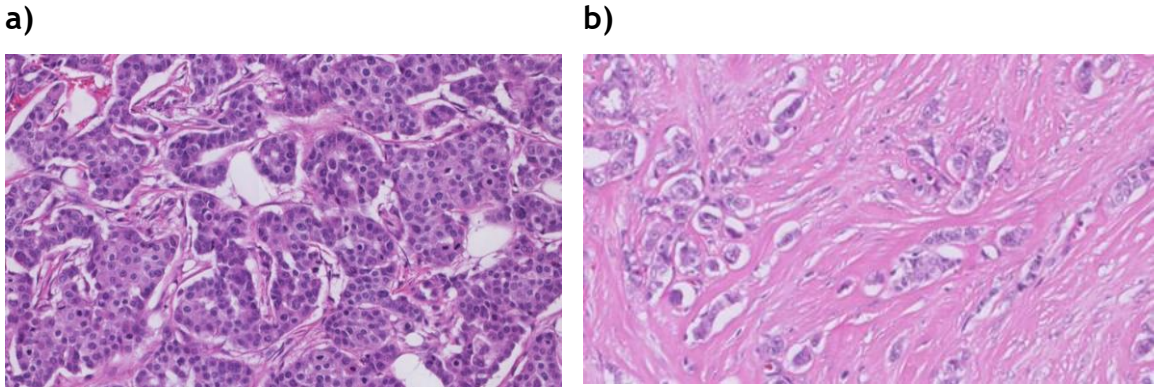

Figure 5-12. Examples of low and high TSP. a) Low TSP, b) high TSP. Images of breast tumour tissue stained with H&E at 20x magnification.

5.3.4.1 Associations with CSS

In the full cohort, patients with high TSP had worse CSS compared to those with low TSP (10yr CSS 77% v 82%, p=0.006; HR 1.42, 95%CI 1.09-1.86, p=0.010). In ER positive disease TSP was not significantly associated with CSS (10yr CSS 81% high TSP v 83% low TSP, p=0.440, HR 1.22, 95%CI 0.87-1.71, p=0.259). In ER negative disease high TSP was associated with worse CSS (10yr CSS 65% v 79%, p=0.005, HR 1.96, 95%CI 1.27-3.01, p=0.002) (**Figure 5-13**).

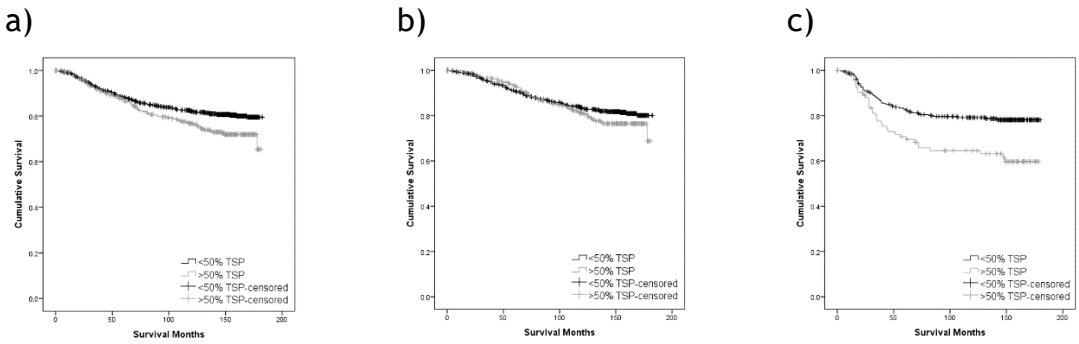

Figure 5-13. The relationship between TSP and CSS in primary operable breast cancer. Kaplan Meier survival graphs for CSS in patients with high compared to low TSP in a) the full cohort (n=1184, **p=0.009**), b) ER positive disease (n=823, p=0.258), and c) ER negative disease (n=358, **p=0.002**).

High TSP was not significantly associated with CSS in ER+/HER2- cancers (10yr CSS 84% v 80%, p=0.216; HR 1.40, 95% CI 0.96-2.06, p=0.083) or ER+/HER2+ cancers (10yr CSS 69% v 75%, p=0.620; HR 0.75, 95% CI 0.28-2.01, p=0.569). High TSP was associated with worse CSS in ER-/HER2+ cancers (10yr CSS 75% v 56%,

p=0.043; HR 2.24, 95% CI 1.05-4.79, p=0.037) and ER-/HER2- cancers (10yr CSS 79% v 65%, p=0.028; HR 1.95, 95% CI 1.13-3.38, p=0.017) (**Figure 5-14**).

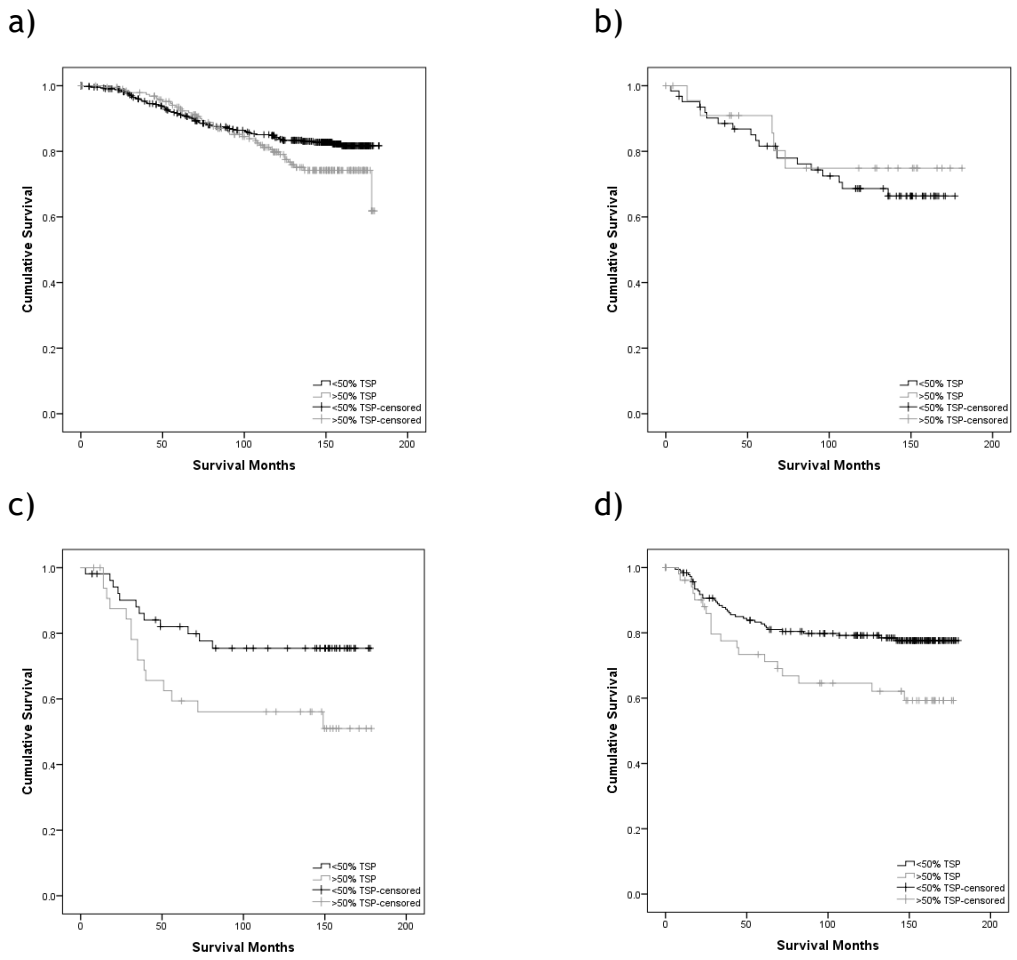

Figure 5-14. The relationship between TSP and CSS in primary operable breast cancer, by receptor subtype. Kaplan Meier survival graphs for CSS in patients with high compared to low TSP in a) ER+/HER2- disease (n=643, p=0.081), b) ER+/HER2+ disease (n=86, p=0.568), c) ER-/HER2+ disease (n=87, **p=0.032**), and d) ER-/HER2- disease (n=238, **p=0.015**).

5.3.4.2 Associations with clinicopathological characteristics

High TSP was associated with nodal positivity (p=0.048) and high budding (p<0.001) but lower tumour grade (p<0.001) and a lower Klintrup-Makinen (KM) score (p<0.001)(**Table 5-3**). In the patients where these markers were available, high budding was associated with low CD4+ lymphocytes (n=679, p=0.022), low CD8+ lymphocytes (n=371, p=0.043) and lower CD68+ cells (n=369, p=0.003).

	Tumour-stroma percentage		p
	Low (≤50%) n=833 (70.1%)	**Low (≤50%)** n=833 (70.1%)	
Age			0.728
<50 years	224 (26.9)	224 (26.9)	
≥50 years	609 (73.1)	609 (73.1)	
Tumour type			0.184
Ductal	752 (90.3)	752 (90.3)	
Lobular	46 (5.5)	46 (5.5)	
Other	35 (4.2)	35 (4.2)	
Invasive tumour size			0.523
≤20mm	446 (53.6)	446 (53.6)	
21-49mm	357 (42.9)	357 (42.9)	
≥50mm	29 (3.5)	29 (3.5)	
Missing data	1	1	
Grade			**<0.001**
I	115 (13.9)	115 (13.9)	
II	338 (40.7)	338 (40.7)	
III	377 (45.4)	377 (45.4)	
Missing data	3	3	
Nodal status			**0.048**
Negative	493 (60.0)	493 (60.0)	
Positive	329 (40.0)	329 (40.0)	
Missing data	11	11	
ER			0.188
Positive	569 (68.6)	569 (68.6)	
Negative	261 (31.4)	261 (31.4)	
Missing data	3	3	
HER2			0.195
Negative	631 (84.6)	631 (84.6)	
Positive	115 (15.4)	115 (15.4)	
Missing data	87	87	
Necrosis			0.075
<25%	477 (57.3)	477 (57.3)	
>25%	356 (42.7)	356 (42.7)	
Tumour budding			**<0.001**
≤20 buds	665 (79.8%)	665 (79.8%)	
>20 buds	168 (20.2%)	168 (20.2%)	
Klintrup-Makinen			**<0.001**
0	186 (22.5)	186 (22.5)	
1	399 (48.2)	399 (48.2)	
2	184 (22.2)	184 (22.2)	
3	59 (7.1)	59 (7.1)	
Missing data	5	5	

Table 5-3. Associations between TSP and clinicopathological characteristics. Table detailing the associations between TSP and other clinicopathological characteristics.

5.3.5 Multivariate survival analysis

Multivariate Cox regression survival analysis was carried out for tumour necrosis, budding and TSP along with other known prognostic factors. In ER positive disease, the only one of the 3 features which was significantly associated with CSS independent of other prognostic factors was tumour necrosis. However, in ER negative disease, all 3 were significantly associated with CSS independent of the other factors (**Table 5-4**).

Factor	ER positive			ER negative		
	n	HR (95% CI)	p	n	HR (95% CI)	p
Tumour size	714		**<0.001**	322		0.155
≤20mm		1 (ref)				
21-49mm		1.70 (1.17-2.48)	**0.006**			
≥50mm		3.51 (1.83-6.78)	**<0.001**			
Tumour grade	714		**0.002**			
I		1 (ref)				
II		1.39 (0.77-2.51)	0.268			
III		2.42 (1.33-4.40)	**0.004**			
Nodal status	714		**<0.001**	322		**<0.001**
Negative		1 (ref)			1 (ref)	
Positive		2.54 (1.76-3.67)			3.19 (1.96-5.22)	
HER2	714		0.246			0.934
Negative						
Positive						
Tumour necrosis	714		**0.033**	322		**0.024**
<25%		1 (ref)			1 (ref)	
>25%		1.46 (1.03-2.08)			2.01 (1.10-3.68)	
Tumour budding	714			322		**0.001**
Low					1 (ref)	
High					2.15 (1.35-3.42)	
TSP	714			322		**0.010**
<50%					1 (ref)	
>50%					1.79 (1.15-2.78)	

Table 5-4. Multivariate survival analysis of necrosis, tumour budding, TSP and other known prognostic pathological factors. Multivariate cox regression survival analysis for prognostic factors ($p \leq 0.05$ on univariate analysis) for CSS in ER positive and ER negative primary operable breast cancer.

5.3.6 A combined score of tumour necrosis and tumour budding

5.3.6.1 Creation of the score

Budding and TSP were combined into a single score (0=both components low, 1=either one component high, 2=both components high). 517 (43.5%) patients had a score of 0, 566 (47.6%) had a score of 1, and 105 (8.8%) had a score of 2.

5.3.6.2 Associations with CSS

In the full cohort, a higher necrosis-budding score was associated with worse CSS (10yr CSS 87% v 80% v 50%, $p<0.001$; score 1 v 0: HR 1.65, 95% CI 1.23-2.23,

p=0.001; score 2 v 0: HR 4.71, 95% CI 3.26-6.79, p<0.001). In ER positive disease, a score of 2 was significantly associated with worse CSS compared to those with a score of 0 (10yr CSS 87% v 82% v 60%, p<0.001; score 1 v 0: HR 1.41, 95% CI 0.99-2.01, p=0.059; score 2 v 0: HR 3.09, 95% CI 1.92-4.96, p<0.001). In ER negative disease, a higher necrosis-budding score was associated with worse CSS (10yr CSS 90% v 78% v 33%, p<0.001; score 1 v 0: HR 2.64, 95% CI 1.26-5.55, p=0.010; Score 2 v 0: HR 10.01, 95% CI 4.52-22.17. p<0.001)(**Figure 5-15**).

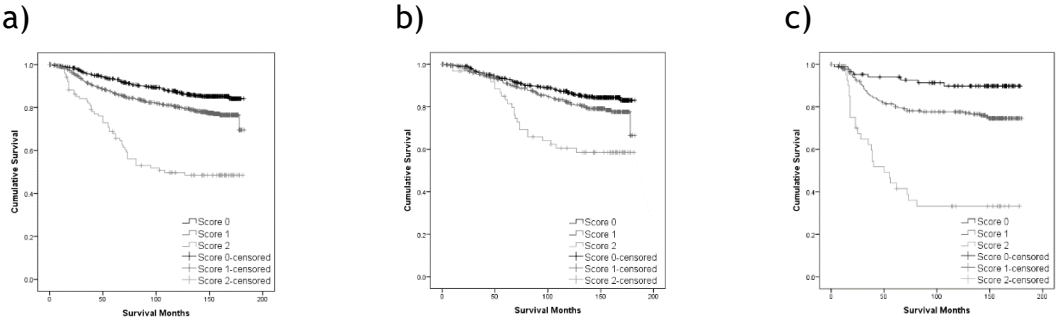

Figure 5-15. The relationship between the necrosis-budding score and CSS in primary operable breast cancer. Kaplan Meier survival graphs for CSS in patients with a necrosis-budding score of 2 compared to 1 compared to 0 in a) the full cohort (n=1184, **p<0.001**), b) ER positive disease (n=823, **p<0.001**), and c) ER negative disease (n=358, **p<0.001**).

In ER+/HER2- cancer, a score of 2 was significantly associated with worse CSS than a score of 0 (10yr CSS 86% v 84% v 61%, p<0.001; score 1 v 0: HR 1.17, 95% CI 0.78-1.76, p=0.448; score 2 v 0: HR 2.82, 95% CI 1.65-4.82, p<0.001). In ER+/HER2+ cancer, a score of 1 was significantly associated with worse CSS than a score of 2 (10yr CSS 80% v 62% v 59%, p=0.048; score 1 v 0: HR 2.77, 95% CI 1.09-7.07, p=0.033; score 2 v 0: HR 2.67, 95% CI 0.85-8.43, p=0.094). In ER-/HER2+ cancers, there was an overall association between high combined necrosis-budding score and worse CSS (10yr CSS 72% v 77% v 26%, p=0.002; score 1 v 0: HR 0.81, 95% CI 0.23-2.81, p=0.735; score 2 v 0: HR 3.60, 95% CI 0.99-13.10, p=0.052). In ER-/HER2- cancers, a higher combined score was associated with worse CSS (10yr CSS 90% v 77% v 38%, p<0.001; score 1 v 0: HR 2.90, 95% CI 1.14-7.36, p=0.025; score 2 v 0: HR 9.15, 95% CI 3.32-25.25, p<0.001).

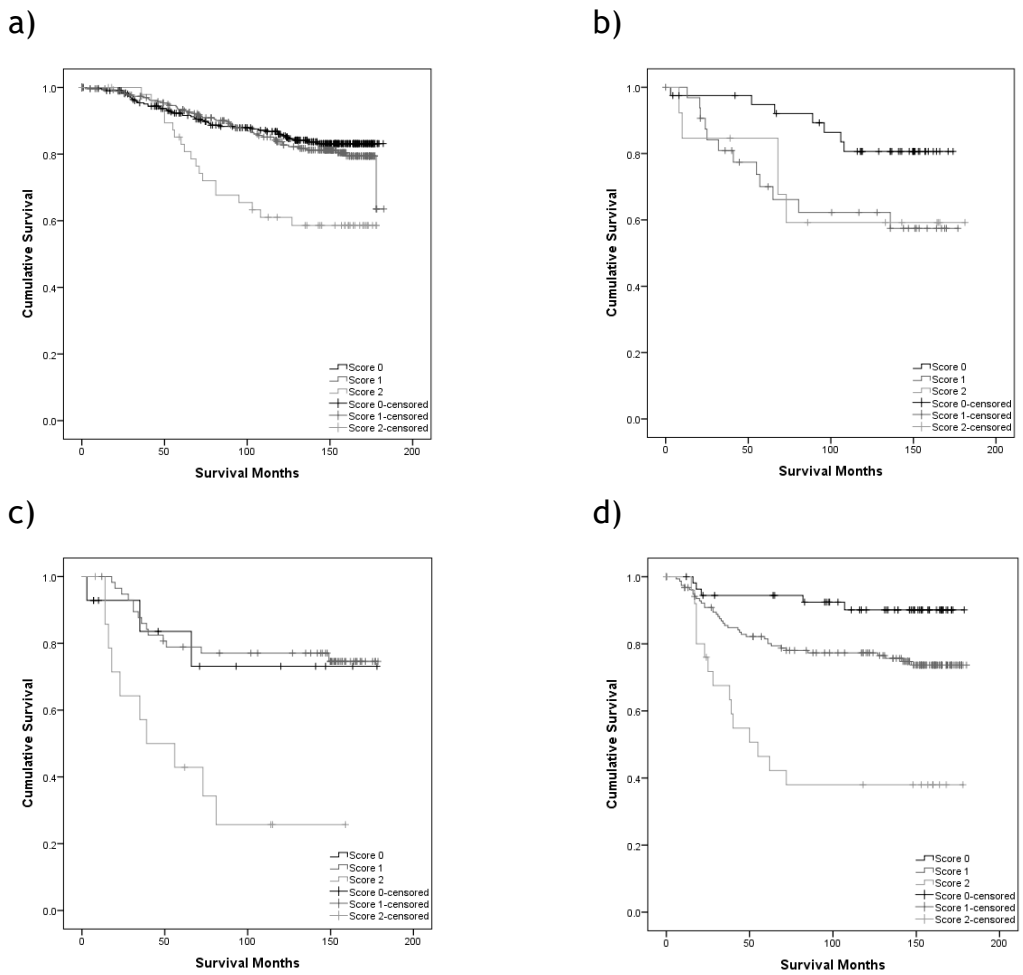

Figure 5-16. The relationship between the necrosis-budding score and CSS in primary operable breast cancer, by receptor subtype. Kaplan Meier survival graphs for CSS in patients with a necrosis-budding score of 2 compared to 1 compared to 0 in a) ER+/HER2- disease (n=643, **p<0.001**), b) ER+/HER2+ disease (n=86 p=0.066), c)ER-/HER2+ disease (n=87, **p<0.001**), and d) ER-/HER2- disease (n=238, **p<0.001**).

5.3.6.3 Associations with clinicopathological characteristics

A high necrosis-budding score was significantly associated with ductal cancer (p=0.022), larger tumour size (p<0.001), higher tumour grade (p<0.001), nodal positivity (p<0.001), ER and PR negativity (p<0.001, p<0.001), HER2 positivity (p=0.001), higher KM grade (p<0.001) and high TSP (p=0.050)(**Table 5-5**).

	Combined necrosis-budding score			p
	0 n=517 (43.5%)	1 n=566 (47.6%)	2 n=105 (8.8%)	
Age				0.067
<50 years	120 (23.2)	166 (29.3)	30 (28.6)	
≥50 years	397 (76.8)	400 (70.7)	75 (71.4)	
Tumour type				**0.022**
Ductal	460 (89.0)	521 (92.0)	103 (98.1)	
Lobular	30 (5.8)	29 (5.1)	1 (1.0)	
Other	27 (5.2)	16 (2.8)	1 (1.0)	
Invasive tumour size				**<0.001**
≤20mm	322 (62.3)	285 (50.4)	42 (40.4)	
21-49mm	186 (36.0)	256 (45.2)	56 (53.8)	
≥50mm	9 (1.7)	25 (4.4)	6 (5.8)	
Missing data	0	0	1	
Grade				**<0.001**
I	116 (22.5)	62 (11.0)	12 (11.4)	
II	221 (42.9)	240 (42.5)	36 (34.3)	
III	178 (34.6)	263 (46.5)	57 (54.3)	
Missing data	2	1	0	
Nodal status				**<0.001**
Negative	318 (63.1)	325 (57.8)	37 (35.6)	
Positive	186 (36.9)	237 (42.2)	67 (64.4)	
Missing data	13	4	1	
ER				**<0.001**
Negative	90 (17.4)	227 (40.2)	42 (40.0)	
Positive	426 (82.6)	337 (59.8)	63 (60.0)	
Missing data	1	2	0	
HER2				**0.001**
Negative	374 (87.4)	434 (82.7)	76 (73.1)	
Positive	54 (12.6)	91 (17.3)	28 (26.9)	
Missing data	89	41	1	
Klintrup-Makinen				**<0.001**
0	180 (35.2)	103 (18.3)	10 (9.5)	
1	262 (51.2)	263 (46.6)	60 (57.1)	
2	55 (10.7)	154 (27.3)	27 (25.7)	
3	15 (2.9)	44 (7.8)	8 (7.6)	
Missing data	5	2	0	

Table 5-5. Associations between the necrosis-budding score and clinicopathological characteristics. Table detailing the associations between the necrosis-budding score and clinicopathological characteristics.

5.3.7 A combined score of tumour necrosis and TSP

5.3.7.1 Creation of the score

Necrosis and TSP were combined into a single score (0=both components low, 1=either one component high, 2=both components high). 477 (40.2%) patients had a score of 0, 579 (48.7%) had a score of 1, and 132 (11.1%) had a score of 2.

5.3.7.2 Associations with CSS

In the full cohort, an increasing combined necrosis-TSP score was associated with worse CSS (10yr CSS 87% v 79% v 62%, p<0.001; score 1 v 0: 1.70, 95% CI 1.2-

2.31, p=0.001; score 2 v 0: 3.63, 95% CI 2.50-5.25, p<0.001). Higher combined score was associated with worse CSS in both ER positive (10yr CSS 87% v 80% v 67%, p=0.001; score 1 v 0: HR1.56, 95% CI 1.09-2.22, p=0.015; score 2 v 0: HR 2.85, 95% CI 1.70-4.77, p<0.001) and ER negative disease (10yr CSS 87% v 77% v 58%; score 1v 0: HR 2.10, 95% CI 1.06-4.16, p=0.033; score 2 v 0: HR 4.54, 95% CI 2.22-9.26, p<0.001)(**Figure 5-17**).

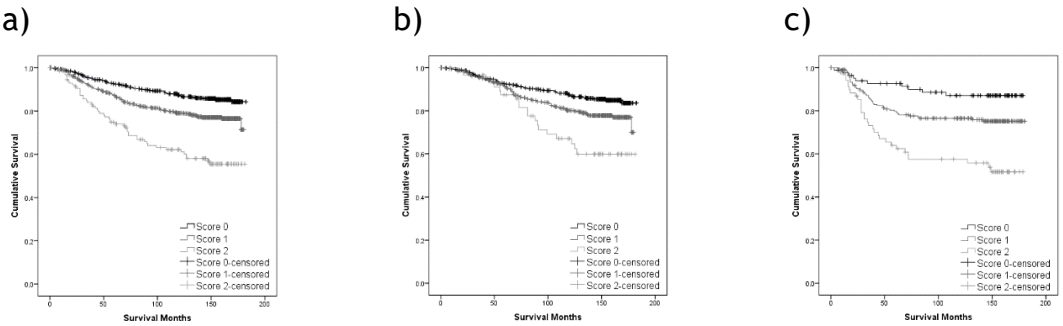

Figure 5-17. The relationship between the necrosis-TSP score and CSS in primary operable breast cancer. Kaplan Meier survival graphs for CSS in patients with a necrosis-TSP score of 2 compared to 1 compared to 0 in a) the full cohort (n=1184, **p<0.001**), b) ER positive disease (n=823, **p<0.001**), and c) ER negative disease (n=358, **p<0.001**).

For those with ER+/HER2- cancer, a higher combined score was associated with worse CSS (10yr CSS 88% v 81% v 65%, p=0.001; score 1 v 0: HR 1.52, 95% CI 1.01-2.29, p=0.044; score 2 v 0: HR 3.24, 95% CI 1.86-5.66, p<0.001). In ER+/HER2+ cancer, there was no significant association between the combined score and CSS (10yr CSS 76% v 63% v 74%, p=0.169; score 1 v 0: HR 2.10, 95% CI 0.88-5.01, p=0.095; score 2 v 0: HR 1.27, 95% CI 0.27-5.97, p=0.765). Similarly, in ER-/HER2+ cancers, the combined score was not significantly associated with CSS (10yr CSS 74% v 75% v 55%, p=0.116; score 1 v 0: HR 0.89, 95% CI 0.25-3.24, p=0.862; score 2 v 0: HR 2.07, 95% CI 0.60-7.21, p=0.252). In ER-/HER2- disease, a score of 2 was significantly associated with worse CSS than a score of 0(10yr CSS 87% v 77% v 56%, p=0.001; score 1 v 0: HR 2.15, 95% CI 0.95-4.85, p=0.065; score 2 v 0: HR 4.95, 95% CI 2.05-11.95, p<0.001).

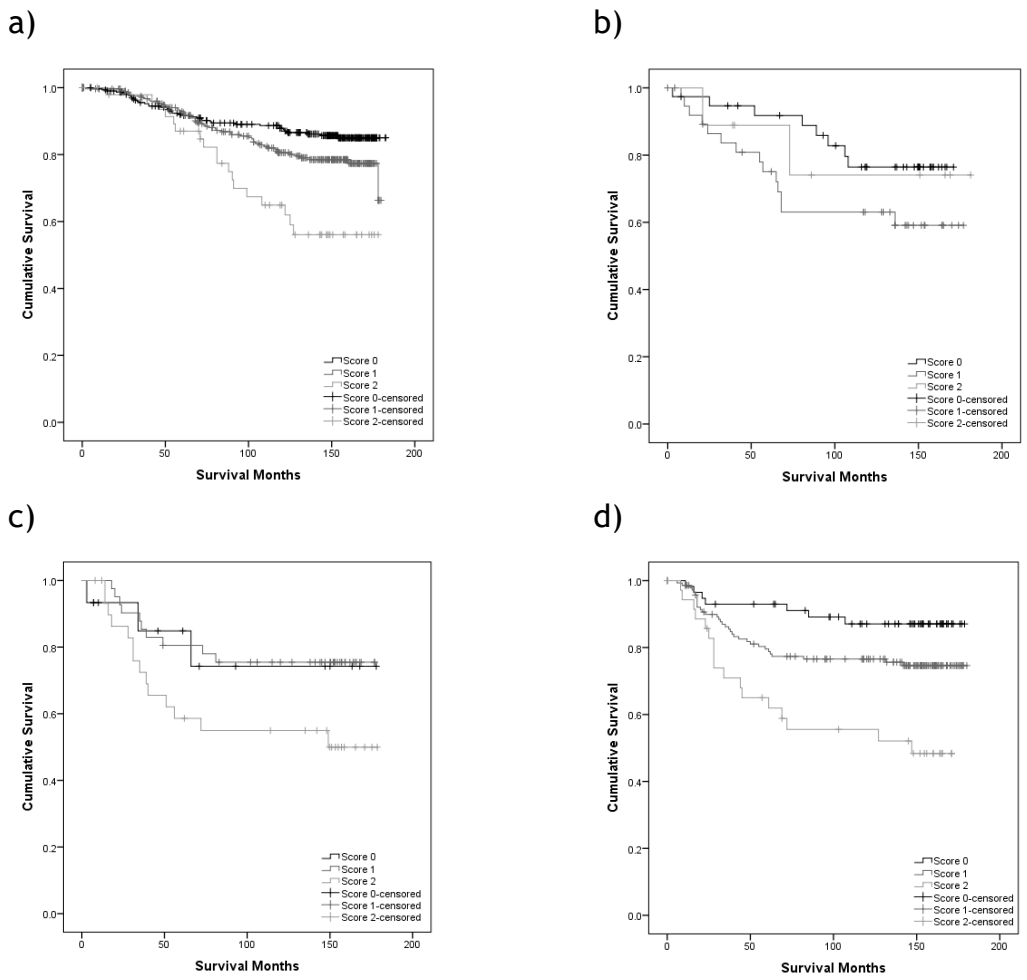

Figure 5-18. The relationship between the necrosis-TSP score and CSS in primary operable breast cancer, by receptor subtype. Kaplan Meier survival graphs for CSS in patients with a necrosis-TSP score of 2 compared to 1 compared to 0 in a) ER+/HER2- disease (n=643, **p<0.001)**, b) ER+/HER2+ disease (n=86, **p=0.220)**, c) ER-/HER2+ disease (n=87, p=0.091), and d) ER-/HER2- disease (n=238, **p<0.001**).

5.3.7.3 Associations with clinicopathological characteristics

A high necrosis-TSP score was significantly associated with ductal tumours (p<0.001), larger tumour size (p<0.001), higher tumour grade (p<0.001), nodal positivity (p=0.001), ER and PR negativity (p<0.001, p<0.001), HER2 positivity (p<0.001) and higher KM grade (p<0.001)(**Table 5-6**).

	Combined necrosis-TSP score			p
	0 n=477 (40.2%)	1 n=579 (48.7%)	2 n=132 (11.1%)	
Age				0.072
<50 years	110 (23.1)	166 (28.7)	40 (30.3)	
≥50 years	367 (76.9)	413 (71.3)	92 (69.7)	
Tumour type				**<0.001**
Ductal	407 (85.3)	548 (94.6)	129 (97.7)	
Lobular	45 (9.4)	14 (2.4)	1 (0.8)	
Other	25 (5.2)	17 (2.9)	2 (1.5)	
Invasive tumour size				**<0.001**
≤20mm	300 (62.9)	283 (49.0)	66 (50.0)	
21-49mm	168 (35.2)	268 (46.4)	62 (47.0)	
≥50mm	9 (1.9)	27 (4.7)	4 (3.0)	
Missing data	0	1	0	
Grade				**<0.001**
I	95 (20.0)	84 (14.5)	11 (8.3)	
II	230 (48.4)	217 (37.5)	50 (37.9)	
III	150 (31.6)	277 (47.9)	71 (53.8)	
Missing data	2	1	0	
Nodal status				**0.001**
Negative	291 (62.2)	331 (58.0)	58 (44.3)	
Positive	177 (37.8)	240 (42.0)	73 (55.7)	
Missing data	9	8	1	
ER				**<0.001**
Negative	86 (18.1)	201 (34.8)	72 (54.5)	
Positive	390 (81.9)	376 (65.2)	60 (45.5)	
Missing data	1	2	0	
HER2				**<0.001**
Negative	366 (87.4)	432 (84.4)	86 (68.3)	
Positive	53 (12.6)	80 (15.6)	40 (31.7)	
Missing data	58	67	6	
Klintrup-Makinen				**<0.001**
0	141 (29.8)	139 (24.1)	13 (9.8)	
1	253 (53.5)	264 (45.8)	68 (51.5)	
2	63 (13.3)	130 (22.6)	43 (32.6)	
3	16 (3.4)	43 (7.5)	8 (6.1)	
Missing data	4	3	0	

Table 5-6. Associations between the necrosis-TSP score and clinicopathological characteristics. Table detailing the associations between the necrosis-TSP score and clinicopathological characteristics.

5.3.8 A combined score of tumour budding and TSP

5.3.8.1 Creation of the score

Budding and TSP were combined into a single score (0=both components low, 1=either one component high, 2=both components high). 665 (56.0%) patients had a score of 0, 403 (33.9%) had a score of 1, and 120 (10.1%) had a score of 2.

5.3.8.2 Associations with CSS

In the full cohort, a higher combined budding-TSP score was associated with worse CSS (10yr CSS 84% v 77% v 71%, p<0.001; score 1 v 0: HR 1.58, 95% CI 1.19-

2.08, p=0.001; score 2 v 0 HR 2.02, 95%CI 1.38-2.97, p<0.001). In ER positive disease, a score of 2 was associated with worse CSS compared to a score of 0 (10yr CSS 83% v 85% v 74%, p=0.110; score 1 v 0: HR 0.99 95% CI 0.69-1.44, p=0.976; score 2 v 0: HR 1.70, 95%CI 1.09-2.66, p=0.021). In ER negative disease, a higher combined budding-TSP score was associated with worse CSS (10yr CSS 86% v 59% v 56%, p<0.001; score 1 v 0 HR 3.28, 95%CI 2.09-5.15, p<0.001; score 2 v 0: HR 3.66, 95%CI 1.75-7.67, p=0.001)(**Figure 5-19**).

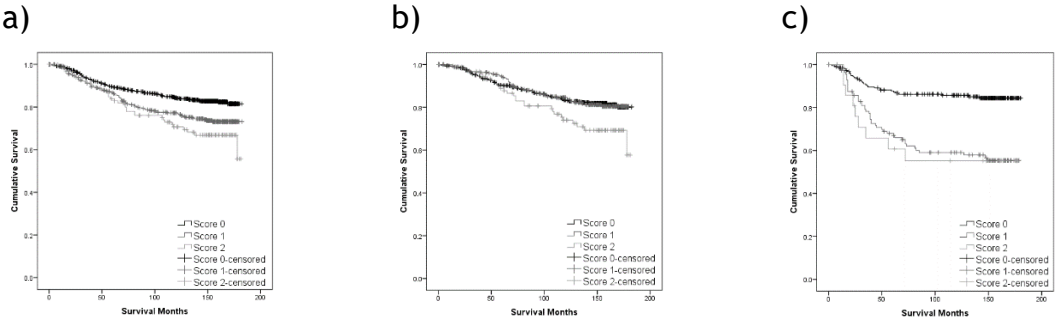

Figure 5-19. The relationship between the budding-TSP score and CSS in primary operable breast cancer. Kaplan Meier survival graphs for CSS in patients with a budding-TSP score of 2 compared to 1 compared to 0 in a) the full cohort (n=1184, **p<0.001**), b) ER positive disease (n=823, **p=0.046**), and c) ER negative disease (n=358, **p<0.001**).

In ER+/HER2- disease, a score of 2 was significantly associated with worse CSS (10yr CSS 83% v 85% v 74%, p=0.211; score 1v 0: HR 1.00, 95% CI 0.66-1.52, p=0.989; score 2 v 0: HR 1.66, 95% CI 1.00-2.75, p=0.050). In ER+/HER2+ disease, the combined budding-TSP score was not significantly associated with CSS (10yr CSS 73% v 66% v 68%, p=0.792; score 1 v 0: HR 1.26, 95% CI 0.52-3.05, p=0.605; score 2 v 0: HR 1.15, 95% CI 0.33-4.02, p=0.833). In ER-/HER2+ cancers, higher combined score was associated with worse CSS (10yr CSS 84% v 58% v 29%, p=0.002; score 1 v 0: HR 3.25, 95% CI 1.27-8.31, p=0.014; score 2 v 0: HR 9.12, 95% CI 2.74-30.35, p<0.001). In ER-/HER2- cancers, a score of 1 was associated with worse CSS than a score of 0 (10yr CSS 85% v 56% v 70%, p<0.001; score 1 v 0: HR 3.50, 95% CI 2.05-5.99, p<0.001; score 2 v 0: HR 1.96, 95% CI 0.68-5.65, p=0.213).

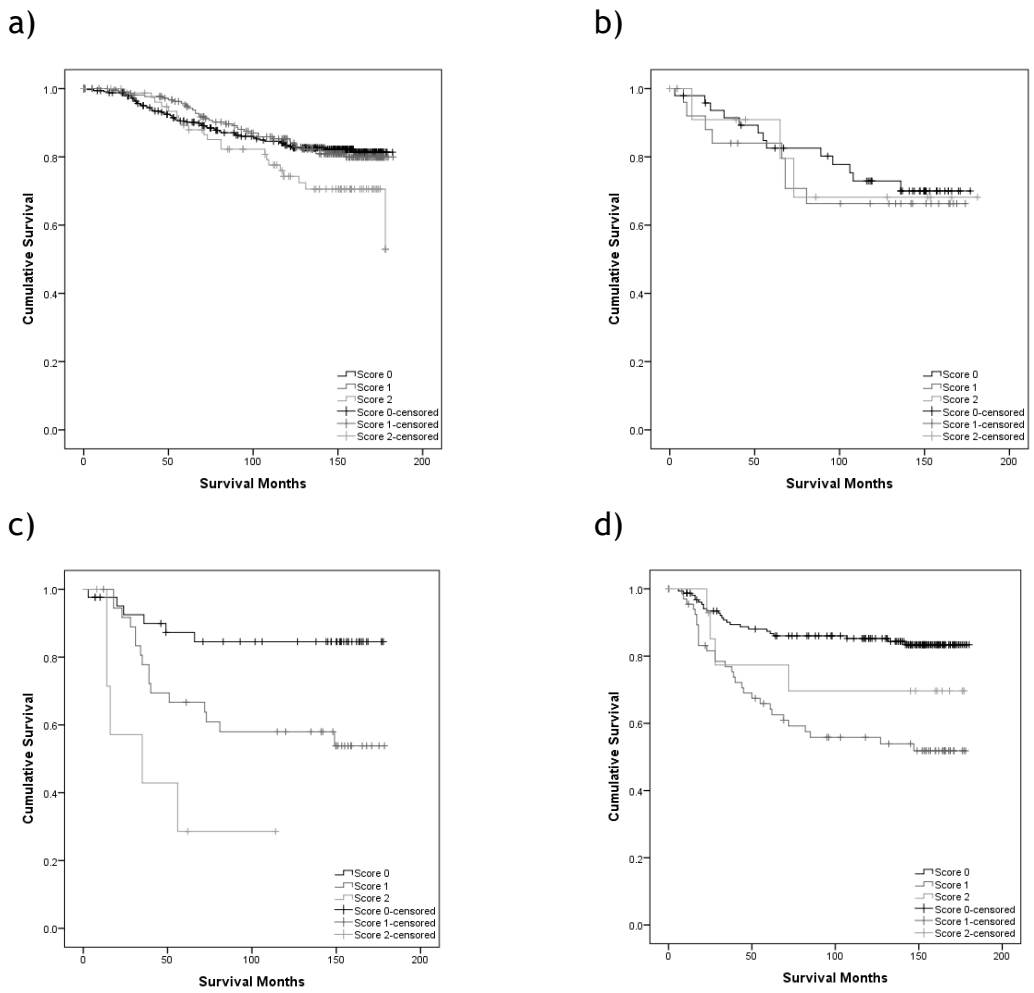

Figure 5-20. The relationship between the budding-TSP score and CSS in primary operable breast cancer, by receptor subtype. Kaplan Meier survival graphs for CSS in patients with a budding-TSP score of 2 compared to 1 compared to 0 in a) ER+/HER2- disease (n=643, p=0.110), b) ER+/HER2+ disease (n=86, p=0.871), c) ER-/HER2+ disease (n=87, **p<0.001**), and d) ER-/HER2- disease (n=238, **p<0.001**).

5.3.8.3 Associations with clinicopathological characteristics

A high budding-TSP score was significantly associated with lobular tumour type (p=0.018), larger tumour size (p=0.015), lower tumour grade (p<0.001), nodal positivity (p=0.001), ER positivity (p=0.006) and lower KM grade (p<0.001) (**Table 5-7**).

	Combined budding-TSP score			p
	0 n=665 (56.0%)	**1** n=403 (33.9%)	**2** n=120 (10.1%)	
Age				0.774
<50 years	181 (27.2)	106 (26.3)	29 (24.2)	
≥50 years	484 (72.8)	297 (73.7)	91 (75.8)	
Tumour type				**0.018**
Ductal	604 (90.8)	375 (93.1)	105 (87.5)	
Lobular	29 (4.4)	19 (4.7)	12 (10.0)	
Other	32 (4.8)	9 (2.2)	3 (2.5)	
Invasive tumour size				**0.015**
≤20mm	348 (52.3)	242 (60.2)	59 (49.2)	
21-49mm	293 (44.1)	152 (37.8)	53 (44.2)	
≥50mm	24 (3.6)	8 (2.0)	8 (6.7)	
Missing data	0	1	0	
Grade				**<0.001**
I	85 (12.8)	80 (19.9)	25 (20.8)	
II	250 (37.8)	181 (44.9)	66 (55.0)	
III	327 (49.4)	142 (35.2)	29 (24.2)	
Missing data	3	0	0	
Nodal status				**0.001**
Negative	409 (62.3)	216 (54.7)	55 (46.2)	
Positive	247 (37.7)	179 (45.3)	64 (53.8)	
Missing data	9	8	1	
ER				**0.006**
Negative	220 (33.2)	116 (28.8)	23 (19.2)	
Positive	442 (66.8)	287 (71.2)	97 (80.8)	
Missing data	3	0	0	
HER2				0.696
Negative	491 (84.5)	298 (82.5)	95 (82.6)	
Positive	90 (15.5)	63 (17.5)	20 (17.4)	
Missing data	84	42	5	
Klintrup-Makinen				**<0.001**
0	158 (23.9)	98 (24.5)	37 (30.8)	
1	297 (44.9)	221 (55.3)	67 (55.8)	
2	153 (23.1)	70 (17.5)	13 (10.8)	
3	53 (8.0)	11 (2.8)	3 (2.5)	
Missing data	4	3	0	

Table 5-7. Associations between the budding-TSP score and clinicopathological characteristics. Table detailing the associations between the budding-TSP score and clinicopathological characteristics.

5.3.9 A combined score of tumour necrosis, tumour budding and TSP

5.3.9.1 Creation of the score

Necrosis, budding and TSP were combined into a single score (0=all components low, 1=any one component high, 2=any two components high, 3=all components high). 372 (31.3%) patients had a score of 0, 543 (45.7%) score 1, 231 (19.4%) score 2 and 42 (3.5%) had a score of 3.

5.3.9.2 Associations with CSS

In the full cohort, a higher score was significantly associated with worse CSS (10yr CSS 87% v 83% v 70% v 44%, p<0.001; score 1 v 0: HR 1.42, 95% CI 0.10-2.01, p=0.053; score 2 v 0: HR 2.79, 95% CI 1.94-4.03, p<0.001; score 3 v 0: HR 5.61, 95% CI 3.35-9.40, p<0.001). In ER positive disease, a score of 3 was significantly associated with worse CSS compared to a score of 0 (10yr CSS 86% v 84% v77% v50%, p<0.001; score 1 v 0: HR 1.22, 95% CI 0.82-1.82, p=0.324; score 2 v 0: HR 1.77, 95% CI 1.13-2.79, p=0.013; score 3 v 0: HR 4.24, 95%CI 2.23-8.07, p<0.001). In ER negative disease, a score of 2 or 3 was significantly associated with worse CSS compared to a score of 0 (10 year CSS 92% v 81% v 57% v 36%, p<0.001; score 1 v 0: HR 2.71, 95% CI 1.06-6.92, p=0.037; score 2 v 0: HR 7.42, 95% CI 2.92-18.83, p<0.001; score 3 v 0: HR 12.91, 95% CI 4.32-38.62, p<0.001)(**Figure 5-21**).

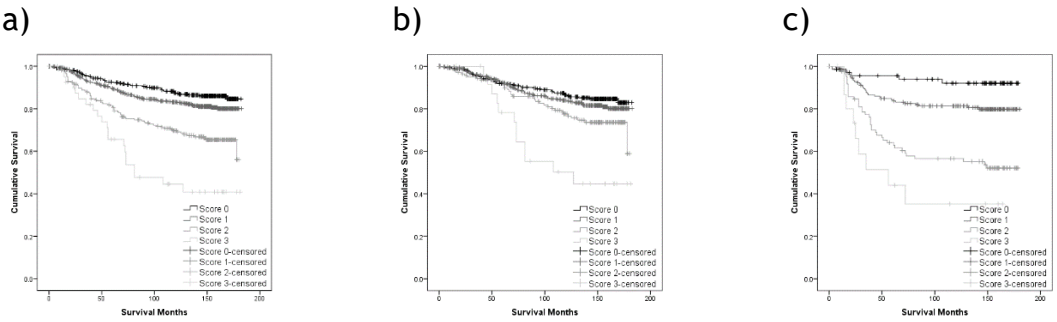

Figure 5-21. The relationship between the necrosis-budding-TSP score and CSS in primary operable breast cancer. Kaplan Meier survival graphs for CSS in patients with a necrosis-budding-TSP score of 3 compared to 2 compared to 1 compared to 0 in a) the full cohort (n=1184, **p<0.001**), b) ER positive disease (n=823, **p<0.001**), and c) ER negative disease (n=358, **p<0.001**).

In ER+/HER2- disease, a score of 3 was significantly associated with worse CSS than a score of 0 (10yr CSS 86% v 85% v 80% v 45%, p<0.001; score 1 v 0: HR 1.17, 95% CI 0.74-1.84, p=0.506; score 2 v 0: HR 1.51, 95% CI 0.90-2.55, p=0.122; score 3 v 0: HR 4.90, 95% CI 2.46-9.75, p<0.001). In ER+/HER2+ cancers, the combined score was not significantly associated with CSS (10yr CSS 79% v 67% v 59% v 75, p=0.181; score 1 v 0: HR 2.17, 95% CI 0.79-5.97, p=0.135; score 2 v 0: HR 2.72, 95% CI 0.91-8.10, p=0.073; HR 1.23, 95% CI 0.15-10.23, p=0.849). In ER-/HER2+ cancers, there was no significant association between the combined score and CSS (score 1 v 0: HR 0.55, 95% CI 0.11-2.74, p=0.467; score 2 v 0: HR 1.91, 95% CI 0.43-8.40, p=0.393; score 3 v 0: HR 4.92, 95% CI 0.95-25.51, p=0.058). In ER-/HER2- disease, a higher combined score was associated with worse CSS (10yr CSS 93% v 80% v56% v 45%, p<0.001; score 1 v 0: HR 3.42, 95% CI 1.04-11.27,

p=0.043; score 2 v 0: HR 9.06 95% CI 2.73-30.12, p<0.001; score 3 v 0 HR 10.46, 95% CI 2.34-46.81, p=0.002).

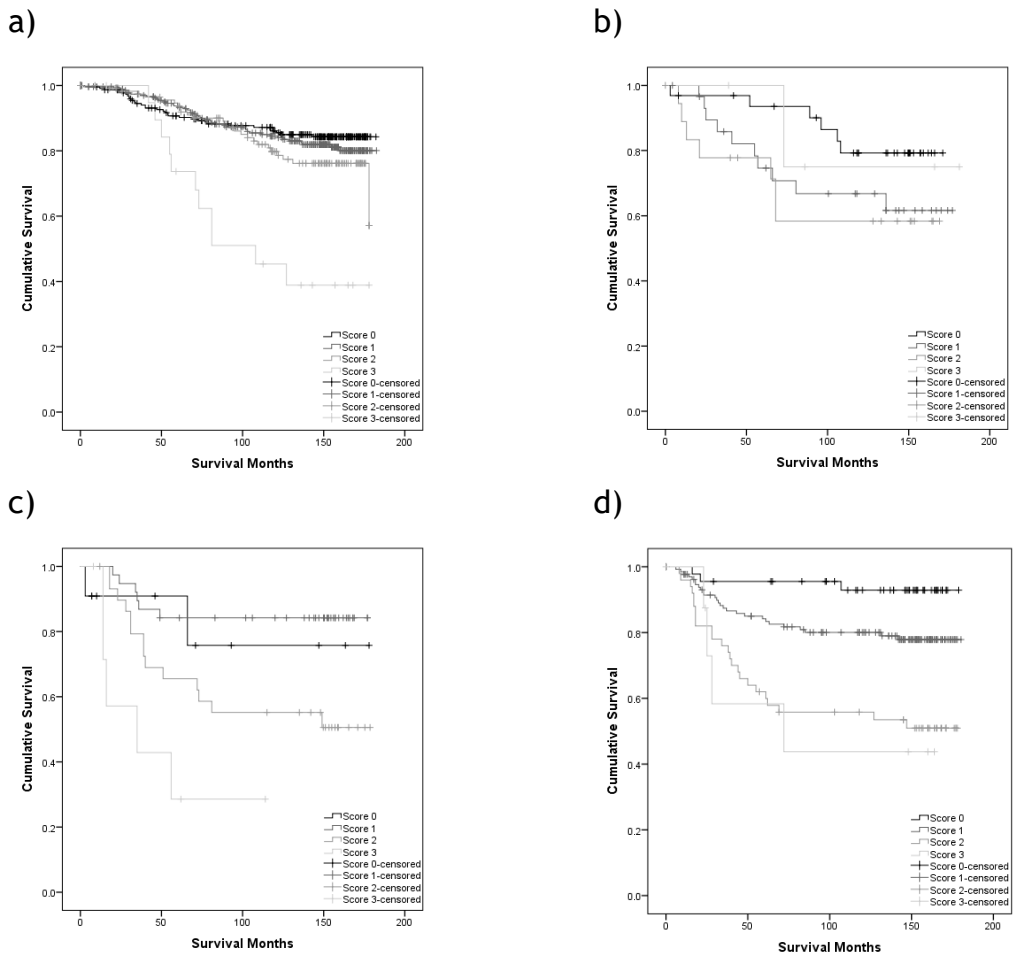

Figure 5-22. The relationship between the necrosis-budding-TSP score and CSS in primary operable breast cancer, by receptor subtype. Kaplan Meier survival graphs for CSS in patients with a necrosis-budding-TSP score of 3 compared to 2 compared to 1 compared to 0 in a) ER+/HER2- disease (n=643, **p<0.001**), b) ER+/HER2+ disease (n=86, p=0.268), c) ER-/HER2+ (n=87, **p=0.001**), and d) ER-/HER2- disease (n=238, **p<0.001**).

As stratification of risk in patients with ER positive lymph node negative disease is of particular clinical interest, we further analysed the combined necrosis-budding-TSP score in this group of patients. In this cohort of 479 patients, a score of 2 or 3 was significantly associated with worse CSS (10yr CSS 95% v 91% v 82% v 58%; score 1 v 0: HR 1.62, 95% CI 0.80-3.28, p=0.185; score 2 v 0: HR 3.58, 95% CI 1.66-7.75, p=0.001; score 3 v 0: HR 7.34, 95% CI 2.07-26.05, p=0.002).

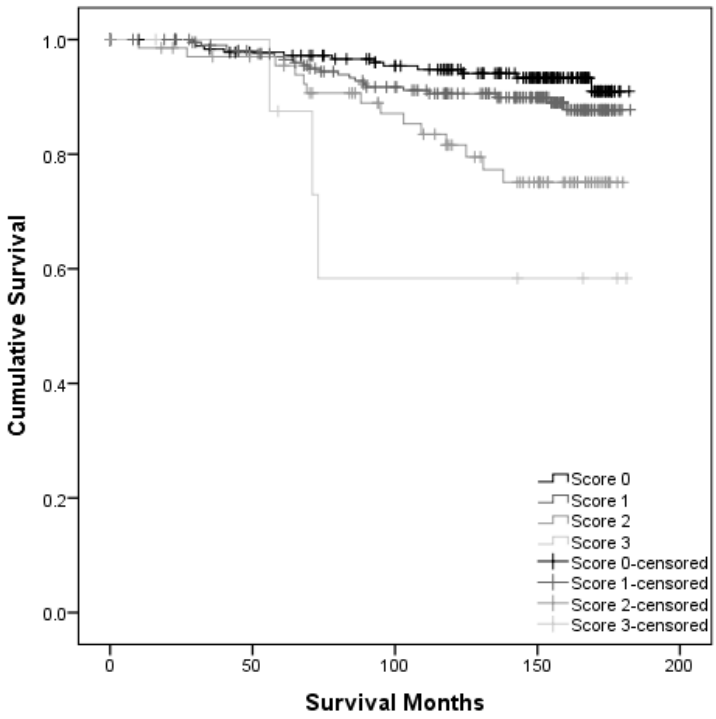

Figure 5-23. The relationship between the necrosis-budding-TSP score and CSS in primary operable ER positive, node negative breast cancer. Kaplan Meier survival graphs for CSS in patients with a necrosis-budding-TSP score of 3 compared to 2 compared to 1 compared to 0, in ER positive, node negative breast cancer (n=429, **p<0.001**).

5.3.9.3 Associations with clinicopathological characteristics

A high combined necrosis-budding-TSP score was associated with ductal subtype (p=0.008), larger tumour size (0.018), nodal (p<0.001) and HER2 positivity (p=0.001), ER negativity (p<0.001) and higher KM score (p<0.001)(**Table 5-8**).

	Combined necrosis-budding-TSP score				p
	0 n=372 (31.3%)	1 n=543 (45.7%)	2 n=231 (19.4%)	3 n=42 (3.5%)	
Age					0.083
<50 years	89 (23.9%)	144 (26.5)	75 (32.5)	8 (19.0)	
≥50 years	283 (76.1)	399 (73.5)	156 (67.5)	34 (81.0)	
Tumour type					**0.008**
Ductal	322 (86.6)	505 (93.0)	217 (93.9)	40 (95.2)	
Lobular	28 (7.5)	20 (3.7)	11 (4.8)	1 (2.4)	
Other	22 (5.9)	18 (3.3)	3 (1.3)	1 (2.4)	
Invasive tumour size					**0.018**
≤20mm	228 (61.3)	286 (52.7)	119 (51.7)	16 (38.1)	
21-49mm	137 (36.8)	236 (43.5)	102 (44.3)	23 (54.8)	
≥50mm	7 (1.9)	21 (3.9)	9 (3.9)	3 (7.1)	
Missing data	0	0	1	0	
Grade					0.163
I	71 (19.2)	83 (15.3)	30 (13.0)	6 (14.3)	
II	162 (43.8)	215 (39.7)	104 (45.0)	16 (38.1)	
III	137 (37.0)	244 (45.0)	97 (42.0)	20 (47.6)	
Missing data	2	1	0	0	
Nodal status					**<0.001**
Negative	231 (63.3)	325 (61.0)	111 (48.1)	13 (31.7)	
Positive	134 (36.7)	208 (39.0)	120 (51.9)	28 (68.3)	
Missing data	7	10	0	1	
ER					**<0.001**
Positive	301 (81.1)	355 (65.6)	145 (62.8)	25 (59.5)	
Negative	70 (18.9)	186 (34.4)	86 (37.2)	17 (40.5)	
Missing data	1	2	0	0	
HER2					**0.001**
Negative	273 (86.4)	412 (85.8)	170 (77.6)	29 (69.0)	
Positive	43 (13.6)	68 (14.2)	49 (22.4)	13 (31.0)	
Missing data	56	63	12	0	
Klintrup-Makinen					**<0.001**
0	119 (32.2)	122 (22.6)	48 (20.8)	4 (9.5)	
1	186 (50.4)	254 (47.1)	120 (51.9)	25 (59.5)	
2	49 (13.3)	124 (23.0)	53 (22.9)	10 (23.8)	
3	15 (4.1)	39 (7.2)	10 (4.3)	3 (7.1)	
Missing data	3	4	0	0	

Table 5-8. Associations between the combined necrosis-budding-TSP score and clinicopathological characteristics. Table showing associations between the necrosis-budding-TSP score and other known prognostic clinicopathological characteristics.

5.3.10 Multivariate survival analysis for the combined necrosis-budding-TSP score

A summary of the univariate survival analysis in ER positive and ER negative disease for each of the individual factors and each of the combined scores analysed above is displayed in **Table 5-9** below, along with other known prognostic factors.

Factor	ER positive			ER negative		
	n	HR (95%CI)	p	n	HR (95%CI)	p
Age	823		0.977	358		0.806
<50 years		1 (ref)			1 (ref)	
≥50 years		1.00 (0.69-1.44)			0.95 (0.62-1.46)	
Tumour type	823		0.328	358		0.904
Ductal		1 (ref)			1 (ref)	
Lobular		0.94 (0.50-1.80)	0.861		0.05 (0.00-483.41)	0. 513
Other		0.37 (0.09-1.51)	0.167		0.05 (0.00-3.19)	0.154
Tumour size	823		**<0.001**	357		**0.005**
≤20mm		1 (ref)			1 (ref)	
21-49mm		2.54 (1.79-3.60)	**<0.001**		1.85 (1.18-2.90)	**0.008**
≥50mm		6.32 (3.44-11.61)	**<0.001**		3.27 (1.36-7.85)	**0.008**
Tumour grade	822		**<0.001**	356		0.893
I		1 (ref)			Incalculable	
II		1.53 (0.89-2.62)	0.121		0.88 (0.53-1.48)	0.637
III		3.38 (1.98-5.75)	**<0.001**		1 (ref)	
Nodal status	807		**<0.001**	356		**<0.001**
Negative		1 (ref)			1 (ref)	
Positive		3.32 (2.36-4.68)			3.87 (2.43-6.16)	
HER2	729		**0.008**	325		0.197
Negative		1 (ref)			1 (ref)	
Positive		1.82 (1.17-2.82)			1.35 (0.86-2.13)	
Necrosis	823		**<0.001**	358		**0.001**
<25%		1 (ref)			1 (ref)	
>25%		2.03 (1.46-2.82)			2.77 (1.54-4.98)	
Budding	823		0.102	358		**<0.001**
Low		1 (ref)			1 (ref)	
High		1.33 (0.94-1.89)			3.05 (1.97-4.73)	
TSP	823		0.259	358		**0.002**
≤50%		1 (ref)			1 (ref)	
>50%		1.22 (0.87-1.71)			1.96 (1.27-3.01)	
Klintrup-Makinen	817		0.199	357		0.155
0		1 (ref)			1 (ref)	
1		1.16 (0.79-1.69)	0.451		6.68 (0.92-48.52)	0.060
2		1.62 (0.99-2.66)	0.057		6.92 (0.95-50.47)	0.056
3		0.71 (0.25-1.98)	0.513		3.89 (0.47-32.30)	0.209
Necrosis-budding score	823		**<0.001**	358		**<0.001**
Both low		(ref)			1 (ref)	
1 low, 1 high		1.41 (0.99-2.01)	0.059		2.64 (1.26-5.55)	**0.010**
Both high		3.09 (1.92-4.96)	**<0.001**		10.01 (4.52-22.17)	**<0.001**
Necrosis-TSP score	823		**<0.001**	358		**<0.001**
Both low		1 (ref)			1 (ref)	
1 high, 1 low		1.56 (1.09-2.22)	**0.015**		2.10 (1.06-4.16)	**0.033**
Both high		2.85 (1.70-4.77)	**<0.001**		4.54 (2.22-9.26)	**<0.001**
Budding-TSP score	823		**0.049**	358		**<0.001**
Both low		1 (ref)			1 (ref)	
1 high, 1 low		0.99 (0.69-1.44)	0.976		3.28 (2.09-5.15)	**<0.001**
Both high		1.70 (1.09-2.66)	**0.021**		3.66 (1.75-7.67)	**0.001**
Combined necrosis-budding-TSP score	823		**<0.001**	358		**<0.001**
All low		1 (ref)			1 (ref)	
1 high		1.22 (0.82-1.82)	0.324		2.71 (1.06-6.92)	**0.037**
2 high		1.77 (1.13-2.79)	**0.013**		7.42 (2.92-18.83)	**<0.001**
All high		4.24 (2.23-8.07)	**<0.001**		12.91 (4.32-38.62)	**<0.001**

Table 5-9. Univariate survival analysis of the relationship between various clinicopathological characteristics, including the combined scores, and CSS in primary operable breast cancer. Univariate analysis for each of the combined scores and other known prognostic clinicopathological characteristics for an outcome of CSS in the ER positive and ER negative cohorts.

Of the individual factors and combined scores investigated in this chapter, the necrosis-budding-TSP score had the highest prognostic power on univariate

analysis. Therefore, multivariate Cox regression survival analysis was carried out for this score with other prognostic clinicopathological factors. The score was significantly associated with CSS, independent of other factors, in both ER positive and ER negative disease (**Table 5-10**).

Factor	ER positive			ER negative		
	n	HR (95% CI)	p	n	HR (95% CI)	p
Tumour size	823		**<0.001**	357		0.173
≤20mm		1 (ref)				
21-49mm		1.67 (1.15-2.44)	**0.008**			0.134
≥50mm		3.70 (1.93-7.10)	**<0.0001**			0.118
Tumour grade	822		**<0.001**			
I		1 (ref)				
II		1.43 (0.79-2.57)	0.234			
III		2.77 (1.53-5.02)	**0.001**			
Nodal status	807		**<0.001**	356		**<0.001**
Negative		1 (ref)			1 (ref)	
Positive		2.44 (1.69-3.55)			3.15 (1.96-5.06)	
HER2	729		0.338			
Negative						
Positive						
Necrosis-budding-TSP score	823		**0.039**	357		**<0.001**
None high		1 (ref)			1 (ref)	
1 component high		1.19 (0.78-1.81)	0.419		2.52 (0.99-6.44)	0.053
2 components high		1.40 (0.87-2.26)	0.170		5.96 (2.34-15.18)	**<0.001**
All components high		2.66 (1.35-5.26)	**0.005**		8.11 (2.68-24.51)	**<0.001**

Table 5-10. Multivariate survival analysis of the necrosis-budding-TSP score and other known prognostic pathological factors. Multivariate cox regression survival analysis for prognostic factors ($p \leq 0.05$ on univariate analysis), including the necrosis-budding-TSP score, for CSS in ER positive and ER negative primary operable breast cancer.

5.4 Discussion

The present chapter involving over 1000 patients confirms the hypothesis that necrosis, tumour budding and TSP have prognostic value in primary operable breast cancer. All 3 features have independent prognostic value in ER negative breast cancer, whilst necrosis also has prognostic value in ER positive disease. A combined score of necrosis, budding and TSP shows particular prognostic power in both ER positive and ER negative disease.

The present study observed that tumour necrosis is associated with worse CSS in both ER positive and ER negative disease. There is little in the literature regarding the prognostic value of tumour necrosis in breast cancer, however these results are in keeping with one smaller study which reported reduced CSS in patients with tumour necrosis(72). The association of necrosis with poor prognosis in other cancers has been reported, including bladder(69), renal(70,

222), lung(71) and colorectal(67). One study in colorectal cancer reported necrosis to be associated with worse outcomes, though this was not independent of systemic and local inflammation, and therefore the authors suggest that the role of necrosis is related to its effect on tumour-related inflammation(68). Similarly, a large but much older cohort of breast cancer patients reported necrosis to be prognostic for survival on univariate analysis but this was not independent of inflammatory cell reaction and known prognostic tumour pathological features(73). In support of this, the present study observed an association between necrosis and high KM score but necrosis was prognostic independent of KM score using Cox regression analysis. It would be interesting, in further work going forward, to determine the associations between necrosis and specific immune cell subtypes. In this study we observed an association between necrosis and high CD4+ lymphocytes and CD68+ macrophages but this analysis could only be carried out in a much smaller subgroup of patients who had had tissue stained for CD4, CD8 and CD68. Larger studies with a broader range of cell markers are required.

The present data has observed that high tumour budding is also associated with worse CSS in primary operable breast cancer, and this is potentiated in ER negative disease. In addition, the current study validates, in a much larger cohort of patients, results previously reported for tumour budding in smaller cohorts of breast cancer(78-80). Tumour budding has been more extensively studied in other solid tumours and has been reported to be associated with worse cancer outcomes in pancreatic(216, 219), oesophageal(208, 211), lung(215, 225), oral squamous(210, 221), and colorectal(209, 217, 223, 224, 226) cancers. In colorectal cancer, whilst budding reporting is not yet in routine use worldwide, the International Tumour Budding Consensus Conference 2016 agreed a single international evidence-based method for tumour budding assessment and reporting, and proposed that the method should be incorporated into colorectal cancer guidelines and staging systems (77). Tumour budding has since been included in the College of American Pathologists guidelines as a feature for reporting in colorectal cancer(75).

Several mechanisms have been proposed regarding the role of tumour budding in cancer growth and dissemination. Budding is observed as a detachment of a

small number of tumour cells at the invasive tumour edge and characteristically these buds show reduced E-cadherin, the cell-cell adhesion molecule. Some evidence suggests that tumour buds may be in a partial epithelial-mesenchymal transition (EMT) state(74)(**Figure 5-24**). There is a potential role for the tumour stroma in establishing a pro-budding microenvironment(75), which is supported by the association between TSP and budding in the present study.

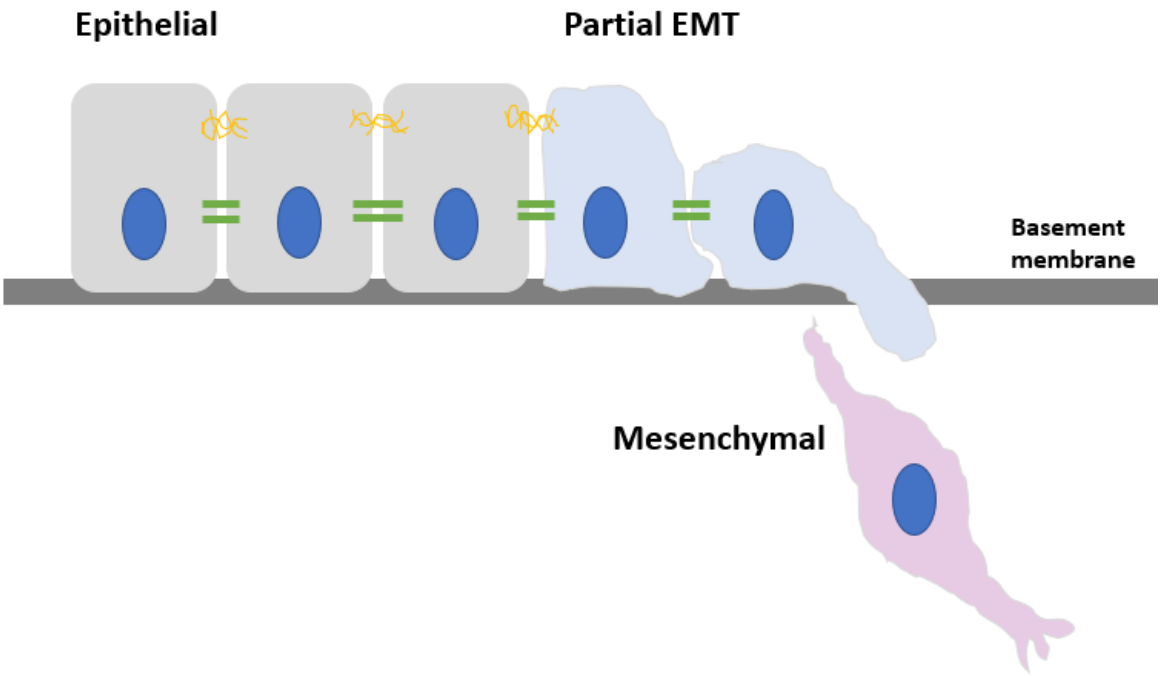

Figure 5-24. Epithelial-mesenchymal transition. Diagram illustrating the process of epithelial-mesenchymal transition. In the epithelial state, tight junctions, adherens junctions and e-cadherin maintain cell-cell adhesion. In the mesenchymal state these are lost and migratory potential is much stronger. Diagram adapted from that in a paper by Leggett et al(227).

TSP was also associated with worse CSS overall, particularly in ER negative patients in the current study. This observation is in accordance with findings of previous studies in breast cancer that also reported TSP to have higher prognostic power in triple-negative tumours(212, 213). High TSP has also been reported to be associated with worse cancer outcomes in colorectal cancer(214, 218, 220). Components of the tumour-associated stroma can promote tumour progression by secretion of growth factors, cytokines and chemokines. These promote cancer cell motility, invasion, resistance to apoptosis, and metastases(228-233). They can also regulate the immune environment to an immunosuppressive, pro-tumourigenic role, and the tumour stroma has been shown to have a role in resistance to systemic therapies in breast cancer(228, 234). Cancer-associated fibroblasts can induce EMT(228), again providing a

potential explanation for the association between TSP and tumour budding observed in the present study. It is interesting to note, with this in mind, that women with high mammographic density breasts (associated with stromal collagen-deposition) have a higher risk of breast cancer(235) and that these tumours differ in terms of cytokine profile and neutrophil recruitment(236).

Given that each of these three factors (necrosis, budding and TSP) were independently associated with worse CSS, they were used in combination to see if a combined score would have additional prognostic value. The combined score of necrosis, budding and TSP had the greatest prognostic power, compared to the combined scores involving only two of these factors. It is interesting to note that, although the only individual factor associated with CSS in ER positive disease was necrosis, which therefore is likely to be the main contributor to the prognostic power of the score in this cohort, the combined score did still have additional prognostic power compared to necrosis alone.

The necrosis-budding-TSP score stratifies ER negative patients into four prognostic groups. It therefore has potential in clinical practice, alongside other established prognostic tumour pathological factors, for risk stratification of patients and therefore to aid discussions around therapeutic options, particularly for patients at high risk from treatment toxicities. With the current move within the breast surgical community to do less surgery in the axilla, the prognostic information from axillary lymph nodes, often used by oncologists to guide treatment decisions such as post-mastectomy radiotherapy, may become less frequently available, adding to the potential for use of this score in clinical practice(45).

Excitingly, this combined score also identifies a high-risk group of patients with ER positive, node negative disease and this may prove useful in decisions regarding chemotherapy for these patients. The advantage of the combined score, over the genomic assays currently in use in this context, is that the only requirement is visual assessment of an H&E slide. Thus it would be cheaper and more readily available for use worldwide. Finally, in the ER positive cohort, it is interesting to note that a score of 3 on the Kaplan Meier graph diverges around the 5 year mark (CSS for those with a score of 3 drops from 78% at 5 years to 50% at 10 years), which is when a number of these patients would have stopped their

endocrine therapy. This suggests another potential clinical use for this score, in identifying patients who may benefit from extended endocrine therapy(51, 237).

Limitations to the present study include retrospective data collection and that it is a cohort of patients from up to 20 years ago when management of breast cancer was different, and therefore there is a question as to whether these results remain applicable in the context of modern treatment regimen. In particular, as this work was carried out on tissue from full resection specimens, it is unclear at present how the prognostic score described could be applied in the setting of neoadjuvant treatment decision-making. Assessment of intratumoral budding on core biopsies has been described(79) but much more work would be required to evaluate scoring of all 3 features on core biopsy specimens, whether their prognostic power was maintained in this setting, and relevance to neoadjuvant treatment decisions. The issue of a historical dataset is weighed against the long follow up period, which is important in breast cancer studies as recurrence can occur many years down the line. In view of the timing of patient accrual to the study, we do not have full HER2 data for all patients and therefore could not carry out detailed analysis within the full molecular subtypes. Work is ongoing to create a tissue microarray for these patients to allow HER2 and Ki67 scoring, and subsequently more detailed subtype analysis, to be carried out.

In conclusion, a combined score of tumour necrosis, tumour budding and TSP shows promise as an inexpensive and readily-available prognostic tool in both ER positive and ER negative operable breast cancer. It requires further validation in other, more recent cohorts, ideally in other regions and with full molecular subtyping. Tumour budding in particular appears to have prognostic power in ER negative breast cancer but what budding represents in currently unknown. This will be further investigated in the following chapter.

6 The relationship between tumour budding and specific gene signatures: a pilot study

6.1 Introduction

The findings in the previous chapter provide evidence that necrosis, TSP and tumour budding are associated with worse CSS in ER negative breast cancer. Of the 3 features, tumour budding was the strongest prognostic feature in ER negative disease in this cohort. Therefore, in this chapter, further investigation into tumour budding is carried out.

As described in the previous chapter, tumour budding represents a phenotype defined in recent colorectal cancer studies as the detachment of buds of 1-5 tumour cells from the main tumour(238-241). It has been implicated in EMT and development of metastases in several cancers including colorectal, pancreatic, oesophageal, lung, head and neck and breast(74), but there is at present little understanding of what this phenotype represents. In this chapter, the aim was to investigate genomic signatures associated with the high budding phenotype in ER negative disease. In view of the suggestion that budding represents a partial EMT state, the hypothesis was that genes associated with EMT would also be associated with high budding. A better understanding of the genomic, transcriptomic and protein pathways associated with the budding phenotype may identify potential therapeutic targets against this aggressive phenotype.

TempOSeq is a targeted sequencing technology based on probe hybridisation(242, 243). Advantages of the technique include the absence of the requirement for RNA extraction, the lack of sensitivity to RNA fragmentation when tissue is formalin fixed and paraffin embedded, and its reproducibility in FFPE compared to frozen specimens is much higher than that associated with RNAseq when RNA has been extracted from the tissue using traditional methods(242, 243). Therefore, this technology can be used to profile gene expression from an area of $\leq 2mm^2$ of the FFPE H&E-stained sections available for our cohort. In this chapter a small pilot study is carried out, using this technique, to investigate the difference in genomic signatures between ER negative cancers with high tumour budding compared to those with no or low budding, and to evaluate the TempOSeq technique in this setting.

6.2 Materials and methods

6.2.1 Cohort selection

Due to financial constraints, only 50 sections could be submitted for RNA sequencing, so this study was carried out as a pilot study of 25 high budding tumours and 25 no/low budding controls. The 1800 cohort was used as this was the cohort for which tissue blocks were still available to our lab. Only patients with ER negative disease were included. They were ordered from highest 'highest bud count' to lowest 'highest bud count' (please refer to chapter 5). Due to the time since the original formation of this cohort, tissue blocks for every patient were not available. Therefore, the high budding cohort was formed by working down the list from the highest bud count patient pulling tissue blocks until 25 high budding patients with tissue blocks were identified. The control cohort was formed in a similar manner, working from the lowest budding count upwards (**Figure 6-1**).

6.2.2 Slide preparation

Tissue sections were cut and fixed as described in chapter 2, prior to transfer to Bioclavis. Sections were labelled with the TMA ID only, to maintain anonymity but to allow data to be linked back to the master database.

6.2.3 RNA sequencing using TempOSeq®

RNA sequencing was carried out at Bioclavis using the protocol detailed in chapter 2. Samples which appeared to have become saturated during amplification were diluted and re-amplified. They were given a suffix of _diluted in the database.

6.2.4 Data analysis

6.2.4.1 Unbiased analysis

Initial analysis was carried out by Bioclavis using the Temp0SeqR data analysis program (BioSpyder technologies, USA). Assay performance metrics were calculated using positive and negative controls. One sample from the high budding cohort was removed prior to analysis because it had a per mapping rate

too close to the negative control (**Figure 6-1, Figure 6-2**). Heatmaps were constructed and principle component analysis was carried out to identify any clustering of samples. Differential expression analysis was carried out using MA plots. The remainder of the analysis was carried out by EM using log2 fold change and adjusted p value data for each of the 22357 genes analysed, using Microsoft® Office Excel 16 (Microsoft, Redmond, WA, USA). Genes with a statistically significant fold change (adjusted $p<0.10$) in the high budding compared to low budding tumours were identified.

6.2.4.2 Biased analysis

A second stage of analysis was carried out to investigate whether genes associated with certain other tumour features/properties were also associated with high tumour budding. In view of the hypothesis that tumour budding may be related to EMT, an EMT-related gene signature reported in the literature was investigated to identify whether any of these genes were associated with tumour budding. Similarly, as the results in chapter 5 reported that high budding is associated with high grade, Klintrup-Makinen grade and TSP, gene signatures reported in the literature for proliferation, inflammation/immunity and stroma were also investigated. Any gene with a log2 fold change of 2 or more in either direction was considered to be of interest in this pilot study, regardless of p value, in view of the small sample size.

6.3 Results

6.3.1 The cohort

Of the 276 patients with ER negative breast cancer, 61 had high tumour budding, of which 25 with tissue blocks available were identified.

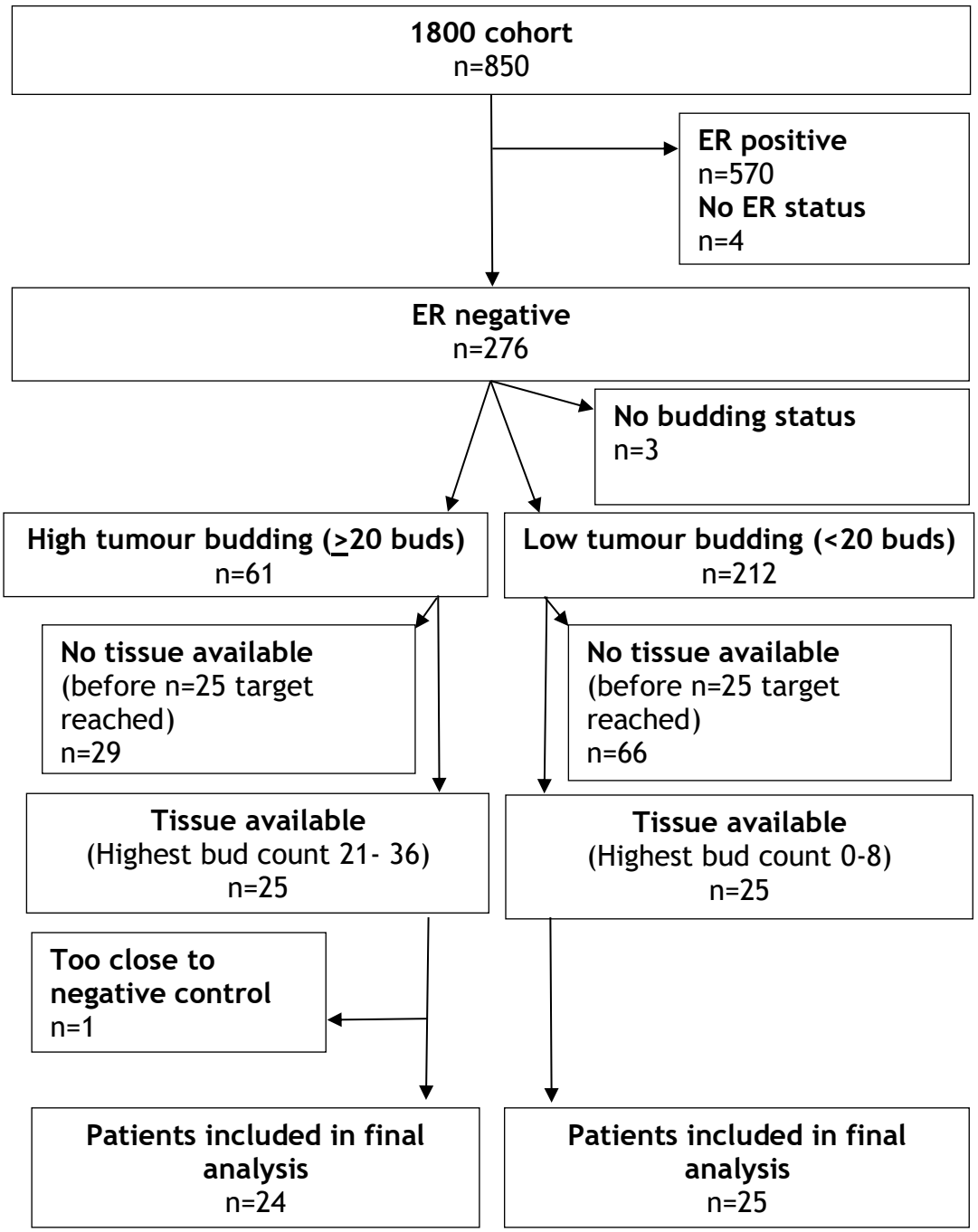

Figure 6-1. Selection of the cohorts for analysis. Flow chart showing how the cohort of 25 high budding patients and the control cohort of 25 low budding patients for transcriptomic analysis were selected.

Quality control metrics were met for all samples but one, which was excluded from further analysis because of its per mapping rate.

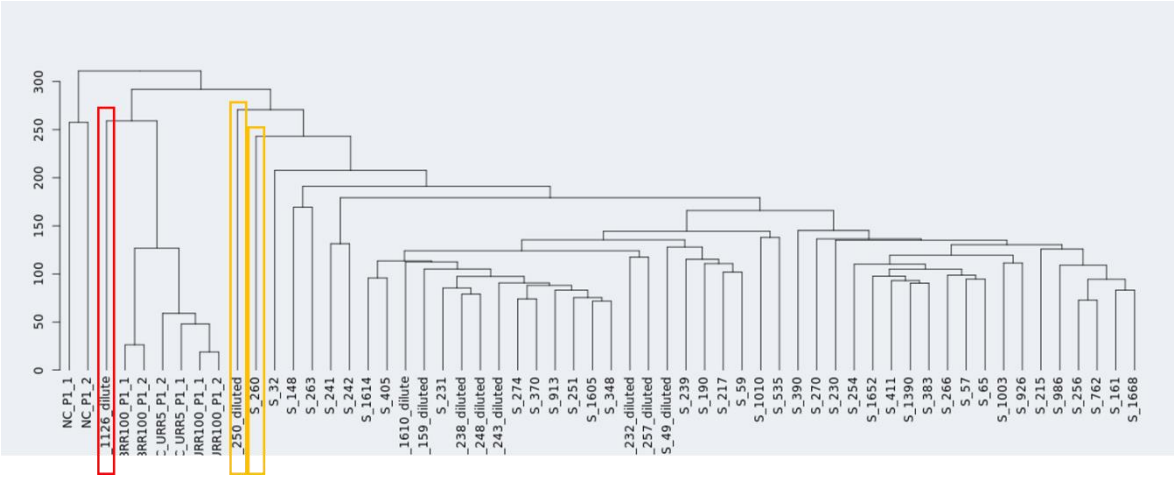

Figure 6-2. Dendrogram of Temp0Seq samples. Dendrogram showing samples which had Temp0Seq carried out. One sample with a per mapping rate close to the negative controls (outlined in red) was excluded from further analysis.

There was no significant difference in clinicopathological features between the high budding and the control cohorts.

	High budding n (%)	Low budding n (%)	p
Number of patients	24	25	
Age			0.644
≤50 years	9 (37.5)	11 (44.0)	
>50 years	15 (62.5)	14 (56.0)	
Tumour type			0.302
Ductal	23 (95.8)	25 (100)	
Lobular	1 (4.2)	0	
Other	0	0	
Invasive tumour size			0.770
≤20mm	9 (37.5)	9 (36.0)	
21-49mm	12 (50.0)	11 (44.0)	
≥50mm	3 (12.5)	5 (20.0)	
Grade			0.397
I	2 (8.3)	1 (4.0)	
II	7 (29.2)	4 (16.0)	
III	15 (62.5)	20 (80.0)	
Nodal status			0.482
Negative	12 (50.0)	15 (60.0)	
Positive	12 (50.0)	10 (40.0)	
PR			0.551
Positive	1 (4.2)	2 (8.3)	
Negative	23 (95.8)	22 (91.7)	
Missing data	0	1	
HER2			0.322
Negative	15 (62.5)	16 (76.2)	
Positive	9 (37.5)	5 (23.8)	
Missing data	0	4	

Table 6-1. Clinicopathological characteristics of the cohorts. Clinicopathological characteristics of the high budding cohort compared to the low budding cohort.

6.3.2 Clustering

When principle component analysis was carried out for all of the samples, no clear clustering of the high budding samples was observed.

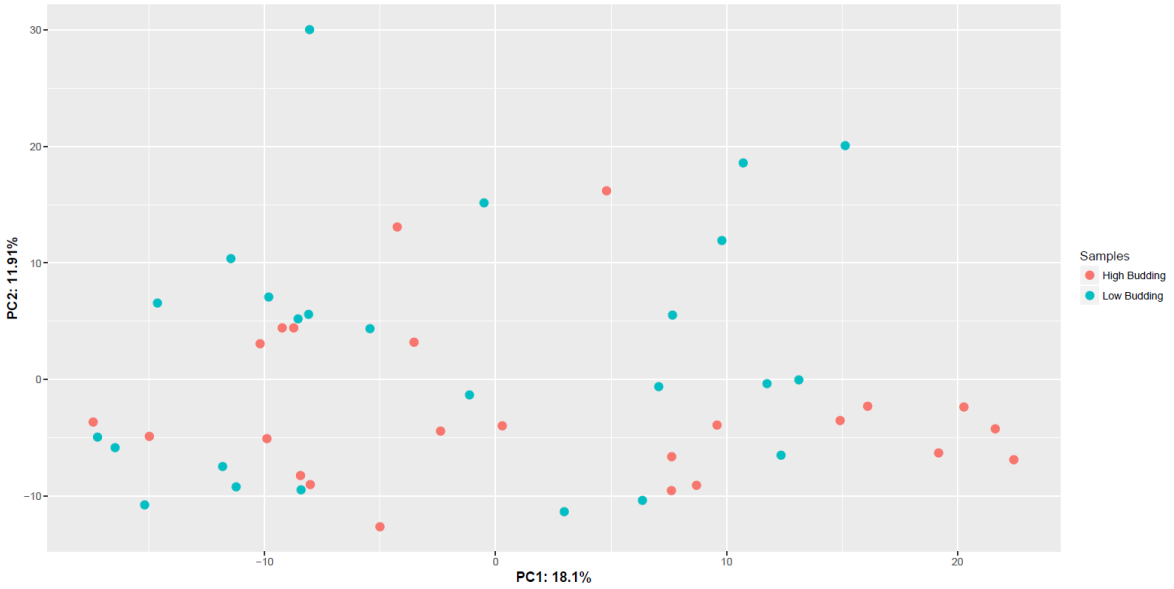

Figure 6-3. Principle component analysis. Scatter plot showing no clear clustering of high budding samples on principle component analysis.

However, when the top 20 or the top 50 genes were analysed (determined by ranking the adjusted p values), clustering of high budding samples was observed, though there was little separation between the groups.

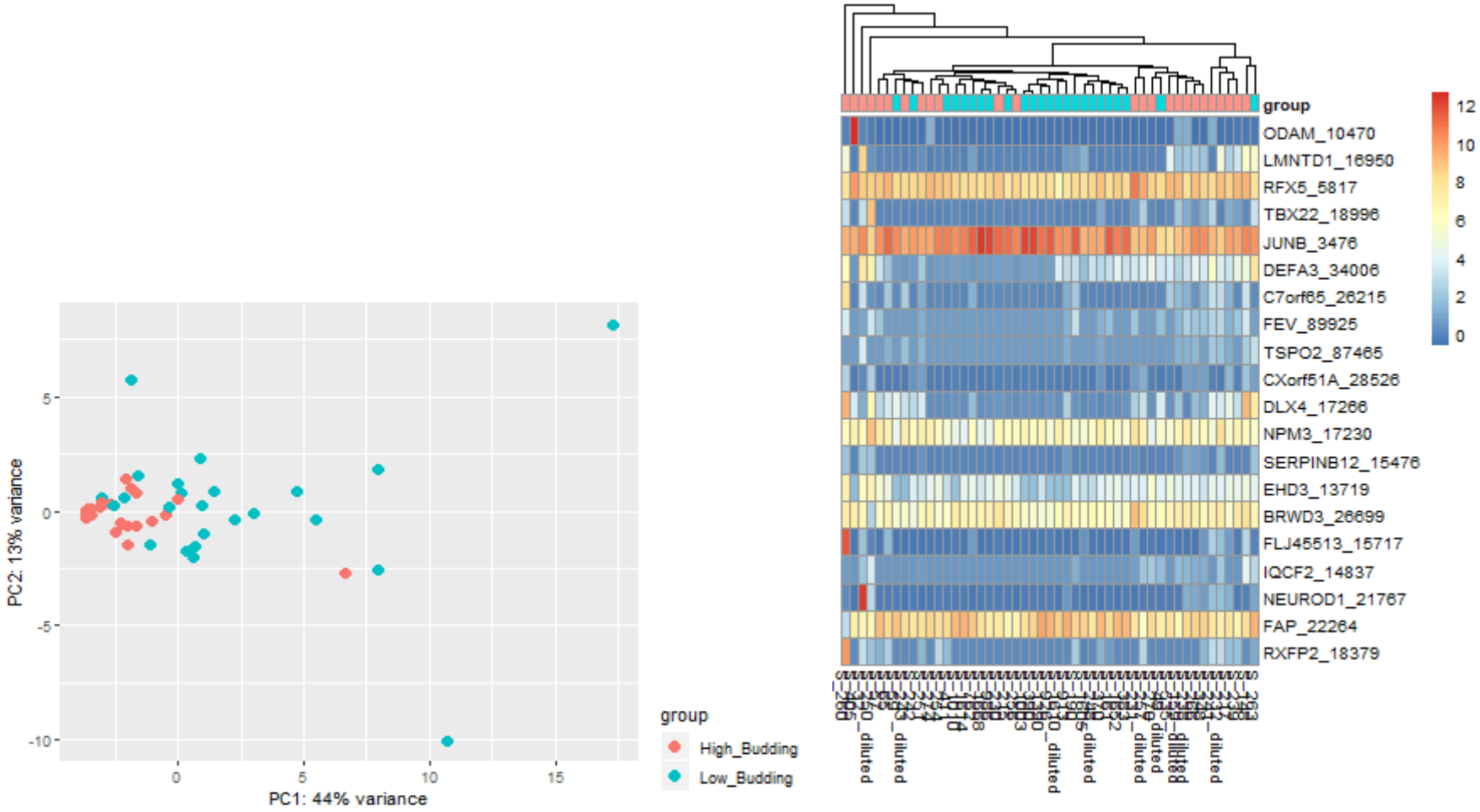

Figure 6-4. Principle component analysis and heat map of top 20 genes. Principle component analysis and heat map of the top 20 differentially expressed genes in high budding tumours compared to low budding tumours, when ranked by adjusted p value.

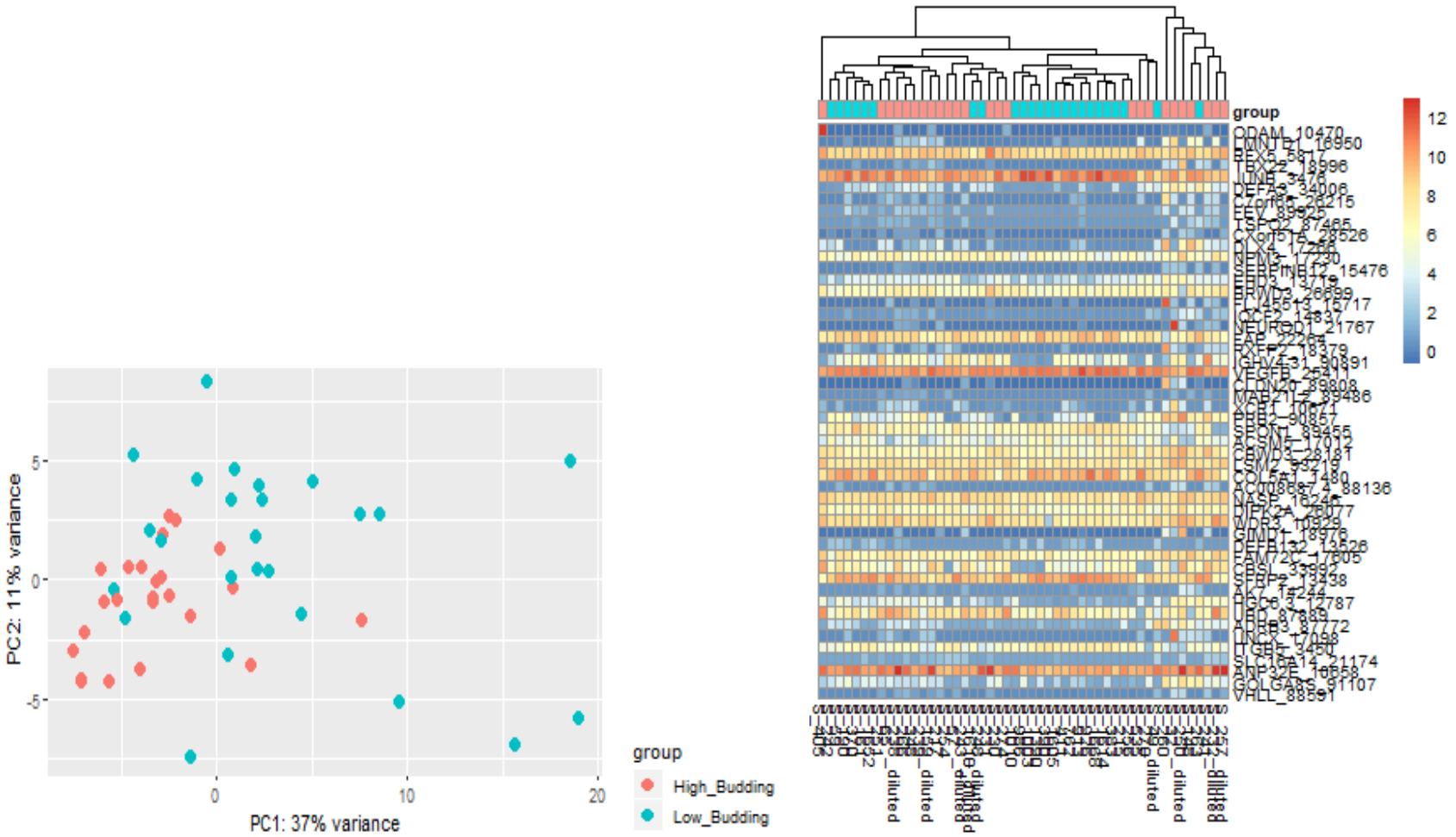

Figure 6-5. Principle component analysis and heat map of top 50 genes. Principle component analysis and heat map of the top 50 differentially expressed genes in high budding tumours compared to low budding tumours, when ranked by adjusted p value

6.3.3 Differential gene expression

On MA plot analysis of the whole genome, 5 genes were differentially expressed, namely ODAM, LMNTD1, RFX5, TBX22 and JUNB (**Figure 6-6**). Despite the low sample size, each of these had statistical significance with adjusted p values <0.05. An additional 4 genes were significantly associated with high tumour budding when significance was defined as p<0.10, namely C7orf65, DEFA3, TSPO2 and FEV (**Table 6-2**). In view of the small sample size, all 9 of these genes were felt to be of interest. JUNB was overexpressed in high budding tumours while the other 8 genes were under-expressed when compared to no/low budding tumours (**Figure 6-7**).

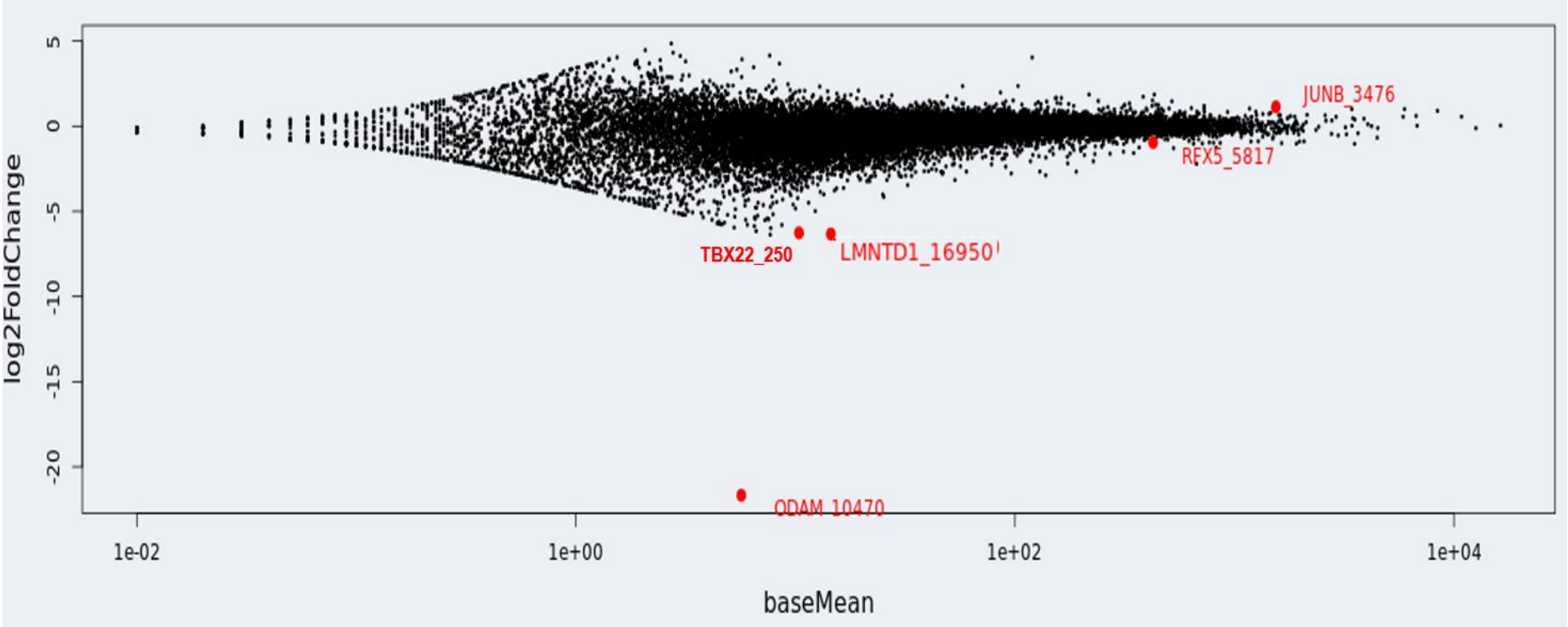

Figure 6-6. Differential gene expression. MA plot showing 5 genes differentially expressed in tumours with high budding.

Gene	Log2 fold change	Adjusted p value
ODAM_10470	-21.67390508	5.08E-10
LMNTD1_16950	-6.327795415	0.001981035
RFX5_5817	-0.957331392	0.005303307
TBX22_18996	-6.266009835	0.019374302
JUNB_3476	1.133353948	0.045423795
C7orf65_26215	-4.981285379	0.07858763
DEFA3_34006	-3.458724686	0.07858763
TSPO2_87465	-5.446552656	0.079250702
FEV_89925	-4.599240538	0.079250702

Table 6-2. Genes associated with high budding. Table to show genes significantly associated with high tumour budding (adjusted p<0.10) with log 2 fold change (negative value = gene under-expressed in high budding samples, positive value = gene over expressed in high budding samples).

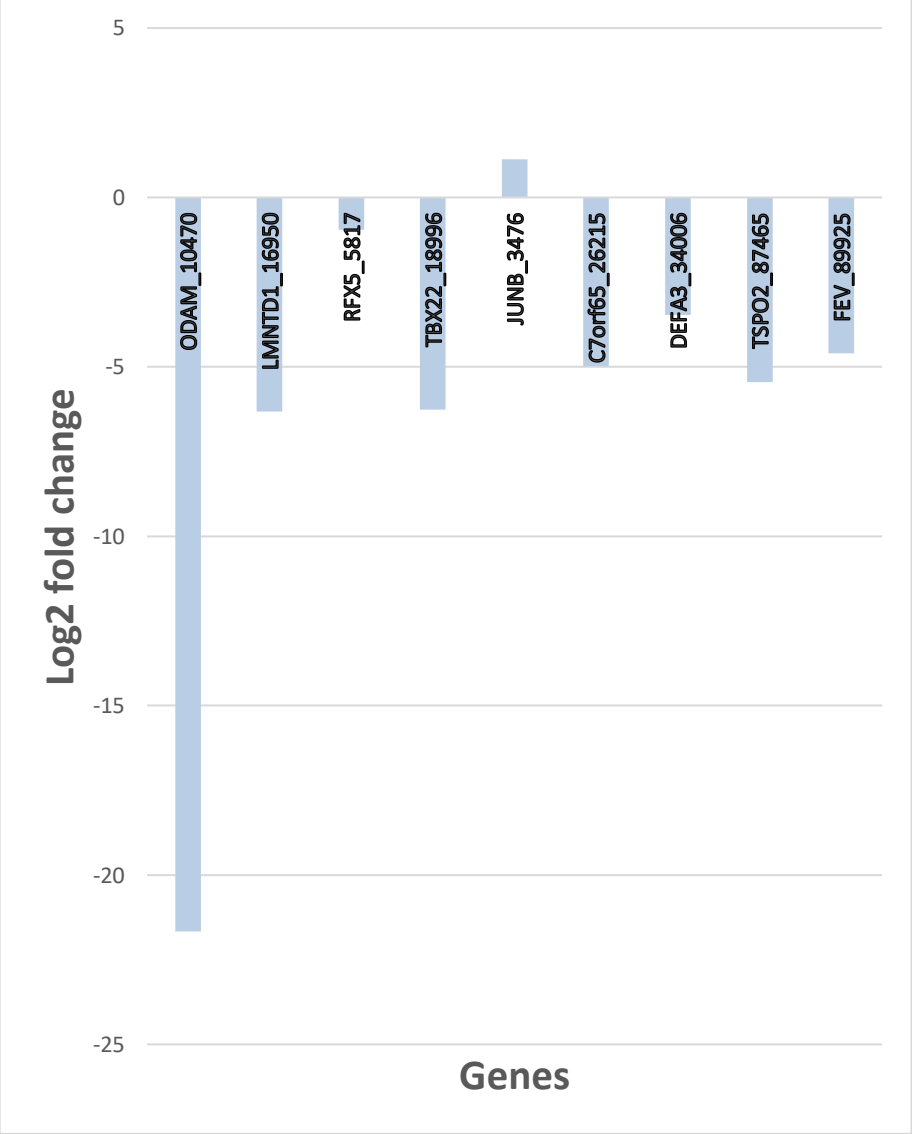

Figure 6-7. Log2 fold changes of genes associated with high tumour budding. Genes significantly (adjusted p<0.10) associated with high tumour budding. Negative log2 fold change indicates gene under-expression, positive log2 fold change indicates gene overexpression.

The top 20 under-expressed genes when ordered by log2fold change, regardless of adjusted p value, are shown in **Table 6-3** and **Figure 6-8**.

Gene	Log2 fold change	Adjusted p value
CXorf51A_28526	-5.469168841	0.137760652
CACNA2D3_10872	-5.495757679	0.411760366
AK7_14244	-5.497712438	0.274411945
B3GNT6_16482	-5.522703217	0.624087369
MUC5AC_33972	-5.603885245	0.753514367
SMR3A_25046	-5.666009126	0.28611906
OR2A5_24846	-5.69576121	0.411760366
OR2T33_28562	-5.717346908	0.411933075
IQCF6_18544	-5.753724239	0.742692709
ABCG2_25072	-5.759850284	0.476318603
RPL10L_21828	-5.788856054	0.382662613
FLJ45513_15717	-5.800807318	0.137760652
SERPINB12_15476	-5.870567158	0.137760652
LGALS16_12287	-5.950707368	0.411760366
NEUROD1_21767	-5.988195633	0.137760652
GIMD1_18976	-6.159071965	0.224803823
TBX22_18996	-6.266009835	**0.019374302**
LMNTD1_16950	-6.327795415	**0.001981035**
CLDN20_89808	-6.369118435	0.186675354
ODAM_10470	-21.67390508	**5.08E-10**

Table 6-3. Top 20 downregulated genes. 20 downregulated genes with highest log2 fold change, regardless of adjusted p value. P values <0.10 are highlighted in bold.

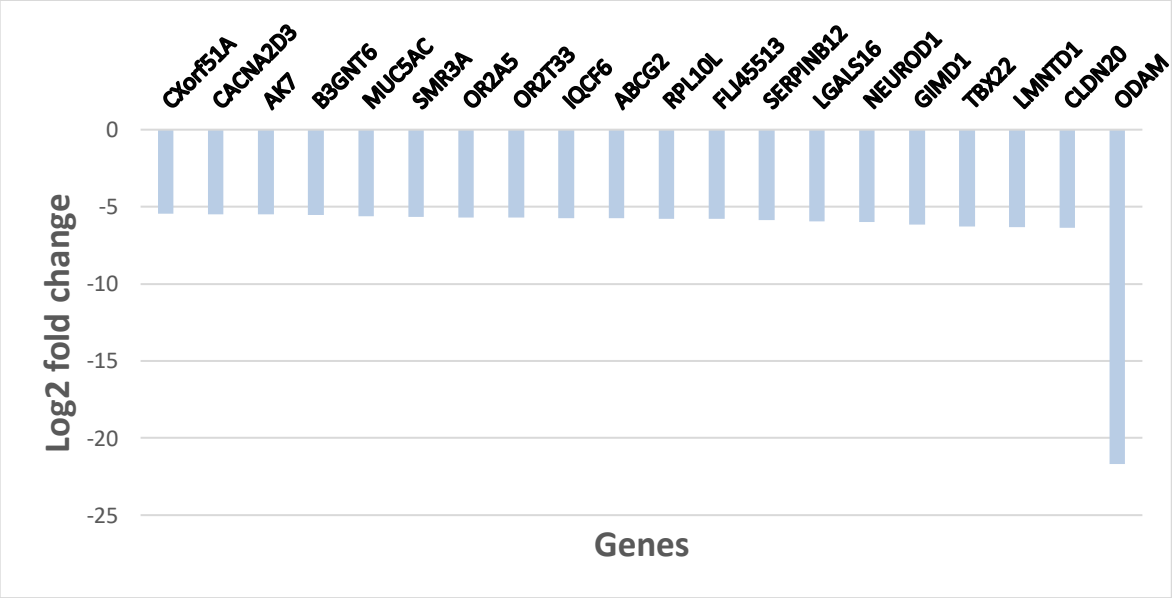

Figure 6-8. Top 20 under-expressed genes. The top 20 under-expressed genes in high budding tumours, ranked by log2 fold change regardless of adjusted p value.

The top 20 over-expressed genes when ordered by log2fold change, regardless of adjusted p value, are shown in **Table 6-4** and **Figure 6-9**.

Gene	Log2 fold change	Adjusted p value
TMEM80_12837	4.857853809	0.722280467
MMP27_26120	4.468012524	0.751797539
TSLP_15791	4.315909273	0.753514367
DEFB132_13526	4.146491249	0.224803823
IGSF22_87763	4.126676816	0.741406955
LGALS9C_33893	4.044036848	0.842257468
CLEC3A_89796	4.040631403	0.476318603
KRT13_90016	3.923890453	0.671678235
SKP1_92580	3.917842063	0.796037379
OR13C8_26182	3.914452784	0.886439732
KCNK18_18748	3.885310945	0.759464518
IL12A_16427	3.850510942	0.771821104
GAGE12H_33626	3.813749585	0.826923871
CLEC12B_12546	3.758917401	0.796037379
ANXA10_10678	3.733644368	0.886439732
CCDC197_88898	3.692522362	0.797471532
PSG4_25648	3.679085901	0.551401805
ZNF577_13278	3.668203113	0.841522977
SERPINA2_18838	3.652173389	0.90766013
ZNF257_12562	3.638369425	0.769561568

Table 6-4. Top 20 upregulated genes. 20 upregulated genes with highest log2 fold change, regardless of adjusted p value. None had p<0.10.

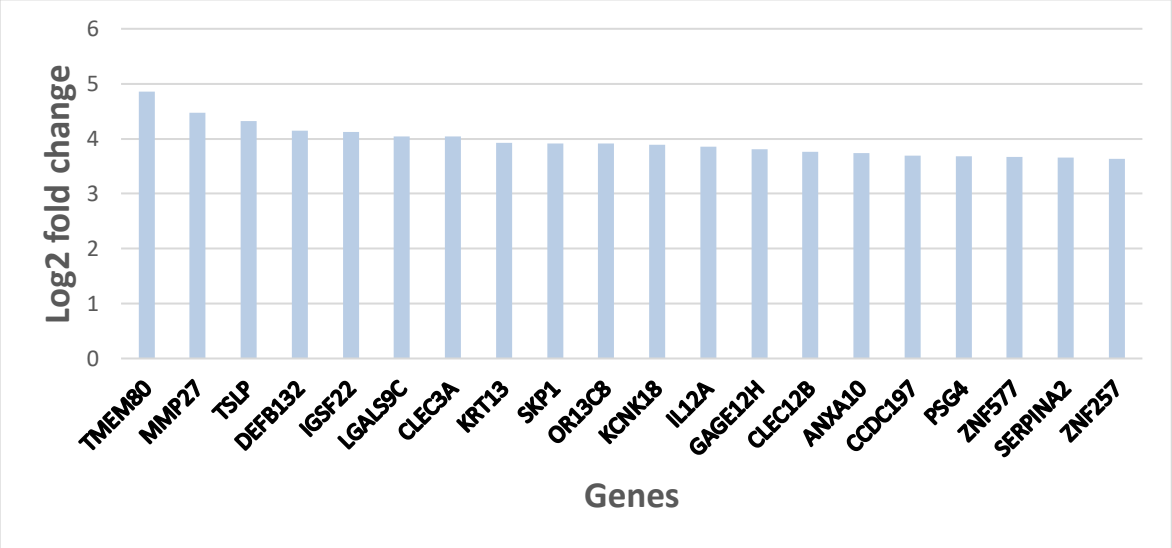

Figure 6-9. Top 20 over-expressed genes. The top 20 over-expressed genes in high budding tumours, ranked by log2 fold change regardless of adjusted p value.

6.3.4 EMT-associated gene expression

As tumour budding has been hypothesised to be related to EMT, EMT associated genes were investigated for their association with tumour budding. The top 20 EMT-associated genes as reported by Zhao and colleagues(244) were selected for analysis. None were associated with high tumour budding either by the definition

of an adjusted p value <0.10 or a log2 fold change of ≥2 in either direction (**Table 6-5, Figure 6-10**).

Gene	Log2 fold change	Adjusted p value
SMAD2_87442	-0.452939559	0.497826542
ERBB2_88307	1.008340544	0.821898969
SMAD7_12470	0.323588783	0.852885718
ILK_28806	-0.247318142	0.867154666
SMAD4_6563	0.557366798	0.882828754
ZEB2_23804	0.309804472	0.893189103
CTNNB1_1633	-0.223141521	0.941573573
SNAI1_24734	-0.542307579	0.949082394
EPAS1_16750	0.392035561	0.952696439
ZEB1_7834	1.030299905	0.973028805
MET_4125	1.196778837	0.973028805
IGF1R_3254	-0.224919614	0.973541439
HIF1A_2945	-0.240403247	0.974907314
SMAD3_6562	0.172699357	0.977577551
TWIST1_20872	0.259923553	0.981902443
AKT1_210	0.192725573	0.981928361
CDH1_1186	0.191330577	0.99417153
EGFR_2063	-0.01669307	0.99963455
SNAI2_24257	0.039971503	0.99963455
TGFB1_27949	-0.052067202	0.99963455

Table 6-5. Top 20 EMT-associated genes. None of the top 20 EMT-associated genes were significantly associated with tumour budding.

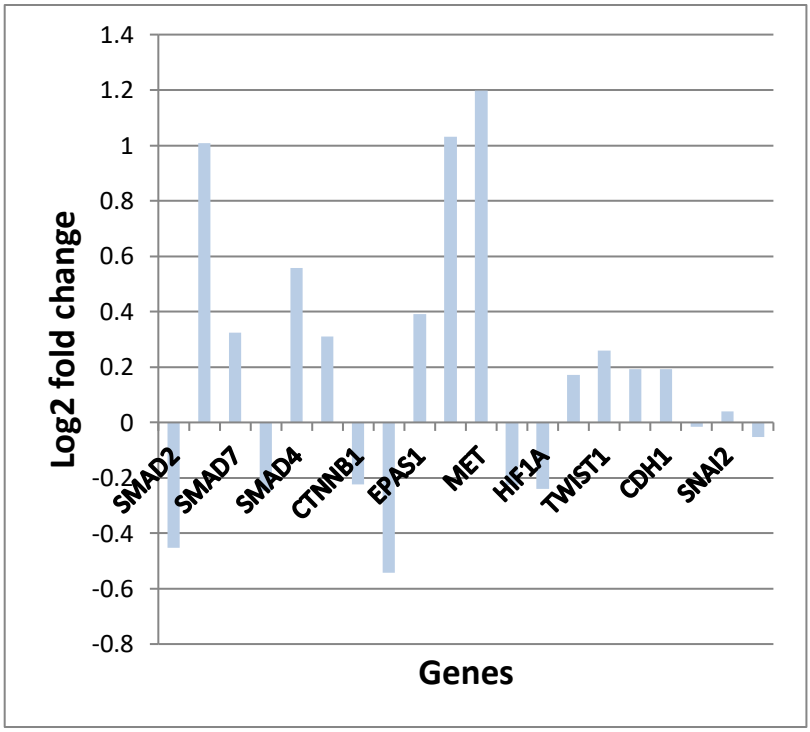

Figure 6-10. Top 20 EMT-associated genes. Differential expression of the top 20 EMT-associated genes in high budding compared to low budding tumours.

6.3.5 Proliferation-associated gene expression

As tumour grade was associated with tumour budding in the previous chapter, proliferation-associated genes were investigated for their relationship with tumour budding. When the genes in the proliferation signature described by Whitfield and colleagues(245) were investigated, none were associated with high tumour budding either by the definition of an adjusted p value <0.10 or a log2 fold change of ≥2 in either direction. The top 20 over or under-expressed genes by log2 fold change are shown in **Table 6-6** and **Figure 6-11** below.

Gene	Log2 fold change	Adjusted p value
CCNE1_1070	0.678180781	0.985609972
MCM6_20957	-0.694336338	0.943562789
MYB_4387	-0.701375987	0.90766013
NASP_16246	-0.705365677	0.216058692
CTPS1_1637	-0.730483094	0.973028805
CDC25C_19441	-0.762438101	0.937246645
CCNB1_1053	-0.76561175	0.933863281
PLK1_5203	-0.830012122	0.782518966
DDX11_13416	-0.831243629	0.794354392
BIRC5_709	-0.835264684	0.969543647
MKI67_28355	-0.882138149	0.86676989
PCNA_4987	-0.953452259	0.923181684
PRIM1_26195	-0.99540237	0.963299143
CDC7_19277	-1.028263705	0.854708164
CKS2_92658	-1.127034735	0.794420592
MCM4_4075	-1.128666354	0.538745025
FEN1_2387	-1.165960135	0.616891593
TYMS_21327	-1.250112629	0.285286658
CENPF_1252	-1.330196597	0.654022047
RRM2_25733	-1.5905154	0.652488961

Table 6-6. Top 20 proliferation-associated genes. None of the top 20 proliferation-associated genes were significantly associated with tumour budding

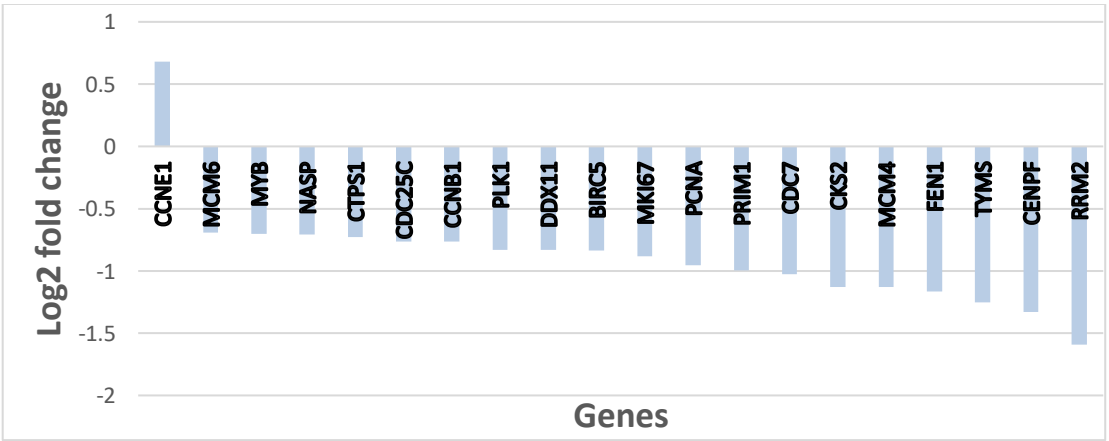

Figure 6-11. Top 20 proliferation-associated genes. Differential expression of the top 20 proliferation-associated genes in high budding compared to low budding tumours.

6.3.6 Inflammation-associated gene expression

In the previous chapter, tumour budding was associated with inflammatory cell infiltrate (Klintrup Makinen grade). Therefore, inflammation-associated genes were investigated for their association with tumour budding. A 17 gene immunity signature reported by Yang and colleagues(246) was selected for investigation. None of the genes were associated with high tumour budding either by the definition of an adjusted p value <0.10 or a log2 fold change of ≥2 in either direction (**Table 6-7, Figure 6-12**).

Gene	Log2 fold change	Adjusted p value
APOBEC3G_11453	0.893210897	0.987131933
CD52_13919	0.27300838	0.979645955
CD2_12308	0.22581409	0.994963222
PTPRC_5605	-0.026939881	0.99963455
GZMK_88700	-0.124475363	0.99963455
PRKCB_17133	-0.300826428	0.981134553
CORO1A_1507	-0.321342479	0.95861623
LCK_21336	-0.345390724	0.971033723
CD3D_1127	-0.50031214	0.949624064
CXCL9_88188	-0.549216484	0.969543647
CD27_87841	-0.6885763	0.893189103
GZMA_88696	-0.761682536	0.783113889
HLA-DMA_27315	-0.848189727	0.852514812
IL2RG_15624	-0.885880944	0.92493824
CCL5_24896	-1.327594711	0.725985453
SH2D1A_20738	-1.454421351	0.933863281
CCR2_88510	-1.744589821	0.59940306

Table 6-7. Immunity-associated genes. None of the 17 immunity-associated genes were significantly associated with tumour budding

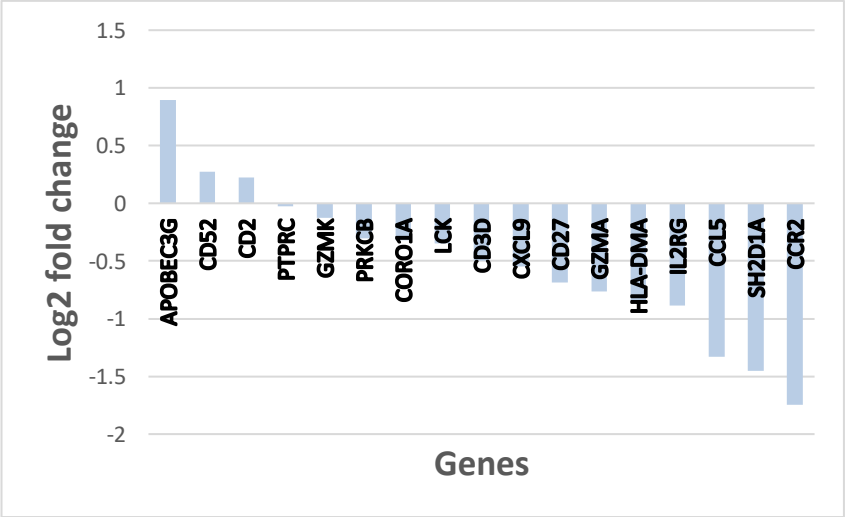

Figure 6-12. Immunity-associated genes. Differential expression of 17 immunity-associated genes in high budding compared to low budding tumours.

6.3.7 Stromal-associated gene expression

As TSP was associated with budding in the previous work, stromal-associated genes were investigated for their association with tumour budding. The top 20 genes (by adjusted p value) in a stromal gene signature described in breast cancer by Winslow and colleagues(247) were selected for investigation. None were associated with tumour budding either by the definition of an adjusted p value <0.10 or a log2 fold change of ≥2 in either direction (**Table 6-8, Figure 6-13**).

Gene	Log2 fold change	Adjusted p value
SFRP2_13438	1.014523743	0.258785
MMP2_4213	0.894817655	0.864873
COL1A2_20081	0.847423878	0.436128
DCN_27099	0.809936235	0.780617
POSTN_20868	0.706350757	0.71678
VCAN_20627	0.698025242	0.551402
DPT_26697	0.674431459	0.790799
COL6A3_13292	0.638170904	0.637922
MMP2_27519	0.635171355	0.583813
COL1A1_1466	0.602504943	0.782467
LUM_17157	0.547305097	0.795848
DCN_27098	0.534879101	0.826924
DCN_1779	0.451157342	0.939316
CTSK_10977	0.430861127	0.848861
CDH11_23329	0.398191959	0.904628
IGLV6-57_89187	0.372736537	0.999635
IGHA1_88367	-0.052550726	0.999635
IGKV1-5_3282	-0.257571765	0.999635
IGLJ3_91164	-0.284814175	0.999635
LOC652493_3838	-0.374086124	0.98561
CCL19_88586	-0.401966663	0.969544
IL7R_3347	-0.479979314	0.977862

Table 6-8. Stroma-associated genes. None of the stroma-associated genes studied were significantly associated with tumour budding

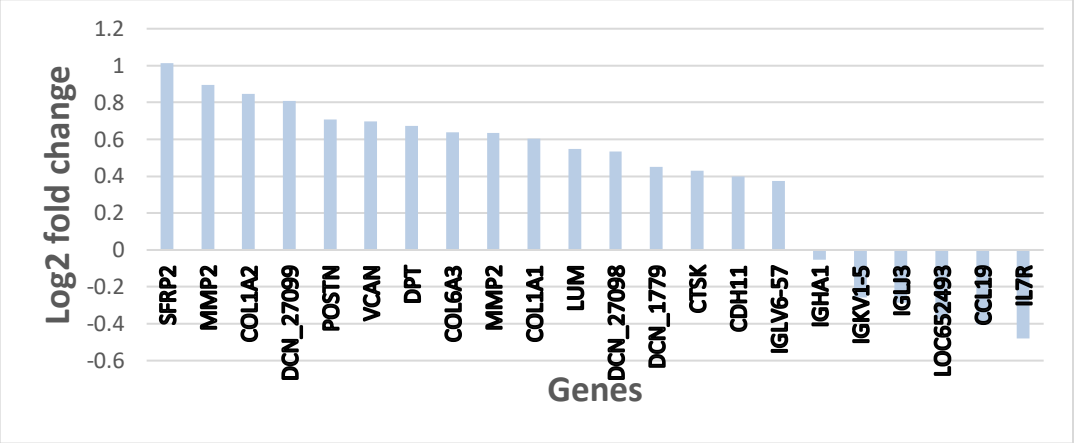

Figure 6-13. Stroma-associated genes. Differential expression of the top 20 proliferation-associated genes in high budding compared to low budding tumours.

6.4 Discussion

This exploratory pilot study of 50 ER negative breast tumours has identified 9 genes associated with tumour budding which warrant further investigation, namely ODAM, LMNTD1, RFX5, TBX22, JUNB, C7orf65, DEFA3, TSPO2 and FEV.

ODAM (Odontogenic ameloblast associated protein) showed the greatest differential expression in this cohort, with under-expression by a log2 fold change of -21.7 in high budding tumours compared to no/low budding tumours. ODAM is a constituent protein of calcifying epithelial odontogenic, glandular and epithelial tissues(248). It is a tight-junction protein which contributes to cell adhesion. There is evidence for a regulatory role in breast cancer tumourigenesis. *In vitro* studies of triple negative MDA-MB-231 breast cancer cells reported that ODAM expression resulted in increased rates of apoptosis, increased adhesion to extracellular matrices, increased cell aggregate formation, reduced cell proliferation (also in MCF-7) reduced migration and invasiveness(249). *In vivo*, ODAM expression in MDA-MB-231 tumours was associated with greatly reduced tumour growth and greatly reduced pulmonary metastatic disease. The tumours had reduced Ki-67 expression and higher levels of caspase-3. The authors of the study suggest that the regulatory effects of ODAM may in part be due to inhibition of Runx2(249). Nuclear ODAM expression has been reported to be associated with improved 5 year survival in breast cancer patients(250).

Under expression of LMNTD1 (lamin tail domain-containing protein 1) was also significantly associated with high tumour budding (log2 fold change -6.32, p=0.002). There is very limited literature related to the role of LMNTD1 in normal or cancer cells. It is however considered to be part of the Pas1c1 gene which is a locus on chromosome 6 which has been implicated in lung cancer in mice(251-253).

Under expression of RFX5 (Regulatory factor X5) was significantly associated with high tumour budding (log2 fold change -0.96, p=0.005). It is a transcriptional activator which has a role in lymphocyte development and, in particular, transcription of the alpha and beta chains of MHC class II(254, 255). This finding

therefore may be relevant to the finding in the previous chapter of an association between tumour budding and KM grade.

Under-expression of TBX22 (T-box transcription factor 22) was associated with high tumour budding (log2 fold change -6.27 p=0.019). The gene encodes a T-box-containing transcription factor, a family of transcription factors which are involved in developmental processes. Mutations in this gene are implicated in X-linked cleft palate(256) and therefore the bulk of available research into this gene is in that field. There is little available literature regarding the role of this gene in cancer. One small Iranian study of colorectal cancers did report it as one of the 10 most amplified markers(257). Conversely, an earlier American study reported TBX22 to be one of the most frequently deleted genes in colorectal cancer(258). Its role in tumourigenesis is currently unknown.

The only gene to be significantly overexpressed in tumours with high budding was JUNB (Transcription factor jun-B) (log2fold change 1.13, p=0.045). In normal cells it is thought to be a growth-arrest mediator with a negative effect on proliferation(259). A recent study in breast cancer reported over-expression of JUNB in circulating tumour cells and in metastases when compared to the primary tumour and has reported its association with poor prognosis(260). Studies have suggested a critical role for JUNB in EMT(261, 262). Another has demonstrated induction of JUNB in response to kinase inhibitors and therefore has suggested a role for the gene in the development of chemotherapy resistance(263). Similarly, it has been implicated as an oncogene in NSCLC(264). Conversely, in other malignancies such as lymphoma, it is postulated to be an anti-oncogene(265).

The other 4 genes significantly under-expressed (when $p<0.10$ rather than 0.05) in high budding tumours were the uncharacterised C7orf65 (Chromosome 7 Open Reading Frame 65), DEFA3 (Defensin Alpha 3) which encodes a protein found in the microbicidal granules of neutrophils(266), TSPO2 (Translocator Protein 2) which binds cholesterol and mediates its redistribution during erythropoiesis(267), and FEV (Fifth Ewing Variant) which is a member of the ETS transcription family and functions as a transcription repressor(268). There is very limited published literature relating to these genes in cancer.

In summary, 9 genes were significantly associated with tumour budding in our study, but 2 are of particular interest in the context of the published literature. Under-expression of ODAM may lead to reduced cell adhesion and increased migration and invasiveness, resulting in the identifiable phenotype of tumour budding. Over-expression of JUNB may be significant in the EMT process thought to be strongly related to budding, and the high expression levels in CTCs and metastases compared to the primary tumour, reported in the literature, support its role in the process of EMT, budding and metastases development.

Despite the identification of differential expression of these genes, clear clustering of genes in high budding patients was not observed. There are several possible reasons for this. There may have been signal dilution as full sections of tumour were used, rather than just analysing the invasive edge where budding takes place. Secondly, it may be that a transient signal occurs which is gone by the time the tumour displays the high budding phenotype. Another possible explanation is that the budding phenotype is not controlled at the gene transcription level but further downstream in cell signalling pathways. Furthermore, the very small numbers in the study will have limited the power of the study to detect significant differences and may explain why no significant findings resulted from the biased analysis.

In conclusion, this small pilot study has identified 9 genes which merit further investigation in relation to tumour budding in ER negative breast cancer, with ODAM and JUNB of particular interest. It has validated the use of the TempOSeq technique in this context and these results should be validated in larger cohorts. The lab group is currently using this data to apply for funding to enable this further work.

7 IL6 and the IL6 receptor in primary operable breast cancer.

7.1 Introduction

Thus far, this thesis has examined the relationships between cancer outcomes and markers of the systemic inflammatory response, the local inflammatory infiltrate, and specific phenotypic features of the tumour and tumour microenvironment. As examples, the neutrophil-lymphocyte ratio, TILs and specifically CD8+ T lymphocytes, and tumour budding have been observed to be associated with CSS. The question therefore arises as to what may link the observed prognostic association of certain inflammatory cells with the poor prognostic associations observed with certain tumour phenotypic features such as necrosis and budding. Cell signalling pathways link external stimuli such as cytokines within the tumour microenvironment with signalling pathways and hence gene expression in tumour cells.

The IL6/JAK/STAT3 pathway is one such pathway. As described in chapter 1, the JAK/STAT3 pathway can be stimulated by numerous ligands, including IL-6. Il-6 binds to the IL6 receptor (IL6R) which may be either membrane-bound or soluble and induces homodimerization of gp130. Receptor-associated JAKs are then activated and can phosphorylate each other as well as allowing autophosphorylation by phosphorylating the intracellular portion of their receptors and other signalling proteins such as STAT3 when in the cytoplasm, permitting STAT3 dimerisation and its translocation to the nucleus where it can bind to regulatory DNA sequences.

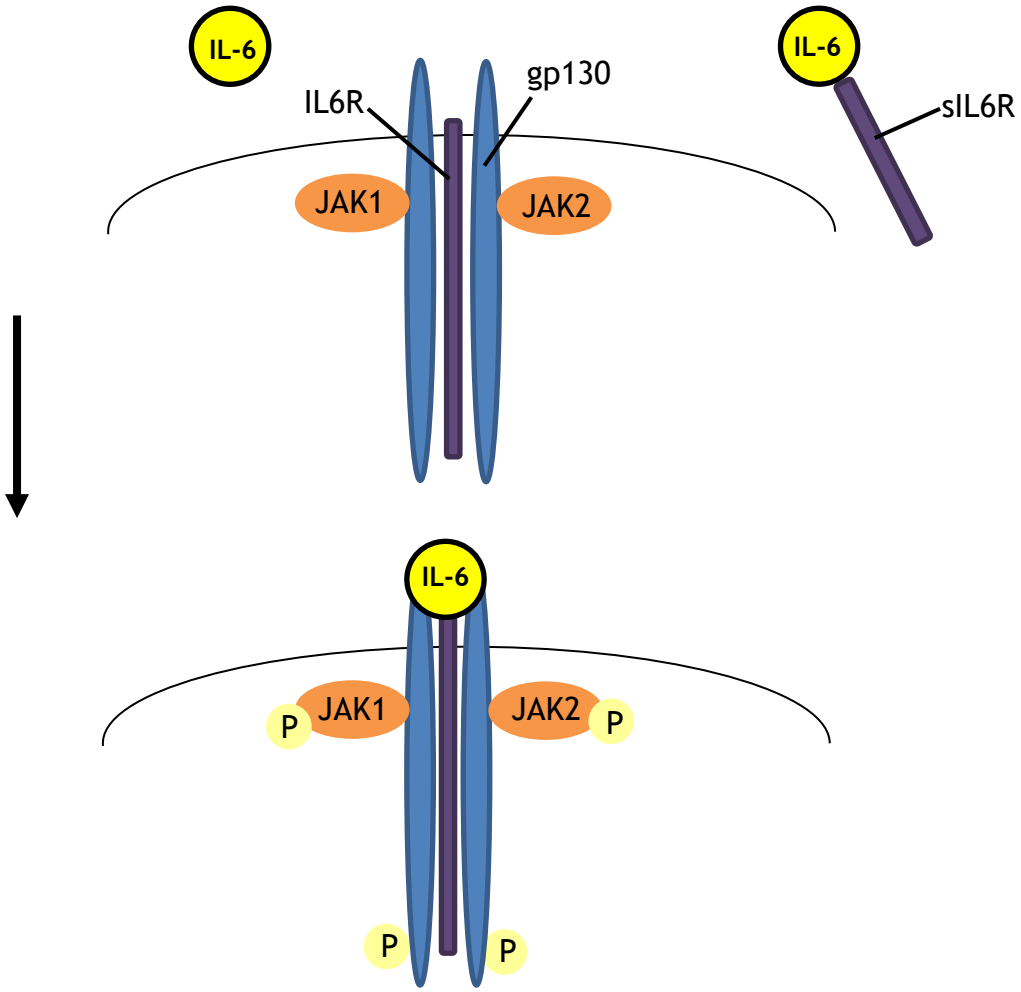

Figure 7-1. Initiation of the IL6/JAK/STAT3 pathway. Diagram illustrating the first stage of the Il6/JAK/STAT3 pathway. IL6 binds with the IL6 receptor leading to activation of JAKs which phosphorylate each other and phosphorylate tyrosine residues of the membrane-bound receptor.

Il-6 is a cytokine with numerous and varied functions including roles in metabolism, haematopoiesis, organ development, immune and inflammatory responses(269). It is produced by immune cells, fibroblasts and various tumour cells(270-272). In classical signalling it binds to the membrane-bound IL6R, which is only expressed by certain cells in the body including hepatocytes and certain immune cells such as macrophages, neutrophils and CD4+ T cells(269). Signal transduction is then mediated by gp130. In the alternative pathway, termed trans-signalling, IL-6 binds to soluble IL6R (sIL6R) and these complexes then have the potential to activate all cells due to the ubiquitous expression of gp130(273). In its most simplistic view, classical signalling has generally been accepted as having anti-inflammatory and regenerative roles whereas trans-signalling has been ascribed a pro-inflammatory role(273). The true situation is likely to be more complex than this however.

In cancer, a role for IL6 in progression and metastatic spread has been recognised(270, 274-277) due to its actions within the tumour microenvironment(275). IL6/IL6R/gp130 blockade is therefore a potential therapeutic option in cancer and various agents have been investigated in certain cancers(270), though rarely in breast cancer to date. However, a number of studies have investigated the role of IL6 in breast cancer. An association between high serum levels of IL6 and poorer prognosis has been reported(270, 274, 278-281). A degree of dependence on IL6 for growth and progression has been observed in breast cancer, particularly in HER2+ and triple negative subtypes(282). IL6 is secreted both by the breast cancer cells themselves and by cells within the tumour microenvironment such as CAFs and mesenchymal stem cells(277, 283-286). IL6 has also been implicated in treatment resistance(287-289). It is therefore important to develop our understanding of the actions of IL6/IL6R/gp130 in breast cancer as it may represent a promising therapeutic target.

With the evidence above in mind, for the present study it was postulated that high expression of IL6 and Il6R would be associated with poorer CSS. Whether IL6 is predominantly expressed in the tumour cells or stromal cells is of interest to try to understand the mechanisms driving tumour growth, The study aimed to describe the expression and distribution of IL6 and IL6R in tumour cells and in the stroma, their associations with each other, with other features of the tumour and tumour microenvironment, and with cancer outcomes in primary operable breast cancer.

7.2 Materials and methods

7.2.1 Patient cohort

The 1800 cohort was used for this study as tissue blocks were available for cutting of a previously constructed TMA. Patient characteristics are detailed in chapter 2.

7.2.2 IL6 expression

7.2.2.1 RNA scope

Due to the secreted nature of IL6, previous efforts in the lab to stain and quantify IL6 expression in cells using IHC were unsuccessful. Therefore for this study, RNA scope, which assesses mRNA expression rather than protein expression, was used to stain fresh TMA slides. The technique is described in chapter 2. TMAs were stained in triplicate.

7.2.2.2 Quantifying expression

Stained slides were scanned and subsequently analysed using HALO™ Image Analysis Software, as described in chapter 2, to quantify probe expression of both IL6 and the housekeeper gene. A normalised ratio (IL6/HK ratio) was formed as described in chapter 2 and used in the analysis.

7.2.3 IL6R expression

7.2.3.1 TMA slide staining and scanning

TMAs were stained in triplicate for IL6R using the IHC technique and antibody detailed in chapter 2. They were scanned into Slidepath software as previously described.

7.2.3.2 Scoring for IL6R expression

Each TMA core was scored by the author using the weighted histoscore method described in chapter 2. Cores which were assessed visually to have >20% of the core missing were not scored. As the IL6 receptor can be membrane-bound or soluble, IL6R expression in tumour cells was scored separately for membranous and cytoplasmic expression. A separate score was also given for expression in stromal cells (differentiation between membranous and cytoplasmic expression in these smaller cells was not reliably possible at 20x magnification).

7.2.4 Molecular subtyping

ER, PR, HER2 and Ki67 profiling had previously been carried out in the lab for this cohort. This data was used to divide the cohort into the four main molecular subtypes of breast cancer, as detailed in chapter 1, for subgroup analysis.

7.2.5 Statistical analysis

Initial analysis using ROC curves and division into tertiles and at the median was carried out to determine the optimum threshold for division into high and low expression groups for further analysis. Analysis of associations with clinicopathological characteristics and with cancer specific survival was carried out as described in chapter 2. This analysis was carried out initially in the full cohort, then in the ER positive and ER negative cohorts separately, and subsequently in the 4 individual molecular subtypes.

7.3 Results

7.3.1 Formation of the cohort for IL6 analysis

Of 850 patients in the cohort, 702 had at least one core assessable for tumour and stromal counts of IL6, while 649 had at least one assessable core for tumour and stromal HK gene probe counts. 645 had calculable tumour IL6/HK ratios and all 649 had calculable stromal IL6/HK ratios.

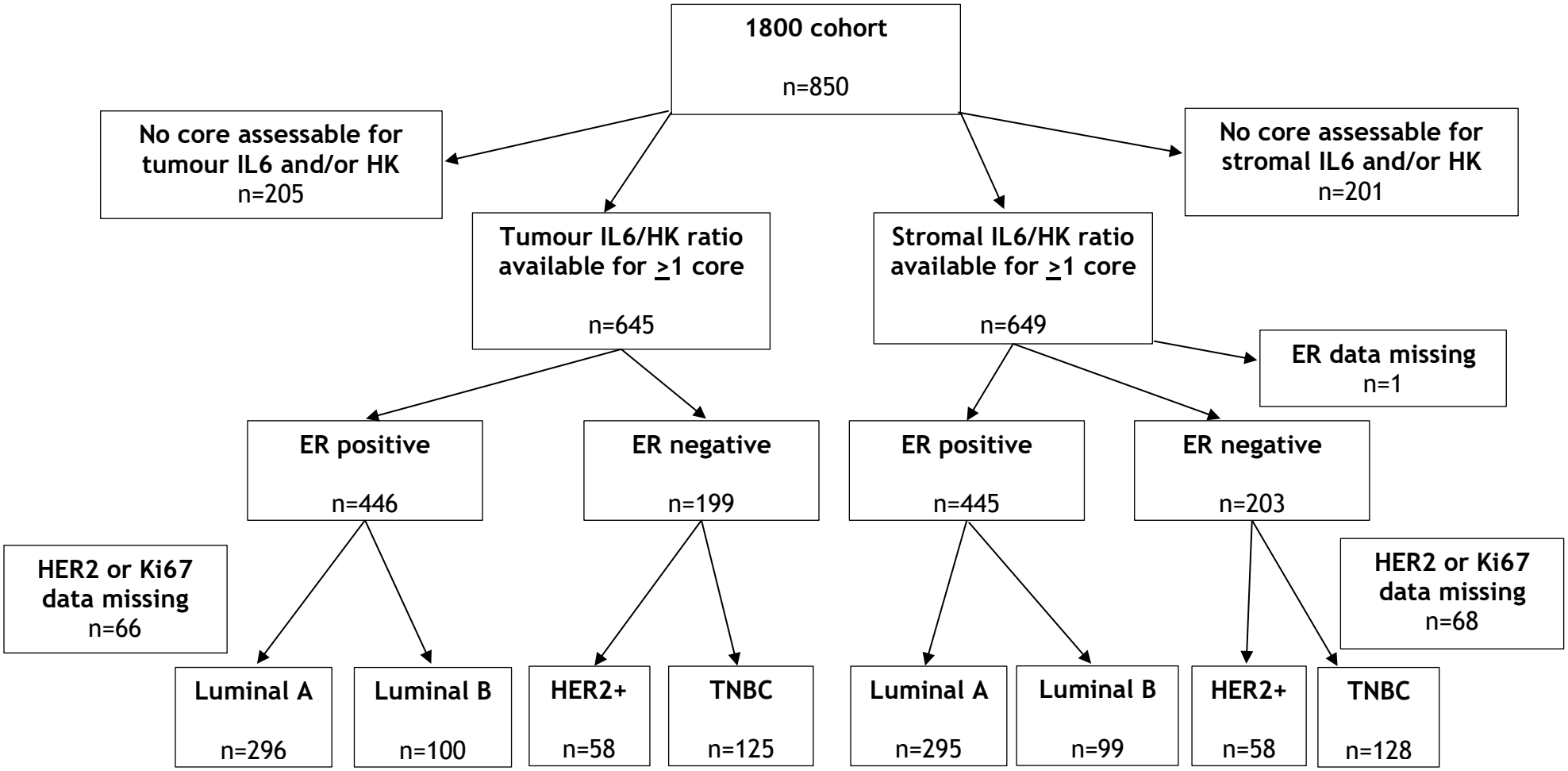

Figure 7-2. Formation of the IL6 cohort. Flow diagram to illustrate the number of patients within the 1800 cohort with at least 1 core which was assessable for IL6 and the housekeeper gene for tumour expression and separately for stromal expression. The numbers available for subgroup analysis by ER status and by molecular subtype are also shown.

7.3.2 IL6 expression

On initial visual inspection of the stained TMA slides, IL6 staining was often present in clusters which could be both in the tumour and the stroma, while in others the staining was sparse. Examples of both are shown below.

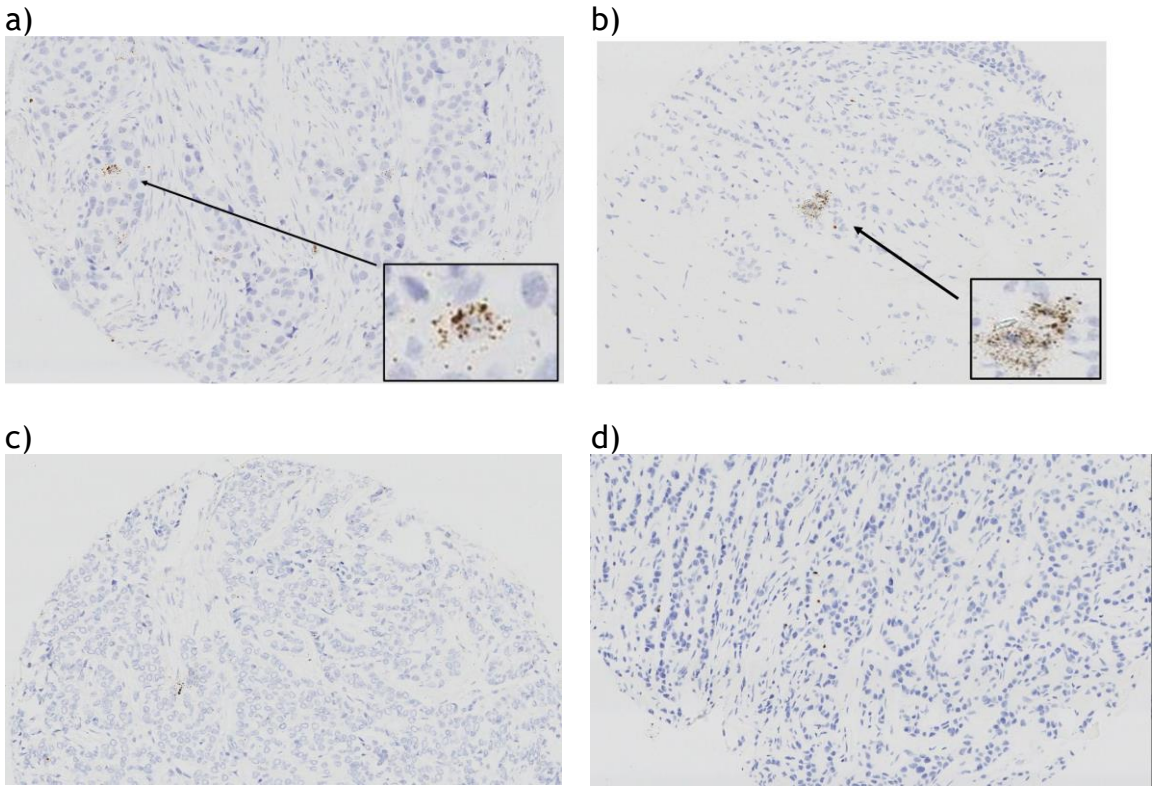

Figure 7-3. TMA cores stained for IL6. Images of TMA cores stained using the RNA scope technique for IL6. a) and b) demonstrate clustering of staining while c) and d) display sparser staining.

The median IL6/HK ratio in tumour was 0.06 (0.00-534.69). Overall, IL6 was more highly expressed in stroma with a median IL6/HK ratio of 0.11 (0.00-170.42), though the range was greater for tumour expression.

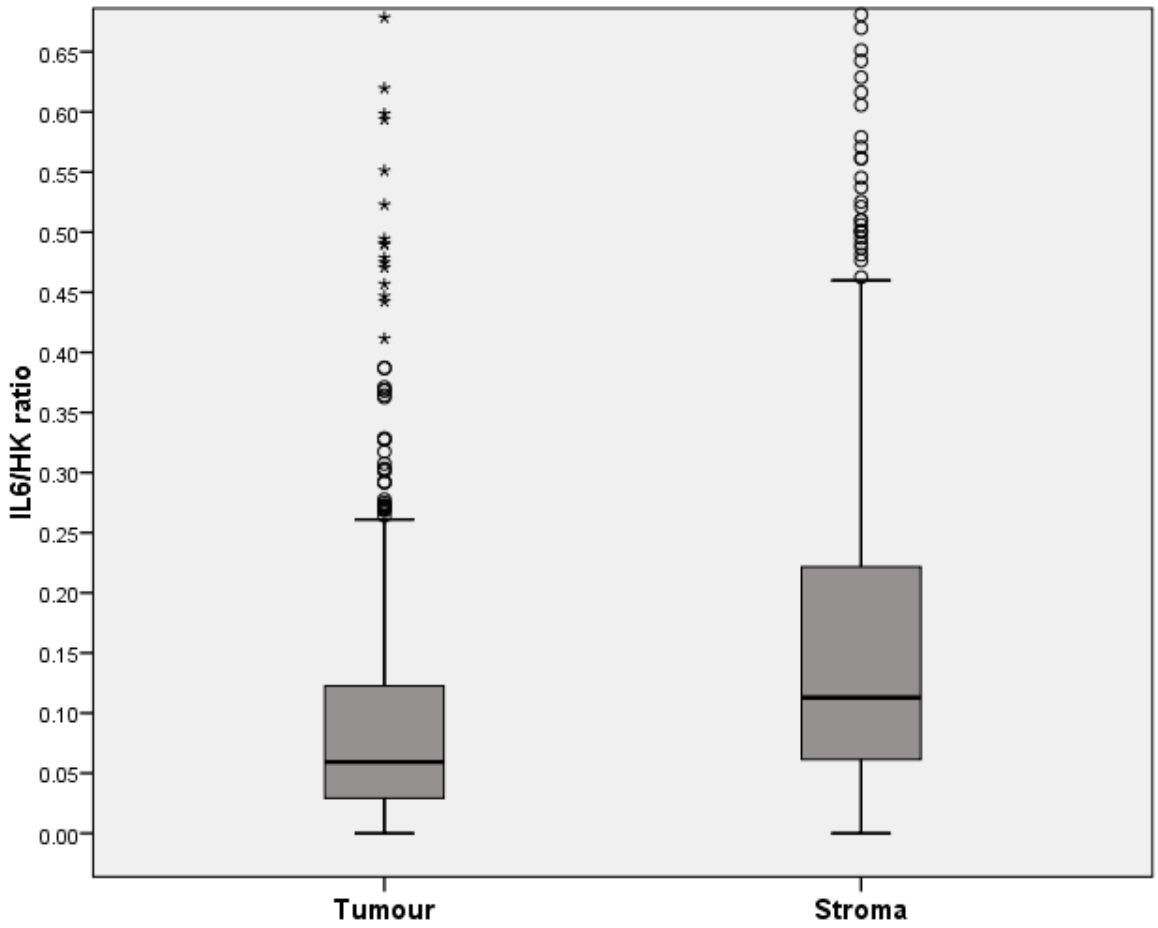

Figure 7-4. Expression of IL6 in tumour and stroma. Box plots illustrating the range of expression levels of IL6 in tumour compared to stroma. Extreme outliers are not shown due to the scale which would be required. Median expression in stroma was higher than that in tumour (**p<0.001**).

There was no significant difference in IL6 expression in tumour between the 4 molecular subtypes.

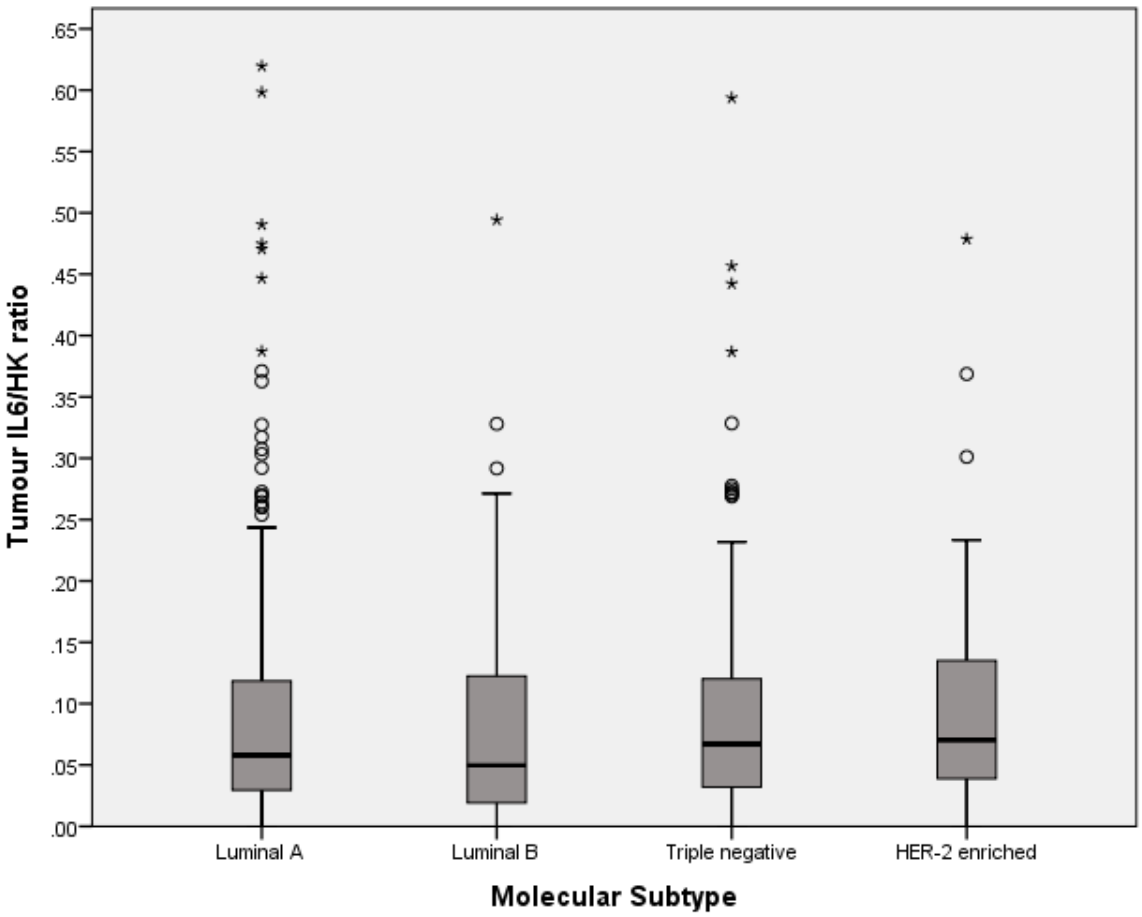

Figure 7-5. Expression of IL6 in tumour by molecular subtype. Box plots illustrating the expression of IL6 in tumour in the 4 molecular subtypes. There was no significant difference between the subtypes (p=0.205).

Overall there was no significant difference in stromal IL6 expression between the molecular subtypes (p=0.070) (**Figure 7-6**). However, when the two subtypes were directly compared, triple negative tumours had significantly higher stromal IL6 expression than luminal B cancers (p=0.014).

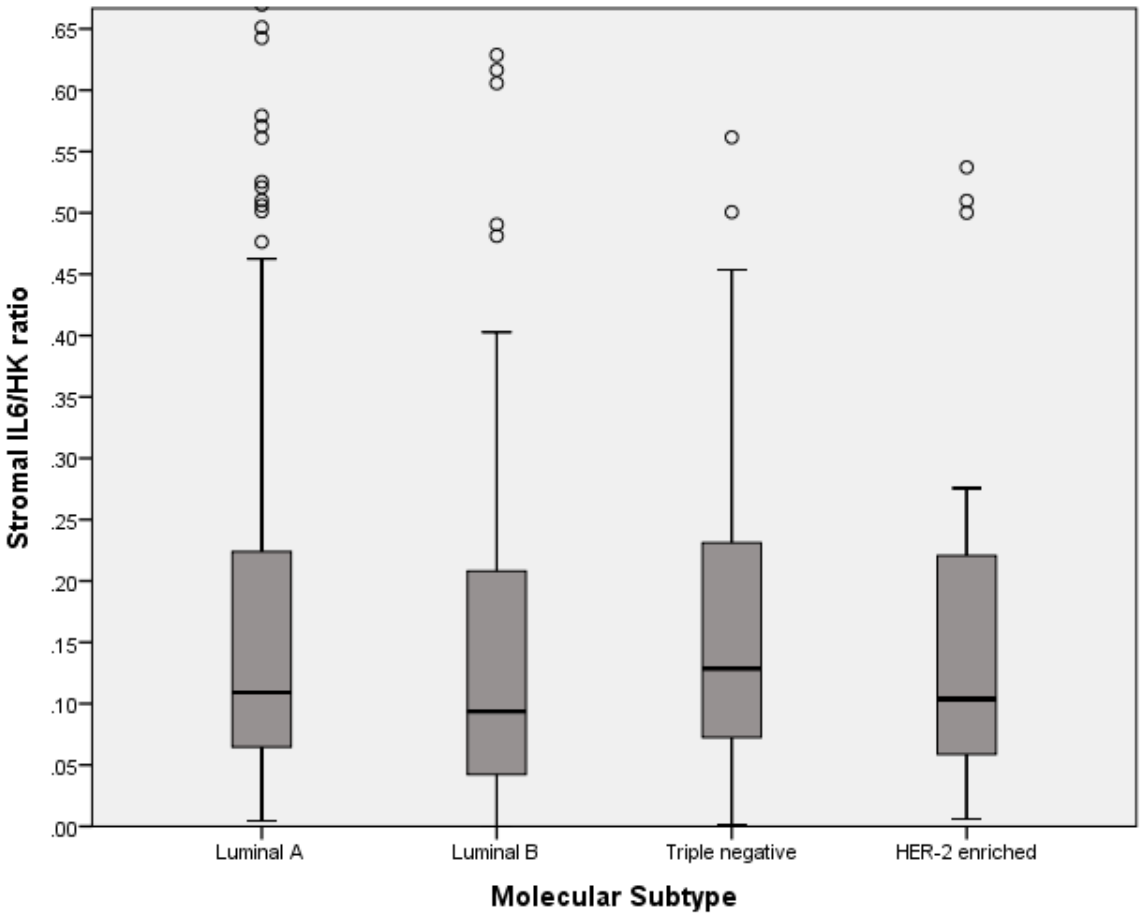

Figure 7-6. Stromal expression of IL6 by molecular subtype. Box plots to illustrate the expression of IL6 in stroma in the different molecular subtypes. There was no significant difference between the subtypes (p=0.070).

There was a strong positive correlation between tumour and stroma IL6/HK ratio (Pearson correlation 0.944, $p<0.001$).

a)

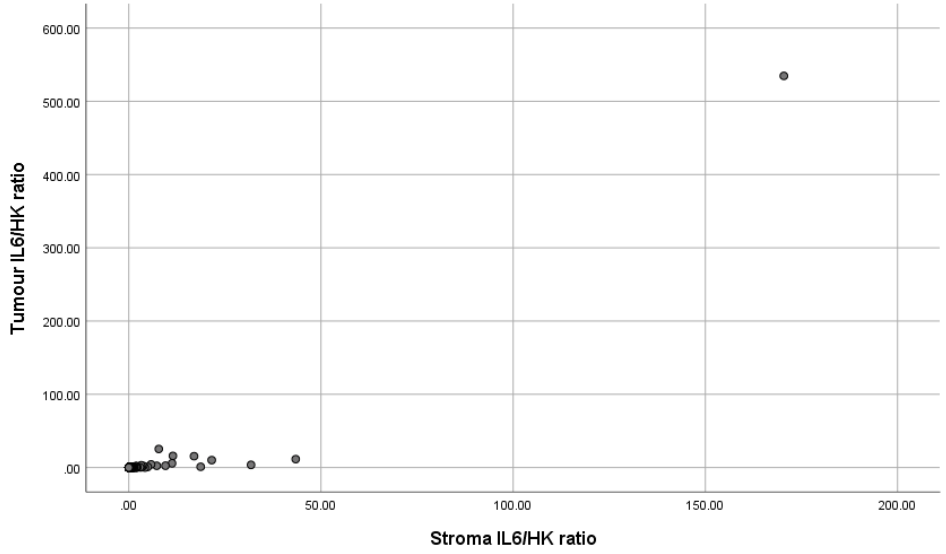

b)

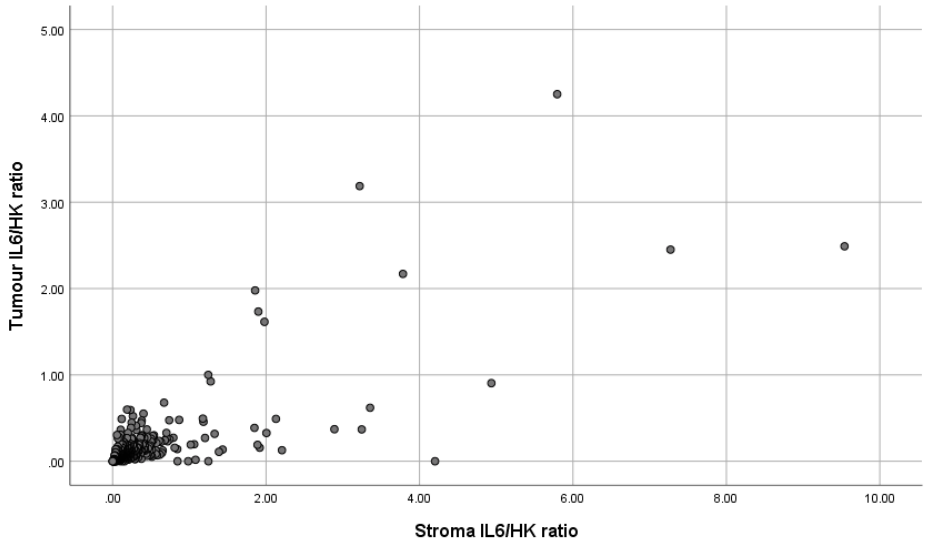

Figure 7-7. Tumour versus stromal IL6 scatterplots. Scatterplots to illustrate the correlation of tumour and stromal IL6/HK ratios, a) includes all cases as at large scale, b) uses a much smaller scale and excludes the major outliers to more clearly illustrate the majority of tumours with lower expression.

7.3.3 The relationship between IL6 and CSS

To determine thresholds to use in further analysis, ROC curves were constructed for tumour and stromal IL6/HK ratios.

a) b)

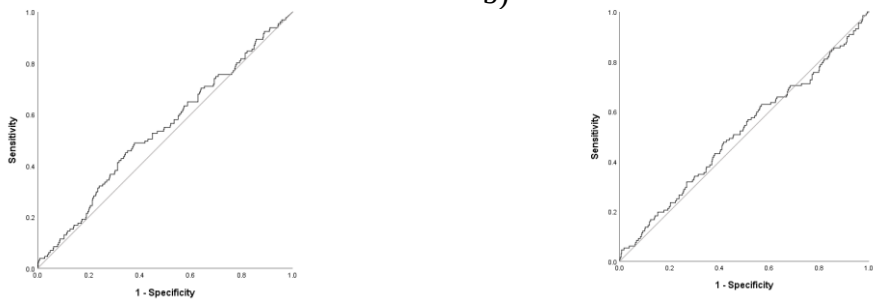

Figure 7-8. ROC curves for IL6 and CSS. ROC curves illustrating the relationships between CSS and a) tumour IL6/HK ratio (AUC 0.539), b) stromal IL6/HK ratio (AUC 0.515).

As no clear threshold was identified from the ROC curves, exploratory analysis using Kaplan Meier curves and divisions at the median, into tertiles and into quartiles was carried out. This identified division into tertiles as the optimum grouping for further survival analysis. Division points for stromal IL6/HK ratio tertiles were 0.07 and 0.18. Tumour IL6/HK ratio was divided at 0.09 which defined the highest tertile.

7.3.3.1 IL6 and CSS in the full cohort

When the whole cohort was analysed, high tumour IL6/HK ratio (≥0.09) was significantly associated with worse CSS (HR 1.45, 95% CI 1.02-2.05, p=0.037)(**Figure 7-9**). There was no association between stromal IL6/HK ratio and CSS (medium v low: HR 1.00, 95% CI 0.65-1.52, p=0.985; high v low: HR 1.09, 95% CI 0.71-1.67, p=0.689)(**Figure 7-10**).

a) b)

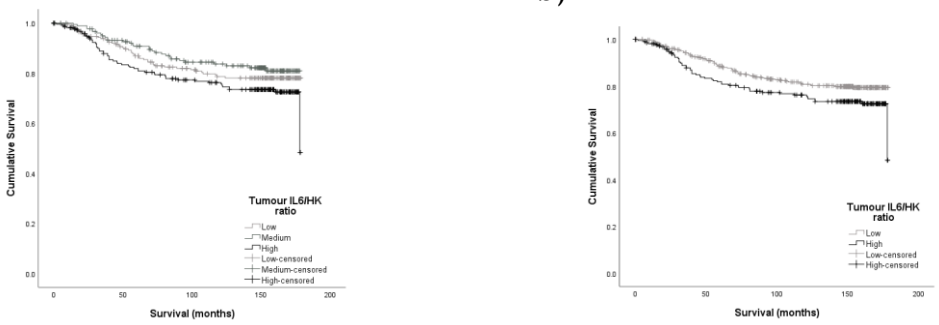

Figure 7-9. Association of tumour IL6 with CSS. Kaplan Meier graphs illustrating the relationship between the tumour IL6/HK ratio and CSS, a) divided into tertiles (low <0.04, medium 0.04-0.08, high ≥0.09), n=645, p=0.080, and b) divided at the highest tertile (low <0.09, high ≥0.09), n=645, **p=0.036**.

a)

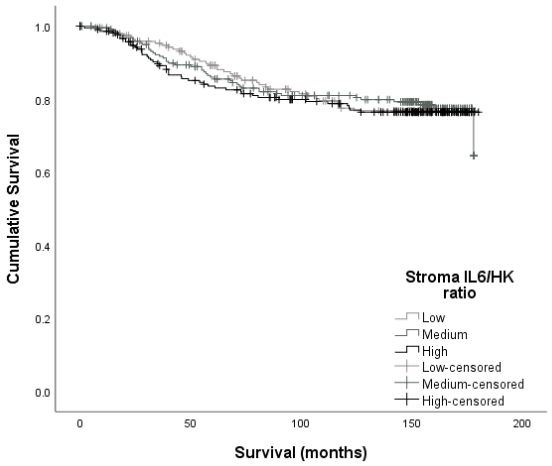

Figure 7-10. Association of stromal IL6 with CSS. Kaplan Meier graphs illustrating the relationship between the stromal IL6/HK ratio and CSS. IL6/HK is divided into tertiles (low <0.07, medium 0.07-0.17, high ≥0.18), n=649, p=0.888.

7.3.3.2 IL6 and CSS by ER status

When analysed separately, there was no significant association observed between tumour IL6/HK ratio and CSS in either ER positive (HR 1.50, 95% CI 0.96-2.36, p=0.077) or ER negative disease (HR 1.32, 95% CI 0.77-2.27, p=0.317). Similarly, no association was observed between stromal IL6/HK ratio and CSS in ER positive (Medium v low: HR 0.78, 95% CI 0.45-1.37, p=0.388; high v low: HR 1.02, 95% CI 0.60-1.74, p=0.946) or ER negative disease (Medium v low: HR 1.22, 95% CI 0.62-2.41, p=0.566; high v low: HR 1.12, 95% CI 0.55-2.27, p=0.749).

a) b)

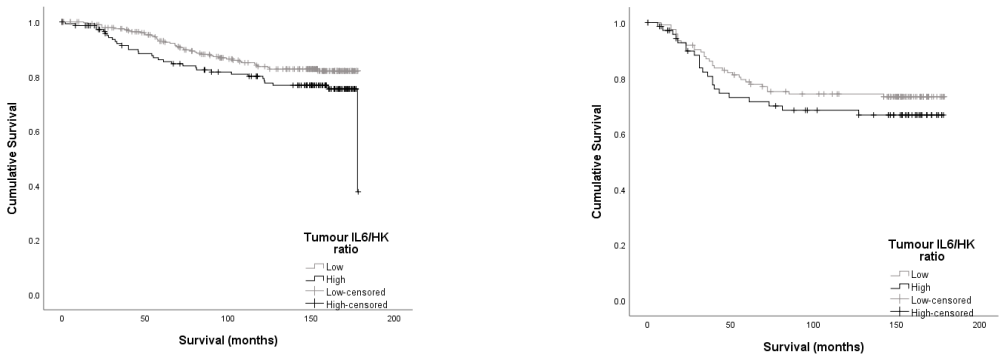

Figure 7-11. Tumour IL6 and CSS by ER status. Kaplan Meier graphs to illustrate the relationship between tumour IL6/HK ratio and CSS in a) ER positive disease (n=446, p=0.075) and b) ER negative disease (n=199, p=0.314).

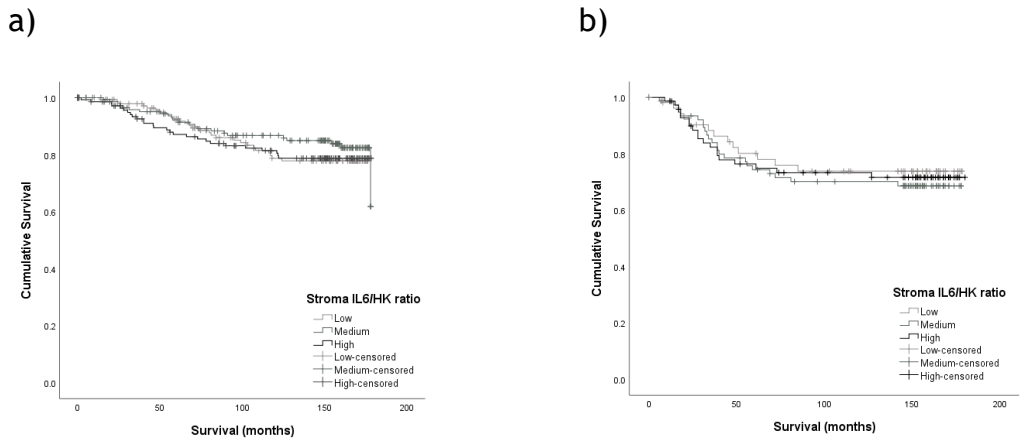

Figure 7-12. Stromal IL6 and CSS by ER status. Kaplan Meier graphs to illustrate the relationship between stromal IL6/HK ratio and CSS in a) ER positive disease (n=445, p=0.589) and b) ER negative disease (n=203, p=0.846).

7.3.3.3 IL6 and CSS by molecular subtype

When analysed individually, there was no association observed between tumour IL6/HK ratio and CSS in luminal A (HR 1.51, 95% CI 0.77-2.95, p=0.227), luminal B (HR 1.55, 95% CI 0.72-3.34, p=0.264), HER2-enriched (HR 1.45, 95% CI 0.59-3.56, p=0.421) or triple negative breast cancer (HR 1.27, 95% CI 0.64-2.53, p=0.502).

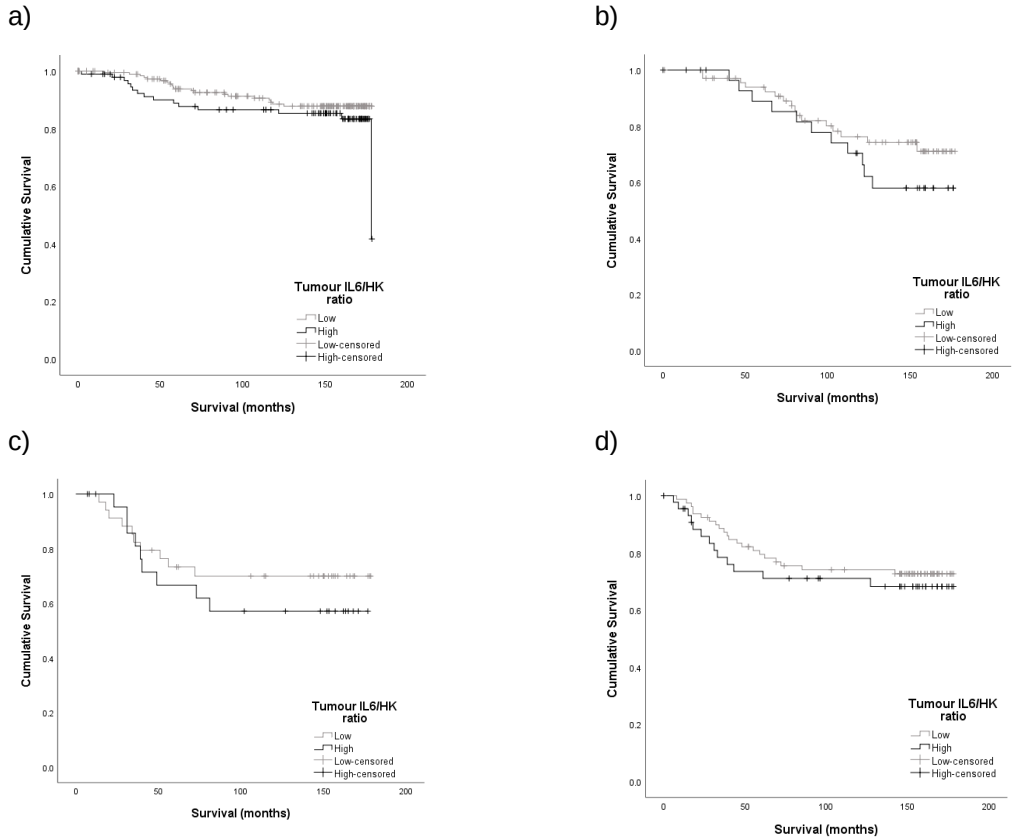

Figure 7-13. Tumour IL6 and CSS by molecular subtype. Kaplan Meier graphs to illustrate the relationship between tumour IL6/HK ratio and CSS in a) luminal A (n=296, p=0.224), b) luminal b (n=100, p=0.260), c) HER2-enriched (n=58, p=0.417) and d) triple negative breast cancer (n=125, p=0.500).

Similarly, there was no association observed between stromal IL6/HK ratio and CSS in luminal A (medium v low: HR 1.07, 95% CI 0.46-2.52, p=0.876; high v low: HR 1.37, 95% CI 0.58-3.20, p=0.474), luminal B (medium v low: HR 0.73, 95% CI 0.26-2.08, p=0.560; high v low: HR 1.03, 95% CI 0.44-2.38, p=0.952), HER2-enriched (medium v low: HR 1.43, 95% CI 0.44-4.70, p=0.552; high v low: HR 1.56, 95% CI 0.51-4.78, p=0.433) or triple negative breast cancer (medium v low: HR 1.18, 95% CI 0.51-2.76, p=0.703; high v low: HR 1.03, 95% CI 0.41-2.55, p=0.954).

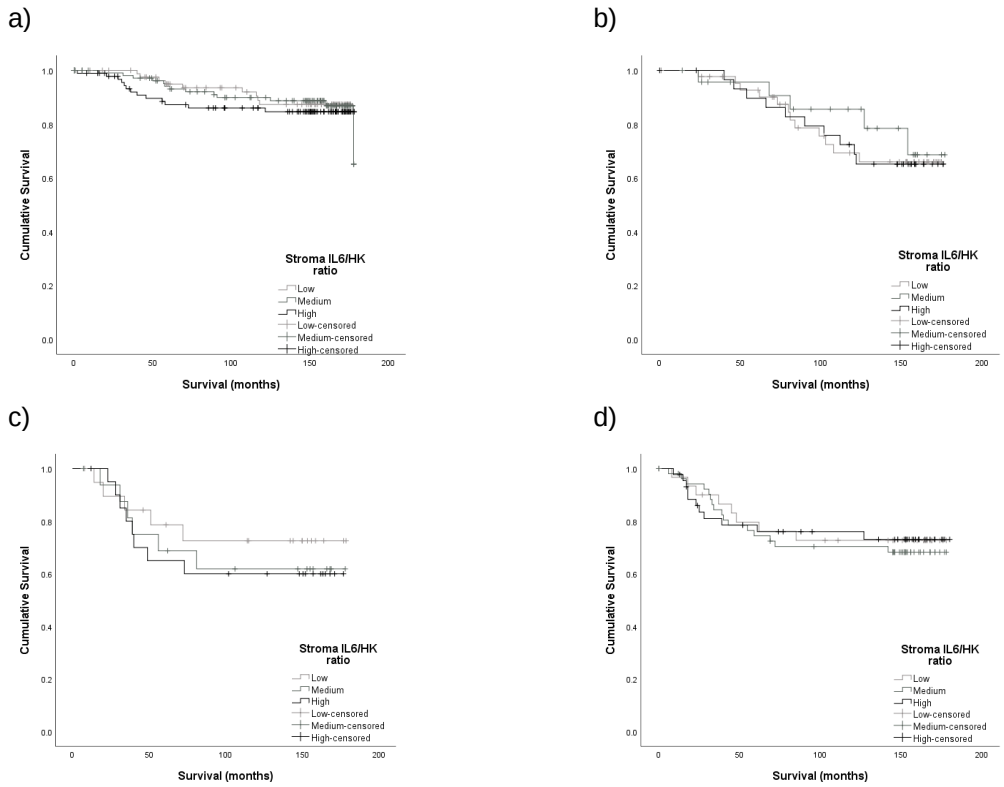

Figure 7-14. Stromal IL6 and CSS by molecular subtype. Kaplan Meier graphs to illustrate the relationship between stromal IL6/HK ratio and CSS in a) luminal A (n=295, p=0.730), b) luminal b (n=99, p=0.806), c) HER2-enriched (n=58, p=0.720) and d) triple negative breast cancer (n=128, p=0.905).

7.3.4 Formation of the cohort for IL6R analysis

678 patients had one or more core assessable for cytoplasmic and membranous IL6R expression. 642 patients had one or more cores which were assessable for stromal IL6R expression.

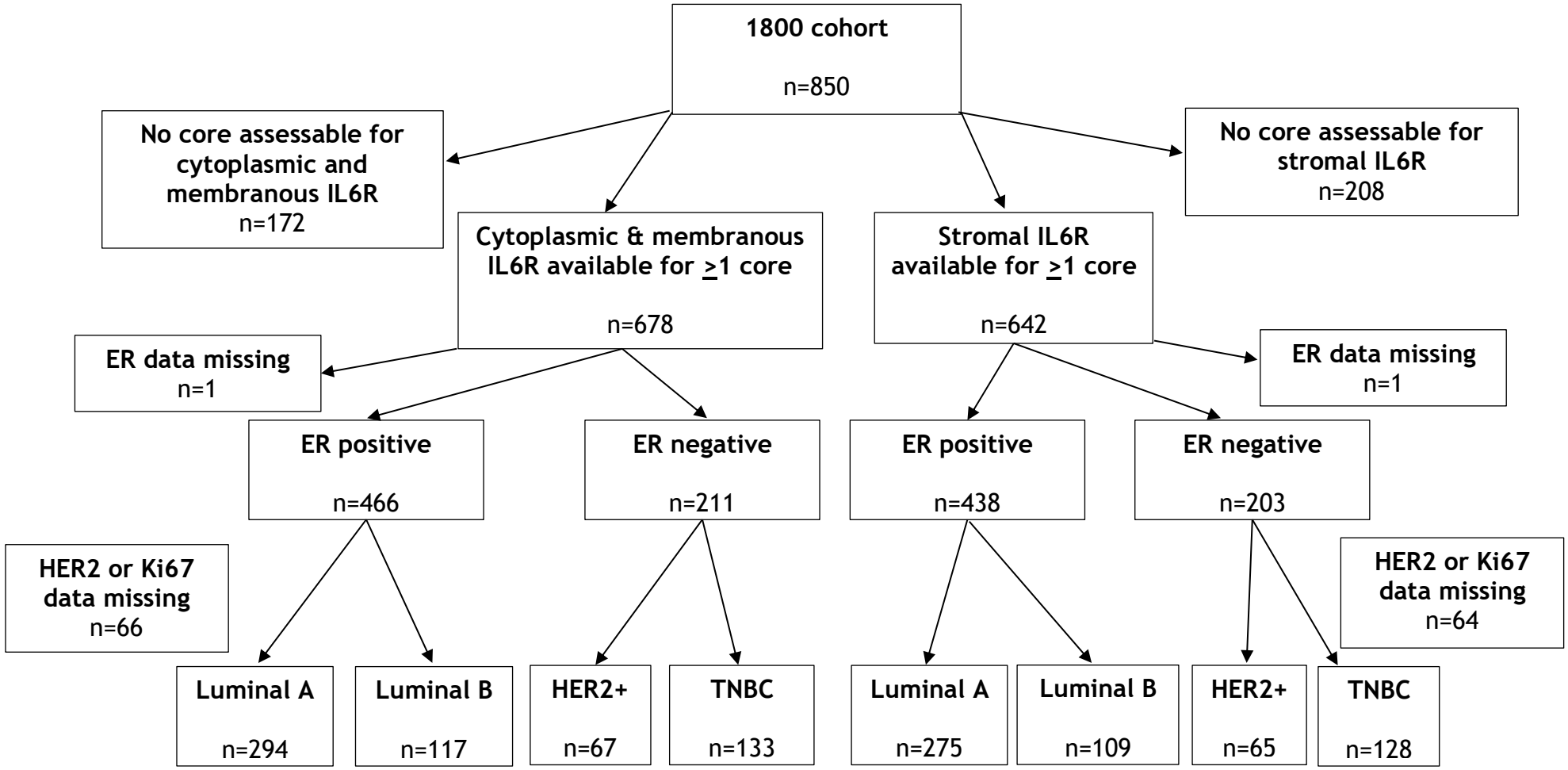

Figure 7-15. Formation of the IL6R cohort. Flow diagram to illustrate the number of patients within the 1800 cohort with at least 1 core which was assessable for IL6R expression in the tumour membrane and cytoplasm, and separately in the stroma. The numbers available for subgroup analysis by ER status and by molecular subtype are also shown.

7.3.5 IL6R expression

No nuclear IL6R expression was observed. Cytoplasmic, membranous and stromal expression were present. Examples of slides stained for IL6R expression using IHC are shown below (**Figure 7-16**).

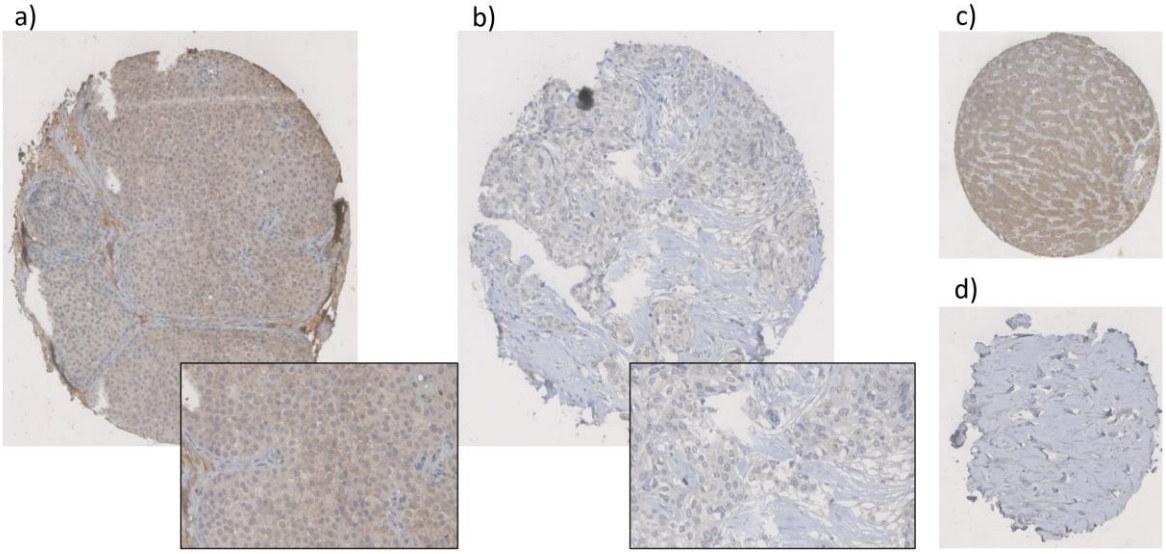

Figure 7-16. Examples of IL6R staining. TMA cores stained using IHC for IL6 receptor: a) breast core with moderate cytoplasmic and moderate and strong membranous staining at 10x magnification with an inset at 40x magnification, b) breast core with weak cytoplasmic staining, c) true positive core (control, liver) at 10x magnification, d) true negative core at 10x magnification.

Highest IL6R expression was in the cytoplasm. Median weighted histoscore was 105 (0-300) for cytoplasmic IL6R expression, 0 (0-150) for membranous expression and 55 (0-202.50) for stromal expression. Expression of IL6R in each location is illustrated in the charts below (**Figure 7-17, Figure 7-18**).

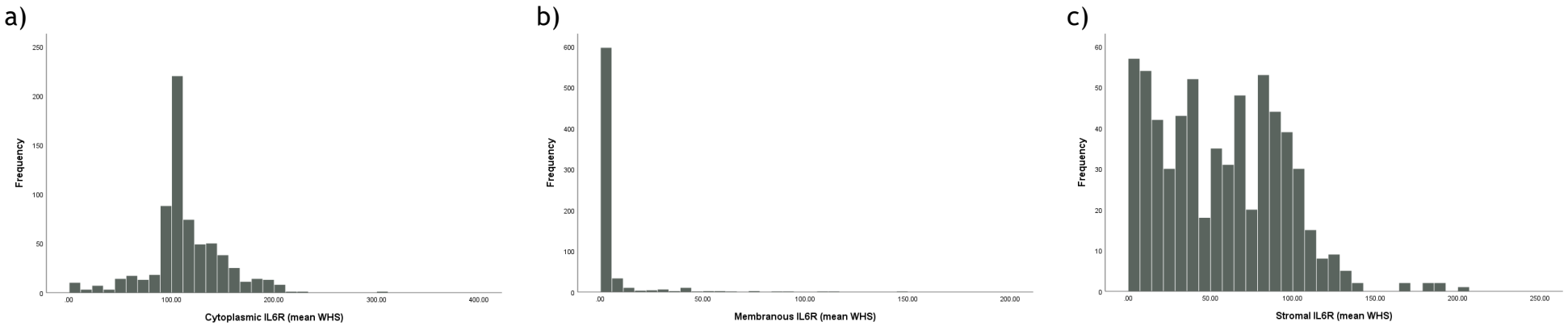

Figure 7-17. Histograms of IL6R expression. Histograms to illustrate IL6R expression in a) tumour cell cytoplasm, b) tumour cell membrane and c) stromal cells.

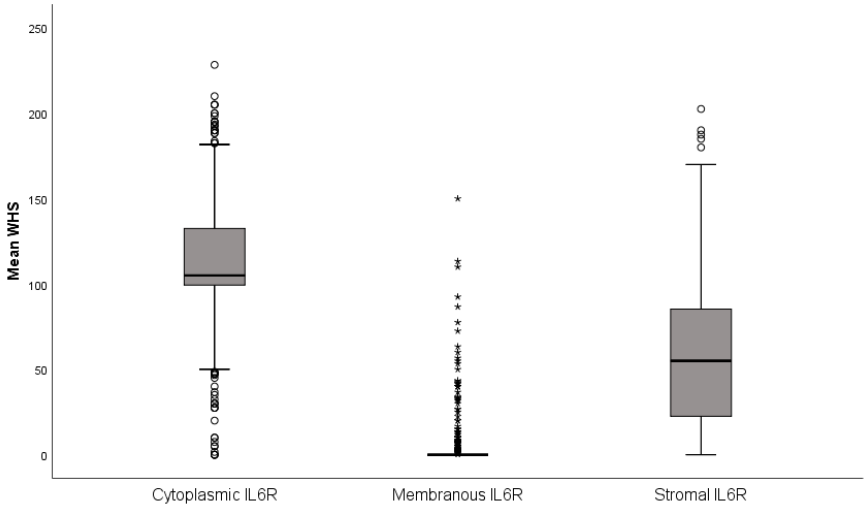

Figure 7-18. Boxplots of IL6R expression. Boxplots to illustrate the expression of IL6R in tumour cell cytoplasm, tumour cell membrane and stromal cells. The highest IL6R expression was observed in cytoplasm (**p<0.001**).

In the molecular subtypes, highest cytoplasmic IL6R expression was in the HER2-enriched subtype (p=0.003).

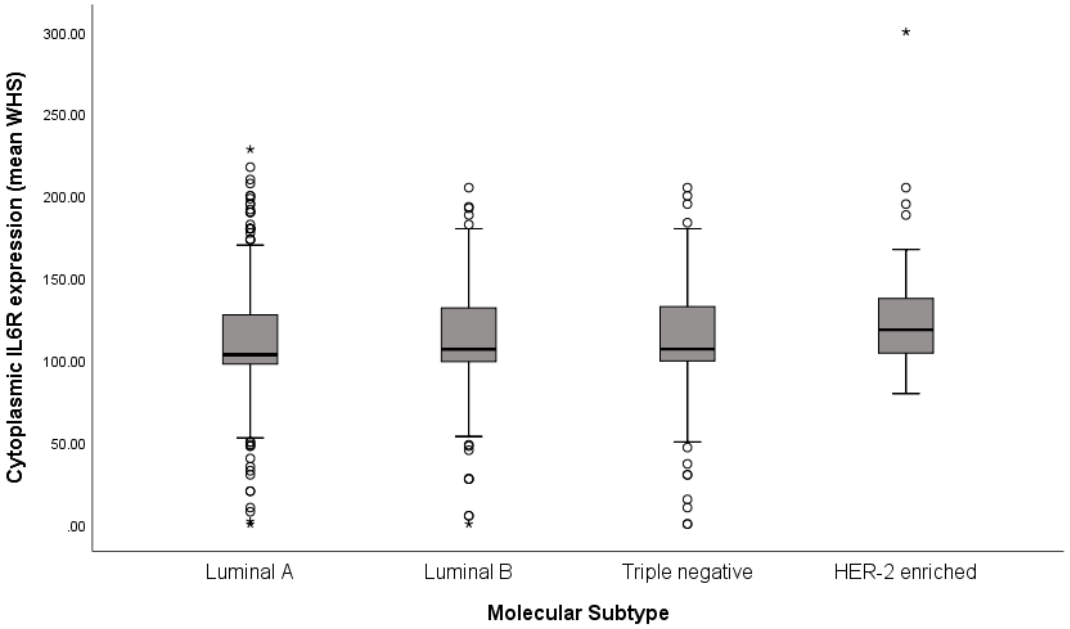

Figure 7-19. Boxplots of cytoplasmic IL6R expression within molecular subtypes. Boxplots to illustrate cytoplasmic IL6R expression within the different molecular subtypes. Highest expression is observed in the HER2-enriched subtype (**p=0.003**).

There was no significant difference in membranous or stromal IL6R expression observed between the molecular subtypes.

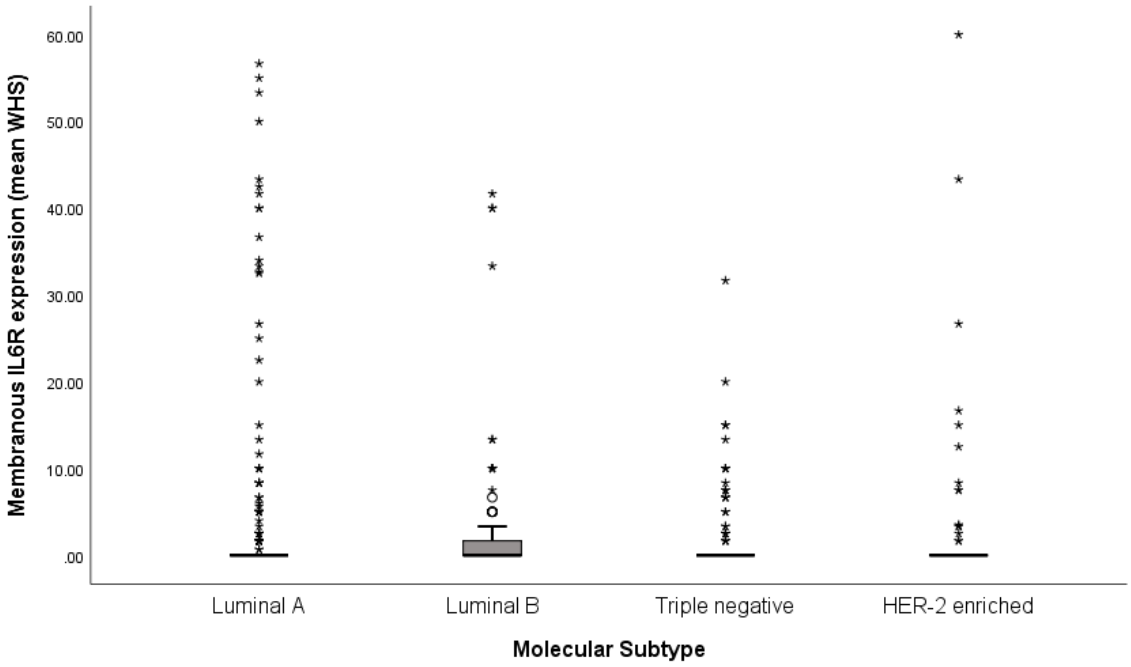

Figure 7-20. Boxplots of membranous IL6R expression within molecular subtypes. Boxplots to illustrate membranous IL6R expression within the different molecular subtypes (p=0.710).

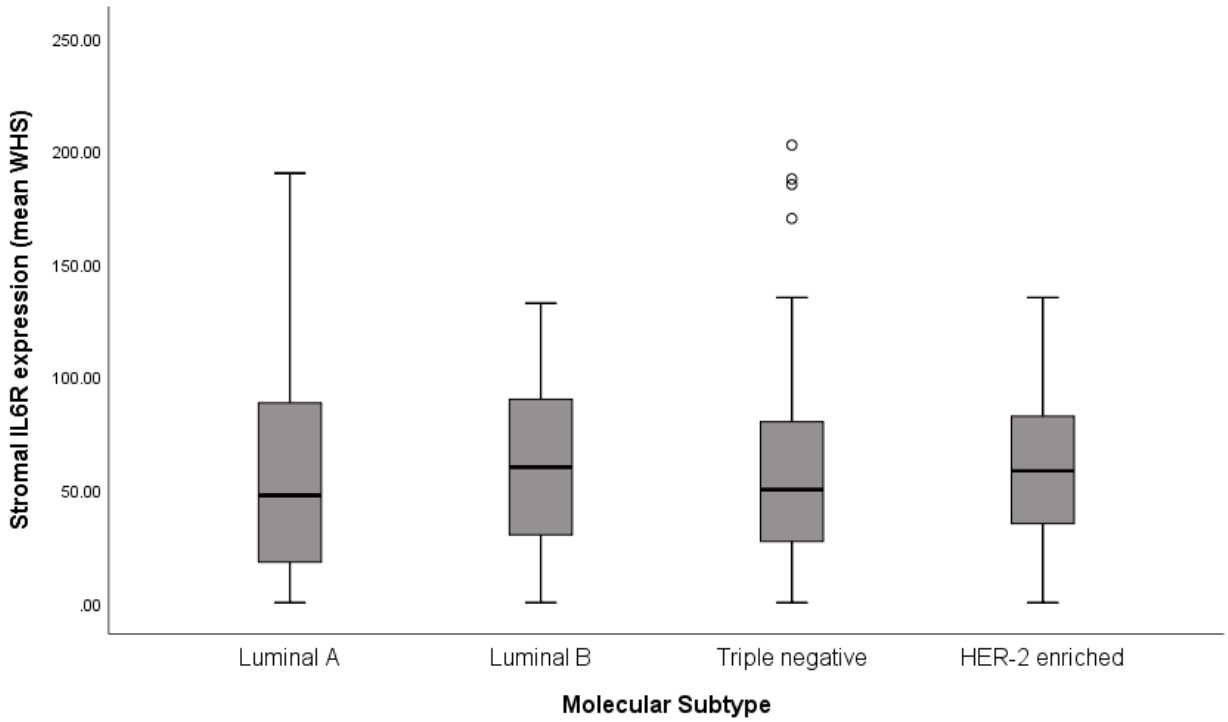

Figure 7-21. Boxplots of stromal IL6R expression within molecular subtypes. Boxplots to illustrate stromal IL6R expression within the different molecular subtypes (p=0.399).

A moderate significant correlation between stromal and cytoplasmic IL6R expression was observed (Pearson correlation coefficient 0.472, $p<0.001$) but no significant correlation was observed between stromal and membranous IL6R expression (Pearson correlation coefficient -0.068, $p=0.086$).

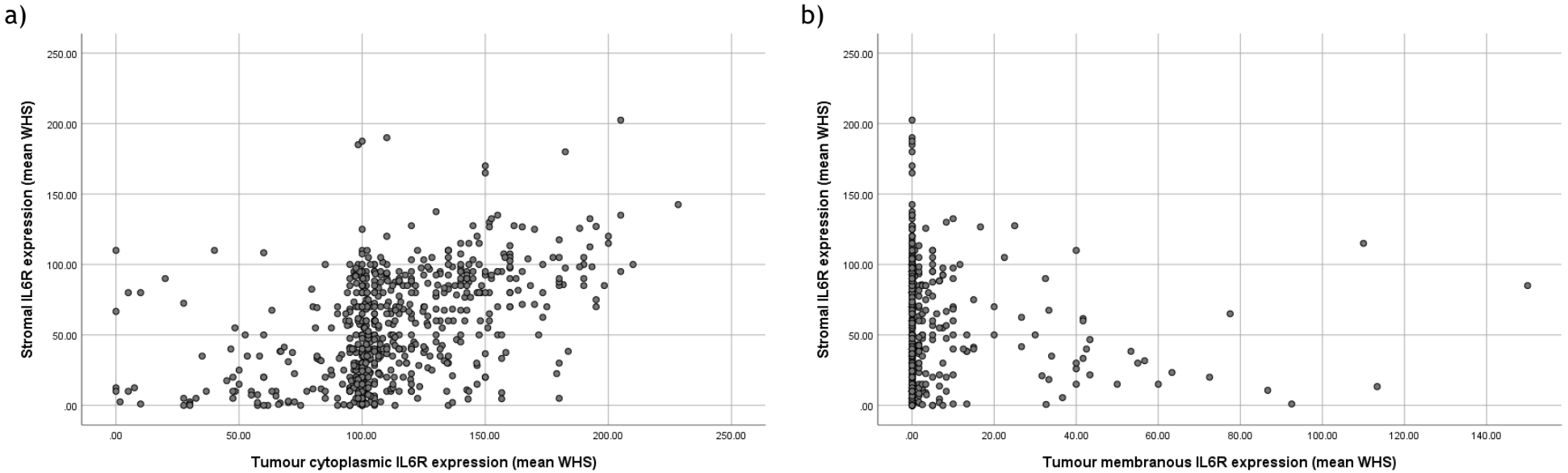

Figure 7-22. Tumour and stromal IL6R expression correlation. Scatter plots to illustrate a) a positive correlation between stromal and tumour cytoplasmic IL6R expression and b) no significant correlation between stromal and tumour membranous IL6R expression.

7.3.6 The relationship between IL6R and CSS

ROC curves for cytoplasmic, membranous and stromal expression of IL6R were constructed with an outcome of CSS to determine suitable thresholds to use in survival analysis going forward. No threshold was identified for cytoplasmic expression. A mean WHS of 2.5 was derived for membranous IL6R and a mean WHS of 82 for stromal IL6R. The median was used to divide patients into high and low cytoplasmic expression groups.

a)

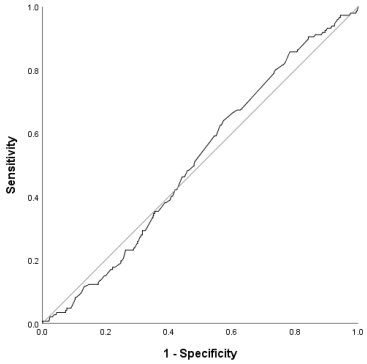

b)

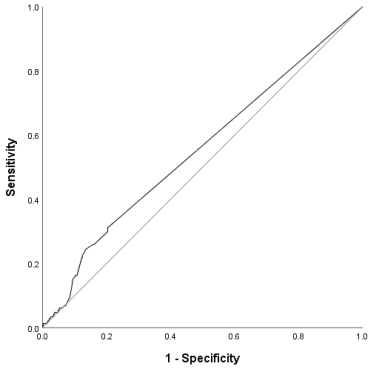

c)

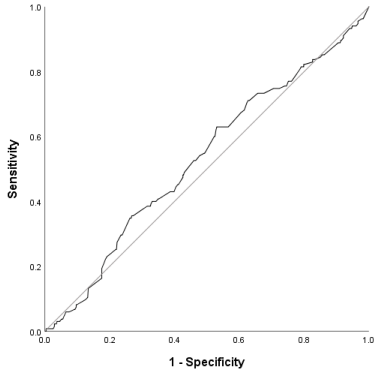

Figure 7-23. ROC curves of IL6R expression and CSS. ROC curves to show the relationship with CSS of IL6R expression in a) tumour cytoplasm (AUC 0.511), b) tumour cell membrane (AUC 0.554) and c) stromal cells (AUC 0.531).

7.3.6.1 Cytoplasmic IL6R expression and CSS

No significant association was observed between cytoplasmic IL6R expression and CSS when analysed divided at the median (HR 1.12, 95% CI 0.81-1.55, p=0.486) or into tertiles (medium v low: HR 1.37, 95% CI 0.93-2.01, p=0.113; high v low: HR 1.05, 95% CI 0.69-1.58, p=0.829) (**Figure 7-24**). This remained the case when analysed in sub-cohorts of ER positive or ER negative disease or within the 4 molecular subtypes (data not shown).

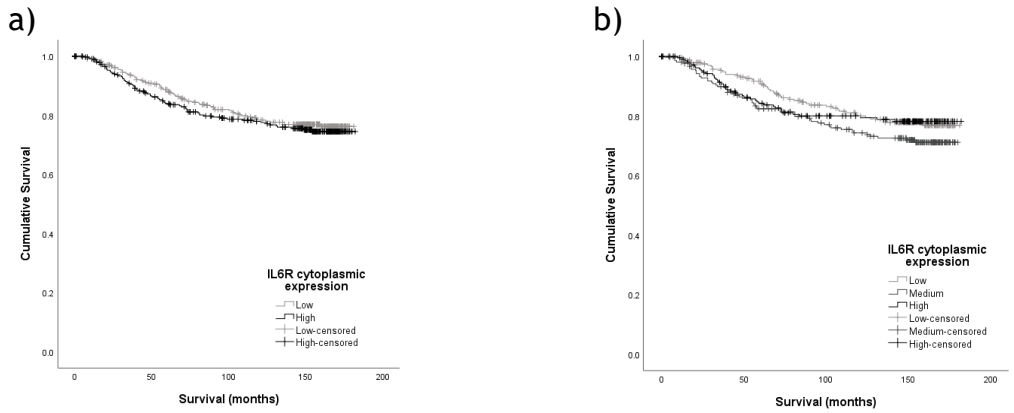

Figure 7-24. The relationship between cytoplasmic IL6R expression and CSS. Kaplan meier graphs to illustrate the relationship between cytoplasmic IL6R expression and CSS when divided a) at the median (p=0.486) or b) into tertiles (p=0.224).

7.3.6.2 Membranous IL6R expression and CSS

When the whole cohort was analysed, high membranous IL6R expression (mean WHS>2.5) was associated with significantly worse CSS (HR 1.90, 95% CI 1.31-2.77, p=0.001). This was the case both in ER positive (HR 1.94, 95% CI 1.19-3.18, p=0.008) and ER negative disease (HR 1.86, 95% CI 1.04-3.32, p=0.037).

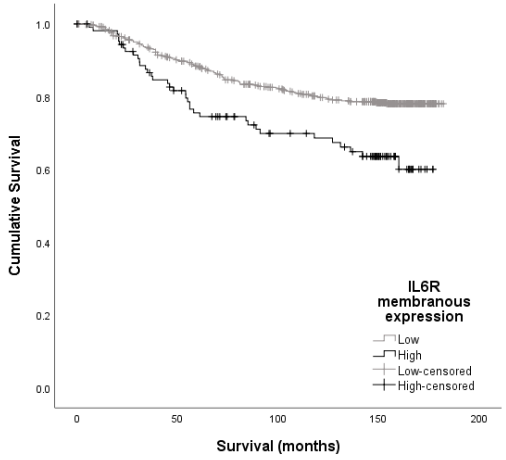

Figure 7-25. The relationship between membranous IL6R expression and CSS. Kaplan meier graph to illustrate the relationship between membranous IL6R expression and CSS in the full cohort (n=678, **p=0.001**).

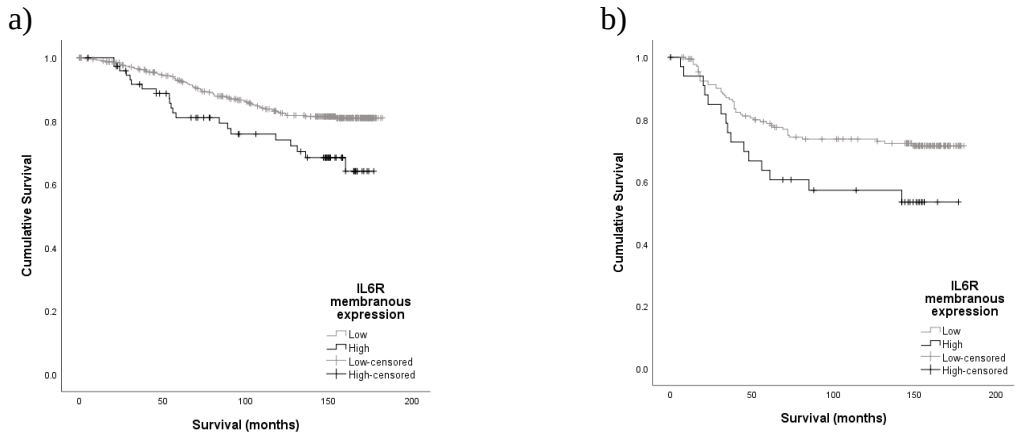

Figure 7-26. The relationship between membranous IL6R expression and CSS by ER status. Kaplan meier graphs to illustrate the relationship between membranous IL6R expression and CSS in a) ER positive (n=466, **p=0.007**) and b) ER negative disease (n=211, **p=0.034**).

When analysed within the molecular subtypes, high membranous IL6R expression was significantly associated with worse CSS in luminal A disease (HR 3.40, 95% CI 1.74-6.65, p<0.001) but not the other 3 subtypes (luminal B: HR 0.86, 95%CI 0.33-2.25, p=0.759; HER2-enriched: HR 1.99, 95% CI 0.78-5.12, p=0.152; TNBC: HR 1.79, 95% CI 0.85-3.78, p=0.124).

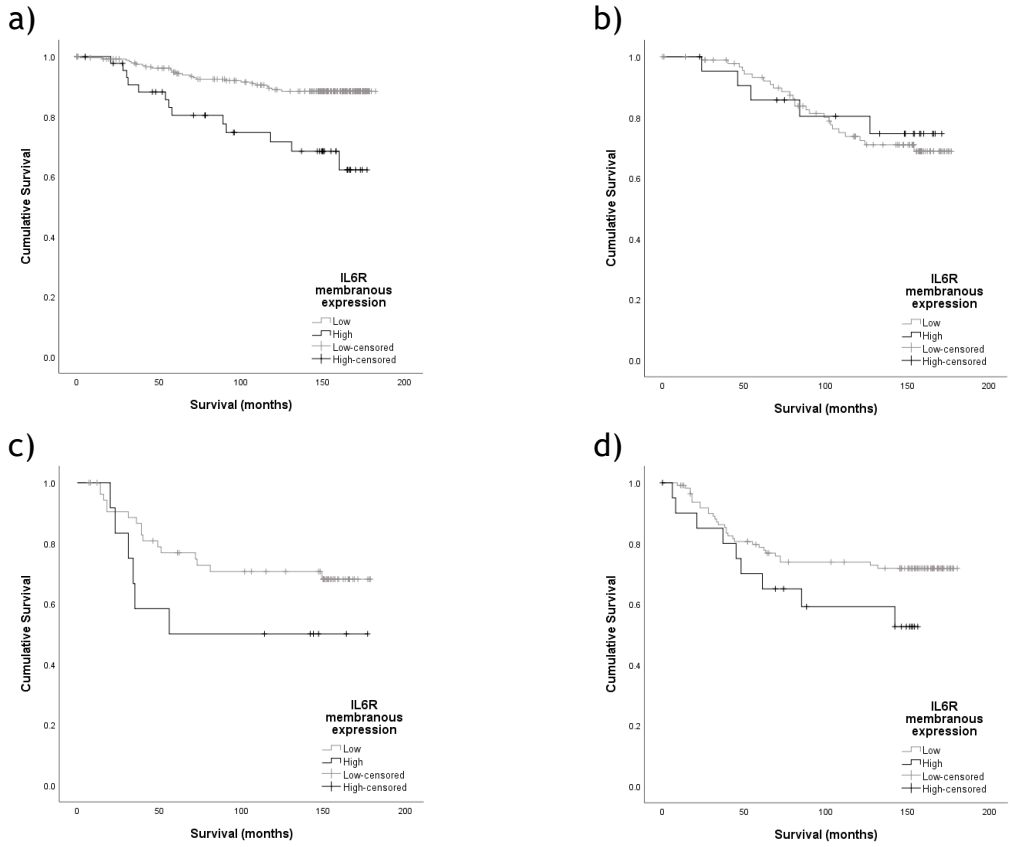

Figure 7-27. The relationship between membranous IL6R expression and CSS by molecular subtype. Kaplan meier graphs to illustrate the relationship between membranous IL6R expression and CSS in a) luminal A (n=294, **p<0.001**), b) luminal B (n=117, p=0.759), c) HER2-enriched (n=67, p=0.143) and d) triple negative breast cancer (n=133, p=0.118).

7.3.6.3 Stromal IL6R expression and CSS

When the whole cohort was analysed, high stromal IL6R expression (mean WHS>82) was associated with significantly worse CSS (HR 1.44, 95% CI 1.02-2.05, p=0.041). However, there was no statistically significant difference when analysed by ER status (ER+: HR 1.54, 95% CI 0.97-2.43, p=0.065; ER-: HR 1.65, 95% CI 0.94-2.90, p=0.082).

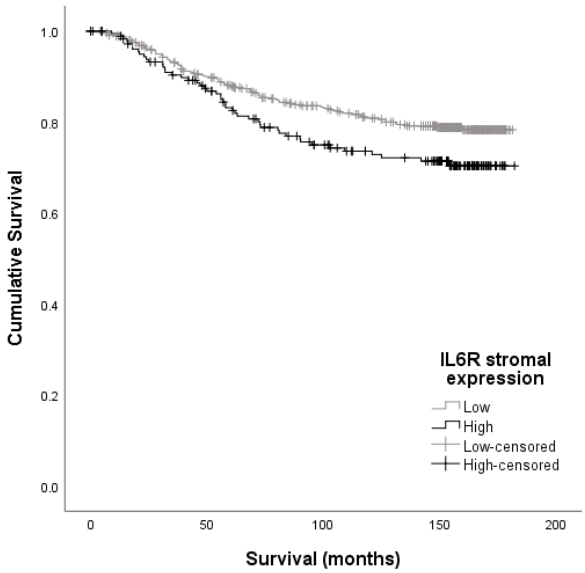

Figure 7-28. The relationship between stromal IL6R expression and CSS. Kaplan meier graph to illustrate the relationship between stromal IL6R expression and CSS in the whole cohort (n=642, **p=0.040**).

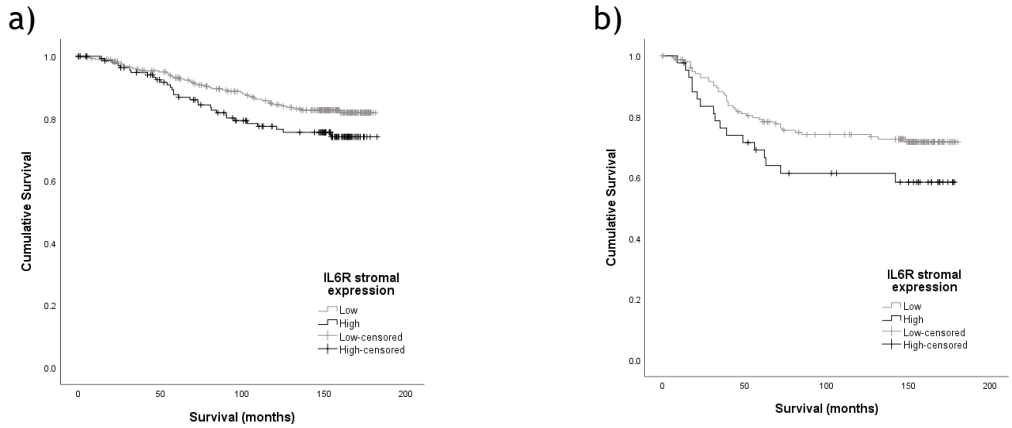

Figure 7-29. The relationship between stromal IL6R expression and CSS by ER status. Kaplan meier graphs to illustrate the relationship between stromal IL6R expression and CCS in a) ER positive (n=438, p=0.063) and b) ER negative disease (n=203, p=0.078).

When analysed within the molecular subtypes, high stromal IL6R was significantly associated with worse CSS in luminal A disease (HR 2.23, 95% CI 1.14-4.38, p=0.019) but not in the other 3 subtypes (luminal B: HR 1.51, 95% CI 0.70-3.26, p=0.291; HER2-enriched: HR 2.14, 95% CI 0.87-5.24, p=0.096; TNBC:

HR 1.30, 95% CI 0.62-2.74, p=0.494), though there was a trend to worse CSS in HER2-enriched disease (**Figure 7-30**).

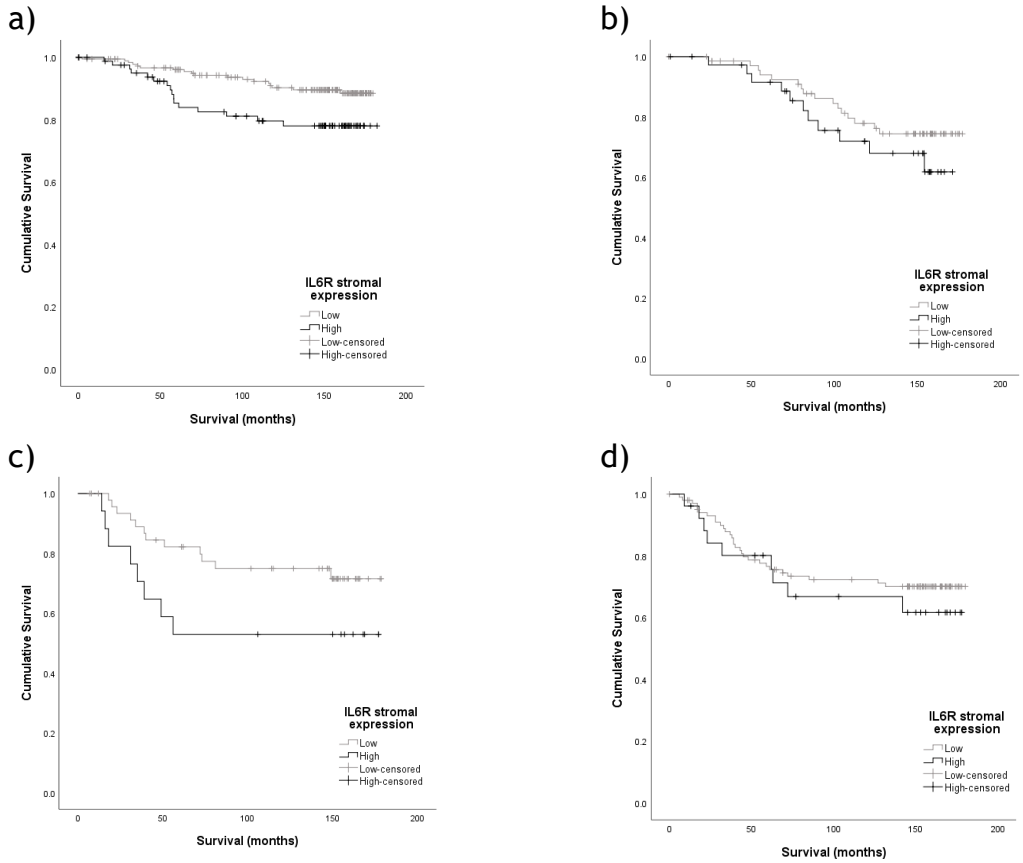

Figure 7-30. The relationship between stromal IL6R expression and CSS by molecular subtype. Kaplan meier graphs to illustrate the relationship between stromal IL6R expression and CCS in a) luminal A (n=275, **p=0.016**), b) luminal B (n=109, p=0.287), c) HER2-enriched (n=65, p=0.088) and d) triple negative breast cancer (n=128, p=0.492).

7.3.6.4 Multivariate survival analysis

On multivariate analysis, controlling for known prognostic clinicopathological factors, membranous IL6R was the only site of IL6 or IL6R expression which was independently associated with worse CSS.

	Univariate analysis		Multivariate analysis	
	HR (95% CI)	p	HR (95% CI)	p
Age		0.755		
≤50yrs				
>50yrs				
Type		**0.029**		
Ductal	1			
Lobular	0.69 (0.38-1.27)	0.236		
Other	0.18 (0.45-0.72)	**0.016**		
Size		**<0.001**		0.126
≤20mm	1			
21-49mm	2.19 (1.59-3.01)	**<0.001**		0.442
≥50mm	4.45 (2.70-7.33)	**<0.001**		0.043
Grade		**<0.001**		0.758
I	1			
II	2.02 (1.14-3.60)	**0.017**		0.476
III	3.95 (2.25-6.93)	**<0.001**		0.477
Nodal status		**<0.001**		**0.002**
Negative	1		1	
Positive	3.24 (2.37-4.44)		2.46 (1.37-4.41)	
ER status		**<0.001**		**0.034**
Negative	1		1	
Positive	0.57 (0.42-0.77)		0.53 (0.30-0.95)	
HER2 status		**0.001**		0.186
Negative	1			
Positive	1.83 (1.28-2.62)			
Necrosis		**<0.001**		**<0.001**
<25%	1		1	
>25%	3.11 (2.24-4.33)		6.20 (2.81-13.63)	
KM score		**0.014**		**0.001**
0	1		1	
1	1.17 (0.74-1.86)	0.497	0.15 (0.06-0.39)	**<0.001**
2	1.80 (1.11-2.94)	**0.018**	0.19 (0.06-0.63)	**0.006**
3	0.78 (0.36-1.68)	0.523	0.14 (0.03-0.59)	**0.008**
CD8+ lymphocytes		**0.002**		**0.015**
Low	1		1	
Medium	0.78 (0.48-1.26)	0.307	0.76 (0.42-1.35)	0.346
High	0.33 (0.18-0.61)	**<0.001**	0.35 (0.18-0.72)	**0.004**
CD4+ lymphocytes		0.216		
Low	1			
Medium	1.27 (0.86-1.88)	0.228		
High	0.91 (0.60-1.38)	0.647		
TSP		**<0.001**		**0.017**
Low	1		1	
High	1.89 (1.39-2.56)		2.00 (1.13-3.54)	
Budding		**<0.001**		**0.001**
≤20 buds	1		1	
>20 buds	1.75 (1.29-2.36)		2.44 (1.43-4.16)	
Tumour IL6		**0.037**		0.868
Low	1			
High	1.45 (1.02-2.05)			
Stromal IL6				
Low	1			
Medium	1.0(0.65-1.52)	0.985		
High	1.09 (0.71-1.67	0.689		
Cytoplasmic IL6R		0.486		
Low	1			
High	1.12 (0.81-1.55)			
Membranous IL6R		**0.001**		**0.047**
Low	1			
High	1.90 (1.31-2.77)		1.86 (1.01-3.44)	
Stromal IL6R		**0.041**		0.330
Low	1			
High	1.44 (1.02-2.05)			

Table 7-1. Survival analysis for IL6, IL6R and other prognostic factors. Univariate and multivariate Cox regression analysis of the relationship between IL6 expression, IL6R expression, other known prognostic clinicopathological factors and CSS. Factors with p<0.05 on univariate analysis were entered into the multivariate analysis.

7.3.7 Associations

High tumour IL6 was associated with larger tumours (p=0.050), low CD8+ lymphocytes (p=0.028) and high stromal IL6 (<0.001). Low membranous IL6R expression was associated with high tumour budding (p=0.031). High stromal IL6R expression was associated with KM score (p=0.001), medium levels of CD8+ lymphocytes (p=0.023), low CD4+ lymphocytes (p=0.017) and tumour cytoplasmic IL6R expression (p<0.001).

	Tumour IL6/HK ratio		p
	Low n(%)	High n(%)	
Age			0.423
≤50yrs	120 (28.3)	56 (25.3)	
>50yrs	304 (71.7)	165 (74.7)	
Type			0.058
Ductal	376 (88.7)	181 (81.9)	
Lobular	31 (7.3)	25 (11.3)	
Other	17 (4.0)	15 (6.8)	
Size			**0.050**
≤20mm	253 (59.8)	122 (55.2)	
21-49mm	153 (36.2)	80 (36.2)	
≥50mm	17 (4.0)	19 (8.6)	
Grade			0.490
I	83 (19.6)	42 (19.1)	
II	184 (43.5)	106 (48.2)	
III	156 (36.9)	72 (32.7)	
Nodal status			0.714
Negative	246 (58.9)	125 (57.3)	
Positive	172 (41.1)	93 (42.7)	
ER status			0.296
Negative	125 (29.5)	74 (33.5)	
Positive	299 (70.5)	147 (66.5)	
HER2 status			0.591
Negative	353 (84.4)	178 (82.8)	
Positive	65 (15.6)	37 (17.2)	
Necrosis			0.354
<25%	228 (55.1)	109 (51.2)	
>25%	186 (44.9)	104 (48.8)	
KM score			0.482
0	63 (15.3)	36 (16.8)	
1	226 (54.9)	109 (50.9)	
2	92 (22.3)	57 (26.6)	
3	31 (7.5)	12 (5.6)	
CD8+ lymphocytes			**0.028**
Low			
Medium	75 (29.1)	39 (40.2)	
High	95 (36.8)	22 (22.7)	
	88 (34.1)	36 (37.1)	
CD4+ lymphocytes			0.603
Low			
Medium	131 (34.0)	67 (33.8)	
High	122 (31.7)	70 (35.4)	
	132 (34.3)	61 (30.8)	
TSP			0.494
Low	289 (69.5)	155 (72.1)	
High	127 (30.5)	60 (27.9)	
Budding			0.826
≤20 buds	275 (66.1)	144 (67.0)	
>20 buds	141 (33.9)	71 (33.0)	
Stromal IL6/HK			**<0.001**
Low	189 (44.8)	14 (6.3)	
Medium	178 (42.2)	55 (24.9)	
High	55 (13.0)	152 (68.8)	
Cytoplasmic IL6R			0.876
Low	197 (51.6)	89 (50.9)	
High	185 (48.4)	86 (49.1)	
Membranous IL6R			0.251
Low	310 (81.2)	149 (85.1)	
High	72 (18.8)	26 (14.9)	
Stromal IL6R			0.536
Low	165 (45.0)	69 (42.1)	
High	202 (55.0)	95 (57.9)	

Table 7-2. Associations between tumour IL6 and other clinicopathological factors. Table detailing the associations between tumour IL6/HK ratio and other clinicopathological factors.

	Membranous IL6R		p
	Low n(%)	High n(%)	
Age			0.279
≤50yrs	172 (30.2)	27 (25.0)	
>50yrs	398 (69.8)	81 (75.0)	
Type			0.473
Ductal	510 (89.5)	95 (88.0)	
Lobular	33 (5.8)	5 (4.6)	
Other	27 (4.7)	8 (7.4)	
Size			0.634
≤20mm	315 (55.4)	61 (56.5)	
21-49mm	228 (40.1)	40 (37.0)	
≥50mm	26 (4.6)	7 (6.5)	
Grade			0.425
I	109 (19.2)	15 (13.9)	
II	244 (43.0)	49 (45.4)	
III	215 (37.9)	44 (40.7)	
Nodal status			0.303
Negative	326 (57.8)	55 (52.4)	
Positive	238 (42.2)	50 (47.6)	
ER status			0.939
Negative	177 (31.1)	34 (31.5)	
Positive	392 (68.9)	74 (68.5)	
HER2 status			0.903
Negative	462 (81.9)	89 (82.4)	
Positive	102 (18.1)	19 (17.6)	
Necrosis			0.902
<25%	276 (49.8)	53 (50.5)	
>25%	278 (50.2)	52 (49.5)	
KM score			0.231
0	78 (14.1)	22 (21.4)	
1	295 (53.2)	46 (44.7)	
2	135 (24.3)	26 (25.2)	
3	47 (8.5)	9 (8.7)	
CD8+ lymphocytes			0.234
Low			
Medium	86 (31.7)	15 (25.4)	
High	97 (35.8)	18 (30.5)	
	88 (32.5)	26 (44.1)	
CD4+ lymphocytes			0.358
Low			
Medium	161 (31.3)	30 (29.1)	
High	186 (36.1)	32 (31.1)	
	168 (32.6)	41 (39.8)	
TSP			0.509
Low	391 (70.2)	71 (67.0)	
High	166 (29.8)	35 (33.0)	
Budding			**0.031**
≤20 buds	366 (65.7)	81 (76.4)	
>20 buds	191 (34.3)	25 (23.6)	
Tumour IL6/HK			0.251
Low	310 (67.5)	72 (73.5)	
High	149 (32.5)	26 (26.5)	
Stromal IL6/HK			0.483
Low	154 (33.5)	37 (37.8)	
Medium	170 (37.0)	30 (30.6)	
High	136 (29.6)	31 (31.6)	
Cytoplasmic IL6R			0.879
Low	291 (51.1)	56 (51.9)	
High	279 (48.9)	52 (48.1)	
Stromal IL6R			0.729
Low	236 (43.8)	47 (45.6)	
High	303 (56.2)	56 (54.4)	

Table 7-3. Associations between membranous IL6R and other clinicopathological factors. Table detailing the associations between membranous IL6R expression and other clinicopathological factors.

	Stromal IL6R		p
	Low n(%)	**High** n(%)	
Age			0.207
≤50yrs	91 (32.2)	99 (27.6)	
>50yrs	192 (67.8)	260 (72.4)	
Type			0.607
Ductal	257 (90.8)	326 (90.8)	
Lobular	16 (5.7)	16 (4.5)	
Other	10 (3.5)	17 (4.7)	
Size			0.607
≤20mm	153 (54.1)	204 (57.0)	
21-49mm	118 (41.7)	136 (38.0)	
≥50mm	12 (4.2)	18 (5.0)	
Grade			0.767
I	51 (18.1)	63 (17.6)	
II	127 (45.0)	153 (42.7)	
III	104 (36.9)	142 (39.7)	
Nodal status			0.759
Negative	160 (57.6)	200 (56.3)	
Positive	118 (42.4)	155 (43.7)	
ER status			0.422
Negative	94 (33.3)	109 (30.4)	
Positive	188 (66.7)	250 (69.6)	
HER2 status			0.221
Negative	234 (83.6)	284 (79.8)	
Positive	46 (16.4)	72 (20.2)	
Necrosis			0.994
<25%	137 (49.5)	173 (49.4)	
>25%	140 (50.5)	177 (50.6)	
KM score			**0.001**
0	27 (9.9)	61 (17.4)	
1	166 (60.6)	162 (46.2)	
2	56 (20.4)	100 (28.5)	
3	25 (9.1)	28 (8.0)	
CD8+ lymphocytes			**0.023**
Low			
Medium	53 (34.0)	42 (25.6)	
High	43 (27.6)	69 (42.1)	
	60 (38.5)	53 (32.3)	
CD4+ lymphocytes			**0.017**
Low			
Medium	67 (25.3)	112 (34.8)	
High	92 (34.7)	112 (34.8)	
	106 (40.0)	98 (30.4)	
TSP			0.597
Low	195 (70.1)	240 (68.2)	
High	83 (29.9)	112 (31.8)	
Budding			0.259
≤20 buds	195 (70.1)	232 (65.9)	
>20 buds	83 (29.9)	120 (34.1)	
Tumour IL6/HK			0.536
Low	165 (70.5)	202 (68.0)	
High	69 (29.5)	95 (32.0)	
Stromal IL6/HK			0.468
Low	75 (31.9)	110 (37.0)	
Medium	88 (37.4)	103 (34.7)	
High	72 (30.6)	84 (28.3)	
Cytoplasmic IL6R			**<0.001**
Low	200 (70.7)	128 (35.7)	
High	83 (29.3)	231 (64.3)	
Membranous IL6R			0.729
Low	236 (83.4)	303 (84.4)	
High	47 (16.6)	56 (15.6)	

Table 7-4. Associations between stromal IL6R and other clinicopathological factors. Table detailing the associations between stromal IL6R expression and other clinicopathological factors.

7.3.8 IL6 and IL6R in combination

To investigate the relationship of different combinations of IL6 expression and IL6R expression site with disease outcome, scores were created for each combination of tumour or stromal IL6 and each of the 3 IL6R receptor sites in the study. When both factors were high there was a significant association with worse CSS with all the possible combinations except stromal IL6 and cytoplasmic IL6R, on univariate analysis. However, on multivariate analysis controlling for known prognostic clinicopathological factors, the only combination independently associated with worse CSS was tumour IL6 and membranous IL6R.

Combined score	Univariate analysis		Multivariate analysis	
	HR (95% CI)	p	HR (95% CI)	p
Tumour IL6 + cytoplasmic IL6R		0.057		
0	1			
1	1.43 (0.94-2.18)	0.093		
2	1.87 (1.11-3.17)	**0.019**		
Tumour IL6+ membranous IL6R		**<0.001**		0.069
0	1			
1	1.39 (0.95-2.03)	0.087	0.95 (0.55-1.64)	0.852
2	4.67 (2.59-8.42)	**<0.001**	2.61 (1.10-6.17)	**0.029**
Tumour IL6 + stromal IL6R		**0.020**		0.425
0	1			
1	1.49 (1.00-2.22)	**0.048**		0.269
2	2.12 (1.20-3.75)	**0.010**		0.648
Stromal IL6 + cytoplasmic IL6R		0.528		
0	1			
1	1.04 (0.60-1.80)	0.901		
2	1.38 (0.80-2.38)	0.254		
3	1.18 (0.61-2.26)	0.625		
Stromal IL6 + membranous IL6R		**0.033**		0.395
0	1			
1	1.20 (0.75-1.91)	0.445		0.818
2	1.16 (0.71-1.89)	0.560		0.365
3	2.69 (1.37-5.29)	**0.004**		0.276
Stromal IL6 + stromal IL6R		**0.027**		0.275
0				
1	1	0.110		0.747
2	1.50 (0.91-2.48)	0.934		0.152
3	1.02 (0.59-1.76)	**0.012**		0.807
	2.31 (1.21-4.43)			

Table 7-5. Associations between combined IL6 and IL6R expression scores and CSS. Table showing univariate and multivariate Cox regression analysis for the association between various scores combining different IL6 and IL6R expression sites and CSS. For the multivariate analysis, scores with p<0.005 were individually (ie. Not alongside another of the scores) entered into a multivariate model with other significant clinicopathological factors detailed in similar analysis earlier in this chapter.

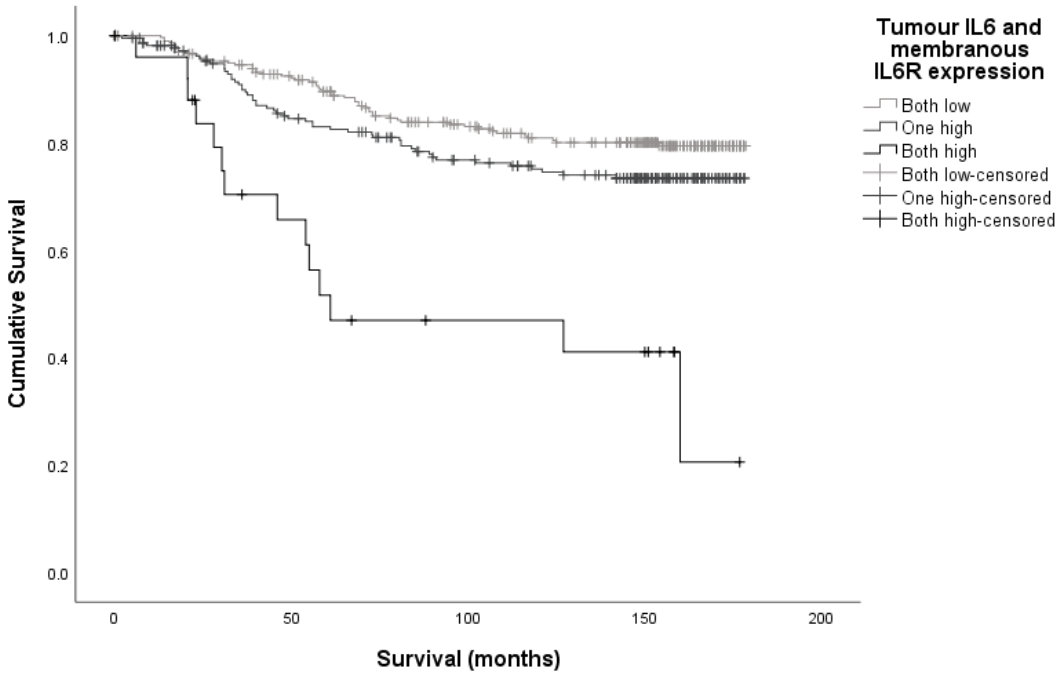

Figure 7-31. The relationship between a combined score of tumour IL6 and membranous IL6R expression and CSS. Kaplan meier graph illustrating the relationship between a combined score of tumour IL6 and membranous IL6R expression and CSS ($p<0.001$).

7.4 Discussion

This study describes the pattern of IL6 and IL6R expression in a cohort of primary operable breast cancers. Higher IL6 expression in stroma compared to tumour was observed and higher stromal expression was observed in the triple negative subtype. Cytoplasmic IL6R expression was generally higher than membranous expression but when high membranous expression was present there was a significant association with worse CSS, particularly when this was combined with high tumour IL6.

The observation that IL6 expression is higher in TNBC is in keeping with some previous research. The triple negative cell line MDA-MB-231 produces IL-6 while the ER positive cell line MCF-7 does not(290-292). One tissue study reported overexpression of multiple cytokines, including IL-6, in ER negative breast cancer(279). This study used a multiplexed flow cytometry method and therefore did not distinguish between the position of the IL6 in the tumour or the stroma. Similarly, in a large genomic study, IL6 expression was reported to be high in TNBC but not in the other molecular subtypes(293). The higher stromal expression observed in this study may represent secretion by immune cells and CAFs in the stroma, which have been shown to express high levels of IL6 in human breast cancer(284), and reflect the more inflammatory nature of triple negative breast cancer compared to the other molecular subtypes. It is interesting to note the positive correlation observed between tumour and stromal IL6 expression. In contrast to the above findings, an early small study reported an association between ER positivity and IL6, with a positive correlation between the levels of ER and IL6 staining(294). However, its measurement of IL6 staining was specifically in tumour cells rather than stroma or both. In the present study no association between ER status and tumour IL6 was observed.

It was observed that membranous IL6R expression on tumour cells was associated with worse CSS independently of other prognostic factors, suggesting that the classical signalling pathway is important in tumour progression. The association with worse CSS was particularly marked in patients who had tumours with both high membranous IL6R and high tumour IL6 expression. This was particularly the case in luminal A disease. This is suggestive of a positive feedback loop whereby

the tumour secretes IL6 which stimulates its own growth and progression via the membranous IL6R receptor and JAK/STAT3 signalling. This is supported by previous work showing that STAT3 activation in tumour cells leads to increased production of IL6(295). Evidence regarding the direct effect of IL6 on tumour growth is mixed with studies reporting growth inhibitory(292, 296) and growth stimulating effects(285, 297). Mechanisms which have been suggested for its pro-tumour effects include alteration of the proliferation/apoptosis balance via an effect on bcl-2 expression(298) and downregulation of tumour suppressor hypermethylated in cancer 1 (HIC1)(299). This conflict suggests the involvement of multiple other influencing factors, such as activation of JAK/STAT3, other components of the tumour microenvironment and the interplay between other cell signalling pathways which IL6 can activate such as the Ras-MAPK, JNK MAPK, PI 3-K-Akt and MEK-ERK5 pathways. This is supported by our study in that tumour IL6 was associated with worse CSS but this was not independent of other prognostic factors. The ability of IL6 to initiate JAK/STAT3 signalling via classical signalling would appear to be important.

On molecular subtype analysis, this association was only significant in luminal A disease. This could simply be because of the higher sample numbers for this subtype, providing more statistical power. However, it is in keeping with previous evidence that ER positive tumours are more sensitive to stimulation by IL6. It has been postulated that this may be due to the longstanding higher exposure of ER negative breast cancer cells to IL6(274). Another reason proposed is that it could be due to difference in IL6R expression with one cell line study reporting that ER positive cells predominantly express sIL6R while in ER negative breast cancer cells the transmembrane receptor predominates(292), but this was not observed in our study. Interestingly, a large genomic study reported high expression of gp130 in luminal A breast cancers but not the other molecular subtypes(293). It is also of interest that IL6 has been reported to increase oestrogen levels(300, 301) and this therefore may be another mechanism by which IL6 stimulates tumour progression in ER positive disease.

It is interesting to note the inverse association between membranous IL6R expression and tumour budding, given that both are reported in this thesis as poor prognostic features. IL6 has been shown to induce EMT in ER positive cell

lines (302) but the finding in this study raises the possibility that once the budding phenotype is established, stimulation by IL6 may become less important.

The association between high tumour IL6, high membranous IL6R and worse CSS observed in this study suggests that therapies which target IL6/IL6R may be beneficial in some patients, particularly those with high-risk ER positive disease or those who have developed resistance to endocrine therapies. As detailed in a review by Heo et al, a number of molecules which target IL6, IL6R or gp130 are available(272). Many of these have shown anti-inflammatory and antitumoural activity in vitro. Several have been approved or are the subject of ongoing trials in autoimmune diseases such as rheumatoid arthritis, systemic lupus and Castleman's disease, providing evidence for their safety in clinical use. Few have undergone clinical trials for cancer, one rare example is the trial of siltuximab in melanoma. Most of the cancer work to date is preclinical and there have been very few studies either in the pre-clinical or clinical setting involving breast cancer. The IL6 inhibitor 6a inhibits STAT3 phosphorylation in IL-6 stimulated MDA-MB-231 cells(303). The IL6R inhibitor tocilizumab inhibited tumour growth in trastuzumab-resistant breast cancer cell lines in mouse models(289). Although adverse effects including infection, cardiovascular toxicity and gastrointestinal perforation have been reported with IL6/IL6R inhibitors, their safe use in certain inflammatory diseases supports further investigation of their potential role in breast cancer.

Limitations of our study include the small patient numbers in the less common molecular subtypes which limit the possibility of identifying significant associations in these groups. Numbers available for final analysis were also limited due to the number of TMA cores which were incomplete or completely floated off during the staining process, perhaps due to the age of the tissue. The nature of TMAs also means that only a tiny section of the tumour is observed and at a single point in time so it may not account for tumour heterogeneity and changes in the tumour as it progresses. This single point in time analysis also makes it difficult to conclude with certainty whether membranous IL6R expression observed represents the membrane-bound IL6R and therefore activation of the classical signalling pathway or whether it actually represents

sIL6R which has formed a complex with IL6 and subsequently bound to the membrane. On the other hand, one advantage of using the RNA scope method to identify IL6 is that it detects the RNA message, and therefore we can be more confident that the IL6 is being produced by the cells in the site it is observed. However, it could also be argued that this message may not be translated to IL6 protein synthesis and secretion as other processes and pathways may interfere and therefore, we may not have a truly accurate recording of the amount of IL6 present.

In summary, the present study has observed higher stromal IL6 expression in TNBC, suggesting that stromal cells such as CAFS and immune cells in this particularly inflammatory tumour type secrete IL6. However, no association between stromal IL6 and CSS was observed. Overall and in luminal A cancer, high membranous expression of IL6R, particularly when combined with high tumour IL6 expression, was associated with worse CSS. This may represent a positive feedback loop driving tumour progression, possibly via the classical signalling pathway. Therefore, further investigation of the role of IL6 and the IL6R in breast cancer is warranted as treatments which target both of these proteins are already in existence and some are in clinical use for other conditions.

8 JAK1 and JAK2 in primary operable breast cancer.

8.1 Introduction

Findings in the previous chapter suggest a role for IL6 and IL6R in the progression of primary operable breast cancer. IL6 can stimulate several different cell signalling pathways but this thesis focuses on the IL6/JAK/STAT3 pathway. Therefore, to better understand the role of this pathway in breast cancer, this chapter will focus further downstream in the pathway, on the Janus kinases (JAKs) 1 and 2.

Four JAKs are known to exist, namely JAKs 1,2, 3 and TYK2(304).They are a subgroup of non-receptor tyrosine kinases(304). As previously described, when a ligand binds to its receptor (in this case IL6 to IL6R), phosphorylation of JAKs occurs at specific tyrosine and serine residues and the JAKs become enzymatically active(304). This leads to phosphorylation of STATs. Structurally, JAKs are made up of a C terminus on which the kinase domain is located, a pseudokinase domain, a SH2 domain and a N terminus which is the part which interacts with the intracellular portion of receptors(304). It is the kinase and pseudokinase domains which led to the name Janus kinase, after the two-faced Roman god Janus(305). Of the 4 JAKs, JAKs 1 and 2 can activate STAT3 in response to IL6(306) and will therefore be the subject of this chapter.

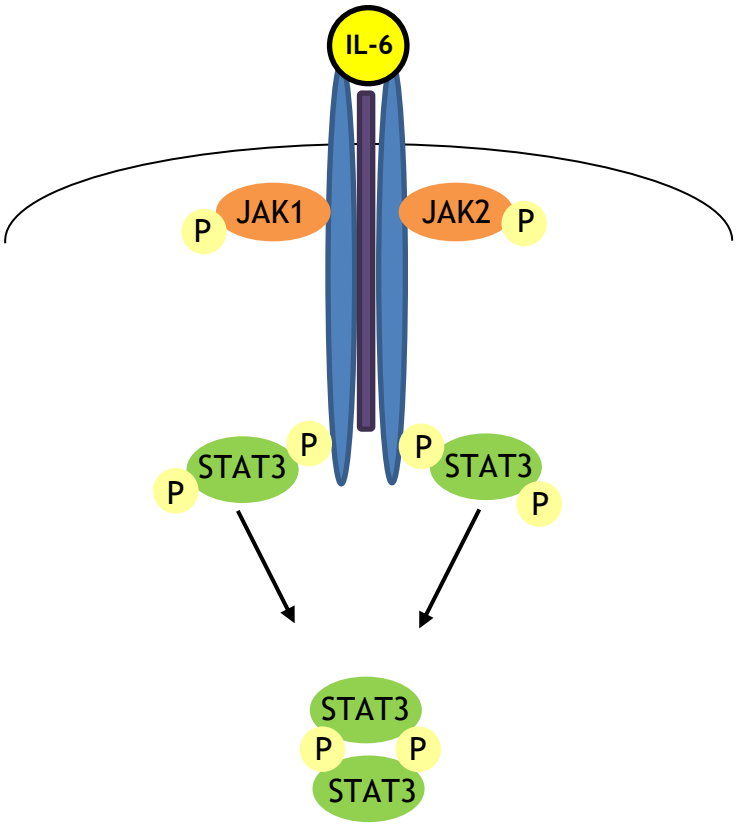

Figure 8-1. Phosphorylation of STAT3 by JAK. Diagram illustrating the next stage of the Il6/JAK/STAT3 pathway. Activated JAKs phosphorylate tyrosine residues of the IL6R, allowing STAT3 to bind. JAKs then phosphorylate STAT3 following which dimerisation of STAT3 occurs.

JAKs have been extensively studied in immune diseases and haematological malignancies and some JAK inhibitors are in clinical use while trials are ongoing in others (304, 307, 308). This raises the question as to whether these agents may be beneficial in breast cancer. There is limited literature regarding the role of JAKs 1 and 2 in breast cancer. In cell line and murine models JAK1 has been identified as a pivotal kinase for the activation of STAT3 resulting in increased invasiveness(306, 309). However studies of human breast cancer tissue have reported lower levels of JAK1 expression in breast cancer compared to normal breast tissue(310) and a correlation with improved cancer outcomes and higher TILs with higher JAK1 expression(311). These latter results raise the possibility that use of JAK1 inhibitors may be counterproductive in breast cancer treatment. Cell line studies of JAK2 have reported conflicting results regarding its effect on STAT3 activation(312, 313). Elevated JAK2 expression is reported to be associated with worse cancer outcomes in triple negative breast cancer and

may be implicated in chemotherapy resistance, suggesting JAK2 specific inhibition may have a role in breast cancer treatment(314).

With this limited evidence in mind, for this study it was postulated that, in a cohort of patients with primary operable breast cancer, high JAK2 expression would be associated with poorer outcomes and, if it is being activated by IL6/IL6R, high JAK2 expression would be correlated with high IL6/IL6R expression. The study therefore aims to describe the expression of JAK1 and JAK2 in primary operable breast cancer and to determine if they are associated with cancer outcomes, with specific clinicopathological features and with IL6 and IL6R expression with a view to better understanding their role within the IL6/JAK/STAT3 pathway in primary operable breast cancer.

8.2 Materials and methods

8.2.1 Patient cohort

The 1800 cohort was used for this study as tissue blocks were available for cutting of a previously constructed TMA. Patient characteristics are detailed in chapter 2.

8.2.2 TMA slide staining and scanning

TMAs were stained in triplicate for JAK1 and separately for JAK2 using the immunohistochemistry technique and antibody detailed in chapter 2. They were scanned into Slidepath software as previously described.

8.2.3 Scoring for JAK1 and JAK2 expression

Each TMA core was scored by the author using the weighted histoscore method described in chapter 2. Cores which were assessed visually to have >20% of the core missing were not scored. For both JAK1 and JAK2, nuclear and cytoplasmic expression in tumour cells was scored separately. A separate score was also given for expression in stromal cells (differentiation between nuclear and cytoplasmic expression in these smaller cells was not reliably possible at 20x magnification).

8.2.4 Molecular subtyping

ER, PR, HER2 and Ki67 profiling had previously been carried out in the lab for this cohort. This data was used to divide the cohort into the four main molecular subtypes of breast cancer, as detailed in chapter 1, for subgroup analysis.

8.2.5 Statistical analysis

Initial analysis using ROC curves and division into tertiles and at the median was carried out to determine the optimum threshold for division into high and low expression groups for further analysis. Analysis of associations with clinicopathological characteristics and with cancer specific survival was carried out as described in chapter 2. This analysis was carried out initially in the full cohort, then in the ER positive and ER negative cohorts separately, and subsequently in the 4 individual molecular subtypes.

8.3 Results

8.3.1 Formation of the cohort

577 patients had at least one core which was assessable for tumour cell nuclear and cytoplasmic JAK1 staining. 531 had at least one core which was assessable for stromal JAK1 expression (**Figure 8-2**).

567 patients had at least one core which was assessable for tumour cell nuclear and cytoplasmic JAK2 expression. 533 patients had at least one core which was assessable for stromal cell JAK2 expression (**Figure 8-3**).

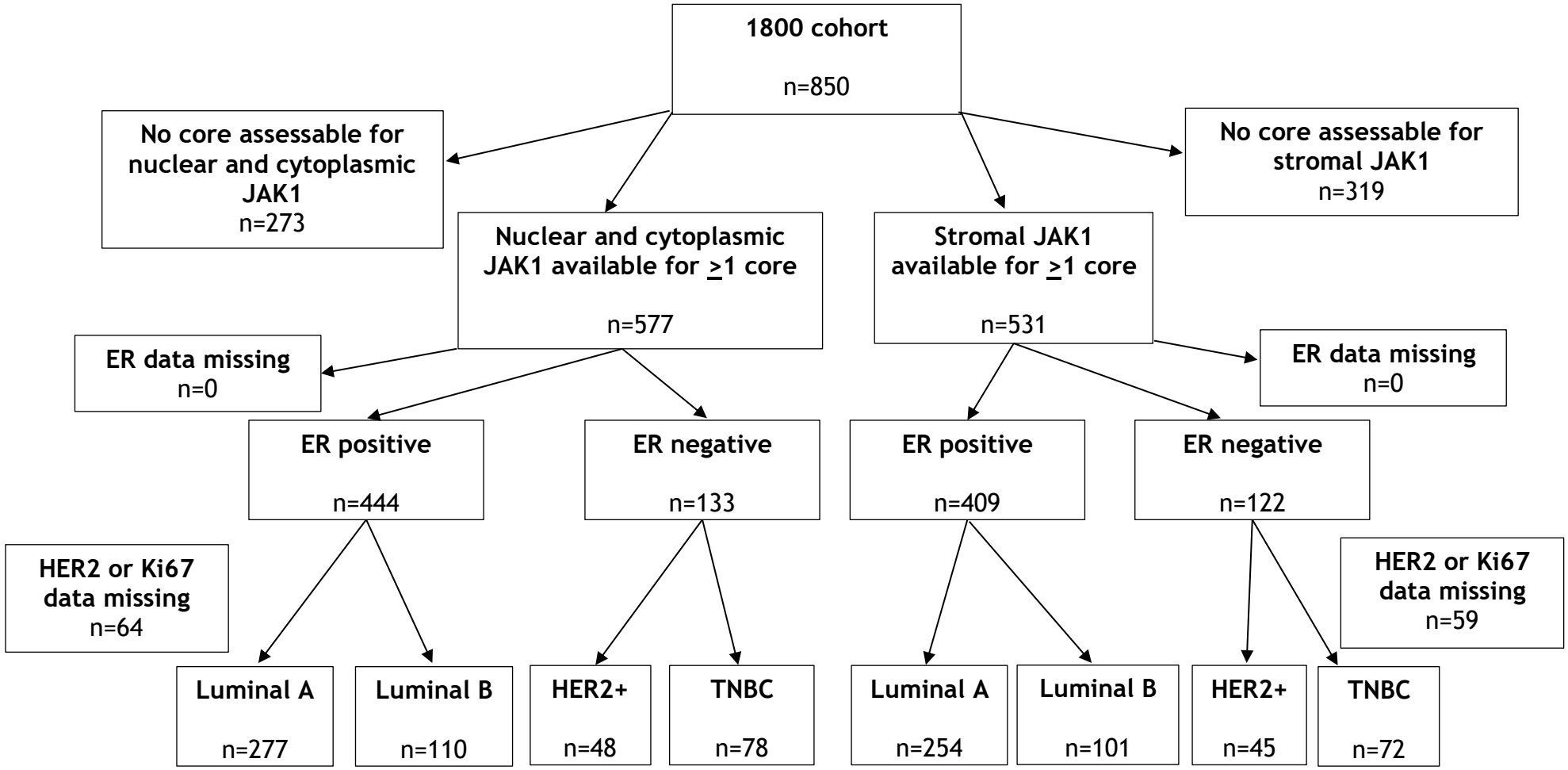

Figure 8-2. Formation of the JAK1 cohort. Flow diagram to illustrate the number of patients within the 1800 cohort with at least 1 core which was assessable for JAK1 expression in the tumour cell nucleus and cytoplasm, and separately in the stroma. The numbers available for subgroup analysis by ER status and by molecular subtype are also shown.

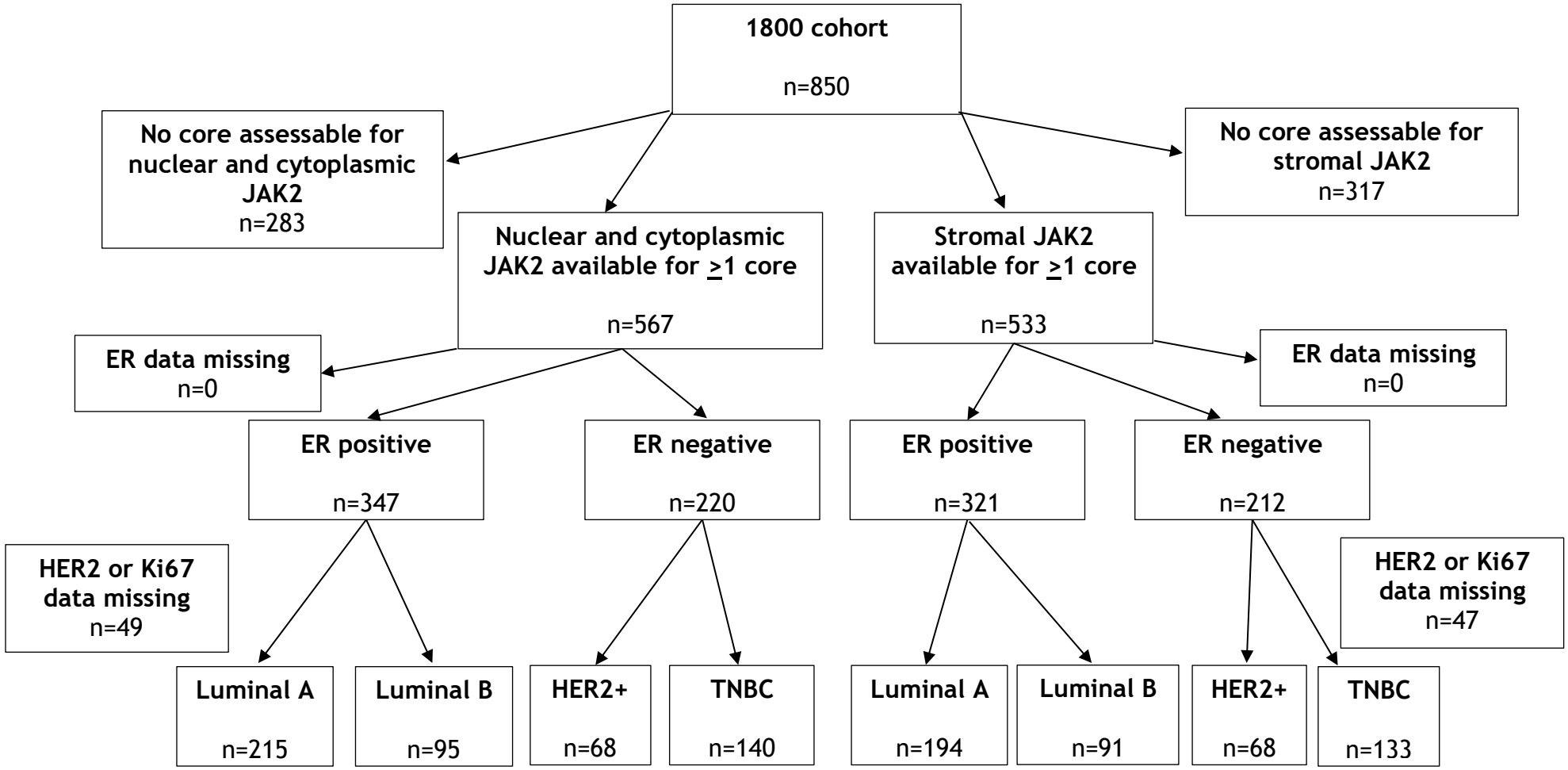

Figure 8-3. Formation of the JAK2 cohort. Flow diagram to illustrate the number of patients within the 1800 cohort with at least 1 core which was assessable for JAK2 expression in the tumour cell nucleus and cytoplasm, and separately in the stroma. The numbers available for subgroup analysis by ER status and by molecular subtype are also shown.

8.3.2 JAK1 expression

JAK1 was predominantly expressed in tumour cytoplasm but some nuclear expression was observed. Examples of TMA cores stained for JAK1 are shown below (**Figure 8-4**).

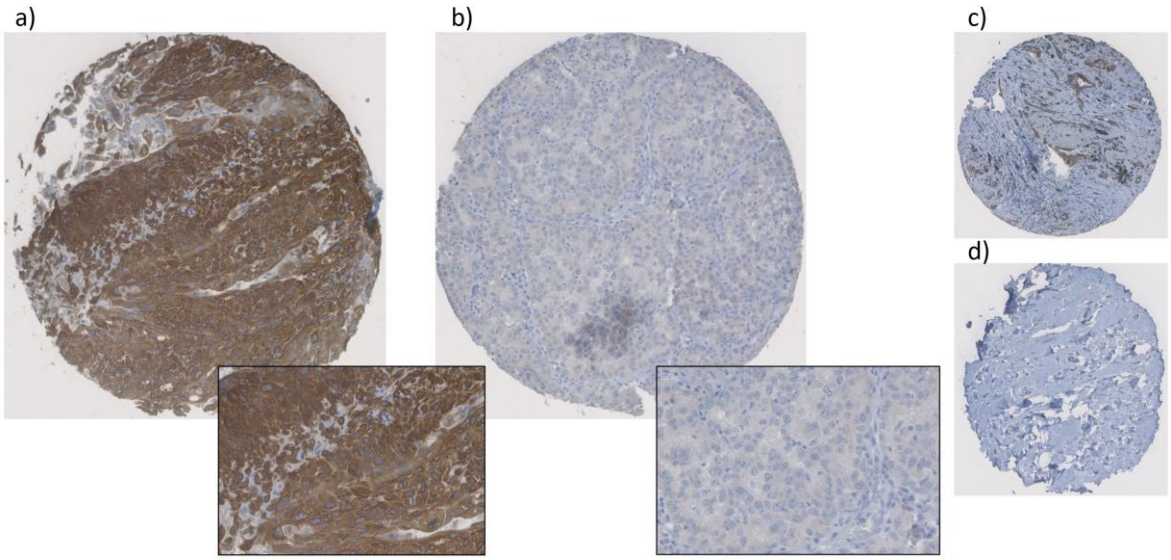

Figure 8-4. Examples of JAK1 staining. TMA cores stained using IHC for JAK1: a) breast core with predominantly moderate and strong cytoplasmic staining at 10x magnification with an inset at 40x magnification, b) breast core with predominantly weak cytoplasmic staining, c) true positive core (control, liver) at 10x magnification, d) true negative core at 10x magnification.

Median WHS for cytoplasmic expression was 101.67 (0-230) compared to 0.33 (0-61.00) for nuclear expression. Median WHS for stromal cell expression was 1.67 (0-130.00). Expression of JAK1 in the different locations described is illustrated in the figures below (**Figure 8-5, Figure 8-6**).

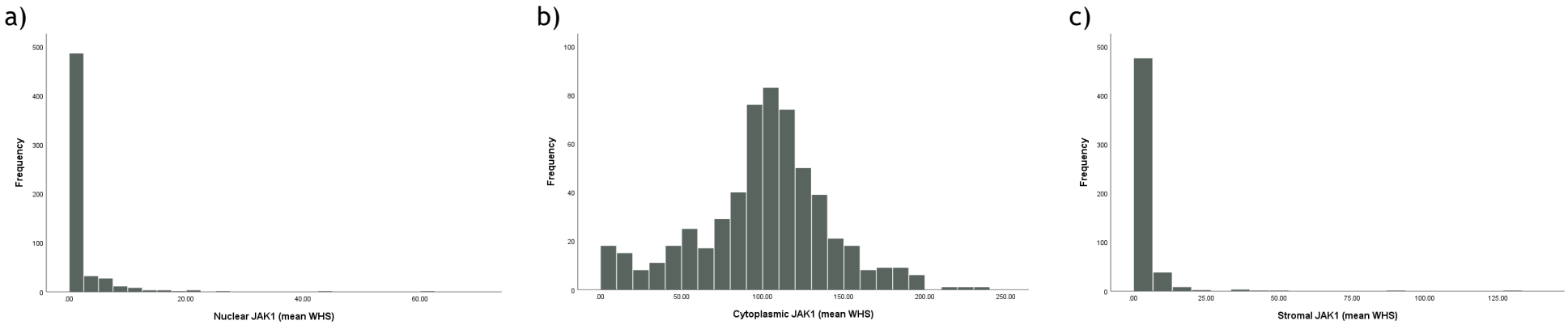

Figure 8-5. Histograms of JAK1 expression. Histograms to illustrate JAK1 expression in a) tumour cell nuclei, b) tumour cell cytoplasm and c) stromal cells.

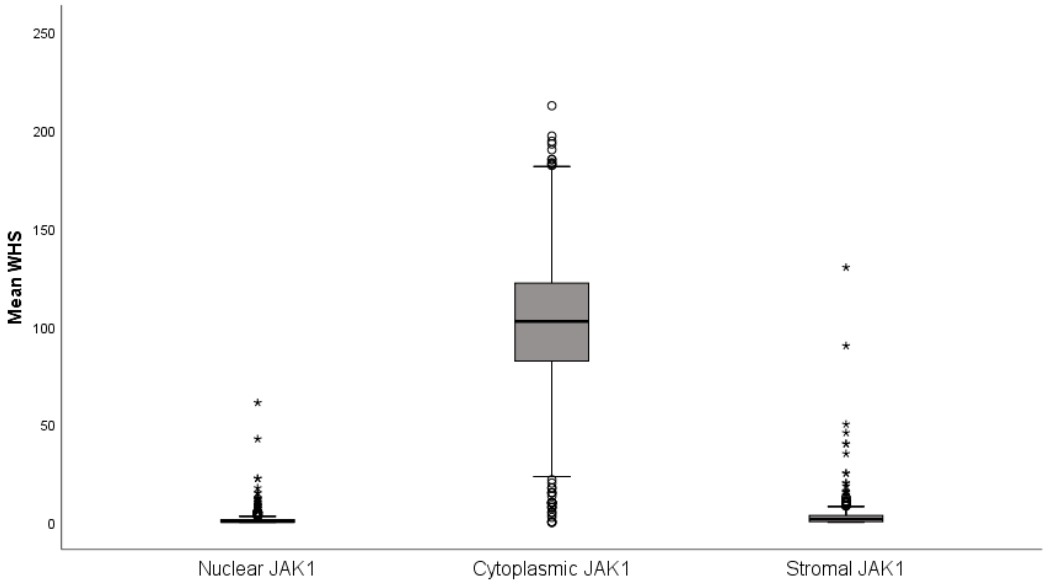

Figure 8-6. Boxplots of JAK1 expression. Boxplots to illustrate the expression of JAK1 in tumour cell nuclei, cytoplasm and stromal cells.

Nuclear JAK1 expression was highest in luminal A cancers (**Figure 8-7**).

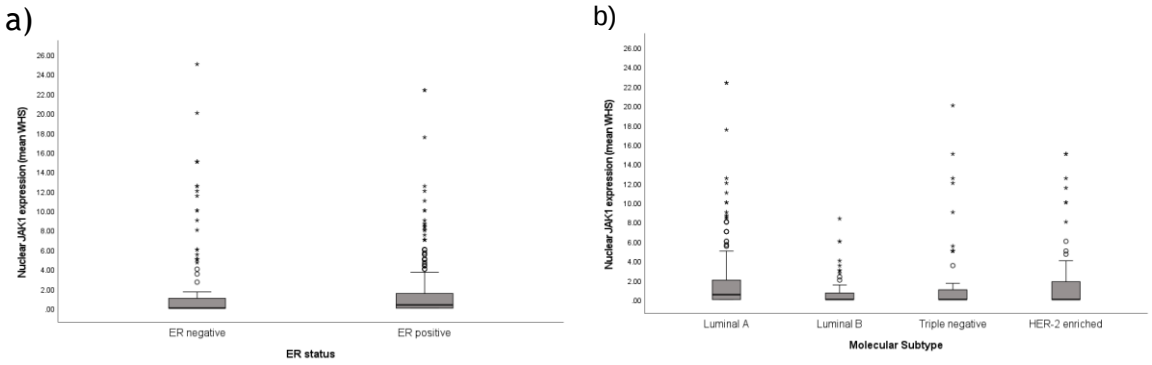

Figure 8-7. Boxplots of nuclear JAK1 by hormone receptor status. Boxplots to illustrate the differences in nuclear JAK1 expression by a) ER status (p=0.646) and b) molecular subtype (**p=0.003**). In both graphs extreme outliers have been excluded to permit an appropriate scale (2 TNBC cases).

Cytoplasmic expression was highest in ER negative tumours and specifically the HER2-enriched subtype (**Figure 8-8**).

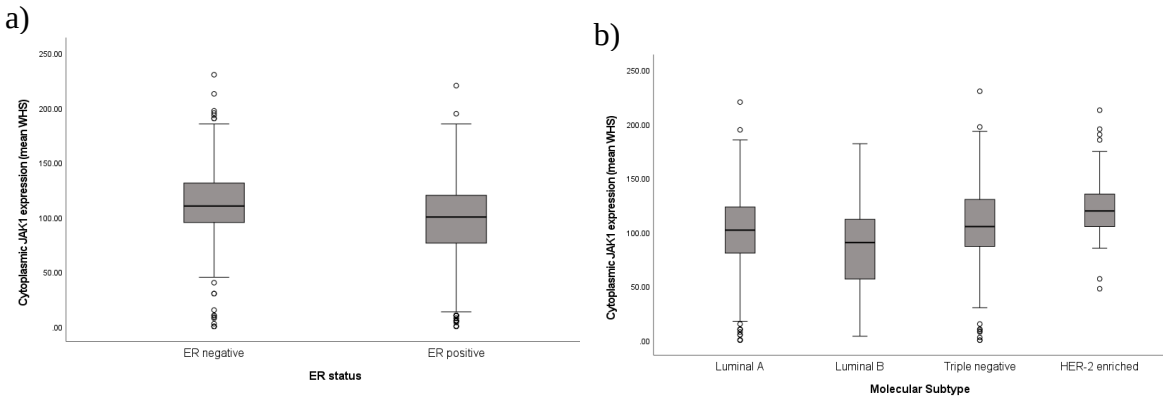

Figure 8-8. Boxplots of cytoplasmic JAK1 by hormone receptor status. Boxplots to illustrate the differences in cytoplasmic JAK1 expression by a) ER status (**p<0.001**) and b) molecular subtype (**p<0.001**).

Stromal expression was highest in luminal A and HER2-enriched cancers (**Figure 8-9**).

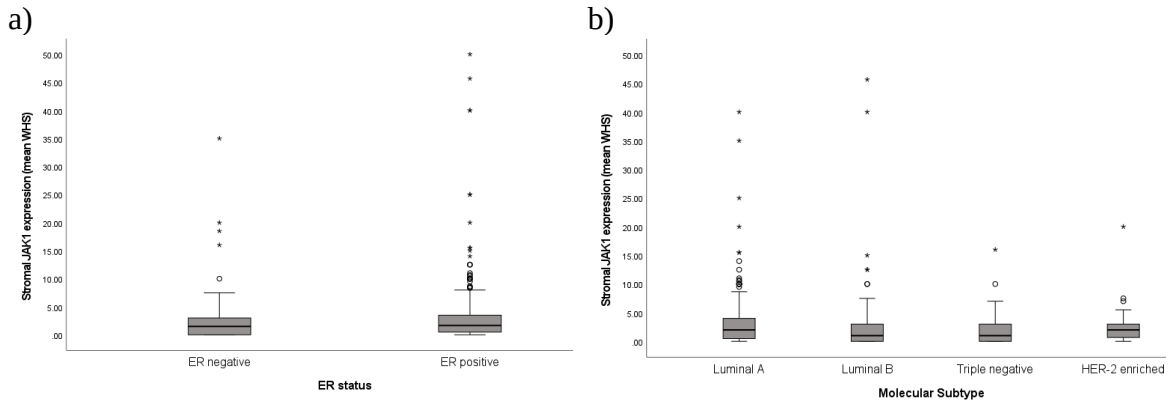

Figure 8-9. Boxplots of stromal JAK1 by hormone receptor status. Boxplots to illustrate the differences in stromal JAK1 expression by a) ER status (p=0.879) and b) molecular subtype (**p=0.017**). In both graphs extreme outliers have been excluded to permit an appropriate scale.

There was a moderate positive correlation between nuclear and cytoplasmic JAK1 expression (Pearson correlation 0.438, p<0.001). There was a weak positive correlation between cytoplasmic and stromal JAK1 expression (Pearson correlation 0.127, p=0.003) but there were significant outliers which may affect this statistic (**Figure 8-10**).

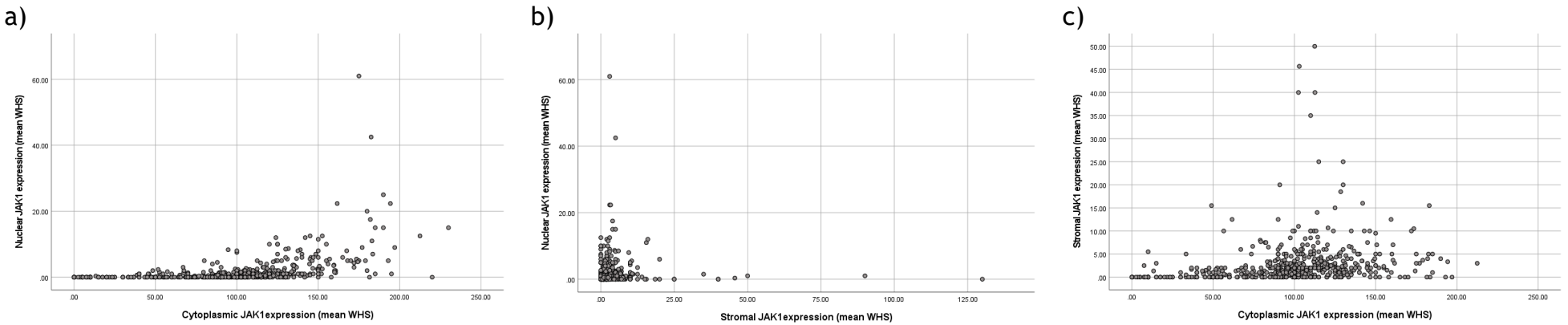

Figure 8-10. Correlation between JAK1 expression sites. Scatter plots to illustrate the correlation between JAK1 expression in different sites: a) nuclear and cytoplasmic expression (Pearson correlation 0.438, **p<0.001**), b) nuclear and stromal expression (Pearson correlation 0.023, p=0.601), c) cytoplasmic and stromal expression (Pearson correlation 0.127, **p=0.003**).

8.3.3 The relationship between JAK1 and CSS

ROC curves were drawn to determine thresholds for division of patients into high and low expression groups for further analysis (**Figure 8-11**). From these, a threshold of 0.17 was derived for nuclear JAK1 expression and a threshold of 0.17 was also derived for stromal JAK1 expression. No threshold could be derived from the ROC curve for cytoplasmic expression so the median of 101.67 was used.

a)

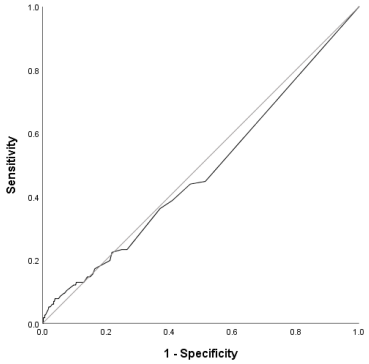

b)

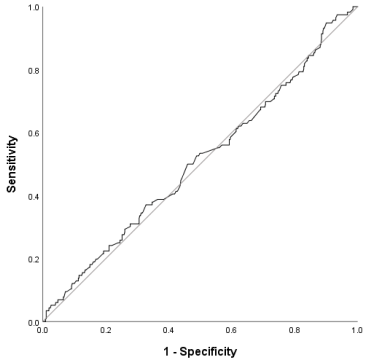

c)

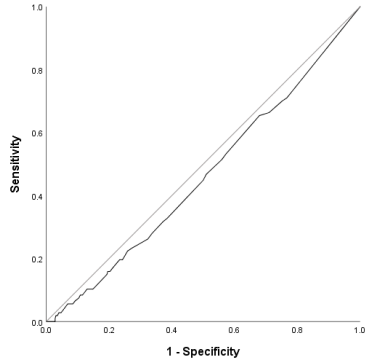

Figure 8-11. ROC curves for JAK1 and CSS. ROC curves to illustrate the relationship between CSS and JAK1 expression in a) tumour cell nuclei (AUC 0.480), b) tumour cell cytoplasm (AUC 0.508) and c) stromal cells (AUC 0.462).

8.3.3.1 Nuclear JAK1 expression and CSS

289 (50.1%) patients had high (mean WHS>0.17) nuclear JAK1 expression. There was no significant association between nuclear JAK1 expression and CSS (high v low: HR 0.79, 95% CI 0.55-1.14, p=0.209). However, when analysed according to ER status, low nuclear expression of JAK1 in tumour cells was significantly associated with worse CSS in ER positive disease (high v low: HR 0.60, 95% CI 0.38-0.95, p=0.029) but not ER negative disease (HR 1.44, 95% CI 0.77-2.68, p=0.249) (**Figure 8-12**). However, when analysed within the molecular subtypes, high nuclear expression of JAK1 was significantly associated with worse CSS in TNBC (HR 2.65, 95% CI 1.19-5.92, p=0.017) but there was no significant association with CSS in the other 3 subtypes (**Figure 8-13**). The associations in ER positive disease and TNBC were not independent of other prognostic variables (p=0.318 and p=0.222 respectively on multivariate analysis).

a)

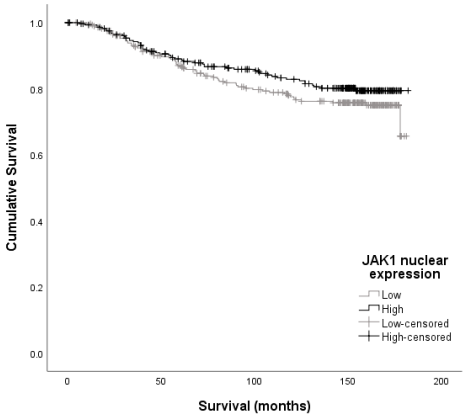

b)

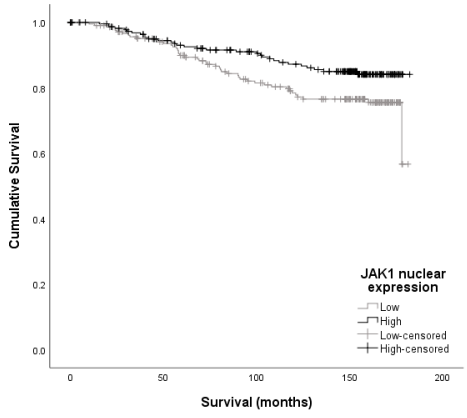

c)

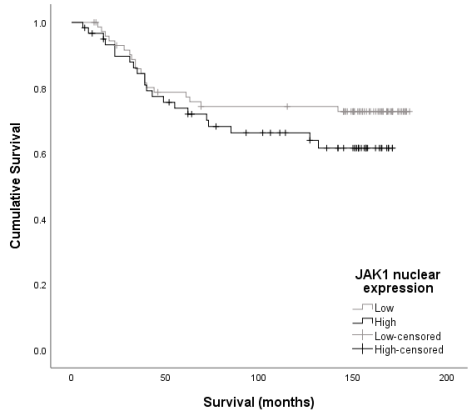

Figure 8-12. The relationship between nuclear JAK1 expression and CSS. Kaplan meier graphs to illustrate the relationship between nuclear JAK1 expression in tumour cells and CSS in a) the full cohort (n=577, p=0.207), b) ER positive disease (n=444, **p=0.028**) and c) ER negative disease (n=133, p=0.245).

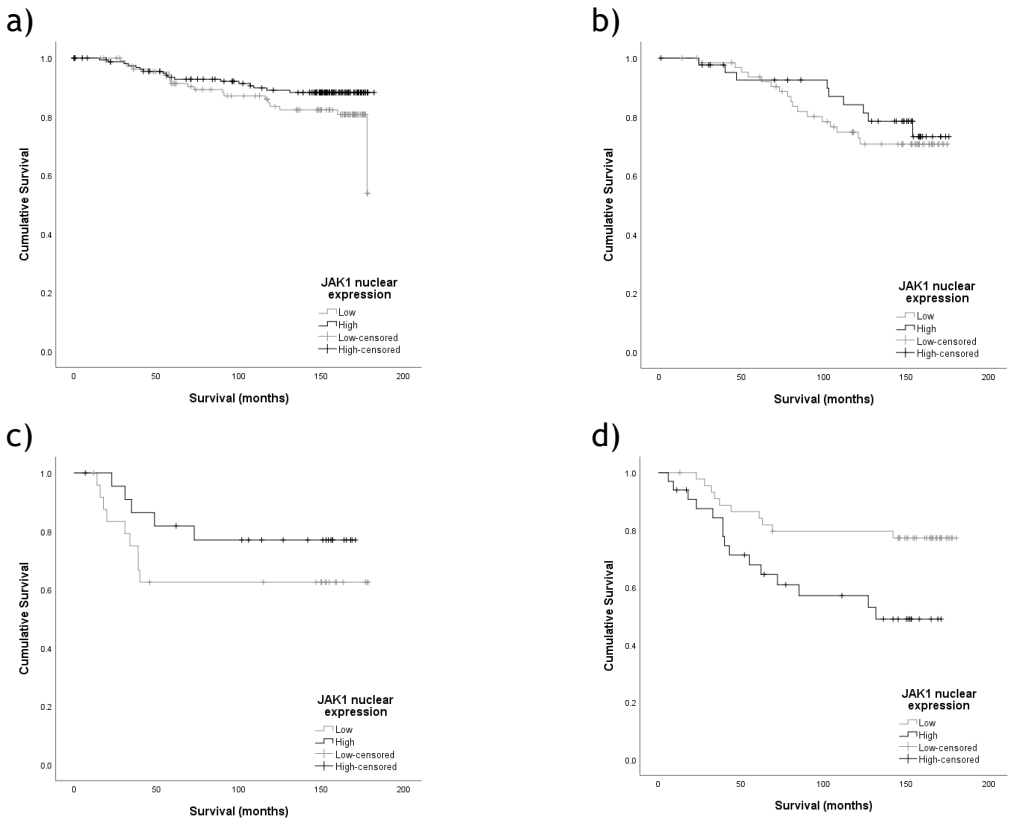

Figure 8-13. The relationship between nuclear JAK1 expression and CSS by molecular subtype. Kaplan meier graphs to illustrate the relationship between nuclear JAK1 expression in tumour cells and CSS in a) luminal A (n=277, p=0.118), b) luminal B (n=110, p=0.514), c) HER2-enriched (n=48, p=0.224) and d) triple negative (n=78, **p=0.013**) breast cancer.

8.3.3.2 Cytoplasmic JAK1 expression and CSS

There was no significant association between cytoplasmic JAK1 expression and CSS in the full cohort (high v low: HR 1.14, 95% CI 0.79-1.64, p=0.480), ER positive (HR 0.87, 95% CI 0.55-1.37, p=0.545) or ER negative disease (HR 1.45, 95% CI 0.72-2.90, p=0.298)(**Figure 8-14**). This was also the case when analysed in the individual molecular subtypes (data not shown).

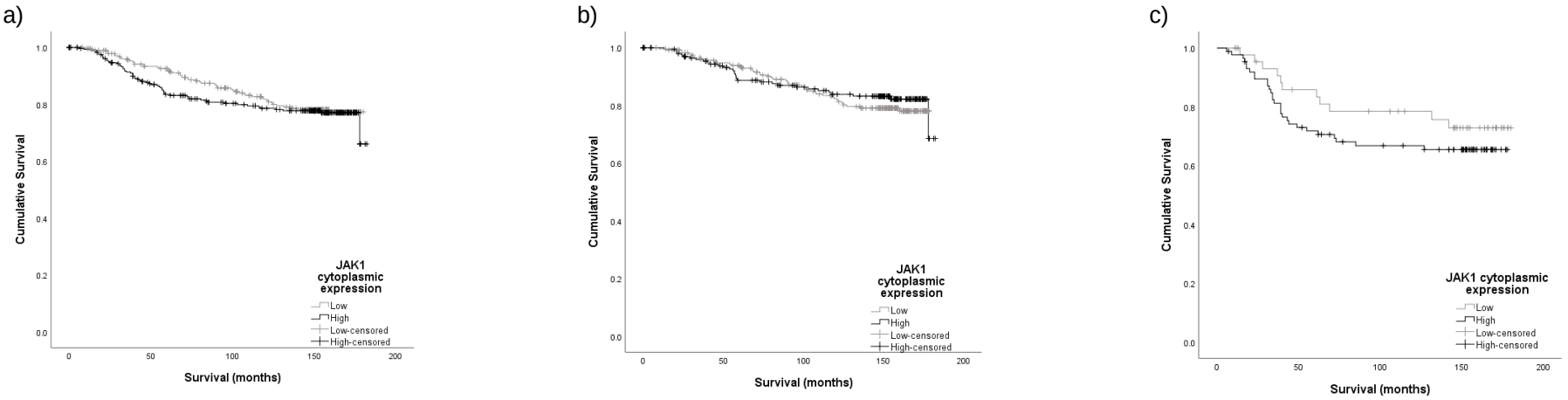

Figure 8-14. The relationship between cytoplasmic JAK1 expression and CSS. Kaplan meier graphs to illustrate the relationship between cytoplasmic JAK1 expression in tumour cells and CSS in a) the full cohort (n=577, p=0.480), b) ER positive disease (n=444, p=0.545) and c) ER negative disease(n=133, p=0.294).

8.3.3.3 Stromal JAK1 expression and CSS

401 (75.5%) patients had high (mean WHS>0.17) stromal expression of JAK1. There was no significant association between stromal JAK1 expression and CSS in the full cohort (high v low: HR 0.79, 95% CI 0.52-1.20, p=0.265). However, when analysed by ER status, low stromal JAK1 expression was significantly associated with worse CSS in ER positive (high v low: HR 0.61, 95% CI 0.37-0.99, p=0.047) but not ER negative disease (HR 1.55, 95% CI 0.70-3.41, p=0.277)(**Figure 8-15**). This was also the case when analysed in the individual molecular subtypes, though there was a trend towards worse CSS with low stromal JAK1 expression in luminal A disease (p=0.057)(**Figure 8-16**). The association in ER positive disease was not independent of other known prognostic variables (p=0.576).

a)

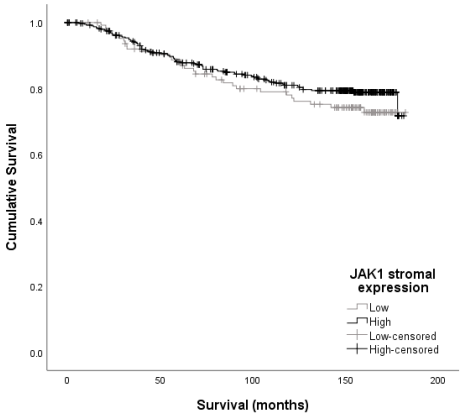

b)

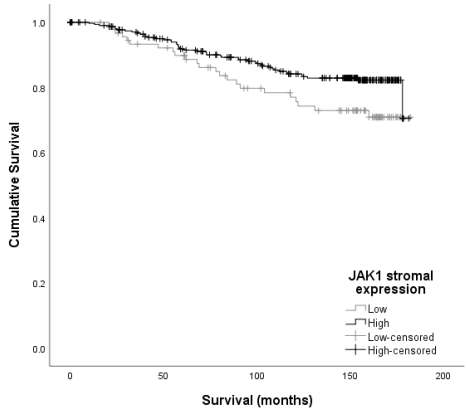

c)

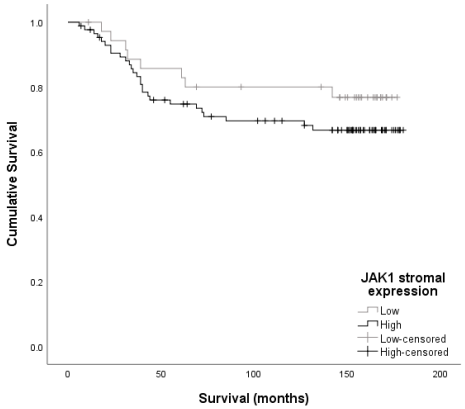

Figure 8-15. The relationship between stromal JAK1 expression and CSS. Kaplan meier graphs to illustrate the relationship between stromal JAK1 expression and CSS in a) the full cohort (n=531, p=0.264), b) ER positive disease (n=409, **p=0.045**) and c) ER negative disease (n=122, p=0.272).

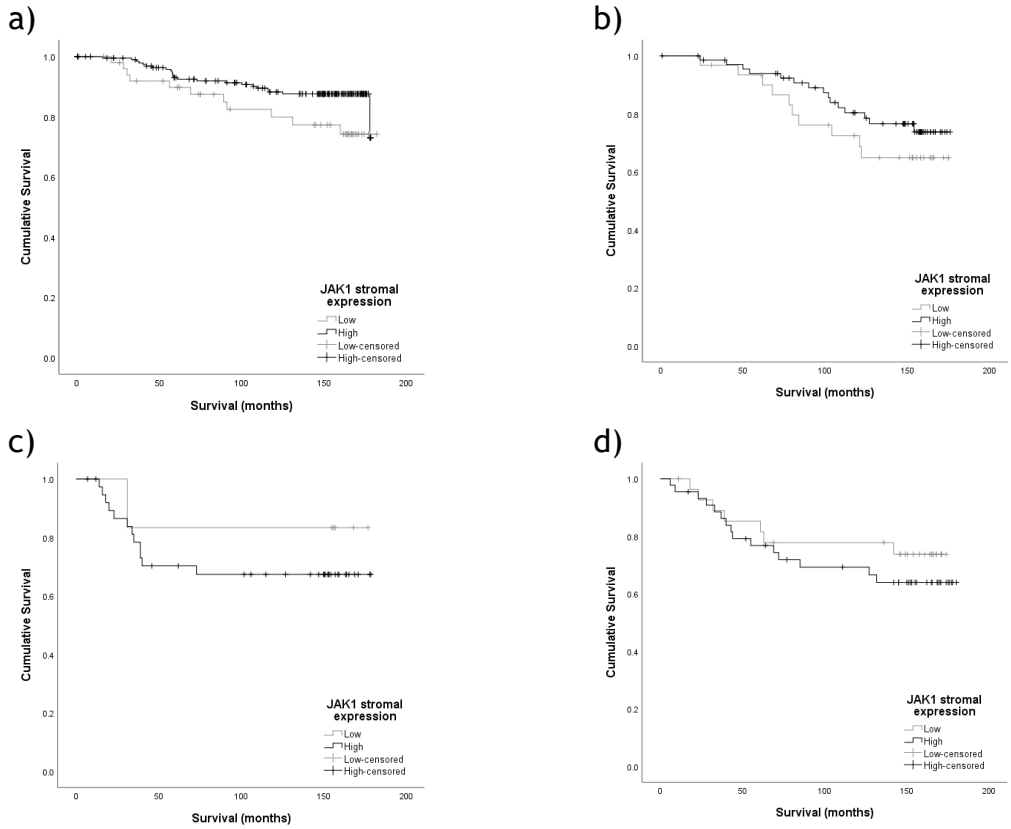

Figure 8-16. The relationship between stromal JAK1 expression and CSS by molecular subtype. Kaplan meier graphs to illustrate the relationship between stromal JAK1 expression and CSS in a) luminal A (n=254, p=0.057), b) luminal B (n=101, p=0.277), c) HER2-enriched (n=45, p=0.457) and d) triple negative (n=72, p=0.423) breast cancer.

8.3.4 Associations between JAK1 expression and clinicopathological characteristics

As nuclear and stromal JAK1 expression were both associated with cancer outcomes, association analysis was carried out for various clinicopathological factors.

High nuclear JAK1 expression was associated with increased age (p=0.032), lobular cancers (p=0.022), lower grade tumours (p=0.006) and low CD4+ lymphocytes (p<0.001) (**Table 8-1**). In ER positive disease it was associated with low grade (p<0.001) and low CD4+ lymphocytes (p<0.001) whereas in TNBC the only significant association was with increased age (p=0.013) (data not shown).

	Nuclear JAK1 expression		p
	Low n(%)	**High** n(%)	
Age			**0.032**
≤50yrs	94 (32.6)	71 (24.6)	
>50yrs	194 (67.4)	218 (75.4)	
Type			**0.022**
Ductal	258 (89.6)	260 (90.0)	
Lobular	11 (3.8)	21 (7.3)	
Other	19 (6.6)	8 (2.8)	
Size			0.752
≤20mm	156 (54.2)	165 (57.3)	
21-49mm	117 (40.6)	109 (37.8)	
≥50mm	15 (5.2)	14 (4.9)	
Grade			**0.006**
I	42 (14.6)	72 (24.9)	
II	141 (49.0)	131 (45.3)	
III	105 (36.5)	86 (29.8)	
Nodal status			0.708
Negative	159 (56.0)	164 (57.5)	
Positive	125 (44.0)	121 (42.5)	
ER status			0.191
Negative	73 (25.3)	60 (20.8)	
Positive	215 (74.7)	229 (79.2)	
HER2 status			0.281
Negative	231 (81.3)	244 (84.7)	
Positive	53 (18.7)	44 (15.3)	
Necrosis			0.060
<25%	143 (51.1)	164 (59.0)	
>25%	137 (48.9)	114 (41.0)	
KM score			0.143
0	51 (18.1)	43 (15.5)	
1	134 (47.7)	159 (57.2)	
2	73 (26.0)	55 (19.8)	
3	23 (8.2)	21 (7.6)	
CD8+ lymphocytes			0.497
Low	44 (31.9)	34 (26.0)	
Medium	47 (34.1)	52 (39.7)	
High	47 (34.1)	45 (34.4)	
CD4+ lymphocytes			**<0.001**
Low	67 (25.5)	111 (41.4)	
Medium	88 (33.5)	91 (34.0)	
High	108 (41.1)	66 (24.6)	
TSP			0.162
Low	192 (67.8)	205 (73.2)	
High	91 (32.2)	75 (26.8)	
Budding			0.422
≤20 buds	192 (67.8)	181 (64.6)	
>20 buds	91 (32.2)	99 (35.4)	

Table 8-1. The association between nuclear JAK1 and clinicopathological characteristics. Table detailing the associations between nuclear JAK1 expression and clinicopathological factors. Statistically significant p values are highlighted in bold.

High stromal JAK1 expression was associated with smaller tumour size (p=0.012), HER2 positivity (p=0.037), high tumour budding (p=0.005) and medium CD8+ lymphocyte counts (p=0.023) (**Table 8-2**).

	Stromal JAK1 expression		p
	Low n(%)	**High** n(%)	
Age			0.838
≤50yrs	38 (29.2)	121 (30.2)	
>50yrs	92 (70.8)	280 (69.8)	
Type			0.375
Ductal	114 (87.7)	368 (91.8)	
Lobular	8 (6.2)	16 (4.0)	
Other	8 (6.2)	17 (4.2)	
Size			**0.012**
≤20mm	60 (46.2)	240 (59.9)	
21-49mm	59 (45.4)	144 (35.9)	
≥50mm	11 (8.5)	17 (4.2)	
Grade			0.052
I	17 (13.1)	92 (22.9)	
II	67 (51.5)	180 (44.9)	
III	46 (35.4)	129 (32.2)	
Nodal status			0.226
Negative	80 (61.5)	218 (55.5)	
Positive	50 (38.5)	175 (44.5)	
ER status			0.141
Negative	36 (27.7)	86 (21.4)	
Positive	94 (72.3)	315 (78.6)	
HER2 status			**0.037**
Negative	114 (88.4)	322 (80.3)	
Positive	15 (11.6)	79 (19.7)	
Necrosis			0.242
<25%	64 (50.8)	223 (56.7)	
>25%	62 (49.2)	170 (43.3)	
KM score			0.408
0	16 (12.8)	66 (16.8)	
1	62 (49.6)	209 (53.0)	
2	34 (27.2)	89 (22.6)	
3	13 (10.4)	30 (7.6)	
CD8+ lymphocytes			**0.023**
Low	21 (31.3)	50 (26.7)	
Medium	16 (23.9)	79 (42.2)	
High	30 (44.8)	58 (31.0)	
CD4+ lymphocytes			0.135
Low	37 (30.6)	117 (31.6)	
Medium	34 (28.1)	134 (36.2)	
High	50 (41.3)	119 (32.2)	
TSP			0.161
Low	94 (74.6)	270 (68.0)	
High	32 (25.4)	127 (32.0)	
Budding			**0.005**
≤20 buds	97 (77.0)	252 (63.5)	
>20 buds	29 (23.0)	145 (36.5)	

Table 8-2. The association between stromal JAK1 and clinicopathological characteristics. Table detailing the associations between stromal JAK1 expression and clinicopathological factors. Statistically significant p values are highlighted in bold.

8.3.5 JAK2 expression

JAK2 expression was predominantly in the cytoplasm with a median WHS 99.00 (0-195.00). Very little nuclear JAK2 expression was observed with median WHS 0.00 (0-22.50). Median WHS for stromal cell JAK2 expression was 20.50 (0-193.00). Examples of TMA cores stained for JAK2 are show below (**Figure 8-17**).

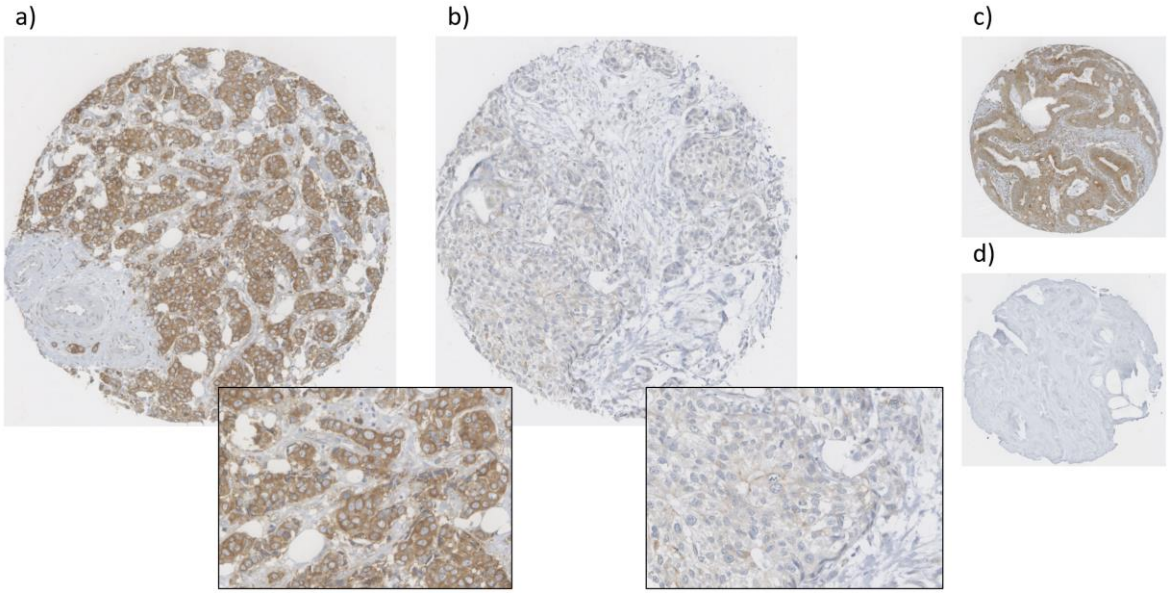

Figure 8-17. Examples of JAK2 staining. TMA cores stained using IHC for JAK2: a) breast core with predominantly moderate and strong cytoplasmic staining at 10x magnification with an inset at 40x magnification, b) breast core with predominantly weak cytoplasmic staining, c) true positive core (control, colon) at 10x magnification, d) true negative core at 10x magnification.

Expression of JAK2 in the different locations described is illustrated in the figures below (**Figure 8-18, Figure 8-19**).

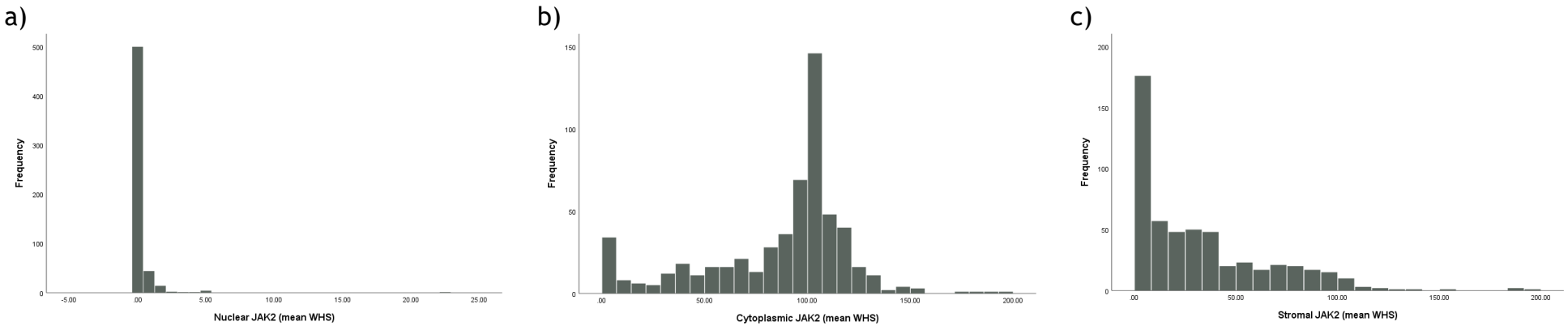

Figure 8-18. Histograms of JAK2 expression. Histograms to illustrate JAK2 expression in a) tumour cell nuclei, b) tumour cell cytoplasm and c) stromal cells.

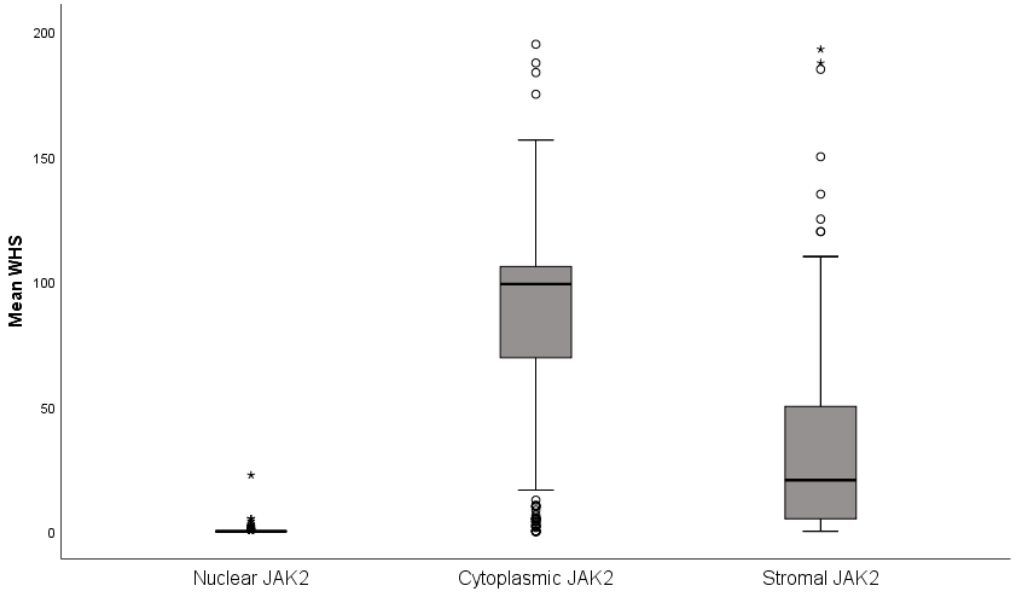

Figure 8-19. Boxplots of JAK2 expression. Boxplots to illustrate the expression of JAK2 in tumour cell nuclei, cytoplasm and stromal cells.

Nuclear expression was higher in the ER positive subtypes (**Figure 8-20**).

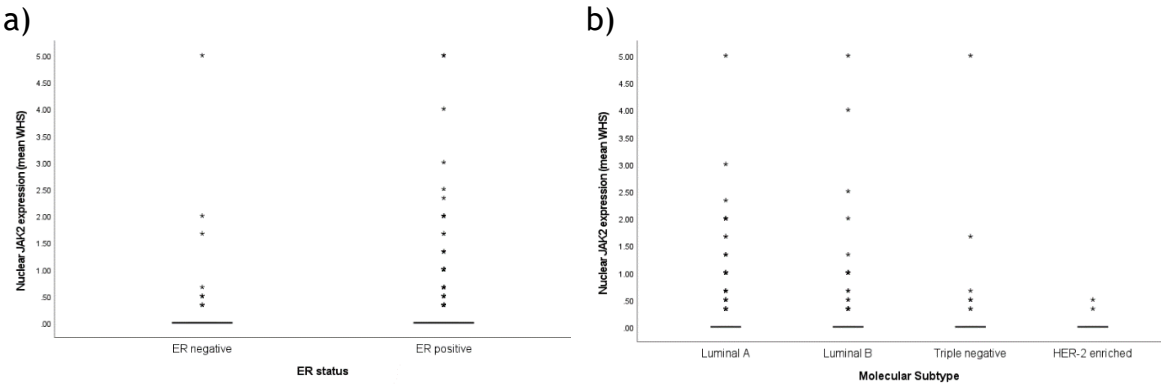

Figure 8-20. Boxplots of nuclear JAK2 by hormone receptor status. Boxplots to illustrate the differences in nuclear JAK2 expression by a) ER status (**p<0.001**) and b) molecular subtype (**p<0.001**). In both graphs extreme outliers have been excluded to permit an appropriate scale.

Cytoplasmic expression was higher in ER positive disease and lowest in the triple negative subtype (**Figure 8-21).**

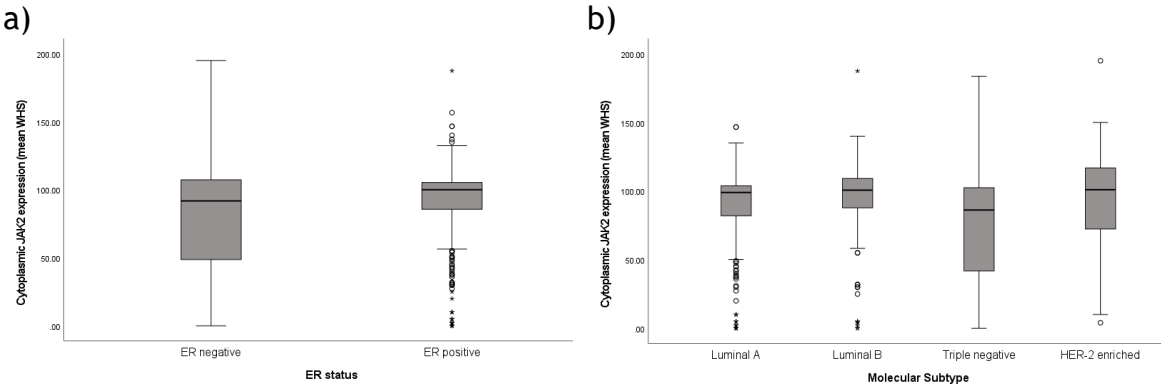

Figure 8-21. Boxplots of cytoplasmic JAK2 by hormone receptor status. Boxplots to illustrate the differences in cytoplasmic JAK2 expression by a) ER status (**p=0.001**) and b) molecular subtype (**p=0.001**).

Similarly, stromal expression was higher in ER positive disease and lowest in the triple negative subtype (**Figure 8-22**).

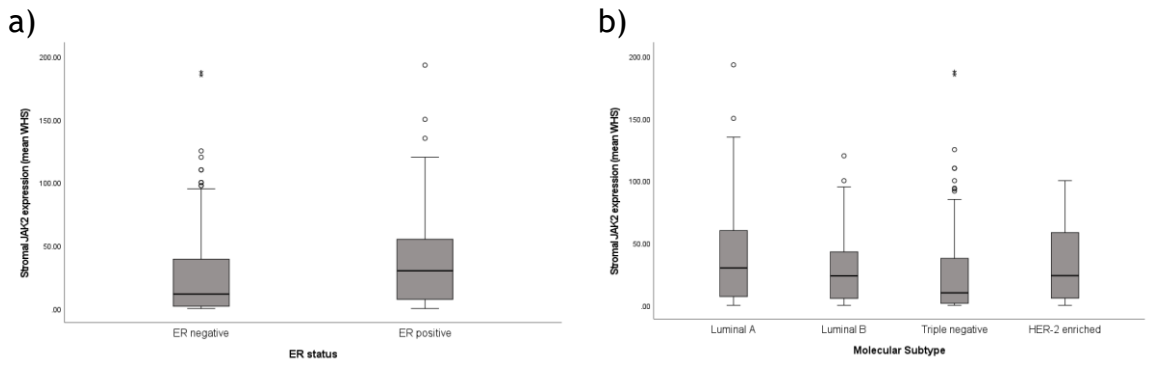

Figure 8-22. Boxplots of stromal JAK2 by hormone receptor status. Boxplots to illustrate the differences in stromal JAK2 expression by a) ER status (**p=0.004**) and b) molecular subtype (**p=0.025**).

There was a weak positive correlation between cytoplasmic and stromal JAK2 expression (Pearson correlation 0.276, p<0.001) (**Figure 8-23**). This was the only statistically significant correlation observed between the JAK2 expression sites.

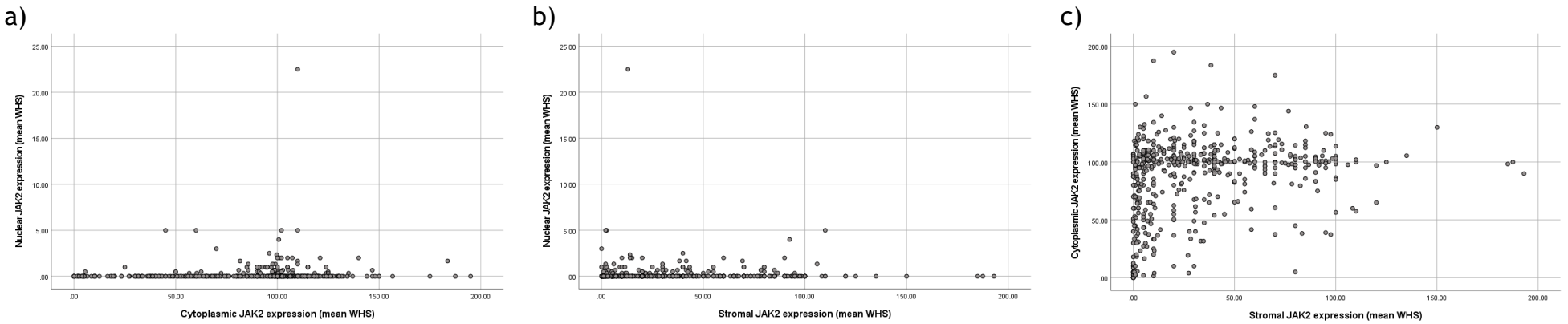

Figure 8-23. Correlation between JAK2 expression sites. Scatter plots to illustrate the correlation between JAK2 expression in different sites: a) nuclear and cytoplasmic expression (Pearson correlation 0.065, p=0.121), b) nuclear and stromal expression (Pearson correlation -0.001, p=0.985), c) cytoplasmic and stromal expression (Pearson correlation 0.276, **p<0.001**).

8.3.6 The relationship between JAK2 and CSS

ROC curves were drawn to determine thresholds for division of patients into high and low expression groups for further analysis (**Figure 8-24)**. From these, a threshold of 0.30 was derived for nuclear JAK2 expression and a threshold of 70.0 was derived for stromal JAK2 expression. No threshold could be derived from the ROC curve for cytoplasmic expression so the median of 99.0 was used.

a)

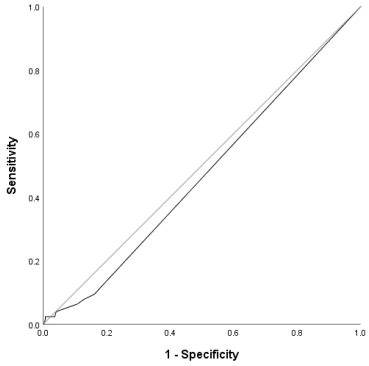

b)

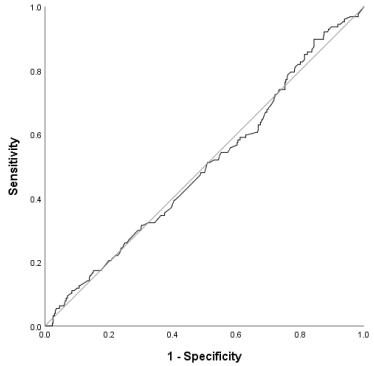

c)

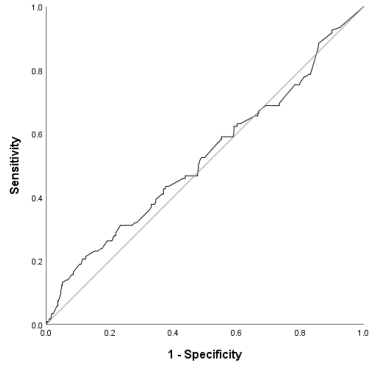

Figure 8-24. ROC curves for JAK2 and CSS. ROC curves to illustrate the relationship between CSS and JAK2 expression in a) tumour cell nuclei (AUC 0.468), b) tumour cell cytoplasm (AUC 0.499) and c) stromal cells (AUC 0.524).

8.3.6.1 Nuclear JAK2 expression and CSS

83 (14.6%) patients had high (mean WHS>0.30) nuclear JAK2 expression. There was no significant association between nuclear JAK2 expression and CSS in the full cohort (high v low: HR 0.61, 95% CI 0.33-1.10, p=0.605). This remained the case in ER positive (HR 0.69, 95% CI 0.34-1.39, p=0.293) and ER negative disease (HR 0.83, 95% CI 0.26-2.65, p=0.757) (**Figure 8-25**) and in each of the molecular subtypes (data not shown).

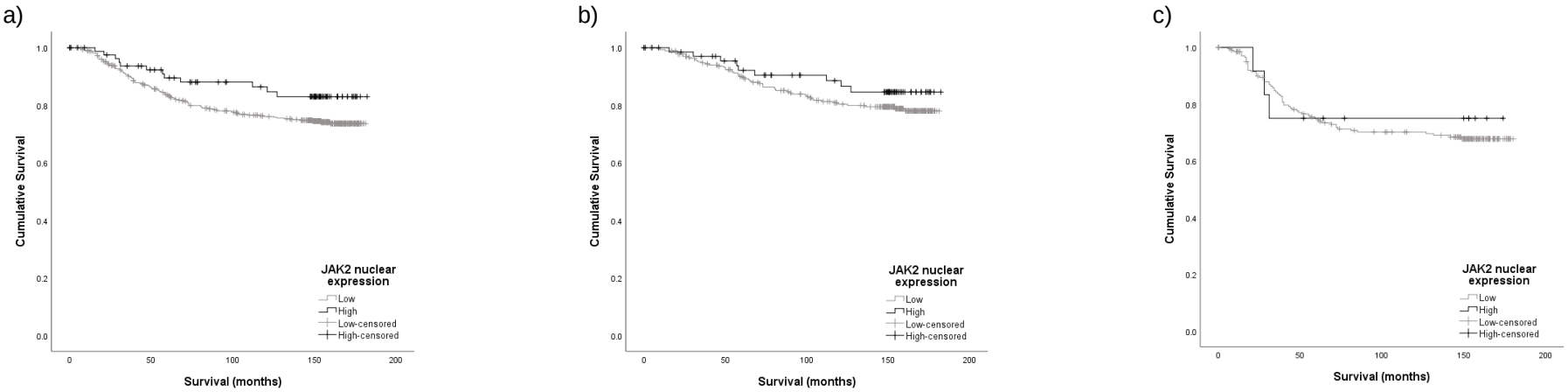

Figure 8-25. The relationship between nuclear JAK2 expression and CSS. Kaplan meier graphs to illustrate the relationship between nuclear JAK2 expression in tumour cells and CSS in a) the full cohort (n=567, p=0.093), b) ER positive disease (n=347, p=0.290) and c) ER negative disease (n=220, p=0.756).

8.3.6.2 Cytoplasmic JAK2 expression and CSS

There was no significant association between cytoplasmic JAK2 expression and CSS in the full cohort (high v low: HR 0.94, 95% CI 0.66-1.33, p=0.719), in ER positive (HR 0.88, 95% CI 0.54-1.45, p=0.615) or in ER negative disease (HR 1.18, 95% CI 0.72-1.92, p=0.511)(**Figure 8-26**). However, when analysed in the individual molecular subtypes, high cytoplasmic JAK2 expression was significantly associated with worse CSS in triple negative disease (HR 1.83, 95% CI 0.99-3.39, p=0.054)(**Figure 8-27**), but this was not independent of other known prognostic factors (p=0.084).

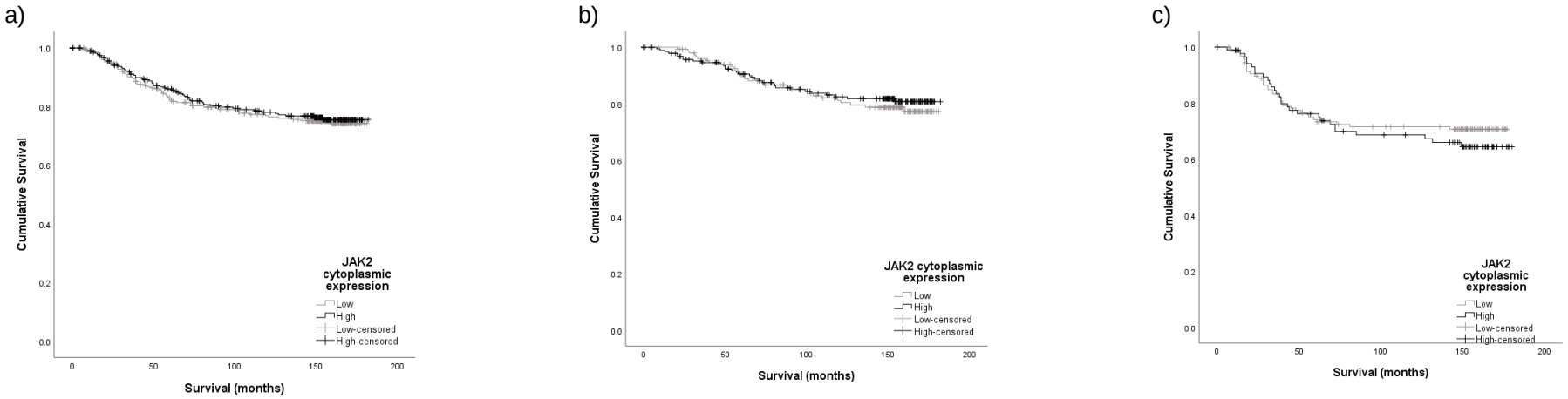

Figure 8-26. The relationship between cytoplasmic JAK2 expression and CSS. Kaplan meier graphs to illustrate the relationship between cytoplasmic JAK2 expression in tumour cells and CSS in a) the full cohort (n=567, p=0.719), b) ER positive disease (n=347, p=0.614) and c) ER negative disease(n=220, p=0.509).

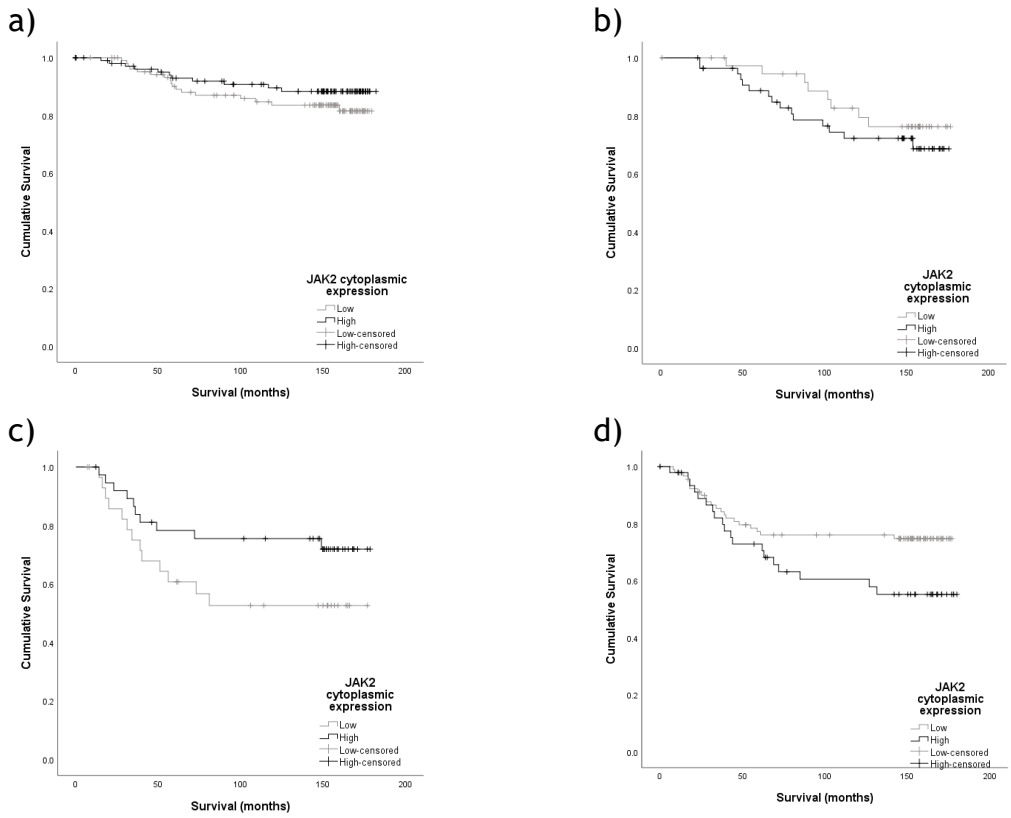

Figure 8-27. The relationship between cytoplasmic JAK2 expression and CSS by molecular subtype. Kaplan meier graphs to illustrate the relationship between cytoplasmic JAK2 expression in tumour cells and CSS in a) luminal A (n=215, p=0.261), b) luminal B (n=95, p=0.389), c) HER2-enriched (n=68, p=0.097) and d) triple negative (n=140, **p=0.049**) breast cancer.

8.3.6.3 Stromal JAK2 expression and CSS

77 (14.4%) patients had high (mean WHS>70) stromal JAK2 expression. In the full cohort, high stromal expression of JAK2 was significantly associated with worse CSS (HR 1.65, 95% CI 1.07-2.54, p=0.024), though this was not independent of other prognostic factors on multivariate analysis (p=0.347). However, when analysed by ER status, high stromal JAK2 expression was only significantly associated with CSS in ER negative (HR 2.38, 95% CI 1.29-4.39, p=0.005), not ER positive disease (HR 1.41, 95% CI 0.76-2.61, p=0.273)(**Figure 8-28**). The association in ER negative disease was not independent of other prognostic factors (p=0.370). When analysed in the molecular subtypes, high stromal JAK2 expression was significantly associated with worse CSS in both luminal B (HR 2.88, 95% CI 1.13-7.31, p=0.026) and HER2-enriched (HR 3.37, 95% CI 1.38-8.23, p=0.008) breast cancer (**Figure 8-29**).

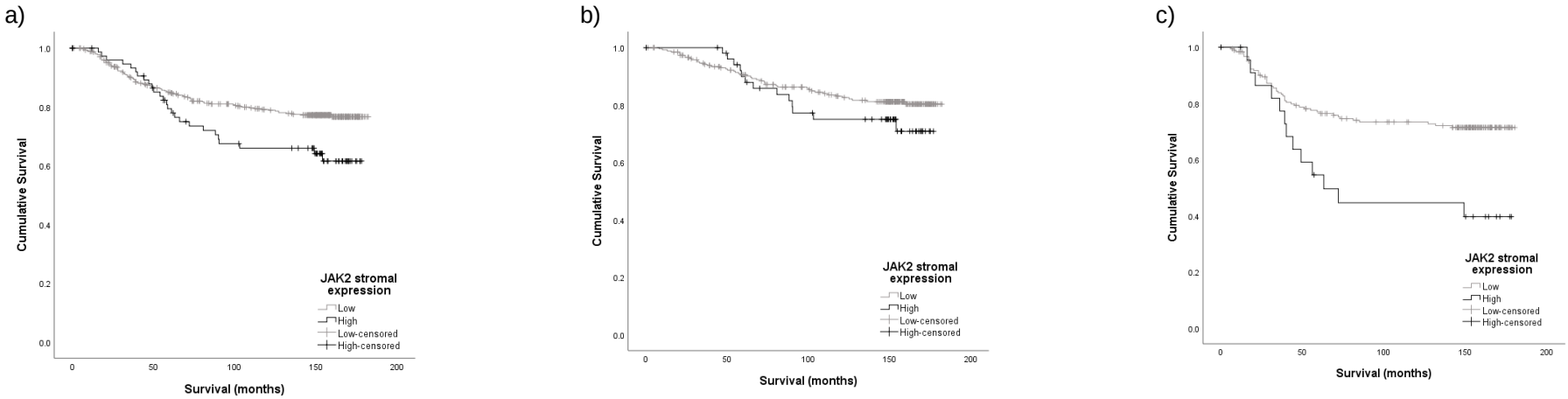

Figure 8-28. The relationship between stromal JAK2 expression and CSS. Kaplan meier graphs to illustrate the relationship between stromal JAK2 expression and CSS in a) the full cohort (n=533, **p=0.023**), b) ER positive disease (n=321, p=0.270) and c) ER negative disease (n=212, **p=0.004**).

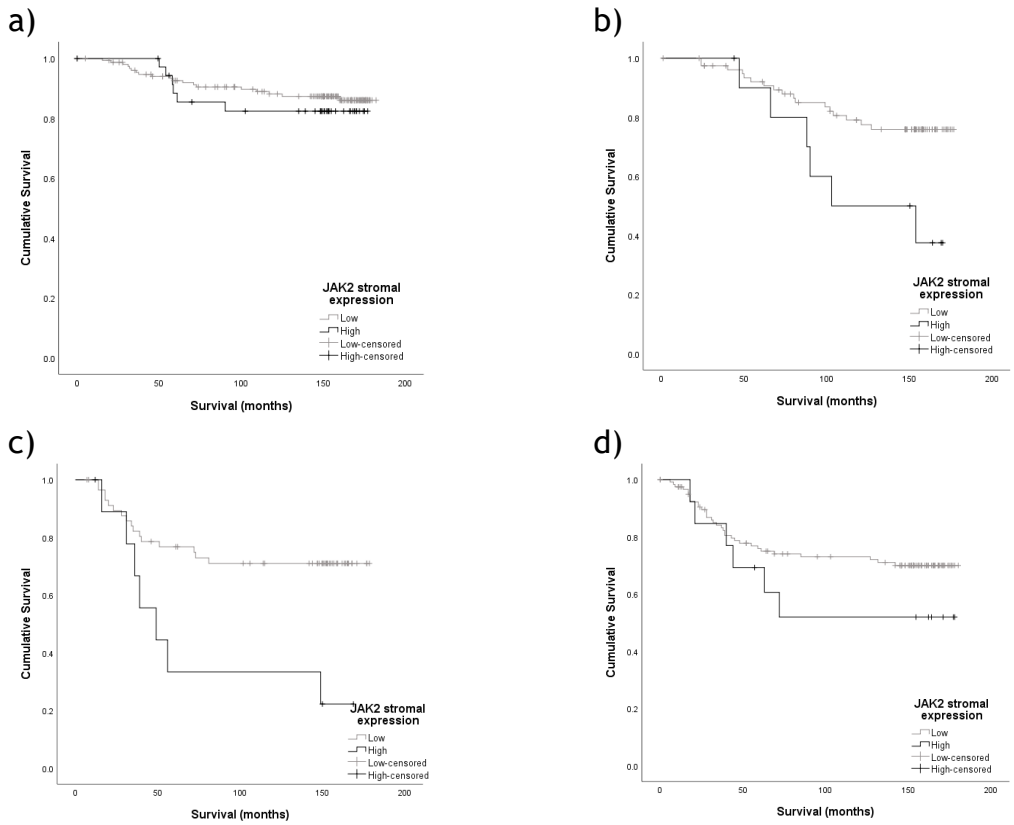

Figure 8-29. The relationship between stromal JAK2 expression and CSS by molecular subtype. Kaplan meier graphs to illustrate the relationship between stromal JAK2 expression and CSS in a) luminal A (n=194, p=0.404), b) luminal B (n=91, **p=0.020**), c) HER2-enriched (n=68, **p=0.005**) and d) triple negative (n=133, p=0.238) breast cancer.

On multivariate analysis, the associations between high stromal JAK2 expression and worse CSS in luminal B (p=0.003, **Table 8-3**) and HER2-enriched (p=0.021, **Table 8-4**) breast cancer were independent of other prognostic factors.

Factor	HR (95% CI)	p
Tumour grade		0.270
I		
II		0.592
III		0.693
Nodal status		**0.007**
Negative	1	
Positive	3.31 (1.39-7.87)	
Necrosis		0.053
<25%		
>25%		
TSP		0.315
<50%		
>50%		
Stromal JAK2 expression		**0.003**
Low	1	
High	4.26 (1.62-11.23)	

Table 8-3. Multivariate analysis for stromal JAK2 expression in luminal B cancer. Table detailing the multivariate survival analysis for stromal JAK2 expression in luminal B breast cancer.

Factor	HR (95% CI)	p
Nodal status		0.430
Negative		
Positive		
Tumour budding		**0.002**
≤20 buds	1	
>20 buds	3.80 (1.65-8.74)	
TSP		**0.036**
<50%	1	
>50%	2.53 (1.06-6.06)	
Stromal JAK2 expression		**0.021**
Low	1	
High	2.99 (1.18-7.56)	

Table 8-4. Multivariate analysis for stromal JAK2 expression in HER2-enriched cancer. Table detailing the multivariate survival analysis for stromal JAK2 expression in HER2-enriched breast cancer.

8.3.7 Associations between JAK2 and clinicopathological characteristics

Cytoplasmic and stromal JAK2 expression were associated with cancer outcomes so their associations with clinicopathological characteristics were assessed.

High cytoplasmic JAK2 expression was significantly associated with ER (p=0.001) and HER2 positivity (p=0.010) and high CD8+ lymphocytes (p=0.004) (**Table 8-5**).

	Cytoplasmic JAK2 expression		p
	Low n(%)	High n(%)	
Age			0.626
≤50yrs	94 (32.9)	87 (31.0)	
>50yrs	192 (67.1)	194 (69.0)	
Type			0.296
Ductal	249 (87.1)	255 (90.7)	
Lobular	18 (6.3)	15 (5.3)	
Other	19 (6.6)	11 (3.9)	
Size			0.936
≤20mm	155 (54.2)	148 (52.9)	
21-49mm	117 (40.9)	117 (41.8)	
≥50mm	14 (4.9)	15 (5.4)	
Grade			0.132
I	44 (15.4)	42 (14.9)	
II	105 (36.8)	126 (44.8)	
III	136 (47.7)	113 (40.2)	
Nodal status			0.259
Negative	162 (57.7)	146 (52.9)	
Positive	119 (42.3)	130 (47.1)	
ER status			**0.001**
Negative	131 (45.8)	89 (31.7)	
Positive	155 (54.2)	192 (68.3)	
HER2 status			**0.010**
Negative	239 (85.1)	214 (76.4)	
Positive	42 (14.9)	66 (23.6)	
Necrosis			0.833
<25%	129 (46.7)	131 (47.6)	
>25%	147 (53.3)	144 (52.4)	
KM score			0.869
0	41 (14.7)	45 (16.4)	
1	133 (47.8)	123 (44.9)	
2	78 (28.1)	77 (28.1)	
3	26 (9.4)	29 (10.6)	
CD8+ lymphocytes			**0.004**
Low	63 (39.1)	22 (20.0)	
Medium	45 (28.0)	40 (36.4)	
High	53 (32.9)	48 (43.6)	
CD4+ lymphocytes			0.960
Low	73 (28.2)	71 (29.3)	
Medium	96 (37.1)	88 (36.4)	
High	90 (34.7)	83 (34.3)	
TSP			0.969
Low	198 (71.0)	197 (71.1)	
High	81 (29.0)	80 (28.9)	
Budding			0.971
≤20 buds	194 (69.5)	193 (69.7)	
>20 buds	85 (30.5)	84 (30.3)	

Table 8-5. The association between cytoplasmic JAK2 and clinicopathological characteristics. Table detailing the associations between cytoplasmic JAK2 expression and clinicopathological factors. Statistically significant p values are highlighted in bold.

High stromal JAK2 expression was associated with low CD8+ (p=0.016) and CD4+ lymphocytes (p<0.001) (**Table 8-6**).

	Stromal JAK2 expression		p
	Low n(%)	**High** n(%)	
Age			0.277
≤50yrs	153 (33.6)	21 (27.3)	
>50yrs	303 (66.4)	56 (72.7)	
Type			0.198
Ductal	403 (88.4)	73 (94.8)	
Lobular	28 (6.1)	3 (3.9)	
Other	25 (5.5)	1 (1.3)	
Size			0.652
≤20mm	250 (54.8)	40 (51.9)	
21-49mm	180 (39.5)	34 (44.2)	
≥50mm	26 (5.7)	3 (3.9)	
Grade			0.977
I	69 (15.2)	11 (14.3)	
II	185 (40.7)	32 (41.6)	
III	201 (44.2)	34 (44.2)	
Nodal status			0.747
Negative	249 (55.3)	40 (53.3)	
Positive	201 (44.7)	35 (46.7)	
ER status			0.095
Negative	188 (41.2)	24 (31.2)	
Positive	268 (58.8)	53 (68.8)	
HER2 status			0.929
Negative	360 (79.8)	61 (80.3)	
Positive	91 (20.2)	15 (19.7)	
Necrosis			0.432
<25%	204 (45.7)	37 (50.7)	
>25%	242 (54.3)	36 (49.3)	
KM score			0.908
0	69 (15.5)	11 (14.9)	
1	207 (46.4)	33 (44.6)	
2	128 (28.7)	21 (28.4)	
3	42 (9.4)	9 (12.2)	
CD8+ lymphocytes			**0.016**
Low	66 (27.8)	12 (52.2)	
Medium	76 (32.1)	8 (34.8)	
High	95 (40.1)	3 (13.0)	
CD4+ lymphocytes			**<0.001**
Low	95 (23.5)	30 (46.9)	
Medium	147 (36.3)	29 (45.3)	
High	163 (40.2)	5 (7.8)	
TSP			0.379
Low	316 (70.4)	49 (65.3)	
High	133 (29.6)	26 (34.7)	
Budding			0.706
≤20 buds	315 (70.2)	51 (68.0)	
>20 buds	134 (29.8)	24 (32.0)	

Table 8-6. The association between stromal JAK2 expression and clinicopathological characteristics. Table detailing the associations between stromal JAK2 expression and clinicopathological factors. Statistically significant p values are highlighted in bold.

8.3.8 The relationship between JAK1 and JAK2

To evaluate the relationship between JAK1 and JAK2 expression, association and correlation analysis was carried out. High nuclear JAK1 expression was associated with high nuclear JAK2 expression (p=0.028) but there were no significant associations observed between the other combinations of JAK1 and JAK2 expression sites (**Table 8-7**).

On correlation analysis, the only significant correlation observed was a very weak negative correlation between nuclear JAK1 and cytoplasmic JAK2 expression (**Figure 8-30**).

	Nuclear JAK1 expression		p	Cytoplasmic JAK1 expression		p	Stromal JAK1 expression		p
	Low	High		Low	High		Low	High	
Nuclear JAK2			**0.028**			0.992			0.876
Low	182 (87.1)	170 (79.1)		166 (83.0)	186 (83.0)		77 (83.7)	249 (83.0)	
High	27 (12.9)	45 (20.9)		34 (17.0)	38 (17.0)		15 (16.3)	51 (17.0)	
Cytoplasmic JAK2			0.420			0.994			0.415
Low	91 (43.5)	102 (47.4)		91 (45.5)	102 (45.5)		44 (47.8)	129 (43.0)	
High	118 (56.5)	113 (52.6)		109 (54.5)	122 (54.5)		48 (52.2)	171 (57.0)	
Stromal JAK2			0.812			0.204			0.347
Low	162 (83.9)	173 (84.8)		159 (86.9)	176 (82.2)		73 (88.0)	242 (83.7)	
High	31 (16.1)	31 (15.2)		24 (13.1)	38 (17.8)		10 (12.0)	47 (16.3)	

Table 8-7. The association between JAK1 and JAK2. Tables detailing the associations between JAK1 and JAK2 in their different expression sites. Significant p values are highlighted in bold.

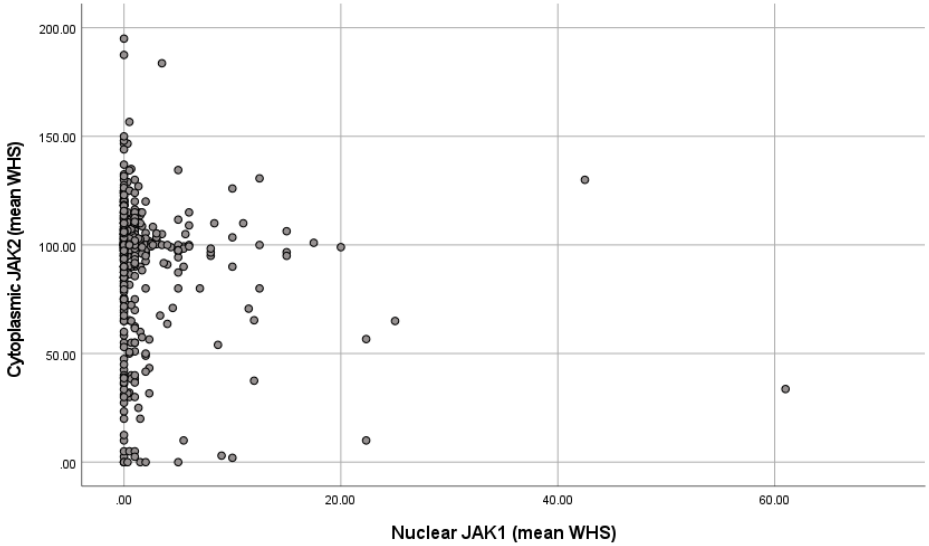

Figure 8-30. The correlation between nuclear JAK1 and cytoplasmic JAK2. Scatter plot illustrating the weak negative correlation between nuclear JAK1 and cytoplasmic JAK2 (Pearson correlation -0.108, **p=0.027**).

8.3.9 The relationship between JAK1, JAK2 and other components of the IL6/JAK/STAT3 pathway

To evaluate the relationship between JAK1 and JAK2 expression and the components of the IL6/JAK/STAT3 pathway studied so far in this thesis, association and correlation analysis was carried out.

8.3.9.1 The relationship between JAK1 and IL6/IL6R expression

High cytoplasmic JAK1 expression was associated with high cytoplasmic and stromal IL6R expression. High stromal JAK1 expression was associated with low membranous IL6R expression (**Table 8-8**).

	Nuclear expression		p	Cytoplasmic expression		p	Stromal expression		p
	Low	High		Low	High		Low	High	
Tumour IL6/HK			0.926			0.829			0.670
Low	165 (69.0)	162 (68.6)		167 (69.3)	160 (68.4)		79 (71.2)	225 (69.0)	
High	74 (31.0)	74 (31.4)		74 (30.7)	74 (31.6)		32 (28.8)	101 (31.0)	
Stromal IL6/HK			0.374			0.955			0.358
Low	92 (38.2)	77 (32.9)		87 (36.0)	82 (35.2)		36 (32.4)	125 (38.3)	
Medium	84 (34.9)	82 (35.0)		83 (34.3)	83 (35.6)		44 (39.6)	106 (32.5)	
High	65 (27.0)	75 (32.1)		72 (29.8)	68 (29.2)		31 (27.9)	95 (29.1)	
Cytoplasmic IL6R			0.136			**0.019**			0.983
Low	128 (46.4)	144 (52.7)		149 (54.6)	123 (44.6)		61 (49.2)	188 (49.1)	
High	148 (53.6)	129 (47.3)		124 (45.4)	153 (55.4)		63 (50.8)	195 (50.9)	
Membranous IL6R			0.331			0.607			**0.028**
Low	234 (84.8)	223 (81.7)		225 (82.4)	232 (84.1)		95 (76.6)	326 (85.1)	
High	42 (15.2)	50 (18.3)		48 (17.6)	44 (15.9)		29 (23.4)	57 (14.9)	
Stromal IL6R			0.854			**0.004**			0.740
Low	176 (68.0)	180 (68.7)		187 (74.5)	169 (62.6)		80 (70.2)	257 (68.5)	
High	83 (32.0)	82 (31.3)		64 (25.5)	101 (37.4)		34 (29.8)	118 (31.5)	

Table 8-8. The association between JAK1 and IL6/IL6R. Table detailing the associations between JAK1 expression in different sites and Il6 and IL6R expression. Significant p values are highlighted in bold.

On correlation analysis using continuous variables, the only significant correlation identified was a very weak positive correlation between stromal JAK1 and IL6R expression but there was a significant outlier which may skew this statistic (**Figure 8-31**).

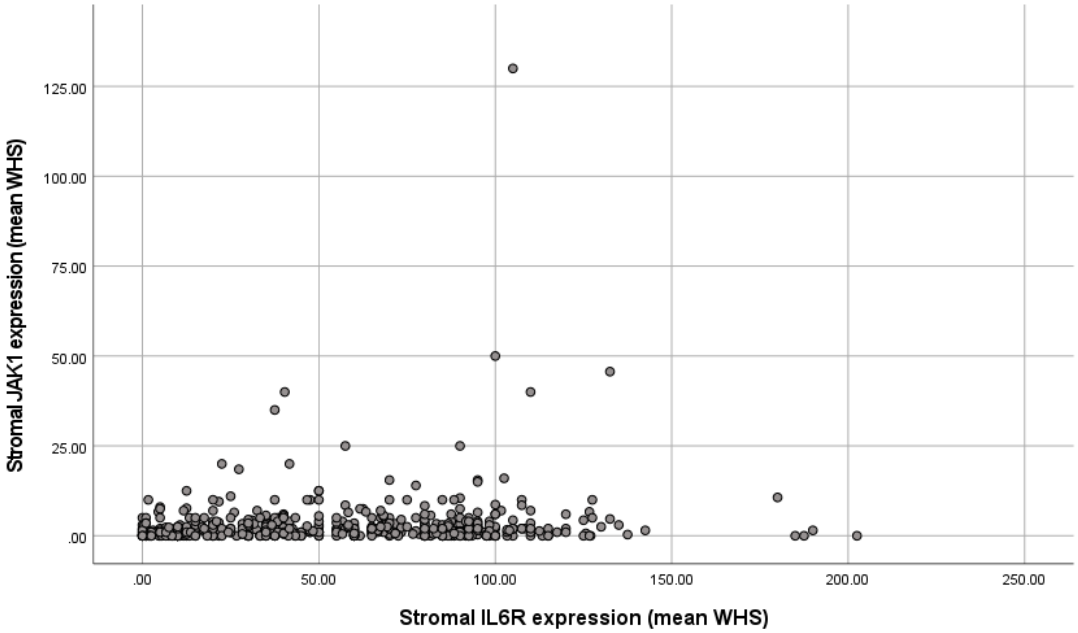

Figure 8-31. The correlation between stromal JAK1 and IL6R expression. Scatter plot to illustrate the correlation between stromal expression of JAK1 and IL6R (Pearson correlation 0.110, **p=0.015**).

8.3.9.2 The relationship between JAK2 and IL6/IL6R expression

High cytoplasmic JAK2 was associated with high cytoplasmic IL6R. High stromal JAK2 was associated with high stromal IL6R and low membranous IL6R (**Table 8-9**).

	Nuclear expression		p	Cytoplasmic expression		p	Stromal expression		p
	Low	High		Low	High		Low	High	
Tumour IL6/HK			0.335			0.452			0.136
Low	254 (66.0)	42 (60.0)		158 (66.7)	138 (63.3)		239 (63.7)	40 (74.1)	
High	131 (34.0)	28 (40.0)		79 (33.3)	80 (36.7)		136 (36.3)	14 (25.9)	
Stromal IL6/HK			0.052			0.055			0.878
Low	128 (33.1)	13 (18.6)		62 (26.1)	79 (36.1)		121 (32.0)	17 (32.1)	
Medium	132 (34.1)	28 (40.0)		92 (38.7)	68 (31.1)		124 (32.8)	19 (35.8)	
High	127 (32.8)	29 (41.4)		84 (35.3)	72 (32.9)		133 (35.2)	17 (32.1)	
Cytoplasmic IL6R			0.299			**<0.001**			0.094
Low	210 (46.9)	39 (53.4)		153 (60.5)	96 (35.8)		189 (45.5)	41 (56.2)	
High	238 (53.1)	34 (46.6)		100 (39.5)	172 (64.2)		226 (54.5)	32 (43.8)	
Membranous IL6R			0.104			0.597			**0.012**
Low	378 (84.4)	56 (76.7)		213 (84.2)	221 (82.5)		337 (81.2)	68 (93.2)	
High	70 (15.6)	17 (23.3)		40 (15.8)	47 (17.5)		78 (18.8)	5 (6.8)	
Stromal IL6R			0.189			0.229			**<0.001**
Low	299 (70.2)	43 (62.3)		172 (71.7)	170 (66.7)		299 (74.2)	28 (40.0)	
High	127 (29.8)	26 (37.7)		68 (28.3)	85 (33.3)		104 (25.8)	42 (60.0)	

Table 8-9. The association between JAK2 and IL6/IL6R. Table detailing the associations between JAK2 expression in different sites and Il6 and IL6R expression. Significant p values are highlighted in bold.

On correlation analysis using continuous variables, weak positive correlations were observed between cytoplasmic JAK2 and cytoplasmic and stromal IL6R, and between stromal JAK2 and stromal IL6R. A weak negative correlation was observed between stromal JAK2 and membranous IL6R (**Figure 8-32**).

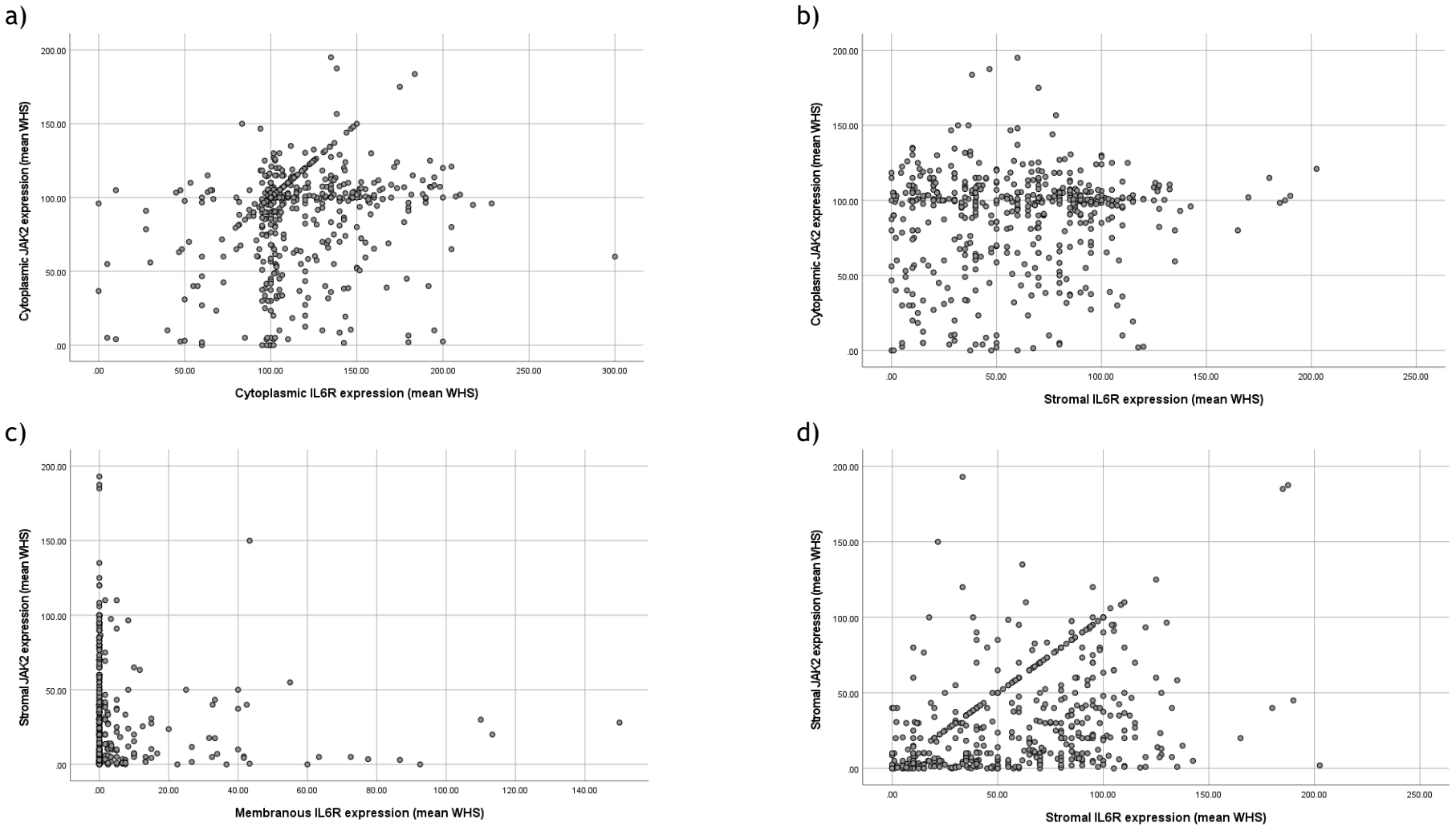

Figure 8-32. The correlation between JAK2 and IL6R. Scatter plots to illustrate the correlation between a) cytoplasmic JAK2 and IL6R expression (Pearson correlation 0.203, **p<0.001**), b) cytoplasmic JAK2 and stromal IL6R expression (Pearson correlation 0.105, **p=0.020**), c) stromal JAK2 and membranous IL6R expression (Pearson correlation -0.105, **p=0.020**), d) stromal JAK2 and IL6R expression (Pearson correlation 0.354, **p<0.001**).

8.4 Discussion

In this study the expression of JAK1 and JAK2 and their associations with clinicopathological factors, CSS and IL6/IL6R expression have been described. JAK1 is predominantly expressed in the cytoplasm but some nuclear expression was also observed. Levels of expression varied between the molecular subtypes. High nuclear JAK1 expression was associated with improved CSS and lower tumour grade in ER+ tumours but with reduced CSS in TNBC. Stromal JAK1 expression was also associated with improved CSS and smaller tumour size in ER+ cancers. Nuclear JAK1 expression was not associated with IL6/IL6R expression whereas cytoplasmic JAK1 expression was. Similarly, JAK2 was predominantly expressed in the cytoplasm and there was negligible nuclear expression observed. Converse to JAK1, stromal JAK2 expression was associated with reduced CSS and with lower CD4+ and CD8+ lymphocytes. Cytoplasmic JAK2 expression was also associated with worse CSS and node positivity in TNBC, as well as IL6 and IL6R expression.

JAK1 was predominantly expressed in the cytoplasm of tumour cells. This is consistent with its widely described role in the JAK/STAT3 pathway mediating phosphorylation of STAT3 in the cytoplasm in response to cytokine signalling. As described in the introduction, binding of cytokines with membrane receptors leads to activation of receptor-associated JAKs via trans-phosphorylation which then phosphorylate sites on the cytoplasmic region of the receptor providing docking sites for STATs and subsequent JAK-mediated STAT3 phosphorylation and activation(315). STAT3 translocates into the nucleus where it influences gene transcription(82, 83). However, JAK1 expression in the nucleus was also observed, more commonly in luminal A cancers and, in this study, it was this expression site which was associated with cancer outcomes. Nuclear JAK expression has been described previously in the literature(316). Initial studies in the late 1990s observed JAK 1 and 2 in the nuclei of CHO cells transfected with the GH receptor(317), JAK2 in nuclei of pancreatic islet cells(318), in cultured liver cells(319) and in mouse oocytes(320). To the knowledge of the author this is the first time that nuclear expression has been reported in breast cancer cells. JAKs are too large to freely diffuse between the cytoplasm and nucleus(316) so they may travel bound to one of their receptors shown to translocate to the nucleus such as growth hormone, prolactin or insulin receptors(316). In diffuse

large B-cell lymphoma (DLBCL), a classical nuclear localisation signal on the N terminus of JAK1 has been described which can be recognised by importin isoforms(321).

Chromatin has been identified as a nuclear target of JAK1 in this tumour type as JAK1 can phosphorylate chromatin on H3Y41 leading to upregulation of the protooncogene transcription factor MYC and consequently to transcription of numerous genes including MYD88 which activates both the NF-κB and p38 MAP kinase pathways(322). In DLBCL nuclear JAK1 was observed to be essential for cell survival. This raises the possibility that the mechanism outlined above may have a role in TNBC, in which subtype the present study observed an association between reduced CSS and high nuclear expression of JAK1. However, the reverse was true in ER+ disease suggesting that in these cancers, genomic targets may differ such that nuclear JAK1 expression leads to inhibition of cancer cell growth and proliferation.

This association between JAK1 and improved survival is in keeping with the findings of a previous small study using human breast cancer tissue which also observed an inverse association between JAK1 expression and tumour size, lymph node status and TNM stage(311). The authors used a qRT-PCR technique to measure mRNA and therefore it is impossible to know the site of JAK1 expression in their study(311). In addition, one other small human tissue study which did, like the present study, use IHC techniques observed high pJAK1 expression in normal breast tissue compared with adjacent breast cancer tissue and low pJAK1 expression was correlated with increased tumour size(310). Both of these findings would seem to support the findings of our study that higher JAK1 expression is associated with better prognosis, at least in ER+ tumours which represent the majority. They also observed an association between high pJAK1 expression and ER negative tumours(310) which would be in keeping with our findings for cytoplasmic but not nuclear JAK1 expression. Like the first study, this one did not report the specific site of the JAK1 expression observed so the present study has the advantage over both of these studies in that regard and in having a far greater sample size. Conversely, a cell line and murine study identified decreased expression of JAK1 in cells whose invasiveness and EMT characteristics had been suppressed by low dose radiation, implicating JAK1 in

the promotion of these characteristics(309). The primary cell line used in the study was the triple negative MDA-MB231 cell line so this would support our finding of worse cancer outcomes with high JAK1 expression in our TNBC patients. Another cell line study in breast cancer reported evidence that JAK1 is key to the oncogenic activation of STAT3 in response to IL6 but this was in a HER2 positive cell line(306), in which subtype the present study did not identify any significant association with CSS. However, the numbers of the HER2-enriched and luminal B subtypes in this cohort are comparatively low so this may be a factor. Cytoplasmic JAK1 expression was observed to be higher in the HER2 enriched subtype.

Nuclear JAK1 expression was not associated with any of the sites of IL6 or IL6R expression and this supports the theory that nuclear JAK1 expression is part of a different, non-canonical pathway, activated by other ligands such as growth hormone(316). On the other hand, cytoplasmic JAK1 was associated with cytoplasmic IL6R suggesting that IL6R signalling via the alternative pathway leads to JAK1 activation in accordance with the widely documented sequence of the IL6/JAK/STAT3 pathway. However, in our study, neither cytoplasmic IL6R nor JAK1 was significantly associated with CSS. It is interesting to note that there was no association between membranous IL6R, the site associated with CSS in the previous chapter, and JAK1 expression, suggesting that classical IL6 signalling via the membrane-bound receptor activates a different pathway. Cytoplasmic JAK1 was also associated with stromal IL6R which may simply reflect IL6 in the tumour microenvironment leading to activation of the IL6/JAK/STAT3 pathway in both tumour and stromal cells.

JAK2 was primarily observed in the tumour cell cytoplasm and there was negligible nuclear expression with, in contrast to nuclear JAK1 expression, no association with CSS observed. Cytoplasmic JAK2 expression was lower in ER negative and particularly TNBC but where expression was high in TNBC, it was associated with worse CSS and nodal positivity. It was also associated and correlated with cytoplasmic IL6R expression and, in TNBC, with tumour IL6 expression. Though the association with worse CSS was not independent of other prognostic features, including nodal status, these findings raise the possibility that, in TNBC, IL6 signalling via the alternative pathway leads to JAK2 activation

and subsequent downstream signalling leads to development of tumour cell characteristics that lead to nodal and distant metastasis such as cell motility, invasiveness, EMT and angiogenesis(323). These findings are in keeping with those of other studies which have observed poorer outcomes with tumours that express high levels of JAK2. In particular, one study of TNBC reported reduced overall and recurrence-free survival in post-chemotherapy patients with JAK2 amplification(314). In longitudinal specimens they noted that JAK2 was selected for during neoadjuvant chemotherapy suggesting a role in chemoresistance. However, they identified STAT6 rather than STAT3 as the key downstream target of JAK2 in this process(314). In the present study we did not observe a significant association between cytoplasmic JAK2 and outcome in ER+ disease but a role for JAK2 and STAT3 has recently been reported in tamoxifen resistance in cell lines and mouse xenografts(312). There is evidence from murine studies that JAK2 activation promotes brain metastasis(324) and the IL6/JAK2/STAT3 pathway is also implicated in the growth of stem cell-like breast cancer cells(325). In contrast, two studies which measured JAK2 mRNA levels reported reduced recurrence rates with higher JAK2 levels(326, 327). However, Miller et al concede that mRNA levels may not reflect JAK2 protein or activated JAK2 levels. High mRNA in that study was correlated with TILs suggesting these may be important in the improved outcomes, rather than JAK2 in the tumour cells themselves(326).

Stromal JAK1 and JAK2 expression was also observed, predominantly in ER+ disease and less in TNBC in the case of JAK2. Differentiation between expression within the cytoplasm or nucleus of these cells was not reliably possible at the magnification available. As with nuclear expression in tumour cells, stromal expression of JAK1 was associated with improved CSS in ER positive disease and was associated with reduced tumour size. Conversely, but similarly to tumour cytoplasmic JAK2 expression, high stromal JAK2 expression was associated with worse CSS overall, in ER- disease and in the luminal B and HER2-enriched subtypes. It was interesting to note that these associations in these two HER2 positive subtypes were the only ones independent of other prognostic factors. Stromal JAK1 and JAK2 expression were weakly correlated with stromal IL6R expression which suggests, while some of the JAK expression is due to IL6R activation, other ligands and receptors are likely to be important. Stromal

expression of both JAKs was associated with membranous ILR expression in tumour cells which may simply reflect the presence of IL6 in the tumour microenvironment. It is interesting to note that high stromal JAK2 expression is associated with lower numbers of CD4+ and CD8+ lymphocytes, suggesting that it is other stromal cell types in which the pathway is being activated, and this may be key to its association with poorer prognosis. For example, it may be that in these tumours there is an imbalance in the stromal cells in the microenvironment with fewer lymphocytes and higher numbers of MSCs, CAFs and other immune cell types. The JAK/STAT pathway has been reported to have a role in homing of MSCs(328) and their cytokine profile(329), in activation of inflammatory CAFS and their crosstalk with tumour cells(330-332), in dendritic cell differentiation and function(333) and in development and maturation of NK cells(334). There is evidence for the involvement of MSCs and CAFs in breast cancer progression, metastases and chemoresistance(335-343).

The findings of the present study suggest both positive and negative roles for the JAKs in tumour progression. Higher expression of JAK1 is predominantly associated with better prognosis, with the exception of TNBC, while JAK2 expression is associated with poorer prognosis. None of the associations with survival observed in this study were independent of other known prognostic factors and therefore, expression of JAK1 or JAK2 alone is unlikely to be of clinical use as a prognostic marker. However, their role in tumour progression suggests a potential role for JAK inhibitors in some breast tumours. They may have a role in TNBC since both nuclear JAK1 and cytoplasmic JAK2 were associated with poor prognosis in this subtype. JAK expression levels could potentially be used as predictive markers for treatment response. Given the complex interplay between different pathways they are likely to be most efficacious in combination with other treatments so further work is warranted in this subtype to fully understand the interplay between these pathways and to establish what treatment combinations may be most effective. In ER positive disease their potential is less clear and certainly, JAK1 inhibition seems likely to be of no benefit or even to be counter-productive so, on the basis of the findings of this study, any investigation into JAK inhibitors in ER positive disease should be with selective JAK2 inhibitors.

Ruxolitinib, a selective JAK1/2 inhibitor, is currently in clinical use for myeloproliferative diseases, which are associated with JAK mutations,(315) but the role of JAK inhibitors in solid tumours has not been fully established and trials are ongoing. Despite promising results with JAK inhibitors in pre-clinical studies of breast cancer(344, 345), some ruxolitinib breast cancer trials were terminated due to lack of clinical response(346-348). The opposing associations with CSS of JAK1 and JAK2 in this study may form part of the explanation for these disappointing results, though one study was in TNBC only(346) in which, based on our findings, we might expect a response. However, the study was in patients with metastatic disease so the disease process may be too advanced at this stage for JAK inhibition to have a significant clinical impact. Two other trials of ruxolitinib in breast cancer remain active at present(349, 350), as well as one investigating its effect on premalignant breast cells (ADH, ALH, LCIS or DCIS)(351). Two studies of the JAK2-specific inhibitor WP1066 in brain tumours are currently active, while two of pacritinib in colorectal cancer and in NSCLC have been terminated(315).

In summary, the present study describes for the first time nuclear expression of JAK1 and 2 in breast cancer cells. It reports an association between high nuclear JAK1 and cytoplasmic JAK2 expression and poor CSS, warranting further investigation of JAK inhibitors in TNBC. Improved CSS is observed in ER+ disease with high nuclear and stromal JAK1 expression so JAK1 inhibitors should be avoided in these cancers. There is evidence for high expression of JAK2 in certain types of stromal cells, in part activated by IL6 signalling, leading to a pro-tumour microenvironment and worse cancer outcomes but further work to determine the stromal cells implicated is indicated. JAK2 inhibition in stromal cells may represent another target for breast cancer therapies going forward.

9 STAT3 in primary operable breast cancer

9.1 Introduction

The previous two chapters have investigated the role of IL6 and JAKs 1 and 2 in primary operable breast cancer. Their downstream target in the IL6/JAK/STAT3 pathway is STAT3. However, as previously discussed, they also activate other cell signalling pathways. Therefore, further investigation of the expression of STAT3 in primary operable breast cancer and its relationship to IL6 and JAK expression is required to more fully describe the role of this pathway in these cancers.

STAT3 is a transcription factor with numerous downstream targets, resulting in key roles in various processes including haematopoiesis, immune development, stem cell maintenance(82, 83), and mammary epithelial cell growth, differentiation, apoptosis and post-lactational mammary involution(84, 85, 352). The pathway can be activated by IL6 receptors but also by tyrosine kinases such as EGFR, serine kinases, G protein coupled receptors, Rho GTPases, cadherin engagement and toll-like receptors(353). Canonically it is phosphorylated by JAKs at a conserved tyrosine residue (Tyr705) leading to STAT3 dimerisation and translocation to the nucleus where it binds to regulatory DNA sequences(82). However, it can also undergo phosphorylation at a serine residue (Ser727) via the p38MAPK and ERK1/2 pathways(87).

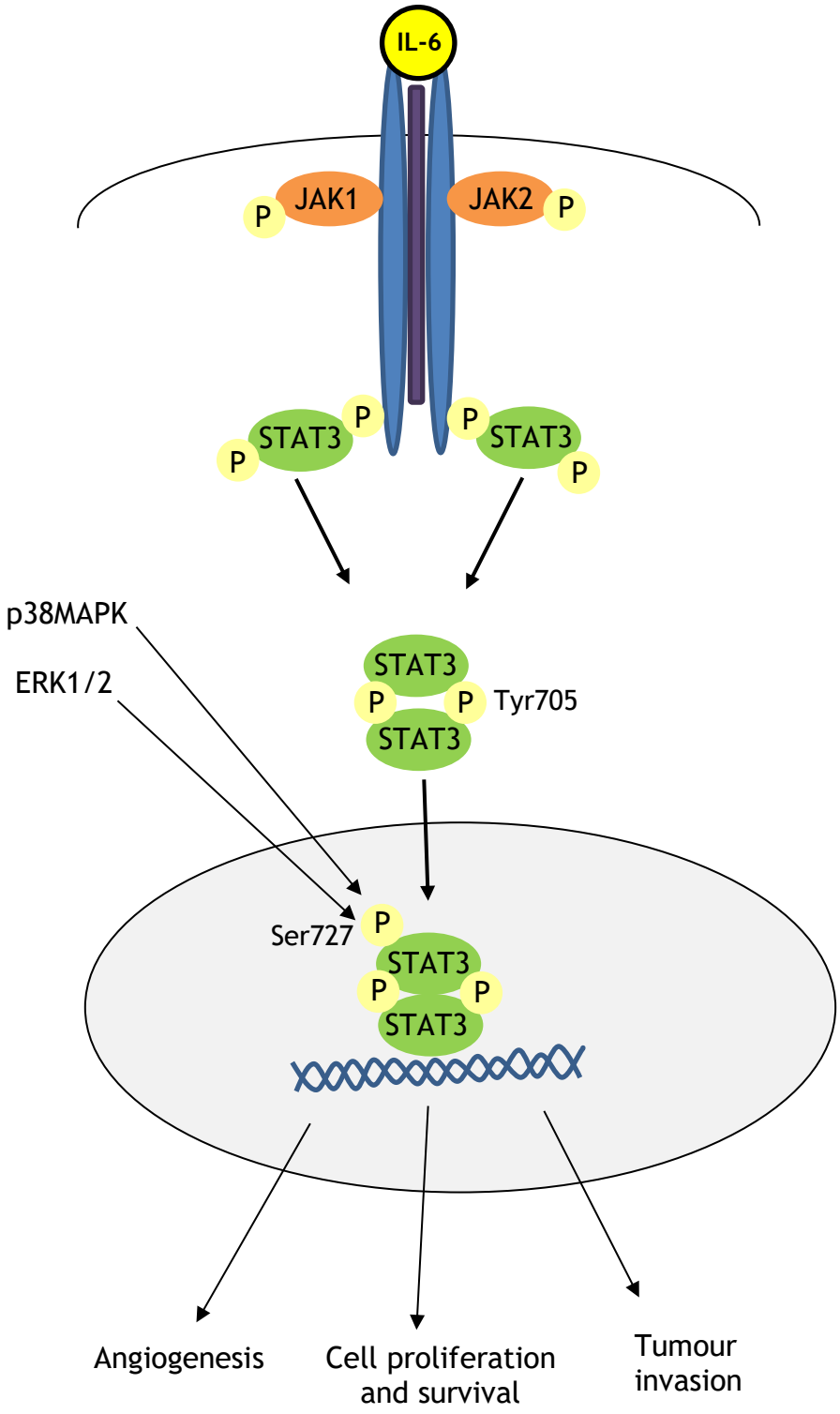

Figure 9-1. Activation of STAT3. Diagram illustrating the final stages of the IL6/JAK/STAT3 pathway. The activated STAT3 dimer translocates into the cell nucleus where it binds to DNA and regulates transcription of various genes. STAT3 can also be phosphorylated at Ser727 via the p38MAPK and ERK 1/2 pathways.

Although STAT3 regulates cell death in breast involution, in breast cancer evidence suggests that it promotes cell survival(352). STAT3 has been observed to be constitutively active in cancer cells(354). Some oncogenic STAT3 target genes include proliferation genes (Bcl-xL, MCL1, survivin), angiogenesis-promoting genes (Hif-1α, VEGF) and EMT-associated genes (vimentin, TWIST, MMP-9)(355). Though evidence from preclinical studies suggests a pro-tumourigenic role for STAT3(91-100), results of clinical studies of STAT3 and pSTAT3 have been mixed(76, 101-107). As detailed in chapter 1, some have reported an association between STAT3 and poorer prognosis(103), some with improved prognosis(76, 104-106), and some observed no statistically significant associations(102, 104). STAT3 inhibitors have yielded promising results in vivo but challenges exist in bringing them to clinical use(356). Early-stage clinical trials in various tumour types have reported conflicting results (357). Therefore, further work is required to better understand the role of STAT3 in breast cancer.

From the preclinical evidence, it could be hypothesised that, in the present cohort of breast cancer patients, high levels of tSTAT3 and pSTAT3 expression would be associated with poorer CSS. However, in view of the mixed results from clinical studies to date, the question arises as to whether the pro or anti tumour activity of STAT3 is influenced by other factors, such as the tumour subtype, the pathway which is activating it and influences from the tumour microenvironment, and the different sites of activation/phosphorylation. Specifically, there is minimal data in the literature regarding the serine 727 phosphorylation site of STAT3 so it could be postulated that phosphorylation at this site may modify the response of activated STAT3 observed in preclinical studies. This study aims to describe the expression of total STAT3 (tSTAT3) and of both its phosphorylated forms, pSTAT3(Tyr705) and pSTAT3(Ser727), and to describe their associations with clinicopathological characteristics, CSS and other components of the IL6/JAK/STAT3 pathway.

9.2 Materials and methods

9.2.1 Patient cohort

A previously constructed TMA from the 1800 cohort was utilised in this study. Patient characteristics are detailed in chapter 2.

9.2.2 TMA slide staining and scanning

TMAs were stained in triplicate for pSTAT3(Tyr705), pSTAT3(Ser727) and total STAT3 (tSTAT3) using the immunohistochemistry technique and antibodies detailed in chapter 2. They were scanned into Slidepath software as previously described.

9.2.3 Scoring for pSTAT3(Tyr705), pSTAT3(Ser727) tSTAT3 expression

Each TMA core was scored by the author using the weighted histoscore method described in chapter 2. Cores with <20% of the core missing by visual assessment were scored. For all three antibodies, nuclear and cytoplasmic expression in tumour cells were scored separately. A separate score was also given for expression in stromal cells (differentiation between nuclear and cytoplasmic expression in these smaller cells was not reliably possible at 20x magnification, so cellular compartments were not assessed).

9.2.4 Molecular subtyping

ER, PR, HER2 and Ki67 profiling was already available. This data was employed to divide the cohort into the four main molecular subtypes of breast cancer, as detailed in chapter 1, for subgroup analysis.

9.2.5 Statistical analysis

Initial analysis using ROC curves, division into tertiles, and the median expression was carried out to determine the optimum threshold for division into high and low expression groups for further analysis. Analysis of associations with clinicopathological characteristics and with cancer specific survival was carried out as described in chapter 2. This analysis was carried out initially in the full cohort, then in the ER positive and ER negative cohorts separately, and subsequently in the 4 individual molecular subtypes.

9.3 Results

9.3.1 Formation of the cohort for tSTAT3

609 patients had at least one core which was assessable for tSTAT3 in tumour nuclei and cytoplasm. 562 had at least 1 core which was assessable for stromal cell tSTAT3 expression (**Figure 9-2**).

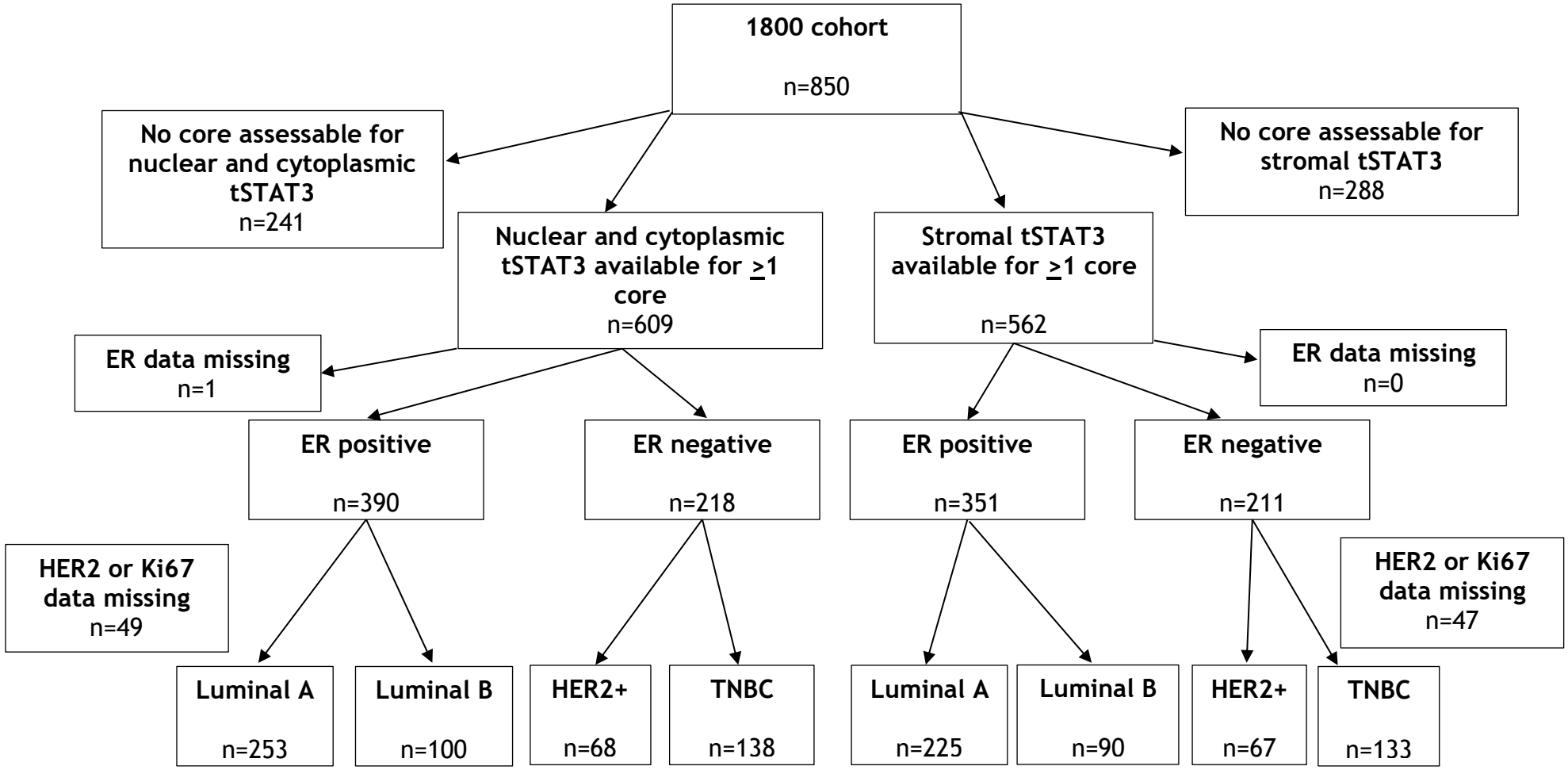

Figure 9-2. Formation of the tSTAT3 cohort. Flow diagram to illustrate the number of patients within the 1800 cohort with at least 1 core which was assessable for tSTAT3 expression in the tumour cell nucleus and cytoplasm, and separately in the stroma. The numbers available for subgroup analysis by ER status and by molecular subtype are also shown.

9.3.2 Total STAT3 expression

tSTAT3 expression was observed in the nucleus and cytoplasm of tumour cells and in stromal cells. Examples of tSTAT3 staining are shown below.

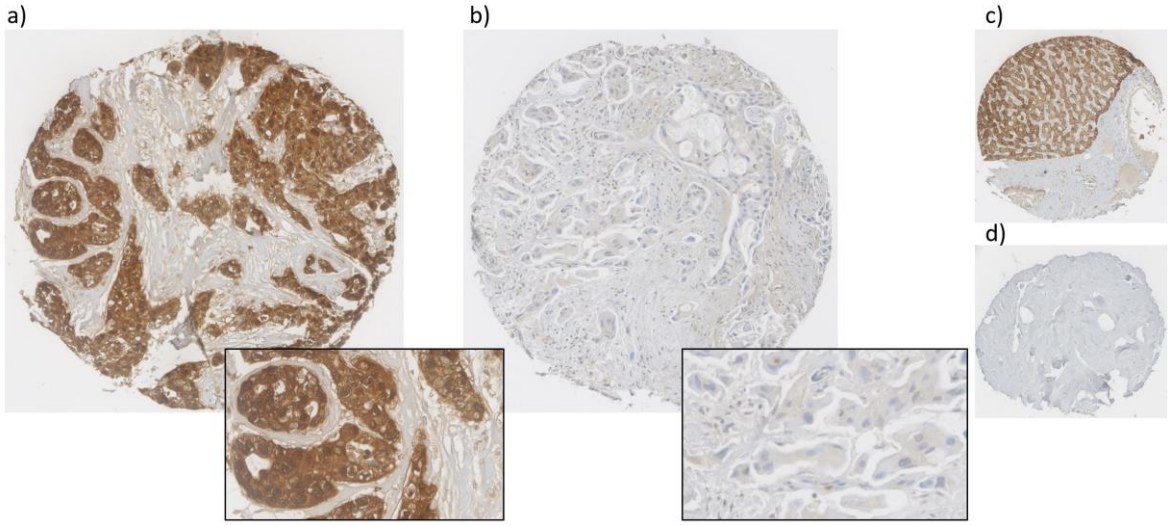

Figure 9-3. Examples of tSTAT3 staining. TMA cores stained using IHC for tSTAT3: a) breast core with moderate and strong nuclear and cytoplasmic staining at 10x magnification with an inset at 40x magnification, b) breast core with weak cytoplasmic staining, c) true positive core (control, liver) at 10x magnification, d) true negative core at 10x magnification.

Median WHS for total STAT3 expression in tumour was 106 (0-260) which was similar to that for cytoplasmic expression which was 105 (0-209.33). Median stromal tSTAT3 WHS was 82.50 (0-205). tSTAT3 expression in the 3 locations across the cohort is illustrated in the figures below (**Figure 9-4, Figure 9-5**).

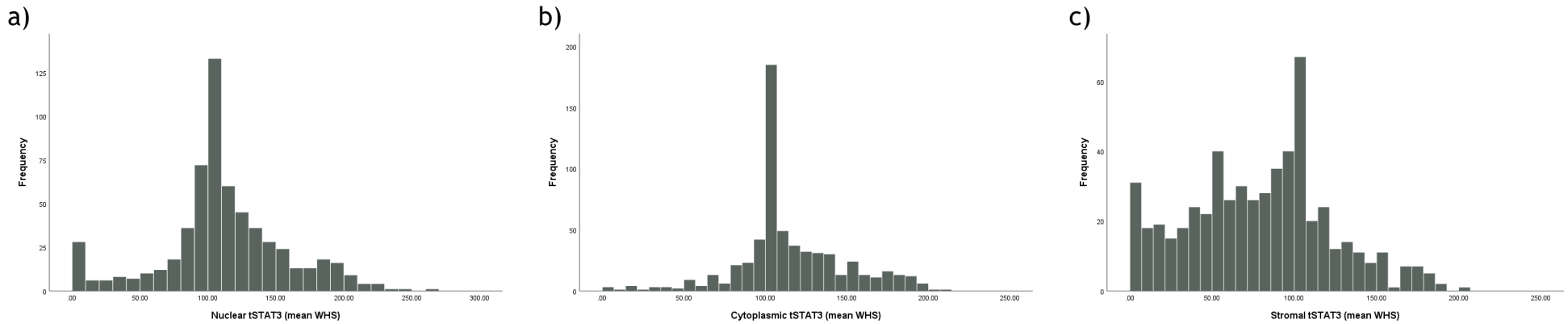

Figure 9-4. Expression of tSTAT3. Histograms to illustrate tSTAT3 expression in a) tumour cell nuclei, b) tumour cell cytoplasm and c) stromal cells.

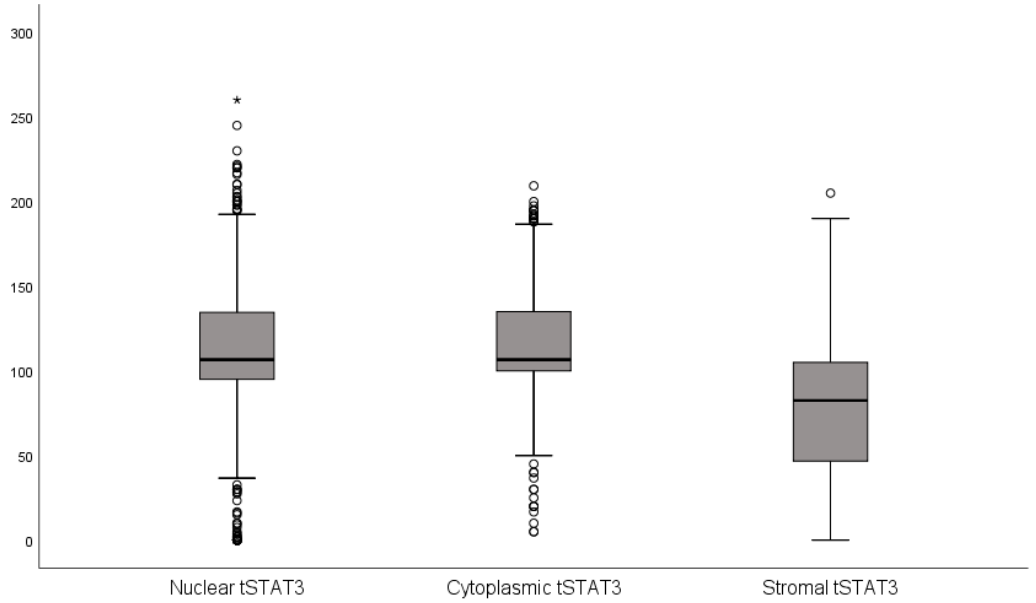

Figure 9-5. Boxplots of tSTAT3 expression. Boxplots to illustrate the comparative expression of tSTAT3 in tumour nuclei, cytoplasm and stromal cells.

Nuclear tSTAT3 expression was higher in ER positive disease and, within the molecular subtypes, highest in luminal A cancers and lowest in HER2-enriched cancers (**Figure 9-6**).

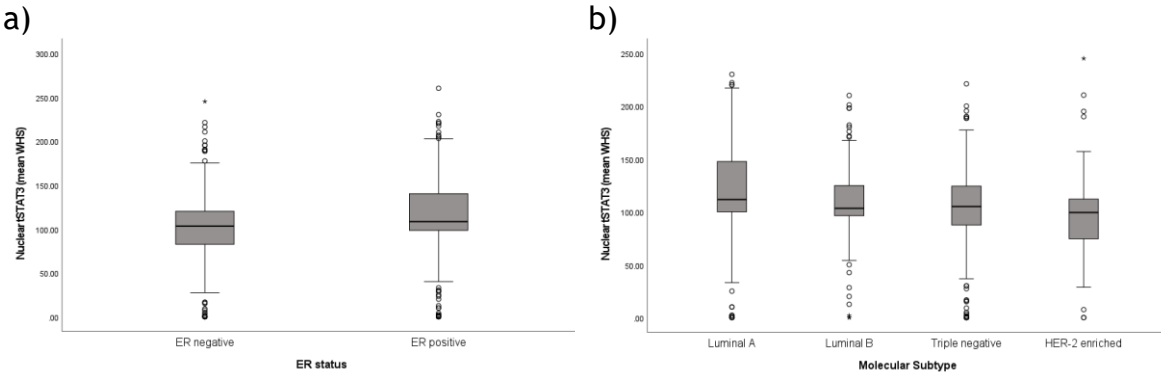

Figure 9-6. Boxplots of nuclear tSTAT3 by receptor status. Boxplots to illustrate the differences in nuclear tSTAT3 expression by a) ER status **(p=0.033**) and b) molecular subtype (**p<0.001**).

There was no difference between the subtypes in cytoplasmic tSTAT3 expression (**Figure 9-7**).

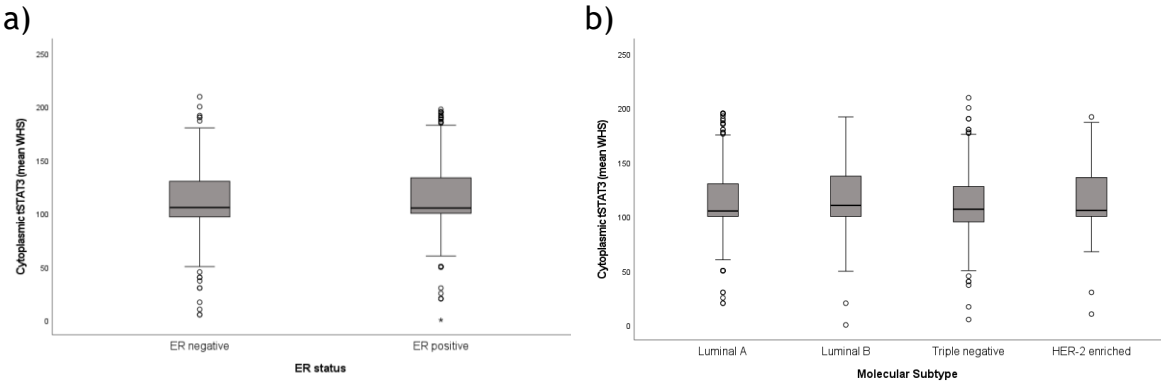

Figure 9-7. Boxplots of cytoplasmic tSTAT3 by receptor status. Boxplots to illustrate the differences in cytoplasmic tSTAT3 expression by a) ER status (p=0.903) and b) molecular subtype (p=0.871).

Stromal expression was higher in ER positive disease with the lowest expression in TNBC (**Figure 9-8**).

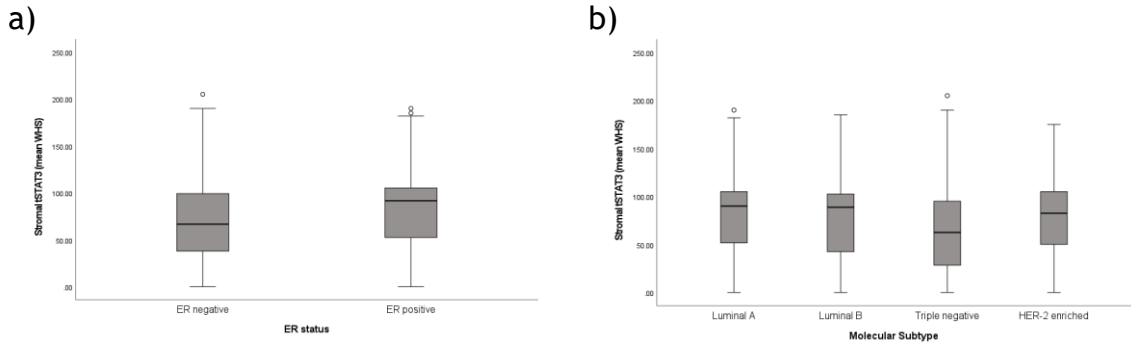

Figure 9-8. Boxplots of stromal tSTAT3 by receptor status. Boxplots to illustrate the differences in stromal tSTAT3 expression by a) ER status (**p<0.001**) and b) molecular subtype (**p=0.001**).

There was moderate positive correlation between each of the tSTAT3 expression sites (**Figure 9-9**).

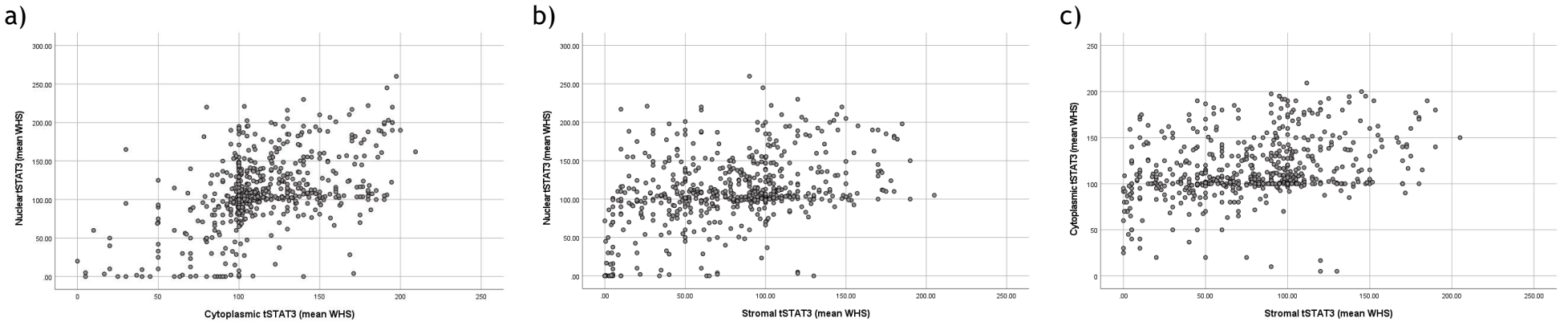

Figure 9-9. Correlation between tSTAT3 expression sites. Scatter plots to illustrate the correlation between tSTAT3 expression in different sites: a) nuclear and cytoplasmic expression (Pearson correlation 0.507, **p<0.001**), b) nuclear and stromal expression (Pearson correlation 0.386, **p<0.001**), c) cytoplasmic and stromal expression (Pearson correlation 0.319, **p<0.001**).

9.3.3 The relationship between total STAT3 and CSS

ROC curves were created to determine thresholds for division of patients into high and low expression groups for further analysis (**Figure 9-10**). From these, a threshold of 111.50 was derived for nuclear tSTAT3 expression and a threshold of 65.50 was derived for stromal tSTAT3 expression. No threshold for cytoplasmic tSTAT3 expression could be derived from the ROC curve so, after some exploratory survival analysis using tertiles and the median, a threshold of 121.33 (the upper tertile) was selected as having the highest prognostic value.

a)

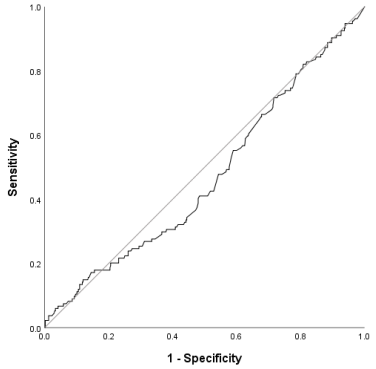

b)

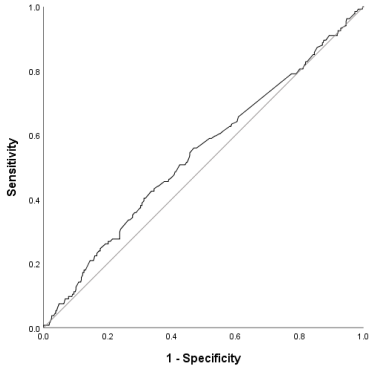

c)

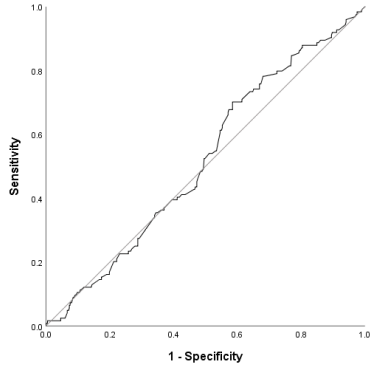

Figure 9-10. ROC curves for tSTAT3 expression and CSS. ROC curves to illustrate the relationship with CSS of tSTAT3 expression in a) tumour cell nuclei (AUC 0.470), b) tumour cell cytoplasm (AUC 0.542) and c) stromal cells (AUCC 0.520).

9.3.3.1 Nuclear tSTAT3 expression and CSS

249 (40.9%) patients had high nuclear tSTAT3 expression (mean WHS>111.50). In the full cohort, low nuclear tSTAT3 expression was associated with worse CSS (high v low: HR 0.66, 95% CI 0.46-0.95, p=0.024) but when analysed by ER status there was no statistically significant association in either ER positive (HR 0.63, 95% CI 0.39-1.04, p=0.071) or ER negative disease (HR 0.75, 95% CI 0.44-1.29, p=0.299) (**Figure 9-11**). This was also the case in each of the individual molecular subtypes (**Figure 9-12**). The association in the full cohort was not independent of other known prognostic factors (p=0.409, data not shown).

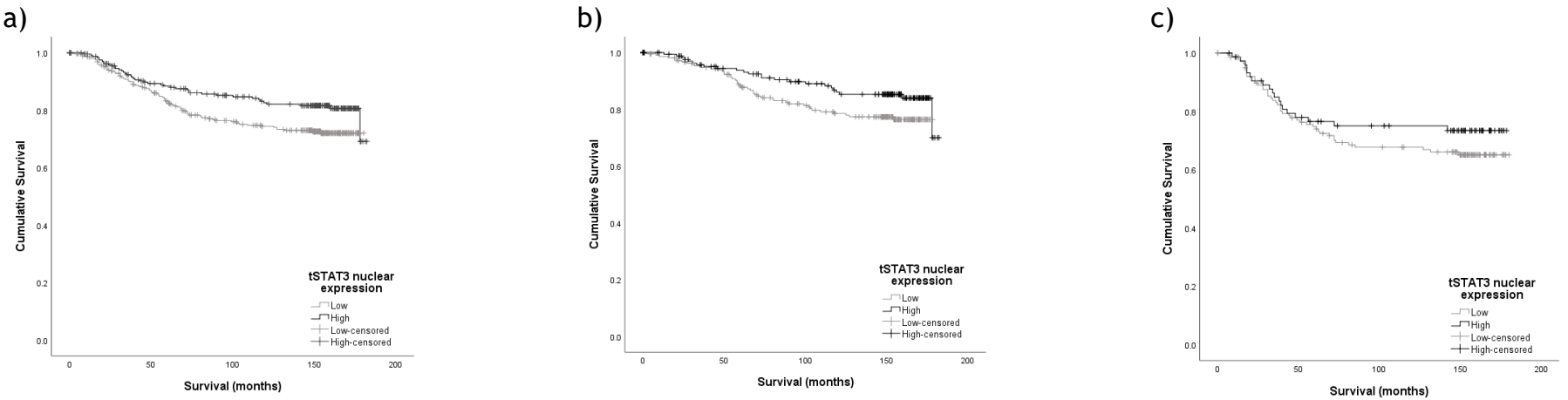

Figure 9-11. The relationship between nuclear tSTAT3 expression and CSS. Kaplan meier graphs to illustrate the relationship between nuclear tSTAT3 expression in tumour cells and CSS in a) the full cohort (n=609**, p=0.023**), b) ER positive disease (n=390, p=0.069) and c) ER negative disease (n=218, p=0.296).

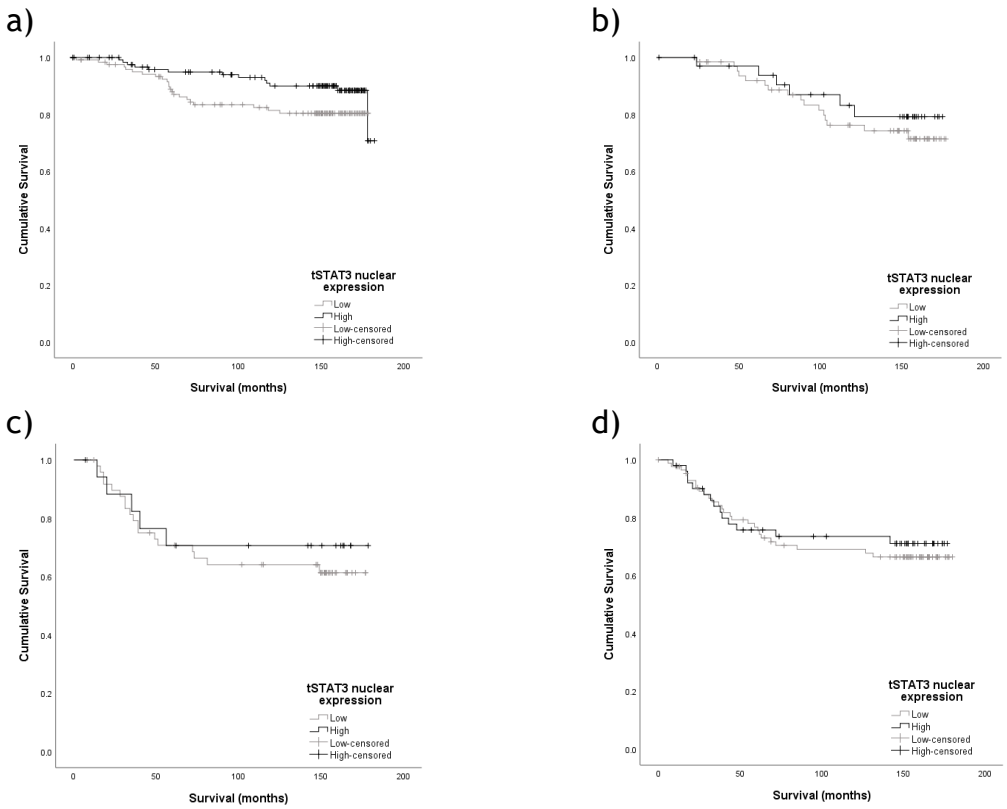

Figure 9-12. The relationship between nuclear tSTAT3 expression and CSS by molecular subtype. Kaplan meier graphs to illustrate the relationship between nuclear tSTAT3 expression in tumour cells and CSS in a) luminal A (n=253, p=0.070), b) luminal B (n=100, p=0.497), c) HER2-enriched (n=68, p=0.600) and d) triple negative (n=138, p=0.662) breast cancer.

9.3.3.2 Cytoplasmic tSTAT3 expression and CSS

203 (33.3%) patients had high cytoplasmic tSTAT3 expression (mean WHS >121.33). In the full cohort, high cytoplasmic expression of tSTAT3 was associated with worse CSS (high v low: HR 1.41, 95% CI 1.00-1.99, p=0.052) and this was particularly the case in ER positive (HR 1.76, 95% CI 1.10-2.82, p=0.020) but not ER negative disease (HR 1.12, 95% CI 0.67-1.87, p=0.674) (**Figure 9-13**). There was no significant relationship between cytoplasmic tSTAT3 expression and CSS in any of the molecular subtypes (**Figure 9-14**). The associations in the full cohort (p=0.105) and in ER positive disease (p=0.144) were not independent of other known prognostic factors (data not shown).

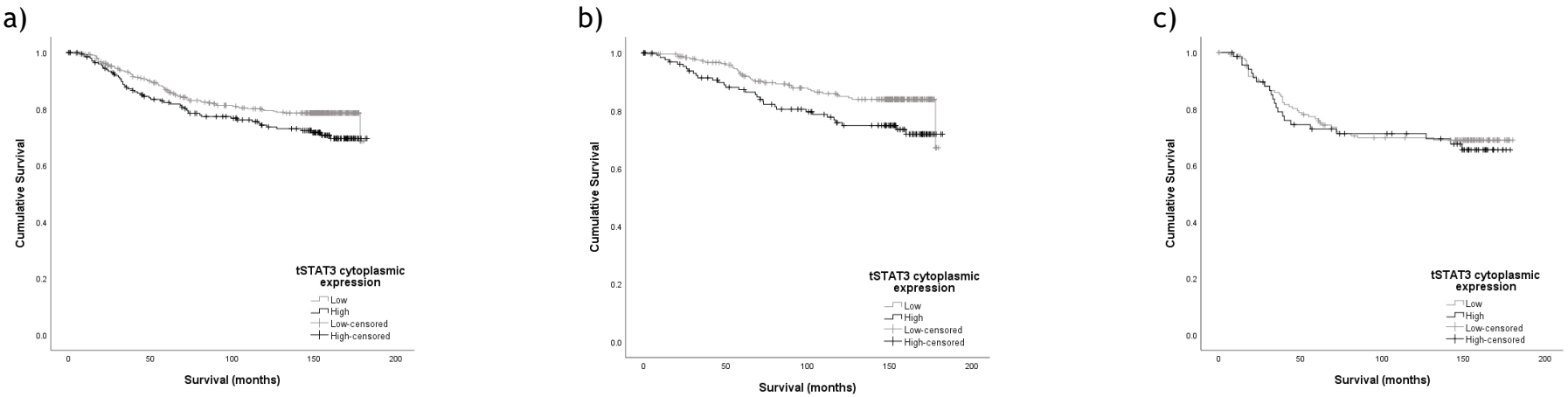

Figure 9-13. The relationship between cytoplasmic tSTAT3 expression and CSS. Kaplan meier graphs to illustrate the relationship between cytoplasmic tSTAT3 expression in tumour cells and CSS in a) the full cohort (n=609, **p=0.050**), b) ER positive disease (n=390, **p0.018**) and c) ER negative disease (n=218, p=0.673).

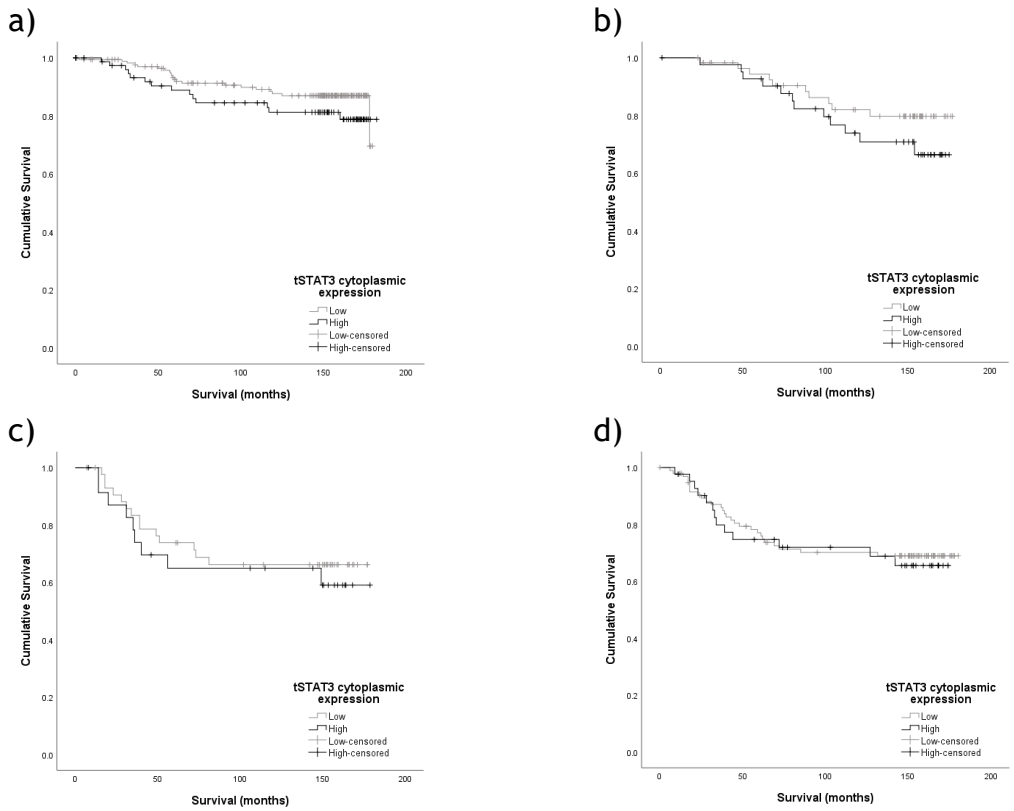

Figure 9-14. The relationship between cytoplasmic tSTAT3 expression and CSS by molecular subtype. Kaplan meier graphs to illustrate the relationship between cytoplasmic tSTAT3 expression in tumour cells and CSS in a) luminal A (n=253, p=0.185), b) luminal B (n=100, p=0.247), c) HER2-enriched (n=68, p=0.595) and d) triple negative (n=138, p=0.764) breast cancer.

9.3.3.3 Stromal tSTAT3 expression and CSS

344 (61.2%) patients had high stromal tSTAT3 expression (mean WHS>65.50). In the full cohort there was a trend towards worse CSS in those with high stromal tSTAT3 expression (high v low: HR 1.46, 95% CI 1.00-2.15, p=0.053). When analysed by ER status, in ER negative disease high stromal tSTAT3 expression was significantly associated with worse CSS (HR 1.96, 95% CI 1.16-3.31, p=0.012) but not in ER positive disease (HR 1.32, 95% CI 0.75-2.34, p=0.340) (**Figure 9-15**). When analysed within the molecular subtypes, high stromal tSTAT3 expression was associated with worse CSS in triple negative disease (HR 2.02, 95% CI 1.05-3.89, p=0.036) but not in the other 3 subtypes (**Figure 9-16**). The associations in ER negative (p=0.242) and triple negative disease (p=0.689) were not independent of other known prognostic factors (data not shown).

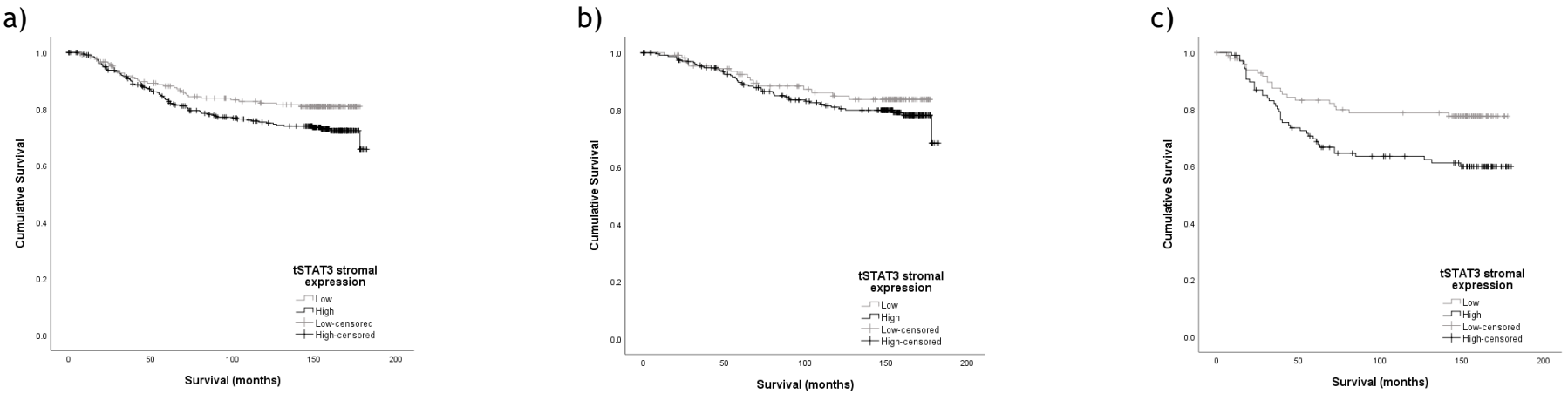

Figure 9-15. The relationship between stromal tSTAT3 expression and CSS. Kaplan meier graphs to illustrate the relationship between stromal tSTAT3 expression and CSS in a) the full cohort (n=562, p=0.051), b) ER positive disease (n=351, p=0.339) and c) ER negative disease (n=211, **p=0.011**).

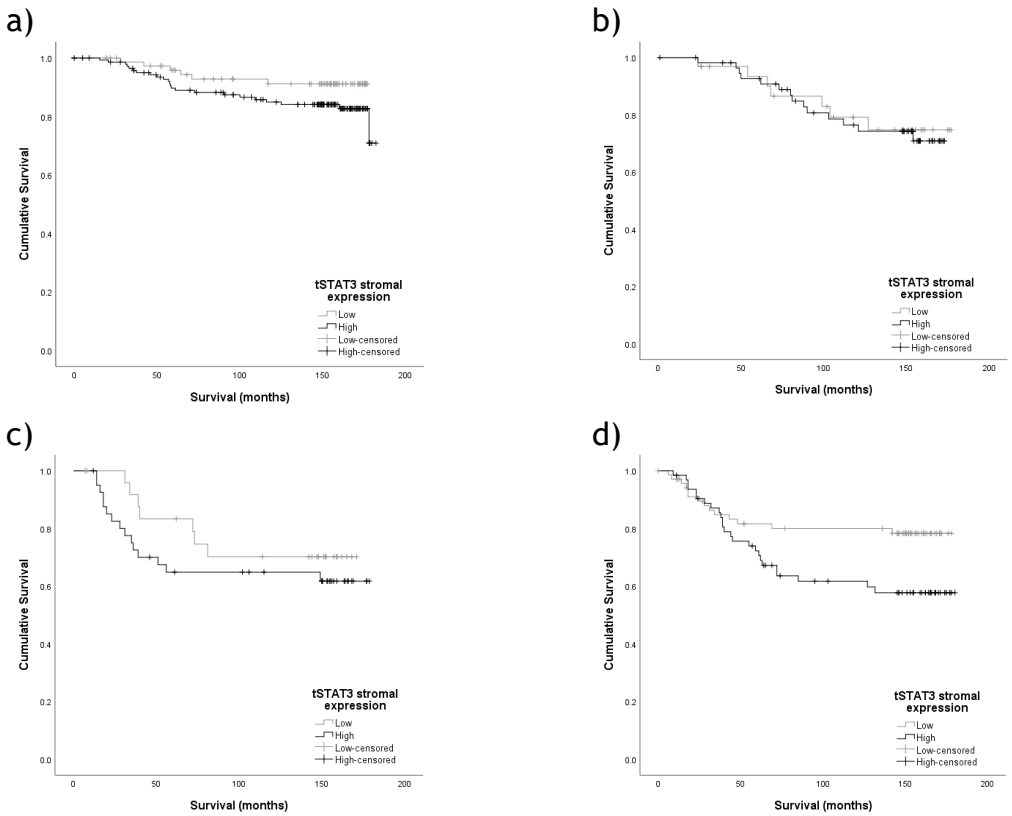

Figure 9-16. The relationship between stromal tSTAT3 expression and CSS by molecular subtype. Kaplan meier graphs to illustrate the relationship between stromal tSTAT3 expression and CSS in a) luminal A (n=225, p=0.132), b) luminal B (n=90, p=0.829), c) HER2-enriched (n=67, p=0.373) and d) triple negative (n=133, **p=0.032**) breast cancer.

9.3.4 Associations between tSTAT3 expression and clinicopathological characteristics

High nuclear tSTAT3 expression was associated with lower grade (p<0.001), ER positivity (p=0.014), HER2 negativity (p=0.001) and low necrosis (p=0.004) (**Table 9-1**). There were no significant associations observed between cytoplasmic tSTAT3 and the clinicopathological characteristics studied (**Table 9-1**).

	Nuclear tSTAT3 expression		p	Cytoplasmic tSTAT3 expression		p
	Low n(%)	**High** n(%)		**Low** n(%)	**High** n(%)	
Age			0.249			0.804
≤50yrs	117 (32.5)	70 (28.1)		126 (31.0)	61 (30.0)	
>50yrs	243 (67.5)	179 (71.9)		280 (69.0)	142 (70.0)	
Type			0.132			0.068
Ductal	324 (90.0)	212 (85.1)		349 (86.0)	187 (92.1)	
Lobular	23 (6.4)	20 (8.0)		35 (8.6)	8 (3.9)	
Other	13 (3.6)	17 (6.8)		22 (5.4)	8 (3.9)	
Size			0.095			0.125
≤20mm	205 (57.1)	127 (51.0)		231 (57.0)	101 (49.8)	
21-49mm	132 (36.8)	112 (45.0)		151 (37.3)	93 (45.8)	
≥50mm	22 (6.1)	10 (4.0)		23 (5.7)	9 (4.4)	
Grade			**<0.001**			0.398
I	40 (11.1)	57 (23.1)		64 (15.8)	33 (16.3)	
II	156 (43.3)	101 (40.9)		179 (44.2)	78 (38.6)	
III	164 (45.6)	89 (36.0)		162 (40.0)	91 (45.0)	
Nodal status			0.427			0.893
Negative	197 (55.3)	143 (58.6)		228 (56.9)	112 (56.3)	
Positive	159 (44.7)	101 (41.4)		173 (43.1)	87 (43.7)	
ER status			**0.014**			0.617
Negative	143 (39.8)	75 (30.1)		148 (36.5)	70 (34.5)	
Positive	216 (60.2)	174 (69.9)		257 (63.5)	133 (65.5)	
HER2 status			**0.001**			0.881
Negative	276 (77.7)	218 (87.9)		330 (82.1)	164 (81.6)	
Positive	79 (22.3)	30 (12.1)		72 (17.9)	37 (18.4)	
Necrosis			**0.004**			0.126
<25%	147 (42.6)	134 (54.7)		195 (49.9)	86 (43.2)	
>25%	198 (57.4)	111 (45.3)		196 (50.1)	113 (56.8)	
KM score			0.094			0.417
0	50 (14.5)	48 (19.6)		71 (18.2)	27 (13.4)	
1	156 (45.1)	121 (49.4)		176 (45.1)	101 (50.2)	
2	105 (30.3)	56 (22.9)		105 (26.9)	56 (27.9)	
3	35 (10.1)	20 (8.2)		38 (9.7)	17 (8.5)	
CD8+ lymphocytes			0.230			0.658
Low	52 (30.4)	38 (31.9)		61 (32.4)	29 (28.4)	
Medium	63 (36.8)	33 (27.7)		59 (31.4)	37 (36.3)	
High	56 (32.7)	48 (40.3)		68 (36.2)	36 (35.3)	
CD4+ lymphocytes			0.806			0.651
Low	96 (30.6)	71 (31.7)		115 (32.0)	52 (29.1)	
Medium	110 (35.0)	82 (36.6)		129 (35.9)	63 (35.2)	
High	108 (34.4)	71 (31.7)		115 (32.0)	64 (35.8)	
TSP			0.646			0.353
Low	247 (71.0)	171 (69.2)		281 (71.5)	137 (67.8)	
High	101 (29.0)	76 (30.8)		112 (28.5)	65 (32.2)	
Budding			0.589			0.883
≤20 buds	237 (68.1)	163 (66.0)		265 (67.4)	135 (66.8)	
>20 buds	111 (31.9)	84 (34.0)		128 (32.6)	67 (33.2)	

Table 9-1. The association between nuclear and cytoplasmic tSTAT3 expression and clinicopathological characteristics. Table detailing the associations between nuclear and cytoplasmic tSTAT3 expression and clinicopathological characteristics. Statistically significant p values are highlighted in bold.

High stromal tSTAT3 expression was associated with HER2 positivity (p=0.024), low CD4+ lymphocytes (p<0.001) and high budding (p=0.049) (**Table 9-2**).

	Stromal tSTAT3 expression		p
	Low n(%)	High n(%)	
Age			0.067
≤50yrs	45 (43.7)	34 (31.5)	
>50yrs	58 (56.3)	74 (68.5)	
Type			0.793
Ductal	95 (92.2)	102 (94.4)	
Lobular	1 (1.0)	1 (0.9)	
Other	7 (6.8)	5 (4.6)	
Size			0.955
≤20mm	48 (46.6)	51 (47.7)	
21-49mm	49 (47.6)	49 (45.8)	
≥50mm	6 (5.8)	7 (6.5)	
Grade			0.271
I	4 (3.9)	1 (0.9)	
II	18 (17.5)	24 (22.6)	
III	81 (78.6)	81 (76.4)	
Nodal status			0.874
Negative	54 (52.9)	56 (51.9)	
Positive	48 (47.1)	52 (48.1)	
HER2 status			**0.024**
Negative	75 (74.3)	63 (59.4)	
Positive	26 (25.7)	43 (40.6)	
Necrosis			0.689
<25%	18 (17.5)	21 (19.6)	
>25%	85 (82.5)	86 (80.4)	
KM score			0.064
0	2 (2.0)	3 (2.8)	
1	32 (31.4)	51 (47.7)	
2	50 (49.0)	43 (40.2)	
3	18 (17.6)	10 (9.3)	
CD8+ lymphocytes			0.357
Low	23 (30.3)	14 (26.9)	
Medium	15 (19.7)	16 (30.8)	
High	38 (50.0)	22 (42.3)	
CD4+ lymphocytes			**<0.001**
Low	5 (5.2)	20 (20.4)	
Medium	26 (27.1)	37 (37.8)	
High	65 (67.7)	41 (41.8)	
TSP			0.793
Low	72 (69.9)	73 (68.2)	
High	31 (30.1)	34 (31.8)	
Budding			**0.049**
≤20 buds	85 (82.5)	76 (71.0)	
>20 buds	18 (17.5)	31 (29.0)	

Table 9-2. The association between stromal tSTAT3 expression and clinicopathological characteristics in ER negative disease. Table detailing the associations between stromal tSTAT3 expression and clinicopathological characteristics in patients with ER negative breast cancer. Statistically significant p values are highlighted in bold.

9.3.5 Formation of the cohort for pSTAT3(Tyr705)

718 patients had at least one core which was assessable for pSTAT3(Tyr 705) expression in tumour cell nuclei and cytoplasm, while 784 had at least one core assessable for stromal expression (**Figure 9-17**).

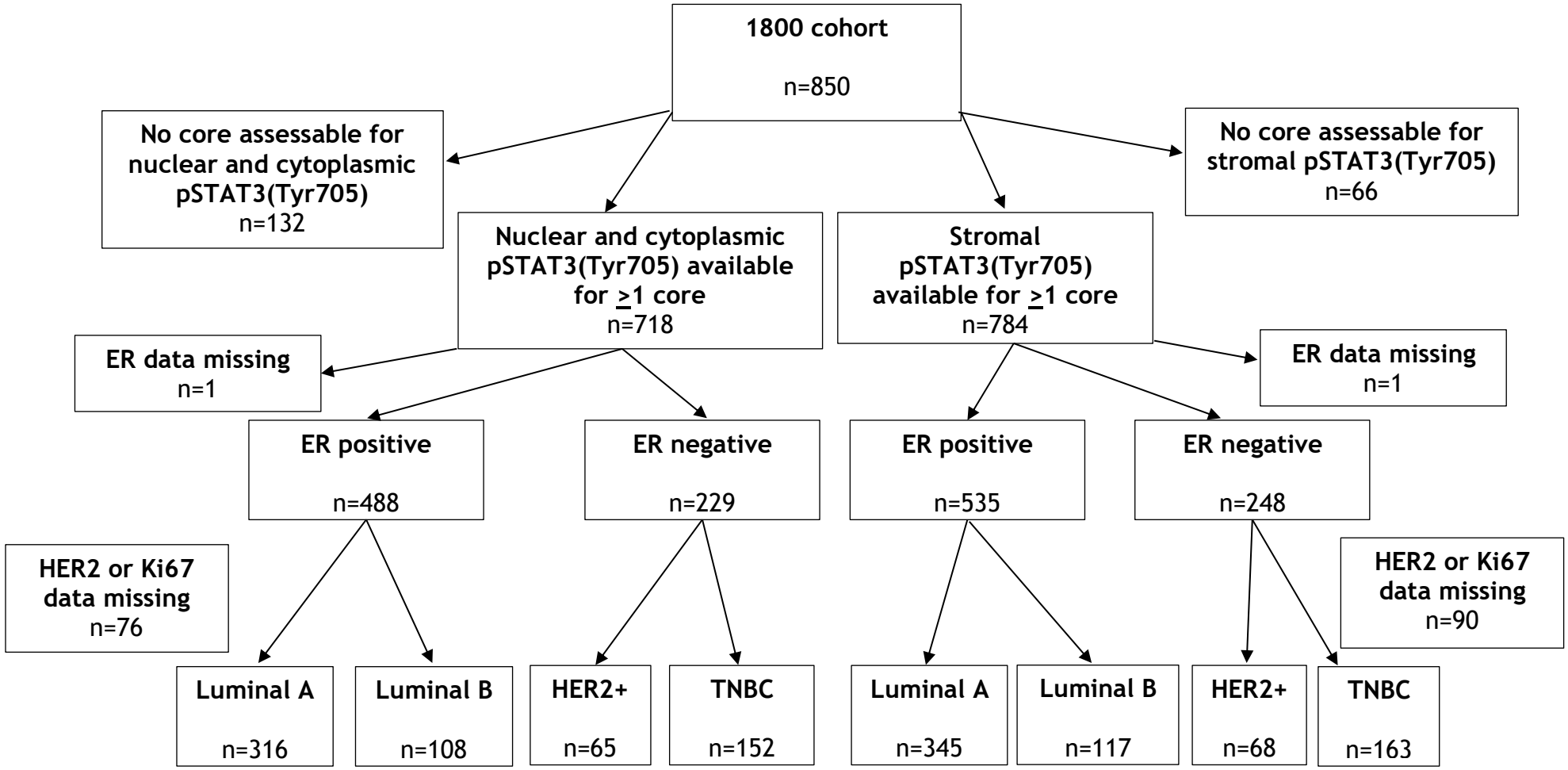

Figure 9-17. Formation of the pSTAT3(Tyr705) cohort. Flow diagram to illustrate the number of patients within the 1800 cohort with at least 1 core which was assessable for pSTAT3(Tyr705) expression in the tumour cell nucleus and cytoplasm, and separately in the stroma. The numbers available for subgroup analysis by ER status and by molecular subtype are also shown.

9.3.6 pSTAT3(Tyr 705) expression

pSTAT3(Tyr705) expression was observed in the nucleus and cytoplasm of tumour cells and in stromal cells. Examples of tSTAT3 staining are shown below.

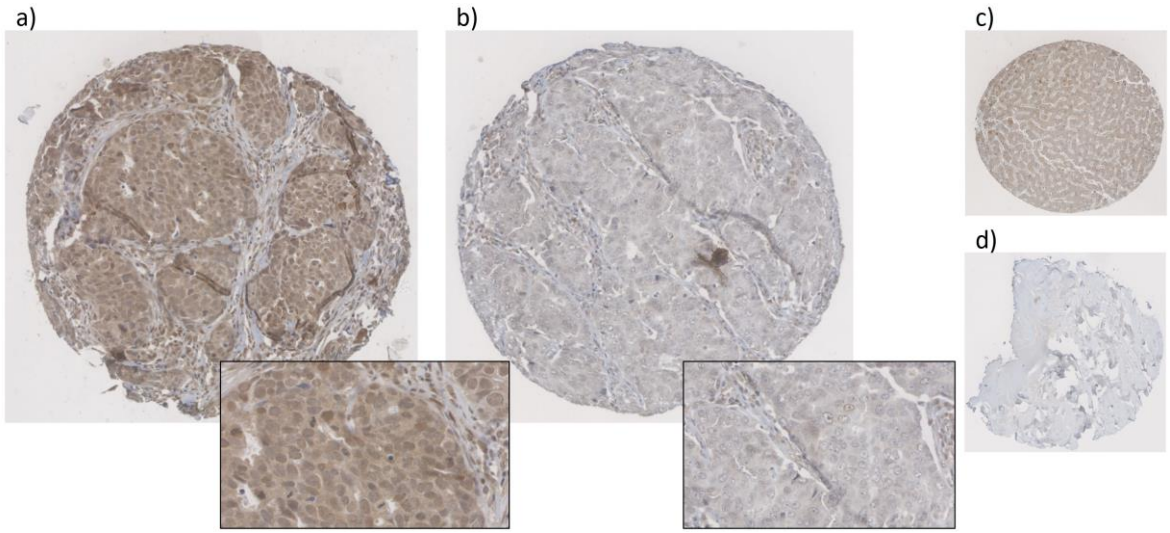

Figure 9-18. Examples of pSTAT3(Tyr 705) staining. TMA cores stained using IHC for pSTAT3(Tyr705): a) breast core with predominantly moderate cytoplasmic staining at 10x magnification with an inset at 40x magnification, b) breast core with predominantly weak cytoplasmic staining, c) true positive core (control, liver) at 10x magnification, d) true negative core at 10x magnification.

Median expression of pSTAT3(Tyr705) was mean WHS 23.33 (0-300) in tumour cell nuclei, 56.67 (0-300) in tumour cell cytoplasm and 6.67 (0-236.67) in stromal cells. pSTAT3(Tyr705) expression in the 3 locations is illustrated in the figures below (**Figure 9-19, Figure 9-20**).

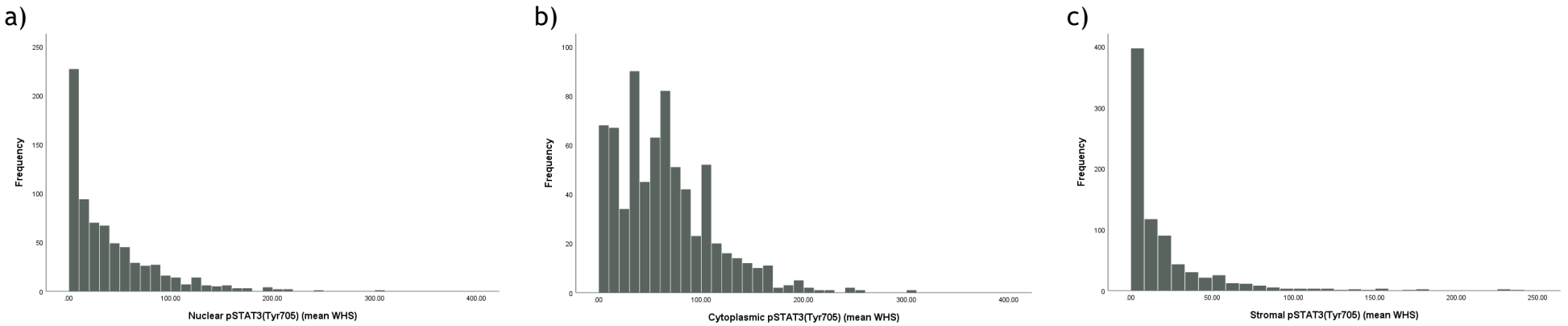

Figure 9-19. Expression of pSTAT3(Tyr705). Histograms to illustrate the expression of pSTAT3(Tyr705) in a) tumour nuclei, b) tumour cytoplasm and c) stroma.

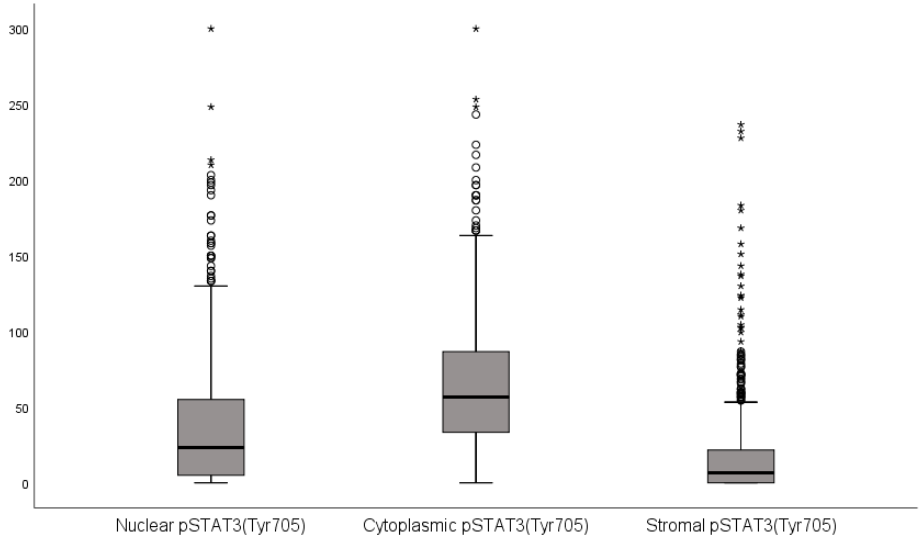

Figure 9-20. Boxplots of pSTAT3(Tyr705) expression. Boxplots to compare the expression of pSTAT3(Tyr705) in tumour nuclei, cytoplasm and in stroma.

There was no significant difference in nuclear pSTAT3(Tyr705) expression between the different ER or molecular subtypes (**Figure 9-21**).

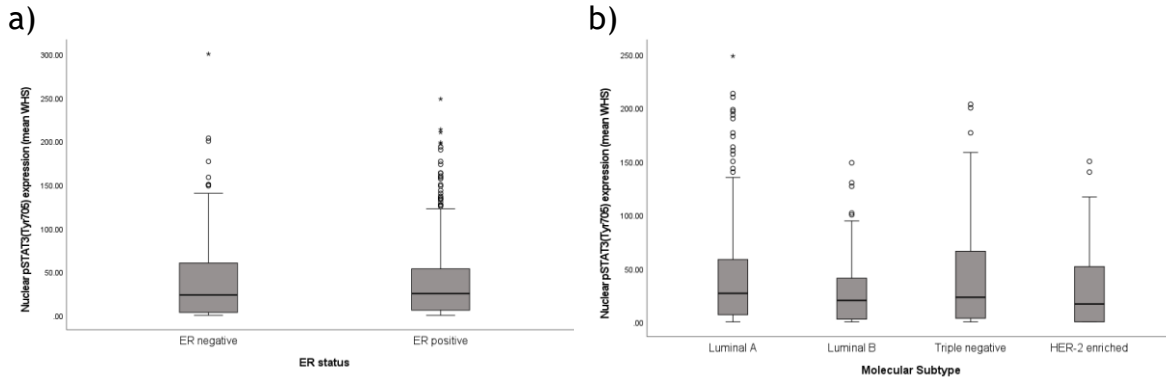

Figure 9-21. Boxplots of nuclear pSTAT3(Tyr705) by receptor status. Boxplots to illustrate the differences in nuclear pSTAT3(Tyr705) expression by a) ER status (p=0.303) and b) molecular subtype (p=0.159).

Similarly, there was no significant difference in cytoplasmic pSTAT3(Tyr705) expression between the different ER or molecular subtypes (**Figure 9-22**).

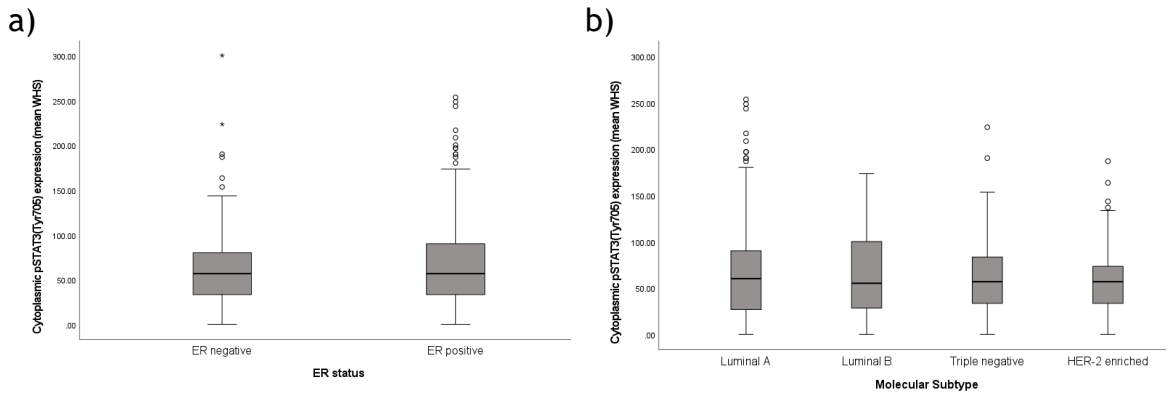

Figure 9-22. Boxplots of cytoplasmic pSTAT3(Tyr705) by receptor status. Boxplots to illustrate the differences in cytoplasmic pSTAT3(Tyr705) expression by a) ER status (p=0.987) and b) molecular subtype (p=0.891).

Stromal pSTAT3(Tyr705) expression was higher in the ER negative subtypes (**Figure 9-23**).

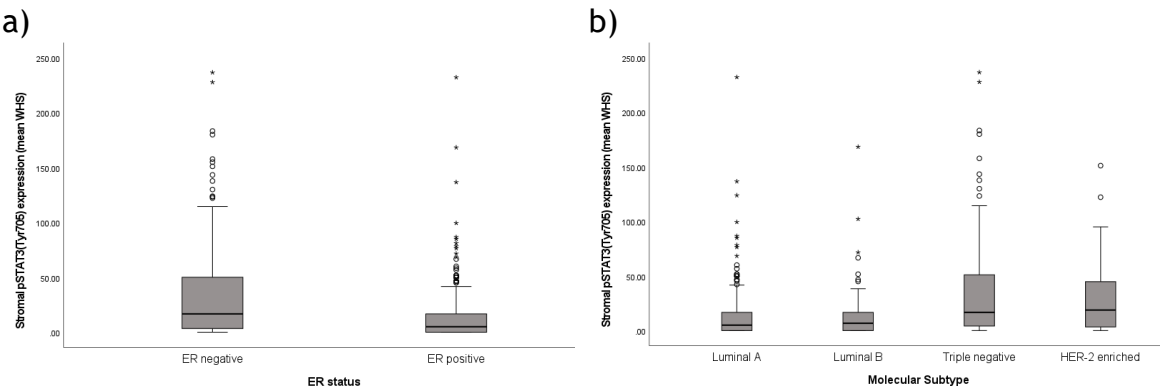

Figure 9-23. Boxplots of stromal pSTAT3(Tyr705) by receptor status. Boxplots to illustrate the differences in stromal pSTAT3(Tyr705) expression by a) ER status (**p<0.001**) and b) molecular subtype (**p<0.001**).

There was a moderate positive correlation between nuclear and cytoplasmic pSTAT3(Tyr705) expression and a weak correlation between each of the tumour cell expression sites and stromal expression (**Figure 9-24**).

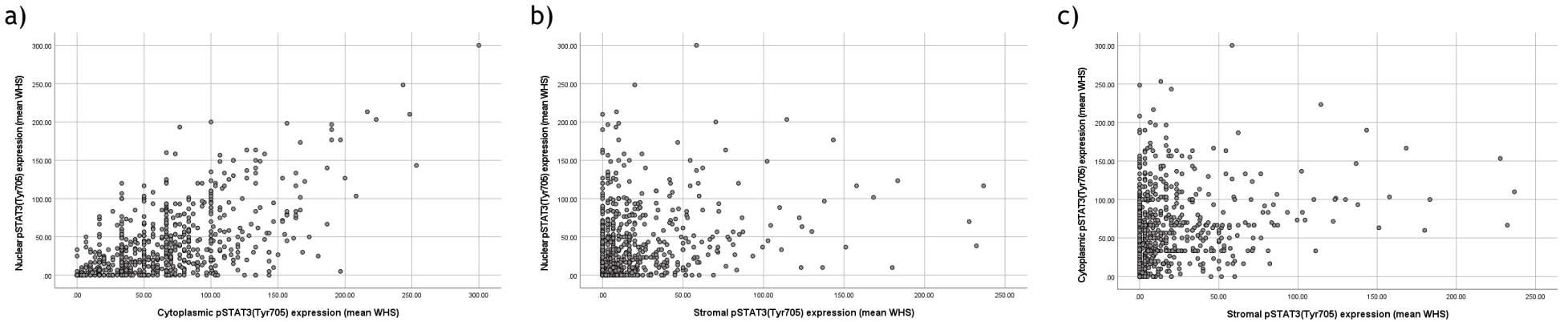

Figure 9-24. Correlation between pSTAT3(Tyr705) expression sites. Scatter plots to illustrate the correlation between pSTAT3(Tyr705) expression in different sites: a) nuclear and cytoplasmic expression (Pearson correlation 0.625, **p<0.001**), b) nuclear and stromal expression (Pearson correlation 0.236, **p<0.001**), c) cytoplasmic and stromal expression (Pearson correlation 0.187, **p<0.001**).

9.3.7 The relationship between pSTAT3(Tyr 705) and CSS

ROC curves were constructed to determine thresholds for division into high and low expression groups for further analysis (**Figure 9-25**). From these, thresholds of a mean WHS of 8.50 and 42.50 were derived for nuclear and cytoplasmic pSTAT3(Tyr705) expression respectively. As no threshold could be derived from the ROC curve for stromal expression, the median (6.67) was used for division into groups.

a)

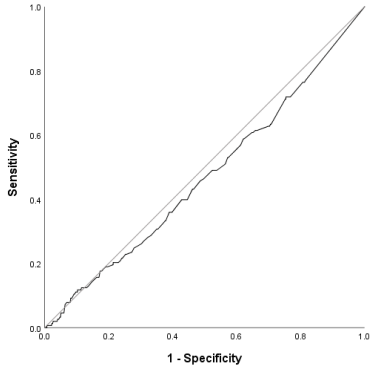

b)

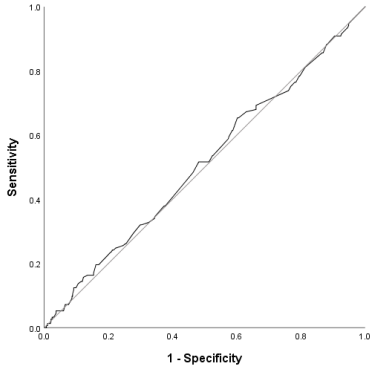

c)

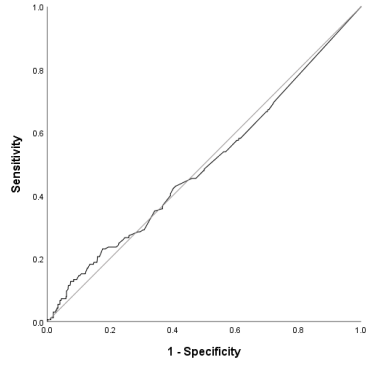

Figure 9-25. ROC curves for pSTAT3(Tyr705) expression and CSS. ROC curves to illustrate the relationship between pSTAT3(Tyr705) and CSS in a) tumour cell nuclei (AUC 0.470), b) tumour cell cytoplasm (AUC 0.510) and c) stromal cells (AUC 0.498).

9.3.7.1 Nuclear pSTAT3(Tyr705) expression and CSS

493 (68.7%) of tumours had high (mean WHS >8.50) nuclear pSTAT3(Tyr705) expression. There was no significant association between nuclear pSTAT3(Tyr705) expression and CSS in the whole cohort or when analysed by ER status (**Figure 9-26**). However, when analysed by molecular subtype, low nuclear pSTAT3(Tyr705) expression was associated with worse CSS in luminal A cancers (high v low: HR 0.53, 95% CI 0.28-1.00, p=0.048) but there was no significant association observed in the other three subtypes (**Figure 9-27**). The association in luminal A disease was not independent of other known pathological prognostic variables on multivariate analysis (p=0.202, data not shown).

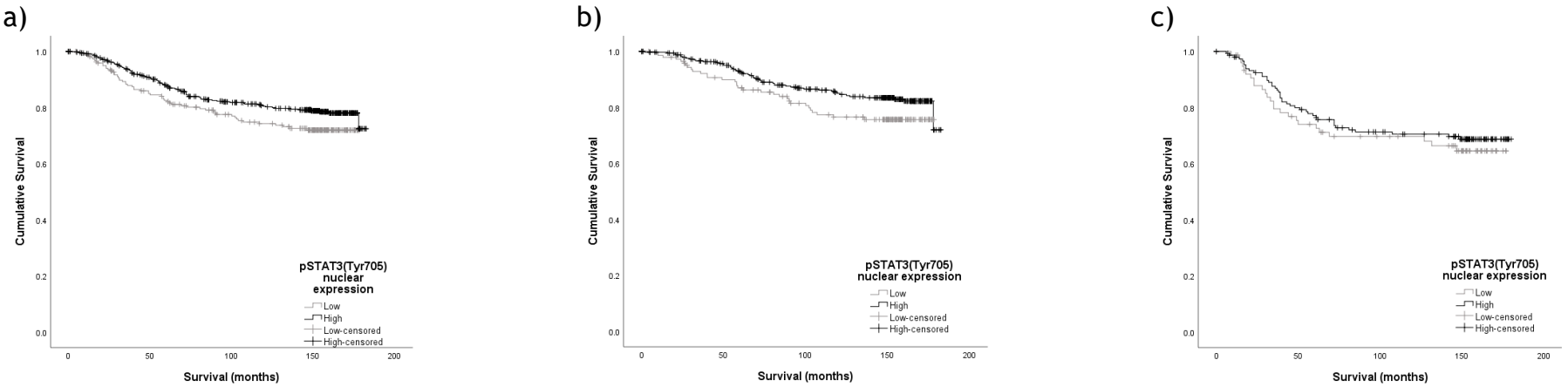

Figure 9-26. The relationship between nuclear pSTAT3(Tyr 705) expression and CSS. Kaplan meier graphs to illustrate the relationship between nuclear pSTAT3(Tyr705) expression in tumour cells and CSS in a) the full cohort (n=718, p=0.063), b) ER positive disease (n=488, p=0.080) and c) ER negative disease (n=229, p=0.502).

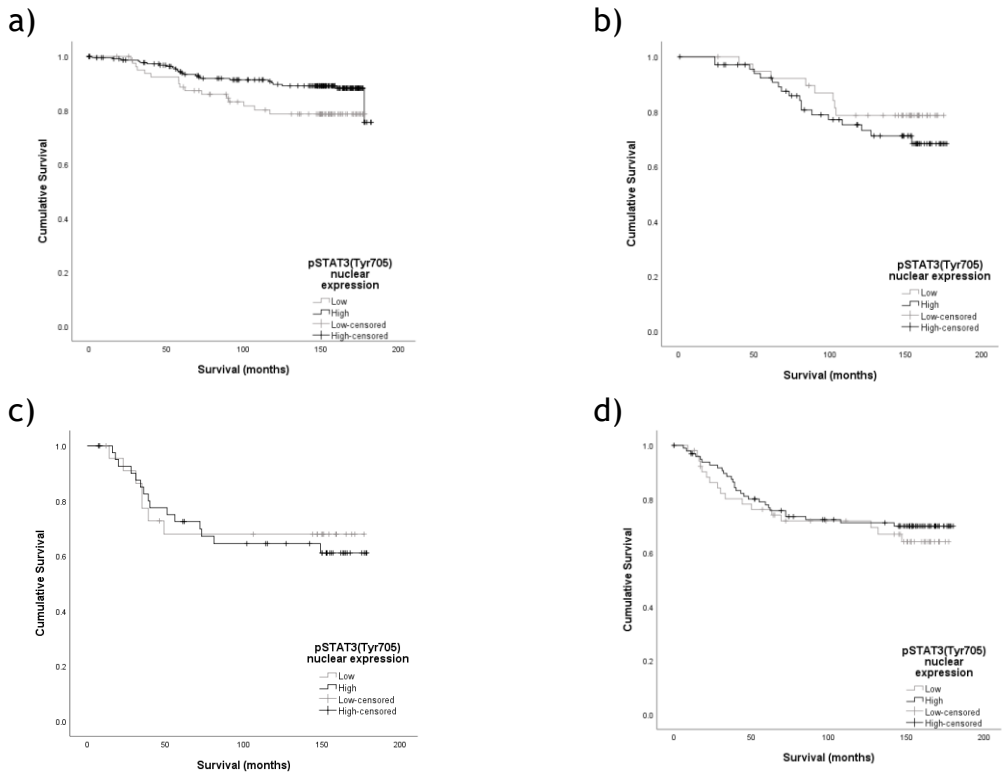

Figure 9-27. The relationship between nuclear pSTAT3(Tyr705) expression and CSS by molecular subtype. Kaplan meier graphs to illustrate the relationship between nuclear pSTAT3(Tyr705) expression and CSS in a) luminal A (n=316, **p=0.045**), b) Luminal B (n=108, p=0.333), c) HER2-enriched (n=65, p=0.788) and d) triple negative (n=152, p=0.534) breast cancer.

9.3.7.2 Cytoplasmic pSTAT3(Tyr705) expression and CSS

440 (61.3%) patients had high (mean WHS >42.50) cytoplasmic pSTAT3(Tyr705) expression. No significant association was observed between cytoplasmic pSTAT3(Tyr705) expression and CSS when analysed in the full cohort, by ER status or by molecular subtype (**Figure 9-28, Figure 9-29**).

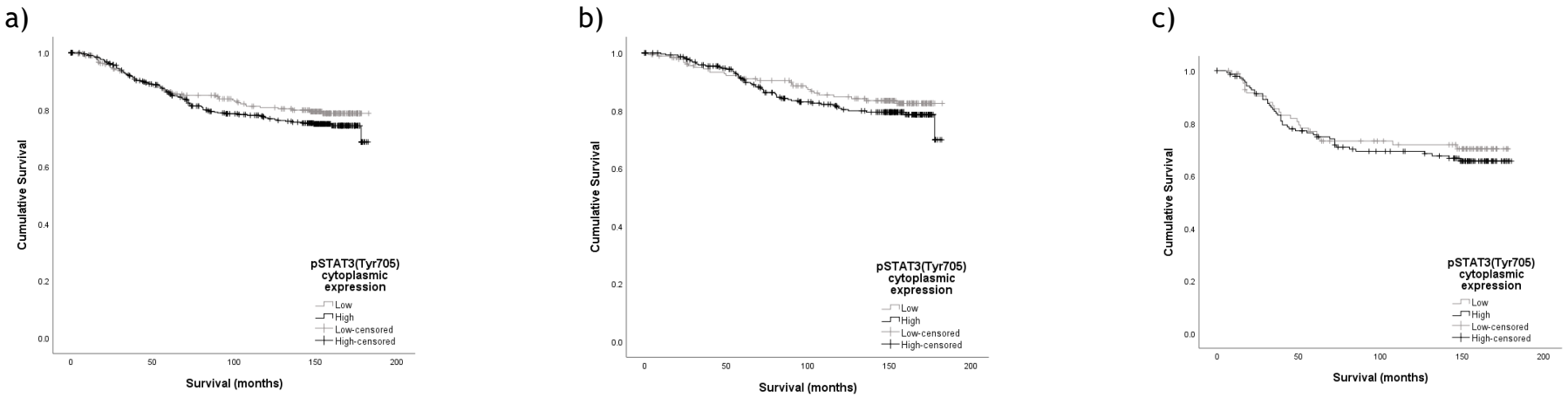

Figure 9-28. The relationship between cytoplasmic pSTAT3(Tyr 705) expression and CSS. Kaplan meier graphs to illustrate the relationship between cytoplasmic pSTAT3(Tyr705) expression in tumour cells and CSS in a) the full cohort (n=718, p=0.243), b) ER positive disease (n=488, p=0.326) and c) ER negative disease (n=229, p=0.555).

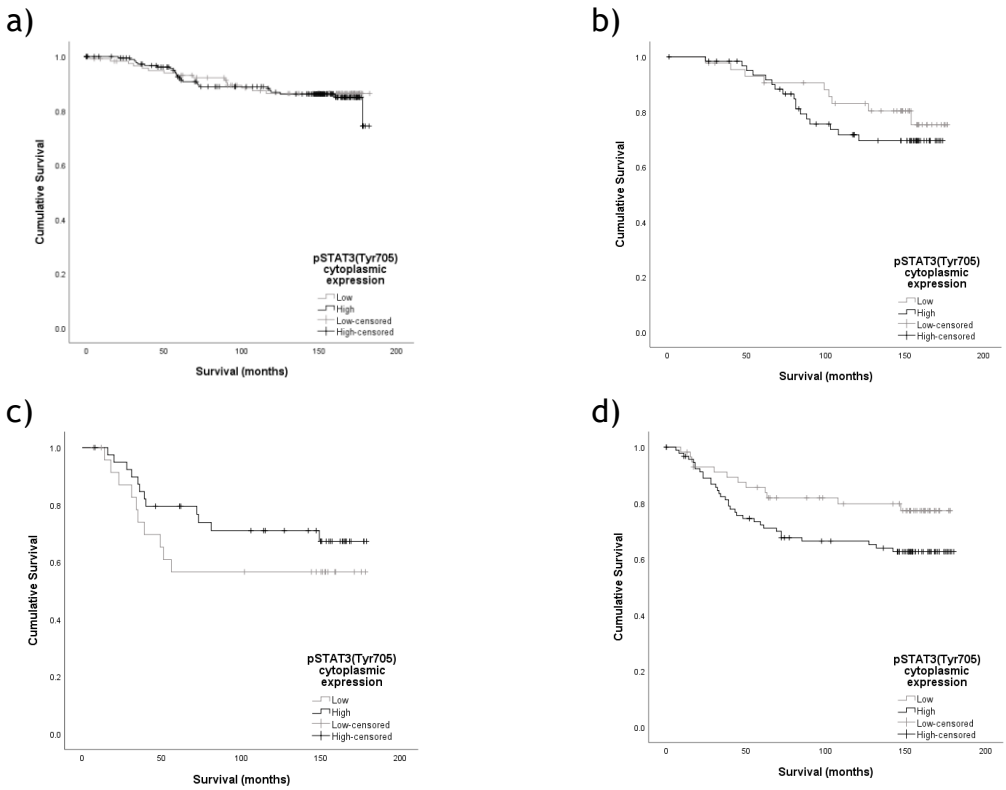

Figure 9-29. The relationship between cytoplasmic pSTAT3(Tyr705) expression and CSS by molecular subtype. Kaplan meier graphs to illustrate the relationship between cytoplasmic pSTAT3(Tyr705) expression and CSS in a) luminal A (n=316, p=0.810), b) Luminal B (n=108, p=0.355), c) HER2-enriched (n=65, p=0.276) and d) triple negative (n=152, p=0.065) breast cancer.

9.3.7.3 Stromal pSTAT3(Tyr705) expression and CSS

No significant association was observed between stromal pSTAT3(Tyr705) expression and CSS when analysed in the full cohort, by ER status or by molecular subtype (**Figure 9-30, Figure 9-31**).

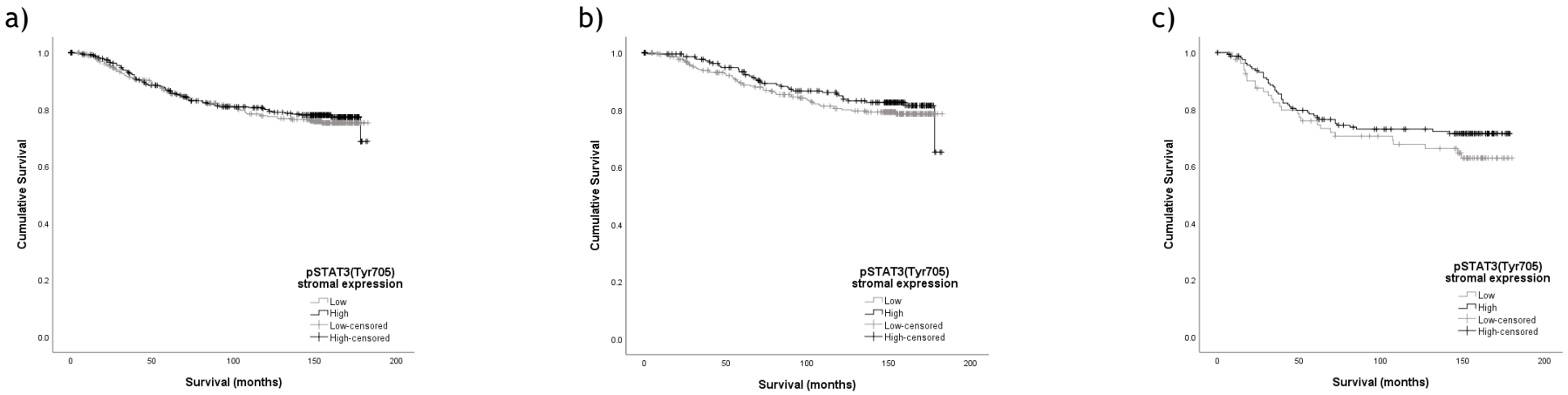

Figure 9-30. The relationship between stromal pSTAT3(Tyr 705) expression and CSS. Kaplan meier graphs to illustrate the relationship between stromal pSTAT3(Tyr705) expression in tumour cells and CSS in a) the full cohort (n=784, p=0.601), b) ER positive disease (n=535, p=0.381) and c) ER negative disease (n=248, p=0.238).

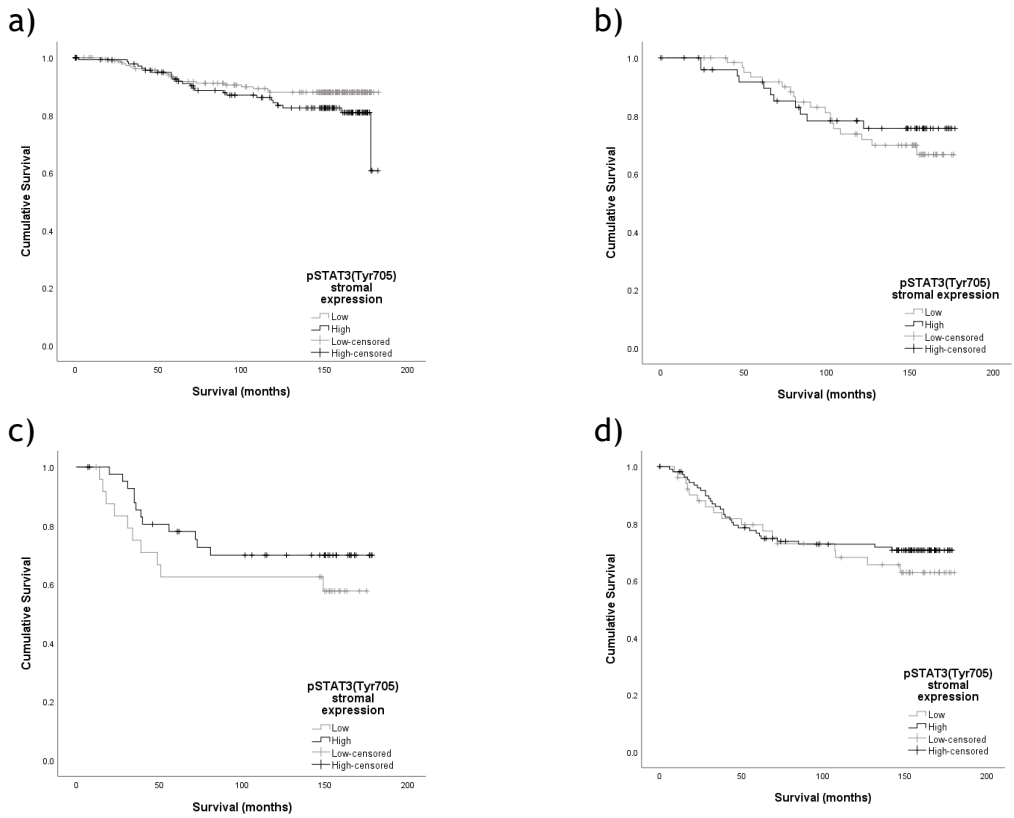

Figure 9-31. The relationship between stromal pSTAT3(Tyr705) expression and CSS by molecular subtype. Kaplan meier graphs to illustrate the relationship between stromal pSTAT3(Tyr705) expression and CSS in a) luminal A (n=345, p=0.126), b) Luminal B (n=117, p=0.568), c) HER2-enriched (n=68, p=0.269) and d) triple negative (n=163, p=0.463) breast cancer.

9.3.8 Associations between pSTAT3(Tyr705) expression and clinicopathological characteristics

High nuclear pSTAT3(Tyr705) expression was associated with younger age (p=0.006), more lobular cancers (p=0.008), low necrosis (p=0.017), lower KM score (p=0.042) and high budding (p<0.001) (**Table 9-3**). In luminal A cancers it was associated with necrosis (p=0.036), age (p=0.005) and tumour type (p=0.020) only.

	Nuclear pSTAT3(Tyr705) expression		p
	Low n(%)	**High** n(%)	
Age			**0.006**
≤50yrs	51 (22.7)	161 (32.7)	
>50yrs	174 (77.3)	332 (67.3)	
Type			**0.008**
Ductal	206 (91.6)	421 (85.4)	
Lobular	6 (2.7)	45 (9.1)	
Other	13 (5.8)	27 (5.5)	
Size			0.288
≤20mm	120 (53.3)	293 (59.6)	
21-49mm	92 (40.9)	176 (35.8)	
≥50mm	13 (5.8)	23 (4.7)	
Grade			0.256
I	33 (14.7)	96 (19.6)	
II	101 (44.9)	216 (44.0)	
III	91 (40.4)	179 (36.5)	
Nodal status			0.902
Negative	129 (58.1)	280 (57.6)	
Positive	93 (41.9)	206 (42.4)	
ER status			0.264
Negative	78 (34.8)	151 (30.6)	
Positive	146 (65.2)	342 (69.4)	
HER2 status			0.835
Negative	187 (83.9)	407 (83.2)	
Positive	36 (16.1)	82 (16.8)	
Necrosis			**0.017**
<25%	96 (44.9)	263 (54.7)	
>25%	118 (55.1)	218 (45.3)	
KM score			**0.042**
0	35 (16.1)	82 (17.2)	
1	94 (43.1)	249 (52.2)	
2	64 (29.4)	113 (23.7)	
3	25 (11.5)	33 (6.9)	
CD8+ lymphocytes			0.310
Low	20 (30.8)	78 (30.0)	
Medium	27 (41.5)	86 (33.1)	
High	18 (27.7)	96 (36.9)	
CD4+ lymphocytes			0.761
Low	62 (35.0)	138 (31.9)	
Medium	57 (32.3)	147 (34.0)	
High	58 (32.8)	147 (34.0)	
TSP			0.844
Low	154 (70.6)	344 (71.4)	
High	64 (29.4)	138 (28.6)	
Budding			**<0.001**
≤20 buds	168 (77.1)	307 (63.7)	
>20 buds	50 (22.9)	175 (36.3)	

Table 9-3. The association between nuclear pSTAT3(Tyr705) expression and clinicopathological characteristics. Table detailing the associations between nuclear pSTAT3(Tyr705) expression and clinicopathological characteristics. Statistically significant p values are highlighted in bold.

9.3.9 Formation of the cohort for pSTAT3(Ser727)

727 patients had at least one core which was assessable for pSTAT3(Ser727) expression in tumour cell nuclei and cytoplasm while 786 had at least one core assessable for stromal expression (**Figure 9-32**).

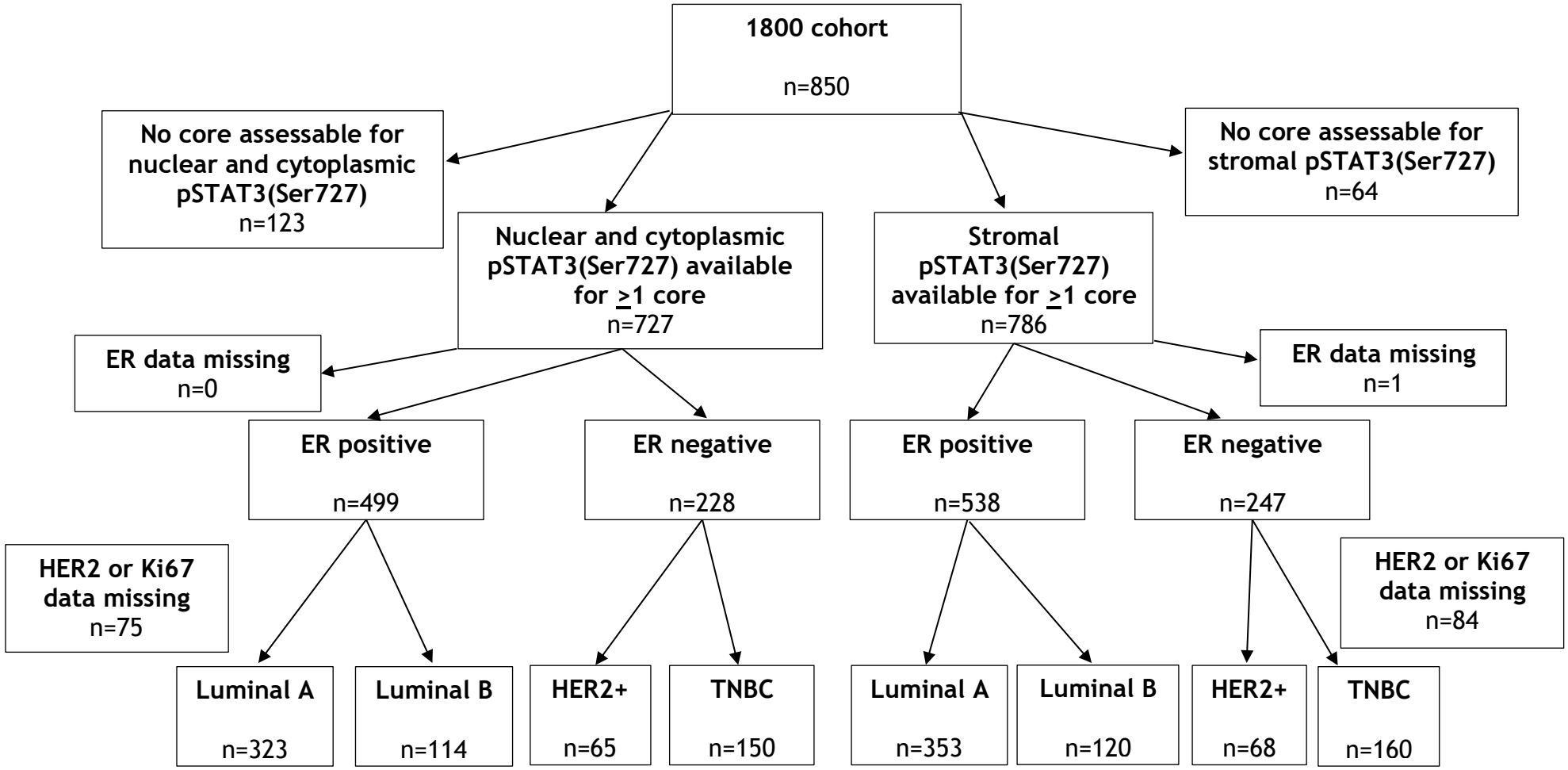

Figure 9-32. Formation of the pSTAT3(Ser727) cohort. Flow diagram to illustrate the number of patients within the 1800 cohort with at least 1 core which was assessable for pSTAT3(Ser727) expression in the tumour cell nucleus and cytoplasm, and separately in the stroma. The numbers available for subgroup analysis by ER status and by molecular subtype are also shown.

9.3.10 pSTAT3(Ser727) expression

pSTAT3(Ser727) expression was observed in the nucleus and cytoplasm of tumour cells and in stromal cells. Examples of tSTAT3 staining are shown below.

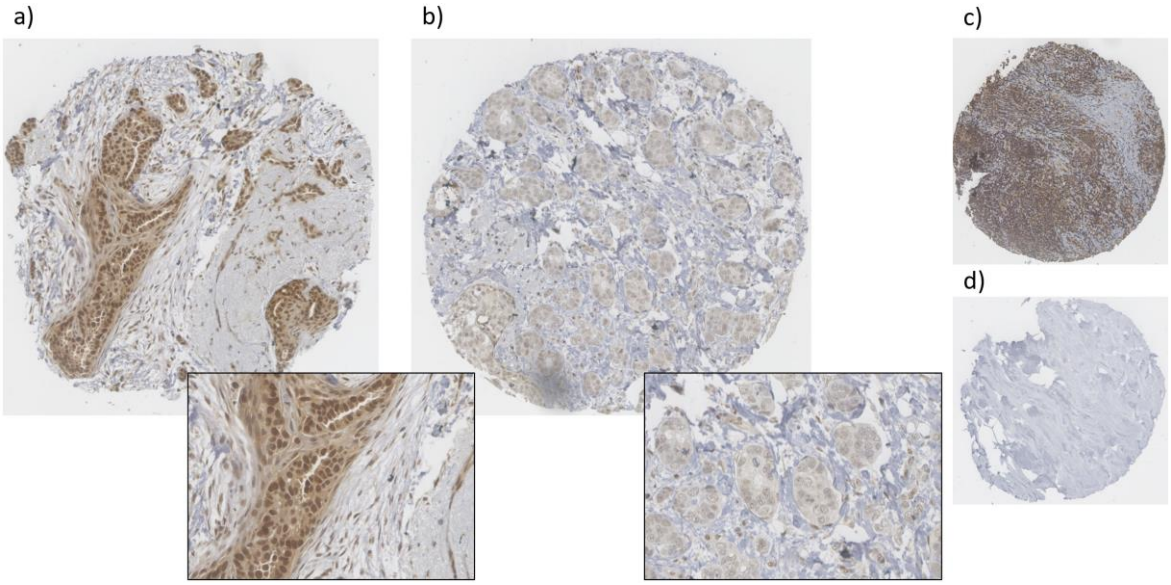

Figure 9-33. Examples of pSTAT3(Ser727) staining. TMA cores stained using IHC for pSTAT3(Ser727): a) breast core with predominantly moderate cytoplasmic staining at 10x magnification with an inset at 40x magnification, b) breast core with predominantly weak cytoplasmic staining, c) true positive core (control, tonsil) at 10x magnification, d) true negative core at 10x magnification.

Median expression of pSTAT3(Ser727) was mean WHS 145 (0-300) in tumour cell nuclei, 120 (0-300) in cytoplasm and 3.33 (0-110) in stroma. pSTAT3(Ser727) expression in the 3 locations is illustrated in the figures below (**Figure 9-34, Figure 9-35**).

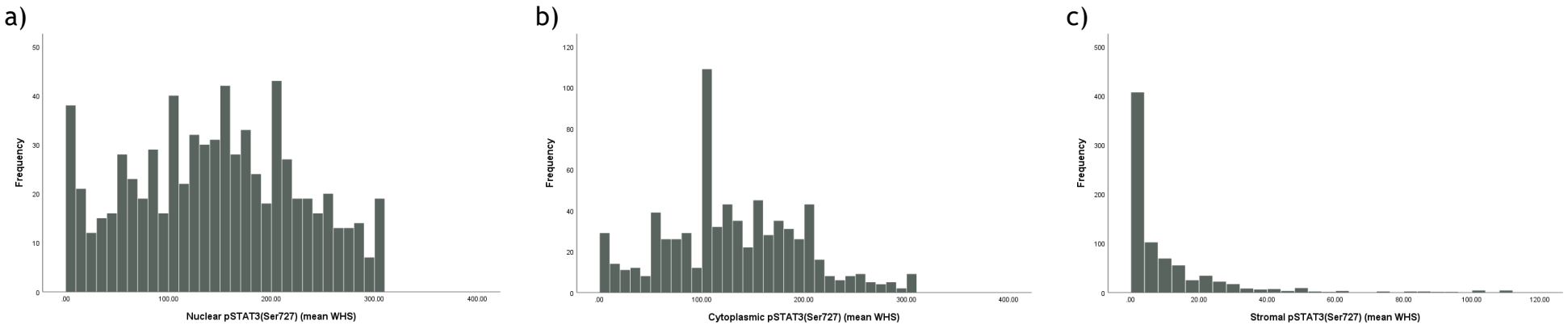

Figure 9-34. Expression of pSTAT3(Ser727). Histograms to illustrate the expression of pSTAT3(ser727) in a) tumour cell nuclei, b) tumour cytoplasm and c) stroma.

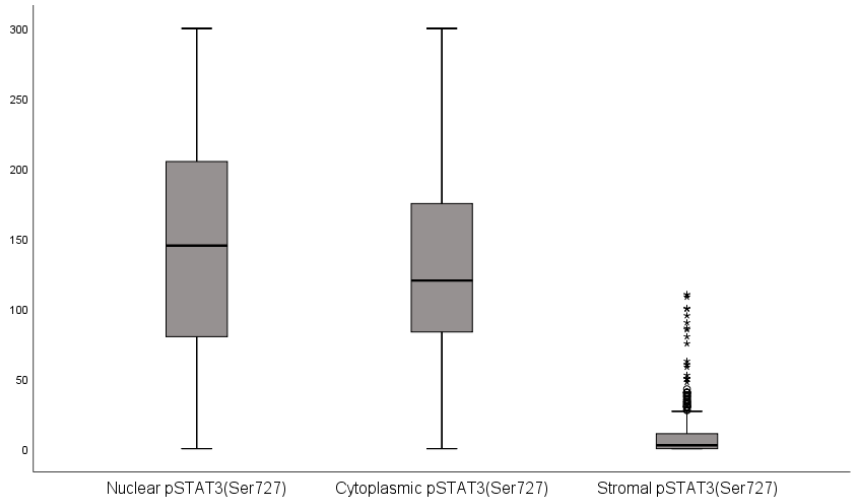

Figure 9-35. Boxplots of pSTAT3(Ser727) expression. Boxplots to compare the expression of pSTAT3(Ser727) in tumour nuclei, cytoplasm and in stroma.

Nuclear pSTAT3(Ser727) expression was higher in ER+ disease and, within the molecular subtypes, was highest in luminal A cancers and lowest in the HER2-enriched subtype (**Figure 9-36**).

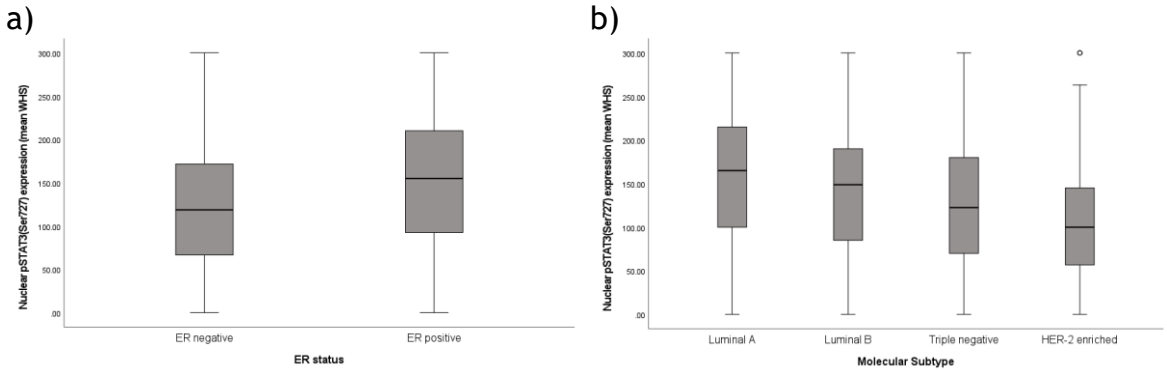

Figure 9-36. Boxplots of nuclear pSTAT3(Ser727) expression by receptor status. Boxplots to illustrate the differences in nuclear pSTAT3(Ser727) expression by a) ER status (**p<0.001**) and b) molecular subtype (**p<0.001**).

Similarly, cytoplasmic pSTAT3(Ser727) expression was higher in ER+ disease and, within the molecular subtypes, was highest in luminal A cancers and lowest in the HER2-enriched subtype (**Figure 9-37**).

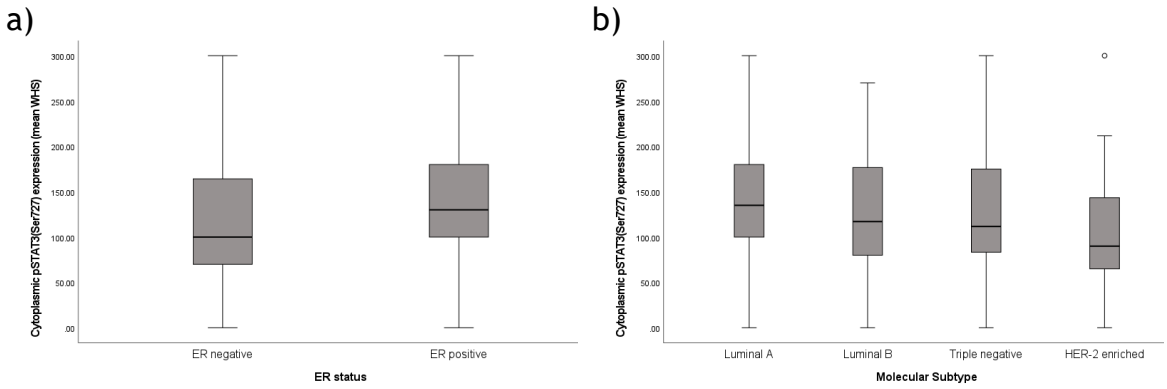

Figure 9-37. Boxplots of cytoplasmic pSTAT3(Ser727) by receptor status. Boxplots to illustrate the differences in cytoplasmic pSTAT3(Ser727) expression by a) ER status (**p<0.001**) and b) molecular subtype (**p<0.001**).

Stromal pSTAT3(Ser727) expression was higher in the ER negative subtypes (**Figure 9-38**).

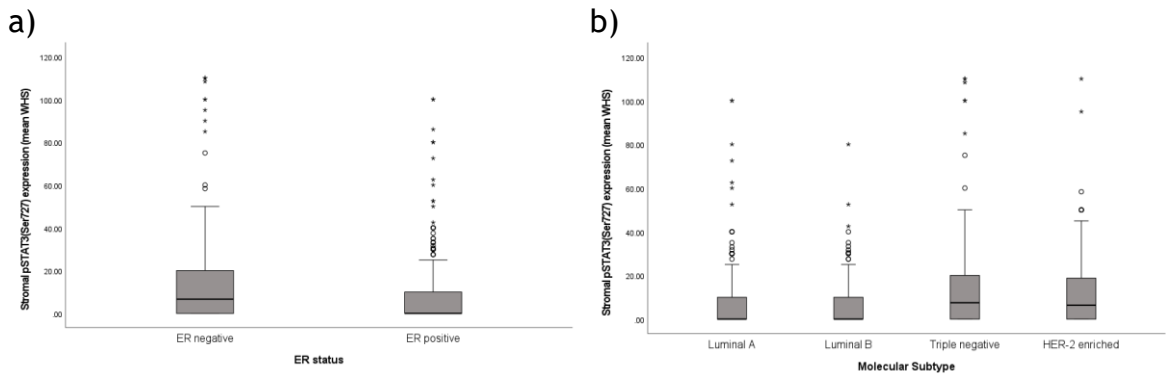

Figure 9-38. Boxplots of stromal pSTAT3(ser727) by receptor status. Boxplots to illustrate the differences in stromal pSTAT3(Ser727) expression by a) ER status (**p<0.001**) and b) molecular subtype (**p<0.001**).

There was a strong positive correlation between nuclear and cytoplasmic pSTAT3(Ser727) expression and a weak positive correlation between each of the tumour cell expression sites and stromal expression (**Figure 9-39**)

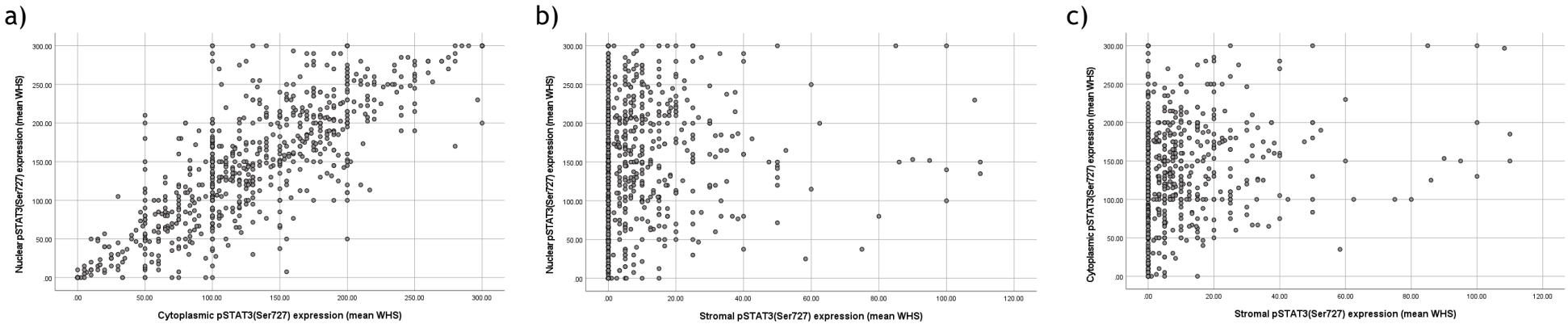

Figure 9-39. Correlation between pSTAT3(Ser727) expression sites. Scatter plots to illustrate the correlation between pSTAT3(Ser727) expression in different sites: a) nuclear and cytoplasmic expression (Pearson correlation 0.810, **p<0.001**), b) nuclear and stromal expression (Pearson correlation 0.142, **p<0.001**), c) cytoplasmic and stromal expression (Pearson correlation 0.239, **p<0.001**).

9.3.11 The relationship between pSTAT3(Ser727) and CSS

ROC curves were constructed to determine thresholds for division into high and low expression groups for further analysis (**Figure 9-40**). From these, thresholds of mean WHS 181.25 for nuclear, 128.75 for cytoplasmic and 0.50 for stromal pSTAT3(Ser727) expression were derived.

a)

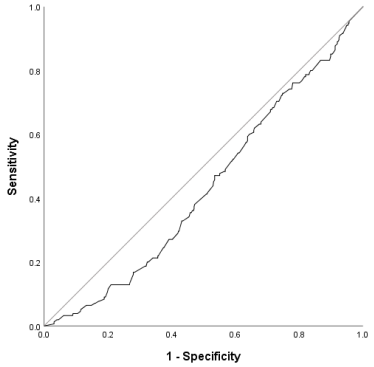

b)

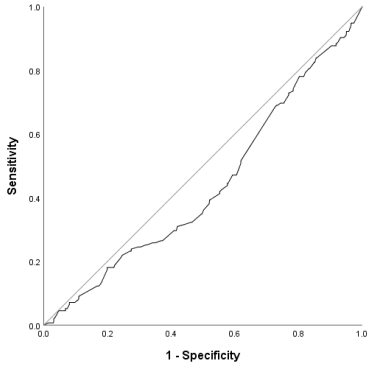

c)

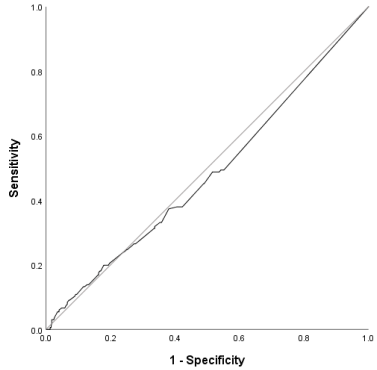

Figure 9-40. ROC curves for pSTAT3(Ser727) expression and CSS. . ROC curves to illustrate the relationship between pSTAT3(Ser727) and CSS in a) tumour cell nuclei (AUC 0.432), b) tumour cell cytoplasm (AUC 0.438) and c) stromal cells (AUC 0.481).

9.3.11.1 Nuclear pSTAT3(Ser727) expression and CSS

242 (33.3%) patients had high (mean WHS>181.25) nuclear pSTAT3(Ser727) expression. High nuclear pSTAT3(Ser727) expression was associated with improved CSS in the full cohort (high v low: HR 0.55, 95% CI 0.38-0.81, p=0.002) and in ER positive (HR 0.56, 95% CI 0.35-0.90, p=0.016) but not ER negative disease (**Figure 9-41**). When analysed within the molecular subtypes, the same was true in luminal A cancers (HR 0.48, 95% CI 0.24-0.95, p=0.036) but not in the other molecular subtypes (**Figure 9-42**).

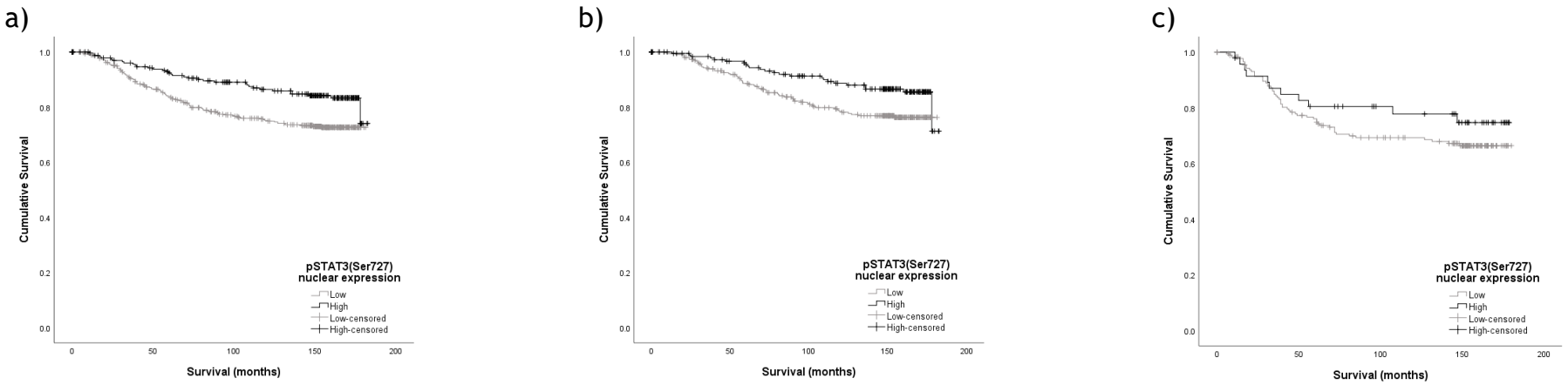

Figure 9-41. The relationship between nuclear pSTAT3(Ser727) expression and CSS. Kaplan meier graphs to illustrate the relationship between nuclear pSTAT3(Ser727) expression in tumour cells and CSS in a) the full cohort (n=727, **p=0.002**), b) ER positive disease (n=499, **p=0.014**) and c) ER negative disease (n=228, p=0.285).

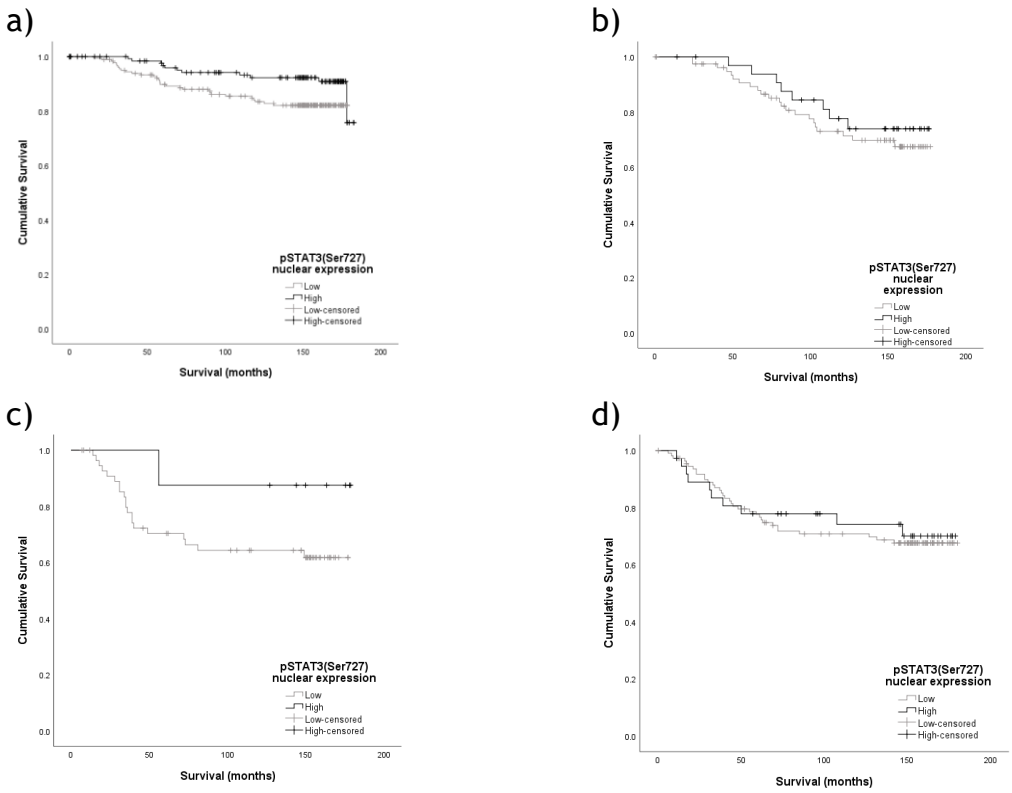

Figure 9-42. The relationship between nuclear pSTAT3(Ser727) expression and CSS by molecular subtype. Kaplan meier graphs to illustrate the relationship between nuclear pSTAT3(Ser727) expression and CSS in a) luminal A (n=323, **p=0.032**), b) Luminal B (n=114, p=0.502), c) HER2-enriched (n=65, p=0.178) and d) triple negative (n=150, p=0.750) breast cancer.

On multivariate analysis, controlling for other known prognostic factors in each subtype, it was only in luminal A disease that nuclear pSTAT3(Ser727) expression was independently associated with CSS (HR 0.38, 95% CI 0.17-0.85, p=0.018) (**Table 9-4**).

Factor	HR (95% CI)	p
Tumour size		**0.010**
≤20mm	1	
21-49mm	1.75 (0.83-3.65)	0.139
≥50mm	5.08 (1.77-14.61)	**0.003**
Tumour grade		**0.007**
I	1	
II	1.25 (0.50-3.15)	0.635
III	3.79 (1.36-10.56)	**0.011**
Nodal status		**0.015**
Negative	1	
Positive	2.34 (1.18-4.65)	
Necrosis		0.509
<25%		
>25%		
TSP		**0.015**
<50%	1	
>50%	2.39 (1.86-4.82)	
Nuclear pSTAT3(Ser727) expression		**0.018**
Low	1	
High	0.38 (0.17-0.85)	

Table 9-4. Multivariate analysis for nuclear pSTAT3(Ser727) in luminal A disease. Table detailing the relationship with CSS of nuclear pSTAT3(Ser727) in luminal A disease when controlling for other known prognostic factors. Factors with p<0.05 on univariate analysis were entered into the equation.

9.3.11.2 Cytoplasmic pSTAT3(Ser727) expression and CSS

337 (46.4%) patients had high (mean WHS>128.75) cytoplasmic pSTAT3(Ser727) expression. Low cytoplasmic pSTAT3(Ser727) expression was associated with worse CSS in the full cohort (high v low: HR 0.58, 95% CI 0.41-0.80, p=0.001), ER positive (HR 0.47, 95% CI 0.31-0.74, p=0.001) and specifically luminal A (HR 0.48, 95% CI 0.26-0.92, p=0.026) cancers (**Figure 9-43, Figure 9-44**).

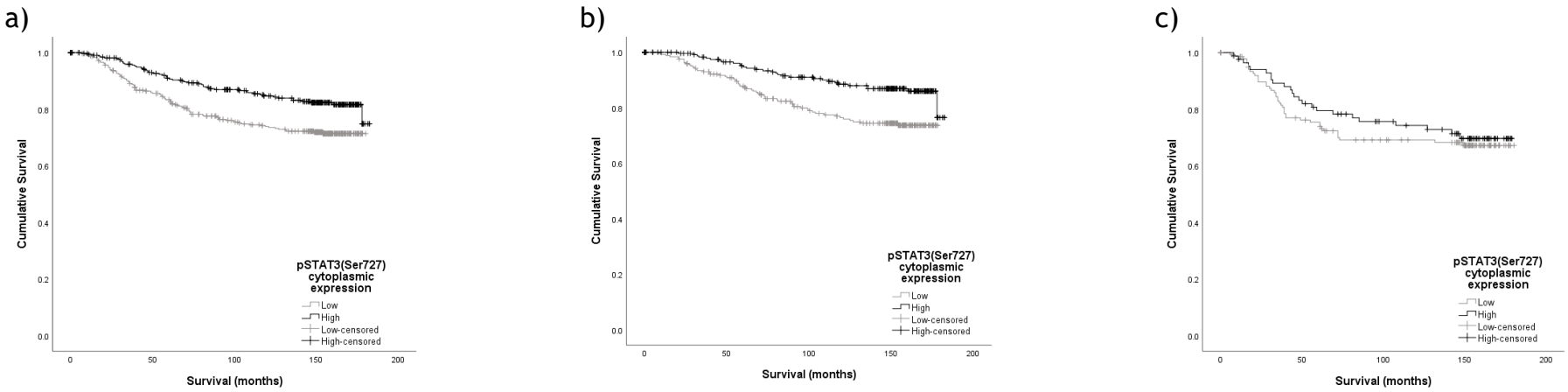

Figure 9-43. The relationship between cytoplasmic pSTAT3(Ser727) expression and CSS. Kaplan meier graphs to illustrate the relationship between cytoplasmic pSTAT3(Ser727) expression in tumour cells and CSS in a) the full cohort (n=727, **p=0.001**), b) ER positive disease (n=499**, p=0.001**) and c) ER negative disease (n=228, p=0.532).

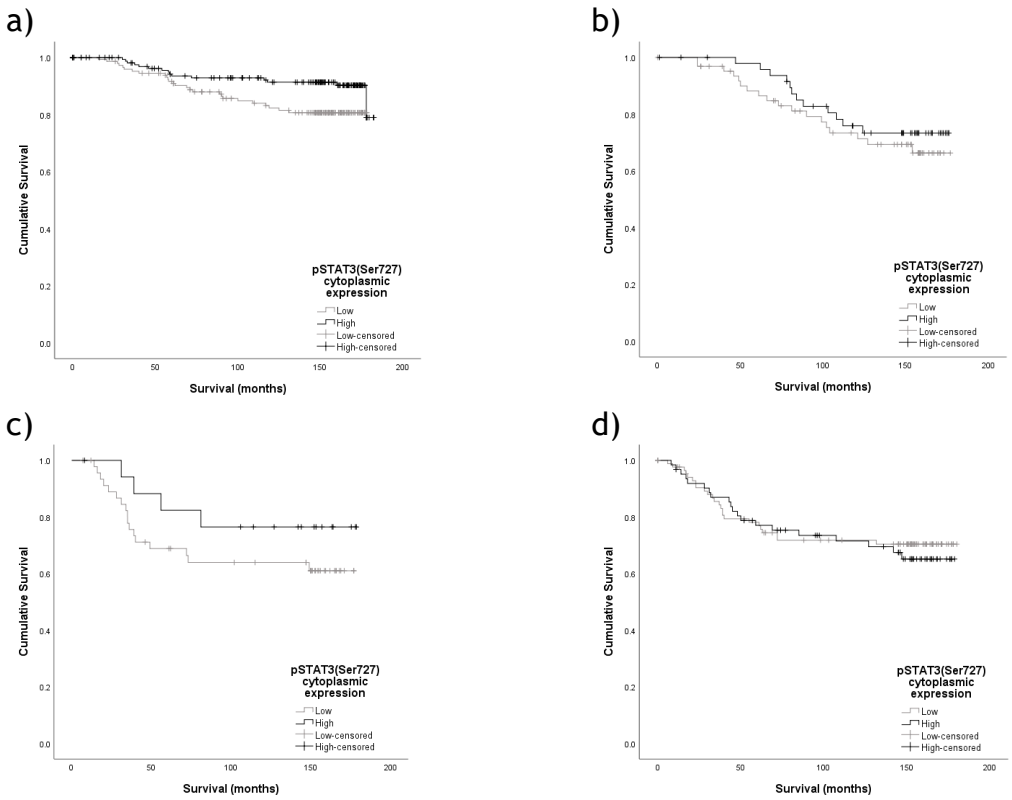

Figure 9-44. The relationship between cytoplasmic pSTAT3(Ser727) expression and CSS by molecular subtype. Kaplan meier graphs to illustrate the relationship between cytoplasmic pSTAT3(Ser727) expression and CSS in a) luminal A (n=323, **p=0.023**), b) Luminal B (n=114, p=0.443), c) HER2-enriched (n=65, p=0.246) and d) triple negative (n=150, p=0.705) breast cancer.

On multivariate analysis, controlling for other known prognostic factors in each subtype, it was only in luminal A disease that cytoplasmic pSTAT3(Ser727) expression was independently associated with CSS (HR 0.37, 95% CI 0.18-0.76, p=0.007) (**Table 9-5**).

Factor	HR (95% CI)	p
Tumour size		**0.007**
≤20mm	1	
21-49mm	1.95 (0.94-4.04)	0.074
≥50mm	5.22 (1.86-14.65_	**0.002**
Tumour grade		**0.008**
I	1	
II	1.22 (0.48-3.08)	0.680
III	3.63 (1.31-10.08)	**0.013**
Nodal status		**0.009**
Negative	1	
Positive	2.49 (1.26-4.94)	
Necrosis		0.524
<25%		
>25%		
TSP		**0.020**
<50%	1	
>50%	2.23 (1.14-4.39)	
Cytoplasmic pSTAT3(Ser727) expression		**0.007**
Low	1	
High	0.37 (0.18-0.76)	

Table 9-5. Multivariate analysis for cytoplasmic pSTAT3(Ser727) in luminal A disease. Table detailing the relationship with CSS of cytoplasmic pSTAT3(Ser727) in luminal A disease when controlling for other known prognostic factors. Factors with p<0.05 on univariate analysis were entered into the equation.

9.3.11.3 Stromal pSTAT3(Ser727) expression and CSS

424 (53.9%) patients had high (mean WHS>0.50) stromal pSTAT3(Ser727) expression. There was no significant association between stromal pSTAT3(Ser727) expression in the full cohort or in ER positive disease but in ER negative disease, low expression was associated with worse CSS (high v low: HR 0.61, 95% CI 0.38-0.97, p=0.037) (**Figure 9-45**). There was no significant association observed within any of the molecular subtypes though there was a trend towards worse CSS in patients with low pSTAT3(Ser727) expression in the HER2-enriched cohort of 68 patients (HR 0.44, 95% CI 0.19-1.03, p=0.059) (**Figure 9-46**). The association in ER negative disease was not independent of other known prognostic factors (p=0.171, data not shown).

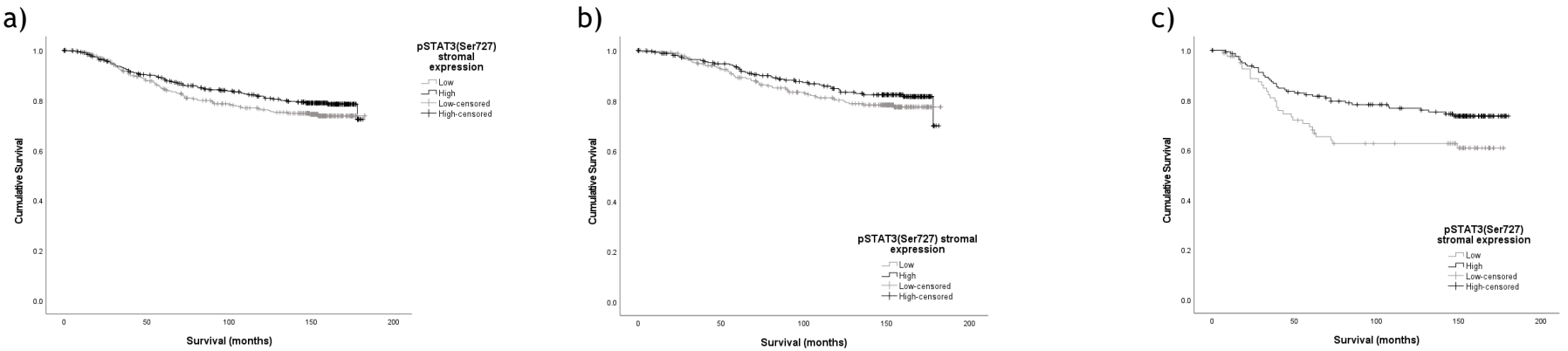

Figure 9-45. The relationship between stromal pSTAT3(Ser727) expression and CSS. Kaplan meier graphs to illustrate the relationship between stromal pSTAT3(Ser727) expression in tumour cells and CSS in a) the full cohort (n=786, p=0.141), b) ER positive disease (n=538, p=0.265) and c) ER negative disease (n=247, **p=0.035**).

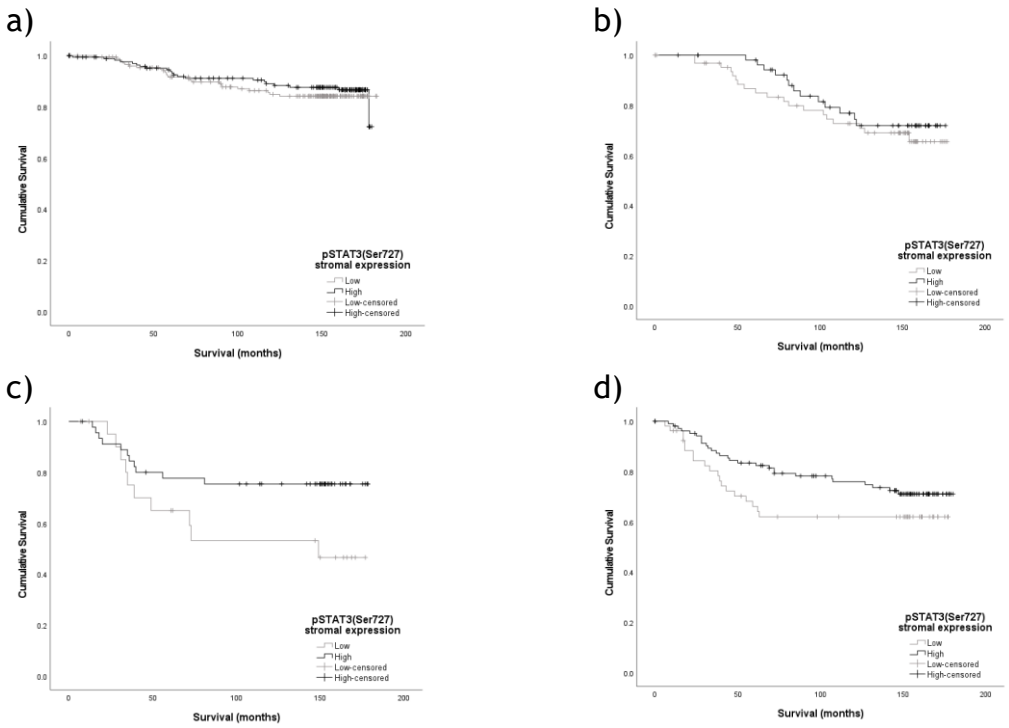

Figure 9-46. The relationship between stromal pSTAT3(Ser727) expression and CSS by molecular subtype. Kaplan meier graphs to illustrate the relationship between stromal pSTAT3(Ser727) expression and CSS in a) luminal A (n=353, p=0.541), b) Luminal B (n=120, p=0.450), c) HER2-enriched (n=68, p=0.051) and d) triple negative (n=160, p=0.134) breast cancer.

9.3.12 Associations between pSTAT3(Ser727) expression and clinicopathological characteristics

High nuclear pSTAT3(Ser727) expression was associated with smaller cancers (p<0.001), lower tumour grade (p<0.001), ER positivity (p<0.001), HER2 negativity (p<0.001), low necrosis (p<0.001), low KM score (p<0.001), low CD8+ lymphocytes (p=0.004) and high budding (p=0.032) (**Table 9-6**).

High cytoplasmic pSTAT3(Ser727) expression was associated with smaller tumours (p=0.011), lower grade (p<0.001), ER positivity (p=0.001), HER2 negativity (p=0.001) and low necrosis (p<0.001) (**Table 9-6**).

	Nuclear pSTAT3(Ser727) expression		p	Cytoplasmic pSTAT3(Ser727) expression		p
	Low n(%)	**High** n(%)		**Low** n(%)	**High** n(%)	
Age			0.830			0.310
≤50yrs	142 (29.3)	69 (28.5)		107 (27.4)	104 (30.9)	
>50yrs	343 (70.7)	173 (71.5)		283 (72.6)	233 (69.1)	
Type			0.078			0.209
Ductal	436 (89.9)	206 (85.1)		352 (90.3)	290 (86.1)	
Lobular	25 (5.2)	23 (9.5)		21 (5.4)	27 (8.0)	
Other	24 (4.9)	13 (5.4)		17 (4.4)	20 (5.9)	
Size			**<0.001**			**0.011**
≤20mm	244 (50.4)	174 (71.9)		204 (52.4)	214 (63.5)	
21-49mm	214 (44.2)	61 (25.2)		165 (42.4)	110 (32.6)	
≥50mm	26 (5.4)	7 (2.9)		20 (5.1)	13 (3.9)	
Grade			**<0.001**			**<0.001**
I	63 (13.0)	67 (27.8)		48 (12.3)	82 (24.5)	
II	212 (43.8)	109 (45.2)		174 (44.6)	147 (43.9)	
III	209 (43.2)	65 (27.0)		168 (43.1)	106 (31.6)	
Nodal status			0.242			0.112
Negative	271 (56.3)	145 (60.9)		214 (55.2)	202 (61.0)	
Positive	210 (43.7)	93 (39.1)		174 (44.8)	129 (39.0)	
ER status			**<0.001**			**0.001**
Negative	181 (37.3)	47 (19.4)		143 (36.7)	85 (25.2)	
Positive	304 (62.7)	195 (80.6)		247 (63.3)	252 (74.8)	
HER2 status			**<0.001**			**0.001**
Negative	384 (79.7)	218 (91.2)		306 (79.1)	296 (88.6)	
Positive	98 (20.3)	21 (8.8)		81 (20.9)	38 (11.4)	
Necrosis			**<0.001**			**<0.001**
<25%	209 (44.5)	158 (66.9)		173 (45.5)	194 (59.5)	
>25%	261 (55.5)	78 (33.1)		207 (54.5)	132 (40.5)	
KM score			**<0.001**			0.242
0	61 (13.0)	50 (21.1)		55 (14.5)	56 (17.1)	
1	216 (46.1)	147 (62.0)		187 (49.3)	176 (53.8)	
2	144 (30.7)	30 (12.7)		102 (26.9)	72 (22.0)	
3	48 (10.2)	10 (4.2)		35 (9.2)	23 (7.0)	
CD8+ lymphocytes			**0.004**			0.709
Low	57 (27.1)	43 (36.8)		55 (31.6)	45 (29.4)	
Medium	64 (30.5)	46 (39.3)		55 (31.6)	55 (35.9)	
High	89 (42.4)	28 (23.9)		64 (36.8)	53 (34.6)	
CD4+ lymphocytes			0.154			0.740
Low	133 (31.0)	70 (36.1)		113 (33.6)	90 (31.4)	
Medium	141 (32.9)	69 (35.6)		109 (32.4)	101 (35.2)	
High	155 (36.1)	55 (28.4)		114 (33.9)	96 (33.4)	
TSP			0.091			0.539
Low	348 (73.6)	160 (67.5)		277 (72.5)	231 (70.4)	
High	125 (26.4)	77 (32.5)		105 (27.5)	97 (29.6)	
Budding			**0.032**			0.138
≤20 buds	333 (70.4)	148 (62.4)		268 (70.2)	213 (64.9)	
>20 buds	140 (29.6)	89 (37.6)		114 (29.8)	115 (35.1)	

Table 9-6. The association between nuclear and cytoplasmic pSTAT3(Ser727) expression and clinicopathological characteristics. Table detailing the associations between nuclear and cytoplasmic pSTAT3(Ser727) expression and clinicopathological characteristics. Significant p values are highlighted in bold.

High stromal pSTAT3(Ser727) expression was associated with high KM score (p=0.037) and high CD4+ lymphocytes (p<0.001) (**Table 9-7**).

	Stromal pSTAT3(Ser727) expression		p
	Low n(%)	**High** n(%)	
Age			0.315
≤50yrs	28 (33.3)	65 (39.9)	
>50yrs	56 (66.7)	98 (60.1)	
Type			0.199
Ductal	78 (92.9)	154 (94.5)	
Lobular	3 (3.6)	1 (0.6)	
Other	3 (3.6)	8 (4.9)	
Size			0.371
≤20mm	42 (50.6)	81 (49.7)	
21-49mm	34 (41.0)	75 (46.0)	
≥50mm	7 (8.4)	7 (4.3)	
Grade			0.802
I	3 (3.6)	7 (4.3)	
II	22 (26.5)	37 (22.8)	
III	58 (69.9)	118 (72.8)	
Nodal status			0.105
Negative	37 (44.0)	89 (54.9)	
Positive	47 (56.0)	73 (45.1)	
HER2 status			0.841
Negative	57 (71.3)	112 (70.0)	
Positive	23 (28.7)	48 (30.0)	
Necrosis			0.618
<25%	22 (26.5)	38 (23.6)	
>25%	61 (73.5)	123 (76.4)	
KM score			**0.037**
0	4 (4.9)	3 (1.9)	
1	42 (51.2)	59 (36.6)	
2	30 (36.6)	74 (46.0)	
3	6 (7.3)	25 (15.5)	
CD8+ lymphocytes			0.365
Low	11 (26.8)	22 (24.2)	
Medium	13 (31.7)	20 (22.0)	
High	17 (41.5)	49 (53.8)	
CD4+ lymphocytes			**<0.001**
Low	17 (23.6)	18 (12.8)	
Medium	32 (44.4)	34 (24.1)	
High	23 (31.9)	89 (63.1)	
TSP			0.128
Low	63 (75.9)	107 (66.5)	
High	20 (24.1)	54 (33.5)	
Budding			0.330
≤20 buds	62 (74.7)	129 (80.1)	
>20 buds	21 (25.3)	32 (19.9)	

Table 9-7. The association between stromal pSTAT3(Ser727) expression and clinicoplathological characteristics in ER negative disease. Table detailing the associations between stromal pSTAT3(Ser727) expression and clinicopathological characteristics in ER negative breast cancer. Statistically significant p values are highlighted in bold.

9.3.13 Associations between STAT3 and CSS in different disease stages

To investigate whether there was any evidence for a different role for STAT3 at different stages of disease, the associations between the different forms and tumour cell expression sites of STAT3 and CSS in the different T and N stages were analysed.

9.3.13.1 Associations between STAT3 and CSS by tumour stage

In T1 breast cancers, high nuclear and cytoplasmic pSTAT3(Ser727) expression were associated with improved CSS (nuclear: HR 0.51, 95% CI 0.28-0.90, p=0.020; cytoplasmic: HR 0.60, 95% CI 0.35-1.01, p=0.052). High nuclear tSTAT3 expression was also associated with improved CSS (HR 0.47, 95% CI 0.24-0.93, p=0.030) (**Figure 9-47**). There was no significant relationship between nuclear and cytoplasmic pSTAT3(Tyr705) or cytoplasmic tSTAT3 expression and CSS (data not shown).

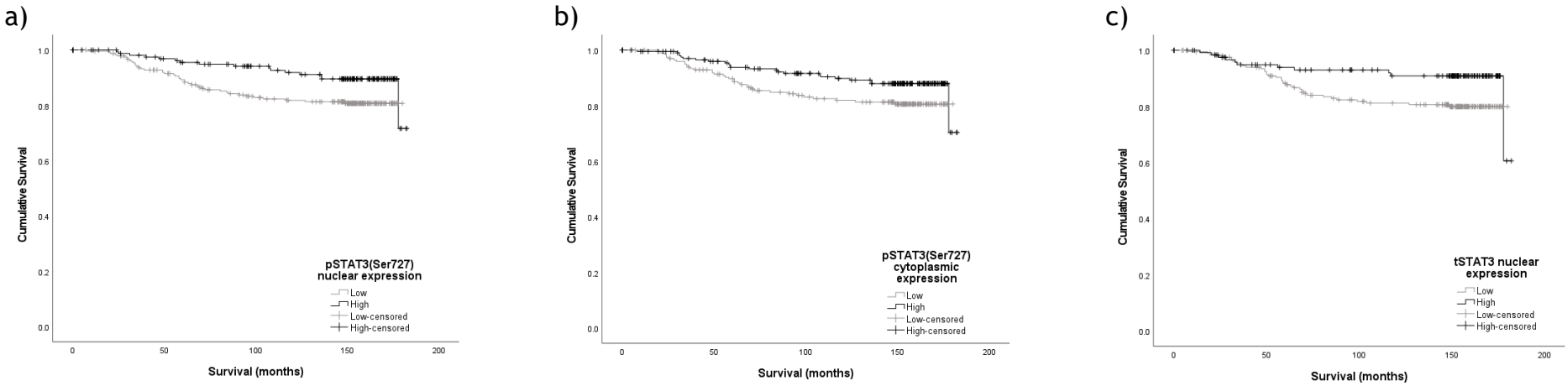

Figure 9-47. Association between STAT3 and CSS in T1 breast cancer. Kaplan meier graphs illustrating the relationship between CSS and a) nuclear pSTAT3(Ser727) expression (**p=0.018**), b) cytoplasmic pSTAT3(Ser727) expression (**p=0.049**) and c) nuclear tSTAT3 expression (**p=0.026**).

In T2 breast cancers, high nuclear pSTAT3(Tyr705) expression was associated with improved CSS (HR 0.64, 95% CI 0.40-1.01, p=0.053) (**Figure 9-48**) and was the only STAT3 form and expression site significantly associated with CSS.

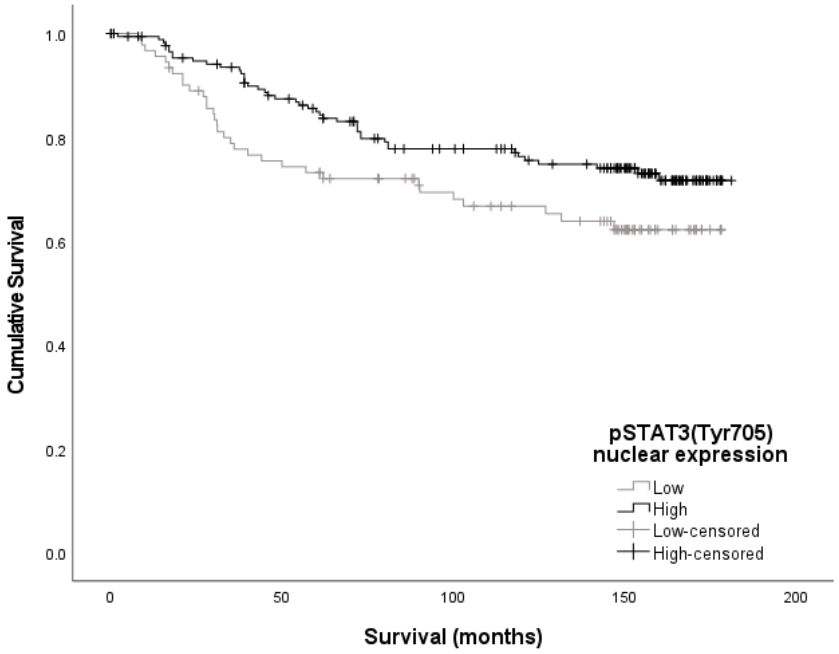

Figure 9-48. Association between nuclear pSTAT3(Tyr705) expression and CSS in T2 breast cancer. Kaplan meier graph to illustrate the relationship between pSTAT3(Tyr705) expression and CSS in T2 breast cancer (**p=0.050**).

In T3 breast cancers, high cytoplasmic tSTAT3 expression was associated with poorer CSS (HR 3.12, 95% CI 1.07-9.06, p=0.037) (**Figure 9-49**) and was the only STAT3 form and expression site significantly associated with CSS in this cohort.

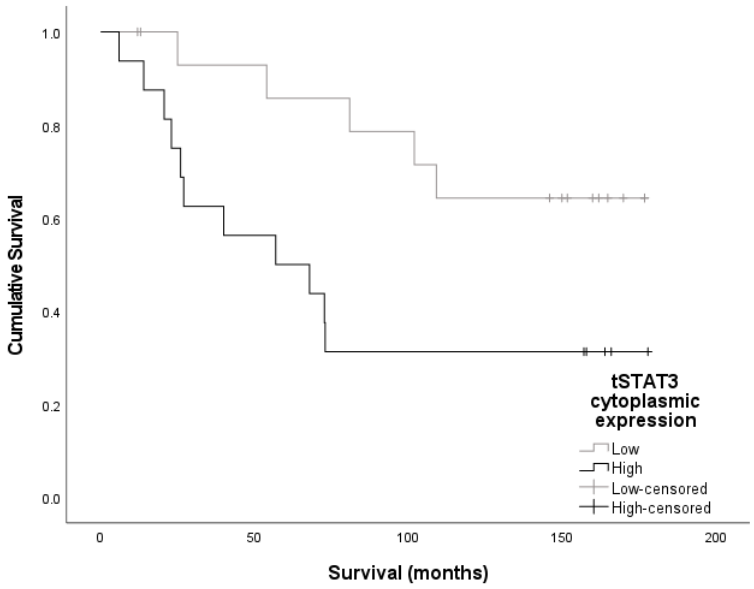

Figure 9-49. Association between cytoplasmic tSTAT3 and CSS in T3 breast cancer. Kaplan meier graph to illustrate the relationship between cytoplasmic tSTAT3 expression and CSS in T3 breast cancer (**p=0.028**).

9.3.13.2 Associations between STAT3 and CSS by nodal stage

In node negative disease, none of the STAT3 forms and expression sites was significantly associated with CSS (data not shown).

In node positive disease both high nuclear and cytoplasmic pSTAT3(Ser727) expression were associated with improved CSS (nuclear: HR 0.52, 95% CI 0.32-0.85, p=0.008; cytoplasmic: HR 0.59, 95% CI 0.39-0.88, p=0.011). High nuclear pSTAT3(Tyr705) (HR 0.59, 95% CI 0.40-0.87, p=0.007) and tSTAT3 expression (HR 0.64, 95% CI 0.41-1.00, p=0.048) were also associated with improved CSS in this cohort (**Figure 9-50**).

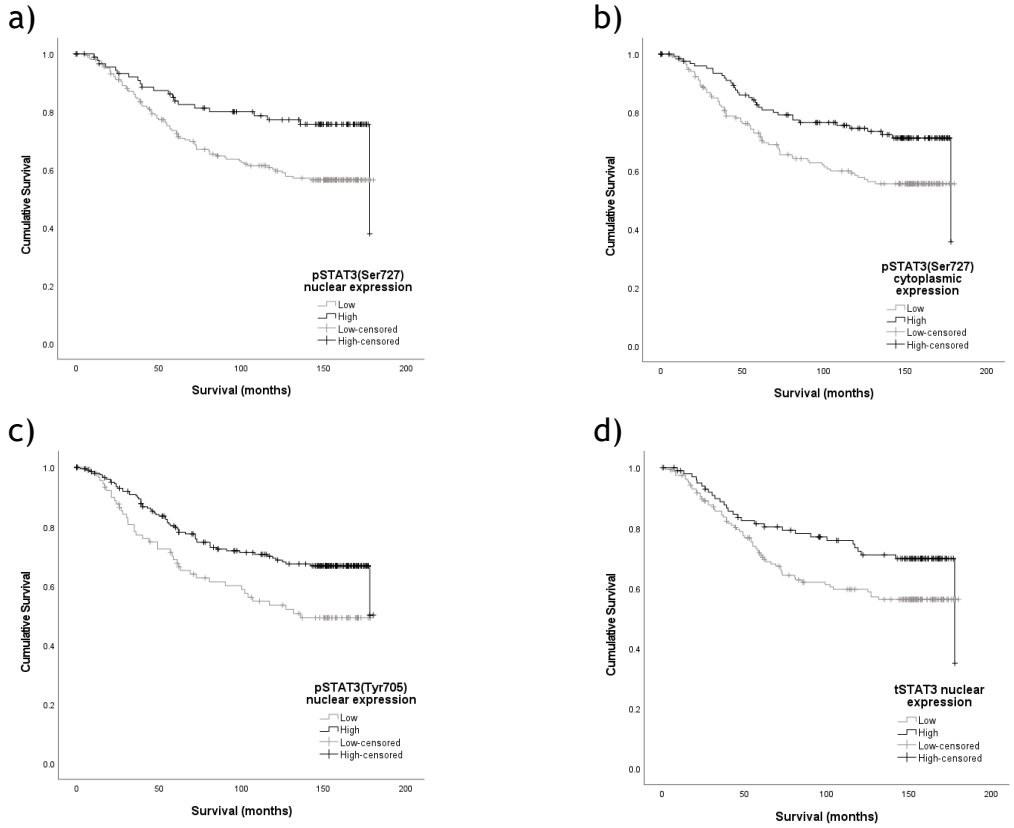

Figure 9-50. Associations between STAT3 and CSS in node positive disease. Kaplan meier graphs illustrating the relationships between CSS and a) nuclear pSTAT3(Ser727) expression (**p=0.007**), b) cytoplasmic pSTAT3(Ser727) expression (**p=0.010**), c) nuclear pSTAT3(Tyr705) expression (**p=0.007**) and d) nuclear tSTAT3 expression (**p=0.046**).

9.3.15 The relationship between pSTAT3(Tyr705), pSTAT3(Ser727) and tSTAT3

The relationship between pSTAT3(Tyr705), pSTAT3(Ser727) and tSTAT3 expression was evaluated using association analysis.

High nuclear pSTAT3(Tyr705) expression was associated with high nuclear ($p<0.001$), cytoplasmic ($p<0.001$) and stromal ($p=0.007$) pSTAT3(Ser727) expression and with high nuclear tSTAT3 expression ($p<0.001$) (**Table 9-8**).

High cytoplasmic pSTAT3(Tyr705) expression was associated with high nuclear ($p=0.010$), cytoplasmic ($p=0.020$) and stromal ($p=0.027$) tSTAT3 expression and with high cytoplasmic pSTAT3(Ser727) expression ($p<0.001$) (**Table 9-8**).

High stromal pSTAT3(Tyr705) expression was associated with high stromal pSTAT3(Ser727) expression ($p<0.001$) (**Table 9-8**).

	Nuclear pSTAT3(Tyr705) expression		p	Cytoplasmic pSTAT3(Tyr705) expression		p	Stromal pSTAT3(Tyr705) expression		p
	Low	High		Low	High		Low	High	
Nuclear pSTAT3(Ser727)			**<0.001**			0.247			0.906
Low	173 (82.0)	292 (62.8)		178 (71.5)	287 (67.2)		245 (67.9)	230 (67.4)	
High	38 (18.0)	173 (37.2)		71 (28.5)	140 (32.8)		116 (32.1)	111 (32.6)	
Cytoplasmic pSTAT3(Ser727)			**<0.001**			**<0.001**			0.080
Low	160 (75.8)	211 (45.4)		173 (69.5)	198 (46.4)		208 (57.6)	174 (51.0)	
High	51 (24.2)	254 (54.6)		76 (30.5)	229 (53.6)		153 (42.4)	167 (49.0)	
Stromal pSTAT3(Ser727)			**0.007**			0.284			**<0.001**
Low	120 (55.0)	211 (44.0)		133 (50.0)	198 (45.8)		200 (52.6)	149 (39.8)	
High	98 (45.0)	269 (56.0)		133 (50.0)	234 (54.2)		180 (47.4)	225 (60.2)	
Nuclear tSTAT3			**<0.001**			**0.010**			0.916
Low	115 (71.0)	219 (54.9)		126 (67.0)	208 (55.8)		169 (59.5)	181 (59.9)	
High	47 (29.0)	180 (45.1)		62 (33.0)	165 (44.2)		115 (40.5)	121 (40.1)	
Cytoplasmic tSTAT3			0.756			**0.020**			0.066
Low	109 (67.3)	263 (65.9)		137 (72.9)	235 (63.0)		180 (63.4)	213 (70.5)	
High	53 (32.7)	136 (34.1)		51 (27.1)	138 (37.0)		104 (36.6)	89 (29.5)	
Stromal tSTAT3			0.693			**0.027**			0.417
Low	57 (38.5)	136 (36.7)		75 (43.9)	118 (33.9)		95 (36.3)	111 (39.6)	
High	91 (61.5)	235 (63.3)		96 (56.1)	230 (66.1)		167 (63.7)	169 (60.4)	

Table 9-8. The association between pSTAT3(Tyr705) expression and the other STAT3 forms. Table detailing the associations between pSTAT3(Tyr705), pSTAT3(Ser727) and tSTAT3 in their different expression sites. Statistically significant p values are highlighted in bold.

Correlation analysis was also carried out. There was a moderate positive correlation between nuclear pSTAT3(Tyr705) expression and both nuclear and cytoplasmic pSTAT3(Ser727) expression (**Figure 9-51**). Other combinations of sites and forms of STAT3 showed no or weak correlation so this data is not illustrated.

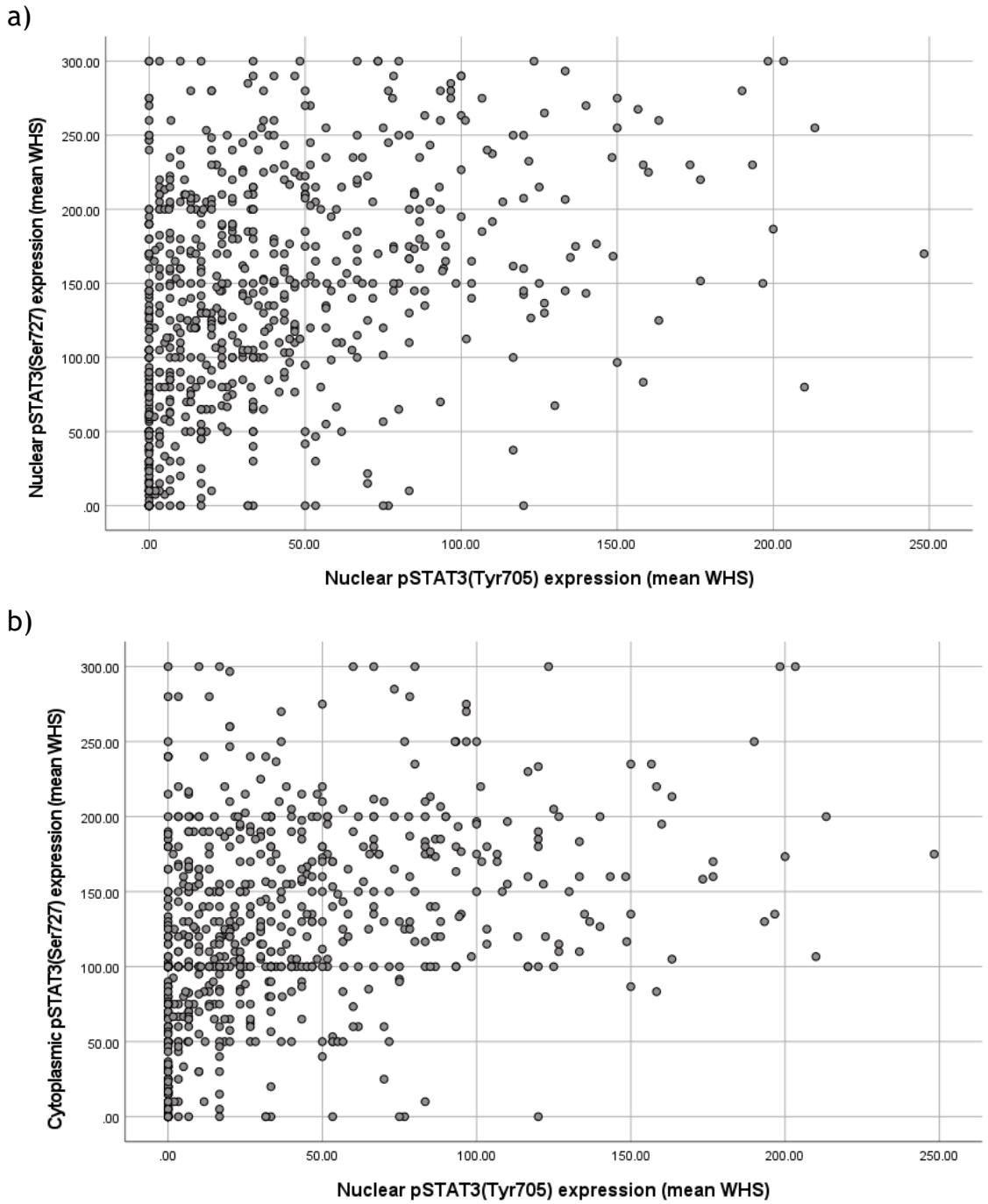

Figure 9-51. Correlation between nuclear pSTAT3(Tyr705) and pSTAT3(Ser727) expression. Scatter plots to illustrate the correlation between nuclear pSTAT3(Tyr705) expression and a) nuclear pSTAT3(Ser727) expression (Pearson correlation 0.377, **p<0.001**) and b) cytoplasmic pSTAT3(Ser727) expression (Pearson correlation 0.357, **p<0.001**).

High nuclear pSTAT3(Ser727) expression was associated with high nuclear tSTAT3 expression ($p<0.001$) (**Table 9-9**).

High cytoplasmic pSTAT3(Ser727) expression was associated with high nuclear ($p<0.001$) and cytoplasmic ($p=0.002$) tSTAT3 expression (**Table 9-9**).

High stromal pSTAT3(Ser727) expression was associated with high cytoplasmic tSTAT3 expression ($p<0.001$) (**Table 9-9**).

The association between pSTAT3(Ser727) and pSTAT3(Tyr705) expression has already been detailed above.

	Nuclear pSTAT3(Ser727) expression		p	Cytoplasmic pSTAT3(Ser727) expression		p	Stromal pSTAT3(Ser727) expression		p
	Low	High		Low	High		Low	High	
Nuclear tSTAT3			**<0.001**			**<0.001**			0.159
Low	258 (65.6)	71 (44.9)		210 (68.0)	119 (49.2)		168 (62.5)	174 (56.7)	
High	135 (34.4)	87 (55.1)		99 (32.0)	123 (50.8)		101 (37.5)	133 (43.3)	
Cytoplasmic tSTAT3			0.078			**0.002**			**<0.001**
Low	272 (69.2)	97 (61.4)		224 (72.5)	145 (59.9)		199 (74.0)	185 (60.3)	
High	121 (30.8)	61 (38.6)		85 (27.5)	97 (40.1)		70 (26.0)	122 (39.7)	
Stromal tSTAT3			0.465			0.352			0.494
Low	139 (38.4)	51 (34.9)		112 (39.2)	78 (35.1)		88 (36.2)	113 (39.1)	
High	223 (61.6)	95 (65.1)		174 (60.8)	144 (64.9)		155 (63.8)	176 (60.9)	

Table 9-9. The association between pSTAT3 (Ser727) and tSTAT3 expression. Table detailing the associations between pSTAT3(Ser727) and tSTAT3 expression in their different expression sites. Significant p values are highlighted in bold.

9.3.16 The relationship between pSTAT3(Tyr705), pSTAT3(Ser727) and tSTAT3 and other components of the IL6/JAK/STAT3 pathway

To evaluate the relationship between pSTAT3(Tyr705), pSTAT3(Ser727) and tSTAT3 expression and the other components of the IL6/JAK/STAT3 pathway studied so far in this thesis, association analysis was carried out.

9.3.16.1 Associations between tSTAT3 expression, IL6/IL6R and JAKs 1 and 2.

High nuclear tSTAT3 expression was associated with high nuclear JAK2 expression (p=0.002) (**Table 9-10**).

High cytoplasmic tSTAT3 expression was associated with the highest and lowest tertiles of stromal IL6 expression (p<0.001), high cytoplasmic (p<0.001) and stromal IL6R (p=0.020), and high cytoplasmic JAK2 expression (p<0.001) (**Table 9-10**).

High stromal tSTAT3 expression was associated with high cytoplasmic (p=0.013) and stromal IL6R (p<0.001), high stromal JAK1 (p=0.039) and high cytoplasmic (p=0.004) and stromal JAK2 (p<0.001) (**Table 9-10**).

	Nuclear expression		p	Cytoplasmic expression		p	Stromal expression		p
	Low	High		Low	High		Low	High	
Tumour IL6/HK			0.318			0.625			0.552
Low	186 (64.1)	139 (68.5)		218 (66.7)	107 (64.5)		122 (65.2)	182 (67.9)	
High	104 (35.9)	64 (31.5)		109 (33.3)	59 (35.5)		65 (34.8)	86 (32.1)	
Stromal IL6/HK			0.273			**<0.001**			0.232
Low	96 (32.9)	63 (31.0)		94 (28.6)	65 (39.2)		55 (29.3)	93 (34.6)	
Medium	105 (36.0)	63 (31.0)		131 (39.8)	37 (22.3)		72 (38.3)	83 (30.9)	
High	91 (31.2)	77 (37.9)		104 (31.6)	64 (38.6)		61 (32.4)	93 (34.6)	
Cytoplasmic IL6R			0.904			**<0.001**			**0.013**
Low	159 (47.9)	107 (48.4)		199 (55.0)	67 (35.1)		105 (54.1)	137 (42.8)	
High	173 (52.1)	114 (51.6)		163 (45.0)	124 (64.9)		89 (45.9)	183 (57.2)	
Membranous IL6R			0.417			0.759			0.073
Low	282 (84.9)	182 (82.4)		305 (84.3)	159 (83.2)		155 (79.9)	275 (85.9)	
High	50 (15.1)	39 (17.6)		57 (15.7)	32 (16.8)		39 (20.1)	45 (14.1)	
Stromal IL6R			0.569			**0.020**			**<0.001**
Low	221 (69.5)	141 (67.1)		249 (72.0)	113 (62.1)		161 (86.6)	179 (57.7)	
High	97 (30.5)	69 (32.9)		97 (28.0)	69 (37.9)		25 (13.4)	131 (42.3)	
Nuclear JAK1			0.574			0.208			0.540
Low	138 (50.2)	85 (47.5)		140 (47.0)	83 (53.2)		69 (47.6)	139 (50.7)	
High	137 (49.8)	94 (52.5)		158 (53.0)	73 (46.8)		76 (52.4)	135 (49.3)	
Cytoplasmic JAK1			0.728			0.921			0.101
Low	126 (45.8)	85 (47.5)		139 (46.6)	72 (46.2)		73 (50.3)	115 (42.0)	
High	149 (54.2)	94 (52.5)		159 (53.4)	84 (53.8)		72 (49.7)	159 (58.0)	
Stromal JAK1			0.449			0.466			**0.039**
Low	63 (24.9)	36 (21.7)		61 (22.5)	38 (25.7)		39 (29.1)	51 (19.8)	
High	190 (75.1)	130 (78.3)		210 (77.5)	110 (74.3)		95 (70.9)	206 (80.2)	
Nuclear JAK2			**0.002**			0.518			0.517
Low	292 (89.3)	177 (79.7)		305 (84.7)	164 (86.8)		166 (84.7)	281 (86.7)	
High	35 (10.7)	45 (20.3)		55 (15.3)	25 (13.2)		30 (15.3)	43 (13.3)	
Cytoplasmic JAK2			0.197			**<0.001**			**0.004**
Low	154 (47.1)	117 (52.7)		199 (55.3)	72 (38.1)		113 (57.7)	145 (44.8)	
High	173 (52.9)	105 (47.3)		161 (44.7)	117 (61.9)		83 (42.3)	179 (55.2)	
Stromal JAK2			0.718			0.149			**<0.001**
Low	265 (85.8)	176 (84.6)		293 (86.9)	148 (82.2)		182 (97.3)	248 (78.5)	
High	44 (14.2)	32 (15.4)		44 (13.1)	32 (17.8)		5 (2.7)	68 (21.5)	

Table 9-10. The association between tSTAT3 and IL6/IL6R and JAK expression. Table detailing the associations between tSTAT3 expression in different sites and Il6, IL6R, JAK1 and JAK2 expression. Significant p values are highlighted in bold.

9.3.16.2 Associations between pSTAT3(Tyr705) expression, IL6/IL6R and JAKs 1 and 2

High nuclear pSTAT3(Tyr705) expression was associated with low tumour (p=0.005) and stromal IL6 (p=0.003), high nuclear JAK1 (p=0.028), low cytoplasmic (p=0.001) and stromal JAK2 (p=0.003) (**Table 9-11**).

High cytoplasmic pSTAT3(Tyr705) expression was associated with low tumour IL6 (p=0.035) and low cytoplasmic JAK2 (p=0.011) (**Table 9-11**).

High stromal pSTAT3(Tyr705) expression was associated with higher stromal IL6 (p=0.020), high membranous IL6R (p=0.006), low stromal JAK1 (p=0.034) and low cytoplasmic (p=0.033) and stromal JAK2 (p<0.001) (**Table 9-11**).

	Nuclear expression		p	Cytoplasmic expression		p	Stromal expression		p
	Low	High		Low	High		Low	High	
Tumour IL6/HK			**0.005**			**0.035**			0.713
Low	89 (59.3)	303 (71.6)		129 (62.9)	263 (71.5)		198 (66.4)	214 (65.0)	
High	61 (40.7)	120 (28.4)		76 (37.1)	105 (28.5)		100 (33.6)	115 (35.0)	
Stromal IL6/HK			**0.003**			0.681			**0.020**
Low	42 (28.2)	151 (35.7)		67 (32.7)	126 (34.3)		109 (36.5)	88 (26.6)	
Medium	46 (30.9)	161 (38.1)		79 (38.5)	128 (34.9)		96 (32.1)	133 (40.2)	
High	61 (40.9)	111 (26.2)		59 (28.8)	113 (30.8)		94 (31.4)	110 (33.2)	
Cytoplasmic IL6R			0.091			0.733			0.814
Low	80 (44.4)	229 (51.9)		112 (50.7)	197 (49.3)		165 (50.8)	160 (49.8)	
High	100 (55.6)	212 (48.1)		109 (49.3)	203 (50.7)		160 (49.2)	161 (50.2)	
Membranous IL6R			0.455			0.938			**0.006**
Low	147 (81.7)	371 (84.1)		184 (83.3)	334 (83.5)		285 (87.7)	256 (79.8)	
High	33 (18.3)	70 (15.9)		37 (16.7)	66 (16.5)		40 (12.3)	65 (20.2)	
Stromal IL6R			0.297			0.383			0.216
Low	114 (68.3)	307 (72.6)		153 (73.6)	268 (70.2)		222 (72.5)	208 (68.0)	
High	53 (31.7)	116 (27.4)		55 (26.4)	114 (29.8)		84 (27.5)	98 (32.0)	
Nuclear JAK1			**0.028**			0.315			0.239
Low	97 (58.1)	174 (47.8)		102 (54.0)	169 (49.4)		148 (49.3)	137 (54.4)	
High	70 (41.9)	190 (52.2)		87 (46.0)	173 (50.6)		152 (50.7)	115 (45.6)	
Cytoplasmic JAK1			0.073			0.160			0.504
Low	92 (55.1)	170 (46.7)		101 (53.4)	161 (47.1)		155 (51.7)	123 (48.8)	
High	75 (44.9)	194 (53.3)		88 (46.6)	181 (52.9)		145 (48.3)	129 (51.2)	
Stromal JAK1			0.171			0.988			**0.034**
Low	31 (20.0)	86 (25.7)		41 (23.8)	76 (23.9)		57 (20.4)	65 (28.5)	
High	124 (80.0)	249 (74.3)		131 (76.2)	242 (76.1)		222 (79.6)	163 (71.5)	
Nuclear JAK2			0.681			0.918			0.176
Low	130 (86.1)	315 (84.7)		140 (84.8)	305 (85.2)		211 (82.7)	252 (86.9)	
High	21 (13.9)	57 (15.3)		25 (15.2)	53 (14.8)		44 (17.3)	38 (13.1)	
Cytoplasmic JAK2			**0.001**			**0.011**			**0.033**
Low	56 (37.1)	199 (53.5)		67 (40.6)	188 (52.5)		113 (44.3)	155 (53.4)	
High	95 (62.9)	173 (46.5)		98 (59.4)	170 (47.5)		142 (55.7)	135 (46.6)	
Stromal JAK2			**0.003**			0.593			**<0.001**
Low	108 (76.6)	306 (87.4)		131 (85.6)	283 (83.7)		189 (79.1)	246 (90.1)	
High	33 (23.4)	44 (12.6)		22 (14.4)	55 (16.3)		50 (20.9)	27 (9.9)	

Table 9-11. The association between pSTAT3(Tyr705) and IL6/IL6R and JAK expression. Table detailing the associations between pSTAT3(Tyr705) expression in different sites and Il6, IL6R, JAK1 and JAK2 expression. Significant p values are highlighted in bold.

9.3.16.3 Associations between pSTAT3(Ser727) expression, IL6/IL6R and JAKs1 and 2.

High nuclear pSTAT3(Ser727) expression was associated with low cytoplasmic (p=0.037) and membranous IL6R (p=0.001) (**Table 9-12**).

High cytoplasmic pSTAT3(Ser727) expression was associated with high cytoplasmic JAK1 (p=0.033) and low stromal JAK2 expression (p=0.026) (**Table 9-12**).

High stromal pSTAT3(Ser727) expression was associated with low stromal IL6 (p=0.024), low nuclear (p=0.007) and high cytoplasmic JAK1 (p=0.044) and low nuclear (p=0.005) and stromal JAK2 (p=0.002) (**Table 9-12**).

	Nuclear expression		p	Cytoplasmic expression		p	Stromal expression		p
	Low	High		Low	High		Low	High	
Tumour IL6/HK			0.232			0.103			0.327
Low	254 (65.6)	130 (70.7)		196 (64.3)	188 (70.7)		188 (67.6)	210 (63.8)	
High	133 (34.4)	54 (29.3)		109 (35.7)	78 (29.3)		90 (32.4)	119 (36.2)	
Stromal IL6/HK			0.300			0.761			**0.024**
Low	119 (30.7)	66 (36.1)		95 (31.1)	90 (34.0)		71 (25.4)	118 (35.6)	
Medium	140 (36.2)	67 (36.6)		112 (36.7)	95 (35.8)		106 (38.0)	112 (33.8)	
High	128 (33.1)	50 (27.3)		98 (32.1)	80 (30.2)		102 (36.6)	101 (30.5)	
Cytoplasmic IL6R			**0.037**			0.475			0.723
Low	209 (47.9)	111 (56.9)		171 (49.4)	149 (52.3)		157 (51.8)	177 (50.4)	
High	227 (52.1)	84 (43.1)		175 (50.6)	136 (47.7)		146 (48.2)	174 (49.6)	
Membranous IL6R			**0.001**			0.328			0.773
Low	351 (80.5)	177 (90.8)		285 (82.4)	243 (85.3)		253 (83.5)	296 (84.3)	
High	85 (19.5)	18 (9.2)		61 (17.6)	42 (14.7)		50 (16.5)	55 (15.7)	
Stromal IL6R			0.336			0.816			0.806
Low	293 (70.8)	138 (74.6)		238 (72.3)	193 (71.5)		203 (72.0)	241 (71.1)	
High	121 (29.2)	47 (25.4)		91 (27.7)	77 (28.5)		79 (28.0)	98 (28.9)	
Nuclear JAK1			0.735			0.247			**0.007**
Low	183 (49.6)	89 (51.1)		152 (52.4)	120 (47.4)		118 (43.4)	158 (54.9)	
High	186 (50.4)	85 (48.9)		138 (47.6)	133 (52.6)		154 (56.6)	130 (45.1)	
Cytoplasmic JAK1			0.918			**0.033**			**0.044**
Low	182 (49.3)	85 (48.9)		155 (53.4)	112 (44.3)		145 (53.3)	129 (44.8)	
High	187 (50.7)	89 (51.1)		135 (46.6)	141 (55.7)		127 (46.7)	159 (55.2)	
Stromal JAK1			0.084			0.090			0.948
Low	88 (26.0)	31 (19.0)		71 (26.8)	48 (20.3)		58 (24.0)	65 (23.7)	
High	250 (74.0)	132 (81.0)		194 (73.2)	188 (79.7)		184 (76.0)	209 (76.3)	
Nuclear JAK2			0.164			0.363			**0.005**
Low	322 (86.6)	116 (81.7)		255 (86.4)	183 (83.6)		201 (80.4)	253 (89.1)	
High	50 (13.4)	26 (18.3)		40 (13.6)	36 (16.4)		49 (19.6)	31 (10.9)	
Cytoplasmic JAK2			0.678			0.069			0.253
Low	181 (48.7)	72 (50.7)		135 (45.8)	118 (53.9)		117 (46.8)	147 (51.8)	
High	191 (51.3)	70 (49.3)		160 (54.2)	101 (46.1)		133 (53.2)	137 (48.2)	
Stromal JAK2			0.362			**0.026**			**0.002**
Low	289 (83.5)	119 (86.9)		221 (81.3)	187 (88.6)		179 (79.6)	248 (89.5)	
High	57 (16.5)	18 (13.1)		51 (18.8)	24 (11.4)		46 (20.4)	29 (10.5)	

Table 9-12. The association between pSTAT3(Ser727) and IL6/IL6R and JAK expression. Table detailing the associations between pSTAT3(Ser727) expression in different sites and Il6, IL6R, JAK1 and JAK2 expression. Significant p values are highlighted in bold.

Correlation analysis was also carried out. There was moderate positive correlation between cytoplasmic tSTAT3 and IL6R expression and between stromal tSTAT3 expression and both stromal IL6R and JAK2 expression (**Figure 9-52**). All other combinations of phosphorylated or total STAT3 and IL6, IL6R, JAK1 and JAK2 showed either no or mild correlation so this data is not illustrated here.

a)

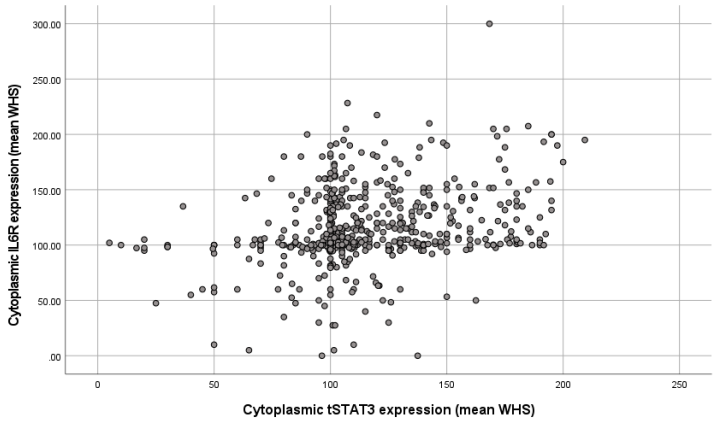

b)

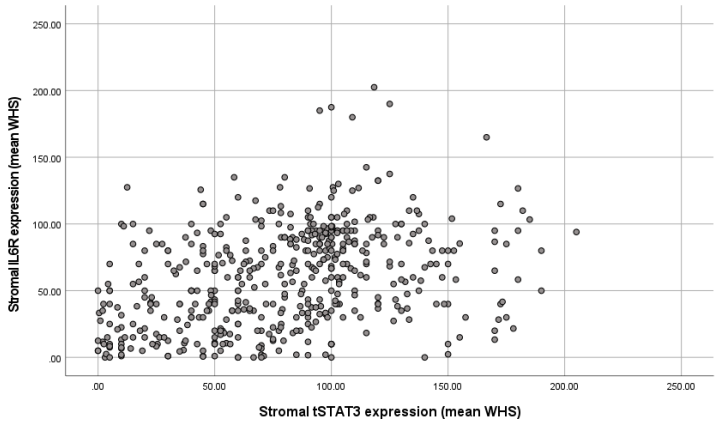

c)

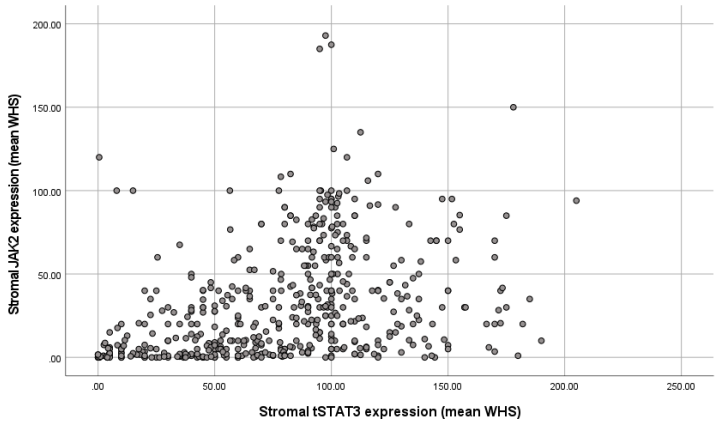

Figure 9-52. Correlation between tSTAT3 and ILR and JAK expression. Scatter plots to illustrate the correlation between a) cytoplasmic tSTAT3 and IL6R expression (Pearson correlation 0.305, **p<0.001**), b) stromal tSTAT3 and IL6R expression (Pearson correlation 0.360, **p<0.001**) and c) stromal tSTAT3 and JAK2 expression (Pearson correlation 0.361, **p<0.001**).

9.3.17 Combining forms of pSTAT3

As both nuclear pSTAT3(Tyr705) and pSTAT3(Ser727) were associated with improved CSS, and there was a positive association observed between the two phosphorylated forms, a score was created combining the two to investigate whether there was additional prognostic power when both were elevated. Patients were divided into three groups where expression of pSTAT3(Tyr705) and pSTAT3(Ser727) were both low, only one was high, or both were high. The relationship with CSS was then examined.

In the full cohort, no significant association with CSS was observed when expression of only one phosphorylation site was high but high expression of both pSTAT3(Tyr705) and pSTAT3(Ser727) was associated with improved CSS (score 1 v 0: HR 0.79, 95% CI 0.55-1.14, p=0.214; score 2 v 0: HR 0.47, 95% CI 0.29-0.76, p=0.002). The same was the case in ER positive (score 1 v 0: HR 0.74, 95% CI 0.45-1.22, p=0.239; score 2 v 0: HR 0.43, 95% CI 0.23-0.81, p=0.010) and luminal A disease (score 1 v 0: HR 0.54, 95% CI 0.26-1.12, p=0.099; score 2 v 0: HR 0.35, 95% CI 0.15-0.85, p=0.020) (**Figure 9-53**). As might be expected from the results for the individual phosphorylation sites detailed above, there was no significant association in ER negative disease or any of the other 3 molecular subtypes (data not shown).

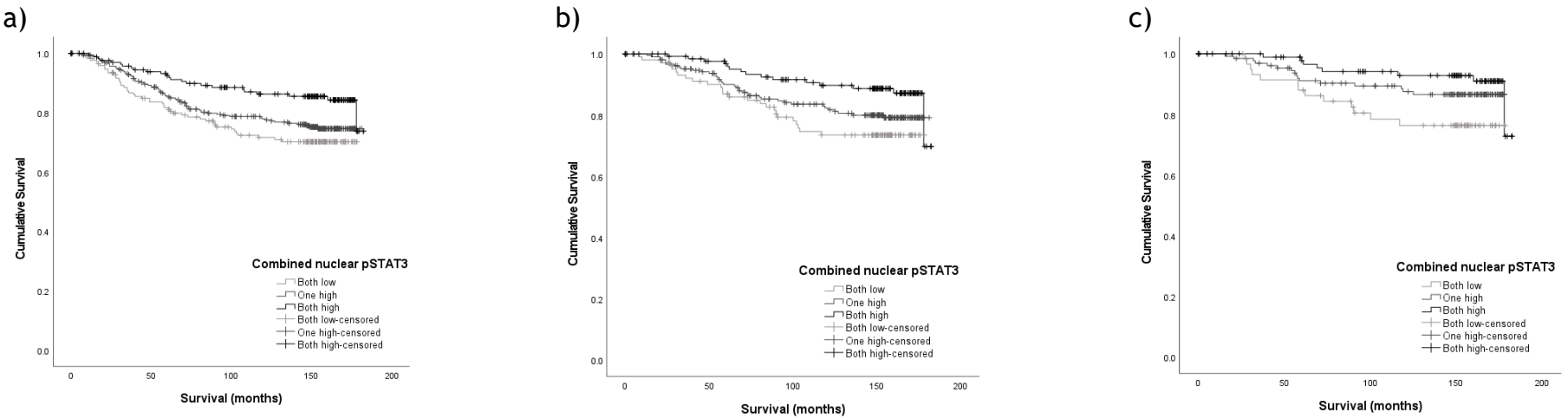

Figure 9-53. The association between a combined pSTAT3 score and CSS. Kaplan meier graphs illustrating the relationship between a combined score of pSTAT3(Tyr705) and pSTAT3(Ser727) expression and CSS in a) the full cohort (n=530 **p=0.008**), b) ER positive disease (n=375**, p=0.030**), and c) luminal A disease (n=256, **p=0.045**).

9.4 Discussion

The work in this chapter has evaluated expression levels of phosphorylated and total STAT3 in primary operable breast cancer, and their associations with survival, clinicopathological characteristics and other components of the IL6/JAK/STAT3 pathway. One principle and novel finding of the study was the association between high nuclear and cytoplasmic expression of pSTAT3(Ser727) and improved CSS in luminal A cancers, independent of other known prognostic features.

In this study, high nuclear and cytoplasmic pSTAT3(Ser727) expression was associated with improved CSS in the full cohort, in ER positive disease and in luminal A cancers but it was only in the luminal A molecular subtype that this was independent of other known prognostic factors. High expression in these sites was also associated with good prognostic features of the tumour including smaller size, lower grade, ER positivity, HER2 negativity and low tumour necrosis. Interestingly though, nuclear expression was also associated with low KM grade, low CD8+ TILs and high tumour budding. These findings suggest a potential regulatory role for serine STAT3 phosphorylation in primary operable breast cancer.

There is very little in the published literature regarding the relationship between the serine phosphorylation of STAT3 and breast cancer outcomes. Of those clinical studies of pSTAT3 in breast cancer, most either investigate pSTAT3(Tyr705)(102, 104-107) or they do not specify the phosphorylation site studied(358). One study which did investigate pSTAT3(Ser727) expression in breast cancer tissues reported higher expression in cancer tissues compared to adjacent normal tissue. In contrast to the present study, they reported higher expression in ER negative compared to ER positive tumours and they also observed a positive rather than negative correlation between pSTAT3(Ser727) expression levels and tumour stage and size and a negative correlation with ER status(101). There are a number of possible explanations for these directly opposing results. Firstly, the Yeh et al study was considerably smaller than this one, analysing tissue from 68 patients(101). Because of the size of their cohort, there were only 6 and 5 patients respectively with stage 1 and stage 3 disease. Their cohort was also dominated by ER negative disease (60.3%) while the cohort

in the present study is more heavily dominated by ER positive disease and it was in ER+ cancers that significant associations with outcome were observed. Finally, the methods for quantifying pSTAT3(Ser727) expression and analysis were quite different as the authors normalised pSTAT3(Ser727) expression against tSTAT3 expression and then analysed the data in groupings related to the difference in expression between cancer tissues and normal breast tissue(101).

Despite the paucity of clinical studies regarding pSTAT3(Ser727) in breast cancer, such that the finding in this study is entirely novel to the literature, the findings are in keeping with the results of some preclinical studies. Early studies reported decreased transcription with serine phosphorylation of STAT3(359-361), supporting the hypothesis of its regulatory role. There is evidence that serine phosphorylation of STAT3 leads to dissociation of pSTAT3(Tyr705) and consequently inactivation of STAT3(362). However, in the present study a positive rather than negative association was observed between both nuclear and cytoplasmic pSTAT3(Ser727) expression and pSTAT3(Tyr705) expression. In opposition to this regulatory role, one breast cancer study concluded that serine phosphorylation is required for the full transcription activity of cyclin D1 expression which leads to increased breast cancer growth(363). There is also evidence of a role for serine phosphorylation of STAT3 in the mitochondria in tumour progression and metastasis(364). Similarly, preclinical studies in other cancers provide evidence for a pro-tumour role for pSTAT3(Ser727), including in haematological malignancies(365, 366), gastric cancer(367, 368) and prostate cancer(369). A study in lung cancer suggested that both phosphorylation sites were important in the process of EMT-MET switch(370) which is interesting to note as nuclear expression of both phosphorylated STAT3 types was associated with higher budding in our study.

In the present study, high nuclear pSTAT3(Ser727) expression was associated with low cytoplasmic and membranous IL6R expression and cytoplasmic expression was associated with low JAK2 expression. This suggests that it is not the IL6/JAK2/STAT3 pathway that leads to serine phosphorylation of STAT3. This is in keeping with the published literature which describes serine phosphorylation of STAT3 via the ERK/MAPK pathway(359), IL6/PKC pathway(360) and by JNK(361). Specifically in breast cancer, one pre-clinical

study reported induction of STAT3 serine phosphorylation by progestins via the c-Src/p42/p44 MAPK pathways(363).

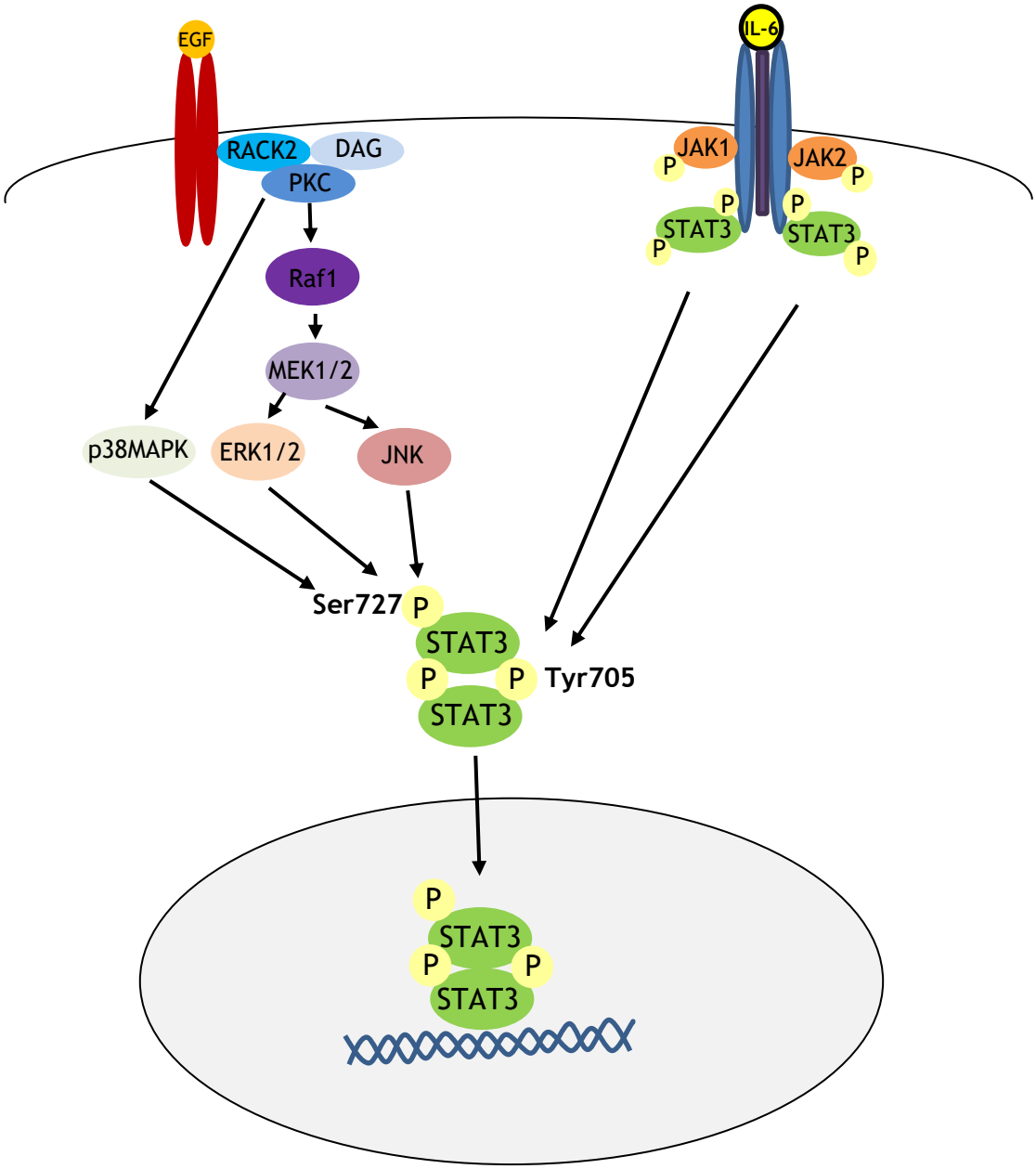

Figure 9-54. Serine phosphorylation of STAT3. Diagram illustrating the proposed mechanisms by which STAT3 is phosphorylated at Ser727 via the ERK/MAPK pathway.

Like pSTAT3(Ser727) expression, high nuclear pSTAT3(Tyr705) expression was associated with improved CSS in luminal A disease, though this was not independent of other known prognostic factors and there was no association with CSS in the full cohort or any of the other subtypes. There was also no association with CSS of cytoplasmic expression. More clinical studies have

examined the relationship between pSTAT3(Tyr705) expression and breast cancer outcomes and, in the main, findings are consistent with the results of this study, reporting either improved outcomes with high expression(104-107) or no significant association(102). The clinical findings are unexpected in the context of some preclinical studies which support a role for tyrosine phosphorylated STAT3 in breast cancer cell migration and metastasis(95), promotion of cell survival via Survivin(371) and promotion of angiogenesis via VEGF(372). However, other studies have reported anti-tumour activity including upregulation of tissue inhibitors of metalloproteinase leading to decreased invasiveness of breast cancer(373), and promotion of apoptosis in mammary epithelial cells(374). Nuclear pSTAT3(Tyr705) expression was associated with high nuclear JAK1 expression, suggesting a relationship between the two, but cell line studies would be required to investigate this further.

While high nuclear tSTAT3 was also associated with improved CSS in this study, high cytoplasmic expression was associated with worse CSS in the full and ER positive cohorts. As in this study the activated, phosphorylated forms of STAT3 seem to be protective, this may simply reflect a higher proportion of inactive STAT3 in these patients. The finding is in keeping with another study which reported worse breast cancer outcomes with higher expression of tSTAT3(103), though a larger study of node negative cancers reported no significant association(104). However, this latter study is also supported by the present study as no significant associations were observed in the subgroup analysis in the lymph node negative cohort. The present study does provide evidence of a varying role for STAT3 in different disease stages as serine phosphorylation was associated with improved survival in T1 disease only, while nuclear pSTAT3(Tyr705) was in T2 disease and in T3 disease, tSTAT3 was actually associated with worse CSS. Somewhat counterintuitively given the associations with better outcomes in lower tumour stage cancers, it was in lymph node positive disease that significant associations were observed between nuclear and cytoplasmic pSTAT3(Ser727), nuclear pSTAT3(Tyr705) and nuclear tSTAT3 expression and improved CSS. This is supported by a study which reported an association between nuclear pSTAT3(Tyr705) expression and improved survival in node positive disease(76). One possible explanation may be that STAT3 plays a

different role in growth of the primary tumour compared to metastasised cells and there has been some published evidence in mice to support this theory(375).

In this study, stromal STAT3 expression was different in several ways to tumour expression. While tumour pSTAT3(Ser727) expression was higher in ER+ cancers, stromal pSTAT3(Tyr705) and pSTAT3(Ser727) expression was higher in ER negative disease. This could simply reflect higher inflammatory infiltrates in these cancers, however stromal tSTAT3 expression was higher in ER positive disease. In ER negative disease, high stromal expression of pSTAT3(Ser727) was associated with improved CSS whereas high tSTAT3 expression was associated with worse CSS, particularly in TNBC. The latter is in keeping with evidence in the literature of the pro-tumourigenic role of JAK/STAT3 in the tumour microenvironment. Pre-clinical studies in breast cancer report that JAK1/STAT3, stimulated by LIF, trigger a switch of fibroblasts to pro-invasive CAFs(332, 376, 377). Other studies provide evidence that activation of STAT3 in various immune cells leads to inhibition of proinflammatory cytokine production by macrophages, reduced DC maturation, suppression of CD8+ lymphocytes, reduced antitumour cytotoxic activity of macrophages, neutrophils and NK cells, and may increase Treg lymphocyte proliferation(295).

Stromal pSTAT3(Tyr705) expression was associated with high stromal IL6 which may represent either or both of increased IL6 production secondary to STAT3 activation or activation of the STAT3 pathway by IL6. Conversely, pSTAT3(Ser727) expression was associated with low stromal IL6, similarly either supporting a regulatory role for serine phosphorylation and therefore less IL6 production, or reflecting stimulation by other ligands. High stromal pSTAT3(Tyr705) was associated with low stromal JAK1 and both phosphorylation sites were associated with low stromal JAK2. Further mechanistic experiments are required to explain this relationship.

In summary, despite preclinical evidence of a pro-tumourigenic role for activated STAT3 in the proliferation, survival, metastasis and invasion and angiogenesis of breast cancer cells(354), this present study, along with other clinical studies, has observed an association between activated STAT3 and improved CSS, suggesting a regulatory anti-tumour role for STAT3. To the knowledge of the author, this is one of the first and the biggest clinical study to

date to investigate the role of pSTAT3(Ser727) in primary operable breast cancer. Nuclear and cytoplasmic pSTAT3(Ser727) expression was associated with improved CSS independently of other prognostic factors in luminal A disease and particularly in T1 and node positive disease meaning that it may have a prognostic role in these patients, for instance in decisions regarding adjuvant chemotherapy in luminal A, node positive disease. It may also serve as a predictive factor as there is evidence that STAT3 is involved in chemoresistance(378, 379), as well as resistance to other systemic therapies(380, 381) and radiotherapy(382), but further research would be required to establish this. Results of preclinical studies raised hopes that STAT3 inhibitors may have a role in breast cancer treatment. However, the findings of this study would caution against their use, particularly in luminal A cancers, and may provide some evidence towards the reasons for the disappointing results seen in trials of STAT inhibitors to date(357). Early phase trials in many cancers, including breast, are ongoing(383). There may be some patient populations in which STAT3 inhibitors could have a role but trials should be targeted at very specific groups, for example those with T3 disease and particularly those with TNBC if the STAT inhibitors can be targeted towards cells in the tumour stroma as well as the tumour cells. tSTAT3 expression could potentially be useful as a predictive marker for response. Similarly, in view of the findings of this study, it would be interesting to include pSTAT3(Ser727) expression in any studies of MAPK inhibitors in breast cancer as cancers under regulatory control by serine phosphorylation of STAT3 could, in theory, be promoted by use of MAPK inhibitors if this is the activating pathway. Again, much more research would be required to establish this and it is clear from this study and the preceding two chapters that it is impossible to wholly isolate one pathway for study and targeting given the complex interplay between different pathways in tumour cells and those of the tumour microenvironment.

In conclusion, this is the first clinical study to report an association between pSTAT3(ser727) and improved CSS so further work into its role as a prognostic marker in certain subtypes of breast cancer is warranted. The results of this study would support the investigation of pSTAT3(Ser727), pSTAT3(Tyr705) and tSTAT3 expression as part of any STAT or MAPK inhibitor studies as there may be a role for one or all of them as predictors of response.

10 Discussion

10.1 General discussion and conclusions

The work of this thesis has focussed on the role in primary operable breast cancer of the systemic inflammatory response, local inflammation, specific phenotypic features of the tumour and the IL6/JAK/STAT3 pathway which is one link between signals in the tumour microenvironment and tumour cells. This exploratory work was carried out with a view to identifying potential prognostic biomarkers to aid in the complex treatment decision-making process in this heterogenous disease, and to identify potential targets for therapy meriting further investigation, either in cancers which have developed resistance to current treatments, or in TNBC for which no targeted treatments are currently available.

Firstly, a number of circulating markers of the systemic inflammatory response were investigated by means of a literature review, meta-analysis and pilot study of 448 West of Scotland patients. The preoperative NLR, albumin and, to a lesser degree, LMR were identified as having a prognostic role in primary operable breast cancer. However, there was insufficient evidence to reach a conclusion regarding suitable thresholds for use in clinical practice, or to ascertain in which molecular subtypes they may best be used. Evidence suggests that systemic inflammation in early-stage breast cancer is an uncommon finding and becomes a more prominent feature in locally advanced and metastatic disease. This further calls into question the likely clinical utility of these markers in primary operable breast cancer. However, they do have the advantage of requiring only a routine blood test and, since the writing of the systematic review, further evidence has been published in support of a prognostic role for NLR in particular(384-390), so it may be that this does find a place in clinical practice due to its simplicity and low cost, for instance in low-resource countries.

In view of the doubts regarding the clinical utility of these markers, the work in this thesis then focussed on the role of the local inflammatory response in primary operable breast cancer. Because its prognostic value in colorectal cancer has been widely reported(183, 184), the Klintrup-Makinen grade was investigated in primary operable breast cancer. In colorectal cancer, higher KM

score is associated with improved prognosis(183, 184), suggesting an anti-tumour role for the inflammatory infiltrate. However, the relationship was more complex in this cohort of breast cancer patients. An association with CSS was observed but this was not independent of other known prognostic factors and it was both the highest and the lowest scores which were associated with the best CSS. There is very little in the published literature regarding the KM score in breast cancer with which to compare, so this finding requires validation in other cohorts. The findings unfortunately do not support the use of the KM grade as a prognostic tool in breast cancer in contrast to that observed with other solid tumours such as colorectal cancer. The composition of the inflammatory infiltrate may be more important. Multiplex IHC would be required to ascertain this composition and also inform us on the spatial relationships between different immune cells. In the current study high CD8+ TILs were associated with improved CSS. TILs are of interest as prognostic and predictive biomarkers in breast cancer and a better understanding of their interactions with the tumour will hopefully lead to improved selection of patients who will benefit from immune checkpoint inhibitors. However, a dedicated International TILs Workshop has recently had a focus on TILs research, so it was decided that this would not be the focus of the current thesis. Instead, the appeal of prognostic markers which only require a single H&E-stained slide led to the investigation of features other than the KM grade which fulfil this specification and have been reported to have a prognostic role in other cancers, namely tumour necrosis, TSP and tumour budding.

In a cohort of over 1000 patients, the work of this thesis has provided evidence of a prognostic role for necrosis in ER positive disease and each of necrosis, TSP and tumour budding in ER negative disease. Additionally, a novel score which combined all 3 features has prognostic value in both ER positive and ER negative disease, and in each of the receptor subtypes except for ER+/HER2+ cancers, though this may be because of a lack of statistical power in this smaller group.

In ER+/HER2- disease the score identifies a poor prognostic group, with all 3 features high, who have significantly worse CSS compared to those with the lower 3 scores. The score may therefore have a role in clinical practice to aid decision making regarding adjuvant chemotherapy and duration of endocrine

therapy. Currently, in the UK, several tools are available to aid these decisions. Predict is an online tool which uses data regarding prognostic factors including tumour size, grade, nodal involvement, ER, HER2, Ki-67 and menopausal status to estimate the benefit from adjuvant treatments in terms of survival gain(39). NICE recommends the use of the gene assays EndoPredict, Oncotype DX Breast Recurrence Score or Prosigna in patients with ER positive, HER2 negative, lymph node negative breast cancer who have an intermediate risk of distant recurrence using Predict or the NPI, if the result would influence the decision regarding adjuvant chemotherapy(52). These tests are not currently recommended for use in lymph node positive disease. However, Optima is a trial currently recruiting in the UK which uses the Prosigna gene score to predict benefit from chemotherapy for ER+/HER2-, lymph node positive patients to see if a proportion of patients with lymph node metastases could avoid chemotherapy(391, 392). These gene assays are expensive and, in the case of Oncotype DX which is used in the West of Scotland, requires a sample to be sent away to a single lab in the USA for testing. The necrosis/TSP/budding score has the advantage of being inexpensive, requiring a single H&E slide, and it can be performed locally. If this score was validated in other cohorts it would then be useful to compare its prognostic power to that of the gene assays as, if equivocal, the use of this score could prove both cost and time efficient. If it did perform similarly, it could be postulated that necrosis, TSP and budding represent phenotypic features influenced by the genes tested in these scores. Alternatively, in view of the fact that the necrosis/TSP/budding score was prognostic independent of the factors used in the Predict tool, it would be interesting to evaluate whether using it in addition to the Predict score could improve prognostic performance and reduce the number of patients requiring Oncotype DX or equivalent.

In ER negative disease, and in particular TNBC, the necrosis/TSP/budding score stratifies patient outcomes. On multivariate analysis, the highest score had a HR of 8.11 in this cohort, compared to those with the lowest score. This compares to a HR of 3.15 for lymph node positivity, the only other factor which was independently prognostic in the ER negative cohort. It therefore may be useful to identify a particularly high-risk group of patients who should be treated aggressively. On the other hand, the cohort with a score of 0 appear to have favourable outcomes and therefore, if validated, this score may be of clinical

utility to identify a cohort of patients who could be treated less aggressively. It should be noted that the scoring in this thesis was carried out on full section slides from resection specimens and therefore its applicability in the setting of neoadjuvant therapy and the possibility of adapting scoring to biopsy specimens is unknown at present.

Given the prognostic power of this score in triple negative breast cancer, a better understanding of the features it comprises may help to develop targeted treatments for this poor prognostic group of patients. Of the 3 components of the score, tumour budding had the highest prognostic power (HR 3.05 on univariate analysis, HR 2.15 on multivariate analysis) and is interesting because the molecular mechanisms driving this phenotype are poorly understood at present. With the aim of gaining a better understanding of the molecular mechanisms driving tumour budding, a small pilot study was carried out for which transcriptomic analysis was performed to compare the transcriptome of patients with high budding to those with low budding. Despite the small sample size (due to financial limitations), 9 genes were identified which justify further investigation. Of particular interest is the ODAM gene which was under-expressed in high budding tumours, which may lead to reduced cell adhesion and increased migration and invasiveness. The other gene of particular interest is JUNB which was over-expressed in high budding tumours and may be significant in EMT. It may be that targeting of these genes could lead to reduced tumour budding and improved prognosis. However, much more work is required to establish this hypothesis and funding is currently being sought in the lab for further research in this area.

Regarding the practicalities of the necrosis/TSP/budding score, the presence or absence of necrosis is frequently commented upon in routine pathology reports, therefore, the routine standardised reporting of this feature should not prove too challenging a step. TSP is a quick and straightforward feature to report. Tumour budding is more time-consuming to quantify. However, there is precedent for its use as it has been recommended for routine reporting in colorectal cancer(75, 77). Another method of assessing tumour budding is pan-cytokeratin staining but further comparison studies of the two methods are required(75). The findings of this thesis require to be validated in other cohorts

with scoring carried out by a qualified pathologist (scoring for the work in this thesis was carried out by two research fellows) but if the findings are confirmed, work to develop automated scoring would be warranted. The advances in digital image analysis provide potential for its use in tumour budding scoring, both in breast and colorectal cancer and discussions are in progress between groups with an interest in this technology and the host lab regarding researching and developing this.

In pursuit of a link between components of the tumour microenvironment, such as the inflammatory infiltrate discussed in chapter 4, and phenotypic features of the tumour associated with poorer prognosis, such as those outlined above, the final three chapters of this thesis investigated the IL6/JAK/STAT3 cell signalling pathway. In this cohort, the findings of this work did not demonstrate clear associations and correlations between expression of all the different components of the pathway. This supports other evidence that numerous signalling pathways within cells interact, with substantial crosstalk. For instance, IL6 can activate other pathways, other ligand and receptor complexes can activate JAKs and other pathways can lead to STAT3 phosphorylation. It is likely to be the balance between activation of these different pathways which is of key importance in cancer progression. However, there were several key findings of note.

Firstly, some significant associations were observed between components of the pathway and some of the phenotypic features investigated in earlier chapters. High membranous IL6R was associated with low tumour budding raising the possibility that one of the pathways involving IL6R may exert a regulatory effect on the development of this phenotype. On the other hand, high nuclear expression of pSTAT3(Ser727) was associated with high budding. STAT3 is phosphorylated at the serine 727 site by pathways other than JAK mediated ones so it may be that one of these pathways is important in the development of budding, justifying further investigation. It was interesting that budding and nuclear pSTAT3(Ser727) were positively associated in the full cohort considering that, in this thesis, budding was a poor prognostic factor while nuclear pSTAT3(Ser727) was a good prognosis factor. However, the former was in ER negative disease and the latter in ER positive disease, and there was no statistically significant association observed when analysed within each of the

two ER subgroups. High stromal JAK1 was also associated with high tumour budding, suggesting a possible influence of stromal cells in the promotion of this phenotype.

In ER positive, or specifically in luminal A disease, a combined score of high tumour IL6 and high membranous IL6R was associated with worse CSS while high nuclear and stromal JAK1, and high nuclear expression of both phosphorylated forms of STAT3 were associated with improved CSS. This suggests a regulatory role on tumour progression of activation of the JAK/STAT3 pathway and implies that IL6 exerts its protumour effects via other pathways. Therefore, these results suggest that there may be a role for IL6 inhibitors in ER positive breast cancers with high IL6 expression, but trials of JAK and STAT3 inhibitors are likely to produce disappointing results in this subset of breast cancer patients. The association with the novel score of tumour IL6 and membranous IL6 and worse CSS, and that of high pSTAT3(Ser727) expression and improved CSS, are new findings not previously described in the literature and raise the possibility that, once validated, they could be used as prognostic tools to aid treatment decisions in some luminal A cancers.

In ER negative, or specifically triple negative breast cancer, high nuclear JAK1 and cytoplasmic JAK2 expression were associated with worse CSS, suggesting that JAK inhibitors may have a role in TNBC. The other significant associations in ER negative breast cancer all involved stromal expression, providing further evidence for the role of the tumour microenvironment in the progression of these tumours. High stromal JAK2 and tSTAT3 expression were associated with worse CSS while high pSTAT3(Ser727) expression was associated with improved CSS.

Throughout this thesis, results have varied between the different molecular (or surrogate receptor) subtypes. This further supports the understanding of breast cancer as a heterogenous disease with subtypes which behave differently and respond to different treatments. Going forward it would seem sensible to focus further research on a specific subtype at one time, rather than breast cancer as a whole.

The majority of the work in this thesis has the strength that it is carried out in a large cohort of patients. This is particularly the case for the work involving Klintrup-Makinen grade, necrosis, TSP and tumour budding for which it was possible to combine two cohorts resulting in over 1000 patients for analysis. However, despite this, small numbers remain in the least common subtypes (luminal B and HER-2 enriched or equivalent surrogate receptor subtypes) so lack of statistical power may affect results in these subtypes. The work is further strengthened by the long length of patient follow up, which is important in breast cancer studies due to late disease recurrence. However, it comes with the trade-off that a historical cohort were managed for their cancer in a different era under different guidelines and with some variation in available treatments compared to modern day practices, which may raise questions as to the applicability of the results in present day practice. Validation in more recent cohorts is required.

In conclusion, a combined score of tumour necrosis, TSP and tumour budding has a prognostic role in both ER positive and ER negative primary operable breast cancer. It is a straightforward and low-cost method to stratify risk and could have a role in decisions regarding adjuvant treatment. Further work is required to better understand tumour budding and to identify therapeutic targets for patients with ER negative cancer and high tumour budding. A combination of high tumour IL6 and high membranous IL6R is associated with worse prognosis in ER positive cancers so IL6 inhibitors may have a role in selected patients. This pro-tumourigenic effect does not appear to be via the JAK/STAT3 pathway. The JAK/STAT3 pathway, and particularly serine phosphorylation of STAT3 via other pathways, may have a regulatory effect on progression of ER positive primary operable breast cancer and therefore JAK and STAT3 inhibitors are unlikely to be of benefit in this group. However, in ER negative disease high expression of JAKs was associated with worse CSS and therefore JAK inhibitors may have a role in selected patients with ER negative breast cancer. There is evidence for an influence of stromal cells on progression of ER negative breast cancers. More work is required, both in pre-clinical and clinical studies, to develop understanding of the complex interactions and crosstalk between different cell signalling pathways in tumour cells, and how they are influenced by factors in

the tumour microenvironment. Further studies investigating the mechanisms would help elucidate specific drivers to tumour progression.

10.2 Further work

The associations with CSS of the necrosis/TSP/budding score require validation in other cohorts, particularly more modern ones. The data in this study suggests that differences in prognosis of the four groups are evident by five years of follow up, if not earlier in ER negative disease, so it should be possible to power a study with shorter follow up than the cohorts in this thesis. Following this, the prognostic performance of the score should be compared to existing prognostic tools to determine in what role it may have most clinical utility. In parallel to this work, it would be useful to investigate the potential to develop automated scoring of the component features of the score and collaborations are being sought with an aim to facilitate this work.

To identify potential therapeutic targets for patients with ER negative breast cancer and high tumour budding, a group with a particularly poor prognosis, further work to identify genes associated with tumour budding is required. The pilot study in this thesis identified 9 genes of potential interest. Funding is being sought to carry out a larger study having verified TempOSeq as an appropriate technique for this work. Gene expression will need to be validated at the protein level in the cohort also.

To better understand the findings of this thesis regarding components of the IL6/JAK/STAT3 pathway, other members in the lab are carrying out IHC work in the same cohort for other cell signalling pathways which should then allow the data to be combined and interactions between the pathways analysed. This will be of particular interest regarding serine phosphorylation of STAT3. Mechanistic cell line studies will also be required to gain a better understanding of the associations observed in the clinical studies.

Appendices

Tumour necrosis, budding and TSP in primary operable ductal cancer

Below is survival and association analysis for necrosis, budding and TSP in ductal cancer, including the combined scores. There was very little difference between these results and those in the full cohort so the analysis is not included in the main thesis.

Associations between necrosis and CSS in ductal breast cancer

In the full cohort, necrosis was associated with worse CSS (10yr CSS 87% v71%, p<0.001; HR 2.28, 95% CI 1.74-2.99, p<0.001). In ER positive disease, this was maintained (10yr CSS 87% v 73%, p<0.001; HR 2.01, 95% CI 1.43-2.83, p<0.001). In ER negative disease, necrosis was associated with worse CSS (10yr CSS 86% v 69%, p=0.001; HR 2.66, 95% CI 1.47-4.79, p=0.001).

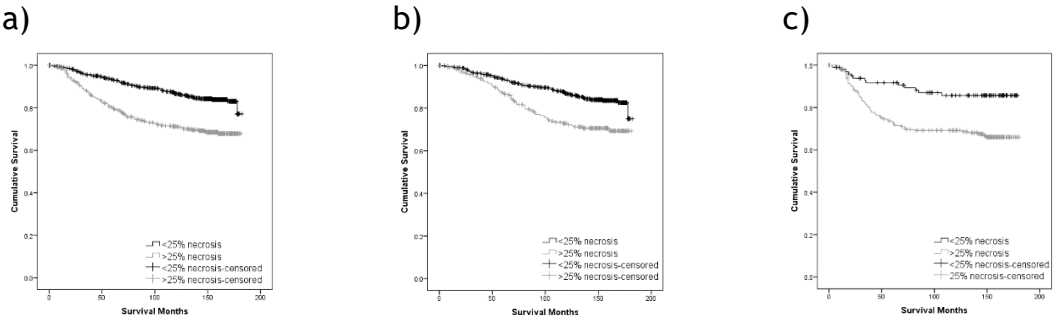

The relationship between tumour necrosis and CSS in primary operable ductal breast cancer. Kaplan Meier survival graphs for CSS in patients with high compared to low necrosis in ductal breast cancer. a) Full cohort n=1080, p<0.001; b) ER positive n=737, p<0.001; c) ER negative n=340, p=0.001

In ER+/HER2- cancers, high necrosis was associated with worse CSS (10yr CSS 87% v 73%, p=0.001; HR 1.89, 95% CI 1.28-2.79, p=0.001) and this was also the case in ER+/HER2+ cancers (10yr CSS 77% v 61%, p=0.040; HR 2.28, 95% CI 1.00-5.20, p=0.051). In ER-/HER2+ cancers, necrosis was not significantly associated with CSS (10yr CSS 72% v 67%; HR 1.25, 95% CI 0.43-3.63, p=0.676). In ER-/HER2- disease, necrosis was associated with worse CSS (10yr CSS 85% v 70%, p=0.006; HR 2.59, HR 1.27-5.27, p=0.009).

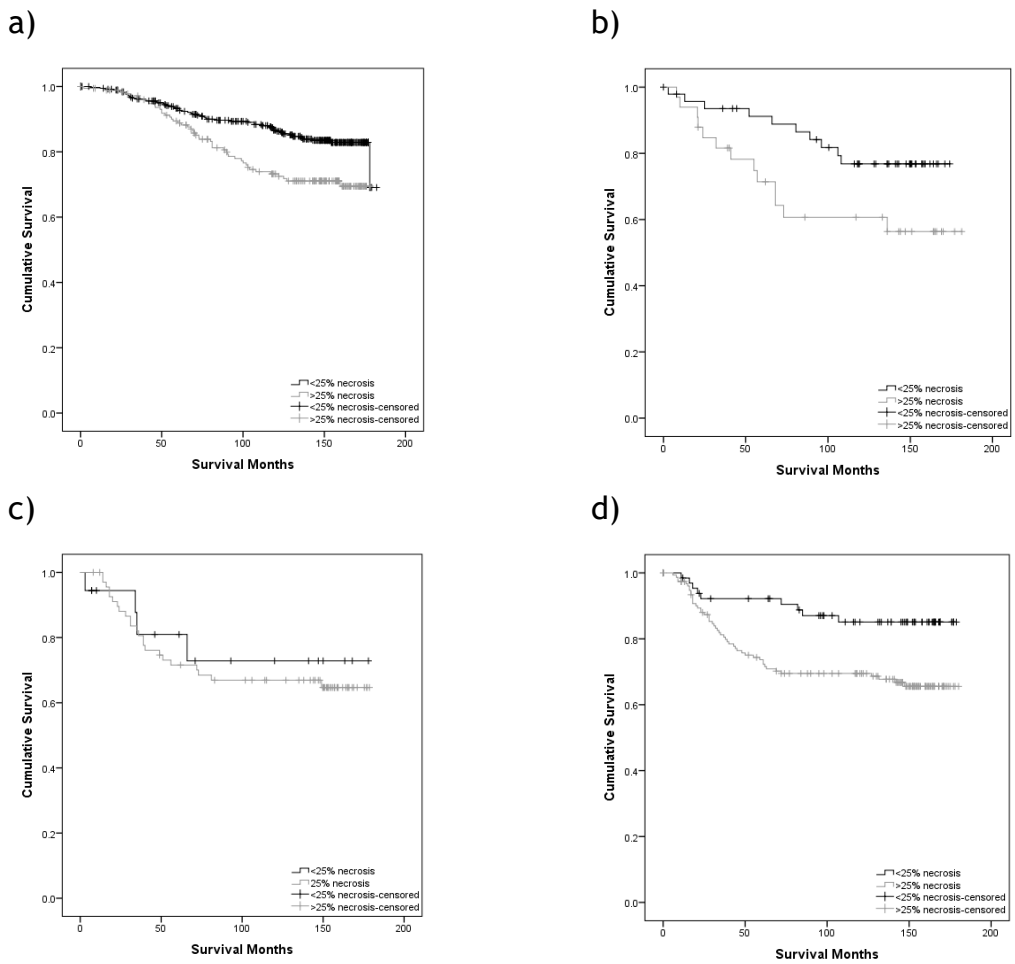

The relationship between tumour necrosis and CSS in primary operable ductal breast cancer, by molecular subtype. Kaplan Meier survival graphs for CSS in patients with high compared to low necrosis in ductal breast cancer. a) ER+/HER2- n=563, p=0.001; b) ER+/HER2+ n=81, p=0.045; c) ER-/HER2+ n=87, p=0.675; d) ER-/HER2- n=221, p=0.006

Associations between necrosis and clinicopathological characteristics in ductal breast cancer

High tumour necrosis was associated with younger age (p=0.001), larger tumour size (p<0.001), higher tumour grade (p<0.001), nodal (p=0.024) and HER2 positivity (p<0.001), ER and PR negativity (p<0.001), a higher Klintrup Makinen (KM) score (p<0.001) and low TSP (p=0.032). In the patients for whom these markers were available, necrosis was associated with high CD4+ lymphocytes (n=592, p<0.001) and high CD68+ cells (n=369, p<0.001).

Associations between budding and CSS in ductal breast cancer

In the full ductal cohort, high tumour budding was associated with worse CSS (10yr CSS 83% v 71%, p<0.001; HR 1.73, 95% CI 1.31-2.29, p<0.001). In ER positive disease, tumour budding was not associated with CSS (10yr CSS 84% v 79%, p=0.148; HR 1.34, 95% CI 0.93-1.93, p=0.117). However, in ER negative disease, high budding was associated with worse CSS (10yr CSS 80% v 47%, p<0.001; HR 3.00, 95% CI 1.94-4.66, p<0.001).

a) b) c)

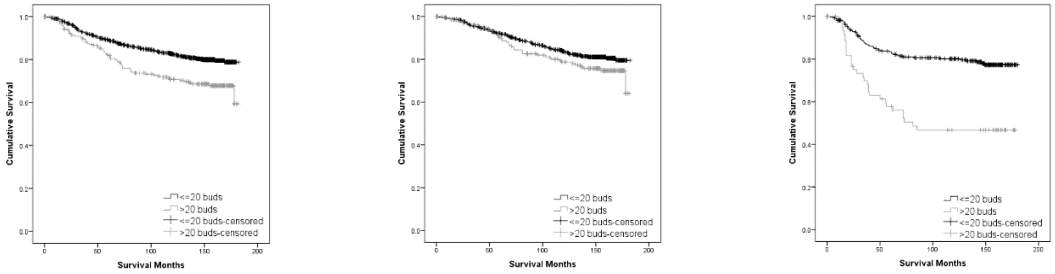

The relationship between tumour budding and CSS in primary operable ductal breast cancer. Kaplan Meier survival graphs for CSS in patients with high compared to low tumour budding in ductal breast cancer. a) Full cohort n=1080, p<0.001; b) ER positive n=737, p=0.116; c) ER negative n=340, p<0.001

High budding was not significantly associated with CSS in either ER+/HER2- (10yr CSS 83% v 80%, p=0.560; HR 1.17, 95% CI 0.77-1.78, p=0.454) or ER+/HER2+ disease (10yr CSS 73% v 62%, p=0.278; HR 1.55, 95% CI 0.66-3.66, p=0.318). High budding was associated with worse CSS in both ER-/HER2+ (10yr CSS 76% v 36%, p=0.003; HR 3.38, 95% CI 1.56-7.32, p=0.002) and ER-/HER2- cancers (10yr CSS 79% v 52%, p=0.002; HR 2.37, 95% CI 1.37-4.10, p=0.002).

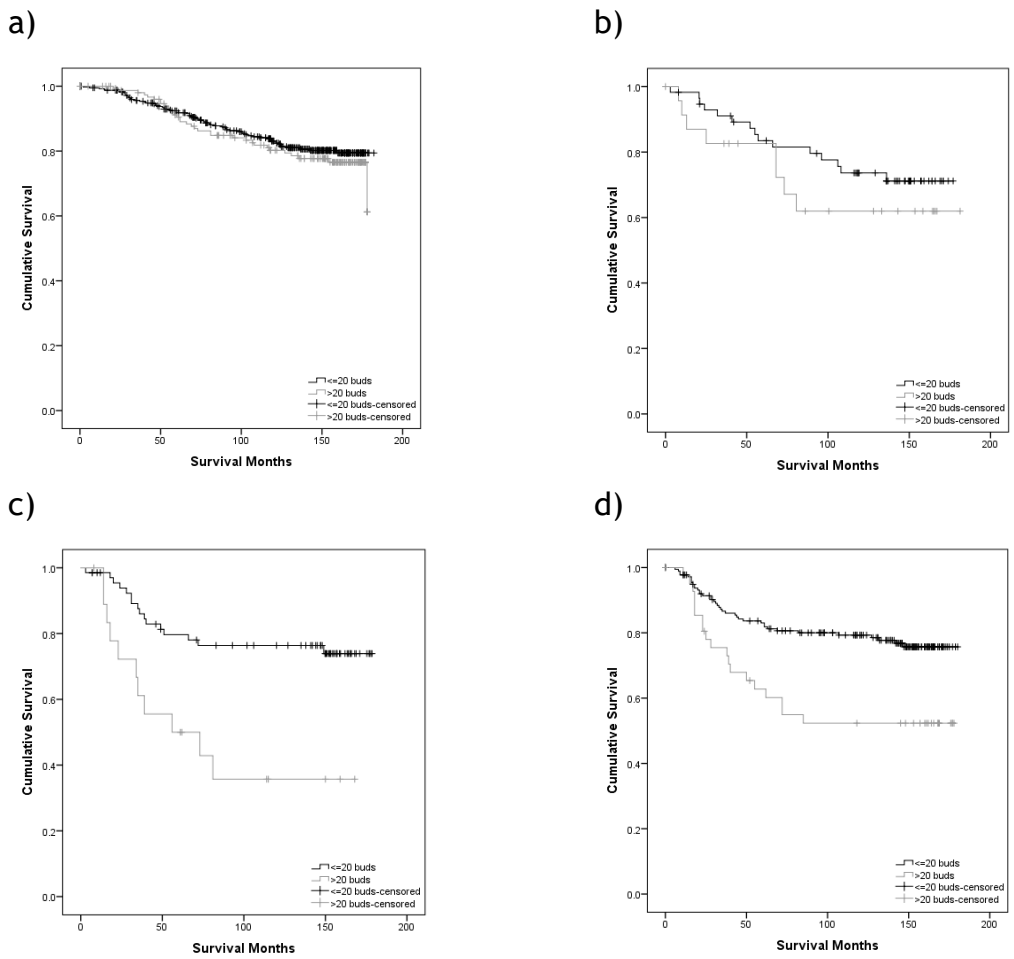

The relationship between tumour budding and CSS in primary operable ductal breast cancer, by molecular subtype. Kaplan Meier survival graphs for CSS in patients with high compared to low tumour budding in ductal breast cancer. a) ER+/HER2- n=563, p=0.453; b) ER+/HER2+ n=81, p=0.314; c) ER-/HER2+ n=87, p=0.001; d) ER-/HER2- n=221, p=0.002

Associations between budding and clinicopathological characteristics in ductal breast cancer

High tumour budding was associated with lower tumour grade (p<0.001), nodal (p=0.001) and ER positivity (p=0.006), high TSP (p<0.001) and lower KM score (p=0.002). In the patients for whom these markers were available, high budding was associated with low CD4+ lymphocytes (n=596, p=0.017) and lower CD8+ lymphocytes (n=371, p=0.027).

Associations between TSP and CSS in ductal breast cancer

In the full ductal cohort, high TSP was associated with worse CSS (95% CI 81% v 76%, p=0.041; HR 1.40, 95% CI 1.07-1.84, p=0.016). In ER positive disease, there was no significant association between TSP and CSS (10yr CSS 83% v 81%, p=0.461; HR 1.23, 95% CI 0.85-1.73, p=0.278). Conversely, in ER negative

disease, high TSP was associated with worse CSS (10yr CSS 78% v 64%, p=0.0101; HR 1.85, 95% CI 1.20-2.84, p=0.005).

a) b) c)

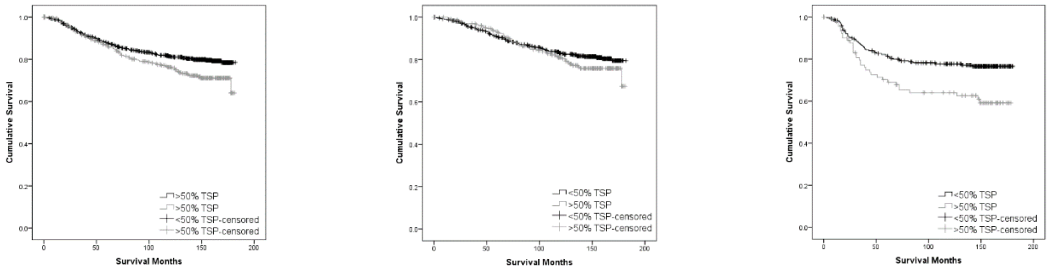

The relationship between TSP and CSS in primary operable ductal breast cancer. Kaplan Meier survival graphs for CSS in patients with high compared to low TSP in ductal breast cancer. a) Full cohort n=1080, p0.015; b) ER positive n=737, p=0.277; c) ER negative n=340, p=0.004.

TSP was not significantly associated with CSS in either ER+/HER2- (10yr CSS 84% v 79%, p=0.147; HR 1.47, 95% CI 0.99-2.19, p=0.055) or ER+/HER2+ cancers (10yr CSS 68% v 77%, p=0.586; HR 0.70, 95% CI 0.24-2.07, p=0.520). High TSP was associated with worse CSS in both ER-/HER2+ (10yr CSS 75% v 56%, p=0.043; HR 2.24, 95% CI 1.05-4.79, p=0.037) and ER-/HER2- cancers (10yr CSS 77% v 64%, p=0.057; HR 1.79, 95% CI 1.04-3.11, p=0.037).

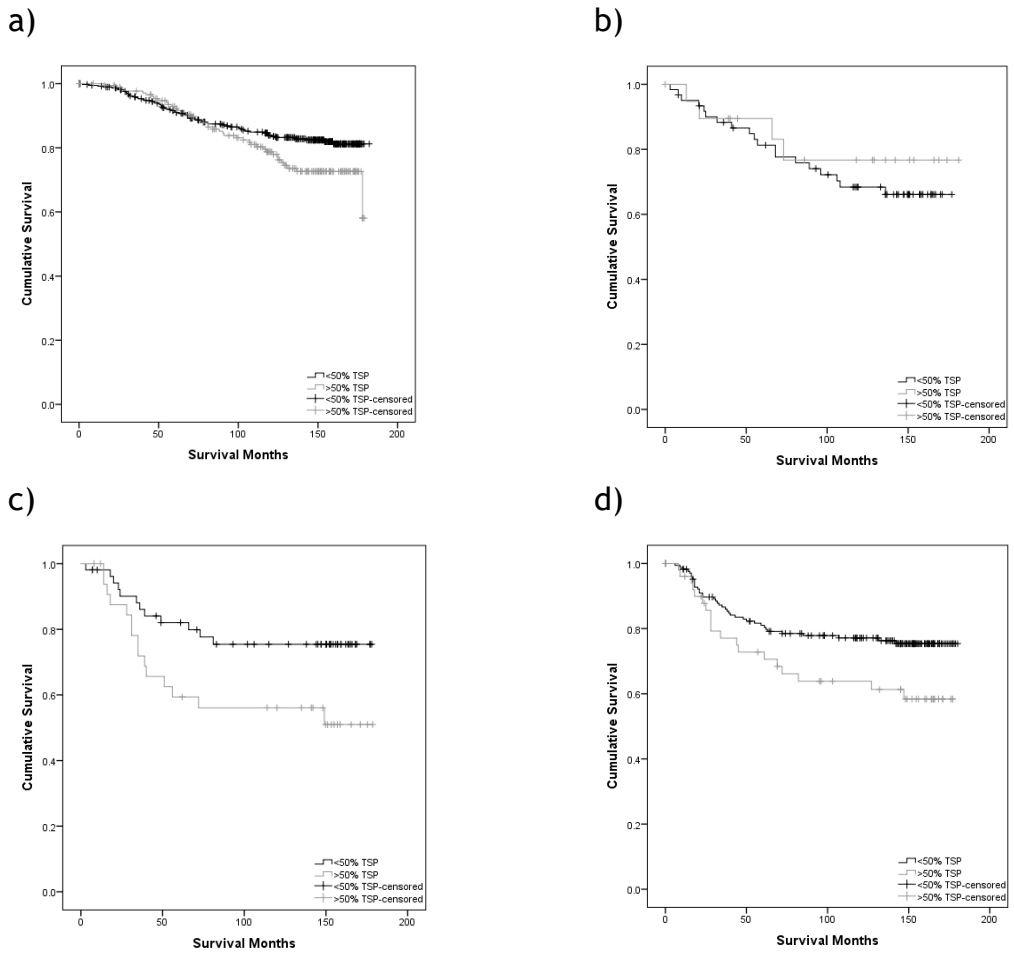

The relationship between TSP and CSS in primary operable ductal breast cancer, by molecular subtype. Kaplan Meier survival graphs for CSS in patients with high compared to low TSP in ductal breast cancer. a) ER+/HER2- n=563, p=0.054; b) ER+/HER2+ n=81, p=0.518; c) ER-/HER2+ n=87, p=0.32; d) ER-/HER2- n=221, p=0.034.

Associations between TSP and clinicopathological characteristics in ductal breast cancer

High TSP was associated with high budding (p<0.001) but lower tumour grade (p<0.001), low or absent necrosis (p=0.032) and a lower Klintrup-Makinen (KM) score (p<0.001). In the patients for whom these markers were available, high TSP was associated with low CD4+ lymphocytes (n=596, p=0.035), low CD8+ (n=371, p=0.043) lymphocytes and lower CD68+ cells (n=369, p=0.003).

Associations between the necrosis-budding score and CSS in ductal breast cancer

In the full ductal cohort, a higher combined necrosis-budding score was associated with worse CSS (10yr CSS 87% v 80% v 49%, p<0.001; score 1 v 0: HR 1.63, 95% CI 1.19-2.23, p=0.002; score 2 v 0: HR 4.63, 95% CI 3.19-6.73, p<0.001). In ER positive disease, a score of 2 was associated with worse CSS than a score of 0 (10yr CSS 86% v 82% v 60%, p<0.001; score 1 v 0: HR 1.35, 95% CI

0.93-1.97, p=0.112; score 2 v 0: HR 3.03, 95% CI 1.87-4.91, p<0.001). In ER negative disease a higher combined necrosis-budding score was associated with worse CSS (10yr CSS 89% v 77% v 31%, p<0.001; score 1 v 0: HR 2.51, 95% CI 1.20-5.28, p=0.015; score 2 v 0: HR 9.48, 95% CI 4.28-20.99, p<0.001).

a) b) c)

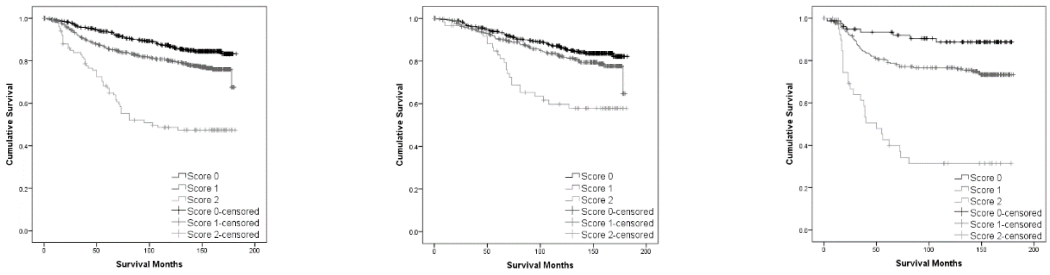

The relationship between the necrosis-budding score and CSS in primary operable ductal breast cancer. Kaplan Meier survival graphs for CSS in patients with a necrosis-budding score of 2 compared to 1 compared to 0, in ductal breast cancer. a) Full cohort n=1080, p<0.001; b) ER positive n=737, p<0.001; c) ER negative n=340, p<0.001

In ER+/HER2- disease, a score of 2 was associated with worse CSS than a score of 0 (10yr CSS 85% v 84% v 60%, p=0.001; score 1 v 0: HR 1.13, 95% CI 0.73-1.74, p=0.583; score 2 v 0: HR 2.73, 95% CI 1.58-4.71, p<0.001). In ER+/HER2+ disease, combined necrosis-budding score was not significantly associated with CSS (10yr CSS 79% v 64% v 59%, p=0.071; score 1 v 0: HR 2.58, 95% CI 1.00-6.69, p=0.051; score 2 v 0: HR 2.55, 95% CI 0.81-8.06, p=0.110). In ER-/HER2+ cancers, a combined score of 2 was associated with worse CSS but this was of borderline statistical significance (10yr CSS 72% v 77% v 26%, p=0.002; score 1 v 0: HR 0.81, 95% CI 0.23-2.81, p=0.735; score 2 v 0: HR 3.60, 95% CI 0.99-13.10, p=0.052). In ER-/HER2- cancers, an increasing combined necrosis-budding score was associated with worse CSS (10yr CSS 89% v 76% v 35%, p<0.001; score 1 v 0: HR 2.67, 95% CI 1.05-6.77, p=0.039; score 2 v 0: HR 8.38, 95% CI 3.04-23.13, p<0.001).

a) b)

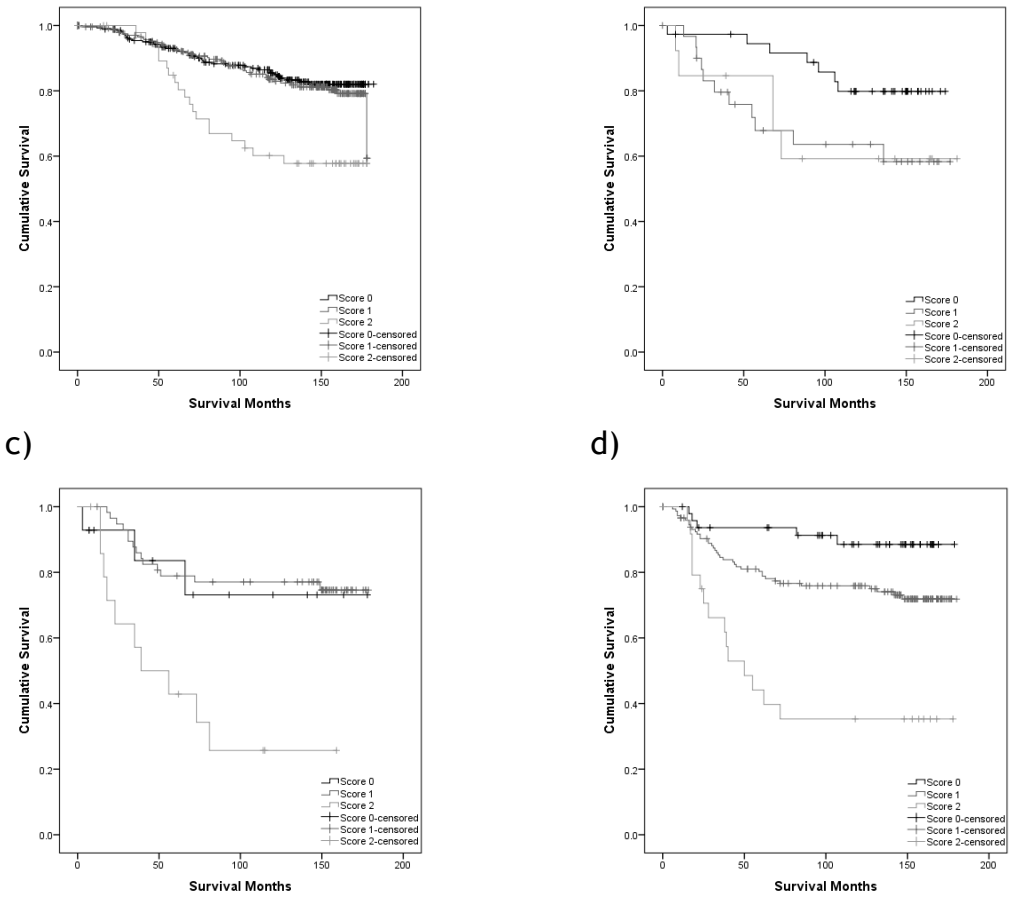

The relationship between the necrosis-budding score and CSS in primary operable ductal breast cancer, by molecular subtype. Kaplan Meier survival graphs for CSS in patients with a necrosis-budding score of 2 compared to 1 compared to 0, in ductal breast cancer. a) ER+/HER2- n=563, p-0.001; b) ER+/HER2+ n=81, p=0.098; c) ER-/HER2+ n=87, p<0.001; d) ER-/HER2- n=221, p<0.001

Associations between the necrosis-budding score and clinicopathological characteristics in ductal breast cancer

A high necrosis-budding score was significantly associated with younger age (p=0.023), larger tumour size (p<0.001), higher tumour grade (p<0.001), nodal positivity (p<0.001), ER and PR negativity (p<0.001, p<0.001), HER2 positivity (p=0.004) and higher KM grade (p<0.001).

Associations between the necrosis-TSP score and CSS in ductal breast cancer

In the full ductal cohort, a higher necrosis-TSP score was associated with worse CSS (10yr CSS 87% v 79% v 61%, p<0.001; score 1 v 0: HR 1.70, 95% CI 1.23-2.34, p=0.001; score 2 v 0: HR 3.61, 95% CI 2.46-5.30, p<0.001). In ER positive disease, a higher necrosis-TSP score was associated with worse CSS (10yr CSS 87% v 80% v 67%, p=0.001; score 1 v 0: HR 1.55, 95% CI 1.07-2.27, p=0.022; score 2 v 0: HR 2.89, 95% CI 1.70-4.90, p<0.001). In ER negative disease, a score of 2 was

associated with worse CSS than a score of 0 (10yr CSS 86% v 76% v 57%, p<0.001; score 1 v 0: HR 1.97, 95% CI 0.99-3.89, p=0.052; score 2 v 0: HR 4.15, 95% CI 2.03-8.47, p<0.001).

a) b) c)

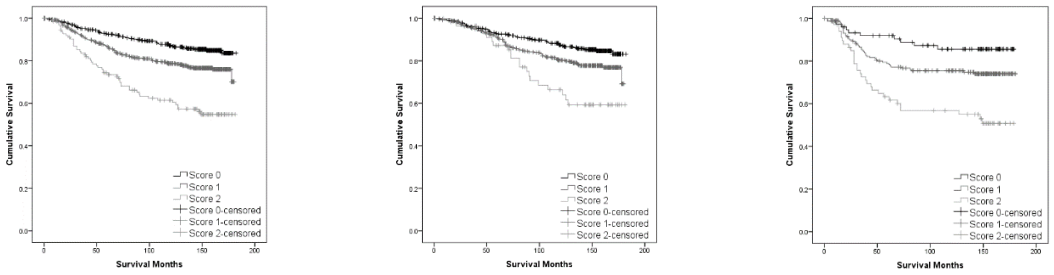

The relationship between the necrosis-TSP score and CSS in primary operable ductal breast cancer. Kaplan Meier survival graphs for CSS in patients with a necrosis-TSP score of 2 compared to 1 compared to 0, in ductal breast cancer. a) Full cohort n=1080, p<0.001; b) ER positive n=737, p<0.001; c) ER negative n=340, p<0.001

In ER+/HER2- disease, a higher score was associated with worse CSS (10yr CSS 88% v 80% v 64%, p=0.001; score 1 v 0: HR 1.57, 95% CI 1.01-2.44, p=0.046; score 2 v 0: HR 3.31, 95% CI 1.86-5.91, p<0.001). In ER+/HER2+ disease, the necrosis-TSP score was not significantly associated with CSS (10yr CSS 76% v 63% v 74%, p=0.173; score 1 v 0: HR 2.11, 95% CI 0.88-5.11, p=0.096; score 2 v 0: HR 1.24, 95% CI 0.26-5.86, p=0.784). In ER-/HER2+ cancers, the necrosis-TSP score was not significantly associated with CSS (10yr CSS 74% v 75% v 55%, p=0.116; score 1 v 0: HR 0.89, 95% CI 0.25-3.24, p=0.862; score 2 v 0: HR 2.07, 95% CI 0.60-7.21, p=0.252). In ER-/HER2- cancer, a score of 2 was associated with worse CSS compared to a score of 0 (10yr CSS 85% v 75% v 54%, p=0.003; score 1 v 0: HR 1.95, 95% CI 0.86-4.39, p=0.108; score 2 v 0: HR 4.35, 95% CI 1.80-10.50, p=0.001).

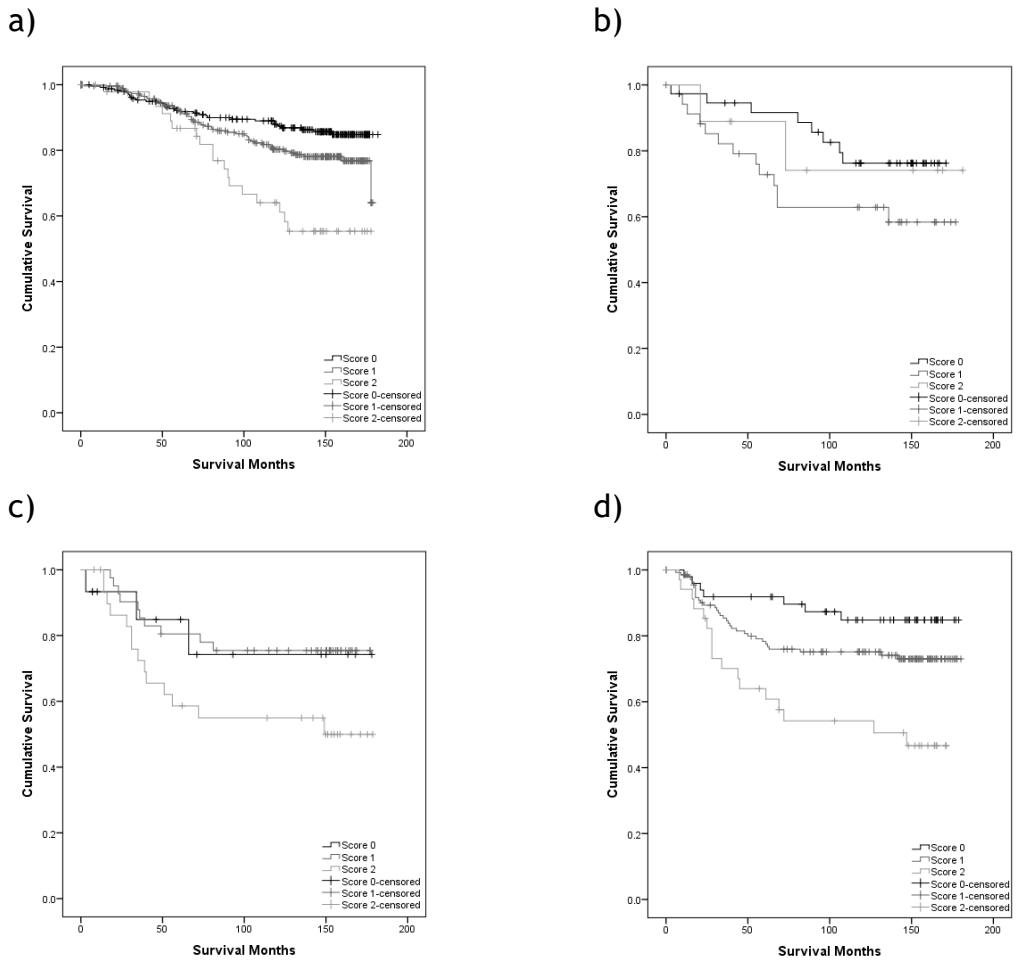

The relationship between the necrosis-TSP score and CSS in primary operable ductal breast cancer, by molecular subtype. Kaplan Meier survival graphs for CSS in patients with a necrosis-TSP score of 2 compared to 1 compared to 0, in ductal breast cancer. a) ER+/HER2- n=563, p<0.001; b) ER+/HER2+ n=81, p=0.222; c) ER-/HER2+ n=87, p=0.091; d) ER-/HER2- n=221, p=0.001

Associations between the necrosis-TSP score and clinicopathological characteristics in ductal breast cancer

A high necrosis-TSP score was significantly associated with larger tumour size (p<0.001), higher tumour grade (p<0.001), nodal positivity (p=0.006), ER and PR negativity (p<0.001, p<0.001), HER2 positivity (p<0.001) and higher KM grade (p<0.001).

Associations between the budding-TSP score and CSS in ductal breast cancer

In the full ductal cohort, a higher budding-TSP score was associated with worse CSS (10yr CSS 84% v 76% v 70%, p=0.001; score 1 v 0: HR 1.58, 95% CI 1.19-2.10, p=0.002; score 2 v 0: HR 2.05, 95% CI 1.38-3.06, p<0.001). In ER positive disease, a score of 2 was significantly associated with worse CSS compared to a score of 0 (10yr CSS 83% v 84% v 74%, p=0.139; score 1 v 0: HR 1.00, 95% CI 0.69-1.47,

p=0.985; score 2 v 0: HR 1.72, 95% CI 1.07-2.76, p=0.026). In ER negative disease, a higher combined score was associated with worse CSS (10yr CSS 85% v 59% v 53%, p<0.001; score 1 v 0: HR 3.07, 95% CI 1.96-4.81, p<0.001; score 2 v 0: HR 3.62, 95% CI 1.73-7.59, p=0.001).

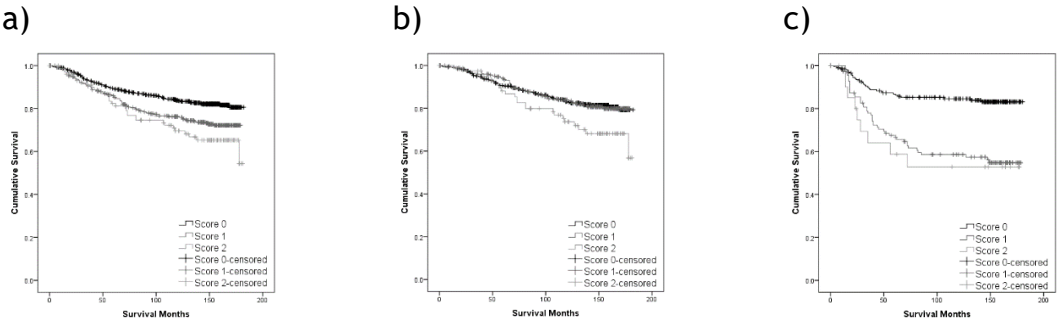

The relationship between the budding-TSP score and CSS in primary operable ductal breast cancer. Kaplan Meier survival graphs for CSS in patients with a budding-TSP score of 2 compared to 1 compared to 0, in ductal breast cancer. a) Full cohort n=1080, p<0.001; b) ER positive n=737, p=0.059; c) ER negative n=340, p<0.001.

In ER+/HER2- disease, a score of 2 was significantly associated with worse CSS than a score of 0 (10yr CSS 83% v 85% v 72%, p=0.120; score 1 v 0: HR 1.01, 95% CI 0.65-1.57, p=0.959; score 2 v 0: HR 1.80, 95% CI 1.06-3.03, p=0.028). In ER+/HER2+ disease, the combined score was not significantly associated with CSS (10yr CSS 72% v 65% v 74%, p=0.717; score 1 v 0: HR 1.32, 95% CI 0.55-3.19, p=0.534; score 2 v 0: HR 0.94, 95% CI 0.21-4.16, p=0.933). In ER-/HER2+ cancers, a higher combined score was associated with worse CSS (10yr CSS 84% v 58% v 29%, p=0.002; score 1 v 0: HR 3.25, 95% CI 1.27-8.31, p=0.014; score 2 v 0: HR 9.12, 95% CI 2.74-30.35, p<0.001). In ER-/HER2- disease, a score of 1 was significantly associated with worse CSS compared to a score of 0 (10yr CSS 84% v 55% v 68%, p<0.001; score 1 v 0: HR 3.17, 95% CI 1.85-5.43, p<0.001; score 2 v 0: HR 1.91, 95% CI 0.66-5.50, p=0.233).

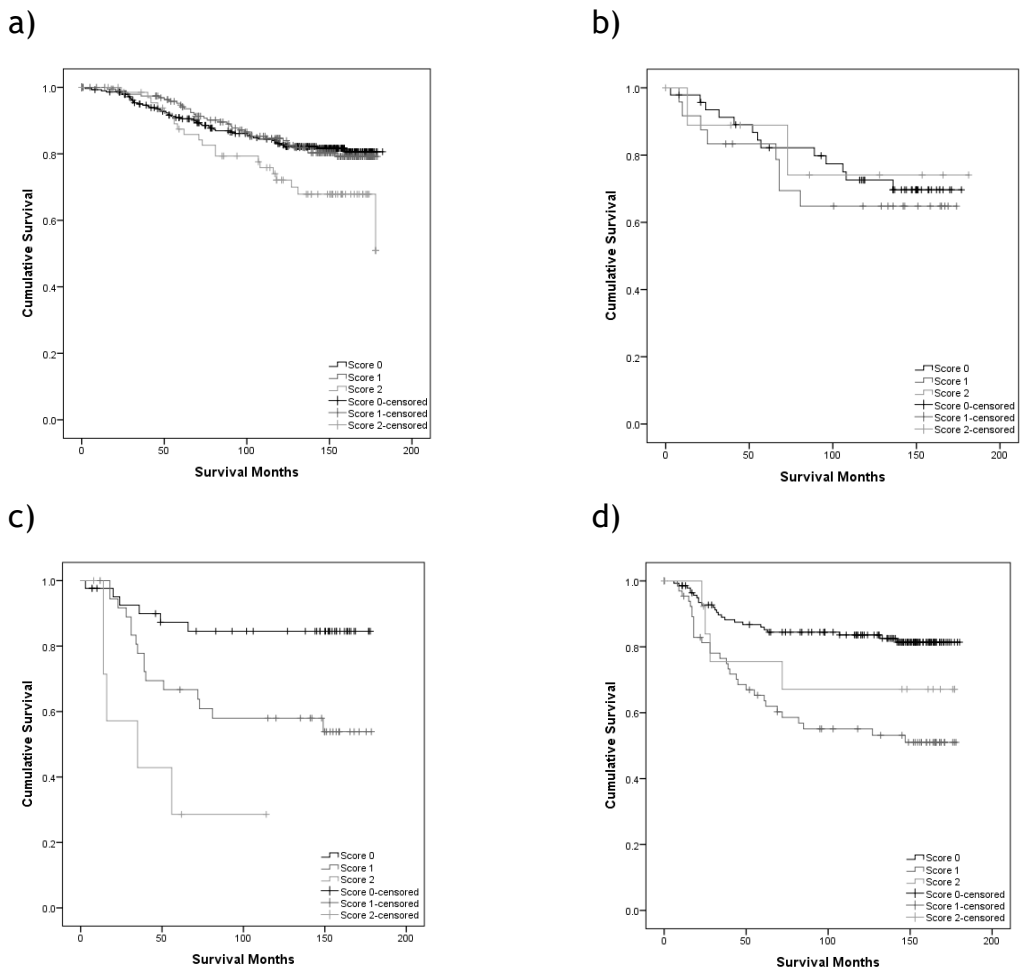

The relationship between the budding-TSP score and CSS in primary operable ductal breast cancer, by molecular subtype. Kaplan Meier survival graphs for CSS in patients with a budding-TSP score of 2 compared to 1 compared to 0, in ductal breast cancer. a) ER+/HER2- n=563, p=0.063; b) ER+/HER2+ n=81, p=0.801; c) ER-/HER2+ n=87, p<0.001; d) ER-/HER2- n=221, p<0.001.

Associations between the budding-TSP score and clinicopathological characteristics in ductal breast cancer

A high budding-TSP score was significantly associated with lower tumour grade (p<0.001), nodal positivity (p=0.006), ER positivity (p=0.023) and lower KM grade (p=0.001).

Associations between the necrosis-budding-TSP score and CSS in ductal breast cancer

In the full ductal cohort, scores of 2 and 3 were associated with worse CSS compared to a score of 0 (10yr CSS 87% v 83% v 69% v 41%, p<0.001; score 1 v 0: HR 1.42, 95% CI 0.98-2.04, p=0.063; score 2 v 0: HR 2.76, 95% CI 1.88-4.04, p<0.001; score 3 v 0: HR 5.85, 95% CI 3.46-9.90, p<0.001). Scores of 2 and 3 were associated with worse CSS compared to a score of 0 in both ER positive (10yr CSS 86% v 84% v 78% v 48%, p<0.001; score 1 v 0: HR 1.21, 95% CI 0.80-1.84,

p=0.370; score 2 v 0: HR 1.73, 95% CI 1.07-2.79, p=0.025; score 3 v 0: HR 4.35, 95% CI 2.26-8.37, p<0.001) and ER negative disease (10yr CSS 91% v 80% v 56% v 31%, p<0.001; score 1 v 0: HR 2.54, 95% CI 1.00-6.49, p=0.051; score 2 v 0: HR 6.58, 95% CI 2.59-16.70, p<0.001; score 3 v 0: HR 13.01, 95% CI 4.35-38.94, p<0.001).

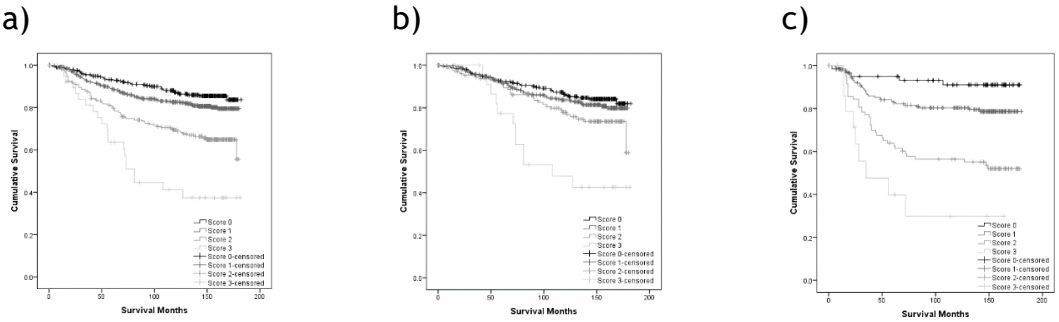

The relationship between the necrosis-budding-TSP score and CSS in primary operable ductal breast cancer. Kaplan Meier survival graphs for CSS in patients with a necrosis-budding-TSP score of 3 compared to 2 compared to 1 compared to 0, in ductal breast cancer. a) Full cohort n=1080, p<0.001; b) ER positive n=737, p<0.001; c) ER negative n=340, p<0.001.

In ER+/HER2- disease, a score of 3 was significantly associated with worse CSS than a score of 0 (10yr CSS 86% v 84% v 79% v 42%, p<0.001; score 1 v 0: HR 1.14, 95% CI 0.70-1.86, p=0.592; score 2 v 0: HR 1.53, 95% CI 0.88-2.66, p=0.129; score 3 v 0: HR 5.04, 95% CI 2.49-10.20, p<0.001). There was no significant association between the combined score and CSS in either ER+/HER2+ (score 1 v 0: HR 2.22, 95% CI 0.81-6.12, p=0.123; score 2 v 0: HR 2.61, 95% CI 0.84-8.11, p=0.097; score 3 v 0: HR 1.21, 95% CI 0.15-10.06, p=0.861), or ER-/HER2+ cancers (10yr CSS 73% v 84% v 55% v 29%, p=0.005; score 1 v 0: HR 0.55, 95% CI 0.11-2.74, p=0.467; score 2 v 0: HR 1.91, 95% CI 0.43-8.40, p=0.393; score 3 v 0: HR 4.92, 95% CI 0.95-25.51, p=0.058). In HER2 negative cancers, a score of 2 or 3 was associated with worse CSS compared to a score of 0 (10yr CSS 92% v 79% v 56% v 36%, p<0.001; score 1 v 0: HR 3.10, 95% CI 0.94-10.21, p=0.063; score 2 v 0: HR 7.53, 95% CI 2.27-25.01, p=0.001; score 3 v 0: HR 10.77, 95% CI 2.40-48.30, p=0.002).

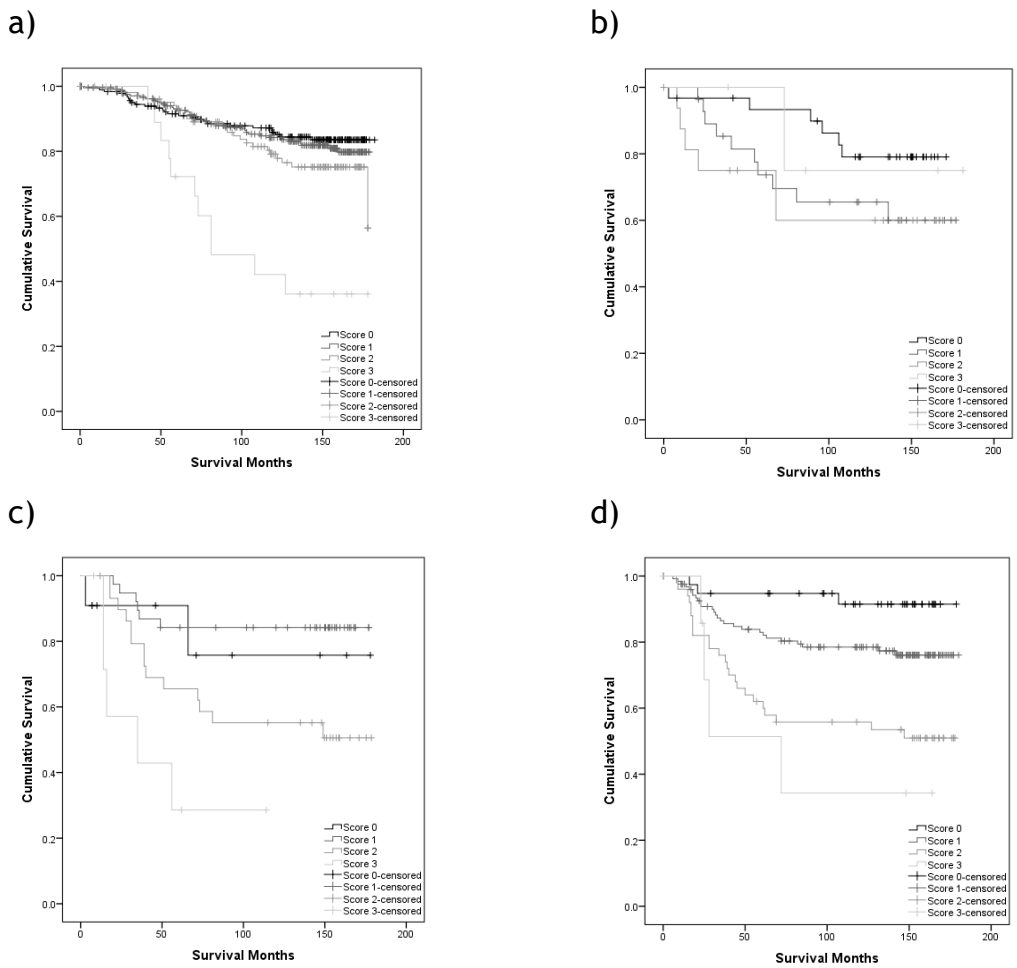

The relationship between the necrosis-budding-TSP score and CSS in primary operable ductal breast cancer, by molecular subtype. Kaplan Meier survival graphs for CSS in patients with a necrosis-budding-TSP score of 3 compared to 2 compared to 1 compared to 0, in ductal breast cancer. a) ER+/HER2- n=563, p<0.001; b) ER+/HER2+ n=81, p=0.296; c) ER-/HER2+ n=87, p=0.001; d) ER-/HER2- n=221, p<0.001.

Associations between the necrosis-budding-TSP score and clinicopathological characteristics in ductal breast cancer

A high combined necrosis-budding-TSP score was associated with larger tumour size (0.003), nodal (p<0.001) and HER2 positivity (p=0.006), ER and PR negativity (p<0.001, p<0.001) and higher KM score (p<0.001).

List of References

1. UK CR. Cancer Research UK Cancer Statistics 2018 [Available from: https://www.cancerresearchuk.org/health-professional/cancer-statistics/statistics-by-cancer-type/breast-cancer.
2. Radiologists TRCo. Guidance on screening and symptomatic breast imaging.: Clinical Radiology; 2019 [updated November 2019. Fourth edition.:[Available from: https://associationofbreastsurgery.org.uk/media/251901/guidance-on-screening-and-symptomatic-breast-imaging-4th-edition.pdf.
3. Brown KF, Rumgay H, Dunlop C, Ryan M, Quartly F, Cox A, et al. The fraction of cancer attributable to modifiable risk factors in England, Wales, Scotland, Northern Ireland, and the United Kingdom in 2015. British journal of cancer. 2018;118(8):1130-41.
4. Koo MM, von Wagner C, Abel GA, McPhail S, Rubin GP, Lyratzopoulos G. Typical and atypical presenting symptoms of breast cancer and their associations with diagnostic intervals: Evidence from a national audit of cancer diagnosis. Cancer epidemiology. 2017;48:140-6.
5. Scotland ISD. Scottish Breast Screening Programme: Information Services Division Scotland; [Available from: https://www.isdscotland.org/Health-Topics/Cancer/Breast-Screening/.
6. Willett A. Best practice guidelines for patients presenting with breast symptoms. In: Michell MJ, editor.: UK Cancer Reform Strategy Breast Cancer Working Group; 2010.
7. (NICE) NIoCE. NICE guideline 101. Early and locally advanced breast cancer:
diagnosis and management: NICE; 2018 [updated 18/07/2018. Available from: https://www.nice.org.uk/guidance/ng101/resources/early-and-locally-advanced-breast-cancer-diagnosis-and-management-pdf-66141532913605.
8. Elston CW, Ellis IO. Pathological prognostic factors in breast cancer. I. The value of histological grade in breast cancer: experience from a large study with long-term follow-up. Histopathology. 1991;19(5):403-10.
9. Williams NS BC, O'Connell PR. Bailey & Love's Short Practice of Surgery. 25th ed: Edward Arnold Ltd.; 2008.
10. Chand N, Cutress RI, Oeppen RS, Agrawal A. Staging Investigations in Breast Cancer: Collective Opinion of UK Breast Surgeons. International journal of breast cancer. 2013;2013:506172.
11. Surgical guidelines for the management of breast cancer. European journal of surgical oncology : the journal of the European Society of Surgical Oncology and the British Association of Surgical Oncology. 2009;35 Suppl 1:1-22.
12. Barter S BP. Recommendations for cross-sectional imaging in cancer management, Second edition. The Royal College of Radiologists; 2014.
13. Patanaphan V, Salazar OM, Risco R. Breast cancer: metastatic patterns and their prognosis. South Med J. 1988;81(9):1109-12.
14. Saini KS, Taylor C, Ramirez AJ, Palmieri C, Gunnarsson U, Schmoll HJ, et al. Role of the multidisciplinary team in breast cancer management: results from a large international survey involving 39 countries. Annals of oncology : official journal of the European Society for Medical Oncology. 2012;23(4):853-9.
15. Taylor C, Shewbridge A, Harris J, Green JS. Benefits of multidisciplinary teamwork in the management of breast cancer. Breast cancer (Dove Medical Press). 2013;5:79-85.

16. Kesson EM, Allardice GM, George WD, Burns HJ, Morrison DS. Effects of multidisciplinary team working on breast cancer survival: retrospective, comparative, interventional cohort study of 13 722 women. BMJ (Clinical research ed). 2012;344:e2718.
17. Li CI, Anderson BO, Daling JR, Moe RE. Trends in incidence rates of invasive lobular and ductal breast carcinoma. Jama. 2003;289(11):1421-4.
18. Williams C, Lin CY. Oestrogen receptors in breast cancer: basic mechanisms and clinical implications. Ecancermedicalscience. 2013;7:370.
19. (NICE) NIfHaCE. Diagnostics Assessment Programme. Gene expression profiling and expanded immunohistochemistry tests to guide selection of chemotherapy regimes in breast cancer management.2011 24/01/2019. Available from: https://www.nice.org.uk/guidance/dg10/documents/gep-and-ihc-tests-for-breast-cancer-assessment-final-scope2.
20. Daniel AR, Hagan CR, Lange CA. Progesterone receptor action: defining a role in breast cancer. Expert review of endocrinology & metabolism. 2011;6(3):359-69.
21. Campbell EJ, Tesson M, Doogan F, Mohammed ZMA, Mallon E, Edwards J. The combined endocrine receptor in breast cancer, a novel approach to traditional hormone receptor interpretation and a better discriminator of outcome than ER and PR alone. British journal of cancer. 2016;115(8):967-73.
22. Blows FM, Driver KE, Schmidt MK, Broeks A, van Leeuwen FE, Wesseling J, et al. Subtyping of breast cancer by immunohistochemistry to investigate a relationship between subtype and short and long term survival: a collaborative analysis of data for 10,159 cases from 12 studies. PLoS Med. 2010;7(5):e1000279.
23. Mohammed H, Russell IA, Stark R, Rueda OM, Hickey TE, Tarulli GA, et al. Progesterone receptor modulates ERalpha action in breast cancer. Nature. 2015;523(7560):313-7.
24. Purdie CA, Quinlan P, Jordan LB, Ashfield A, Ogston S, Dewar JA, et al. Progesterone receptor expression is an independent prognostic variable in early breast cancer: a population-based study. British journal of cancer. 2014;110(3):565-72.
25. Mitri Z, Constantine T, O'Regan R. The HER2 Receptor in Breast Cancer: Pathophysiology, Clinical Use, and New Advances in Therapy. Chemotherapy research and practice. 2012;2012:743193.
26. Goldhirsch A, Wood WC, Coates AS, Gelber RD, Thürlimann B, Senn HJ. Strategies for subtypes--dealing with the diversity of breast cancer: highlights of the St. Gallen International Expert Consensus on the Primary Therapy of Early Breast Cancer 2011. Annals of oncology : official journal of the European Society for Medical Oncology. 2011;22(8):1736-47.
27. Network SIG. Treatment of primary breast cancer. A national clinical guideline. 2013.
28. Pilewskie M, Morrow M. Margins in breast cancer: How much is enough? Cancer. 2018;124(7):1335-41.
29. Jatoi I, Proschan MA. Randomized trials of breast-conserving therapy versus mastectomy for primary breast cancer: a pooled analysis of updated results. Am J Clin Oncol. 2005;28(3):289-94.
30. Morrow ES, Stallard S, Doughty J, Malyon A, Barber M, Dixon JM, et al. Oncoplastic breast conservation occupies a niche between standard breast conservation and mastectomy - A population-based prospective audit in Scotland. European journal of surgical oncology : the journal of the European Society of Surgical Oncology and the British Association of Surgical Oncology. 2019.

31. Waljee JF, Hu ES, Ubel PA, Smith DM, Newman LA, Alderman AK. Effect of esthetic outcome after breast-conserving surgery on psychosocial functioning and quality of life. Journal of clinical oncology : official journal of the American Society of Clinical Oncology. 2008;26(20):3331-7.
32. Losken A, Hart AM, Broecker JS, Styblo TM, Carlson GW. Oncoplastic Breast Reduction Technique and Outcomes: An Evolution over 20 Years. Plastic and reconstructive surgery. 2017;139(4):824e-33e.
33. Romics L, Macaskill EJ, Fernandez T, Simpson L, Morrow E, Pitsinis V, et al. A population-based audit of surgical practice and outcomes of oncoplastic breast conservations in Scotland - An analysis of 589 patients. European journal of surgical oncology : the journal of the European Society of Surgical Oncology and the British Association of Surgical Oncology. 2018;44(7):939-44.
34. Campbell EJ, Romics L. Oncological safety and cosmetic outcomes in oncoplastic breast conservation surgery, a review of the best level of evidence literature. Breast cancer (Dove Medical Press). 2017;9:521-30.
35. Robb GL. Immediate versus delayed breast reconstruction. Breast Cancer Research. 2007;9(1):S9.
36. Baskar R, Dai J, Wenlong N, Yeo R, Yeoh KW. Biological response of cancer cells to radiation treatment. Frontiers in molecular biosciences. 2014;1:24.
37. Bryan J. From breast cancer treatment to prevention: the story of tamoxifen. The Pharmaceutical Journal. 2009;282:137.
38. Howell A, Cuzick J, Baum M, Buzdar A, Dowsett M, Forbes JF, et al. Results of the ATAC (Arimidex, Tamoxifen, Alone or in Combination) trial after completion of 5 years' adjuvant treatment for breast cancer. Lancet. 2005;365(9453):60-2.
39. Cambridge Uo. Predict. Breast Cancer [2.1:[Available from: https://breast.predict.nhs.uk/tool.
40. NICE. Pertuzumab for the neoadjuvant treatment of HER2-positive breast cancer [TA424} 2016 [updated October 2020. Available from: https://www.nice.org.uk/guidance/ta424.
41. NICE. Pertuzumab for adjuvant treatment of HER2-positive early stage breast cancer [TA569] 2019 [updated 20/03/2019. Available from: https://www.nice.org.uk/guidance/ta569.
42. von Minckwitz G, Huang C-S, Mano MS, Loibl S, Mamounas EP, Untch M, et al. Trastuzumab Emtansine for Residual Invasive HER2-Positive Breast Cancer. New England Journal of Medicine. 2018;380(7):617-28.
43. Swoboda A, Nanda R. Immune Checkpoint Blockade for Breast Cancer. Cancer treatment and research. 2018;173:155-65.
44. Wein L, Luen SJ, Savas P, Salgado R, Loi S. Checkpoint blockade in the treatment of breast cancer: current status and future directions. British journal of cancer. 2018;119(1):4-11.
45. Kunkler IH, Dixon JM, Maclennan M, Russell NS. European interpretation of North American post mastectomy radiotherapy guideline update. European journal of surgical oncology : the journal of the European Society of Surgical Oncology and the British Association of Surgical Oncology. 2017;43(10):1805-7.
46. Gray E, Donten A, Payne K, Hall PS. Survival estimates stratified by the Nottingham Prognostic Index for early breast cancer: a systematic review and meta-analysis of observational studies. Systematic Reviews. 2018;7(1):142.
47. Green AR, Soria D, Powe DG, Nolan CC, Aleskandarany M, Szász MA, et al. Nottingham prognostic index plus (NPI+) predicts risk of distant metastases in

primary breast cancer. Breast cancer research and treatment. 2016;157(1):65-75.
48. Cambridge Uo. Predict Breast Cancer Tool [2.2:[Available from: https://breast.predict.nhs.uk/tool.
49. Gray E, Marti J, Brewster DH, Wyatt JC, Hall PS, the SAG. Independent validation of the PREDICT breast cancer prognosis prediction tool in 45,789 patients using Scottish Cancer Registry data. British journal of cancer. 2018;119(7):808-14.
50. Candido Dos Reis FJ, Wishart GC, Dicks EM, Greenberg D, Rashbass J, Schmidt MK, et al. An updated PREDICT breast cancer prognostication and treatment benefit prediction model with independent validation. Breast cancer research : BCR. 2017;19(1):58.
51. Excellence NIfHaC. Nice Guideline 101. Early and locally advanced breast cancer: diagnosis and management2018 September 2018. Available from: nice.org.uk/guidance/ng101.
52. Evidence NIoC. Tumour profiling tests to guide adjuvant chemotherapy decisions in early breast cancer. Diagnostics Guidance [DG34] 2018 [updated 19/12/2018. Available from: https://www.nice.org.uk/guidance/dg34/chapter/1-Recommendations.
53. Health G. Oncotype DX Breast Recurrence Score 2004 [updated 2021. Available from: https://www.oncotypeiq.com/en-GB/breast-cancer/healthcare-professionals/oncotype-dx-breast-recurrence-score/.
54. Sparano JA, Gray RJ, Makower DF, Pritchard KI, Albain KS, Hayes DF, et al. Adjuvant Chemotherapy Guided by a 21-Gene Expression Assay in Breast Cancer. New England Journal of Medicine. 2018;379(2):111-21.
55. Hanahan D, Weinberg RA. Hallmarks of cancer: the next generation. Cell. 2011;144(5):646-74.
56. McAllister SS, Weinberg RA. The tumour-induced systemic environment as a critical regulator of cancer progression and metastasis. Nature cell biology. 2014;16(8):717-27.
57. Coussens LM, Werb Z. Inflammation and cancer. Nature. 2002;420(6917):860-7.
58. Jiang X, Shapiro DJ. The immune system and inflammation in breast cancer. Molecular and cellular endocrinology. 2014;382(1):673-82.
59. LeBien TW, Tedder TF. B lymphocytes: how they develop and function. Blood. 2008;112(5):1570-80.
60. Zúñiga-Pflücker JC. T-cell development made simple. Nature reviews Immunology. 2004;4(1):67-72.
61. Golubovskaya V, Wu L. Different Subsets of T Cells, Memory, Effector Functions, and CAR-T Immunotherapy. Cancers (Basel). 2016;8(3).
62. Morrow ES, Roseweir A, Edwards J. The role of gamma delta T lymphocytes in breast cancer: a review. Transl Res. 2019;203:88-96.
63. Annaratone L, Cascardi E, Vissio E, Sarotto I, Chmielik E, Sapino A, et al. The Multifaceted Nature of Tumor Microenvironment in Breast Carcinomas. Pathobiology. 2020;87(2):125-42.
64. Huang Y, Ma C, Zhang Q, Ye J, Wang F, Zhang Y, et al. CD4+ and CD8+ T cells have opposing roles in breast cancer progression and outcome. Oncotarget. 2015;6(19):17462-78.
65. Miyashita M, Sasano H, Tamaki K, Hirakawa H, Takahashi Y, Nakagawa S, et al. Prognostic significance of tumor-infiltrating CD8+ and FOXP3+ lymphocytes in residual tumors and alterations in these parameters after neoadjuvant

chemotherapy in triple-negative breast cancer: a retrospective multicenter study. Breast cancer research : BCR. 2015;17(1):124.
66. Yu X, Zhang Z, Wang Z, Wu P, Qiu F, Huang J. Prognostic and predictive value of tumor-infiltrating lymphocytes in breast cancer: a systematic review and meta-analysis. Clinical & translational oncology : official publication of the Federation of Spanish Oncology Societies and of the National Cancer Institute of Mexico. 2016;18(5):497-506.
67. Pollheimer MJ, Kornprat P, Lindtner RA, Harbaum L, Schlemmer A, Rehak P, et al. Tumor necrosis is a new promising prognostic factor in colorectal cancer. Human pathology. 2010;41(12):1749-57.
68. Richards CH, Roxburgh CS, Anderson JH, McKee RF, Foulis AK, Horgan PG, et al. Prognostic value of tumour necrosis and host inflammatory responses in colorectal cancer. The British journal of surgery. 2012;99(2):287-94.
69. Hodgson A, Xu B, Satkunasivam R, Downes MR. Tumour front inflammation and necrosis are independent prognostic predictors in high-grade urothelial carcinoma of the bladder. Journal of clinical pathology. 2018;71(2):154-60.
70. Frank I, Blute ML, Cheville JC, Lohse CM, Weaver AL, Zincke H. An outcome prediction model for patients with clear cell renal cell carcinoma treated with radical nephrectomy based on tumor stage, size, grade and necrosis: the SSIGN score. The Journal of urology. 2002;168(6):2395-400.
71. Swinson DE, Jones JL, Richardson D, Cox G, Edwards JG, O'Byrne KJ. Tumour necrosis is an independent prognostic marker in non-small cell lung cancer: correlation with biological variables. Lung cancer (Amsterdam, Netherlands). 2002;37(3):235-40.
72. Gujam FJ, Edwards J, Mohammed ZM, Going JJ, McMillan DC. The relationship between the tumour stroma percentage, clinicopathological characteristics and outcome in patients with operable ductal breast cancer. British journal of cancer. 2014;111(1):157-65.
73. Carlomagno C, Perrone F, Lauria R, de Laurentiis M, Gallo C, Morabito A, et al. Prognostic significance of necrosis, elastosis, fibrosis and inflammatory cell reaction in operable breast cancer. Oncology. 1995;52(4):272-7.
74. Grigore AD, Jolly MK, Jia D, Farach-Carson MC, Levine H. Tumor Budding: The Name is EMT. Partial EMT. Journal of clinical medicine. 2016;5(5).
75. Zlobec I, Lugli A. Tumour budding in colorectal cancer: molecular rationale for clinical translation. Nature reviews Cancer. 2018;18(4):203-4.
76. Sonnenblick A, Shriki A, Galun E, Axelrod JH, Daum H, Rottenberg Y, et al. Tissue microarray-based study of patients with lymph node-positive breast cancer shows tyrosine phosphorylation of signal transducer and activator of transcription 3 (tyrosine705-STAT3) is a marker of good prognosis. Clinical & translational oncology : official publication of the Federation of Spanish Oncology Societies and of the National Cancer Institute of Mexico. 2012;14(3):232-6.
77. Lugli A, Kirsch R, Ajioka Y, Bosman F, Cathomas G, Dawson H, et al. Recommendations for reporting tumor budding in colorectal cancer based on the International Tumor Budding Consensus Conference (ITBCC) 2016. Modern pathology : an official journal of the United States and Canadian Academy of Pathology, Inc. 2017;30(9):1299-311.
78. Gujam FJ, McMillan DC, Mohammed ZM, Edwards J, Going JJ. The relationship between tumour budding, the tumour microenvironment and survival in patients with invasive ductal breast cancer. British journal of cancer. 2015;113(7):1066-74.

79. Salhia B, Trippel M, Pfaltz K, Cihoric N, Grogg A, Ladrach C, et al. High tumor budding stratifies breast cancer with metastatic properties. Breast cancer research and treatment. 2015;150(2):363-71.
80. Liang F, Cao W, Wang Y, Li L, Zhang G, Wang Z. The prognostic value of tumor budding in invasive breast cancer. Pathology, research and practice. 2013;209(5):269-75.
81. O'Shea JJ, Schwartz DM, Villarino AV, Gadina M, McInnes IB, Laurence A. The JAK-STAT pathway: impact on human disease and therapeutic intervention. Annual review of medicine. 2015;66:311-28.
82. Rawlings JS, Rosler KM, Harrison DA. The JAK/STAT signaling pathway. Journal of cell science. 2004;117(Pt 8):1281-3.
83. Harrison DA. The Jak/STAT pathway. Cold Spring Harbor perspectives in biology. 2012;4(3).
84. Chapman RS, Lourenco P, Tonner E, Flint D, Selbert S, Takeda K, et al. The role of Stat3 in apoptosis and mammary gland involution. Conditional deletion of Stat3. Advances in experimental medicine and biology. 2000;480:129-38.
85. Turkson J, Jove R. STAT proteins: novel molecular targets for cancer drug discovery. Oncogene. 2000;19(56):6613-26.
86. Mihara M, Hashizume M, Yoshida H, Suzuki M, Shiina M. IL-6/IL-6 receptor system and its role in physiological and pathological conditions. Clinical science (London, England : 1979). 2012;122(4):143-59.
87. Decker T, Kovarik P. Serine phosphorylation of STATs. Oncogene. 2000;19(21):2628-37.
88. Yu H, Pardoll D, Jove R. STATs in cancer inflammation and immunity: a leading role for STAT3. Nature reviews Cancer. 2009;9(11):798-809.
89. Garcia R, Yu CL, Hudnall A, Catlett R, Nelson KL, Smithgall T, et al. Constitutive activation of Stat3 in fibroblasts transformed by diverse oncoproteins and in breast carcinoma cells. Cell Growth Differ. 1997;8(12):1267-76.
90. Sartor CI, Dziubinski ML, Yu CL, Jove R, Ethier SP. Role of epidermal growth factor receptor and STAT-3 activation in autonomous proliferation of SUM-102PT human breast cancer cells. Cancer research. 1997;57(5):978-87.
91. Li L, Shaw PE. Autocrine-mediated activation of STAT3 correlates with cell proliferation in breast carcinoma lines. The Journal of biological chemistry. 2002;277(20):17397-405.
92. Burke WM, Jin X, Lin HJ, Huang M, Liu R, Reynolds RK, et al. Inhibition of constitutively active Stat3 suppresses growth of human ovarian and breast cancer cells. Oncogene. 2001;20(55):7925-34.
93. Garcia R, Bowman TL, Niu G, Yu H, Minton S, Muro-Cacho CA, et al. Constitutive activation of Stat3 by the Src and JAK tyrosine kinases participates in growth regulation of human breast carcinoma cells. Oncogene. 2001;20(20):2499-513.
94. Ranger JJ, Levy DE, Shahalizadeh S, Hallett M, Muller WJ. Identification of a Stat3-dependent transcription regulatory network involved in metastatic progression. Cancer research. 2009;69(17):6823-30.
95. Barbieri I, Pensa S, Pannellini T, Quaglino E, Maritano D, Demaria M, et al. Constitutively active Stat3 enhances neu-mediated migration and metastasis in mammary tumors via upregulation of Cten. Cancer research. 2010;70(6):2558-67.
96. Barbieri I, Quaglino E, Maritano D, Pannellini T, Riera L, Cavallo F, et al. Stat3 is required for anchorage-independent growth and metastasis but not for

mammary tumor development downstream of the ErbB-2 oncogene. Mol Carcinog. 2010;49(2):114-20.
97. Ling X, Arlinghaus RB. Knockdown of STAT3 expression by RNA interference inhibits the induction of breast tumors in immunocompetent mice. Cancer research. 2005;65(7):2532-6.
98. Song H, Wang R, Wang S, Lin J. A low-molecular-weight compound discovered through virtual database screening inhibits Stat3 function in breast cancer cells. Proceedings of the National Academy of Sciences of the United States of America. 2005;102(13):4700-5.
99. Zhao W, Jaganathan S, Turkson J. A cell-permeable Stat3 SH2 domain mimetic inhibits Stat3 activation and induces antitumor cell effects in vitro. The Journal of biological chemistry. 2010;285(46):35855-65.
100. Lin L, Hutzen B, Zuo M, Ball S, Deangelis S, Foust E, et al. Novel STAT3 phosphorylation inhibitors exhibit potent growth-suppressive activity in pancreatic and breast cancer cells. Cancer research. 2010;70(6):2445-54.
101. Yeh YT, Ou-Yang F, Chen IF, Yang SF, Wang YY, Chuang HY, et al. STAT3 ser727 phosphorylation and its association with negative estrogen receptor status in breast infiltrating ductal carcinoma. International journal of cancer. 2006;118(12):2943-7.
102. Sato T, Neilson LM, Peck AR, Liu C, Tran TH, Witkiewicz A, et al. Signal transducer and activator of transcription-3 and breast cancer prognosis. American journal of cancer research. 2011;1(3):347-55.
103. Sheen-Chen SM, Huang CC, Tang RP, Chou FF, Eng HL. Prognostic value of signal transducers and activators of transcription 3 in breast cancer. Cancer epidemiology, biomarkers & prevention : a publication of the American Association for Cancer Research, cosponsored by the American Society of Preventive Oncology. 2008;17(9):2286-90.
104. Dolled-Filhart M, Camp RL, Kowalski DP, Smith BL, Rimm DL. Tissue microarray analysis of signal transducers and activators of transcription 3 (Stat3) and phospho-Stat3 (Tyr705) in node-negative breast cancer shows nuclear localization is associated with a better prognosis. Clinical cancer research : an official journal of the American Association for Cancer Research. 2003;9(2):594-600.
105. Gujam FJ, McMillan DC, Edwards J. The relationship between total and phosphorylated STAT1 and STAT3 tumour cell expression, components of tumour microenvironment and survival in patients with invasive ductal breast cancer. Oncotarget. 2016;7(47):77607-21.
106. Aleskandarany MA, Agarwal D, Negm OH, Ball G, Elmouna A, Ashankyty I, et al. The prognostic significance of STAT3 in invasive breast cancer: analysis of protein and mRNA expressions in large cohorts. Breast cancer research and treatment. 2016;156(1):9-20.
107. Sonnenblick A, Uziely B, Nechushtan H, Kadouri L, Galun E, Axelrod JH, et al. Tumor STAT3 tyrosine phosphorylation status, as a predictor of benefit from adjuvant chemotherapy for breast cancer. Breast cancer research and treatment. 2013;138(2):407-13.
108. Ikpatt O, Ndoma-Egba R, Collan Y. Prognostic value of necrosis in Nigerian breast cancer. Adv Clin Path. 2002;6(1):31-7.
109. UK CR. Cancer Research UK Cancer Statistics 2017 [Available from: http://www.cancerresearchuk.org/health-professional/cancer-statistics/statistics-by-cancer-type/breast-cancer.
110. Page DL. Prognosis and breast cancer. Recognition of lethal and favorable prognostic types. The American journal of surgical pathology. 1991;15(4):334-49.

111. Rosen PP, Groshen S, Kinne DW, Norton L. Factors influencing prognosis in node-negative breast carcinoma: analysis of 767 T1N0M0/T2N0M0 patients with long-term follow-up. Journal of clinical oncology : official journal of the American Society of Clinical Oncology. 1993;11(11):2090-100.
112. Simpson JF, Page DL. Status of breast cancer prognostication based on histopathologic data. American journal of clinical pathology. 1994;102(4 Suppl 1):S3-8.
113. Fitzgibbons PL, Page DL, Weaver D, Thor AD, Allred DC, Clark GM, et al. Prognostic factors in breast cancer. College of American Pathologists Consensus Statement 1999. Archives of pathology & laboratory medicine. 2000;124(7):966-78.
114. Rakha EA, El-Sayed ME, Lee AH, Elston CW, Grainge MJ, Hodi Z, et al. Prognostic significance of Nottingham histologic grade in invasive breast carcinoma. Journal of clinical oncology : official journal of the American Society of Clinical Oncology. 2008;26(19):3153-8.
115. Paik S, Tang G, Shak S, Kim C, Baker J, Kim W, et al. Gene expression and benefit of chemotherapy in women with node-negative, estrogen receptor-positive breast cancer. Journal of clinical oncology : official journal of the American Society of Clinical Oncology. 2006;24(23):3726-34.
116. Dowsett M, Cuzick J, Wale C, Forbes J, Mallon EA, Salter J, et al. Prediction of risk of distant recurrence using the 21-gene recurrence score in node-negative and node-positive postmenopausal patients with breast cancer treated with anastrozole or tamoxifen: a TransATAC study. Journal of clinical oncology : official journal of the American Society of Clinical Oncology. 2010;28(11):1829-34.
117. Sparano JA, Gray RJ, Makower DF, Pritchard KI, Albain KS, Hayes DF, et al. Prospective Validation of a 21-Gene Expression Assay in Breast Cancer. The New England journal of medicine. 2015;373(21):2005-14.
118. Coussens LM, Werb Z. Inflammation and cancer. Nature. 2002;420(6917):860-7.
119. DeNardo DG, Coussens LM. Inflammation and breast cancer. Balancing immune response: crosstalk between adaptive and innate immune cells during breast cancer progression. Breast cancer research : BCR. 2007;9(4):212.
120. Dolan RD, McSorley ST, Horgan PG, Laird B, McMillan DC. The role of the systemic inflammatory response in predicting outcomes in patients with advanced inoperable cancer: Systematic review and meta-analysis. Critical reviews in oncology/hematology. 2017;116:134-46.
121. Shinko D, Diakos CI, Clarke SJ, Charles KA. Cancer-related systemic inflammation: The challenges and therapeutic opportunities for personalized medicine. Clinical pharmacology and therapeutics. 2017.
122. Cihan YB, Arslan A, Cetindag MF, Mutlu H. Lack of prognostic value of blood parameters in patients receiving adjuvant radiotherapy for breast cancer. Asian Pac J Cancer Prev. 2014;15(10):4225-31.
123. Wulaningsih W, Holmberg L, Garmo H, Malmstrom H, Lambe M, Hammar N, et al. Prediagnostic serum inflammatory markers in relation to breast cancer risk, severity at diagnosis and survival in breast cancer patients. Carcinogenesis. 2015;36(10):1121-8.
124. Wariss BR, de Souza Abrahao K, de Aguiar SS, Bergmann A, Thuler LCS. Effectiveness of four inflammatory markers in predicting prognosis in 2374 women with breast cancer. Maturitas. 2017;101:51-6.

125. Wen J, Ye F, Huang X, Li S, Yang L, Xiao X, et al. Prognostic Significance of Preoperative Circulating Monocyte Count in Patients With Breast Cancer: Based on a Large Cohort Study. Medicine (Baltimore). 2015;94(49):e2266.
126. Taucher S, Salat A, Gnant M, Kwasny W, Mlineritsch B, Menzel RC, et al. Impact of pretreatment thrombocytosis on survival in primary breast cancer. Thrombosis and haemostasis. 2003;89(6):1098-106.
127. Gu ML, Yuan CJ, Liu XM, Zhou YC, Di SH, Sun FF, et al. Pre-treatment Elevated Platelet Count Associates with HER2 Overexpression and Prognosis in Patients with Breast Cancer. Asian Pac J Cancer Prev. 2015;16(13):5537-40.
128. Liu C, Huang Z, Wang Q, Sun B, Ding L, Meng X, et al. Usefulness of neutrophil-to-lymphocyte ratio and platelet-to-lymphocyte ratio in hormone-receptor-negative breast cancer. OncoTargets and therapy. 2016;9:4653-60.
129. Krenn-Pilko S, Langsenlehner U, Thurner EM, Stojakovic T, Pichler M, Gerger A, et al. The elevated preoperative platelet-to-lymphocyte ratio predicts poor prognosis in breast cancer patients. British journal of cancer. 2014;110(10):2524-30.
130. Lee SK, Choi MY, Bae SY, Lee JH, Lee HC, Kil WH, et al. Immediate postoperative inflammation is an important prognostic factor in breast cancer. Oncology. 2015;88(6):337-44.
131. Suppan C, Bjelic-Radisic V, La Garde M, Groselj-Strele A, Eberhard K, Samonigg H, et al. Neutrophil/Lymphocyte ratio has no predictive or prognostic value in breast cancer patients undergoing preoperative systemic therapy. BMC Cancer. 2015;15:1027.
132. Takeuchi H, Kawanaka H, Fukuyama S, Kubo N, Hiroshige S, Yano T. Comparison of the prognostic values of preoperative inflammation-based parameters in patients with breast cancer. PLoS One. 2017;12(5):e0177137.
133. Azab B, Shah N, Radbel J, Tan P, Bhatt V, Vonfrolio S, et al. Pretreatment neutrophil/lymphocyte ratio is superior to platelet/lymphocyte ratio as a predictor of long-term mortality in breast cancer patients. Med Oncol. 2013;30(1):432.
134. Noh H, Eomm M, Han A. Usefulness of pretreatment neutrophil to lymphocyte ratio in predicting disease-specific survival in breast cancer patients. Journal of breast cancer. 2013;16(1):55-9.
135. Forget P, Bentin C, Machiels JP, Berliere M, Coulie PG, De Kock M. Intraoperative use of ketorolac or diclofenac is associated with improved disease-free survival and overall survival in conservative breast cancer surgery. Br J Anaesth. 2014;113 Suppl 1:i82-7.
136. Nakano K, Hosoda M, Yamamoto M, Yamashita H. Prognostic significance of pre-treatment neutrophil: Lymphocyte ratio in japanese patients with breast cancer. Anticancer Research. 2014;34(7):3819-24.
137. Koh YW, Lee HJ, Ahn JH, Lee JW, Gong G. Prognostic significance of the ratio of absolute neutrophil to lymphocyte counts for breast cancer patients with ER/PR-positivity and HER2-negativity in neoadjuvant setting. Tumour Biol. 2014;35(10):9823-30.
138. Dirican A, Kucukzeybek BB, Alacacioglu A, Kucukzeybek Y, Erten C, Varol U, et al. Do the derived neutrophil to lymphocyte ratio and the neutrophil to lymphocyte ratio predict prognosis in breast cancer? Int J Clin Oncol. 2015;20(1):70-81.
139. Yao M, Liu Y, Jin H, Liu X, Lv K, Wei H, et al. Prognostic value of preoperative inflammatory markers in Chinese patients with breast cancer. OncoTargets and therapy. 2014;7:1743-52.

140. Koh CH, Bhoo-Pathy N, Ng KL, Jabir RS, Tan GH, See MH, et al. Utility of pre-treatment neutrophil-lymphocyte ratio and platelet-lymphocyte ratio as prognostic factors in breast cancer. British journal of cancer. 2015;113(1):150-8.
141. Hong J, Mao Y, Chen X, Zhu L, He J, Chen W, et al. Elevated preoperative neutrophil-to-lymphocyte ratio predicts poor disease-free survival in Chinese women with breast cancer. Tumour Biol. 2016;37(3):4135-42.
142. Jia W, Wu J, Jia H, Yang Y, Zhang X, Chen K, et al. The Peripheral Blood Neutrophil-To-Lymphocyte Ratio Is Superior to the Lymphocyte-To-Monocyte Ratio for Predicting the Long-Term Survival of Triple-Negative Breast Cancer Patients. PLoS ONE [Electronic Resource]. 2015;10(11):e0143061.
143. Krenn-Pilko S, Langsenlehner U, Stojakovic T, Pichler M, Gerger A, Kapp KS, et al. The elevated preoperative derived neutrophil-to-lymphocyte ratio predicts poor clinical outcome in breast cancer patients. Tumor Biology. 2016;37(1):361-8.
144. Ni XJ, Zhang XL, Ou-Yang QW, Qian GW, Wang L, Chen S, et al. An elevated peripheral blood lymphocyte-to-monocyte ratio predicts favorable response and prognosis in locally advanced breast cancer following neoadjuvant chemotherapy. PLoS ONE [Electronic Resource]. 2014;9(11):e111886.
145. Al Murri AM, Wilson C, Lannigan A, Doughty JC, Angerson WJ, McArdle CS, et al. Evaluation of the relationship between the systemic inflammatory response and cancer-specific survival in patients with primary operable breast cancer. British journal of cancer. 2007;96(6):891-5.
146. Allin KH, Nordestgaard BG, Flyger H, Bojesen SE. Elevated pre-treatment levels of plasma C-reactive protein are associated with poor prognosis after breast cancer: a cohort study. Breast Cancer Research. 2011;13(3):R55.
147. Sicking I, Edlund K, Wesbuer E, Weyer V, Battista MJ, Lebrecht A, et al. Prognostic influence of pre-operative C-reactive protein in node-negative breast cancer patients. PLoS ONE [Electronic Resource]. 2014;9(10):e111306.
148. Liu X, Meng QH, Ye Y, Hildebrandt MA, Gu J, Wu X. Prognostic significance of pretreatment serum levels of albumin, LDH and total bilirubin in patients with non-metastatic breast cancer. Carcinogenesis. 2015;36(2):243-8.
149. Lis CG, Grutsch JF, Vashi PG, Lammersfeld CA. Is serum albumin an independent predictor of survival in patients with breast cancer? JPEN Journal of parenteral and enteral nutrition. 2003;27(1):10-5.
150. Azab BN, Bhatt VR, Vonfrolio S, Bachir R, Rubinshteyn V, Alkaied H, et al. Value of the pretreatment albumin to globulin ratio in predicting long-term mortality in breast cancer patients. Am J Surg. 2013;206(5):764-70.
151. Watt DG, Proctor MJ, Park JH, Horgan PG, McMillan DC. The neutrophil-platelet score (NPS) predicts survival in primary operable colorectal cancer and a variety of common cancers. PLoS ONE. 2015;10 (11) (no pagination)(e0142159).
152. Templeton AJ, McNamara MG, Seruga B, Vera-Badillo FE, Aneja P, Ocana A, et al. Prognostic Role of Neutrophil-to-Lymphocyte Ratio in Solid Tumors: A Systematic Review and Meta-Analysis. Journal of the National Cancer Institute. 2014;106(6):1-11.
153. Ethier JL, Desautels D, Templeton A, Shah PS, Amir E. Prognostic role of neutrophil-to-lymphocyte ratio in breast cancer: a systematic review and meta-analysis. Breast cancer research : BCR. 2017;19(1):2.
154. Schmidt H, Suciu S, Punt CJ, Gore M, Kruit W, Patel P, et al. Pretreatment levels of peripheral neutrophils and leukocytes as independent predictors of overall survival in patients with American Joint Committee on Cancer Stage IV Melanoma: results of the EORTC 18951 Biochemotherapy Trial. Journal of clinical

oncology : official journal of the American Society of Clinical Oncology. 2007;25(12):1562-9.
155. Teramukai S, Kitano T, Kishida Y, Kawahara M, Kubota K, Komuta K, et al. Pretreatment neutrophil count as an independent prognostic factor in advanced non-small-cell lung cancer: an analysis of Japan Multinational Trial Organisation LC00-03. European journal of cancer (Oxford, England : 1990). 2009;45(11):1950-8.
156. Atzpodien J, Royston P, Wandert T, Reitz M. Metastatic renal carcinoma comprehensive prognostic system. British journal of cancer. 2003;88(3):348-53.
157. Fogar P, Sperti C, Basso D, Sanzari MC, Greco E, Davoli C, et al. Decreased total lymphocyte counts in pancreatic cancer: an index of adverse outcome. Pancreas. 2006;32(1):22-8.
158. Ray-Coquard I, Cropet C, Van Glabbeke M, Sebban C, Le Cesne A, Judson I, et al. Lymphopenia as a prognostic factor for overall survival in advanced carcinomas, sarcomas, and lymphomas. Cancer research. 2009;69(13):5383-91.
159. De Larco JE, Wuertz BR, Furcht LT. The potential role of neutrophils in promoting the metastatic phenotype of tumors releasing interleukin-8. Clinical cancer research : an official journal of the American Association for Cancer Research. 2004;10(15):4895-900.
160. Muller I, Munder M, Kropf P, Hansch GM. Polymorphonuclear neutrophils and T lymphocytes: strange bedfellows or brothers in arms? Trends in immunology. 2009;30(11):522-30.
161. Dunn GP, Old LJ, Schreiber RD. The immunobiology of cancer immunosurveillance and immunoediting. Immunity. 2004;21(2):137-48.
162. Morgan RA, Dudley ME, Wunderlich JR, Hughes MS, Yang JC, Sherry RM, et al. Cancer regression in patients after transfer of genetically engineered lymphocytes. Science (New York, NY). 2006;314(5796):126-9.
163. Proctor MJ, McMillan DC, Morrison DS, Fletcher CD, Horgan PG, Clarke SJ. A derived neutrophil to lymphocyte ratio predicts survival in patients with cancer. British journal of cancer. 2012;107(4):695-9.
164. Gupta D, Lis CG. Pretreatment serum albumin as a predictor of cancer survival: a systematic review of the epidemiological literature. Nutrition journal. 2010;9:69.
165. Seaton K. Albumin concentration controls cancer. Journal of the National Medical Association. 2001;93(12):490-3.
166. Laursen I, Briand P, Lykkesfeldt AE. Serum albumin as a modulator on growth of the human breast cancer cell line, MCF-7. Anticancer Res. 1990;10(2a):343-51.
167. Sonnenschein C, Soto AM, Michaelson CL. Human serum albumin shares the properties of estrocolyone-I, the inhibitor of the proliferation of estrogen-target cells. The Journal of steroid biochemistry and molecular biology. 1996;59(2):147-54.
168. Jamieson NB, Glen P, McMillan DC, McKay CJ, Foulis AK, Carter R, et al. Systemic inflammatory response predicts outcome in patients undergoing resection for ductal adenocarcinoma head of pancreas. British journal of cancer. 2005;92(1):21-3.
169. Crumley ABC, McMillan DC, McKernan M, Going JJ, Shearer CJ, Stuart RC. An elevated C-reactive protein concentration, prior to surgery, predicts poor cancer-specific survival in patients undergoing resection for gastro-oesophageal cancer. British journal of cancer. 2006;94(11):1568-71.
170. Schmid M, Schneitter A, Hinterberger S, Seeber J, Reinthaller A, Hefler L. Association of elevated C-reactive protein levels with an impaired prognosis in

patients with surgically treated endometrial cancer. Obstetrics and gynecology. 2007;110(6):1231-6.
171. Polterauer S, Grimm C, Tempfer C, Sliutz G, Speiser P, Reinthaller A, et al. C-reactive protein is a prognostic parameter in patients with cervical cancer. Gynecologic oncology. 2007;107(1):114-7.
172. Roxburgh CS, McMillan DC. Role of systemic inflammatory response in predicting survival in patients with primary operable cancer. Future oncology (London, England). 2010;6(1):149-63.
173. Coombes RC, Powles TJ, Gazet JC, Ford HT, Sloane JP, Laurence DJ, et al. Biochemical markers in human breast cancer. Lancet. 1977;1(8003):132-4.
174. Williams MR, Turkes A, Pearson D, Griffiths K, Blamey RW. An objective biochemical assessment of therapeutic response in metastatic breast cancer: a study with external review of clinical data. British journal of cancer. 1990;61(1):126-32.
175. Albuquerque KV, Price MR, Badley RA, Jonrup I, Pearson D, Blamey RW, et al. Pre-treatment serum levels of tumour markers in metastatic breast cancer: a prospective assessment of their role in predicting response to therapy and survival. European journal of surgical oncology : the journal of the European Society of Surgical Oncology and the British Association of Surgical Oncology. 1995;21(5):504-9.
176. Al Murri AM, Bartlett JM, Canney PA, Doughty JC, Wilson C, McMillan DC. Evaluation of an inflammation-based prognostic score (GPS) in patients with metastatic breast cancer. British journal of cancer. 2006;94(2):227-30.
177. Proctor MJ, Morrison DS, Talwar D, Balmer SM, Fletcher CD, O'Reilly DS, et al. A comparison of inflammation-based prognostic scores in patients with cancer. A Glasgow Inflammation Outcome Study. European journal of cancer (Oxford, England : 1990). 2011;47(17):2633-41.
178. Azab B, Camacho-Rivera M, Taioli E. Average values and racial differences of neutrophil lymphocyte ratio among a nationally representative sample of United States subjects. PLoS One. 2014;9(11):e112361.
179. Bain B, Seed M, Godsland I. Normal values for peripheral blood white cell counts in women of four different ethnic origins. Journal of clinical pathology. 1984;37(2):188-93.
180. Bain BJ. Ethnic and sex differences in the total and differential white cell count and platelet count. Journal of clinical pathology. 1996;49(8):664-6.
181. Goldhirsch A, Wood WC, Coates AS, Gelber RD, Thurlimann B, Senn HJ. Strategies for subtypes--dealing with the diversity of breast cancer: highlights of the St. Gallen International Expert Consensus on the Primary Therapy of Early Breast Cancer 2011. Annals of oncology : official journal of the European Society for Medical Oncology. 2011;22(8):1736-47.
182. Dai X, Li T, Bai Z, Yang Y, Liu X, Zhan J, et al. Breast cancer intrinsic subtype classification, clinical use and future trends. American journal of cancer research. 2015;5(10):2929-43.
183. Klintrup K, Makinen JM, Kauppila S, Vare PO, Melkko J, Tuominen H, et al. Inflammation and prognosis in colorectal cancer. European journal of cancer (Oxford, England : 1990). 2005;41(17):2645-54.
184. Alexander PG, McMillan DC, Park JH. The local inflammatory response in colorectal cancer - Type, location or density? A systematic review and meta-analysis. Cancer treatment reviews. 2020;83:101949.
185. Teng F, Meng X, Wang X, Yuan J, Liu S, Mu D, et al. Expressions of CD8+TILs, PD-L1 and Foxp3+TILs in stage I NSCLC guiding adjuvant chemotherapy decisions. Oncotarget. 2016;7(39):64318-29.

186. Zhao Y, Ge X, He J, Cheng Y, Wang Z, Wang J, et al. The prognostic value of tumor-infiltrating lymphocytes in colorectal cancer differs by anatomical subsite: a systematic review and meta-analysis. World J Surg Oncol. 2019;17(1):85.
187. Goeppert B, Frauenschuh L, Zucknick M, Stenzinger A, Andrulis M, Klauschen F, et al. Prognostic impact of tumour-infiltrating immune cells on biliary tract cancer. British journal of cancer. 2013;109(10):2665-74.
188. Savas P, Salgado R, Denkert C, Sotiriou C, Darcy PK, Smyth MJ, et al. Clinical relevance of host immunity in breast cancer: from TILs to the clinic. Nat Rev Clin Oncol. 2016;13(4):228-41.
189. Shou J, Zhang Z, Lai Y, Chen Z, Huang J. Worse outcome in breast cancer with higher tumor-infiltrating FOXP3+ Tregs : a systematic review and meta-analysis. BMC Cancer. 2016;16(1):687.
190. Dutta S, Going JJ, Crumley AB, Mohammed Z, Orange C, Edwards J, et al. The relationship between tumour necrosis, tumour proliferation, local and systemic inflammation, microvessel density and survival in patients undergoing potentially curative resection of oesophageal adenocarcinoma. British journal of cancer. 2012;106(4):702-10.
191. Qayyum T, McArdle P, Hilmy M, Going J, Orange C, Seywright M, et al. A prospective study of the role of inflammation in bladder cancer. Curr Urol. 2013;6(4):189-93.
192. Kotoula V, Chatzopoulos K, Lakis S, Alexopoulou Z, Timotheadou E, Zagouri F, et al. Tumors with high-density tumor infiltrating lymphocytes constitute a favorable entity in breast cancer: a pooled analysis of four prospective adjuvant trials. Oncotarget. 2016;7(4):5074-87.
193. Pruneri G, Gray KP, Vingiani A, Viale G, Curigliano G, Criscitiello C, et al. Tumor-infiltrating lymphocytes (TILs) are a powerful prognostic marker in patients with triple-negative breast cancer enrolled in the IBCSG phase III randomized clinical trial 22-00. Breast cancer research and treatment. 2016;158(2):323-31.
194. Asano Y, Kashiwagi S, Goto W, Takada K, Takahashi K, Hatano T, et al. Prediction of survival after neoadjuvant chemotherapy for breast cancer by evaluation of tumor-infiltrating lymphocytes and residual cancer burden. BMC Cancer. 2017;17(1):888.
195. Krishnamurti U, Wetherilt CS, Yang J, Peng L, Li X. Tumor-infiltrating lymphocytes are significantly associated with better overall survival and disease-free survival in triple-negative but not estrogen receptor-positive breast cancers. Human pathology. 2017;64:7-12.
196. Salgado R, Denkert C, Demaria S, Sirtaine N, Klauschen F, Pruneri G, et al. The evaluation of tumor-infiltrating lymphocytes (TILs) in breast cancer: recommendations by an International TILs Working Group 2014. Annals of oncology : official journal of the European Society for Medical Oncology. 2015;26(2):259-71.
197. Hendry S, Salgado R, Gevaert T, Russell PA, John T, Thapa B, et al. Assessing Tumor-infiltrating Lymphocytes in Solid Tumors: A Practical Review for Pathologists and Proposal for a Standardized Method From the International Immunooncology Biomarkers Working Group: Part 1: Assessing the Host Immune Response, TILs in Invasive Breast Carcinoma and Ductal Carcinoma In Situ, Metastatic Tumor Deposits and Areas for Further Research. Adv Anat Pathol. 2017;24(5):235-51.
198. Yang X, Rao J, Yang W, Shui R. Evaluation of the Predictive and Prognostic Values of Stromal Tumor-Infiltrating Lymphocytes in HER2-Positive Breast

Cancers treated with neoadjuvant chemotherapy. Target Oncol. 2018;13(6):757-67.
199. Mao Y, Qu Q, Zhang Y, Liu J, Chen X, Shen K. The value of tumor infiltrating lymphocytes (TILs) for predicting response to neoadjuvant chemotherapy in breast cancer: a systematic review and meta-analysis. PLoS One. 2014;9(12):e115103.
200. Bense RD, Sotiriou C, Piccart-Gebhart MJ, Haanen J, van Vugt M, de Vries EGE, et al. Relevance of Tumor-Infiltrating Immune Cell Composition and Functionality for Disease Outcome in Breast Cancer. Journal of the National Cancer Institute. 2017;109(1).
201. Durgeau A, Virk Y, Corgnac S, Mami-Chouaib F. Recent Advances in Targeting CD8 T-Cell Immunity for More Effective Cancer Immunotherapy. Frontiers in immunology. 2018;9:14.
202. Shaw TN, Houston SA, Wemyss K, Bridgeman HM, Barbera TA, Zangerle-Murray T, et al. Tissue-resident macrophages in the intestine are long lived and defined by Tim-4 and CD4 expression. J Exp Med. 2018;215(6):1507-18.
203. Zhen A, Krutzik SR, Levin BR, Kasparian S, Zack JA, Kitchen SG. CD4 ligation on human blood monocytes triggers macrophage differentiation and enhances HIV infection. J Virol. 2014;88(17):9934-46.
204. UK CR. Cancer Research UK Cancer Statistics 2018 [Available from: https://www.cancerresearchuk.org/health-professional/cancer-statistics/statistics-by-cancer-type/breast-cancer.
205. Goldhirsch A, Wood WC, Coates AS, Gelber RD, Thürlimann B, Senn H. Strategies for subtypes—dealing with the diversity of breast cancer: highlights of the St Gallen International Expert Consensus on the Primary Therapy of Early Breast Cancer 2011. Annals of oncology : official journal of the European Society for Medical Oncology. 2011;22(8):1736-47.
206. Sparano JA, Gray RJ, Makower DF, Pritchard KI, Albain KS, Hayes DF, et al. Adjuvant Chemotherapy Guided by a 21-Gene Expression Assay in Breast Cancer. The New England journal of medicine. 2018;379(2):111-21.
207. Roxburgh CS, McMillan DC. The role of the in situ local inflammatory response in predicting recurrence and survival in patients with primary operable colorectal cancer. Cancer treatment reviews. 2012;38(5):451-66.
208. Almangush A, Karhunen M, Hautaniemi S, Salo T, Leivo I. Prognostic value of tumour budding in oesophageal cancer: a meta-analysis. Histopathology. 2016;68(2):173-82.
209. Beaton C, Twine CP, Williams GL, Radcliffe AG. Systematic review and meta-analysis of histopathological factors influencing the risk of lymph node metastasis in early colorectal cancer. Colorectal disease : the official journal of the Association of Coloproctology of Great Britain and Ireland. 2013;15(7):788-97.
210. Boxberg M, Jesinghaus M, Dorfner C, Mogler C, Drecoll E, Warth A, et al. Tumour budding activity and cell nest size determine patient outcome in oral squamous cell carcinoma: proposal for an adjusted grading system. Histopathology. 2017;70(7):1125-37.
211. Brown M, Sillah K, Griffiths EA, Swindell R, West CM, Page RD, et al. Tumour budding and a low host inflammatory response are associated with a poor prognosis in oesophageal and gastro-oesophageal junction cancers. Histopathology. 2010;56(7):893-9.
212. de Kruijf EM, van Nes JG, van de Velde CJ, Putter H, Smit VT, Liefers GJ, et al. Tumor-stroma ratio in the primary tumor is a prognostic factor in early

breast cancer patients, especially in triple-negative carcinoma patients. Breast cancer research and treatment. 2011;125(3):687-96.
213. Dekker TJ, van de Velde CJ, van Pelt GW, Kroep JR, Julien JP, Smit VT, et al. Prognostic significance of the tumor-stroma ratio: validation study in node-negative premenopausal breast cancer patients from the EORTC perioperative chemotherapy (POP) trial (10854). Breast cancer research and treatment. 2013;139(2):371-9.
214. Huijbers A, Tollenaar RA, v Pelt GW, Zeestraten EC, Dutton S, McConkey CC, et al. The proportion of tumor-stroma as a strong prognosticator for stage II and III colon cancer patients: validation in the VICTOR trial. Annals of oncology : official journal of the European Society for Medical Oncology. 2013;24(1):179-85.
215. Kadota K, Nitadori J, Woo KM, Sima CS, Finley DJ, Rusch VW, et al. Comprehensive pathological analyses in lung squamous cell carcinoma: single cell invasion, nuclear diameter, and tumor budding are independent prognostic factors for worse outcomes. Journal of thoracic oncology : official publication of the International Association for the Study of Lung Cancer. 2014;9(8):1126-39.
216. Karamitopoulou E, Zlobec I, Born D, Kondi-Pafiti A, Lykoudis P, Mellou A, et al. Tumour budding is a strong and independent prognostic factor in pancreatic cancer. European journal of cancer (Oxford, England : 1990). 2013;49(5):1032-9.
217. Lai YH, Wu LC, Li PS, Wu WH, Yang SB, Xia P, et al. Tumour budding is a reproducible index for risk stratification of patients with stage II colon cancer. Colorectal disease : the official journal of the Association of Coloproctology of Great Britain and Ireland. 2014;16(4):259-64.
218. Mesker WE, Junggeburt JM, Szuhai K, de Heer P, Morreau H, Tanke HJ, et al. The carcinoma-stromal ratio of colon carcinoma is an independent factor for survival compared to lymph node status and tumor stage. Cellular oncology : the official journal of the International Society for Cellular Oncology. 2007;29(5):387-98.
219. O'Connor K, Li-Chang HH, Kalloger SE, Peixoto RD, Webber DL, Owen DA, et al. Tumor budding is an independent adverse prognostic factor in pancreatic ductal adenocarcinoma. The American journal of surgical pathology. 2015;39(4):472-8.
220. Park JH, Richards CH, McMillan DC, Horgan PG, Roxburgh CS. The relationship between tumour stroma percentage, the tumour microenvironment and survival in patients with primary operable colorectal cancer. Annals of oncology : official journal of the European Society for Medical Oncology. 2014;25(3):644-51.
221. Seki M, Sano T, Yokoo S, Oyama T. Tumour budding evaluated in biopsy specimens is a useful predictor of prognosis in patients with cN0 early stage oral squamous cell carcinoma. Histopathology. 2017;70(6):869-79.
222. Sengupta S, Lohse CM, Leibovich BC, Frank I, Thompson RH, Webster WS, et al. Histologic coagulative tumor necrosis as a prognostic indicator of renal cell carcinoma aggressiveness. Cancer. 2005;104(3):511-20.
223. Syk E, Lenander C, Nilsson PJ, Rubio CA, Glimelius B. Tumour budding correlates with local recurrence of rectal cancer. Colorectal disease : the official journal of the Association of Coloproctology of Great Britain and Ireland. 2011;13(3):255-62.
224. van Wyk HC, Park JH, Edwards J, Horgan PG, McMillan DC, Going JJ. The relationship between tumour budding, the tumour microenvironment and survival in patients with primary operable colorectal cancer. British journal of cancer. 2016;115(2):156-63.

225. Weichert W, Kossakowski C, Harms A, Schirmacher P, Muley T, Dienemann H, et al. Proposal of a prognostically relevant grading scheme for pulmonary squamous cell carcinoma. The European respiratory journal. 2016;47(3):938-46.
226. Swets M, Kuppen PJK, Blok EJ, Gelderblom H, van de Velde CJH, Nagtegaal ID. Are pathological high-risk features in locally advanced rectal cancer a useful selection tool for adjuvant chemotherapy? European journal of cancer (Oxford, England : 1990). 2018;89:1-8.
227. Leggett SE, Hruska AM, Guo M, Wong IY. The epithelial-mesenchymal transition and the cytoskeleton in bioengineered systems. Cell Communication and Signaling. 2021;19(1):32.
228. McCuaig R, Wu F, Dunn J, Rao S, Dahlstrom JE. The biological and clinical significance of stromal-epithelial interactions in breast cancer. Pathology. 2017;49(2):133-40.
229. Bussard KM, Mutkus L, Stumpf K, Gomez-Manzano C, Marini FC. Tumor-associated stromal cells as key contributors to the tumor microenvironment. Breast cancer research : BCR. 2016;18(1):84.
230. Liu R, Li J, Xie K, Zhang T, Lei Y, Chen Y, et al. FGFR4 promotes stroma-induced epithelial-to-mesenchymal transition in colorectal cancer. Cancer research. 2013;73(19):5926-35.
231. De Wever O, Mareel M. Role of tissue stroma in cancer cell invasion. The Journal of pathology. 2003;200(4):429-47.
232. Zlobec I, Lugli A. Invasive front of colorectal cancer: dynamic interface of pro-/anti-tumor factors. World journal of gastroenterology. 2009;15(47):5898-906.
233. Hemmings C. Is carcinoma a mesenchymal disease? The role of the stromal microenvironment in carcinogenesis. Pathology. 2013;45(4):371-81.
234. Majidinia M, Yousefi B. Breast tumor stroma: A driving force in the development of resistance to therapies. Chemical biology & drug design. 2017;89(3):309-18.
235. Boyd NF, Dite GS, Stone J, Gunasekara A, English DR, McCredie MR, et al. Heritability of mammographic density, a risk factor for breast cancer. The New England journal of medicine. 2002;347(12):886-94.
236. Garcia-Mendoza MG, Inman DR, Ponik SM, Jeffery JJ, Sheerar DS, Van Doorn RR, et al. Neutrophils drive accelerated tumor progression in the collagen-dense mammary tumor microenvironment. Breast cancer research : BCR. 2016;18(1):49.
237. Goldvaser H, AlGorashi I, Ribnikar D, Seruga B, Templeton AJ, Ocana A, et al. Efficacy of extended adjuvant therapy with aromatase inhibitors in early breast cancer among common clinicopathologically-defined subgroups: A systematic review and meta-analysis. Cancer treatment reviews. 2017;60:53-9.
238. Koelzer VH, Zlobec I, Berger MD, Cathomas G, Dawson H, Dirschmid K, et al. Tumor budding in colorectal cancer revisited: results of a multicenter interobserver study. Virchows Arch. 2015;466(5):485-93.
239. Prall F, Nizze H, Barten M. Tumour budding as prognostic factor in stage I/II colorectal carcinoma. Histopathology. 2005;47(1):17-24.
240. Zlobec I, Hädrich M, Dawson H, Koelzer VH, Borner M, Mallaev M, et al. Intratumoural budding (ITB) in preoperative biopsies predicts the presence of lymph node and distant metastases in colon and rectal cancer patients. British journal of cancer. 2014;110(4):1008-13.
241. Koelzer VH, Zlobec I, Lugli A. Tumor budding in colorectal cancer--ready for diagnostic practice? Human pathology. 2016;47(1):4-19.

242. BioSpyder. TEMPO-SEQ Workflow [Available from: https://www.biospyder.com/tempo-seq-workflow.
243. BioClavis. TEMPO-SEQ 2020 [Available from: https://www.bioclavis.co.uk/overview.
244. Zhao M, Kong L, Liu Y, Qu H. dbEMT: an epithelial-mesenchymal transition associated gene resource. Sci Rep. 2015;5:11459.
245. Whitfield ML, George LK, Grant GD, Perou CM. Common markers of proliferation. Nature reviews Cancer. 2006;6(2):99-106.
246. Yang B, Chou J, Tao Y, Wu D, Wu X, Li X, et al. An assessment of prognostic immunity markers in breast cancer. NPJ breast cancer. 2018;4:35.
247. Winslow S, Leandersson K, Edsjo A, Larsson C. Prognostic stromal gene signatures in breast cancer. Breast cancer research : BCR. 2015;17:23.
248. Kestler DP, Foster JS, Macy SD, Murphy CL, Weiss DT, Solomon A. Expression of odontogenic ameloblast-associated protein (ODAM) in dental and other epithelial neoplasms. Mol Med. 2008;14(5-6):318-26.
249. Kestler DP, Foster JS, Bruker CT, Prenshaw JW, Kennel SJ, Wall JS, et al. ODAM Expression Inhibits Human Breast Cancer Tumorigenesis. Breast Cancer (Auckl). 2011;5:73-85.
250. Siddiqui S, Bruker CT, Kestler DP, Foster JS, Gray KD, Solomon A, et al. Odontogenic ameloblast associated protein as a novel biomarker for human breast cancer. Am Surg. 2009;75(9):769-75; discussion 75.
251. Devereux TR, Wiseman RW, Kaplan N, Garren S, Foley JF, White CM, et al. Assignment of a locus for mouse lung tumor susceptibility to proximal chromosome 19. Mamm Genome. 1994;5(12):749-55.
252. Gariboldi M, Manenti G, Canzian F, Falvella FS, Radice MT, Pierotti MA, et al. A major susceptibility locus to murine lung carcinogenesis maps on chromosome 6. Nat Genet. 1993;3(2):132-6.
253. Manenti G, Dragani TA. Pas1 haplotype-dependent genetic predisposition to lung tumorigenesis in rodents: a meta-analysis. Carcinogenesis. 2005;26(5):875-82.
254. Mach B, Steimle V, Martinez-Soria E, Reith W. Regulation of MHC class II genes: lessons from a disease. Annu Rev Immunol. 1996;14:301-31.
255. Gajiwala KS, Chen H, Cornille F, Roques BP, Reith W, Mach B, et al. Structure of the winged-helix protein hRFX1 reveals a new mode of DNA binding. Nature. 2000;403(6772):916-21.
256. NCBI. TBX22.
257. Brim H, Abu-Asab MS, Nouraie M, Salazar J, Deleo J, Razjouyan H, et al. An integrative CGH, MSI and candidate genes methylation analysis of colorectal tumors. PLoS One. 2014;9(1):e82185.
258. Ashktorab H, Schaffer AA, Daremipouran M, Smoot DT, Lee E, Brim H. Distinct genetic alterations in colorectal cancer. PLoS One. 2010;5(1):e8879.
259. Passegue E, Wagner EF. JunB suppresses cell proliferation by transcriptional activation of p16(INK4a) expression. Embo j. 2000;19(12):2969-79.
260. Kallergi G, Tsintari V, Sfakianakis S, Bei E, Lagoudaki E, Koutsopoulos A, et al. The prognostic value of JUNB-positive CTCs in metastatic breast cancer: from bioinformatics to phenotypic characterization. Breast cancer research : BCR. 2019;21(1):86.
261. Gervasi M, Bianchi-Smiraglia A, Cummings M, Zheng Q, Wang D, Liu S, et al. JunB contributes to Id2 repression and the epithelial-mesenchymal transition in response to transforming growth factor-beta. J Cell Biol. 2012;196(5):589-603.

262. Lian S, Shao Y, Liu H, He J, Lu W, Zhang Y, et al. PDK1 induces JunB, EMT, cell migration and invasion in human gallbladder cancer. Oncotarget. 2015;6(30):29076-86.
263. Hicks M, Hu Q, Macrae E, DeWille J. JUNB promotes the survival of Flavopiridol treated human breast cancer cells. Biochem Biophys Res Commun. 2014;450(1):19-24.
264. Pei H, Guo Z, Wang Z, Dai Y, Zheng L, Zhu L, et al. RAC2 promotes abnormal proliferation of quiescent cells by enhanced JUNB expression via the MAL-SRF pathway. Cell Cycle. 2018;17(9):1115-23.
265. Szremska AP, Kenner L, Weisz E, Ott RG, Passegue E, Artwohl M, et al. JunB inhibits proliferation and transformation in B-lymphoid cells. Blood. 2003;102(12):4159-65.
266. NCBI. DEFA3.
267. Fan J, Rone MB, Papadopoulos V. Translocator protein 2 is involved in cholesterol redistribution during erythropoiesis. The Journal of biological chemistry. 2009;284(44):30484-97.
268. NCBI. FEV.
269. Su H, Lei C-T, Zhang C. Interleukin-6 Signaling Pathway and Its Role in Kidney Disease: An Update. Frontiers in immunology. 2017;8(405).
270. Yao X, Huang J, Zhong H, Shen N, Faggioni R, Fung M, et al. Targeting interleukin-6 in inflammatory autoimmune diseases and cancers. Pharmacol Ther. 2014;141(2):125-39.
271. Santhanam U, Ghrayeb J, Sehgal PB, May LT. Post-translational modifications of human interleukin-6. Arch Biochem Biophys. 1989;274(1):161-70.
272. Heo TH, Wahler J, Suh N. Potential therapeutic implications of IL-6/IL-6R/gp130-targeting agents in breast cancer. Oncotarget. 2016;7(13):15460-73.
273. Wolf J, Rose-John S, Garbers C. Interleukin-6 and its receptors: a highly regulated and dynamic system. Cytokine. 2014;70(1):11-20.
274. Dethlefsen C, Højfeldt G, Hojman P. The role of intratumoral and systemic IL-6 in breast cancer. Breast cancer research and treatment. 2013;138(3):657-64.
275. Guo Y, Xu F, Lu T, Duan Z, Zhang Z. Interleukin-6 signaling pathway in targeted therapy for cancer. Cancer treatment reviews. 2012;38(7):904-10.
276. Taniguchi K, Karin M. IL-6 and related cytokines as the critical lynchpins between inflammation and cancer. Semin Immunol. 2014;26(1):54-74.
277. Di GH, Liu Y, Lu Y, Liu J, Wu C, Duan HF. IL-6 secreted from senescent mesenchymal stem cells promotes proliferation and migration of breast cancer cells. PLoS One. 2014;9(11):e113572.
278. Benoy I, Salgado R, Colpaert C, Weytjens R, Vermeulen PB, Dirix LY. Serum interleukin 6, plasma VEGF, serum VEGF, and VEGF platelet load in breast cancer patients. Clin Breast Cancer. 2002;2(4):311-5.
279. Chavey C, Bibeau F, Gourgou-Bourgade S, Burlinchon S, Boissière F, Laune D, et al. Oestrogen receptor negative breast cancers exhibit high cytokine content. Breast cancer research : BCR. 2007;9(1):R15.
280. Salgado R, Junius S, Benoy I, Van Dam P, Vermeulen P, Van Marck E, et al. Circulating interleukin-6 predicts survival in patients with metastatic breast cancer. International journal of cancer. 2003;103(5):642-6.
281. Zhang GJ, Adachi I. Serum interleukin-6 levels correlate to tumor progression and prognosis in metastatic breast carcinoma. Anticancer Res. 1999;19(2b):1427-32.

282. Hartman ZC, Poage GM, den Hollander P, Tsimelzon A, Hill J, Panupinthu N, et al. Growth of triple-negative breast cancer cells relies upon coordinate autocrine expression of the proinflammatory cytokines IL-6 and IL-8. Cancer research. 2013;73(11):3470-80.
283. Korkaya H, Liu S, Wicha MS. Breast cancer stem cells, cytokine networks, and the tumor microenvironment. J Clin Invest. 2011;121(10):3804-9.
284. Erez N, Glanz S, Raz Y, Avivi C, Barshack I. Cancer associated fibroblasts express pro-inflammatory factors in human breast and ovarian tumors. Biochem Biophys Res Commun. 2013;437(3):397-402.
285. Studebaker AW, Storci G, Werbeck JL, Sansone P, Sasser AK, Tavolari S, et al. Fibroblasts isolated from common sites of breast cancer metastasis enhance cancer cell growth rates and invasiveness in an interleukin-6-dependent manner. Cancer research. 2008;68(21):9087-95.
286. Lieblein JC, Ball S, Hutzen B, Sasser AK, Lin HJ, Huang TH, et al. STAT3 can be activated through paracrine signaling in breast epithelial cells. BMC Cancer. 2008;8:302.
287. Shah N, Jin K, Cruz LA, Park S, Sadik H, Cho S, et al. HOXB13 mediates tamoxifen resistance and invasiveness in human breast cancer by suppressing ERα and inducing IL-6 expression. Cancer research. 2013;73(17):5449-58.
288. Conze D, Weiss L, Regen PS, Bhushan A, Weaver D, Johnson P, et al. Autocrine production of interleukin 6 causes multidrug resistance in breast cancer cells. Cancer research. 2001;61(24):8851-8.
289. Korkaya H, Kim GI, Davis A, Malik F, Henry NL, Ithimakin S, et al. Activation of an IL6 inflammatory loop mediates trastuzumab resistance in HER2+ breast cancer by expanding the cancer stem cell population. Mol Cell. 2012;47(4):570-84.
290. Faggioli L, Costanzo C, Merola M, Bianchini E, Furia A, Carsana A, et al. Nuclear factor kappa B (NF-kappa B), nuclear factor interleukin-6 (NFIL-6 or C/EBP beta) and nuclear factor interleukin-6 beta (NFIL6-beta or C/EBP delta) are not sufficient to activate the endogenous interleukin-6 gene in the human breast carcinoma cell line MCF-7. Comparative analysis with MDA-MB-231 cells, an interleukin-6-expressing human breast carcinoma cell line. Eur J Biochem. 1996;239(3):624-31.
291. Robinson EK, Sneige N, Grimm EA. Correlation of interleukin 6 with interleukin 1alpha in human mammary tumours, but not with oestrogen receptor expression. Cytokine. 1998;10(12):970-6.
292. Chiu JJ, Sgagias MK, Cowan KH. Interleukin 6 acts as a paracrine growth factor in human mammary carcinoma cell lines. Clinical cancer research : an official journal of the American Association for Cancer Research. 1996;2(1):215-21.
293. Fertig EJ, Lee E, Pandey NB, Popel AS. Analysis of gene expression of secreted factors associated with breast cancer metastases in breast cancer subtypes. Sci Rep. 2015;5:12133.
294. Fontanini G, Campani D, Roncella M, Cecchetti D, Calvo S, Toniolo A, et al. Expression of interleukin 6 (IL-6) correlates with oestrogen receptor in human breast carcinoma. British journal of cancer. 1999;80(3-4):579-84.
295. Yu H, Kortylewski M, Pardoll D. Crosstalk between cancer and immune cells: role of STAT3 in the tumour microenvironment. Nature reviews Immunology. 2007;7(1):41-51.
296. Danforth DN, Jr., Sgagias MK. Interleukin-1 alpha and interleukin-6 act additively to inhibit growth of MCF-7 breast cancer cells in vitro. Cancer research. 1993;53(7):1538-45.

297. Jiang XP, Yang DC, Elliott RL, Head JF. Down-regulation of expression of interleukin-6 and its receptor results in growth inhibition of MCF-7 breast cancer cells. Anticancer Res. 2011;31(9):2899-906.
298. Garcia-Tuñón I, Ricote M, Ruiz A, Fraile B, Paniagua R, Royuela M. IL-6, its receptors and its relationship with bcl-2 and bax proteins in infiltrating and in situ human breast carcinoma. Histopathology. 2005;47(1):82-9.
299. Sun X, Qu Q, Lao Y, Zhang M, Yin X, Zhu H, et al. Tumor suppressor HIC1 is synergistically compromised by cancer-associated fibroblasts and tumor cells through the IL-6/pSTAT3 axis in breast cancer. BMC Cancer. 2019;19(1):1180.
300. Singh A, Purohit A, Ghilchik MW, Reed MJ. The regulation of aromatase activity in breast fibroblasts: the role of interleukin-6 and prostaglandin E2. Endocr Relat Cancer. 1999;6(2):139-47.
301. Purohit A, Newman SP, Reed MJ. The role of cytokines in regulating estrogen synthesis: implications for the etiology of breast cancer. Breast cancer research : BCR. 2002;4(2):65-9.
302. Sullivan NJ, Sasser AK, Axel AE, Vesuna F, Raman V, Ramirez N, et al. Interleukin-6 induces an epithelial–mesenchymal transition phenotype in human breast cancer cells. Oncogene. 2009;28(33):2940-7.
303. Zinzalla G, Haque MR, Basu BP, Anderson J, Kaye SL, Haider S, et al. A novel small-molecule inhibitor of IL-6 signalling. Bioorg Med Chem Lett. 2010;20(23):7029-32.
304. Furumoto Y, Gadina M. The arrival of JAK inhibitors: advancing the treatment of immune and hematologic disorders. BioDrugs. 2013;27(5):431-8.
305. Wilks AF, Harpur AG, Kurban RR, Ralph SJ, Zürcher G, Ziemiecki A. Two novel protein-tyrosine kinases, each with a second phosphotransferase-related catalytic domain, define a new class of protein kinase. Mol Cell Biol. 1991;11(4):2057-65.
306. Wehde BL, Rädler PD, Shrestha H, Johnson SJ, Triplett AA, Wagner KU. Janus Kinase 1 Plays a Critical Role in Mammary Cancer Progression. Cell reports. 2018;25(8):2192-207.e5.
307. Senkevitch E, Durum S. The promise of Janus kinase inhibitors in the treatment of hematological malignancies. Cytokine. 2017;98:33-41.
308. Roskoski R, Jr. Janus kinase (JAK) inhibitors in the treatment of inflammatory and neoplastic diseases. Pharmacol Res. 2016;111:784-803.
309. Kaushik N, Kim MJ, Kim RK, Kumar Kaushik N, Seong KM, Nam SY, et al. Low-dose radiation decreases tumor progression via the inhibition of the JAK1/STAT3 signaling axis in breast cancer cell lines. Sci Rep. 2017;7:43361.
310. Yeh YT, Ou-Yang F, Chen IF, Yang SF, Su JH, Hou MF, et al. Altered p-JAK1 expression is associated with estrogen receptor status in breast infiltrating ductal carcinoma. Oncol Rep. 2007;17(1):35-9.
311. Chen B, Lai J, Dai D, Chen R, Li X, Liao N. JAK1 as a prognostic marker and its correlation with immune infiltrates in breast cancer. Aging (Albany NY). 2019;11(23):11124-35.
312. Zhu N, Zhang J, Du Y, Qin X, Miao R, Nan J, et al. Loss of ZIP facilitates JAK2-STAT3 activation in tamoxifen-resistant breast cancer. Proceedings of the National Academy of Sciences of the United States of America. 2020;117(26):15047-54.
313. Xie J, LeBaron MJ, Nevalainen MT, Rui H. Role of tyrosine kinase Jak2 in prolactin-induced differentiation and growth of mammary epithelial cells. The Journal of biological chemistry. 2002;277(16):14020-30.
314. Balko JM, Schwarz LJ, Luo N, Estrada MV, Giltnane JM, Dávila-González D, et al. Triple-negative breast cancers with amplification of JAK2 at the 9p24

locus demonstrate JAK2-specific dependence. Sci Transl Med. 2016;8(334):334ra53.
315. Qureshy Z, Johnson DE, Grandis JR. Targeting the JAK/STAT pathway in solid tumors. Journal of Cancer Metastasis and Treatment. 2020;6:27.
316. Zouein FA, Duhé RJ, Booz GW. JAKs go nuclear: emerging role of nuclear JAK1 and JAK2 in gene expression and cell growth. Growth Factors. 2011;29(6):245-52.
317. Lobie PE, Ronsin B, Silvennoinen O, Haldosén LA, Norstedt G, Morel G. Constitutive nuclear localization of Janus kinases 1 and 2. Endocrinology. 1996;137(9):4037-45.
318. Sorenson RL, Stout LE. Prolactin receptors and JAK2 in islets of Langerhans: an immunohistochemical analysis. Endocrinology. 1995;136(9):4092-8.
319. Ram PA, Waxman DJ. Interaction of growth hormone-activated STATs with SH2-containing phosphotyrosine phosphatase SHP-1 and nuclear JAK2 tyrosine kinase. The Journal of biological chemistry. 1997;272(28):17694-702.
320. Ito M, Nakasato M, Suzuki T, Sakai S, Nagata M, Aoki F. Localization of janus kinase 2 to the nuclei of mature oocytes and early cleavage stage mouse embryos. Biol Reprod. 2004;71(1):89-96.
321. Zhu F, Hwang B, Miyamoto S, Rui L. Nuclear Import of JAK1 Is Mediated by a Classical NLS and Is Required for Survival of Diffuse Large B-cell Lymphoma. Mol Cancer Res. 2017;15(3):348-57.
322. Rui L, Drennan AC, Ceribelli M, Zhu F, Wright GW, Huang DW, et al. Epigenetic gene regulation by Janus kinase 1 in diffuse large B-cell lymphoma. Proceedings of the National Academy of Sciences. 2016;113(46):E7260.
323. Martin TA YL, Sanders AJ et al. Cancer Invasion and Metastasis: Molecular and Cellular Perspective. 2013. In: Madame Curie Bioscience Database [Internet]. Austin (TX): Landes Bioscience. Available from: https://www.ncbi.nlm.nih.gov/books/NBK164700/.
324. Wang S, Liang K, Hu Q, Li P, Song J, Yang Y, et al. JAK2-binding long noncoding RNA promotes breast cancer brain metastasis. J Clin Invest. 2017;127(12):4498-515.
325. Marotta LL, Almendro V, Marusyk A, Shipitsin M, Schemme J, Walker SR, et al. The JAK2/STAT3 signaling pathway is required for growth of $CD44^{+}CD24^{-}$ stem cell-like breast cancer cells in human tumors. J Clin Invest. 2011;121(7):2723-35.
326. Miller CP, Thorpe JD, Kortum AN, Coy CM, Cheng WY, Ou Yang TH, et al. JAK2 expression is associated with tumor-infiltrating lymphocytes and improved breast cancer outcomes: implications for evaluating JAK2 inhibitors. Cancer Immunol Res. 2014;2(4):301-6.
327. López-Ozuna VM, Hachim IY, Hachim MY, Lebrun JJ, Ali S. Prolactin Pro-Differentiation Pathway in Triple Negative Breast Cancer: Impact on Prognosis and Potential Therapy. Sci Rep. 2016;6:30934.
328. Popielarczyk TL, Huckle WR, Barrett JG. Human Bone Marrow-Derived Mesenchymal Stem Cells Home via the PI3K-Akt, MAPK, and Jak/Stat Signaling Pathways in Response to Platelet-Derived Growth Factor. Stem Cells Dev. 2019;28(17):1191-202.
329. Zacharaki D, Ghazanfari R, Li H, Lim HC, Scheding S. Effects of JAK1/2 inhibition on bone marrow stromal cells of myeloproliferative neoplasm (MPN) patients and healthy individuals. Eur J Haematol. 2018;101(1):57-67.

330. von Ahrens D, Bhagat TD, Nagrath D, Maitra A, Verma A. The role of stromal cancer-associated fibroblasts in pancreatic cancer. J Hematol Oncol. 2017;10(1):76.
331. Biffi G, Oni TE, Spielman B, Hao Y, Elyada E, Park Y, et al. IL1-Induced JAK/STAT Signaling Is Antagonized by TGFβ to Shape CAF Heterogeneity in Pancreatic Ductal Adenocarcinoma. Cancer Discov. 2019;9(2):282-301.
332. Kuzet SE, Gaggioli C. Fibroblast activation in cancer: when seed fertilizes soil. Cell Tissue Res. 2016;365(3):607-19.
333. Heine A, Held SA, Daecke SN, Wallner S, Yajnanarayana SP, Kurts C, et al. The JAK-inhibitor ruxolitinib impairs dendritic cell function in vitro and in vivo. Blood. 2013;122(7):1192-202.
334. Gotthardt D, Trifinopoulos J, Sexl V, Putz EM. JAK/STAT Cytokine Signaling at the Crossroad of NK Cell Development and Maturation. Frontiers in immunology. 2019;10:2590.
335. Papaccio F, Paino F, Regad T, Papaccio G, Desiderio V, Tirino V. Concise Review: Cancer Cells, Cancer Stem Cells, and Mesenchymal Stem Cells: Influence in Cancer Development. Stem Cells Transl Med. 2017;6(12):2115-25.
336. Chang AI, Schwertschkow AH, Nolta JA, Wu J. Involvement of mesenchymal stem cells in cancer progression and metastases. Curr Cancer Drug Targets. 2015;15(2):88-98.
337. Hass R. Role of MSC in the Tumor Microenvironment. Cancers (Basel). 2020;12(8).
338. El-Haibi CP, Bell GW, Zhang J, Collmann AY, Wood D, Scherber CM, et al. Critical role for lysyl oxidase in mesenchymal stem cell-driven breast cancer malignancy. Proceedings of the National Academy of Sciences of the United States of America. 2012;109(43):17460-5.
339. Zhang T, Lee YW, Rui YF, Cheng TY, Jiang XH, Li G. Bone marrow-derived mesenchymal stem cells promote growth and angiogenesis of breast and prostate tumors. Stem Cell Res Ther. 2013;4(3):70.
340. Karnoub AE, Dash AB, Vo AP, Sullivan A, Brooks MW, Bell GW, et al. Mesenchymal stem cells within tumour stroma promote breast cancer metastasis. Nature. 2007;449(7162):557-63.
341. Dittmer A, Hohlfeld K, Lützkendorf J, Müller LP, Dittmer J. Human mesenchymal stem cells induce E-cadherin degradation in breast carcinoma spheroids by activating ADAM10. Cell Mol Life Sci. 2009;66(18):3053-65.
342. Orimo A, Gupta PB, Sgroi DC, Arenzana-Seisdedos F, Delaunay T, Naeem R, et al. Stromal fibroblasts present in invasive human breast carcinomas promote tumor growth and angiogenesis through elevated SDF-1/CXCL12 secretion. Cell. 2005;121(3):335-48.
343. Houthuijzen JM, Jonkers J. Cancer-associated fibroblasts as key regulators of the breast cancer tumor microenvironment. Cancer Metastasis Rev. 2018;37(4):577-97.
344. Mumin NH, Drobnitzky N, Patel A, Lourenco LM, Cahill FF, Jiang Y, et al. Overcoming acquired resistance to HSP90 inhibition by targeting JAK-STAT signalling in triple-negative breast cancer. BMC Cancer. 2019;19(1):102.
345. Doheny D, Sirkisoon S, Carpenter RL, Aguayo NR, Regua AT, Anguelov M, et al. Combined inhibition of JAK2-STAT3 and SMO-GLI1/tGLI1 pathways suppresses breast cancer stem cells, tumor growth, and metastasis. Oncogene. 2020;39(42):6589-605.
346. Stover DG, Gil Del Alcazar CR, Brock J, Guo H, Overmoyer B, Balko J, et al. Phase II study of ruxolitinib, a selective JAK1/2 inhibitor, in patients with metastatic triple-negative breast cancer. NPJ breast cancer. 2018;4:10.

347. O'Shaughnessy J, DeMichele A, Ma CX, Richards P, Yardley DA, Wright GS, et al. A randomized, double-blind, phase 2 study of ruxolitinib or placebo in combination with capecitabine in patients with advanced HER2-negative breast cancer and elevated C-reactive protein, a marker of systemic inflammation. Breast cancer research and treatment. 2018;170(3):547-57.
348. Lin NU, Gelman RS, Brock JE, Bardia A, Mayer EL, Overmoyer B, et al. Phase II study of ruxolitinib in patients with pStat3+ breast cancer. Journal of Clinical Oncology. 2013;31(15_suppl):TPS1134-TPS.
349. A Phase 1 Study of PD-1 Inhibition With Pembrolizumab Combined With JAK2 Inhibition in Triple Negative Breast Cancer [Internet]. 2017 [cited 11/11/2020]. Available from: https://clinicaltrials.gov/ct2/show/NCT03012230.
350. Phase I/II Trial of Ruxolitinib in Combination With Trastuzumab in Metastatic HER2 Positive Breast Cancer [Internet]. 2014 [cited 11/11/2020]. Available from: https://clinicaltrials.gov/ct2/show/NCT02066532.
351. TBCRC 042 - A Randomized Phase II Window-of-Opportunity Trial of Ruxolitinib in Patients With High Risk and Premalignant Breast Conditions [Internet]. 2016 [cited 11/11/2020]. Available from: https://clinicaltrials.gov/ct2/show/NCT02928978.
352. Hughes K, Watson CJ. The Multifaceted Role of STAT3 in Mammary Gland Involution and Breast Cancer. International journal of molecular sciences. 2018;19(6).
353. Yuan J, Zhang F, Niu R. Multiple regulation pathways and pivotal biological functions of STAT3 in cancer. Sci Rep. 2015;5:17663.
354. Banerjee K, Resat H. Constitutive activation of STAT3 in breast cancer cells: A review. International journal of cancer. 2016;138(11):2570-8.
355. Groner B, von Manstein V. Jak Stat signaling and cancer: Opportunities, benefits and side effects of targeted inhibition. Molecular and cellular endocrinology. 2017;451:1-14.
356. Wake MS, Watson CJ. STAT3 the oncogene - still eluding therapy? Febs j. 2015;282(14):2600-11.
357. Segatto I, Baldassarre G, Belletti B. STAT3 in Breast Cancer Onset and Progression: A Matter of Time and Context. International journal of molecular sciences. 2018;19(9).
358. Zhang N, Ma ZP, Wang J, Bai HL, Li YX, Sun Q, et al. Human papillomavirus infection correlates with inflammatory Stat3 signaling activity and IL-17 expression in patients with breast cancer. American journal of translational research. 2016;8(7):3214-26.
359. Jain N, Zhang T, Fong SL, Lim CP, Cao X. Repression of Stat3 activity by activation of mitogen-activated protein kinase (MAPK). Oncogene. 1998;17(24):3157-67.
360. Jain N, Zhang T, Kee WH, Li W, Cao X. Protein kinase C delta associates with and phosphorylates Stat3 in an interleukin-6-dependent manner. The Journal of biological chemistry. 1999;274(34):24392-400.
361. Lim CP, Cao X. Serine phosphorylation and negative regulation of Stat3 by JNK. The Journal of biological chemistry. 1999;274(43):31055-61.
362. Yang J, Kunimoto H, Katayama B, Zhao H, Shiromizu T, Wang L, et al. Phospho-Ser727 triggers a multistep inactivation of STAT3 by rapid dissociation of pY705-SH2 through C-terminal tail modulation. Int Immunol. 2020;32(2):73-88.
363. Tkach M, Rosemblit C, Rivas MA, Proietti CJ, Díaz Flaqué MC, Mercogliano MF, et al. p42/p44 MAPK-mediated Stat3Ser727 phosphorylation is required for

progestin-induced full activation of Stat3 and breast cancer growth. Endocr Relat Cancer. 2013;20(2):197-212.
364. Zhang Q, Raje V, Yakovlev VA, Yacoub A, Szczepanek K, Meier J, et al. Mitochondrial localized Stat3 promotes breast cancer growth via phosphorylation of serine 727. The Journal of biological chemistry. 2013;288(43):31280-8.
365. Rozovski U, Harris DM, Li P, Liu Z, Jain P, Veletic I, et al. Constitutive Phosphorylation of STAT3 by the CK2-BLNK-CD5 Complex. Mol Cancer Res. 2017;15(5):610-8.
366. Balic JJ, White CL, Dawson R, Gough D, McCormack MP, Jenkins BJ. STAT3-driven hematopoiesis and lymphopoiesis abnormalities are dependent on serine phosphorylation. Cytokine. 2020;130:155059.
367. Balic JJ, Garama DJ, Saad MI, Yu L, West AC, West AJ, et al. Serine-Phosphorylated STAT3 Promotes Tumorigenesis via Modulation of RNA Polymerase Transcriptional Activity. Cancer research. 2019;79(20):5272-87.
368. Balic JJ, Saad MI, Dawson R, West AJ, McLeod L, West AC, et al. Constitutive STAT3 Serine Phosphorylation Promotes Helicobacter-Mediated Gastric Disease. The American journal of pathology. 2020;190(6):1256-70.
369. Hsu FN, Chen MC, Lin KC, Peng YT, Li PC, Lin E, et al. Cyclin-dependent kinase 5 modulates STAT3 and androgen receptor activation through phosphorylation of Ser^{727} on STAT3 in prostate cancer cells. Am J Physiol Endocrinol Metab. 2013;305(8):E975-86.
370. Lin WH, Chang YW, Hong MX, Hsu TC, Lee KC, Lin C, et al. STAT3 phosphorylation at Ser727 and Tyr705 differentially regulates the EMT-MET switch and cancer metastasis. Oncogene. 2020.
371. Gritsko T, Williams A, Turkson J, Kaneko S, Bowman T, Huang M, et al. Persistent activation of stat3 signaling induces survivin gene expression and confers resistance to apoptosis in human breast cancer cells. Clinical cancer research : an official journal of the American Association for Cancer Research. 2006;12(1):11-9.
372. Niu G, Wright KL, Huang M, Song L, Haura E, Turkson J, et al. Constitutive Stat3 activity up-regulates VEGF expression and tumor angiogenesis. Oncogene. 2002;21(13):2000-8.
373. Dien J, Amin HM, Chiu N, Wong W, Frantz C, Chiu B, et al. Signal transducers and activators of transcription-3 up-regulates tissue inhibitor of metalloproteinase-1 expression and decreases invasiveness of breast cancer. The American journal of pathology. 2006;169(2):633-42.
374. Chapman RS, Lourenco PC, Tonner E, Flint DJ, Selbert S, Takeda K, et al. Suppression of epithelial apoptosis and delayed mammary gland involution in mice with a conditional knockout of Stat3. Genes Dev. 1999;13(19):2604-16.
375. Jhan JR, Andrechek ER. Stat3 accelerates Myc induced tumor formation while reducing growth rate in a mouse model of breast cancer. Oncotarget. 2016;7(40):65797-807.
376. Albrengues J, Bertero T, Grasset E, Bonan S, Maiel M, Bourget I, et al. Epigenetic switch drives the conversion of fibroblasts into proinvasive cancer-associated fibroblasts. Nat Commun. 2015;6:10204.
377. Yoshida GJ. Regulation of heterogeneous cancer-associated fibroblasts: the molecular pathology of activated signaling pathways. Journal of experimental & clinical cancer research : CR. 2020;39(1):112.
378. Wang T, Fahrmann JF, Lee H, Li YJ, Tripathi SC, Yue C, et al. JAK/STAT3-Regulated Fatty Acid β-Oxidation Is Critical for Breast Cancer Stem Cell Self-Renewal and Chemoresistance. Cell Metab. 2018;27(1):136-50.e5.

379. Real PJ, Sierra A, De Juan A, Segovia JC, Lopez-Vega JM, Fernandez-Luna JL. Resistance to chemotherapy via Stat3-dependent overexpression of Bcl-2 in metastatic breast cancer cells. Oncogene. 2002;21(50):7611-8.
380. Kettner NM, Vijayaraghavan S, Durak MG, Bui T, Kohansal M, Ha MJ, et al. Combined Inhibition of STAT3 and DNA Repair in Palbociclib-Resistant ER-Positive Breast Cancer. Clinical cancer research : an official journal of the American Association for Cancer Research. 2019;25(13):3996-4013.
381. Sonnenblick A, Brohee S, Fumagalli D, Vincent D, Venet D, Ignatiadis M, et al. Constitutive phosphorylated STAT3-associated gene signature is predictive for trastuzumab resistance in primary HER2-positive breast cancer. BMC medicine. 2015;13:177.
382. Lu L, Dong J, Wang L, Xia Q, Zhang D, Kim H, et al. Activation of STAT3 and Bcl-2 and reduction of reactive oxygen species (ROS) promote radioresistance in breast cancer and overcome of radioresistance with niclosamide. Oncogene. 2018;37(39):5292-304.
383. Qin JJ, Yan L, Zhang J, Zhang WD. STAT3 as a potential therapeutic target in triple negative breast cancer: a systematic review. Journal of experimental & clinical cancer research : CR. 2019;38(1):195.
384. Fujimoto Y, Ozawa H, Higuchi T, Miyagawa Y, Bun A, Imamura M, et al. Improved prognosis of low baseline neutrophil-to-lymphocyte ratio is significantly exclusive in breast cancer patients with high absolute counts of lymphocytes. Mol Clin Oncol. 2019;10(2):275-84.
385. Patel DA, Xi J, Luo J, Hassan B, Thomas S, Ma CX, et al. Neutrophil-to-lymphocyte ratio as a predictor of survival in patients with triple-negative breast cancer. Breast cancer research and treatment. 2019;174(2):443-52.
386. Ferroni P, Roselli M, Buonomo OC, Spila A, Portarena I, Laudisi A, et al. Prognostic Significance of Neutrophil-to-lymphocyte Ratio in the Framework of the 8th TNM Edition for Breast Cancer. Anticancer Res. 2018;38(8):4705-12.
387. Geng SK, Fu SM, Fu YP, Zhang HW. Neutrophil to lymphocyte ratio is a prognostic factor for disease free survival in patients with breast cancer underwent curative resection. Medicine (Baltimore). 2018;97(35):e11898.
388. Losada B, Guerra JA, Malón D, Jara C, Rodriguez L, Del Barco S. Pretreatment neutrophil/lymphocyte, platelet/lymphocyte, lymphocyte/monocyte, and neutrophil/monocyte ratios and outcome in elderly breast cancer patients. Clinical & translational oncology : official publication of the Federation of Spanish Oncology Societies and of the National Cancer Institute of Mexico. 2019;21(7):855-63.
389. Moldoveanu D, Pravongviengkham V, Best G, Martínez C, Hijal T, Meguerditchian AN, et al. Dynamic Neutrophil-to-Lymphocyte Ratio: A Novel Prognosis Measure for Triple-Negative Breast Cancer. Ann Surg Oncol. 2020;27(10):4028-34.
390. Qiu X, Song Y, Cui Y, Liu Y. Increased neutrophil-lymphocyte ratio independently predicts poor survival in non-metastatic triple-negative breast cancer patients. IUBMB Life. 2018;70(6):529-35.
391. Unit WCT. Optimal personalised treatment of early breast cancer using multiparameter analysis (OPTIMA) ISRCTN registry2012 [Available from: https://www.isrctn.com/ISRCTN42400492.
392. Stein RC, Dunn JA, Bartlett JM, Campbell AF, Marshall A, Hall P, et al. OPTIMA prelim: a randomised feasibility study of personalised care in the treatment of women with early breast cancer. Health Technol Assess. 2016;20(10):xxiii-xxix, 1-201.